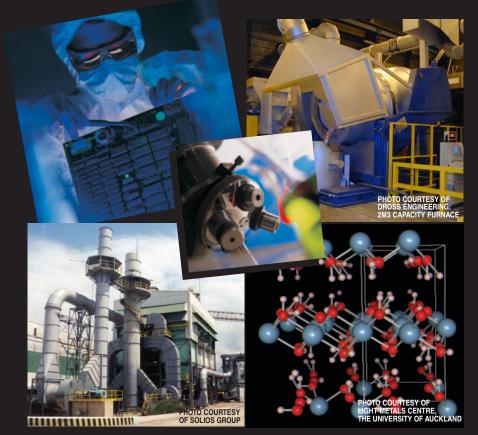


# **133rd Annual Meeting & Exhibition**

The Minerals, Metals & Materials Society welcomes you to the TECHNICAL PROGRAM for the 133<sup>rd</sup> TMS Annual Meeting & Exhibition, to be held March 14–18, 2004, in Charlotte, North Carolina.



## For your convenience, we have also included details on

- Meeting Activities and Registration
- Conference Proceedings
- Our Exhibition
- TMS Membership
- Additional On-line Resources that You May Utilize

All designed to help you prepare for and optimally benefit from one of the world's premier metals and materials events.

# This document comprises MONDAY'S TECHNICAL PROGRAM

Including fully text-searchable paper titles, abstracts, and author names with affiliations

# **See you in Charlotte!**





http://www.tms.org/ AnnualMeeting.html

# The Improved Web Resource for Every TMS Publication...

# The New On-Line TMS Document Center

Customized to meet your unique needs and now upgraded to provide faster service and easier navigation, the On-Line TMS Document Center provides detailed information and on-line purchasing opportunities for TMS proceedings volumes, textbooks, journals, software programs, video series, and reports. If you need information, you've got to try the new TMS Document Center.

Check out these great new features:



## Find, Select, and Check Out the Products You Want FAST

The new TMS Document Center provides easier navigation and faster service for an overall improved shopping experience.



## Sample Articles Before You Buy

Not sure if a particular article is the one you need? Click on the PDF icon to view the first page of the article and know that you will be satisfied with your purchase.

## TMS Members: View JOM On-Line Free of Charge

TMS members can view the journal for free through the new TMS Document Center. Simply log in and articles from past and current issues are instantly at your fingertips to browse, read, and print out, free of charge!

## Purchase Download Suites

Purchase downloads in sets of 10, 25, 50, or 100, and use them to download any files in the TMS Document Center (for less than it would cost to download that many papers individually!). Download suites can be used all at once, over a series of visits to the site, or to create your own custom publication.



## **Create Your Own Custom Publication**

Gather individual papers and articles from TMS proceedings volumes, *JOM*, *Journal of Electronic Materials*, and *Metallurgical and Materials Transactions A* and *B* to create a one-of-a-kind publication that meets your needs. TMS will compile them in either a softcover book or on a CD-ROM—it's your choice.

## Coming in 2004: TMS Letters

*TMS Letters* is a peer-reviewed, on-line-only journal featuring technical updates of hitherto unpublished research presented at TMS meetings. Available free-of-charge to TMS members (and by subscription to nonmembers), the journal comprises two-page technical updates, including text and graphics. Visit the TMS Document Center for additional information about *TMS Letters*!

See it for yourself! Visit the new TMS Document Center today.

# http://doc.tms.org

## AN INTERNATIONAL EVENT IN SCIENCE AND ENGINEERING

During the week of March 14–18, the 2004 TMS Annual Meeting & Exhibition will host approximately 4,000 science and engineering professionals, representing more than 70 different countries. They are convening at the Charlotte Convention Center to attend a field-spanning array of metals and materials symposia containing more than 200 sessions and 1,900 individual technical presentations.

#### This year's meeting will feature programming by

- TMS Electronic, Magnetic & Photonic Materials Division
- TMS Extraction & Processing Division
- TMS Light Metals Division
- TMS Materials Processing & Manufacturing Division
- TMS Structural Materials Division
- TMS Education Committee
- TMS Young Leaders Committee
- ASM International's Materials Science Critical Technologies Sector
- International Titanium Association
- International Magnesium Association
- National Science Foundation
- TMS Public & Governmental Affairs Committee

# In addition to the technical programming featured on the following pages, attendees will have the opportunity to

- Tour the Exhibition of more than 160 Companies Displaying New Products and Services
- Attend Special Lectures and Tutorials
- Participate in Short Courses on Metal Matrix Composites, Introduction to Nanomanufacturing and Nanotechnology, Technology Transfer Seminar, Smelter Grade Alumina from the Smelting Perspective and Computational Modelling for the Materials Professional
- Enjoy Special Luncheons, Dinners, and Social Functions, including events honoring Didier de Fontaine, R.J. Arsenault, A.L. Roytburd and Roger D. Doherty
- Network Extensively
- **Experience** the Charm and Amenities of Charlotte

#### Extensive details about these and all conference-related activities can be found on the 2004 TMS Annual Meeting Web Site.

## WANT TO BE PART OF THE ACTION?

#### Registration is easy.

Just complete and mail or fax the Annual Meeting Registration Form that appears in this document. Or, visit the meeting web site to register immediately (and securely) on-line.

To register in advance, your submission must reach TMS not later than **February 16, 2004.** After this date, it will be necessary to register at the meeting site.

The **Westin Charlotte Hotel** is the TMS headquarters hotel. Special conference rates have been contracted with this hotel and others in the area surrounding the **Charlotte Convention Center.** To receive special rates, use the TMS 2004 Housing Reservation Form that appears in this document and that can be found on the meeting web site.

**Special Opportunity for TMS Nonmember Registrants:** All nonmember registrants automatically receive a one-year introductory associate membership in TMS for 2004. Membership benefits include a subscription to *JOM* (print and on-line versions) and significant discounts on TMS products and services.

More on the benefits of membership appears on the <u>TMS Membership Web Pages</u>.

## INTERESTED IN BUSINESS OPPORTUNITIES?

The 2004 TMS Annual Meeting & Exhibition presents businesses, universities, institutions, agencies, consultants, and others with myriad opportunities to partner in effective marketing communication. Such opportunities to reach thousands of meeting attendees include:

- Placing a **Booth** in the Exhibition
- Placing an Ad in the Official Conference Publication and At-Meeting Program: JOM
- Sponsoring High-Profile Attendee Services, such as the CyberCenter, Coffee Breaks, Signage, and Prize Drawings.
- Hosting a Hospitality Suite

More information on these opportunities is available on the 2004 TMS Annual Meeting Sponsorship Web Pages.

CONFERENCE PROCEEDINGS: THE **RECORDS OF EVENTS** 

The technical program of each TMS Annual Meeting yields numerous conference proceedings that document many presentations delivered in session rooms. Such publications can be ordered both before and after the meeting via the meeting registration form and/or the TMS Document Center.

The following symposium proceedings will be available in tandem with the meeting:

#### ADVANCED MATERIALS FOR ENERGY CONVERSION II

Dhanesh Chandra, Renato G. Bautista, and Louis Schlapbach, editors ISBN 0-87339-574-3 • Approx. 560 pp., illus., index, softcover Order No. 04-5743 • Weight 3 lbs M \$112 + S \$89 + L \$160

#### ADVANCES IN SUPERPLASTICITY AND

SUPERPLASTIC FORMING

Eric M. Taleff, Paul E. Krajewski, and Peter A. Friedman, editors ISBN 0-87339-564-6 • Approx. 436 pp., illus., index, softcover Order No. 04-5646 • Weight 2 lbs M \$115 + S \$91 + L \$164

#### **BULK METALLIC GLASSES**

Peter K. Liaw and Raymond A. Buchanan, editors ISBN 0-87339-573-5 • Approx. 256 pp., illus., index, softcover Order No. 04-5735 • Weight 2 lbs M \$125 + S \$99 + L \$179

#### **EPD CONGRESS 2004**

Mark Schlesinger, editor

Includes the proceedings from the following symposia: Electrochemical Mea-surements and Processing of Materials, General Pyrometallurgy, Materials Processing Fundamentals, Solid and Aqueous Wastes, Sustainable Development session of Recent Advances in Non-Ferrous Metals Processing, and General Recycling session of Recycling.

ISBN 0-87339-565-4 • Approx. 1,020 pp., CD-ROM Order No. 04-5654-CD • Weight 1 lb M \$71 + S \$56 + L \$101

LATERITE NICKEL SYMPOSIUM 2004 D.M. Lane and W.P. Imrie, editors ISBN 0-87339-550-6 • Approx. 1,144 pp., illus., index, hardcover Order No. 04-5506 • Weight 4 lbs M \$119 + S \$94 + L \$170

#### **LIGHT METALS 2004**

A.T. Tabereaux, editor

Includes the proceedings from the following symposia Alumina & Bauxite, Aluminum Can Recycling, Aluminum Reduction Technology, Carbon Technol-ogy, Cast House Technology, Reactive Metals session of Recent Advances in Non-Ferrous Metals Processing, Aluminum and Aluminum Dross Processing

sessions of Recycling. ISBN 0-87339-567-0 • Approx. 1,150 pp., illus., hardcover & CD-ROM Order No. 04-5670-G • Weight 7 lbs M \$150 + S \$125 + Ľ \$225

#### **MAGNESIUM TECHNOLOGY 2004**

Alan A. Luo, editor

ISBN 0-87339-568-9 • Approx. 436 pp., illus., hardcover & CD-ROM Order No. 04-5689-G • Weight 3 lbs M \$101 + S \$80 + L \$144

#### SOLIDIFICATION OF ALUMINUM ALLOYS

Men G. Chu, Douglas A. Granger, and Qingyou Han, editors ISBN 0-87339-569-7 • Approx. 440 pp., illus., softcover Order No. 04-5697 • Weight 2 lbs M \$118 + S \$93 + L \$168

#### **MULTIPHASE PHENOMENA AND CFD MODELING AND** SIMULATION IN MATERIALS PROCESSES L. Nastac and B. Li. editors

Includes the proceedings from the following symposia: Multiphase Phenomena in Materials Processing and CFD Modeling and Simulation of Engineering Processes.

ISBN 0-87339-570-0 • Approx. 760 pp., illus., softcover Order No. 04-5700 • Weight 4 lbs M \$132 + \$ \$105 + L \$189

#### SOLIDIFICATION PROCESSES AND MICROSTRUCTURES: A SYMPOSIUM IN HONOR OF PROF. W. KURZ

M. Rappaz, C. Beckermann, and R. Trivedi, editors ISBN 0-87339-572-7 • Approx. 432 pp., softcover Order No. 04-5727 • Weight 2 lbs M \$112 + S \$88 + L \$159

#### THE FIFTH GLOBAL INNOVATIONS SYMPOSIUM ON **MATERIALS PROCESSING AND MANUFACTURING:** SURFACES AND INTERFACES IN NANOSTRUCTURED MATERIALS AND TRENDS IN LIGA, MINIATURIZATION, AND NANOSCALE MATERIALS

Sharmila M. Mukhopadhyay, John Smugeresky, Sudipta Seal, Narendra B. Dahotre, and Arvind Agarwal, editors

Includes the proceedings from the following symposia: Surfaces and Interfaces in Nanostructured Materials and the Fifth Global Innovations Symposium on Materials Processing and Manufacturing: Trends in LIGA, Miniaturization, and Nanoscale Materials

ISBN 0-87339-566-2 • Approx. 720 pp., illus., softcover Order No. 04-5662 • Weight 4 lbs M \$118 + S \$93 + L \$168

#### **ULTRAFINE GRAINED MATERIALS III**

Yuntian Theodore Zhu, Terence G. Langdon, and Ruslan Z. Valiev, editors ISBN 0-87339-571-9 • Approx. 824 pp., illus., index, softcover Order No. 04-5719 • Weight 4 lbs M \$124 + S \$98 + L \$177

#### M /Member + S / Student + L / List

The following proceedings are planned for publication in TMS journals after the meeting:

#### In the Journal of Electronic Materials

Challenges in Advanced Thin Films: Microstructures. Interfaces. and Reactions

Lead-Free Solders and Processing Issues Relevant to Microelectronic Packaging

Phase Stability, Phase Transformation, and Reactive Phase Formation in Electronic Materials III

#### In Metallurgical and Materials Transactions

**Beyond Nickel-Base Superalloys** 

Hume-Rothery Symposium: Structural and Diffusional Growth Phase Transformations and Deformation in Magnesium Alloys

#### In TMS Letters

Processing and Properties of Powder-Based Materials

Other symposia eligible for TMS Letters:

Cost-Affordable Titanium

Dislocations

Educational Issues in Transport Phenomena in Materials Processing **General Abstracts** 

General Poster Session

Internal Stresses and Thermo-Mechanical Behavior in Multi-Component Materials Systems

Roytburd Symposium on Polydomain Stryctures

Symposium in Honor of Prof. Roger D. Doherty

The Didier de Fontaine Symposium on the Thermodynamics of Alloys The Role of Grain Boundaries in Material Design

Detailed information about these publications, and many others, can be found in the TMS Document Center.

## ADDITIONAL RESOURCES

On-line answers to any of your 2003 TMS Annual Meeting & Exhibition questions can be found at

- 2003 TMS Annual Meeting & Exhibition Web Site: Get up-to-the-minute meeting details and complete registration materials at http://www.tms.org/AnnualMeeting.html
- TMS Personal Conference Scheduler: Review the most-up-to-date version of the technical program, examine the calendar of events, and create your own personalized itinerary by visiting <u>http://pcs.tms.org</u>

- TMS Document Center: Review the complete tables of contents for conference proceedings and order publications by visiting <u>http://doc.tms.org</u>
- TMS Membership: Learn more about the benefits of membership by touring <u>http://www.tms.org/Society/membership.html</u>
- TMS Business-to-Business Partnering: Learn how TMS can help your organization maximize its impact by viewing <u>http://www.tms.org/Meetings/Annual-04/Exhibit2004/Annual04-exhibit-home.html</u>

#### If you want to contact a person, more details are available at

TMS Meetings Department The Minerals, Metals & Materials Society 184 Thorn Hill Road, Warrendale, PA 15086 USA Telephone: 1-800-759-4867 (in the U.S. and Canada) or (724) 776-9000, ext. 243 Fax: (724) 776-3770

# TMSLETTERS

#### A valuable new resource for members

#### A distinguished publication venue for authors

Timely, relevant, and rigorously reviewed, *TMS Letters* is a unique technical journal that presents cutting-edge research in succinct, informative technical updates.

The peer-reviewed journal will be available exclusively in on-line format through the TMS Document Center (*doc.tms.org*) and will be accessible free-of-charge to all TMS members as a benefit of membership. *TMS Letters* will be composed entirely of two-page technical updates, including text and graphics, of research presented at TMS meetings that are not published in any other book or journal.

The first issue of *TMS Letters* will consist exclusively of technical updates presented at the 2004 TMS Annual Meeting, to be held March 14–18, 2004. Presenters at the 2004 TMS Annual Meeting, whose work will not be published in any other book or journal, may submit their work for publication in the inaugural issue of *TMS Letters*.

To learn more about *TMS Letters* or to submit a technical update, contact: Dan Thoma Editor, *TMS Letters* c/o TMS 184 Thorn Hill Road, Warrendale, PA 15086 E-mail: tmsletters@tms.org Web: www.tms.org/tmsletters.html

www.tms.org/tmsletters.html

Visit this web site often, as more details will be made available throughout the year, including author instructions for submitting papers to the journal and non-member subscription information.

March 14-18, 2004 • Charlotte, N				Figure 16, 2004         Payment must accompany form.         AMC           Forms received past this date will be processed at the on-site         Forms received past this date will be processed at the on-site         Forms received past this date will be processed at the on-site         Forms received past this date will be processed at the on-site         Forms received past this date will be processed at the on-site         Forms received past this date will be processed at the on-site         Forms received past this date will be processed at the on-site         Forms received past this date will be processed at the on-site         Forms received past this date will be processed at the on-site         Forms received past this date will be processed at the on-site         Forms received past this date will be processed at the on-site         Forms received past this date will be processed at the on-site         Forms received past this date will be processed at the on-site         Forms received past this date will be processed at the on-site         Forms received past this date will be processed at the on-site         Forms received past this date will be processed at the on-site         Forma received past this date will be processed at the on-site         Forma received past this date will be processed at the on-site         Forma received past this date will be processed at the on-site         Forma received past this date will be processed at the on-site         Forma received past this date will be processed at the on-site         Forma received past this date will be processed at the on-site         Forma received past this date will be processed at the on-site         Forma received past this date will be proces the past the past t	04-TECH
http://www.tms.org	<b>1.</b> P	Member of: rof.	: TMS	AIST SME SPE Member Number:	
Web registration requires credit card payment.	Mr. M	Irs. 🗌 Ms	Last Name	First Name Middle	e Initial
<b>USA:</b> 724-776-3770	Informal First Na	ame to Appear	on Badge:	Date of Birth:	
Fax registration requires				Title:	
credit card payment.					
<b>Return with</b> TMS, Meeting Services				te/Province:Zip/Postal Code:Country:	
payment to: 184 Thorn Hill Road Warrendale, PA 15086	lelephone:			Fax:E-Mail:	
				Guests do not receive admission to technical se	essions.
2. Registration Fees: unti	Advance Fees il February 16, 2004	On-Site after Februar	v 16. 2004	3. Social Function Tickets: Fee Quantity Total	FD
Member Non-member Author*				Bigg Didier de Fontaine Honorary Dinner       \$60       \$         Bigg Sc R.J. Arsenalt Honorary Dinner       \$60       \$         Roger Doherty Honorary Dinner       \$60       \$	JD
Non-member *	\$550 NM	\$650	NML	Roger Doherty Honorary Dinner\$60 \$	DD
Student Member ##	\$0 STU \$25 STUN	\$0 \$ \$25 \$	STUL	TMS-AIME Banguet\$60 \$	AD
TMS Senior Member	\$250 RM	\$250 I	RML	Tables of 8 \$480 \$	AD8
Exhibit Booth Personnel	\$0 E	\$0 H	EL	Provide Sign to Read	
			EOL	المجارة         <	_ EP EP8
Registration TOTAL \$ _				Table Sign to Read	0
* Includes TMS membership for 2004	aal'a atudant idantifiaatia	n oord		t	LM
## Students must attach a copy of their sch		n calu.		<b>§</b> Eight Medias Division Educateon	_ LM8
<b>4. Tutorial Luncheon Tickets:</b> Monday 3/15/04	Fee	Quantity	Total	률도 Table Sign to Read	RD
The Young Leader Tutorial Lecture is free. You may purchase the optional box lunch for	\$25		\$ EM		_
			·	Social Function TOTAL \$	
5. Publication Orders: All order Order Number Title	ers that are not indicated	for shipment o	n this form mu	Shipping Subtotal At-Meeting List Subt	total ice
04-5654-CD EPD Congress 2004 (CD-R	OM)				
04-5506 Laterite Nickel 2004	,				
04-5670-G Light Metals 2004 (Book and	d CD-ROM Set)				
04-5689-G Magnesium Technology 200					
04-5743 Advanced Materials for Ene					
04-5662 Fifth Global Symposium on in Nanostructured Materials	Materials Processing an and Trends in LIGA Mir	id Manutacturin	ig: Surfaces a nd Nanoscale	nd Interfaces Materials 4 \$118 \$168 \$	
04-5719 Ultrafine Grained Materials					
04-5727 Solidification Processes and					
04-5697 Solidification of Aluminum A					
04-5735 Bulk Metallic Glasses					
04-5646 Advances in Superplasticity 04-5700 Multiphase Phenomena and					
	ND ZONE CHART			Subtotal \$	
Weight USA Canada Mexico	Western J. A. NZ Europe	EE, C/S Am, Pac. Rim,	Middle East, Africa	If books are to be shipped, please complete the following.	
1 \$4.50 \$4.00 \$5.00 2 \$5.00 \$7.50 \$9.50	\$4.50 \$5.00 \$8.50 \$9.50	\$5.50 \$10.50	\$7.50 \$14.50		
3 \$5.50 \$11.00 \$14.00 4 \$6.00 \$14.50 \$18.50	\$12.50 \$14.00 \$16.50 \$18.50	\$15.50 \$20.50	\$21.50 \$28.50	Total Weight Calculate shipping fees from the chart (at left) \$	
5 \$6.50 \$18.00 \$23.00	\$20.50 \$23.00 \$24.50 \$27.50	\$25.50 \$30.50	\$35.50 \$42.50	One-time \$5 handling fee per order shipped \$	
6 \$7.00 \$21.50 \$27.50 7 \$7.50 \$25.00 \$32.00 8 \$8.00 \$28.50 \$36.50	\$28.50 \$32.00 \$32.50 \$36.50	\$35.50 \$40.50	\$49.50 \$56.50	NOTE: If your order exceeds 12 pounds, add the amount	
9 \$8.50 \$32.00 \$41.00	\$36.50 \$41.00 \$40.50 \$45.50	\$45.50	\$63.50	that it is over from the chart (at the left) to reach the total weight of your order. [Example: 16 lbs. (delivered in U.S.A.)	
10 \$9.00 \$35.50 \$45.50 11 \$9.50 \$39.00 \$50.00 12 \$10.00 \$42.50 \$54.50	\$40.50 \$44.50 \$50.00 \$48.50 \$54.50	\$50.50 \$55.50 \$60.50	\$70.50 \$77.50 \$84.50	would be 12 lbs. (\$10.00) + 4 lbs (\$6.00) = 16 lbs. (\$16.00)] Publications TOTAL \$	
6. Continuing Education Short (	Courses: Sunday, Mar Advance Fees	ch 14, 2004 On-Site	Fees	7. 2004 Membership Dues: For current TMS members only Full Member	FM
	til February 16, 2004 ember Non-member	after Februa Member No		□ Sunor Member	ST
1. Metal Matrix Composites		\$525	\$610	8. Payment enclosed:	
2. Introduction to	. UOC\$ C1+4	φ020	φυτυ	Check, Bank Draft, Money Order	
Nanomanufacturing and	¢475 ¢500	¢EOE	<b>0010</b>	Make checks payable to TMS. Payment shall be made in USA dollars drawn on a USA bank.	
Nanotechnology	\$475 \$560	\$525	\$610	Credit Card Expiration Date:	
3. Technology Transfer Seminar	\$475 \$560	\$525	\$610	Card No.:	
4. Smelter Grade Alumina from				□ Visa □ MasterCard □ Diners Club □ American Express	
the Smelting Perspective	\$475 \$560	\$525	\$610	Cardholder Name:	
the Materials Professionals	\$475 \$560	\$525	\$610	Signature:	
				9. TOTAL FEES PAID	

Short Course TOTAL \$ \_\_\_\_\_ \$ \_\_\_\_\_

Refund policy: Writer requests must be mailed to TMS, post-marked no later than February 16, 2004. A \$50 processing fee will be charged for all cancellations. No refunds will be processed after February 16, 2004.



#### **133rd Annual International Meeting & Exhibition** March 14-18, 2004 • Charlotte, North Carolina, USA

Making your reservation is easier than ever through Travel Planners' real-time Internet reservation system! Just log on to www.tms.org, and follow the link to Travel Planners. You will be able to view actual

## **HOUSING RESERVATION FORM**

Mail or fax this housing form to: Travel Planners, Inc., 381 Park Ave. South, New York, NY 10016 FAX: 212-779-6128 • PHONE: 800-221-3531 (in 212, 718, 516, 914, 631 or international call 212-532-1660) (CHOOSE ONLY ONE OPTION)

availability, learn about your hotel's features and services, and obtain local city and sightseeing information. Most importantly, you will receive instant confirmation of your reservation!

#### Reservations must be received at Travel Planners by: Monday, February 16, 2004

Indicate 1st, 2nd, & 3rd hotel choice:       Type of Accomodations: (check one)       Image: Single 1 person/1bed □ Double 2 people/1bed □ Twin 2 people/2 beds       at the headquarters hotel, More with ear the headquarters hotel, More with Head and as with Head Head wachead housing ear the head hear ward wary acc	Arrival Date	Departure Date	
Street	ast Name	First Name	MI
City	Company		
Daytime Phone	Street	Address	
Additional Room Occupants	City	State/CountyZip/Postal Code	Country
<ul> <li>E-nail</li></ul>	Daytime Phone	Fax	
Non-Smoking Room Requested	Additional Room Occupants		
Indicate 1st, 2nd, & 3rd hotel choice:          Type of Accomadations: (check one)         [_]	E-mail		(confirmation will be sent via e-mail if address is provided
Indicate 1st, 2nd, & 3rd hotel choice:          Type of Accomodations: (check one)         Single 1 person/tbed □ Double 2 people/tbed □ Twin 2 people/2 beds         The 9 people/2	Non-Smoking Room Requested	Special Needs	
<ul> <li>HEADQUARTERS</li> <li>Westin Charlotte Hotel \$179/single • \$194/double</li> <li>Hilton Charlotte Hotel \$154/single • \$174/double</li> <li>Milton Charlotte Hotel \$154/single • \$174/double</li> <li>Minito Charlotte Hotel \$129/single • \$174/double</li> <li>Mariot Elized under the second state of the second state of</li></ul>		☐ Single 1 person/1bed ☐ Double 2 people/1bed ☐ Twin 2 peo ☐ Triple 3 people/2 beds ☐ Quad 4 people/2 beds If all three (3) requested hotels are unavailable, please process t	a financial liability for any and al rooms in that block that are no reserved. You are strongly encour aged to reserve your room(s) at the hotels listed to limit our financial liabil ity. Please help TMS achieve overal success with the 133rd TMS Annua
W. First St. E. First St. CHARLOTTE CONVENTION CENTER anajor credit card or deposit of one night and tax payable to Travel Planners, Inc.	<ol> <li>Westin Charlotte Hotel \$179/single • \$194/double</li> <li>Hilton Charlotte Hotel \$154/single • \$174/double</li> <li>Omni Hotel \$129/single • \$129/double</li> <li>Adams Mark Hotel \$125/single • \$125/double</li> <li>Holiday Inn Center City \$115/single • \$115/double</li> <li>Marriott City Center Hotel</li> </ol>	W. Trade St. E. Tride St. W. Fourth St. W. Fourth St. W. First St. W. First St. E. First St. W. First St. E. First St.	<ul> <li>reservation at one of the listed hotels prior to the advance housing deadline Thank you.</li> <li>Confirmations: Confirmations will be e-mailed faxed or mailed to you from Travel Planners, Inc.</li> <li>Changes/Cancellations: All changes and cancellations in hotel reservations must be madwith Travel Planners, Inc.</li> <li>Changes/Cancellations: All changes and cancellations in hotel reservations must be madwith Travel Planners, Inc.</li> <li>Changes/Cancellations: All changes and cancellations in hotel reservations must be madwith Travel Planners, Inc.</li> <li>Changes/Cancellations: All changes and cancellations in hotel reservations must be madwith Travel Planners, Inc. up until 3 business day prior to arrival and are subject to the individue hotel's cancellation policies. Cancellations and changes within 3 days of arrival MUST be madwith your hotel directly. Many hotels are now imposing fees for early departure. This rate is set by each hotel and may vary accordingly Please reconfirm your departure date at the time</li> </ul>

Deposit Payment: Check American Express MasterCard VISA Discover Diners

Account Number \_

Card Holder Name \_\_\_

\_\_ Expiration Date \_

form per com required. Make additional copies if needed.

\_\_\_\_ Authorized Signature \_\_\_\_

Monday	March 15	Tuesday-	GRID March 16	Wednesda	v-March 17	Thursday-March 18	
AM	PM	AM	PM	AM	PM	AM	
					Materials Analysis: Understanding the Columbia Disaster		
Dislocations: Modeling and Simulation Fundamentals	Dislocations: Simulation and Observation of Fundamental Mechanisms	Dislocations: Dislocation Structures and Patterning	Dislocations: Novel Experimental Methods	Dislocations: Plasticity, Voids, and Fracture	Dislocations: Dislocations in Complex Materials		
	Advances in Superplasticity and Superplastic Forming: Dvlp. of Advanced Superplastic Forming Processes	Advances in Superplasticity and Superplastic Forming: Advances in Superplastic Al-Mg Materials	Advances in Superplasticity and Superplastic Forming: Advances in Superplastic Forming of Light Alloys	Advances in Superplasticity and Superplastic Forming: Advd. Superplastic Matls. & the Sci. of Superplasticity	Advances in Superplasticity and Superplastic Forming: Modeling of Superplas- tic Forming Processes and Materials	General Abstracts: Session IX	-
Computational Thermodynamics and Phase Transformations: Grain Growth and Particle Coarsening	Computational Thermodynamics and Phase Transformations: Interfaces and Grain Boundaries	Computational Thermodynamics and Phase Transformations: Phase Field Modeling I	Computational Thermodynamics and Phase Transformations: Phase Field Modeling II	Computational Thermodynamics and Phase Transformations: Phase Equilibria and Thermodynamic Assessments	Computational Thermodynamics and Phase Transformations: Thermodynamics and Phase Transformation		
General Pyrometallurgy: Session I	5th Global Innovations Symposium: Plenary: Trends: Past, Present, and Future	5th Global Innovations Symposium: Small Volume Deformation	5th Global Innovations Symposium: Properties & Characterization of Matls. for Microsys./ LIGA Applications	5th Global Innovations Symposium: Properties, Processes, and Modeling	5th Global Innovations Symposium: Manufacturing and Evaluation of Layered Nano-Scale Materials		
Advanced Materials for Energy Conversion II: Energy Issues & Metal Hydrides I	Advanced Materials for Energy Conversion II: Metal Hydrides II	Advanced Materials for Energy Conversion II: Complex Hydrides I	Advanced Materials for Energy Conversion II: Complex Hydrides II	Advanced Materials for Energy Conversion II: Metal Hydrides III	Advanced Materials for Energy Conversion II: Metal Hydrides IV- Dynamics of Metal Hydrides &Tritium Gettering	Advanced Materials for Energy Conversion II: Thermoelectrics, Superconductors, and Piezoelectrics Materials	Т
Magnesium Technology 2004: Automotive Applications/Welding	Magnesium Technology 2004: Wrought Magnesium Alloys I	Magnesium Technology 2004: Wrought Magnesium Alloys II/Corrosion and Coatings	Magnesium Technology 2004: Primary Processing and Environmental Issues	Magnesium Technology 2004: Casting Processes and Properties	Magnesium Technology 2004: Fundamental Research	Magnesium Technology 2004: Alloy Development	
General Abstracts: Session I	General Abstracts: Session II	General Abstracts: Session IV	General Abstracts: Session V	Advanced Materials for Energy Conversion II: Thermodynamics, Superconductors & Batteries	Advanced Materials for Energy Conversion II: Magnetic Materials & Hydrogen Permeation	Advd. Matls. for Energy Conversion II: Metal Hydrides V-Thermal Energy Storage & Containment Matls.	У
Recent Advances in Non-Ferrous Metals Processing: Reactive Metals	Recent Advances in Non-Ferrous Metals Processing: Sustainable Development	Phase Transformations and Deformation in Mg Alloys: Solidification and Precipitation	Phase Transformations and Deformation in Mg Alloys: Plastic Deformation and Texture	Phase Transformations and Deformation in Mg Alloys: Creep Deformation	Phase Transformations and Deformation in Mg Alloys: Deformation and Strengthening		_
CFD Modeling and Simulation of Engineering Processes: Advanced Casting and Solidification Processes I	CFD Modeling and Simulation of Engineering Processes: Remelt Processes	CFD Modeling and Simulation of Engineering Processes: MEMS/ Microfluidics	CFD Modeling and Simulation of Engineering Processes: Advanced Casting and Solidification Processes II	CFD Modeling and Simulation of Engineering Processes: Process Modeling I	CFD Modeling and Simulation of Engineering Processes: Process Modeling II		
Cost-Affordable Titanium Symposium Dedicated to Prof. Harvey Flower: Overview and Innovative Processes	Cost-Affordable Titanium Symposium Dedicated to Prof. Harvey Flower: Break Through Technologies	Cost-Affordable Titanium Symposium Dedicated to Prof. Harvey Flower: Titanium Economics	Cost-Affordable Titanium Symposium Dedicated to Prof. Harvey Flower: Creative Processing	Cost-Affordable Titanium Symposium Dedicated to Prof. Harvey Flower: Creative Fabrication	Cost-Affordable Titanium Symposium Dedicated to Prof. Harvey Flower: Low Cost Titanium	Cost-Affordable Titanium Symposium Dedicated to Prof. Harvey Flower: Property Enhancement	
Third International Symposium on Ultrafine Grained Aterials: Processing I: Fundamentals and Technology	Third International Symposium on Ultrafine Grained Materials: Processing II: Structural Evolution	Third International Symposium on Ultrafine Grained Materials: UFG Material Fundamentals	Third International Symposium on Ultrafine Grained Materials: Microstruc- ture and Properties	Third International Symposium on Ultrafine Grained Materials: Mechanical Properties	Third International Symposium on Ultrafine Grained Materials: Superplas- ticity, Creep & Thermal Stability		
Materials Issues in Fuel Cells: State-of-the-Art	Materials Issues in Fuel Cells: Materials Challenges	Solidification of Aluminum Alloys: Microstructural Evolution I	Solidification of Aluminum Alloys: Microstructural Evolution II	Solidification of Aluminum Alloys: Solidification Cracking/ Mechanical Properties	Solidification of Aluminum Alloys: Gas Porosity/Micro- Macro Segregation	Solidification of Aluminum Alloys: Special Effects	

GRID							
	Monday-		Tuesday-		Wednesda	-	Thursday-March 18
	AM	PM	AM	PM	AM	PM	AM
207D	Solidification Processes and Microstructures: A Symp. in Honor of Prof. W. Kurtz: Processes	Solidification Processes and Microstructures: A Symp. in Honor of Prof. W. Kurtz: Mushy Zone Dynamics	Solidification Processes and Microstructures: A Symp. in Honor of Prof. W. Kurtz: Microstructures	Solidification Processes and Microstructures: A Symp. in Honor of Prof. W. Kurtz: Rapid Solidification	Solidification Processes and Microstructures: A Symp. in Honor of Prof. W. Kurtz: Phase Field	General Abstracts: Session VIII	
208A	Hume Rothery Symp.: Struct. & Diffusional Growth Mechanisms of Irrational Interphase Boundaries: Session I	Hume Rothery Symp.: Struct. & Diffusional Growth Mechanisms of Irrational Interphase Boundaries: Session II	Hume Rothery Symp.: Struct. & Diffusional Growth Mechanisms of Irrational Interphase Boundaries: Session III	Hume Rothery Symp.: Struct. & Diffusional Growth Mechanisms of Irrational Interphase Boundaries: Session IV	Hume Rothery Symp.: Struct. & Diffusional Growth Mechanisms of Irrational Interphase Boundaries: Session V	Hume Rothery Symp.: Struct. & Diffusional Growth Mechanisms of Irrational Interphase Boundaries: Session VI	
208B		Processing, Microstructure and Properties of Powder- Based Materials: Session I	Processing, Microstructure and Properties of Powder- Based Materials: Session II	Processing, Microstructure and Properties of Powder- Based Materials: Session III	General Abstracts: Session VI	General Abstracts Session VII	
209A	Bulk Metallic Glasses: Processing I	Bulk Metallic Glasses: Processing II	Bulk Metallic Glasses: Fatigue and Fracture	Bulk Metallic Glasses: Theoretical Modeling and Shear Bands	Bulk Metallic Glasses: Bio, Corrosion, and Fracture Behavior	Bulk Metallic Glasses: Phase Transformation and Alloy Design	Bulk Metallic Glasses: Mechanical Behavior
209B	Internal Stresses & Thermo-Mech. Behavior in Multi-Component Matls. Sys.: Electronic Thin Films & Pkgg. Matls. I	Internal Stresses & Thermo-Mech. Behavior in Multi-Component Matls. Sys.: Electronic Thin Films & Pkgg. Matls. II	Internal Stresses & Thermo-Mech. Behavior in Multi-Component Matls. Sys.: Creep and Plasticity I	in Multi-Component		Educational Issues in Transport Phenomena in Materials Processing: Presentations and Panel Discussion	
210A	Automotive Alloys 2004: Session I	Automotive Alloys 2004: Session II	Automotive Alloys 2004: Session III	Automotive Alloys 2004: Session IV	High Risk Technologies in Metallurgy with Commercial Potential: Session I	High Risk Technologies in Metallurgy with Commercial Potential: Session II	
210B	Materials by Design: Atoms to Applications: Materials Chemistry and Alloy Design	Materials by Design: Atoms to Applications: Materials Character- ization and Microstruc- tural Modeling	Computational and	Materials by Design: Atoms to Applications: Designing Nanostructures	Materials by Design: Atoms to Applications: Design for Mechanical Functionality I	Materials by Design: Atoms to Applications: Design for Mechanical Functionality II	
211A	R.J. Arsenault Symposium on Materials Testing and Evaluation: Session I	R.J. Arsenault Symposium on Materials Testing and Evaluation: Session II	R.J. Arsenault Symposium on Materials Testing and Evaluation: Session III	R.J. Arsenault Symposium on Materials Testing and Evaluation: Session IV	Failure of Structural Materials: Fundamentals	Failure of Structural Materials: Fatigue	Failure of Structural Materials: General
211B	Beyond Ni-Base Superalloys: Superalloys and Niobium Silicides	Beyond Ni-Base Superalloys: Molybdenum Silicides I	Beyond Ni-Base Superalloys: Precious Metal Alloys	Beyond Ni-Base Superalloys: Molybdenum Silicides II	Beyond Ni-Base Superalloys: Niobium Silicides	Beyond Ni-Base Superalloys: Other Systems and Physical Properties of Silicides	
212A		General Abstracts: Session III	Electrochemical Measurements and Processing of Materials: Electrodepo- sition Processes	Electrochemical Measurements and Processing of Materials: Electro- chemical Refining	Electrochemical Measurements and Processing of Materials: Electro- chemical Metal Production	Electrochemical Measurements and Processing of Materials: Electro- chemical Sensors and Measurements	
212B	Materials Processing Fundamentals: Solidification and Casting	Materials Processing Fundamentals: Deformation Processing	Materials Processing Fundamentals: Liquid Metal Processing	Materials Processing Fundamentals: Smelting and Refining	Materials Processing Fundamentals: Aqueous Processing	Materials Processing Fundamentals: Powders, Composites, Coatings and Measurements	
213A	Carbon Technology: Cathode Material and Corrosion	Carbon Technology: Anode Raw Materials	Carbon Technology: Green Anodes and Soderberg Paste	Carbon Technology: Anode Baking	Carbon Technology: Anode Quality and Performance	Aluminum Reduction Technology: Materials and Fundamentals	
213B/C	Cast Shop Technology: Melting and Refractories	Cast Shop Technology: Modeling of Casting Processes	Cast Shop Technology: Casting	Cast Shop Technology: Metal Treatment	Cast Shop Technology: Alloying and Furnace Processing	Cast Shop Technology: Grain Refining	Cast Shop Technology: Foundry
Ц				450			

GRID								
Monday-I AM	March 15 PM	Tuesday-I AM	March 16 PM	Wednesday AM	r-March 17 PM	Thursday-March 18 AM		
Aluminum Reduction - Potroom Improvements	Aluminum Reduction Technology: Cell Development and Operations	Aluminum Reduction Technology: Pot Control	Aluminum Reduction Technology: Modeling - Industry Trends	Aluminum Reduction Technology: Emerging Technologies	Aluminum Reduction Technology: Environmental	Aluminum Reduction Technology: Modeling	213D	
Phase Stability, Phase Transformation, and Reactive Phase Formation in Electronic Materials III Session I	Phase Stability, Phase Transformation, and Reactive Phase Formation in Electronic Materials III Session II	Phase Stability, Phase Transformation, and Reactive Phase Formation in Electronic Materials III Session III	Phase Stability, Phase Transformation, and Reactive Phase Formation in Electronic Materials III Session IV	Phase Stability, Phase Transformation, and Reactive Phase Formation in Electronic Materials III Session V	Solid and Aqueous Wastes from Non- Ferrous Metals Industry: Session I	Solid and Aqueous Wastes from Non- Ferrous Metals Industry: Session II	214	
Nanostructured Magnetic Matls.: Recent Progress in Magnetic Nanostructures	Nanostructured Mag- netic Matls.: Synthesis & Characterization of Nanostructured Magnetic Matls.	Nanostructured Mag- netic Matls.: Magnetic Tunnel Junctions and Semiconductor Spintronics	Nanostructured Magnetic Matls.: Self Assembly and Patterned Nanostructures	Metals for the Future: Structural Materials	Metals for the Future: Functional Materials	Metals for the Future: Processing and Bio- Materials	215	
Symp. on Microstruc- tural Stability in Honor of Prof. Roger D. Doherty: Microstruc- tural Stability: Recrystallization	Symp. on Microstruc- tural Stability in Honor of Prof. Roger D. Doherty: Microstruc- tural Stability: Texture Development	Symp. on Microstruc- tural Stability in Honor of Prof. Roger D. Doherty: Microstruc- tural Stability: Plastic Deformation	Symp. on Microstruc- tural Stability in Honor of Prof. Roger D. Doherty: Microstructl. Stability: Precipitation & Other Topics	Roytburd Symposium on Polydomain Structures: Elastic Domains in Structural Materials	Roytburd Symposium on Polydomain Structures: Domains in Ferroelectrics and Magnetics		216A	
The Didier de Fontaine Symp. on the Thermo- dynamics of Alloys: Fundamentals of Alloy Theory	The Didier de Fontaine Symp. on the Thermo- dynamics of Alloys: Experimental Techniques	The Didier de Fontaine Symp. on the Thermo- dynamics of Alloys: First Principle Calcul- ations & Cluster Expansion Techniques	The Didier de Fontaine Symp. on the Thermo- dynamics of Alloys: Interatomic Potentials and Cluster Expansion Techniques	The Didier de Fontaine Symp. on the Thermo- dynamics of Alloys: Jt. Session w/Computatl. Thermodynamics & Phase Transformations I	The Didier de Fontaine Symp. on the Thermo- dynamics of Alloys: Jt. Session w/Computatl. Thermodynamics & Phase Transformations II		216B	
		Surfaces & Interfaces in Nanostructured Matls.: General Phenomena & Processes	Surfaces & Interfaces in Nanostructured Matls.: Grain & Phase Boundaries	Surfaces & Interfaces in Nanostructured Matls.: Synthesis & Processing	Surfaces & Interfaces in Nanostructured Matls.: Coatings and Surface Modification	Surfaces & Interfaces in Nanostructured Matls.: Self-Organized & Biological Materials		
International Laterite Nickel Symposium - 2004: Economics and Project Assessment	International Laterite Nickel Symposium - 2004: Mineralogy and Geometallurgy/Panel Discussion	International Laterite Nickel Symposium - 2004: Pressure Acid Leaching	International Laterite Nickel Symposium - 2004: Process Development for Prospective Projects	International Laterite Nickel Symposium - 2004: Process and Operational Lessons Learned - Part I	International Laterite Nickel Symposium - 2004: Process and Operational Lessons Learned - Part II	International Laterite Nickel Symposium - 2004: Atmospheric Leaching/Slurry Rheology, Solution Extraction and Other	217B/C	
Recycling: General Recycling	Recycling: Aluminum and Aluminum Dross Processing	Aluminum Can Recycling: Session I	International Laterite Nickel Symposium - 2004: Roasting and Smelting	Materials Education to Revitalize the Workforce: Session I	Materials Education to Revitalize the Workforce: Session II		217D	
Alumina and Bauxite: Bayer Plant Operations: Red Side	Alumina and Bauxite: Process Modeling and Control	Alumina and Bauxite: Bayer Plant Operations: White Side	Alumina and Bauxite: Technology and Future Trends	The Role of Grain Boundaries in Material Design: Grain Boundary Character	The Role of Grain Boundaries in Material Design: Grain Boundary Segregation, Diffusion, Damage	The Role of Grain Boundaries in Material Design: Simulation of Grain Boundary Effects of Properties	218A	
Challenges in Advd. Thin Films: Microstruc- tures, Interfaces & Reactions: Advances in Photonic & Opto- elect. Matls. & Proc.	Challenges in Advd. Thin Films: Microstruct., Interfaces & Reactions: Microstruct., Prop. & Reliability of Microelec. Devices	Challenges in Advd. Thin Films: Microstruc- tures, Interfaces and Reactions: Modifica- tion, Characterization, and Modeling	Challenges in Advd. Thin Films: Micro- struct., Interfaces & Reactions: Design, Proc. & Property Control	Multiphase Phenomena in Materials Processing: Session I	Multiphase Phenomena in Materials Processing: Session II	Multiphase Phenomena in Materials Processing Session III	218B	
Nanostructured Materials for Biomedical Applications: Session I	Nanostructured Materials for Biomedical Applications: Session II	Nanostructured Materials for Biomedical Applications: Session III	Nanostructured Materials for Biomedical Applications: Session IV	Nanostructured Materials for Biomedical Applications: Session V	Nanostructured Materials for Biomedical Applications: Session VI	Nanostructured Materials for Biomedical Applications: Session VII	219A	
Lead-Free Solders & Procg. Issues Rele- vant to Microelectronic Pkgg.: Fundamentals, Phases, Wetting & Solidification	Lead-Free Solders & Procg. Issues Relevant to Microelect. Pkgg.: Envionmental & Matls. Issues for Lead-Free	Lead-Free Solders & Procg. Issues Relevant to Microelect. Pkgg.: Mechanical Properties & Fatigue Behavior	Lead-Free Solders & Procg. Issues Relevant to Microelect. Pkgg.: Electromigration and Creep in Leadfree Solders	Lead-Free Solders & Procg. Issues Relevant to Microelect. Pkgg.: Interfacial Interactions, Intermetallics & Substrates	Lead-Free Solders & Procg. Issues Relevant to Microelect. Pkgg.: Microstructural Characterization & Evolution		219B	
		1			1	1		

# Table of Contents

(In Order By Technical Track)

SESSION TITLE	ROOM	DAY	PAGE
Hot-Topic Track: Building MSE Synergies			
High Risk Technologies in Metallurgy with Commercial Potential: Session I	210A	Wed-AM	369
High Risk Technologies in Metallurgy with Commercial Potential: Session II	210A	Wed-PM	414
Materials Analysis: Understanding the Columbia Disaster	Ballroom B	Wed-PM	418
Materials by Design: Atoms to Applications: Materials Chemistry and Alloy Design	210B	Mon-AM	192
Materials by Design: Atoms to Applications: Materials Characterization and Microstructural Modeling	210B	Mon-PM	234
Materials by Design: Atoms to Applications: Computational and Experimental Strategies	210B	Tues-AM	288
Materials by Design: Atoms to Applications: Designing Nanostructures	210B	Tues-PM	334
Materials by Design: Atoms to Applications: Design for Mechanical Functionality I	210B	Wed-AM	376
Materials by Design: Atoms to Applications: Design for Mechanical Functionality II	210B	Wed-PM	419
Materials Education to Revitalize the Workforce: Session I	217D	Wed-AM	377
Materials Education to Revitalize the Workforce: Session II	217D	Wed-PM	420
Materials Issues in Fuel Cells: State-of-the-Art	207B/C	Mon-AM	193
Materials Issues in Fuel Cell: Materials Challenges	207B/C	Mon-PM	235
Metals for the Future: Structural Materials	215	Wed-AM	379
Metals for the Future: Functional Materials	215	Wed-PM	422
Metals for the Future: Processing and Bio-Materials	215	Thurs-AM	445
Advanced Materials			
Advanced Materials for Energy Conversion II: Energy Issues & Metal Hydrides I	203A	Mon-AM	169
Advanced Materials for Energy Conversion II: Metal Hydrides II	203A	Mon-PM	210
Advanced Materials for Energy Conversion II: Complex Hydrides I	203A	Tues-AM	262
Advanced Materials for Energy Conversion II: Complex Hydrides II	203A	Tues-PM	309
Advanced Materials for Energy Conversion II: Metal Hydrides III	203A	Wed-AM	353
Advanced Materials for Energy Conversion II: Thermodynamics, Superconductors & Batteries	204	Wed-AM	354
Advanced Materials for Energy Conversion II: Metal Hydrides IV - Dynamics of Metal Hydrides, and Tritium Gettering	203A	Wed-PM	395
Advanced Materials for Energy Conversion II: Magnetic Materials & Hydrogen Permeation	204	Wed-PM	396
Advanced Materials for Energy Conversion II: Thermoelectrics, Superconductors, and Piezoelectric Materials	203A	Thurs-AM	435
Advanced Materials for Energy Conversion II: Metal Hydrides V, Thermal Energy Storage and Containment Materials	204	Thurs-AM	436
Beyond Nickel-Base Superalloys: Superalloys and Niobium Silicides	211B	Mon-AM	174
Beyond Nickel-Base Superalloys: Molybdenum Silicides I	211B	Mon-PM	215

SESSION TITLE	ROOM	DAY	PAGE
Advanced Materials continued			
Beyond Nickel-Base Superalloys: Precious Metal Alloys	211B	Tues-AM	269
Beyond Nickel-Base Superalloys: Molybdenum Silicides II	211B	Tues-PM	315
Beyond Nickel-Base Superalloys: Niobium Silicides	211B	Wed-AM	357
Beyond Nickel-Base Superalloys: Other Systems and Physical Properties of Silicides	211B	Wed-PM	400
Bulk Metallic Glasses: Processing I	209A	Mon-AM	175
Bulk Metallic Glasses: Processing II	209A	Mon-PM	216
Bulk Metallic Glasses: Fatigue and Fracture	209A	Tues-AM	270
Bulk Metallic Glasses: Theoretical Modeling and Shear Bands	209A	Tues-PM	316
Bulk Metallic Glasses: Bio, Corrosion, and Fracture Behavior	209A	Wed-AM	359
Bulk Metallic Glasses: Phase Transformation and Alloy Design	209A	Wed-PM	402
Bulk Metallic Glasses: Mechanical Behavior	209A	Thurs-AM	438
Processing, Microstructure and Properties of Powder-Based Materials: Session I	208B	Mon-PM	242
Processing, Microstructure and Properties of Powder-Based Materials: Session II	208B	Tues-AM	295
Processing, Microstructure and Properties of Powder-Based Materials: Session III	208B	Tues-PM	340
Roytburd Symposium on Polydomain Structures: Elastic Domains in Structural Materials	216A	Wed-AM	384
Roytburd Symposium on Polydomain Structures: Domains in Ferroelectrics and Magnetics	216A	Wed-PM	425
Electronic Materials			
Challenges in Advanced Thin Films: Microstructures, Interfaces, and Reactions: Advances in Photonic and Optoelectronic Materials and Processes	218B	Mon-AM	179
Challenges in Advanced Thin Films: Microstructures, Interfaces, and Reactions: Microstructures, Properties, and Reliability of Microelectronic Devices	218B	Mon-PM	220
Challenges in Advanced Thin Films: Microstructures, Interfaces, and Reactions: Modification, Characterization, and Modeling	218B	Tues-AM	274
Challenges in Advanced Thin Films: Microstructures, Interfaces, and Reactions: Design, Process, and Property Control of Functional and Structural Thin-Films	218B	Tues-PM	320
Lead-Free Solders and Processing Issues Relevant to Microelectronic Packaging: Fundamentals, Phases, Wetting and Solidification	219B	Mon-AM	189
Lead-Free Solders and Processing Issues Relevant to Microelectronic Packaging: Environmental and Materials Issues for Lead-Free	219B	Mon-PM	231
Lead-Free Solders and Processing Issues Relevant to Microelectronic Packaging: Mechanical Properties and Fatigue Behavior	219B	Tues-AM	285
Lead-Free Solders and Processing Issues Relevant to Microelectronic Packaging: Electromigration and Creep in Leadfree Solders	219B	Tues-PM	331
Lead-Free Solders and Processing Issues Relevant to Microelectronic Packaging: Interfacial Interactions, Intermetallics and Substrates	219B	Wed-AM	373
Lead-Free Solders and Processing Issues Relevant to Microelectronic Packaging: Microstructural Characterization and Evolution	219B	Wed-PM	416
Phase Stability, Phase Transformation, and Reactive Phase Formation in Electronic Materials III: Session I	214	Mon-AM	198
Phase Stability, Phase Transformation, and Reactive Phase Formation in Electronic Materials III: Session II	214	Mon-PM	240

SESSION TITLE	ROOM	DAY	PAGE
Electronic Materials continued			
Phase Stability, Phase Transformation, and Reactive Phase Formation in Electronic Materials III: Session III	214	Tues-AM	293
Phase Stability, Phase Transformation, and Reactive Phase Formation in Electronic Materials III: Session IV	214	Tues-PM	338
Phase Stability, Phase Transformation, and Reactive Phase Formation in Electronic Materials III: Session V	214	Wed-AM	382
Extraction and Processing			
Educational Issues in Transport Phenomena in Materials Processing: Presentations and Panel Discussion	209B	Wed-PM	408
General Pyrometallurgy: Session I	202B	Mon-AM	185
International Laterite Nickel Symposium - 2004: Economics and Project Assessment	217B/C	Mon-AM	188
International Laterite Nickel Symposium - 2004: Mineralogy and Geometallurgy	217B/C	Mon-PM	230
International Laterite Nickel Symposium - 2004: Panel Discussion	217B/C	Mon-PM	231
International Laterite Nickel Symposium - 2004: Pressure Acid Leaching	217B/C	Tues-AM	284
International Laterite Nickel Symposium - 2004: Process Development for Prospective Projects	217B/C	Tues-PM	328
International Laterite Nickel Symposium - 2004: Roasting and Smelting	217D	Tues-PM	330
International Laterite Nickel Symposium - 2004: Process and Operational Lessons Learned - Part I	217B/C	Wed-AM	372
International Laterite Nickel Symposium - 2004: Process and Operational Lessons Learned - Part II	217B/C	Wed-PM	415
International Laterite Nickel Symposium - 2004: Atmospheric Leaching	217B/C	Thurs-AM	443
International Laterite Nickel Symposium - 2004: Slurry Rheology, Solution Extraction and Other	217B/C	Thurs-AM	443
Materials Processing Fundamentals: Solidification and Casting	212B	Mon-AM	194
Materials Processing Fundamentals: Deformation Processing	212B	Mon-PM	236
Materials Processing Fundamentals: Liquid Metal Processing	212B	Tues-AM	289
Materials Processing Fundamentals: Smelting and Refining	212B	Tues-PM	335
Materials Processing Fundamentals: Aqueous Processing	212B	Wed-AM	378
Materials Processing Fundamentals: Powders, Composites, Coatings and Measurements	. 212B	Wed-PM	420
Recent Advances in Non-Ferrous Metals Processing: Reactive Metals	205	Mon-AM	199
Recent Advances in Non-Ferrous Metals Processing: Sustainable Development	205	Mon-PM	244
Recycling: General Recycling	217D	Mon-AM	200
Recycling: Aluminum and Aluminum Dross Processing	217D	Mon-PM	244
Solid and Aqueous Wastes from Non-Ferrous Metal Industry: Session I	214	Wed-PM	426
Solid and Aqueous Wastes from Non-Ferrous Metal Industry: Session II	214	Thurs-AM	448
Light Metals			
Alumina and Bauxite: Bayer Plant Operations: Red Side	218A	Mon-AM	170
Alumina and Bauxite: Process Modeling and Control	218A	Mon-PM	212

SESSION TITLE	ROOM	DAY	PAGE
Light Metals continued			
Alumina and Bauxite: Bayer Plant Operations: White Side	218A	Tues-AM	265
Alumina and Bauxite: Technology and Future Trends	218A	Tues-PM	311
Aluminum Can Recycling: Session I	217D	Tues-AM	266
Aluminum Reduction - Potroom Improvements	213D	Mon-AM	171
Aluminum Reduction Technology: Cell Development and Operations	213D	Mon-PM	212
Aluminum Reduction Technology: Pot Control	213D	Tues-AM	267
Aluminum Reduction Technology: Modeling - Industry Trends	213D	Tues-PM	312
Aluminum Reduction Technology: Emerging Technologies	213D	Wed-AM	356
Aluminum Reduction Technology: Environmental	213D	Wed-PM	398
Aluminum Reduction Technology: Materials and Fundamentals	213A	Wed-PM	399
Aluminum Reduction Technology: Modeling	213D	Thurs-AM	437
Automotive Alloys 2004: Session I	210A	Mon-AM	172
Automotive Alloys 2004: Session II	210A	Mon-PM	213
Automotive Alloys 2004: Session III	210A	Tues-AM	268
Automotive Alloys 2004: Session IV	210A	Tues-PM	313
Carbon Technology: Cathode Material and Corrosion	213A	Mon-AM	176
Carbon Technology: Anode Raw Materials	213A	Mon-PM	217
Carbon Technology: Green Anodes and Soderberg Paste	213A	Tues-AM	272
Carbon Technology: Anode Baking	213A	Tues-PM	317
Carbon Technology: Anode Quality and Performance	213A	Wed-AM	360
Cast Shop Technology: Melting and Refractories	213B/C	Mon-AM	177
Cast Shop Technology: Modeling of Casting Processes	213B/C	Mon-PM	218
Cast Shop Technology: Casting	213B/C	Tues-AM	272
Cast Shop Technology: Metal Treatment	213B/C	Tues-PM	318
Cast Shop Technology: Alloying and Furnace Processing	213B/C	Wed-AM	361
Cast Shop Technology: Grain Refining	213B/C	Wed-PM	403
Cast Shop Technology: Foundry	213B/C	Thurs-AM	439
Cost-Affordable Titanium Symposium Dedicated to Prof. Harvey Flower: Overview and Innovative Processes.	206B	Mon-AM	182
Cost-Affordable Titanium Symposium Dedicated to Prof. Harvey Flower: Break Through Technologies	206B	Mon-PM	223
Cost-Affordable Titanium Symposium Dedicated to Prof. Harvey Flower: Titanium Economics	206B	Tues-AM	278
Cost-Affordable Titanium Symposium Dedicated to Prof. Harvey Flower: Creative Processing	206B	Tues-PM	323
Cost-Affordable Titanium Symposium Dedicated to Prof. Harvey Flower: Creative Fabrication	206B	Wed-AM	364

SESSION TITLE	ROOM	DAY	PAGE
Light Metals continued			
Cost-Affordable Titanium Symposium Dedicated to Prof. Harvey Flower: Low Cost Titanium	206B	Wed-PM	406
Cost-Affordable Titanium Symposium Dedicated to Prof. Harvey Flower: Property Enhancement	206B	Thurs-AM	440
Magnesium Technology 2004: Automotive Applications/Welding	203B	Mon-AM	191
Magnesium Technology 2004: Wrought Magnesium Alloys I	203B	Mon-PM	233
Magnesium Technology 2004: Wrought Magnesium Alloys II/Corrosion and Coatings	203B	Tues-AM	287
Magnesium Technology 2004: Primary Processing and Environmental Issues	203B	Tues-PM	332
Magnesium Technology 2004: Casting Processes and Properties	203B	Wed-AM	375
Magnesium Technology 2004: Fundamental Research	203B	Wed-PM	417
Magnesium Technology 2004: Alloy Development	203B	Thurs-AM	444
Phase Transformations and Deformation in Magnesium Alloys: Solidification and Precipitation	205	Tues-AM	294
Phase Transformations and Deformation in Magnesium Alloys: Plastic Deformation and Texture	205	Tues-PM	339
Phase Transformations and Deformation in Magnesium Alloys: Creep Deformation	205	Wed-AM	383
Phase Transformations and Deformation in Magnesium Alloys: Deformation and Strengthening	205	Wed-PM	425
Solidification of Aluminum Alloys: Microstructural Evolution I	207B/C	Tues-AM	298
Solidification of Aluminum Alloys: Microstructural Evolution II	207B/C	Tues-PM	343
Solidification of Aluminum Alloys: Solidification Cracking/Mechanical Properties	207B/C	Wed-AM	385
Solidification of Aluminum Alloys: Gas Porosity/Micro-Macro Segregation	207B/C	Wed-PM	427
Solidification of Aluminum Alloys: Special Effects	207B/C	Thurs-AM	449
Micro- and Nanoscale Technologies			
5th Global Innovations Symposium: Trends in LIGA, Miniaturization, and Nano-Scale Materials, Devices and Technologies: Plenary: Trends: Past, Present, and Future	202B	Mon-PM	209
5th Global Innovations Symposium: Trends in LIGA, Miniaturization, and Nano-Scale Materials, Devices and Technologies: Small Volume Deformation	202B	Tues-AM	261
5th Global Innovations Symposium: Trends in LIGA, Miniaturization, and Nano-Scale Materials, Devices and Technologies: Properties and Characterization of Materials for Microsystem/LIGA Applications	202B	Tues-PM	308
5th Global Innovations Symposium: Trends in LIGA, Miniaturization, and Nano-Scale Materials, Devices and Technologies: Properties, Processes, and Modeling	202B	Wed-AM	352
5th Global Innovations Symposium: Trends in LIGA, Miniaturization, and Nano-Scale Materials, Devices and Technologies: Manufacturing and Evaluation of Layered Nano-Scale Materials	202B	Wed-PM	394
Nanostructured Magnetic Materials: Recent Progress in Magnetic Nanostructures	215	Mon-AM	195
Nanostructured Magnetic Materials: Synthesis and Characterization of Nanostructured Magnetic Materials	t	Mon-PM	237
Nanostructured Magnetic Materials: Magnetic Tunnel Junctions and Semiconductor Spintronics		Tues-AM	290
Nanostructured Magnetic Materials: Self Assembly and Patterned Nanostructures	215	Tues-PM	336
Nanostructured Materials for Biomedical Applications: Session I	219A	Mon-AM	197

SESSION TITLE F	ROOM	DAY	PAGE
Micro- and Nanoscale Technologies continued			
Nanostructured Materials for Biomedical Applications: Session II	219A	Mon-PM	239
Nanostructured Materials for Biomedical Applications: Session III	219A	Tues-AM	291
Nanostructured Materials for Biomedical Applications: Session IV	219A	Tues-PM	337
Nanostructured Materials for Biomedical Applications: Session V	219A	Wed-AM	381
Nanostructured Materials for Biomedical Applications: Session VI	219A	Wed-PM	424
Nanostructured Materials for Biomedical Applications: Session VII	219A	Thurs-AM	447
Surfaces and Interfaces in Nanostructured Materials: General Phenomena & Processes	217A	Tues-AM	301
Surfaces and Interfaces in Nanostructured Materials: Grain & Phase Boundaries	217A	Tues-PM	346
Surfaces and Interfaces in Nanostructured Materials: Synthesis & Processing	217A	Wed-AM	388
Surfaces and Interfaces in Nanostructured Materials: Coatings and Surface Modification	. 217A	Wed-PM	428
Surfaces and Interfaces in Nanostructured Materials: Self-Organized and Biological Materials	2174	Thurs-AM	450
	2178	THUIS-AW	430
Third International Symposium on Ultrafine Grained Materials: Processing I: Fundamentals and Technology	207A	Mon-AM	206
Third International Symposium on Ultrafine Grained Materials: Processing II: Structural Evolution	207A	Mon-PM	251
Third International Symposium on Ultrafine Grained Materials: Posters	207A	Mon-PM/Tue/Wed	253
Third International Symposium on Ultrafine Grained Materials: UFG Material Fundamentals	207A	Tues-AM	305
Third International Symposium on Ultrafine Grained Materials: Microstructure and Properties	207A	Tues-PM	349
Third International Symposium on Ultrafine Grained Materials: Mechanical Properties	207A	Wed-AM	391
Third International Symposium on Ultrafine Grained Materials: Superplasticity, Creep & Thermal Stability	207A	Wed-PM	432
Physical Metallurgy			
Advances in Superplasticity and Superplastic Forming: Development of Advanced Superplastic Forming Processes	201B	Mon-PM	211
Advances in Superplasticity and Superplastic Forming: Advances in Superplastic Al-Mg Materials	201B	Tues-AM	264
Advances in Superplasticity and Superplastic Forming: Advances in Superplastic			
Forming of Light Alloys	2018	Tues-PM	310
Advances in Superplasticity and Superplastic Forming: Advanced Superplastic Materials and the Science of Superplasticity	201B	Wed-AM	355
Advances in Superplasticity and Superplastic Forming: Modeling of Superplastic Forming Processes and Materials	201B	Wed-PM	397
CFD Modeling and Simulation of Engineering Processes: Advanced Casting and Solidification Processes I	206A	Mon-AM	178
CFD Modeling and Simulation of Engineering Processes: Remelt Processes	206A	Mon-PM	219
CFD Modeling and Simulation of Engineering Processes: MEMS/Microfluidics	206A	Tues-AM	273
CFD Modeling and Simulation of Engineering Processes: Advanced Casting and Solidification Processes II	206A	Tues-PM	319
CFD Modeling and Simulation of Engineering Processes: Process Modeling I	206A	Wed-AM	362
CFD Modeling and Simulation of Engineering Processes: Process Modeling II	206A	Wed-PM	404

SESSION TITLE	ROOM	DAY	PAGE
Physical Metallurgy continued			
Computational Thermodynamics and Phase Transformations: Grain Growth and Particle Coarsening	202A	Mon-AM	180
Computational Thermodynamics and Phase Transformations: Interfaces and Grain Boundaries	202A	Mon-PM	222
Computational Thermodynamics and Phase Transformations: Phase Field Modeling I	202A	Tues-AM	276
Computational Thermodynamics and Phase Transformations: Phase Field Modeling II	202A	Tues-PM	322
Computational Thermodynamics and Phase Transformations: Phase Equilibria and Thermodynamic Assessments	202A	Wed-AM	363
Computational Thermodynamics and Phase Transformations: Joint Session with The Didier de Fontaine Symposium on the Thermodynamics of Alloys I	216B	Wed-AM	389
Computational Thermodynamics and Phase Transformations: Thermodynamics and Phase Transformations	202A	Wed-PM	405
Computational Thermodynamics and Phase Transformations: Joint Session with The Didier de Fontaine Symposium on the Thermodynamics of Alloys II	216B	Wed-PM	430
Dislocations: Modeling and Simulation Fundamentals	201A	Mon-AM	182
Dislocations: Simulation and Observation of Fundamental Mechanisms	201A	Mon-PM	224
Dislocations: Dislocation Structures and Patterning	201A	Tues-AM	278
Dislocations: Novel Experimental Methods	201A	Tues-PM	324
Dislocations: Plasticity, Voids, and Fracture	201A	Wed-AM	365
Dislocations: Dislocations in Complex Materials	201A	Wed-PM	407
Electrochemical Measurements and Processing of Materials: Electrodeposition Processes	212A	Tues-AM	280
Electrochemical Measurements and Processing of Materials: Electrochemical Refining	212A	Tues-PM	325
Electrochemical Measurements and Processing of Materials: Electrochemical Metal Production	212A	Wed-AM	366
Electrochemical Measurements and Processing of Materials: Electrochemical Sensors and Measurements	212A	Wed-PM	409
Failure of Structural Materials: Fundamentals	211A	Wed-AM	367
Failure of Structural Materials: Fatigue	211A	Wed-PM	410
Failure of Structural Materials: General	211A	Thurs-AM	441
Hume Rothery Symposium: Structure and Diffusional Growth Mechanisms of Irrational Interphase Boundaries: Session I	208A	Mon-AM	186
Hume Rothery Symposium: Structure and Diffusional Growth Mechanisms of Irrational Interphase Boundaries: Session II	208A	Mon-PM	228
Hume Rothery Symposium: Structure and Diffusional Growth Mechanisms of Irrational Interphase Boundaries: Session III	208A	Tues-AM	282
Hume Rothery Symposium: Structure and Diffusional Growth Mechanisms of Irrational Interphase Boundaries: Session IV	208A	Tues-PM	327
Hume Rothery Symposium: Structure and Diffusional Growth Mechanisms of Irrational Interphase Boundaries: Session V	208A	Wed-AM	370
Hume Rothery Symposium: Structure and Diffusional Growth Mechanisms of Irrational Interphase Boundaries: Session VI	208A	Wed-PM	415

SESSION TITLE	ROOM	DAY	PAGE
Physical Metallurgy continued			
Internal Stresses and Thermo-Mechanical Behavior in Multi-Component Materials Systems: Electronic Thin Films and Packaging Materials I	209B	Mon-AM	187
Internal Stresses and Thermo-Mechanical Behavior in Multi-Component Materials Systems: Electronic Thin Films and Packagaing Materials II	209B	Mon-PM	229
Internal Stresses and Thermo-Mechanical Behavior in Multi-Component Materials Systems: Creep and Plasticity I	209B	Tues-AM	283
Internal Stresses and Thermo-Mechanical Behavior in Multi-Component Materials Systems: Creep and Plasticity II	209B	Tues-PM	327
Internal Stresses and Thermo-Mechanical Behavior in Multi-Component Materials Systems: Anisotropy and Residual Stresses	209B	Wed-AM	371
Multiphase Phenomena in Materials Processing: Session I	218B	Wed-AM	379
Multiphase Phenomena in Materials Processing: Session II	218B	Wed-PM	423
Multiphase Phenomena in Materials Processing: Session III	218B	Thurs-AM	446
R.J. Arsenault Symposium on Materials Testing and Evaluation: Session I	211A	Mon-AM	201
R.J. Arsenault Symposium on Materials Testing and Evaluation: Session II	211A	Mon-PM	246
R.J. Arsenault Symposium on Materials Testing and Evaluation: Session III	211A	Tues-AM	296
R.J. Arsenault Symposium on Materials Testing and Evaluation: Session IV	211A	Tues-PM	342
Solidification Processes and Microstructures: A Symposium in Honor of Prof. W. Kurz: Processes	207D	Mon-AM	202
Solidification Processes and Microstructures: A Symposium in Honor of Prof. W. Kurz: Mushy Zone Dynamics	207D	Mon-PM	247
Solidification Processes and Microstructures: A Symposium in Honor of Prof. W. Kurz: Microstructures	207D	Tues-AM	299
Solidification Processes and Microstructures: A Symposium in Honor of Prof. W. Kurz: Rapid Solidification	207D	Tues-PM	344
Solidification Processes and Microstructures: A Symposium in Honor of Prof. W. Kurz: Phase Field	207D	Wed-AM	386
Symposium on Microstructural Stability in Honor of Prof. Roger D. Doherty: Microstructural Stability: Recrystallization	216A	Mon-AM	204
Symposium on Microstructural Stability in Honor of Prof. Roger D. Doherty: Microstructural Stability: Texture Development	216A	Mon-PM	249
Symposium on Microstructural Stability in Honor of Prof. Roger D. Doherty: Microstructural Stability: Plastic Deformation	216A	Tues-AM	302
Symposium on Microstructural Stability in Honor of Prof. Roger D. Doherty: Microstructural Stability: Precipitation and Other Topics	216A	Tues-PM	347
The Didier de Fontaine Symposium on the Thermodynamics of Alloys: Fundamentals of Alloy Theory	216B	Mon-AM	205
The Didier de Fontaine Symposium on the Thermodynamics of Alloys: Experimental Techniques	216B	Mon-PM	250
The Didier de Fontaine Symposium on the Thermodynamics of Alloys: First Principle Calculations and Cluster Expansion Techniques	216B	Tues-AM	304
The Didier de Fontaine Symposium on the Thermodynamics of Alloys: Interatomic Potentials and Cluster Expansion Techniques	216B	Tues-PM	348
The Didier de Fontaine Symposium on the Thermodynamics of Alloys: Joint Session with Computational Thermodynamics and Phase Transformations I	216B	Wed-AM	389

SESSION TITLE	ROOM	DAY	PAGE
Physical Metallurgy continued			
The Didier de Fontaine Symposium on the Thermodynamics of Alloys: Joint Session with Computational Thermodynamics and Phase Transformations II	216B	Wed-PM	430
The Role of Grain Boundaries in Material Design: Grain Boundary Character	218A	Wed-AM	390
The Role of Grain Boundaries in Material Design: Grain Boundary Segregation, Diffusion, Damage	218A	Wed-PM	431
The Role of Grain Boundaries in Material Design: Simulation of Grain Boundary Effects of Properties	218A	Thurs-AM	451
General Abstracts			
General Abstracts: Session I	204	Mon-AM	184
General Abstracts: Session II	204	Mon-PM	225
General Abstracts: Session III	212A	Mon-PM	226
General Abstracts: Session IV	204	Tues-AM	281
General Abstracts: Session V	204	Tues-PM	326
General Abstracts: Session VI	208B	Wed-AM	368
General Abstracts: Session VII	208B	Wed-PM	411
General Abstracts: Session VIII	207D	Wed-PM	412
General Abstracts: Session IX	201B	Thurs-AM	441
General Poster Session			
General Poster Session	Ballroom Foyer	MonPM-WedPM	453

# **Table of Contents**

## (Alphabetical Order)

SESSION TITLE	ROOM	DAY	PAGE
5th Global Innovations Symposium: Trends in LIGA, Miniaturization, and Nano-Scale Materials, Devices and Technologies: Plenary: Trends: Past, Present, and Future	202B	Mon-PM	209
5th Global Innovations Symposium: Trends in LIGA, Miniaturization, and Nano-Scale Materials, Devices and Technologies: Small Volume Deformation	202B	Tues-AM	261
5th Global Innovations Symposium: Trends in LIGA, Miniaturization, and Nano-Scale Materials, Devices and Technologies: Properties and Characterization of Materials for Microsystem/LIGA Applications	202B	Tues-PM	308
5th Global Innovations Symposium: Trends in LIGA, Miniaturization, and Nano-Scale Materials, Devices and Technologies: Properties, Processes, and Modeling	202B	Wed-AM	352
5th Global Innovations Symposium: Trends in LIGA, Miniaturization, and Nano-Scale Materials, Devices and Technologies: Manufacturing and Evaluation of Layered Nano-Scale Materials	202B	Wed-PM	394
		Mon-AM	
Advanced Materials for Energy Conversion II: Energy Issues & Metal Hydrides I			169
Advanced Materials for Energy Conversion II: Metal Hydrides II		Mon-PM	210
Advanced Materials for Energy Conversion II: Complex Hydrides I	203A	Tues-AM	262
Advanced Materials for Energy Conversion II: Complex Hydrides II	203A	Tues-PM	309
Advanced Materials for Energy Conversion II: Metal Hydrides III	203A	Wed-AM	353
Advanced Materials for Energy Conversion II: Thermodynamics, Superconductors & Batteries	204	Wed-AM	354
Advanced Materials for Energy Conversion II: Metal Hydrides IV - Dynamics of Metal Hydrides, and Tritium Gettering	203A	Wed-PM	395
Advanced Materials for Energy Conversion II: Magnetic Materials & Hydrogen Permeation	204	Wed-PM	396
Advanced Materials for Energy Conversion II: Thermoelectrics, Superconductors, and Piezoelectric Materials		Thurs-AM	435
Advanced Materials for Energy Conversion II: Metal Hydrides V, Thermal Energy Storage and Containment Materials	204	Thurs-AM	436
Advances in Superplasticity and Superplastic Forming: Development of Advanced Superplastic Forming Processes	201B	Mon-PM	211
Advances in Superplasticity and Superplastic Forming: Advances in Superplastic Al-Mg Materials	201B	Tues-AM	264
Advances in Superplasticity and Superplastic Forming: Advances in Superplastic Forming of Light Alloys	201B	Tues-PM	310
Advances in Superplasticity and Superplastic Forming: Advanced Superplastic Materials and the Science of Superplasticity	201B	Wed-AM	355
Advances in Superplasticity and Superplastic Forming: Modeling of Superplastic Forming Processes and Materials	201B	Wed-PM	397
Alumina and Bauxite: Bayer Plant Operations: Red Side	218A	Mon-AM	170
Alumina and Bauxite: Process Modeling and Control	218A	Mon-PM	212
Alumina and Bauxite: Bayer Plant Operations: White Side	218A	Tues-AM	265
Alumina and Bauxite: Technology and Future Trends		Tues-PM	311

SESSION TITLE	ROOM	DAY	PAGE
Aluminum Can Recycling: Session I	217D	Tues-AM	266
Aluminum Reduction - Potroom Improvements	213D	Mon-AM	171
Aluminum Reduction Technology: Cell Development and Operations	213D	Mon-PM	212
Aluminum Reduction Technology: Pot Control	213D	Tues-AM	267
Aluminum Reduction Technology: Modeling - Industry Trends	213D	Tues-PM	312
Aluminum Reduction Technology: Emerging Technologies	213D	Wed-AM	356
Aluminum Reduction Technology: Environmental	213D	Wed-PM	398
Aluminum Reduction Technology: Materials and Fundamentals	213A	Wed-PM	399
Aluminum Reduction Technology: Modeling	213D	Thurs-AM	437
Automotive Alloys 2004: Session I	210A	Mon-AM	172
Automotive Alloys 2004: Session II	210A	Mon-PM	213
Automotive Alloys 2004: Session III	210A	Tues-AM	268
Automotive Alloys 2004: Session IV	210A	Tues-PM	313
Beyond Nickel-Base Superalloys: Superalloys and Niobium Silicides	211B	Mon-AM	174
Beyond Nickel-Base Superalloys: Molybdenum Silicides I	211B	Mon-PM	215
Beyond Nickel-Base Superalloys: Precious Metal Alloys	211B	Tues-AM	269
Beyond Nickel-Base Superalloys: Molybdenum Silicides II	211B	Tues-PM	315
Beyond Nickel-Base Superalloys: Niobium Silicides	211B	Wed-AM	357
Beyond Nickel-Base Superalloys: Other Systems and Physical Properties of Silicides	211B	Wed-PM	400
Bulk Metallic Glasses: Processing I	209A	Mon-AM	175
Bulk Metallic Glasses: Processing II	209A	Mon-PM	216
Bulk Metallic Glasses: Fatigue and Fracture	209A	Tues-AM	270
Bulk Metallic Glasses: Theoretical Modeling and Shear Bands	209A	Tues-PM	316
Bulk Metallic Glasses: Bio, Corrosion, and Fracture Behavior	209A	Wed-AM	359
Bulk Metallic Glasses: Phase Transformation and Alloy Design	209A	Wed-PM	402
Bulk Metallic Glasses: Mechanical Behavior	209A	Thurs-AM	438
Carbon Technology: Cathode Material and Corrosion	213A	Mon-AM	176
Carbon Technology: Anode Raw Materials	213A	Mon-PM	217
Carbon Technology: Green Anodes and Soderberg Paste	213A	Tues-AM	272
Carbon Technology: Anode Baking	213A	Tues-PM	317
Carbon Technology: Anode Quality and Performance	213A	Wed-AM	360
Cast Shop Technology: Melting and Refractories	213B/C	Mon-AM	177
Cast Shop Technology: Modeling of Casting Processes	213B/C	Mon-PM	218
Cast Shop Technology: Casting	213B/C	Tues-AM	272
Cast Shop Technology: Metal Treatment	213B/C	Tues-PM	318
Cast Shop Technology: Alloying and Furnace Processing	213B/C	Wed-AM	361

SESSION TITLE	ROOM	DAY	PAGE
Cast Shop Technology: Grain Refining	213B/C	Wed-PM	403
Cast Shop Technology: Foundry	213B/C	Thurs-AM	439
CFD Modeling and Simulation of Engineering Processes: Advanced Casting and Solidification Processes I	. 206A	Mon-AM	178
CFD Modeling and Simulation of Engineering Processes: Remelt Processes	. 206A	Mon-PM	219
CFD Modeling and Simulation of Engineering Processes: MEMS/Microfluidics	206A	Tues-AM	273
CFD Modeling and Simulation of Engineering Processes: Advanced Casting and Solidification Processes II	. 206A	Tues-PM	319
CFD Modeling and Simulation of Engineering Processes: Process Modeling I	206A	Wed-AM	362
CFD Modeling and Simulation of Engineering Processes: Process Modeling II	206A	Wed-PM	404
Challenges in Advanced Thin Films: Microstructures, Interfaces, and Reactions: Advances in Photonic and Optoelectronic Materials and Processes	. 218B	Mon-AM	179
Challenges in Advanced Thin Films: Microstructures, Interfaces, and Reactions: Microstructures, Properties, and Reliability of Microelectronic Devices	. 218B	Mon-PM	220
Challenges in Advanced Thin Films: Microstructures, Interfaces, and Reactions: Modification, Characterization, and Modeling	218B	Tues-AM	274
Challenges in Advanced Thin Films: Microstructures, Interfaces, and Reactions: Design, Process, and Property Control of Functional and Structural Thin-Films	218B	Tues-PM	320
Computational Thermodynamics and Phase Transformations: Grain Growth and Particle Coarsening	. 202A	Mon-AM	180
Computational Thermodynamics and Phase Transformations: Interfaces and Grain Boundaries	202A	Mon-PM	222
Computational Thermodynamics and Phase Transformations: Phase Field Modeling I	. 202A	Tues-AM	276
Computational Thermodynamics and Phase Transformations: Phase Field Modeling II	. 202A	Tues-PM	322
Computational Thermodynamics and Phase Transformations: Phase Equilibria and Thermodynamic Assessments	202A	Wed-AM	363
Computational Thermodynamics and Phase Transformations: Joint Session with The Didier de Fontaine Symposium on the Thermodynamics of Alloys I	216B	Wed-AM	389
Computational Thermodynamics and Phase Transformations: Thermodynamics and Phase Transformations	. 202A	Wed-PM	405
Computational Thermodynamics and Phase Transformations: Joint Session with The Didier de Fontaine Symposium on the Thermodynamics of Alloys II	216B	Wed-PM	430
Cost-Affordable Titanium Symposium Dedicated to Prof. Harvey Flower: Overview and Innovative Processes.	206B	Mon-AM	182
Cost-Affordable Titanium Symposium Dedicated to Prof. Harvey Flower: Break Through Technologies	206B	Mon-PM	223
Cost-Affordable Titanium Symposium Dedicated to Prof. Harvey Flower: Titanium Economics	206B	Tues-AM	278
Cost-Affordable Titanium Symposium Dedicated to Prof. Harvey Flower: Creative Processing	206B	Tues-PM	323
Cost-Affordable Titanium Symposium Dedicated to Prof. Harvey Flower: Creative Fabrication	206B	Wed-AM	364
Cost-Affordable Titanium Symposium Dedicated to Prof. Harvey Flower: Low Cost Titanium	206B	Wed-PM	406
Cost-Affordable Titanium Symposium Dedicated to Prof. Harvey Flower: Property Enhancement	. 206B	Thurs-AM	440

SESSION TITLE	ROOM	DAY	PAGE
Dislocations: Modeling and Simulation Fundamentals	201A	Mon-AM	182
Dislocations: Simulation and Observation of Fundamental Mechanisms	201A	Mon-PM	224
Dislocations: Dislocation Structures and Patterning	201A	Tues-AM	278
Dislocations: Novel Experimental Methods	201A	Tues-PM	324
Dislocations: Plasticity, Voids, and Fracture	201A	Wed-AM	365
Dislocations: Dislocations in Complex Materials	201A	Wed-PM	407
Educational Issues in Transport Phenomena in Materials Processing: Presentations and Panel Discussion	209B	Wed-PM	408
Electrochemical Measurements and Processing of Materials: Electrodeposition Processes	212A	Tues-AM	280
Electrochemical Measurements and Processing of Materials: Electrochemical Refining	212A	Tues-PM	325
Electrochemical Measurements and Processing of Materials: Electrochemical Metal Production	212A	Wed-AM	366
Electrochemical Measurements and Processing of Materials: Electrochemical Sensors and Measurements	212A	Wed-PM	409
Failure of Structural Materials: Fundamentals	211A	Wed-AM	367
Failure of Structural Materials: Fatigue	211A	Wed-PM	410
Failure of Structural Materials: General	211A	Thurs-AM	441
General Abstracts: Session I	204	Mon-AM	184
General Abstracts: Session II	204	Mon-PM	225
General Abstracts: Session III	212A	Mon-PM	226
General Abstracts: Session IV	204	Tues-AM	281
General Abstracts: Session V	204	Tues-PM	326
General Abstracts: Session VI	208B	Wed-AM	368
General Abstracts: Session VII	208B	Wed-PM	411
General Abstracts: Session VIII	207D	Wed-PM	412
General Abstracts: Session IX	201B	Thurs-AM	441
General Poster Session	Ballroom Foyer	MonPM-WedPM	453
General Pyrometallurgy: Session I	202B	Mon-AM	185
High Risk Technologies in Metallurgy with Commercial Potential: Session I	210A	Wed-AM	369
High Risk Technologies in Metallurgy with Commercial Potential: Session II	210A	Wed-PM	414
Hume Rothery Symposium: Structure and Diffusional Growth Mechanisms of Irrational Interphase Boundaries: Session I	208A	Mon-AM	186
Hume Rothery Symposium: Structure and Diffusional Growth Mechanisms of Irrational Interphase Boundaries: Session II	208A	Mon-PM	228
Hume Rothery Symposium: Structure and Diffusional Growth Mechanisms of Irrational Interphase Boundaries: Session III	208A	Tues-AM	282
Hume Rothery Symposium: Structure and Diffusional Growth Mechanisms of Irrational Interphase Boundaries: Session IV	208A	Tues-PM	327
Hume Rothery Symposium: Structure and Diffusional Growth Mechanisms of Irrational Interphase Boundaries: Session V	208A	Wed-AM	370

SESSION TITLE	ROOM	DAY	PAGE
Hume Rothery Symposium: Structure and Diffusional Growth Mechanisms of Irrational Interphase Boundaries: Session VI	208A	Wed-PM	415
Internal Stresses and Thermo-Mechanical Behavior in Multi-Component Materials Systems: Electronic Thin Films and Packaging Materials I	209B	Mon-AM	187
Internal Stresses and Thermo-Mechanical Behavior in Multi-Component Materials Systems: Electronic Thin Films and Packagaing Materials II	209B	Mon-PM	229
Internal Stresses and Thermo-Mechanical Behavior in Multi-Component Materials Systems: Creep and Plasticity I	209B	Tues-AM	283
Internal Stresses and Thermo-Mechanical Behavior in Multi-Component Materials Systems: Creep and Plasticity II	209B	Tues-PM	327
Internal Stresses and Thermo-Mechanical Behavior in Multi-Component Materials Systems: Anisotropy and Residual Stresses	209B	Wed-AM	371
International Laterite Nickel Symposium - 2004: Economics and Project Assessment	217B/C	Mon-AM	188
International Laterite Nickel Symposium - 2004: Mineralogy and Geometallurgy	217B/C	Mon-PM	230
International Laterite Nickel Symposium - 2004: Panel Discussion	217B/C	Mon-PM	231
International Laterite Nickel Symposium - 2004: Pressure Acid Leaching	217B/C	Tues-AM	284
International Laterite Nickel Symposium - 2004: Process Development for Prospective Projects	217B/C	Tues-PM	328
International Laterite Nickel Symposium - 2004: Roasting and Smelting	217D	Tues-PM	330
International Laterite Nickel Symposium - 2004: Process and Operational Lessons Learned - Part I	217B/C	Wed-AM	372
International Laterite Nickel Symposium - 2004: Process and Operational Lessons Learned - Part II	217B/C	Wed-PM	415
International Laterite Nickel Symposium - 2004: Atmospheric Leaching	217B/C	Thurs-AM	443
International Laterite Nickel Symposium - 2004: Slurry Rheology, Solution Extraction and Other	217B/C	Thurs-AM	443
Lead-Free Solders and Processing Issues Relevant to Microelectronic Packaging: Fundamentals, Phases, Wetting and Solidification	219B	Mon-AM	189
Lead-Free Solders and Processing Issues Relevant to Microelectronic Packaging: Environmental and Materials Issues for Lead-Free	219B	Mon-PM	231
Lead-Free Solders and Processing Issues Relevant to Microelectronic Packaging: Mechanical Properties and Fatigue Behavior	219B	Tues-AM	285
Lead-Free Solders and Processing Issues Relevant to Microelectronic Packaging: Electromigration and Creep in Leadfree Solders	219B	Tues-PM	331
Lead-Free Solders and Processing Issues Relevant to Microelectronic Packaging: Interfacial Interactions, Intermetallics and Substrates	219B	Wed-AM	373
Lead-Free Solders and Processing Issues Relevant to Microelectronic Packaging: Microstructural Characterization and Evolution	219B	Wed-PM	416
Magnesium Technology 2004: Automotive Applications/Welding	203B	Mon-AM	191
Magnesium Technology 2004: Wrought Magnesium Alloys I	203B	Mon-PM	233
Magnesium Technology 2004: Wrought Magnesium Alloys II/Corrosion and Coatings	203B	Tues-AM	287
Magnesium Technology 2004: Primary Processing and Environmental Issues	203B	Tues-PM	332
Magnesium Technology 2004: Casting Processes and Properties	203B	Wed-AM	375
Magnesium Technology 2004: Fundamental Research	203B	Wed-PM	417
Magnesium Technology 2004: Alloy Development	203B	Thurs-AM	444

SESSION TITLE	ROOM	DAY	PAGE
Materials Analysis: Understanding the Columbia Disaster	Ballroom B	Wed-PM	418
Materials by Design: Atoms to Applications: Materials Chemistry and Alloy Design	210B	Mon-AM	192
Materials by Design: Atoms to Applications: Materials Characterization and Microstructural Modeling	210B	Mon-PM	234
Materials by Design: Atoms to Applications: Computational and Experimental Strategies	210B	Tues-AM	288
Materials by Design: Atoms to Applications: Designing Nanostructures	210B	Tues-PM	334
Materials by Design: Atoms to Applications: Design for Mechanical Functionality I	210B	Wed-AM	376
Materials by Design: Atoms to Applications: Design for Mechanical Functionality II	210B	Wed-PM	419
Materials Education to Revitalize the Workforce: Session I	217D	Wed-AM	377
Materials Education to Revitalize the Workforce: Session II	217D	Wed-PM	420
Materials Issues in Fuel Cells: State-of-the-Art	207B/C	Mon-AM	193
Materials Issues in Fuel Cell: Materials Challenges	207B/C	Mon-PM	235
Materials Processing Fundamentals: Solidification and Casting		Mon-AM	194
Materials Processing Fundamentals: Deformation Processing	212B	Mon-PM	236
Materials Processing Fundamentals: Liquid Metal Processing		Tues-AM	289
Materials Processing Fundamentals: Smelting and Refining		Tues-PM	335
Materials Processing Fundamentals: Aqueous Processing		Wed-AM	378
Materials Processing Fundamentals: Powders, Composites, Coatings and Measurement		Wed-PM	420
Metals for the Future: Structural Materials		Wed-AM	379
Metals for the Future: Functional Materials		Wed-PM	422
Metals for the Future: Processing and Bio-Materials		Thurs-AM	445
Multiphase Phenomena in Materials Processing: Session I		Wed-AM	379
Multiphase Phenomena in Materials Processing: Session II		Wed-AM	423
Multiphase Phenomena in Materials Processing: Session III		Thurs-AM	446
Nanostructured Magnetic Materials: Recent Progress in Magnetic Nanostructures	215	Mon-AM	195
Nanostructured Magnetic Materials: Synthesis and Characterization of Nanostructured Magnetic Materials	215	Mon-PM	237
Nanostructured Magnetic Materials: Magnetic Tunnel Junctions and Semiconductor Spintronics	215	Tues-AM	290
Nanostructured Magnetic Materials: Self Assembly and Patterned Nanostructures	215	Tues-PM	336
Nanostructured Materials for Biomedical Applications: Session I	219A	Mon-AM	197
Nanostructured Materials for Biomedical Applications: Session II	219A	Mon-PM	239
Nanostructured Materials for Biomedical Applications: Session III	219A	Tues-AM	291
Nanostructured Materials for Biomedical Applications: Session IV	219A	Tues-PM	337
Nanostructured Materials for Biomedical Applications: Session V	219A	Wed-AM	381
Nanostructured Materials for Biomedical Applications: Session VI	219A	Wed-PM	424
Nanostructured Materials for Biomedical Applications: Session VII	219A	Thurs-AM	447
Phase Stability, Phase Transformation, and Reactive Phase Formation in Electronic Materials III: Session I	214	Mon-AM	198

SESSION TITLE	ROOM	DAY	PAGE
Phase Stability, Phase Transformation, and Reactive Phase Formation in Electronic Materials III: Session II	214	Mon-PM	240
Phase Stability, Phase Transformation, and Reactive Phase Formation in Electronic Materials III: Session III	214	Tues-AM	293
Phase Stability, Phase Transformation, and Reactive Phase Formation in Electronic Materials III: Session IV	214	Tues-PM	338
Phase Stability, Phase Transformation, and Reactive Phase Formation in Electronic Materials III: Session V	214	Wed-AM	382
Phase Transformations and Deformation in Magnesium Alloys: Solidification and Precipitation	205	Tues-AM	294
Phase Transformations and Deformation in Magnesium Alloys: Plastic Deformation and Texture	205	Tues-PM	339
Phase Transformations and Deformation in Magnesium Alloys: Creep Deformation	205	Wed-AM	383
Phase Transformations and Deformation in Magnesium Alloys: Deformation and Strengthening	205	Wed-PM	425
Processing, Microstructure and Properties of Powder-Based Materials: Session I	208B	Mon-PM	242
Processing, Microstructure and Properties of Powder-Based Materials: Session II	208B	Tues-AM	295
Processing, Microstructure and Properties of Powder-Based Materials: Session III	208B	Tues-PM	340
Recent Advances in Non-Ferrous Metals Processing: Reactive Metals	205	Mon-AM	199
Recent Advances in Non-Ferrous Metals Processing: Sustainable Development	205	Mon-PM	244
Recycling: General Recycling	217D	Mon-AM	200
Recycling: Aluminum and Aluminum Dross Processing	217D	Mon-PM	244
Roytburd Symposium on Polydomain Structures: Elastic Domains in Structural Materials .	216A	Wed-AM	384
Roytburd Symposium on Polydomain Structures: Domains in Ferroelectrics and Magnetic	cs 216A	Wed-PM	425
R.J. Arsenault Symposium on Materials Testing and Evaluation: Session I	211A	Mon-AM	201
R.J. Arsenault Symposium on Materials Testing and Evaluation: Session II	211A	Mon-PM	246
R.J. Arsenault Symposium on Materials Testing and Evaluation: Session III	211A	Tues-AM	296
R.J. Arsenault Symposium on Materials Testing and Evaluation: Session IV	211A	Tues-PM	342
Solid and Aqueous Wastes from Non-Ferrous Metal Industry: Session I	214	Wed-PM	426
Solid and Aqueous Wastes from Non-Ferrous Metal Industry: Session II	214	Thurs-AM	448
Solidification of Aluminum Alloys: Microstructural Evolution I	207B/C	Tues-AM	298
Solidification of Aluminum Alloys: Microstructural Evolution II	207B/C	Tues-PM	343
Solidification of Aluminum Alloys: Solidification Cracking/Mechanical Properties	207B/C	Wed-AM	385
Solidification of Aluminum Alloys: Gas Porosity/Micro-Macro Segregation	207B/C	Wed-PM	427
Solidification of Aluminum Alloys: Special Effects	207B/C	Thurs-AM	449
Solidification Processes and Microstructures: A Symposium in Honor of Prof. W. Kurz: Processes	207D	Mon-AM	202
Solidification Processes and Microstructures: A Symposium in Honor of Prof. W. Kurz: Mushy Zone Dynamics	207D	Mon-PM	247
Solidification Processes and Microstructures: A Symposium in Honor of Prof. W. Kurz: Microstructures	207D	Tues-AM	299

SESSION TITLE	ROOM	DAY	PAGE
Solidification Processes and Microstructures: A Symposium in Honor of Prof. W. Kurz: Rapid Solidification	207D	Tues-PM	344
Solidification Processes and Microstructures: A Symposium in Honor of Prof. W. Kurz: Phase Field	207D	Wed-AM	386
Surfaces and Interfaces in Nanostructured Materials: General Phenomena & Processes	217A	Tues-AM	301
Surfaces and Interfaces in Nanostructured Materials: Grain & Phase Boundaries	217A	Tues-PM	346
Surfaces and Interfaces in Nanostructured Materials: Synthesis & Processing	217A	Wed-AM	388
Surfaces and Interfaces in Nanostructured Materials: Coatings and Surface Modification	. 217A	Wed-PM	428
Surfaces and Interfaces in Nanostructured Materials: Self-Organized and Biological Materials	217A	Thurs-AM	450
Symposium on Microstructural Stability in Honor of Prof. Roger D. Doherty: Microstructural Stability: Recrystallization	216A	Mon-AM	204
Symposium on Microstructural Stability in Honor of Prof. Roger D. Doherty: Microstructural Stability: Texture Development	216A	Mon-PM	249
Symposium on Microstructural Stability in Honor of Prof. Roger D. Doherty: Microstructural Stability: Plastic Deformation	216A	Tues-AM	302
Symposium on Microstructural Stability in Honor of Prof. Roger D. Doherty: Microstructural Stability: Precipitation and Other Topics	216A	Tues-PM	347
The Didier de Fontaine Symposium on the Thermodynamics of Alloys: Fundamentals of Alloy Theory	216B	Mon-AM	205
The Didier de Fontaine Symposium on the Thermodynamics of Alloys: Experimental Techniques	216B	Mon-PM	250
The Didier de Fontaine Symposium on the Thermodynamics of Alloys: First Principle Calculations and Cluster Expansion Techniques	216B	Tues-AM	304
The Didier de Fontaine Symposium on the Thermodynamics of Alloys: Interatomic Potentials and Cluster Expansion Techniques	216B	Tues-PM	348
The Didier de Fontaine Symposium on the Thermodynamics of Alloys: Joint Session with Computational Thermodynamics and Phase Transformations I	216B	Wed-AM	389
The Didier de Fontaine Symposium on the Thermodynamics of Alloys: Joint Session with Computational Thermodynamics and Phase Transformations II	216B	Wed-PM	430
The Role of Grain Boundaries in Material Design: Grain Boundary Character	218A	Wed-AM	390
The Role of Grain Boundaries in Material Design: Grain Boundary Segregation, Diffusion, Damage	218A	Wed-PM	431
The Role of Grain Boundaries in Material Design: Simulation of Grain Boundary Effects of Properties	218A	Thurs-AM	451
Third International Symposium on Ultrafine Grained Materials: Processing I: Fundamentals and Technology	207A	Mon-AM	206
Third International Symposium on Ultrafine Grained Materials: Processing II: Structural Evolution	207A	Mon-PM	251
Third International Symposium on Ultrafine Grained Materials: Posters	207A	Mon-PM/Tue/Wed	253
Third International Symposium on Ultrafine Grained Materials: UFG Material Fundamentals	207A	Tues-AM	305
Third International Symposium on Ultrafine Grained Materials: Microstructure and Properties	207A	Tues-PM	349
Third International Symposium on Ultrafine Grained Materials: Mechanical Properties	207A	Wed-AM	391
Third International Symposium on Ultrafine Grained Materials: Superplasticity, Creep & Thermal Stability	207A	Wed-PM	432

# **TECHNICAL PROGRAM**

Charlotte Convention Center; Charlotte, North Carolina USA; March 14-18, 2004

# MONDAY

#### Advanced Materials for Energy Conversion II: Energy Issues & Metal Hydrides I

Sponsored by: Light Metals Division, LMD-Reactive Metals Committee

*Program Organizers:* Dhanesh Chandra, University of Nevada, Metallurgical & Materials Engineering, Reno, NV 89557 USA; Renato G. Bautista, University of Nevada, Metallurgical and Materials Engineering, Reno, NV 89557-0136 USA; Louis Schlapbach, EMPA Swiss Federal, Laboratory for Materials Testing and Research, Duebendorf CH-8600 Switzerland

Monday AM	Room: 203A
March 15, 2004	Location: Charlotte Convention Center

Session Chairs: Renato G. Bautista, University of Nevada, Matls. & Metalurgl. Engrg., Reno, NV 89557 USA; Dhanesh Chandra, University of Nevada, Metallurgl. & Matls. Engrg., Reno, NV 89557 USA; Louis Schlapbach, EMPA, Swiss Federal Lab for Matls. Testing & Rsch., Duebendorf Switzerland

#### 8:30 AM Plenary

**Overview of Advanced Materials for Energy Conversion II Symposium**: *Dhanesh Chandra*<sup>1</sup>; Renato G. Bautista<sup>1</sup>; Louis Schlapbach<sup>2</sup>; <sup>1</sup>University of Nevada, Metallurgl. & Matls. Engrg., MS 388, Coll. of Engrg., Reno, NV 89557 USA; <sup>2</sup>EMPA, Swiss Federal Lab. for Matls. Testing & Rsch., Duebendorf Switerzland

An overview of Advanced Materials For Energy Conversion II Symposium, that includes storage will be presented. In this symposium we emphasize fields of materials related to energy conversion, fundamentals as well as applied research and industrial practices. Recent advances in methodology used in neutron scattering to characterize the hydrides, such as in-situ type experiments. The symposium sessions will include Hydrogen and Tritium Storage in intermetallics, alantes, and other hydrides, Batteries, Fuel Cells, Superconductors, Magnets, Membrane Materials, Thermal Energy Storage Materials, Photovoltaics and others. Several advances have been made in fuel cell materials, and we will highlight some of the key advances. Several adavnces have been made in hydrogen and tritum storage materials, we will empahsize light weight Alanate hydrides; Li based hydrides seem to be promising materials for storage. In addition Uranium hydride kinteics and other issues will be presented in thsi sympsoium. Fundamental understanding of the hydriding mechanisms will be discussed. We also have sessions devoted to materials for other Thermal Energy Storage Materials such as solid state organic phase change materials, photovoltaics, and thermoelectric materials will be be presented.

#### 8:45 AM Plenary

Energy Crisis - Fact or Fiction: *Bhakta B. Rath*<sup>1</sup>; <sup>1</sup>Naval Research Laboratory, Matls. Sci. & Component Tech. Direct., Code 6000, Washington, DC 20375-5341 USA

Global consumption of energy is staggering. The U.S. Department of Energy projects the total world consumption to rise by 59% between 1999 and 2020, from 382 to 607 quads per year (one quad being defined as 1015 BTU and equivalent to more than 7 billion gallons of petroleum). The same report predicts a 20% increase of carbon dioxide equivalent to approximately ten billion metric pounds of carbon. Another complication in the energy equation is that global population will increase from 6.0 to 7.5 billion. The impact of these projections may have long-range and profound implications. In the United States, hydrocarbon-based fuel use is twice that of coal or natural gas consumption and four times greater than the use of nuclear energy or renewable energy resources. Virtually the entire existing energy related infrastructure for the United States relies on fossil fuels. Undoubtedly, we will remain dependent on hydrocarbon combustion for the foreseeable future. As such, the country can not afford to ignore the long-term impacts of continued hydrocarbon combustion. It is essential to develop a long-term plan to deal with the use of alternative energy sources.

#### 9:15 AM Plenary

Advanced Materials Research in Photovoltaics: Progress and Challenges: *Thomas Surek*<sup>1</sup>; <sup>1</sup>National Renewable Energy Laboratory, Golden, CO 80401 USA

Photovoltaics (PV) is solar electric power - a semiconductor-based technology that converts sunlight to electricity. Three decades of research has led to the discovery of new materials and devices and new processing techniques for low-cost manufacturing. This has resulted in improved sunlight-to-electricity conversion efficiencies, improved outdoor reliability, and lower module and system costs. The manufacture and sale of PV has grown into a \$4 billion industry worldwide, with more than 560 megawatts of PV modules shipped in 2002. This paper reviews the most significant advances in PV materials and devices research over the past 30 years and examines the research challenges to reach the ultimate potential of current-generation (crystalline silicon), next-generation (thin films), and future-generation PV technologies. The latter include innovative materials and device concepts that hold the promise of significantly higher conversion efficiencies and/or much lower costs.

#### 9:45 AM Plenary

Advances in Fuel Cell Materials: Solid Electrolytes, Anodes and Cathodes, for Distributed and Portable Power: G. Jeffrey Snyder<sup>1</sup>; <sup>1</sup>Caltech/JPL, MS 277-207, Pasadena, CA 91109 USA

Fuel cells have emerged as the most promising alternative to the combustion engine to reduce the environmental impact and dependence on fossil fuels. Fuel cells directly convert the chemical energy of fuels to electrical energy with high efficiency. Many types of fuels can be used with hydrogen most widely considered. The primary components of a fuel cell are an ion conducting electrolyte, a cathode, and an anode. Advances in the materials that make up these components are of fundamental importance for improving fuel cell performance and are a focus of research at Caltech. The solid acid and solid oxide electrolytes are ideal for elevated temperature, high efficiency fuel cells. Improved power densities are achieved with microstructure engineered cathode and anode materials. With advanced thermal management techniques, single chamber fuel cells have been demonstrated that are small enough for hand-held electronics.

#### 10:15 AM Break

#### 10:30 AM Keynote

A New Means of Chemical Energy Conversion by Semiconductors: *V. V. Styrov*<sup>1</sup>; A. E. Kabansky<sup>1</sup>; <sup>1</sup>Priazovsky State Technical University, Dept. of Physics, University Str. 7, Mariupol, Donetsky Reg. 87500 Ukraine

The reaction of recombination of hydrogen atoms from the gas phase on solid surfaces (the energy release up to 4,48eV) leads to generation of electron-hole pairs in solids (Ge, CdS, ZnSe, ZnS). Thus one can observe during the surface chemical reaction all the effects known under optical excitation (chemoluminescence, longitudinal chemovoltaic effect on p-n junction, transversal chemovoltaic effect and so on). We have found the gas-solid system (atomic hydrogen+germanium) with extremely high efficiency of e-p pairs generation approaching unity per recombination. This system is perspective for chemical-to-electric energy conversion on Ge-based p-n junctions. The efficiency of chemical-to-light conversion in the system of atomic hydrogen+ZnS-Tm reaches one quantum (478,5nm) per 100 recombination. A solid-state laser can be designed under certain conditions with "chemical pumping". One more group of chemoeffects consists in electron emission stimulated by the surface reaction. The solids with the negative electron affinity are promising for chemical-to-electric energy conversion.

#### 10:55 AM Keynote

#### Hydrogen Storage-A Critical Challenge for the Hydrogen Economy: Russell H. Jones<sup>1</sup>; <sup>1</sup>Pacific Northwest National Laboratory, Matls. Scis., PO Box 999, Richland, WA 99352 USA

Vehicle range on a single tank of hydrogen is critical for the economic viability of hydrogen fueled vehicles. A range of 500 kilometers is projected for economic viability and this requires the storage of 4 kg of H2. Hydrogen storage concepts being considered and evaluated include: 1) compressed H2, 2) liquid H2, 3) bulk storage in hydrides, 4) surface adsorption on carbon and boron nitride nanotubes and 5) generation by chemical reaction of a hydride with water. Compressed H2 tanks with a capacity of about 2 kg of H2 stored at 350 bar of pressure have been certified while tanks with higher capacity stored at 700 bar are being developed. Liquidified H2 tanks can store more H2 in a vehicle than compressed H2 but liquifying H2 requires considerable energy and boil-off of the liquid H2 is a concern, especially in enclosed spaces. Storage of H2 in bulk hydrides or on the surface of carbon or boron nitride nanotubes are attractive because of the low pressures involved. Recent studies have shown that NaAlH4 can be reversibly charged and discharged with H2 100's of times but the capacity of this hydride material is only about 1/2 of that needed. Storage of H2 on the surfaces of carbon nanotubes has shown great promise but verification of the storage capacities has not occurred. However, carbon nanotubes have the potential to store about 80% of the desired quantity of H2 so it remains a viable storage material. Generation of H2 by chemical reaction of a hydride such as LiH with water to produce H2 is also attractive because of the significant amounts of H2 that can be generated by this process. The key issues for this process of generating H2 is the need to reprocess the reaction products and the cost associated with transportation and reprocessing this product. There are several options for storing hydrogen on-board a vehicle but as summarized above considerable development work is needed before the hydrogen economy can be realized. Critical materials issues associated with H2 storage will be presented.

#### 11:20 AM Keynote

International Hydrogen Storage R&D in IEA Task 17: Gary Sandrock<sup>1</sup>; <sup>1</sup>SunaTech, Inc., IEA Task 17 Operating Agent, 113 Kraft Pl., Ringwood, NJ 07456 USA

The International Energy Agency Agreement on the Production and Utilization of Hydrogen is marking its 25th anniversary. This presentation summarizes the R&D activities in currently active Annex 17 - Solid and Liquid State Hydrogen Storage Materials. Task 17 was chartered in 2001 and sets as its main target the development of reversible hydrogen storage media capable of delivering 5 wt.% H at less than 80°C. Nine countries are official participants: Canada, Japan, Lithuania, Norway, Spain, Sweden, Switzerland, the United Kingdom and the United States. The nine national participations are represented by 28 research centers representing universities, national laboratories and industries. Internationally collaborative R&D are being performed under 28 projects divided into three categories of H-storage media: hydrides, carbon and combined hydrides plus carbon. Included in the Task 17 activities is the IEA/DOE/SNL Hydride Information Center, an extensive series of online databases of hydride properties and applications.

#### 11:45 AM Invited

Nanoscale Selective, Highly Efficient Doped and Metal Atom Seeded Visible Light Tunable Nanoparticles: Application to Sensors, Microreactors, and Solar Cells: James L. Gole<sup>1</sup>; John Stout<sup>1</sup>; Clemens Burda<sup>2</sup>; <sup>1</sup>Georgia Institute of Technology, Sch. of Physics, 837 State St., Atlanta, GA 30332-0430 USA; <sup>2</sup>Case Western Reserve, Dept. of Chmst., Cleveland, OH USA

An exciting aspect of research at the nanoscale results as nanostructures hold the potential to display an enhanced and unexpected reactivity relative to that at the micron scale and bulk phase. Further, their formation and interaction may be accompanied by phase transformations not commonly observed in bulk systems. These factors can lead to unusual surface oxidation states, routes for highly efficient metallization, and the potential use of metastable phases as they apply to catalysis and energy conversion in environmentally benign systems. We have used a modified-flow tube furnace configuration carefully calibrated for temperature, temperature gradients, entrainment gas flow rate, and total pressure, and variable Si/SiO2 mixtures to generate silica (SiOx) nanospheres which are found to display enhanced catalytic activity and unexpected oxidation state distributions and reactivity. These structures can be agglomerated to wire-like configurations subsequently providing a means to grow silica nanotubes. Layered Sn/SnO mixtures to generate SnOx nanostructures at pressures of a few hundred Torr, display a phase coexistence between rutile and orthohombic crystal structures normally observed at pressures in excess of 150 kbar in the bulk. These observations have suggested a nanoscale exclusive synthesis route. In seconds, at room temperature, we produce nitrogen doped, stable, and environmentally benign TiO2xNx photocatalysts whose optical response can be tuned across the entire visible region. This synthesis, which can be simultaneously accompanied by metal atom seeding, can be accomplished through the direct nitration of anatase TiO2 nanostructures with alkyl ammonium salts. Tunability throughout the visible depends on the degree of TiO2 nanoparticle agglomeration and the influence of metal seeding. The introduction of a small quantity of palladium in the form of the acetate, chloride, or nitrate catalyzes further nitrogen uptake, appears to lead to a partial phase transformation, displays a counterion effect, and produces a material absorbing well into the near infrared. Silver introduced as the nitrate into a TiO2 or TiO2-xNx nanostructure framework, forms seeded AgxO - TiO2 or TiO2-xNx nanostructure mixtures which can be induced to self-assemble to agglomerate nanoneedle and planar arrays using select metals. Surprisingly, no organics are incorporated into the final TiO2-xNx products. These visible light absorbing photocatalysts readily photodegrade methylene blue and gaseous acetaldehyde. They can be transformed from liquids to gels and placed on the surfaces of sensor and microreactor based configurations to 1) produce an improved photocatalytically induced solar based sensor response, and 2) facilitate catalytically induced disinfection of airborne pathogens. In contrast to a nitration process which is facile at the nanoscale, we find little or no direct nitridation of micrometer sized anatase or rutile TiO2 powders at room temperature. Thus, we demonstrate an example of how a traversal to the nanoscale can vastly improve the efficiency for producing important submicron particles.

# Alumina and Bauxite: Bayer Plant Operations: Red Side

Sponsored by: Light Metals Division, LMD-Aluminum Committee Program Organizers: Travis Galloway, Century Aluminum, Hawesville, KY 42348 USA; David Kirkpatrick, Kaiser Aluminum & Chemical Group, Gramercy, LA 70052-3370 USA; Alton T. Tabereaux, Alcoa Inc., Process Technology, Muscle Shoals, AL 35661 USA

Monday AM	Room: 2	18A		
March 15, 2004	Location:	Charlotte	Convention	Center

Session Chair: Fred S. Williams, CMIS Corporation, Victoria, TX 77904 USA

#### 8:30 AM

Wollastonite as a Substitute for Lime in Phosphorus Control During Digestion and as Precoat or Filter-Aid for Pregnant Liquor Filtration in the Bayer Process: *Guy Forté*<sup>1</sup>; <sup>1</sup>Alcan International Ltd., Arvida R&D Ctr., 1955 Blvd. Mellon, PO Box 1250, Jonquiere, Quebec G7S 4K8 Canada

The use of wollastonite, a calcium silicate, was considered as a substitute for lime to control phosphorus in Bayer digestion and as precoat or filter-aid in the Bayer filtration process. Its stability in Bayer liquor and efficiency to control phosphorus was studied and will be reported. Bayer liquor filtration rate against wollastonite dosage will be presented and compared to standard lime precoat or filter-aid.

#### 8:55 AM

Effect of Pre-Desilication and Digestion Conditions on Silica Level in Bayer Liquor: *Eric Tizon*<sup>1</sup>; Philippe Clerin<sup>1</sup>; Benoît Cristol<sup>1</sup>; <sup>1</sup>Aluminium Pechiney, Direction de la Recherche et du Développement, BP- 54, Gardanne 13541 France

Controlling silica level in Bayer liquor is critical in order to prevent scaling or alumina quality issues. Experiments carried out in industrial liquor with metasilicate and kaolin were undertaken to simulate silica metabolism during pre-desilication and digestion operations. Effects of factors such as pre-desilication residence time, alumina and caustic concentration and digestion temperature have been studied. Depending on pre-desilication and digestion conditions, silica solubilisation during digestion has been attributed to kaolin, unstable zeolite or even sodalite dissolution for high caustic and alumina concentrations. The percentage of kaolin to DSP conversion often has the greatest influence on silica solubilisation during digestion. This can be limited by lack of residence time or accessibility of the kaolin in bauxite. It has been found that other factors, including the degree of maturation of the DSP from zeolite A to sodalite and its solubility in the digestion conditions, can also influence silica solubilisation in the digestion process.

#### 9:20 AM

#### Combination of Hydroxamate and Polyacrylamide Based Flocculents for Settler Performance Improvement in ADG Alumina Refinery: Jean-Marc Rousseaux<sup>1</sup>; B. Cristol<sup>1</sup>; S. Torsiello<sup>2</sup>; <sup>1</sup>Aluminium Pechiney, BP 54, 13541 Gardanne France; <sup>2</sup>Aluminium De Grèce, Paralia Distomou, 32003 Beotia Greece

HX® is a well-known settler flocculent, which has proven its efficiency in many alumina refineries. It has been found that a judicious combination of a well-chosen PAM with HX can significantly reduce the dosage without detrimental effects on settling rate, clarification and mud compaction. Three key parameters are to be considered to achieve the PAM + HX combination. Firstly, the right PAM anionicity and molecular weight should be determined. Besides the caustic level of the liquor (with respect to anionicity), chemical mud characteristics play a major role in the choice of the two PAM properties. Secondly, the choice of the respective PAM and HX proportions will have a significant effect on flocculation performances. Finally, for optimal results, it is necessary to pre-mix the PAM and HX flocculants before addition in feed-line and feed-well. Lab test results and industrial application in ADG refinery are detailed in this paper.

#### 9:45 AM

Continued Efforts on the Development of Salicylic Acid Containing Red Mud Flocculants: Everett C. Phillips<sup>1</sup>; <sup>1</sup>Ondeo Nalco Co., Mining & Mineral Process Chem., One Ondeo Nalco Ctr., Naperville, IL 60563-1198 USA

New digestion and process technology (such as high rate and pressure decantation) and the desire to increase liquor productivity, even while processing cheaper and lower grade bauxite ores, continues to increase demands on the red mud clarification process. As previously reported in 2003, Ondeo Nalco Co. has developed a range of new high molecular weight flocculants containing salicylic acid chemistry that promise substantial improvements for the clarification of red mud slurries when used alone or in combination with other chemistries. This paper summarizes further progress in this area. Efforts to explore the benefits of these new flocculants relative to those currently used in the industry and applications strategies to maximize their performance in combination with other flocculants will be discussed. The results of several plant evaluations will also be summarized.

#### 10:10 AM Break

#### 10:20 AM

Adsorption of Calcium on Red Mud and Gibbsite in the Bayer Process: Marie Raty<sup>1</sup>; *Kenneth T. Stanton*<sup>1</sup>; B. K. Hodnett<sup>1</sup>; M. Loan<sup>1</sup>; <sup>1</sup>University of Limerick, Matl. Sci. & Tech. Dept., Plassey Technological Park, Limerick Ireland

There is some evidence that calcium can be added to Bayer liquor in order to prevent scaling and losses of product in the mud circuit as calcium seems to modify gibbsite (Al2O3.3H2O) crystallisation. Calcium carbonate (CaCO3) was determined to have a solubility equilibrium from 5 to 30 ppm of Ca2+ in solutions of different causticity. Calcium adsorption on red mud and gibbsite surface was investigated. Results showed that Ca2+ adsorbed to a small degree on red mud surface (0.02 mg/g at equilibrium) and that the adsorption is at least ten times higher on gibbsite is similar to the dissolution rate of CaCO3 in the caustic solution at 70°C. This study shows that gibbsite has a pronounced affinity for calcium adsorption compared to red mud, although it is unclear at this stage how Ca2+ affects its growth rate.

#### 10:45 AM

Benefits of the Utilization of Cleaning Liquor in Red Side of CVG-Bauxilum: *Ricardo Alfredo Galarraga*<sup>1</sup>; Rodolfo José Díaz<sup>1</sup>; <sup>1</sup>CVG-Bauxilum, Gerencia de Producción, Zona Industrial Matanzas, Puerto Ordaz, Bolivar 8015 Venezuela

CVG-Bauxilum, in trying to reduce the maintenance costs and the cleaning time of equipment, has made changes to the original cleaning system with the purpose of obtaining a more versatile chemical cleaning system with caustic liquor to pipes and equipment with incrustations. The revised system has the possibility of making at least ten individuals circuits. The present work approaches mainly three topics: 1. comparison of costs between manual cleaning, cleaning with high pressure water and cleaning pipes with caustic liquor; 2. main circuits used to guarantee scale removal, higher levels of production and cur-

rent reliability of equipment; 3. previous analysis made in the laboratory to optimize and to guarantee results. The exact knowledge of the characteristics of material to remove, the magnitude of the incrustations in each one of the cases and the appropriate conditions of liquor for the effective accomplishment of the removal constitute essentially the beginning of this work.

#### 11:10 AM

Mechanochemistry and the Bayer Process of Alumina Production: Rakesh Kumar<sup>1</sup>; T. C. Alex<sup>1</sup>; M. K. Jha<sup>1</sup>; Z. H. Khan<sup>1</sup>; S. P. Mahapatra<sup>2</sup>; C. R. Mishra<sup>2</sup>; <sup>1</sup>National Metallurgical Laboratory, Nonferrous Process Div., Burmamines, Jamshedpur, Jharkhand 831007 India; <sup>2</sup>National Aluminium Company, P1, Nayapali, Bhubaneswar, Orissa 761013 India

The concept of mechanical activation has been applied to the traditional Bayer process of alumina production. The basic idea has been to achieve moderation in process conditions, reduce alumina and soda losses in the red mud, and alter the rheological character of red mud to improve its settling behaviour. The research pursued has primarily focussed on: (a) the particle breakage and structural changes in bauxite due to attrition milling; and (b) alumina recovery in simultaneous milling and leaching experiments. Particle breakage dominates during the initial stage (3-5 min) of the milling. Both XRD and TEM studies have indicated that the gibbsite present in the bauxite undergoes structural changes due to the milling. In typical 'simultaneous milling and leaching' experiments, it is found that almost all the alumina can be dissolved in alkali at 90°C after 15 minutes. Unlike the plant red mud, that was found to contain gibbsite as the dominant mineral, the solid residue produced in the laboratory experiments contained hematite as the dominant mineral.

#### 11:35 AM

**Preheators and Digestors in the Bayer Digestion Process:** Songqing Gu<sup>1</sup>; Zhonglin Yin<sup>1</sup>; <sup>1</sup>Zhengzhou Light Metal Research Institute, Chalco, No. 82 Jiyuan Rd., Shangjie Dist., Zhengzhou, Henan 450041 China

The existing preheaters and digesters applied in Bayer digestion processes are classified and investigated in this paper. The characteristics and mineral compositions of bauxite to be treated have great effects on the performance and operational efficiency of the preheaters and digesters. Therefore, the design concept and selection principle of Bayer digestion facilities and whole systems should be considered thoroughly on the basis of analysis of chemical and mineral compositions of bauxites and the results of studying behaviors of the minerals in bauxites in the preheating and digestion process.

#### **Aluminum Reduction - Potroom Improvements**

Sponsored by: Light Metals Division, LMD-Aluminum Committee Program Organizers: Alton T. Tabereaux, Alcoa Inc., Process Technology, Muscle Shoals, AL 35661 USA; Tom Alcorn, Noranda Aluminum Inc., New Madrid, MO 63869 USA

Monday AM	Room: 213D
March 15, 2004	Location: Charlotte Convention Center

Session Chair: Tom Alcorn, Noranda Aluminum Inc., New Madrid, MO 63869 USA

#### 8:30 AM

N

Automated Positioning of Prebaked Anodes in Electrolysis Cells, Part 1: Jean-Pierre Gagne<sup>1</sup>; Marc-Andre Thibault<sup>1</sup>; Robin Boulianne<sup>1</sup>; Gilles Dufour<sup>2</sup>; Gauthier Claude<sup>3</sup>; <sup>1</sup>Societe de Technologies de l'Aluminium STAS, 1846 rue outarde, Chicoutimi, Quebec Canada; <sup>2</sup>Alcoa Canada, 1 Place Ville Marie, Montreal, Quebec Canada; <sup>3</sup>Alcoa Canada, Aluminerie Deschambault, 1 Blvd. des Sources, Deschambault, Quebec Canada

During the production of aluminum in smelters, the anodes used in the electrolysis cells need to be frequently replaced. At the present time this is done manually, which not only is a most labour intensive task but also is subject to human error. Even though the operations are highly mechanized, human intervention is essential to ensure proper positioning of the anodes upon replacement (anode gaging). Even with the best trained operating crew, such an operation is prone to variability and lack of consistency given the number of people involved and the methods used. For the last two years, STAS and Alcoa Canada, have been working on the development of an automated system aimed at the vertical positioning of the carbon anodes upon their replacement on electrolysis cells. The control system is based on a precise measurement of the anodes and anode butts within the anode replacement cycle. The measurement system is relying upon the use of artificial vision. This paper will present the system developed by STAS and installed and tested on a pot tending machine at Alcoa Deschambault, Québec.

#### 8:55 AM

**Tomago Aluminum AP22 Project**: *Claude Vanvoren*<sup>1</sup>; Laurent Fiot<sup>2</sup>; Nigel Backhouse<sup>2</sup>; Chris Jamey<sup>2</sup>; <sup>1</sup>Aluminium Pechiney, Rsch. Ctr. LRF, BP 114, 73300 Saint Jean de Maurienne France; <sup>2</sup>Tomago Aluminum Company Pty Limited, Tomago Rd., Raymond Terrace, NSW 2325 Australia

Late April 2002, Tomago Aluminium announced the expansion of its production capacity by 70 000 tpy. This project is based on the AP22 Pechiney reduction cell technology, developped late 90's as reengineered technology for the well known AP18 cell. The project entered in its active phase early 2003 with the start up of a 20 pots trial section. Over and above the fine tuning of final operating setpoint, the purpose of this trial section is to pilot anode and anode assemblies transition phase, which, in such a large plant (3 potlines, 840 cells), requires to master both logistic and transient cell operating target. Progressive production increase will take place from 2004 and full production (530 000 tpy) is planned to be achieved in 2007 after lining turnover completion. Project progress, technical performance of the trial section as well as technical options on the cell and its surrounding will be discussed.

#### 9:20 AM

#### **Summer Potroom Efficiency Improvements**: Craig Anthony Lightle<sup>1</sup>; Mike Muncy<sup>1</sup>; Lon Ramsey<sup>1</sup>; John Browning<sup>1</sup>; Tom Saunders<sup>1</sup>; Chuck Tommey<sup>1</sup>; <sup>1</sup>Century Aluminum Corp, Ravenswood Reduction Plant, PO Box 98, Ravenswood, WV 26164 USA

In order for older U.S. reduction plants to remain in a competitive position, they must implement continuous improvement programs. At Century Aluminum of West Virginia, one program that has proven to be very successful and critical to making our operating plan has been "Victory Over Summer". Achieving monthly production and efficiency goals throughout the summer has always been difficult at the Ravenswood Facility due to excessively hot and humid conditions. Month goals have become tighter over the years and more critical to meet or exceed. As a result, a joint team of Potroom Operations and Potroom Technical personnel proposed a summer "campaign" focusing on maintaining and exceeding standard practices through increased monitoring and auditing, while also emphasizing early detection of operational concerns. This campaign due to measurable results has become a part of summer operation at the Ravenswood Facility. This presentation will outline the procedures utilized and the level of improvement attained.

#### 9:45 AM

**Exhaustion, Pneumatic Conveyor and Storage of Carbonaceous Waste Materials**: *Paulo Douglas S. de Vasconcelos*<sup>1</sup>; <sup>1</sup>Albras Alumínio Brasileiro S/A, Barcarena, Pará - Brazil, Rod. Pa 483 Km 21 - 68447-000

In smelters that use prebaked anodes, operations such as butt cleaning, butt and anode reject crushing and grinding, handling of coke packing material in the bake furnace, floor sweeping and discharge of dust from bake furnace cranes cause significant problems with the high generation of carbon dust and consequent environmental pollution. To control the dust pollution is a very difficult task. Another problem, meanwhile, is how to convey and store the dust collected. This paper presents the problem existing in the carbon plant of Albras, describing the pneumatic conveyor system developed by the Carbon Plant Engineering department, and the storage of the dust collected in the carbon plant. Examples of application of the system are the sale of carbon dust to the cement industry, or to generate steam for our alumina And/ or carbon plant in the future.

#### 10:10 AM Break

#### 10:20 AM

Experience with Power Saving in the Soderberg Lines at Hydro Aluminium Karmøy: *Knut A. Paulsen*<sup>1</sup>; Egil Furu<sup>1</sup>; Kristian Rolland<sup>1</sup>; *Ola Tratteberg*<sup>1</sup>; Marvin Bugge<sup>2</sup>; <sup>1</sup>Hydro Aluminium, Karmøy Plant, N-4265 Håvik Norway; <sup>2</sup>Norsk Hydro a.s, Rsch. Ctr., N-3901 Porsgrunn Norway

Due to very little rainfall during the fall of 2002, the water power production was severely reduced in Norway during the winter 2002/2003. The aluminium plants were asked to reduce their consumption. This paper describes the experiences gained in the Soderberg lines at Hydro Aluminium Karmøy when the line current was lowered from 135 kA and kept at 120 kA for a four months period. In order to save

additional energy the bath chemistry was adjusted to less surplus aluminiumfluoride and the cell voltage lowered considerably. Several challenges were initiated as the cells adjusted to the new heat balance situation. An immediate response from the cells was that the number of cathode failures/leakages and red-hot cathodeshieldspots dropped to zero. The side ledge thickness increased, particularly in the upper part. The super heat was lower, causing alumina dissolution problems and building up of heaps at the point feeding positions. This affected the anode effect frequency. Due to the adjusted bath chemistry with less aluminiumfluoride the temperature increased from 960-965 up to about 970°C, and above. A considerable decrease in dust and fluoride emissions was observed. Also, a decrease in the iron content in the metal produced was observed. The sodium content in the metal produced increased by 30% as the cell performance stabilized with low bath acidity. In the paper the experiences gained and the actions taken to cope with the operational challenges are discussed. During such an energy saving period, there are positive and negative effects observed. All three periods, the lowering of the current and energy input, the low energy period and the period bringing the cell lines back to normal current and production have their own challenges.

#### 10:45 AM

**Process Improvements to Raise the Line Current at Albras**: *Guilherme Epifânio da Mota*<sup>1</sup>; José Eduardo Macedo Blasques<sup>1</sup>; <sup>1</sup>ALBRAS - Alumínio Brasileiro S.A., Estrada PA 483 Km 21- Vila Murucupi, Barcarena, Pará 68447-000 Brasil

After the cut back made during the power-rationing period that occurred in Brazil in 2001, the Albras potlines were given current increases of up to 26 kA to reestablish and further increase metal production. During the ramping up period, problems with some equipments and process limitations were encountered. The dry scrubbers exhaustion rate reached the limit and the cell ACDs needed adjustment. With the line tending to heat up it was necessary to make key changes very quickly. Amongst these changes were a reduction in anode cover and a new audit practice in order to guarantee a better cover homogeneity, which would not compromise the anode consumption and the metal purity. Another implementation was the use of bath cavity cleaners during anode changes to facilitate reaching new ACD targets. This paper presents how the main process variables responded to the current increases and the new operational practices.

#### 11:10 AM

Experience with Booster Pots in the Prebake Line at Hydro Aluminium Karmøy: *Jørn Tonheim*<sup>1</sup>; Ove Kobbeltvedt<sup>1</sup>; Knut Arne Paulsen<sup>1</sup>; Marvin Bugge<sup>2</sup>; Sara Thornblad Mathisen<sup>2</sup>; <sup>1</sup>Hydro Aluminium Karmøy, N-4265 Håvik Norway; <sup>2</sup>Hydro Aluminium Porsgrunn, N-3901 Porsgrunn Norway

In September 1999 five booster pots were introduced in the Karmøy prebake line. These pots have been operated with 5.5 to 17.5 kA extra amperage, and are currently (June 2003) operated at 210 kA (which is +15.5 kA). The anode size and the stub size have been increased. Anodes with slots have been tested at both 204.5 kA and 210 kA. The pots were operated to 200 kA without modifications of the cathode lining. During September to November 2001 three pots were relined, and the cathode lining were modified. In January 2002 the current was increased to 210 kA. Two of the pots are still operated with the original cathode lining. The sideledge thickness has decreased in the test pots with old cathode lining. Operational performance has been good.

#### Automotive Alloys 2004: Session I

Sponsored by: Light Metals Division, LMD-Aluminum Committee Program Organizer: Subodh K. Das, Secat, Inc., Coldstream Research Campus, Lexington, KY 40511 USA

Monday AM	Room: 210A
March 15, 2004	Location: Charlotte Convention Center

Session Chair: Subodh K. Das, Secat Inc., Coldstream Rsch. Campus, Lexington, KY 40511 USA

#### 8:30 AM

Assuring Continued Recyclability of Automotive Aluminum Alloys: Chemical-Composition—Based Batching of Wrought Alloy Compositions from Al Scrap Shred Recovered from Nonmagnetic Shredder Fraction and AIVs: Adam Jan Gesing<sup>1</sup>; Benjamin AuBuchon<sup>1</sup>; Paul Torek<sup>1</sup>; Ron Dalton<sup>1</sup>; Richard Wolanski<sup>1</sup>; <sup>1</sup>Huron Valley Steel Corporation, 41000 Huron River Dr., Belleville, MI 48111 USA

There is continuing development at HVSC of recycling technologies needed to assure continued, high-value recyclability of all present and future automotive alloys - particularly wrought alloys as the use of these increases in the aluminum intensive vehicle (AIV). Here we add to our series of papers presenting the sort results from a prototype industrial sorter that uses laser induced breakdown spectroscopy (LIBS) to chemically analyze and sort each shredded scrap particle. This time we concentrate on the results that demonstrate the quality of the composition and the product recoveries that are achievable by the current prototype sorter sorting the Al shred recovered from both commercially available nonmagnetic shredder fraction and from the shredded AIVs.

#### 9:00 AM

Assuring Continued Recyclability of Automotive Aluminum Alloys: X-Ray-Absorption-Based Grouping of Light Metal Shredded Scrap: Adam Jan Gesing<sup>1</sup>; Tako P.R. de Jong<sup>2</sup>; Wijnand L. Dalmijn<sup>3</sup>; Richard Wolanski<sup>1</sup>; <sup>1</sup>Huron Valley Steel Corporation, 41000 Huron River Dr., Belleville, MI 48111 USA; <sup>2</sup>Delft University of Technology, Fac. of Civil Engrg. & Geoscis., Mijnbouwstraat 120, 2628 RX, Delft The Netherlands; <sup>3</sup>Delft University of Technology, Fac. of Mining & Petroleum Engrg., Mijnbouwstraat 120, 2628 RX, Delft The Netherlands

As the proportion of light metals used in automobile construction increases, so does the economic incentive to separate and group Al and Mg scrap recovered from shredded auto hulks into value-added alloy groupings. Dual-wavelength x-ray absorption imaging improved our ability to resolve small differences in material density, thickness and average atomic number. It is routinely applied to bone density scan measurements and to airport luggage inspection. In this paper we demonstrate the capability of the dual wavelength x-ray imaging technique to resolve differences between different light metal alloys in shredded metal scrap.

#### 9:30 AM

Processing and Properties of Ti-38-644 Alloy for Titanium Automotive Suspension Springs: Victor R. Jablokov<sup>1</sup>; J. Randolph Wood<sup>1</sup>; Brian G. Drummond<sup>2</sup>; <sup>1</sup>ATI Allvac, R&D, 2020 Ashcraft Ave., PO Box 5030, Monroe, NC 28111 USA; <sup>2</sup>ATI Allvac, Business Dvlp., 2020 Ashcraft Ave., PO Box 5030, Monroe, NC 28111 USA

The metastable beta titanium alloy Ti-38-644 has a long history of use for aerospace springs and fasteners. A vast range of mechanical properties is attainable for this alloy by manipulating the processing parameters and adjusting subsequent thermal treatments. The present work focuses on adjusting the thermomechanical processing procedures of Ti-38-644 to improve its viability and cost for the automotive suspension spring market. Particular attention has been given to cold drawing after the hot rolling process and conducting thermal aging treatments on the order of 30 minutes to 6 hours. Short aging times are less disruptive to the manufacturing cycle and offer the potential for elimination of post-process pickling procedures which are common for aerospace titanium spring parts. It is anticipated that the improved processing and associated cost reduction of Ti-38-644 will be beneficial for near-future automotive vehicle applications.

#### 9:55 AM

Synthesis of Closed-Cell Aluminum Microfoams: Halil Berberoglu<sup>1</sup>; Hélène Ruckebusch<sup>1</sup>; Jonathan Chang<sup>1</sup>; Aram Agrapetian<sup>1</sup>; Laurent Pilon<sup>1</sup>; <sup>1</sup>University of California, Mech. & Aeros. Engrg. Dept., 37-132 Engineering IV - Box 951597, Los Angeles, CA 90095-1597 USA

Aluminum foams have been identified as potential lightweight materials with adequate mechanical, thermal, and non-corroding properties to be used in various applications such as crash energy absorber, noise control, machine construction, sporting equipment, and biomedical applications. Aluminum foams should have controllable, homogeneous, and uniform morphology. However, current processes do not repeatedly produce metal foams with the desired characteristics. A novel technique for making closed-cell aluminum microfoams is presented. The process consists of stirring molten aluminum at highspeed in an inert atmosphere. During spinning, the inert gas is drawn into the aluminum melt and is broken into microscopic bubbles. These bubbles get trapped in the bulk in an orderly fashion as the melt solidifies.

#### 10:20 AM

Fatigue Life Prediction of Cast A356 Automotive Components: Jianzhang Yi<sup>1</sup>; Yunxin Gao<sup>1</sup>; Peter D. Lee<sup>1</sup>; Daan M. Maijer<sup>2</sup>; Harvey M. Flower<sup>1</sup>; Trevor C. Lindley<sup>1</sup>; <sup>1</sup>Imperial College London, Dept. of Matls., Prince Consort Rd., London SW7 2BP UK; <sup>2</sup>University of British Columbia, Dept. of Metals & Matls. Engrg., Frank Forward Bldg., 309-6350 Stores Rd., Vancouver V6T 1Z4 Canada

The fatigue design of cast components has traditionally been based on an extensive material property database together with experience from in-service performance. However, such an approach requires a significant amount of fatigue S-N testing in view of the complex shapes of cast components and the corresponding large variation in microstructures and defect populations. Also, this approach does not incorporate the flexibility necessary for product design optimisation. In the present study, a new methodology is proposed which allows prediction of fatigue life of automotive components made from cast aluminium-silicon alloys. Experimentally, a wide range of microstructure (secondary dendrite arm spacing) and defects (pores, inter-metallic particles) were introduced in a cast A356 aluminium-silicon alloy by using a wedge cast mould and carefully controlling the casting conditions and eutectic modifier addition. Analysis of experimental results and finite element analysis were used to identify the crack initiating defect and to characterise the development of fatigue damage including interactions between the different defect types. A fatigue life prediction model has been developed which relates porosity, eutectic modification and secondary dendrite arm spacing to fatigue life. This model was used in conjunction with finite element stress analysis to predict the fatigue life of a cast A356 brake calliper with reasonable correlation to experimental results.

#### 10:45 AM

Improvement in Bake Hardening Response of a Twin Roll Cast Al-Mg-Si Sheet: Yucel Birol<sup>1</sup>; Canan Inel<sup>2</sup>; <sup>1</sup>Marmara Research Center, Matls. & Chem. Tech. Rsch. Inst., Gebze, Kocaeli 41470 Turkey; <sup>2</sup>Assan Aluminum, Quality Sys. Lab., E-5 Karayolu 32. Km Tuzla, Istanbul Turkey

Body panel sheet is expected to have a low and stable yield strength in the as-delivered condition for easy stamping and a high yield strength after the paint bake cycle for high dent resistance required in service. The heat-treatable Al-Mg-Si aluminum alloys are increasingly used for automotive body panel applications owing to their ability to meet in large part, these conflicting demands. The age hardening potential of these alloys, however, can not be fully exploited in paint bake cycles at automobile plants due to the low temperatures and short times involved. Hence, the microstructure in the conventional T4 condition must be modified after the solution heat treatment so as to improve the aging kinetics and the paint bake response. The present work was undertaken to improve the paint bake response of a twin roll cast 6016 sheet. Different pre-aging treatments were employed and the critical process parameters were identified.

#### 11:10 AM

Aluminum High-Speed Train: Aureliu Panaitescu<sup>1</sup>; Augustin Moraru<sup>1</sup>; Alexandru Ionescu<sup>2</sup>; *Ileana Panaitescu*<sup>3</sup>; <sup>1</sup>"Politehnica" University of Bucharest, Elect. Engrg. Dept., Splaiul Independentei 313, Bucharest 060032 Romania; <sup>2</sup>Iveco Fiat, Torino Italy; <sup>3</sup>Isvor Fiat, Engrg. Processes & ICT, Corso Dante 103, Turin 10126 Italy

This paper distinguishes itself by focusing on a new high-speed public transportation system and not on the aluminum alloys used for its construction. There are many regions around world where the transportation problem between far urban locations might be solved with high-speed trains (v > 190-250 mph) safe in operation and non-polluting. The expectations for the linear motor trains with magnetic levitation didn't prevail commercially even in recent days. The vehicle here presented may become, we believe, a very convenient solution because its constructive simplicity and the acceptable investments needed for its construction; should be of great interest for both the aluminum alloys producers and the engineers involved within the ground transportation. There are presented the main operation characteristics and compared with the French high speed train characteristics (TGV).

#### 11:35 AM

Infrared Imaging Investigation of Foam Removal Mechanism in Lost Foam Aluminum Process: *Qi Zhao*<sup>1</sup>; *Thomas W. Gustafson*<sup>2</sup>; <sup>1</sup>Metal Casting Technology, 127 Old Wilton Rd., Milford, NH 03055 USA; <sup>2</sup>General Motors, GM Powertrain/CDVC, 1629 N. Washington Ave., Saginaw, MI 48605-5073 USA

A high-speed infrared camera was used to measure and record variations in thermal profile across the surfaces of ceramic coating coated foam plates during the lost foam aluminum casting. The real time images were analyzed to gain the insight of the process fundamentals. The results were compared with the observations in the past vacuumassisted foundry experiments. The process kinetics information acquired from the real time IR imaging verified that foam removal in the lost foam aluminum casting, regardless vacuum-assisted or gravity

# Beyond Nickel-Base Superalloys: Superalloys and Niobium Silicides

Sponsored by: Structural Materials Division, SMD-Corrosion and Environmental Effects Committee-(Jt. ASM-MSCTS), SMD-High Temperature Alloys Committee, SMD-Mechanical Behavior of Materials-(Jt. ASM-MSCTS), SMD-Refractory Metals Committee *Program Organizers*: Joachim H. Schneibel, Oak Ridge National Laboratory, Oak Ridge, TN 37831-6115 USA; David A. Alven, Lockheed Martin - KAPL, Inc., Schenectady, NY 12301-1072 USA; David U. Furrer, Ladish Company, Cudahy, WI 53110 USA; Dallis A. Hardwick, Air Force Research Laboratory, AFTL/MLLM, Wright-Patterson AFB, OH 45433 USA; Martin Janousek, Plansee AG Technology Center, Reutte, Tyrol A-6600; Yoshinao Mishima, Tokyo Institute of Technology, Precision and Intelligence Laboratory, Yokohama, Kanagawa 226 Japan; John A. Shields, HC Stark, Cleveland, OH 44117 USA; Peter F. Tortorelli, Oak Ridge National Laboratory, Oak Ridge, TN 37831-6156 USA

 Monday AM
 Room: 211B

 March 15, 2004
 Location: Charlotte Convention Center

Session Chairs: Yoshinao Mishima, Tokyo Institute of Technology, Dept. of Matls. Sci. & Engrg., Yokohama, Kanagawa 226-8502 Japan; Peter F. Tortorelli, Oak Ridge National Laboratory, Metals & Ceram. Div., Oak Ridge, TN 37831 USA

## 8:30 AM Introduction - by Joachim H. Schneibel

#### 8:45 AM Invited

Superalloys: Evolution and Revolution for the Future: *Hiroshi Harada*<sup>1</sup>; 'NIMS, High Temp. Matls. 21 Project, Sengen 1-2-1, Tsukuba Science City, Ibaraki 305-0047 Japan

The temperature capability of Ni-base superalloys has been improved by more than 300C since the invention in early 1940's. Despite a view that the superalloy has reached its limitation in temperature capability, recent efforts of alloy development are again lifting up the temperature capability, e.g., fourth generation superalloys with platinum group metals (Ru or Ir) additions capable up to 1100C, suggesting further evolutions in future. Also, platinum group metals base superalloys, namely, refractory superalloys, proposed by the author and some of his group members have resulted in revolutionary improvements in temperature capability, reaching 1800C. This paper describes the present status of the superalloy developments and tries to provide a view of the future possibilities.

#### 9:15 AM

Effect of Ru on Elemental Partitioning Behaviour and Phase Stability of Ni-Based Superalloys: An-Chou Yeh<sup>1</sup>; Sammy Tin<sup>1</sup>; <sup>1</sup>University of Cambridge, Rolls-Royce Univ. Tech. Ctr., Dept. of Matls., New Museum Site, Pembroke St., Cambridge UK

Nickel-base single crystal superalloys are predominately used as materials for turbine blades in aero-engines because of its excellent mechanical properties at elevated temperatures. Due to the elevated levels of refractory alloying additions, precipitation of intermetallic Topologically-Close-Packed (TCP) phases that eventually degrade the mechanical properties occurs after prolonged exposure at elevated temperatures. Recent studies have shown that additions of the platinum group metal; ruthenium offers the possibility to increase the stability of the microstructure and creep resistance of this class of alloys at high temperatures. The present investigation carefully details the influence of Ru on the stability and elemental partitioning behaviour of Ni-base superalloys. Microstructures in both as-cast and solution-treated conditions were carefully characterized, and Electron-Probe Micro-Analysis was performed to study the elemental segregation behaviour in as-cast samples. Compositional differences between the g-g' phases were quantified using a variety of chemical analysis techniques. The long-term phase stability of the alloys was investigated over a wide range of thermal exposures and TEM analysis was performed to identify the various TCP phases present in Ru-containing alloys. Underlying mechanisms of how ruthenium addition improves the properties of Ni-based superalloys are discussed.

#### 9:30 AM

Microstructures and Mechanical Properties in Ni<sub>3</sub>Al-Ni<sub>3</sub>Ti-Ni<sub>3</sub>V-Based Multi-Intermetallic Alloys: *Takayuki Takasugi*<sup>1</sup>; Yoshinari Nunomura<sup>1</sup>; Yasuyuki Kaneno<sup>1</sup>; <sup>1</sup>Osaka Prefecture University, Dept. of Metall. & Matls. Sci., 1-1 Gakuen-cho, Sakai, Osaka 599-8531 Japan

The phase relation, microstructures, high-temperature deformation and oxidation behavior of intermetallic alloys based on Ni<sub>3</sub>Al-Ni<sub>3</sub>Ti-Ni<sub>3</sub>V pseudo-ternary alloy system were investigated. As the constituent intermetallic phases, L12(Ni3Al), D024(Ni3Ti), D022(Ni3V) and hcp(Ni<sub>3</sub>Ti<sub>0.65</sub>V<sub>0.35</sub>) were identified at 1273K, and then their phase fields were discussed, based on the electrical and geometrical factors of constituent atoms. Among four intermetallic phases, five kinds of twophase relations and two kinds of three-phase relations were found to exist. Also, D024(Ni3Ti) phase extended up to concentration field in which a majority of constituent Ti elements were replaced by Al and V elements. The prepared alloys exhibited widely different microstructures, depending on the number and the kind of the constituent intermetallic phases, and also heat trea tment. Particularly, the alloys which contain low Ti content and have bi-modal three-phase fine microstructures composed of L12(Ni3Al), D024(Ni3Ti) and D022(Ni3V) showed extremely superior high-temperature strength and ductility, and also reasonable corrosion and oxidation properties.

#### 9:45 AM

**Oxidation Resistance - One Barrier to Moving Beyond Ni-Base Alloys:** *Bruce A. Pint*<sup>1</sup>; Ian G. Wright<sup>1</sup>; <sup>1</sup>Oak Ridge National Laboratory, Metals & Ceram., 1 Bethel Valley Rd., MS 6156, Oak Ridge, TN 37831-6156 USA

The implementation of new high-temperature materials is often hampered by their lack of oxidation or environmental resistance. In fact, this failing is one of the strongest barriers to moving beyond Nibase superalloys. In practice, high-temperature alloys have at least reasonable, inherent oxidation resistance. In the case of the current generation of superalloys, these alloys have sufficient oxidation resistance to provide limited protection but, for reliable maximum-temperature operation, they are coated with an oxidation-resistant metallic coating and an outer ceramic thermal barrier layer. In the materials development process, the considerations of microstructural and compositional demands to provide increased high-temperature strength are paramount, and result in the needs for oxidation resistance, along with other realities, being given minor attention. The assumption made is that an oxidation-resistant coating will be available to protect these substrates. For many systems, this assumption is seriously flawed as interactions with the substrate or mechanical degradation of the coating lead to insufficient reliability for critical components. Examples are given for currently-used materials and materials classes with critical oxidation resistance problems.

#### 10:00 AM Break

#### 10:30 AM

**Computational Design of Oxidation Resistant Niobium Alloys**: John E. Morral<sup>1</sup>; Yunzhi Wang<sup>1</sup>; <sup>1</sup>Ohio State University, Matls. Sci. & Engrg., 2041 College Rd., Columbus, OH 43210 USA

Computer software is now available that can predict the microstructural evolution that accompanies gas-solid reactions. Accordingly, with the proper databases the software could predict whether or not an alloy will form a protective oxide film on the surface of an alloy. Using the niobium system as an example, it will be shown how calculated phase diagrams, diffusion constants and the assumptions of "local equilibrium" and "zero stress" can be combined to screen which combination of two, three, or more elements in niobium is likely to form a protective alumina scale. Further screening is possible via phase field modeling in which both non-equilibrium and the formation of residual stresses can be considered.

#### 10:45 AM

Influence of Microstructure on High Temperature Oxidation in Multicomponent Nb Alloys: Sarath K. Menon<sup>1</sup>; Triplicane A. Parthasarathy<sup>1</sup>; Madan G. Mendiratta<sup>1</sup>; <sup>1</sup>UES Inc., Matl. Procg. Div., 4401 Dayton-Xenia Rd., Dayton, OH 45432-1894 USA

Nb-based metal/silicide alloys (Nb-Ti-Si-Cr-Al-Hf-Sn) are being explored to extend the temperature capability of the current Ni-based superalloys in jet engines. One of the serious concerns in the application of Nb based alloys is their poor oxidation resistance at elevated temperatures. In this paper an overview of the high temperature oxidation resistance of these multiphase alloys will be provided. These alloys contain a distribution of the Nb<sub>5</sub>Si<sub>3</sub> phase in  $\beta$  matrix. The Nb-Si phase diagram is characterized by a high temperature eutectoid reaction, Nb<sub>3</sub>Si >  $\beta$  + Nb<sub>5</sub>Si<sub>3</sub>, however the reaction has been found to be extremely sluggish. Our studies on ternary Nb-Si-Ti alloys have shown that this eutectoid reaction had occurred to completion in some ternary alloys indicating that the extremely sluggish eutectoid reaction had been considerably accelerated with the addition of Ti. The eutec-

#### 11:00 AM

Chlorination of Mo-Nb-Si-B intermetallic Alloys to Improve Oxidation Resistance: Vikas Behrani<sup>1</sup>; Andrew J. Thom<sup>1</sup>; Matthew J. Kramer<sup>1</sup>; Mufit Akinc<sup>1</sup>; <sup>1</sup>Iowa State University, Ames Lab., Matls. Chmst./Dept. of Matls. Sci. & Engrg., Spedding Hall, Ames, IA 50011 USA

Recent studies showed that quaternary Mo-Nb-Si-B system is not oxidation resistant. The difference in oxidation resistance between Mo-Si-B and Mo-Nb-Si-B may be interpreted in terms of the volatility of the oxide. Chlorination is a novel processing technique to selectively remove Nb2O5 from the scale as volatile NbCl5. This work studied the chlorination of oxidized Mo-Nb-Si-B alloy of nominal composition 63(Nb,Mo)-30Si-7B;Nb/Mo=1 (at%) comprised of three phase microstructure of (Nb,Mo)5Si3Bx(T1)-(Nb,Mo)5(Si,B)3(T2)-(Nb,Mo)5Si3Bx(D88). Oxidation behavior of these alloys in air has been studied before and after chlorination. Results show that Nb2O5 can be selectively removed from scale leaving a borosilicate rich scale. Linear oxidation rate of the chlorinated alloys were reduced by up to ~3 times no-treated alloy under identical conditions. Chlorination will form a dense scale after heat treatment at 1000°C in argon. Microstructure analysis shows that borosilicate glass reflowed to fill voids created by v olatilized Nb2O5, thus reducing oxidation rate.

#### 11:15 AM

Oxidation Behavior of the Multi Component Nb-Si-Ti-Al-Cr-X Alloys for High Temperature Aeroengine Applications: *Raghvendra Tewari*<sup>1</sup>; Hyojin Song<sup>1</sup>; Amit Chatterjee<sup>2</sup>; P. I. Rosales<sup>1</sup>; Vijay K. Vasudevan<sup>1</sup>; <sup>1</sup>University of Cincinnati, Dept. of Chem. & Matls. Engrg., Cincinnati, OH 45221-0012 USA; <sup>2</sup>Rolls-Royce Corporation, 2001 S. Tibbs Ave., Indianapolis, IN 46241 USA

Nb-based silicides possess a good combination of properties which make them potential materials for high temperature applications. However, these silicides exhibit poor oxidation at elevated temperatures. Present paper reports the oxidation behavior of the multi-component Nb-Si-Ti-Al-Cr-X alloys. The as cast specimens which have been oxidized at different temperatures, showed the presence of two types of oxides under cyclic as well as static conditions. The chemical composition and in depth profile analysis of the oxide layer have shown presence of different oxides scales. Cross sectional examination of oxides has revealed cracks in the oxide layer and deep penetration of oxygen in to the matrix phase. Elemental mapping of these oxides have clearly revealed that many elements, like Cr, Si, do not constitute substantially into the oxide layer. XPS results showed different oxidation states of the Ti and Al elements indicating a complex nature of the oxide. Based on these observations, a possible mechanism of oxidation of these alloys has been proposed.

#### 11:30 AM

Study of the Effects of Cr, Al and Ta Additions on the Microstructure and Oxidation Behaviour of Nb-Silicide Based In Situ Composites: Kostas Zelenitsas<sup>1</sup>; Panayiotis Tsakiropoulos<sup>1</sup>; <sup>1</sup>University of Surrey, Sch. of Engrg., Mech. & Aeros. Engrg., Metall. Rsch. Grp., Guildford, Surrey GU2 7XH England

Niobium silicide based in situ composites have been designed to study the synergistic effects of Cr, Al and Ta on phase selection in Nb-Ti-Si alloys in the as solidified condition and after heat treatment. The alloys were prepared using clean melting and casting in water-cooled copper crucibles/moulds. Tantalum offers solid solution strengthening and Cr and Al play important roles in phase selection and oxidation behaviour. In our study particular attention has been paid to segregation phenomena in ingots and on phase equilibria involving the Nbss and the Nb3Si, Nb5Si3 and Laves phases. Selected alloys have also been evaluated for their oxidation behaviour using isothermal oxidation tests that cover the whole range from pest, to intermediate to high temperature oxidation. The results of microstructural characterization using XRD, EPMA and TEM will be presented and discussed together with preliminary results of our oxidation studies.

#### 11:45 AM

Applicability of Mo(Si,Al)2-Base Oxidation Resistant Coating Onto Nb-Base Structural Materials: *Tatsuo Tabaru*<sup>1</sup>; Jin-Hak Kim<sup>1</sup>; Kazuhisa Shobu<sup>1</sup>; Michiru Sakamoto<sup>1</sup>; Hisatoshi Hirai<sup>1</sup>; Shuji Hanada<sup>2</sup>; <sup>1</sup>National Institute of Advanced Industrial Science and Technology, Inst. for Structural & Engrg. Matls., 807-1 Shuku, Tosu, Saga 841-0052 Japan; <sup>2</sup>Tohoku University, Inst. for Matls. Rsch., 2-1-1 Katahira, Aoba, Sendai, Miyagi 980-8577 Japan

Applicability of Mo(Si,Al)<sub>2</sub>-base oxidation resistant coating for Nb-base materials were investigated focusing on the oxidation resistance, thermal expansion behavior and interfacial stability with Nb. Mo(Si,Al)<sub>2</sub> with various substitution ratios of Al for Si exhibit a good oxidation resistance due to a protective alumina scale formation at temperatures up to 1673 K, and the parabolic rate constants are an order lower than that for NiAl. Average coefficients of thermal expansion (CTEs) between 298 and 1723 K are (9.2~10.5) x 10<sup>-6</sup> /K, while those for some Nb alloys are (8.2~8.7) x 10<sup>-6</sup> /K. The satisfactory oxidation resistance and small CTE mismatch with Nb suggest that Mo(Si,Al)<sub>2</sub> is a promising candidate for the oxidation resistant coating on Nb-base materials. Joining of Mo(Si,Al)<sub>2</sub> and Nb-base alloys, however, forms an diffusion-reaction layer consisting of Nb<sub>5</sub>Si<sub>3</sub> and Mo<sub>5</sub>Si<sub>3</sub>. Effect of an interlayer to suppress such reaction-layer formation is also described.

#### Bulk Metallic Glasses: Processing I

Sponsored by: Structural Materials Division, ASM International: Materials Science Critical Technology Sector, SMD-Mechanical Behavior of Materials-(Jt. ASM-MSCTS) Program Organizers: Peter K. Liaw, University of Tennessee,

Department of Materials Science and Engineering, Knoxville, TN 37996-2200 USA; Raymond A. Buchanan, University of Tennessee, Department of Materials Science and Engineering, Knoxville, TN 37996-2200 USA

Monday AM	Room: 209A
March 15, 2004	Location: Charlotte Convention Center

Session Chairs: Raymond A. Buchanan, University of Tennessee, Matls. Sci. & Engrg., Knoxville, TN 37996-2200 USA; Daniel Miracle, Air Force Research Laboratory, Matls. & Mfg. Direct., Wright-Patterson AFB, OH 45433 USA

#### 8:30 AM Invited

Principles for the Constitution, Structure and Stability of Metallic Glasses: Daniel Miracle<sup>1</sup>; Oleg Senkov<sup>2</sup>; Stephane Gorsse<sup>3</sup>; Wynn S. Sanders<sup>1</sup>; Kevin Kendig<sup>1</sup>; <sup>1</sup>Air Force Research Laboratory, Matls. & Mfg. Direct., 2230 Tenth St., Wright-Patterson AFB, OH 45433 USA; <sup>2</sup>UES, Inc., 4401 Dayton-Xenia Rd., Dayton, OH USA; <sup>3</sup>University of Bordeaux, ICMCB, Bordeaux France

The current understanding of the stability of metallic glasses relies heavily upon empirical ideas such as electron-to-atom ratio and the number of constituents, or upon isolated models based on features such as atom size, enthalpy of mixing, or reduced glass transition temperature. There is at present no clear rationale for determining the relative importance of these models, or for providing a credible link between these separate concepts. The objective of this presentation will be to highlight recent developments in the understanding of principles that influence the constitution, structure and stability of metallic glasses, and to describe an approach to unify these ideas into a single conceptual framework. Modification of an earlier model based on atomic level lattice strains will be combined with the more recent principle of efficient atomic packing to provide specific insight into the composition and local atomic structure of metallic glasses. Although earlier efforts to relate thermodynamic quantities to glass formability via simple relationships have been shown to be inadequate, a new methodology will be developed that provides a direct quantitative link between traditional thermodynamic quantities and atomic size. Together, the principles of atomic level strains, efficient atomic packing and thermodynamic modeling will be shown to provide a unified framework to more clearly understand the constitution, structure and stability of metallic glasses.

#### 8:55 AM Invited

A Guide to Optimum Compositions for Bulk Metallic Glass Formation: Z. P. Lu<sup>1</sup>; C. T. Liu<sup>1</sup>; 'Oak Ridge National Laboratory, Metals & Ceram. Div., Oak Ridge, TN 37831 USA

In the development of new bulk metallic glasses (BMGs) and other non-crystalline materials, it is vitally important for us to understand the nature of glass formation and know how to locate optimum compositions for glass formation. Considerable efforts have been devoted to this area; however, no reliable approaches have been developed to analyze the glass-forming ability (GFA) for various materials. In this study, a comprehensive expression to predict glass forming ability for various glass-forming systems,  $\lambda = T_x/(T_g+T_l)$ , has been derived from characteristic features of TTT (time-temperature-transformation) curves with considerations of all transformation kinetics, wherein  $T_{\star}$  is the crystallization temperature, Tg is the glass transition temperature and  $T_1$  is the liquidus temperature. This approach is not only verified by Fe-based glass-forming alloys developed recently but also strongly supported by the experimental data reported by other groups for various metallic glass systems. The current physical metallurgy approach will also help us attain a comprehensive understanding of the nature of glass formation from a basic science standpoint, and paves a new avenue in synthesizing novel bulk metallic glasses.

#### 9:20 AM

**Thermal Tempering of Bulk Metallic Glasses - I: Modeling:** *Cahit C. Aydiner*<sup>1</sup>; Ersan Ustundag<sup>1</sup>; <sup>1</sup>Caltech, Matls. Sci., MC 138-78, Pasadena, CA 91125 USA

Recently developed bulk metallic glasses (BMGs) possess exceptional glass formation ability and can be processed into large dimensions. This, however, can generate large residual stresses. The BMG processing typically involves casting an alloy into a thin-walled mold followed by severe quenching. This procedure leads to large thermal gradients due to the low thermal conductivity of BMG. In addition, the alloy experiences large changes in its viscosity within a small temperature range during glass transition. All of these parameters lead to 'thermal tempering' which generates compressive surface residual stresses balanced with mid-tension. We have modeled the development of these stresses using several approaches: (i) instant freezing model; (ii) viscoelastic model; and (iii) structural model. The results show that significant surface residual stresses approaching several hundred MPa can be generated in typical BMG specimens. The predictions of these models will be compared with each other and with experimental data.

#### 9:45 AM

Thermal Tempering of Bulk Metallic Glasses - II: Residual Stress Measurements: Cahit C. Aydiner<sup>1</sup>; Ersan Ustundag<sup>1</sup>; <sup>1</sup>Caltech, Matls. Sci., MC 138-78, Pasadena, CA 91125 USA

Bulk metallic glasses (BMGs) can be processed into large dimensions by casting into a thin-walled mold followed by severe quenching. This procedure leads to large thermal gradients due to the low thermal conductivity of BMG. In addition, the alloy experiences large changes in its viscosity within a small temperature range during glass transition. All of these lead to 'thermal tempering' which generates compressive surface residual stresses balanced with mid-tension. Since neither photoelasticity nor diffraction can be applied to BMGs, we employed a mechanical relaxation method, the crack compliance (slitting) technique which yielded excellent accuracy and spatial resolution. It will be shown that surface compression in excess of 300 MPa can be generated in BMGs under certain processing conditions. Then, results from bending experiments will be discussed about the effects of such high residual stresses on the mechanical properties of BMGs. The results will also be compared to modeling predictions.

#### 10:10 AM

Stability of Ni-Based Bulk Metallic Glasses: *Michelle L. Tokarz*<sup>1</sup>; Scott Speakman<sup>2</sup>; E. Andrew Payzant<sup>2</sup>; Wallace Porter<sup>2</sup>; John C. Bilello<sup>1</sup>; <sup>1</sup>University of Michigan, Matls. Sci. & Engrg., 3062 H H Dow Bldg., Ann Arbor, MI 48109 USA; <sup>2</sup>Oak Ridge National Laboratory, High Temp. Matls. Lab., PO Box 2008, MS6064, Oak Ridge, TN 37831-6064 USA

Ni-based bulk metallic glasses of varying concentrations were studied in order to understand their stability at elevated temperatures. The x-ray scattering patterns of several of these metallic glasses showed evidence of intermediate range order, which is atypical. This study explores the connection between this order and the subsequent phase transformations that occur at elevated temperatures. DSC scans provided glass transition temperatures, which were used as a reference. A number of x-ray diffraction patterns were obtained at constant temperatures below Tg, (for times from 5 to 36 hours). These showed the appearance and growth of crystalline peaks. Additionally, the characteristics of the amorphous scattering signal changes, during an isothermal hold, were tracked. Further experiments were performed on polished samples to distinguish any potential surface effects. Finally, these data are compared to those obtained from Vitreloy-106 (a well characterized traditional bulk metallic glass) such that differences can be identified and understood.

#### 10:35 AM

Glass Forming Ability and Thermal Stability of a Ti Containing Zr-Based Bulk Amorphous Alloy: Jun Shen<sup>1</sup>; <sup>1</sup>University of Sydney, CAMT, Sch. of Aeros., Mech. & Mechatronic Engrg., Sydney, NSW 2006 Australia

The apparent activation energies for crystallization of bulk Zr59Cu18Ni13A110 and Zr56.6Cu17.3Ni12.5Al9.6Ti4 alloys are Ec??295.6kJ/mol and Ec??248.5kJ/mol?Crespectively. The crystallization kinetics of bulk Zr56.6Cu17.3Ni12.5Al9.6Ti4 amorphous alloy is composed of two stages, in each stage the Avrami exponent is around 1.0?'2.5, indicating that the crystallization is controlled by limit nucleation and steady growth process. While the activation energy for nucleation and growth for bulk Zr56.6Cu17.3Ni12.5Al9.6Ti4 alloy are 364.8kJ/mol and254.6kJ/mol, respectively. It can be therefore concluded that the addition of Ti to bulk Zr-Cu-Ni-Al amorphous alloy has a role of suppressing the nucleation process on one hand, which is in favor of promoting GFA. On the other hand, the crystallization process is accelerated by Ti addition and consequently resulting in lowering of the stability of the amorphous phase.

#### 11:00 AM

The Thermal Stability of Zr-Cu-Ni-Ti-Be-Y Bulk Metallic Glasses: *Chun Huei Tsau*<sup>1</sup>; <sup>1</sup>Chinese Culture University, Inst. of Matls. Sci. & Mfg., 1, No, 55 Hwa Kang Rd., Yang Ming Shan, Taipei Taiwan

Five compositions of Zr-Cu-Ni-Ti-Be-Y amorphous alloys with 3 mm in thickness were made by arc-melting and die-casting processes. The thermal properties and mechanical properties of these alloys were examined and calculated their transformation temperature and activation energies. Results revealed that the increasing of content of Be could increase both of the Tx and ?'T (?'T=Tx-Tg). These exhibited that increasing the content of Be resulted in increasing the glass formability of the alloys in the present study. The hardness of these alloys at amorphous and crystallizing states was about 500 DPH and 450DPH, respectively. Compositions had no significantly effect on the hardness of these alloys. In addition, the alloys with the content of Be more than 20 at.% would crystallize while they annealed at elevated temperature for several hours, even though the annealing temperature was below the Tx point.

#### 11:25 AM Invited

Mg-Based Bulk Metallic Glass Composites with Plasticity and High Strength: Jian Xu<sup>1</sup>; Han Ma<sup>1</sup>; Evan Ma<sup>2</sup>; <sup>1</sup>Chinese Academy of Sciences, Inst. of Metal Rsch., Shenyang Natl. Lab. for Matls. Sci., 72 Wenhua Rd., Shenyang, Liaoning 110016 China; <sup>2</sup>Johns Hopkins University, Dept. of Matls. Sci. & Engrg., Baltimore, MD 21218 USA

Composite alloys of  $(Mg_{0.65}Cu_{0.075}Ni_{0.075}Zn_{0.05}Ag_{0.05}Y_{0.1})_{100-x}Fe_x(x=9,13)$ have been produced through copper mold casting, based on a good bulk metallic glass former and a new composite design scheme. Upon cooling the melt, an  $\alpha$ -Fe solid solution precipitates uniformly with sizes in the 1 to 8  $\mu$ m range while the remaining melt undergoes a glass transition to yield the in situ composite. Compressive strength of the composite approaches 1 GPa, a factor of 1.6 higher than the single-phase metallic glass. In contrast to all the previous Mg-based monolithic glasses that always fail in the elastic regime, a plastic strain to failure of the order of 1% was obtained for the composite. We used a new BMG composite design scheme that takes advantage of the immiscibility of the components. It is the first time that the very brittle Mgbased BMGs have ever exhibited usable plasticity.

## Carbon Technology: Cathode Material and Corrosion

Sponsored by: Light Metals Division, LMD-Aluminum Committee Program Organizers: Markus Meier, R&D Carbon, Sierre CH 3960 Switzerland; Amir A. Mirchi, Alcan Inc., Arvida Research and Development Centre, Jonquiere, QC G7S 4K8 Canada; Alton T. Tabereaux, Alcoa Inc., Process Technology, Muscle Shoals, AL 35661 USA

Monday AM	Room: 213A
March 15, 2004	Location: Charlotte Convention Center

Session Chair: Stefan A. Vogt, Alcoa Aluminio Espanol, San Ciprian (Lugo) 27890 Spain

#### NOTE: Session begins at 10:20 AM

10:20 AM

<sup>3-</sup>D Modelling of Thermal and Sodium Expansion in Soderberg Aluminium Reduction Cells: Yang Sun<sup>1</sup>; Karl G. Forslund<sup>2</sup>; Morten

**MONDAY AM** 

Sørlie<sup>3</sup>; Harald Oye<sup>1</sup>; <sup>1</sup>Norwegian University of Science and Technology, Dept. of Matls. Tech., Trondheim 7491 Norway; <sup>2</sup>Elkem Aluminium ANS Lista, PO Box 128, Farsund N-4551 Norway; <sup>3</sup>ELKEM ASA Aluminium Research, PO Box 8040, Vagsbygd 4675 Norway

A three dimensional transient mathematical model of a Soderberg aluminium reduction cell was developed to study cathode changes during heat up and early operation by using the ANSYS program. In this nonlinear finite element model, material non-linearity and the influence of temperature on the material's mechanical properties were taken into account. First thermal field distribution and sodium concentration distribution in the cathode carbon block with time were calculated, and then the stress distribution and deformation were calculated and analyzed. Points where the construction should be strengthened and area of high stress are pointed out. It is also shown that thermal excursions and sodium expansion can cause a gap under the cathode carbon block, allowing bath to fill the void and reacting with the refractory to crystalline compounds, result in a push-up of the cathode carbon block that may result in a permanent bottom heave over time.

#### 10:45 AM

Cathode Quality Improvement by Application of an Intensive Homogenizer for Green Mix Preparation: Frank Hiltmann<sup>1</sup>; Johann Daimer<sup>1</sup>; Berthold Hohl<sup>2</sup>; Roman Nowak<sup>3</sup>; Janusz Tomala<sup>3</sup>; <sup>1</sup>SGL Carbon GmbH, Griesheim Plant, Frankfurt 65933 Germany; <sup>2</sup>Maschinenfabrik Gustav Eirich, Hardheim 74732 Germany; <sup>3</sup>ZEW S.A., a member of SGL Carbon Group, Raciborz 47-400 Poland

As a part of the continuous quality improvement program of SGL CARBON's Racibórz facility, the process unit steps in the green shop were analysed and a potential for further process efficiency and product homogeneity improvement attributed to the existing green mix buffer silo. ZEW has successfully commissioned a batchwise-operated EIRICH mixer DW 29/4 as a homogenizer, downstream of the existing sigma-blade kneading mixers. As the homogenizer allows to control feeding of the vibrocompacting mould as well, the existing intermediate silo could be replaced. After an installation period of only four weeks, the redesigned paste mixing line came into operation. Compared to the original situation, the green plant now shows a significantly better performance in terms of stability of green production process and product characteristics. This paper presents the technical solution and the operational results before and after the start-up of the new equipment.

#### 11:10 AM

**Erosion Rate Testing of Graphite Cathode Materials**: *Siegfried Wilkening*<sup>1</sup>; Pierre Reny<sup>2</sup>; <sup>1</sup>Hydro Aluminium T & P, PO Box 2468, Bonn 53014 Germany; <sup>2</sup>Aluminery Alouette Inc., Case postale 1650, Sept Iles (Quebec) G4R5M9 Canada

The operational advantages of graphite cathode blocks in highamperage aluminium reduction cells are accompanied by an increased and uneven wear phenomenon. By means of a laboratory testing method it could be shown that the graphite erosion rate depends on the AIF3 content of the electrolytic melt and the current density. A decrease in the erosion rate can be achieved by the intercalation of durable and densifying coke residues from pitch and resin impregnation in the open pore structure of the graphite blocks. The deposition of some finely dispersed TiO2 in the graphite pores reduces the erosion rate significantly.

#### 11:35 AM

Variable Resistivity Cathode Against Graphite Erosion: Jean Michel Dreyfus<sup>1</sup>; Loig Rivoaland<sup>1</sup>; Serge Lacroix<sup>1</sup>; <sup>1</sup>Carbone Savoie-LRE, BP 16, Venissieux Cedex 69631 France

Pre-baked electrolysis cells equipped with graphite cathodes exhibit a reduction in lifetime compared to cells built with graphitic grades. This limitation is clearly related today to a wear mechanism induced by an electrochemical reaction. The importance of the current density peak on the wear celerity has been highlighted and led to the development of new concepts aimed at a better balance of the current density in the cell. The variable resistivity graphite cathode is one of the most promising ways, which can be offered by the cathode supplier. The actual technology development, resistivity pattern, current peak balance and erosion rate improvements are discussed through simulation models, products properties and in situ erosion measurements.

#### Cast Shop Technology: Melting and Refractories

Sponsored by: Light Metals Division, LMD-Aluminum Committee Program Organizers: Corleen Chesonis, Alcoa Inc., Alcoa Technical Center, Alcoa Center, PA 15069 USA; Jean-Pierre Martin, Aluminum Technologies Centre, c/o Industrial Materials Institute, Boucherville, QC J4B 6Y4 Canada; Alton T. Tabereaux, Alcoa Inc., Process Technology, Muscle Shoals, AL 35661 USA

Monday AM	Room: 213B/C
March 15, 2004	Location: Charlotte Convention Center

*Session Chairs:* Pierre Proulx, Universite de Sherbrooke, Chem. Engrg., Sherbrooke, Quebec J1K 2R1 Canada; Chris Bickert, Pechiney Group, Neuilly Sur Seine 92200 France

#### NOTE: Session begins at 8:55 AM

#### 8:55 AM

Energy Efficiency Tests in Aluminum Combination Melting and Holding Furnaces: Cynthia K. Belt<sup>1</sup>; <sup>1</sup>Commonwealth Aluminum, 7319 Newport Rd. SE, Uhrichsville, OH 44683 USA

Natural gas efficiency is extremely important in reverbatory furnaces. Most efforts are made to reduce gas usage in pure melting furnaces while holding and combination furnaces have been largely ignored. Tests were run during production to improve the energy efficiency of the aluminum combination melting and holding furnaces located at the Newport facility of Commonwealth Aluminum. These tests included idle modes, reduced excess air, reduced fire rate, reduced flue temperature, pilot relight burners, and reduced flue size. The variables stressed are less expensive process, control, and equipment changes that can be easily cost justified. The testing ran for over two years. Results of these real-world tests will be discussed.

#### 9:20 AM

**Corrosion Kinetics of Refractory by Molten Aluminium**: Jingguo Gao<sup>1</sup>; Saïed Afshar<sup>1</sup>; *Claude Allaire*<sup>1</sup>; <sup>1</sup>Ecole Polytechnique of Montreal, 8475 Christophe Colomb St., Montreal, Quebec H2M 2N9 Canada

Alumino-silicate refractories for aluminum cast-house applications are exposed to severe corrosion conditions in service. This research work was performed with a new set of samples issued from an improved formulation technique. To predict the service life of refractory material and to improve the properties, the corrosion kinetics of aluminosilicate materials was first studied under static conditions in Al-5wt.%Mg. It is suggested that the silica content inside refractories has little influence on the incubation time prior to the chemical attack. The latter appeared to be controlled by diffusion process. To verify the dynamic solicitation influence on the corrosion, special cylinder shape alumino-silicate refractory castables were submitted to the same above alloy, under both static and dynamic testing conditions. These tests were performed under protective gas such as argon or nitrogen.

#### 9:45 AM

High Temperature Confinement Composite Refractories: Jean-Benoît Pineault<sup>2</sup>; Claude Allaire<sup>1</sup>; <sup>1</sup>Ecole Polytechnique of Montreal, 8475 Christophe Colomb Rd., Montreal, Quebec H2M 2N9 Canada; <sup>2</sup>Groupe Refraco Inc., 1207 Antonio-Lemaire, Chicoutimi, Quebec G7K 1J2 Canada

In many high temperature industrial applications, such as primary aluminum treatment furnaces and launders, composite refractories with varying properties between their hot and cold faces would be beneficial. Such composites with varying mechanical, thermal and chemical properties along their thickness have recently been developed according to an improved technique. Examples of such materials as well as their properties are presented in this paper.

#### 10:10 AM Break

#### 10:45 AM

Room and High Temperature Measurement of the Elastic Properties of Refractories Using a New Apparatus and Set-Up: Claude Allaire<sup>1</sup>; *Jonathan Allaire*<sup>1</sup>; Alain Carbonneau<sup>1</sup>; <sup>1</sup>Ecole Polytechnique of Montreal, 8475 Christophe Colomb St., Montreal, Quebec H2M 2N9 Canada

Knowing the elastic properties of materials is of prime importance. These properties do not only reflect the extent of bonding in the material, but also permit to characterize its behavior under stress. For refractories, the measurement of such properties may be difficult due to their heterogeneous nature. This paper presents a new apparatus and set-up allowing the measurement of the Elastic and Shear Modulus, as well as the Poisson's ratio of refractories, at room and high temperature, according to a non destructive acoustic technique. Examples of results obtained from different types of refractory castables, suitable for the lining of aluminum treatment furnaces and/ or launders, are presented. The effects of the material pre-firing temperature and composition, as well as the sample's dimensions are discussed. Finally, the results obtained at room temperature with the new apparatus and set-up are compared to those obtained using the Grindo Sonic apparatus, as a reference.

## 11:10 AM

Refractories for Aluminium Melting and Holding Furnaces: The Importance of Materials Testing: Marcel Hogenboom<sup>1</sup>; Marcel Spreij<sup>1</sup>; <sup>1</sup>Corus Research Development & Technology, Ceram. Rsch. Ctr., PO Box 10.000, IJmuiden 1970 CA The Netherlands

Refractory lining lifetime of melting and holding furnaces and downtime due to refractory re-linings, are important parameters for increasing the aluminium output of casthouses and decreasing costs. When optimising the refractory linings to value for money, performance and downtime, testing of refractory materials plays an important role. Since process installation are not devised for revealing information on refractory performance, laboratory testing is essential. Failure risk can be decreased significantly by using relevant laboratory testing as a basis for materials selection. The importance of refractory materials testing is illustrated by examples of improvements made in refractory lining concepts, introduction of alternative materials, quality control and evaluation of new developments.

#### 11:35 AM

Effect of Corrosion by Molten Al-5wt%Mg on Mechanical and Physical Properties of Aluminosilicate Refractories: N. Ntakaburimvo<sup>1</sup>; *Claude Allaire*<sup>1</sup>; <sup>1</sup>Ecole Polytechnique of Montreal, 8475 Christophe Colomb St., Montreal, Quebec H2M 2N9 Canada

In addition to refractory corrosion classification based on the traditional criteria which are depth penetration, discoloration aspect and/ or cracking and friability level, the present work focussed on the aluminosilicate refractories properties modification due to corrosion by molten Al-5% Mg alloy. After corrosion, samples were cooled inside the furnace to avoid the effect of thermal shock on residual properties. The measured material properties before and after corrosion were the strength, the elastic modulus, the apparent porosity, as well as the apparent and bulk density. The material strength was measured at room temperature and at 900°C for both cases. The obtained results showed that the residual mechanical properties are much more improved in case of most corroded materials. However, the residual hot modulus of rupture was reduced in the case of two castables, and this may be attributed to the nature of formed phases during corrosion process. Considering together the overall tested materials, the relative porosity was reduced within 21% to 38%, while the relative bulk density was increased by 5% to 9%. This suggests the necessity of the combination of the traditional experimental refractory corrosion resistance criteria and the measurement of the material's strength after corrosion in its nearly service conditions.

# CFD Modeling and Simulation of Engineering Processes: Advanced Casting and Solidification Processes I

Sponsored by: Materials Processing & Manufacturing Division, ASM/MSCTS-Materials & Processing, MPMD/EPD-Process Modeling Analysis & Control Committee, MPMD-Solidification Committee, MPMD-Computational Materials Science & Engineering-(Jt. ASM-MSCTS)

*Program Organizers:* Laurentiu Nastac, Concurrent Technologies Corporation, Pittsburgh, PA 15219-1819 USA; Shekhar Bhansali, University of South Florida, Electrical Engineering, Tampa, FL 33620 USA; Adrian Vasile Catalina, BAE Systems, SD46 NASA-MSFC, Huntsville, AL 35812 USA

 Monday AM
 Room: 206A

 March 15, 2004
 Location: Charlotte Convention Center

*Session Chairs:* Laurentiu Nastac, Concurrent Technologies Corporation, Pittsburgh, PA 15219-1819 USA; Andreas Ludwig, University of Leoben, Dept. of Ferrous Metall., Leoben A-8700 Austria

8:30 AM Opening Remarks - Laurentiu Nastac

#### 8:35 AM Invited

Programs and Opportunities at ATP Focusing on Modeling and Simulation of Engineering Processes: *Dilip Kumar Banerjee*<sup>1</sup>; <sup>1</sup>National Institute of Standards and Technology (NIST), Advd. Tech. Prog. (ATP), 100 Bureau Dr., MS 4730, Gaithersburg, MD 20899-4730 USA

This paper will discuss ATP's contribution over the last decade to the development and use of process modeling as a tool to address some of the challenges faced by the US metal casting industries. Particular attention will be given to highlight how process modeling can be used to improve the manufacturability of components needed for high performance and critical applications. The challenges associated with the design and production of thin walled cast parts with intricate and complex internal geometries will be discussed. Modeling issues associated with the control of the final grain structure in the solidified parts will also be addressed. This paper will discuss the advantages of using appropriate mathematical models for designing new alloys for use in various applications. Finally, the author would discuss the role of ATP over the last decade in uplifting the US technological base by forming useful partnership with various industries to fund high-risk research in order to bring to market new and improved products for the broader benefit of the nation.

#### 9:10 AM Invited

A 3D-FEM Solver for Non-Steady State Navier-Stokes Equations With Free Surface: Application to Mold Filling Simulation in Casting Processes: *Michel Bellet*<sup>1</sup>; Estelle Saez<sup>1</sup>; Olivier Jaouen<sup>2</sup>; Thierry Coupez<sup>1</sup>; <sup>1</sup>Ecole des Mines de Paris, CEMEF, BP 207, Sophia Antipolis F-06904 France; <sup>2</sup>Transvalor S.A., 694 Ave. du Dr. Maurice Donat, Mougins F-06255 France

The paper presents a 3D finite element solver for non steady state fluid flow. The thermomechanical simulation package REM3D® has been initially developed to model Stokes-flow for polymer injection. The mechanical module is based on a Eulerian velocity-pressure formulation. The spatial discretization uses P1+/P1 tetrahedral elements. The front tracking module consists of the resolution of a transport equation, thanks to an original space-time discontinuous Galerkin formulation. It includes mesh adaptation, which permits a dynamic refinement at the fluid interface, thus controling the numerical diffusion. The same approach is used to solve heat transfer. In this paper, we focus on the specific adaptations done to treat Navier-Stokes flow in casting. The treatment of inertia terms is detailed, as well as the implementation of sliding conditions at mould surface, using conservative normals. Validation examples and application to industrial mold filling cases are presented.

#### 9:40 AM Invited

Application of CFD Technique for Modeling of Globular Equiaxed Solidification in Binary and Decomposition in Monotectic Alloys: Andreas Ludwig<sup>1</sup>; Menghuai Wu<sup>1</sup>; <sup>1</sup>University of Leoben, Dept. of Metall., Franz-Josef-Str. 18, Leoben Austria

Phase separation is frequently occurring during solidification accompanied by phenomena like melt convection, sedimentation or with two liquids Marangoni driven motion. In order to describe these phase separation phenomena a two-phase volume averaging model was designed specially for globular equiaxed solidification of binary alloys and decomposition and solidification of hyper-monotectic alloys. The model considers nucleation and growth of equiaxed grains or second phase droplets, motion and sedimentation of grains or droplet, feeding flow and solute transport by diffusion and convection. It allows the prediction of macrosegregations and the distributions of grain size or droplet size. Evaluations were made by comparing the predictions gained with simulation with experimental results. For example it is shown that the numerically predicted grain size distribution in a plate casting (Al-4wt%Cu) agrees reasonably well with the experimental analyses.

# 10:10 AM Break

#### 10:30 AM

Melt Flow and its Effect on Interface Curvature in a Horizontal Unidirectional Solidification System: *Taiming Guo*<sup>1</sup>; Hongmin Li<sup>1</sup>; M. J. Braun<sup>1</sup>; G-X. Wang<sup>1</sup>; <sup>1</sup>The University of Akron, Dept. of Mech. Engrg., Akron, OH 44325-3903 USA

This paper presents an experimental and numerical investigation on natural convection and melt flow near the solid/liquid interface during horizontal unidirectional solidification. In particular, the analysis is focusing on the melt flow near the solid/liquid interface under various channel heights (H) and temperature differences across the hot and cold ends (DT) of the samples and their effects on the interface shape. One horizontal unidirectional solidification system with succinonitrile is constructed so that interface shape and melt flow near the interface can be observed from the top through the microscope and from the side through the telescope at the same time. Experiments on samples with channel height of 1, 3.2 and 5 mm, respectively, have been conducted under various temperature differences across the hot and cold ends. The fluid velocity and interface shape are then quantified. Experimental observations show that the interface shape is significantly influenced by the channel height and temperature difference, both of which strongly affect the melt flow near the interface. Curved interfaces are observed for large channel height and high temperature difference, while an almost flat vertical interface is observed when the channel height is pretty small. A two-dimensional numerical simulation has been performed using the commercial CFD package, Fluent. The enthalpy-porosity solidification model is used to track the phase change between the liquid and solid. The effects of channel height and temperature difference on interface shape and melt flow are analyzed through variation of Rayleigh number (RaH). Good agreements between the numerical predictions and the experimental measurements have been achieved.

# 11:00 AM

**Directional Solidification of a Silicon Ingot: Modeling and Experimental Validation**: *Harald Laux*<sup>1</sup>; <sup>1</sup>SINTEF Materials Technology, Flow Tech., Alfred Getz vei 2, Trondheim 7465 Norway

The industrial production of wafers for solar cells is mostly based on multi-crystalline silicon produced by directional solidification in specialized furnaces. Today there is still room for considerable improvements of the quality of cast ingots, and small improvements may already result in large cost reductions for the final product. One means of improving the average ingot quality is to optimize solidification and furnace operation parameters. In this respect controlled experiments and process simulation by means of CFD will help to understand the fundamentals of the process and to improve it accordingly. This work presents first results of the modeling activities in a five-year research programme. Among others, one goal of the programme is to develop and validate a mathematical model that can simulate industrial furnaces for production of silicon ingots and that is complex enough to assess the final ingot quality from the CFD results for a given set of solidification and furnace operation parameters. At this early stage the process will be simulated using a standard enthalpyporosity method, and the CFD results will be validated against temperature measurements in controlled in-house experiments. The evolution of the temperature distribution in the furnace, the solidification front and residual stresses will be computed with the model. The validation will show if the chosen model is sufficient accurate and useful for future extension to model also the distribution of solutes and the precipitation of particle phases.

# 11:30 AM

Numerical Calculation of the Drag Force Acting on a Solid Particle Pushed by a Solid/Liquid Interface: Adrian Vasile Catalina<sup>1</sup>; Doru Michael Stefanescu<sup>2</sup>; Subhayu Sen<sup>1</sup>; <sup>1</sup>BAE SYSTEMS Analytical Solutions, SD46 NASA Marshall Space Flight Ctr., Huntsville, AL 35812 USA; <sup>2</sup>University of Alabama, Metallurgl. & Matls. Engrg., Tuscaloosa, AL 35487 USA

The distribution of insoluble particles in metal castings depends on the interaction of the particles with the advancing solid/liquid (SL) interface. The balance of the forces acting on a particle determines whether it is engulfed or pushed by the solidification front. An important component of this force balance is the drag force, FD, generated by the particle motion in front of the SL interface. Previous mathematical models for particle/interface interaction made use of steadystate solutions of FD provided by the lubrication theory. However, as recently demonstrated by both theoretical and experimental work, a dynamic analysis of the process is more appropriate. In this paper we report a numerical investigation on FD acting on a spherical particle undergoing an accelerated motion in front of SL interface. We account for a non-planar interface due to the particle/liquid thermal conductivity mismatch and assume a microgravity environment to eliminate the influence of natural convection.

# Challenges in Advanced Thin Films: Microstructures, Interfaces, and Reactions: Advances in Photonic and Optoelectronic Materials and Processes

Sponsored by: Electronic, Magnetic & Photonic Materials Division, EMPMD-Thin Films & Interfaces Committee *Program Organizers:* N. M. (Ravi) Ravindra, New Jersey Institute of Technology, Department of Physics, Newark, NJ 07102 USA; Seung H. Kang, Agere Systems, Device and Module R&D, Allentown, PA 18109 USA; Choong-Un Kim, University of Texas, Materials Science and Engineering, Arlington, TX 76019 USA; Jud Ready, Georgia Tech Research Institute - EOEML, Atlanta, GA 30332-0826 USA; Anis Zribi, General Electric Global Research Center, Niskayuna, NY 12309 USA

Monday AM	Room: 218B
March 15, 2004	Location: Charlotte Convention Center

Session Chairs: Anis Zribi, General Electric, Global Rsch. Ctr., Niskayuna, NY 12309 USA; Seung H. Kang, Agere Systems, IC Device Tech., Allentown, PA 18109 USA; N. M. (Ravi) Ravindra, New Jersey Institute of Technology, Dept. of Physics, Newark, NJ 07102 USA

# 8:30 AM Opening Remarks by Ravindra et al.

# 8:40 AM Invited

Photonic Crystals and Nano-Plasmonics: Enabling New Technology Through Materials Engineering: Matthew C. Nielsen<sup>1</sup>; Xiaolei Shi<sup>1</sup>; Ivan Celanovic<sup>1</sup>; Min-Yi Shih<sup>1</sup>; <sup>1</sup>General Electric, Global Rsch. Ctr., Niskayuna, NY 12309 USA

Data storage and transmission fuels many aspects of the world's economy. For example, 75% of IT spending in 2003 for large corporations is expected to be on data storage. In this paper, novel material structures will be presented that could dramatically change the way light interacts with materials, effecting how we store and transport data. Recent advances being made in the area of photonic crystals will first be presented. By building materials with a highly ordered structure, it is possible to create optical bands. Use of the band structure has been demonstrated for optical waveguides, filters, and lighting applications. While the promise exists for radical innovations in optical devices using the photonic crystals, we will present some of their limitations, mainly arising from current manufacturing processes. Another exciting area of photonics and materials research is nanoplasmonics. We will also describe how the interaction of light with materials can be controlled with plasmonics on the nano-scale, mainly for applications in data storage.

# 9:05 AM Invited

**Optical Nanostructures**: *Gernot S. Pomrenke*<sup>1</sup>; <sup>1</sup>Air Force Office of Scientific Research, Arlington, VA USA

Advances in understanding fundamental physics and engineering on the nanoscale are viewed as critical to the development of next generation devices and systems. Progress in nanotechnology is enabled by the remarkable success in semiconductor materials growth, nanoscale patterning, device fabrication, polymers and coating technology. It is now possible to fabricate, literally atom-by-atom, semiconductor materials that do not exist in nature and with properties that are near ideal for application in electronics, optics and magnetics. Nanotechnology as applied to optoelectronics offers an area ripe with opportunities and challenges. In one area the convergence of nanotechnology, material processing, tools, and applications is driving the realization of integrated photonics and the all photonics chip. Part of this approach is photonic crystals. Building these crystals requires creating periodic structures from dielectric materials that repeat themselves exactly and at regular intervals. If the matrix is made precisely, the resulting structure may have a photonic bandgap (PBG), a range of forbidden frequencies within which a particular wavelength may be blocked, and the electromagnetic radiation is reflected. Photonic bandgap structures and the associated nanofabrication allows photonics to advance optoelectronic miniaturization, light localization, and highly integrated optical devices and components. Integrated 3-D photonic crystal structures form the basis for the fabrication of a photonic chip utilizing the important 1.5 micron wavelength associated with micro-photonic circuits, computers, optical interconnects, micronets, and communication systems.

# 9:30 AM

**Optical Properties of Novel Glasses**: *Sufian Abedrabbo*<sup>1</sup>; D. Arafah<sup>1</sup>; N. M. Ravindra<sup>2</sup>; <sup>1</sup>University of Jordan, Dept. of Physics, Amman 11942 Jordan; <sup>2</sup>New Jersey Institute of Technology, Dept. of Physics, Newark, NJ 07102 USA

Ion-exchange methods have been deployed to form glasses with desired optical properties. The objective of this study is to utilize these glasses for optics and optical communication applications. We will address, specifically, areas such as imaging diagnostics, charge-coupled devices and optical fibers.

#### 9:45 AM Break

# 10:00 AM Invited

GaN Device Performance Based on Thin Film/Substrate Interface for Heterojunction and Homojunction Structures: Danielle Merfeld<sup>1</sup>; <sup>1</sup>GE Global Research, 1 Rsch. Cir., Bldg. KW-C1325, Niskayuna, NY 12309 USA

GaN material has been the subject of intense research over the last decade due to it's unique properties, which are particularly beneficial in optoelectronic and high-power microwave applications. Thin film properties of epitaxially grown GaN and other III-N compounds are highly dependent on the interface at the substrate, and commonly a buffer layer is incorporated into the growth recipe to assist in optimizing the initial island growth conditions as well as to reduce defects brought on by the lattice mismatch between GaN and the substrate. An analysis of various optoelectonic and high-power microwave devices explore the dependence of device performance and reliability on interface properties as measured by various analytical techniques (eg. TEM, SEM, X-ray topography). A comparison between the various methods of reducing the dislocations in the epitaxial III-N films is explored, including growth on bulk GaN substrates. Lastly, the potential benefit of homoepitaxial structures on device performance is analyzed.

#### 10:25 AM

Radiative Properties of Wide Bandgap Materials: N. M. Ravindra<sup>1</sup>; Anthony T. Fiory<sup>1</sup>; <sup>1</sup>New Jersey Institute of Technology, Dept. of Physics, Newark, NJ 07102 USA

A spectral emissometer operating in the wavelength range of 1 to 20 microns and temperature range of 30 to 2000°C has been utilized to measure the reflectance, transmittance and emittance of AlN, Diamond Like Carbon, Erbium Oxide and Sapphire. Interpretation of the measured data has been sought from bandstructure calculations.

#### 10:40 AM

Cold Welding of Organic Light Emitting Devices: Modeling and Reliability: Y. Cao<sup>1</sup>; C. Kim<sup>2</sup>; S. Sethiaraj<sup>3</sup>; O. Akogwu<sup>1</sup>; S. Forrest<sup>2</sup>; *Winston O. Soboyejo*<sup>1</sup>; <sup>1</sup>Princeton University, MAE, D404 Engrg. Quad., Olden St., Princeton, NJ 08544 USA; <sup>2</sup>Princeton University, Dept. of Elect. Engrg., Princeton, NJ 08544 USA; <sup>3</sup>University of Botswana, Dept. of Physics, Gaborone, Botswana Africa

This paper presents the results of a combined experimental and computational study of cold welding. Numerical finite element methods are used to study the effects of dust particle size and holding time on cold welding. These utilize material property measurements that are obtained from nano-indentation experiments. An interfacial fracture mechanics approach is then used to characterize the reliability of Au/Au cold welds. The interfacial fracture toughness of such welds is shown to depend on mode mixity and welding parameters. The implications of the results are also discussed for the reliability testing of organic light emitting devices that are fabricated using cold welding techniques.

# 10:55 AM Invited

**Some Si Based Heterostructures for Optical Applications**: *Magnus Willander*<sup>1</sup>; <sup>1</sup>Chalmers University of Technology and Gothenburg University, Lab. of Phys. Elect. & Photonics, Physics & Engrg. Physics, Dept. of Physics & Engrg. Physics, SE-412 96, Gothenburg Sweden

In this invited talk we will present our research on the growth and characterization of Si based heterostructures for optical and photonic devices. The heterostructures to be included are thin films as well as low dimensional heterostructures. The performance and functionality extension of Si technology due to the development of such heterostructures will be presented and discussed. The heterostructures include strained as well as poly-crystalline-Si1-xGex in addition to ZnO nano-wires and thin films all grown on Si and SiO2 substrates. We will present our growth and characterization for both heterostructures. We will concentrate on structural and optical characterization results in connection to device properties. The structural characterization includes x-ray diffraction for assessment of the crystallinity and the

stress in the films as well as secondary ion mass spectrometery for chemical analysis. In addition, results using photoluminescence as an optical characterization tool will be shown. The device application of these then films includes detectors, lasers, and other light emitting devices. Some of the Si-based heteorstructures to be presented are to include devices emitting and detecting up to the blue-green and violet wave lengths.

#### 11:20 AM Invited

Light-Emitting Composite SiOx/Si Films Produced by Vacuum Evaporation: I. Z. Indutnyy<sup>1</sup>; I. P. Lisovskyy<sup>1</sup>; D. O. Mazunov<sup>1</sup>; *Galyna Yurivna Rudko*<sup>1</sup>; P. E. Shepelyavyj<sup>1</sup>; V. A. Dan'ko<sup>1</sup>; <sup>1</sup>NAS of Ukraine, Inst. of Semiconductor Physics, 41, Nauky prosp., Kyiv 03028 Ukraine

Silicon oxide films with nanocrystalline silicon inclusions are a perspective optoelectronic material compatible with integrated circuit technology. Among the variety of methods used for their production the vacuum thermal evaporation of silicon monoxide is a promising one due to high mechanical and chemical stability of the films and to possibility of large-area Si-based displays fabrication. SiOx/Si films were deposited by evaporating SiO (Cerac Inc.) of 99.9% purity in vacuum at the residual pressure of 2.10-3 Pa and annealed in argon atmosphere. The analysis of the content of Si<sup>-</sup>COy<sup>-</sup>CSi4<sup>-</sup>Cy(1  $\stackrel{.}{i}$ Ú y $\stackrel{.}{i}$ Ú 4) molecular complexes in the structural network of the SiOx matrix by infrared transmission showed that the films consist of SiO2 with Si inclusions surrounded by SiOx interface layers. The photoluminescence spectra exhibit a broad band that ranges from 600 nm to beyond 980 nm.

# 11:45 AM

**Modeling of Photovoltaic Devices Based on Organic Materials**: *Dejan Karabasevic*<sup>1</sup>; Rifat Ramovic<sup>2</sup>; <sup>1</sup>Copper Institute Bor, 19210 Bor Serbia; <sup>2</sup>Faculty of Electrical Engineering, 11000 Belgrade Serbia

Optoelectronic devices based on organic materials have made very rapid progress in the last several years. With field-effect mobility and current on/off ratio values comparable to amorphous silicon, organic optoelectronic devices will find use in broad area optoelectronics applications. Further improvements of devices performances are possible in several areas such as improving device reliability and uniformity and in developing low-cost fabrication processes. It is also important to develop accurate analytical/numerical models that can be used to simulate devices and circuits. While analytical models are useful in understanding basic device operation, numerical simulation is often essential to understand the subtrashold characteristics, and to be able to design more complicated device structures. In this paper analytical model for organic photovoltaic devices based on a model used for a silicon thin-film transistors (TFT's) is proposed. One of the main problems of describing charge transport in molecular system by a semiconductor device simulation tool is mobility which is taken to be an energy and temperature dependent parameter just like in silicon, with the understanding that the underlying physics of transport that gives rise to these mobilities is totally different. On base of this model, simulation was made for pentacene organic TFT, and some of results such as current on/off response and trashold voltage characteristics, when the device is carried into the light beam, are presented.

# Computational Thermodynamics and Phase Transformations: Grain Growth and Particle Coarsening

Sponsored by: ASM International: Materials Science Critical Technology Sector, Electronic, Magnetic & Photonic Materials Division, Materials Processing & Manufacturing Division, Structural Materials Division, MPMD-Computational Materials Science & Engineering-(Jt. ASM-MSCTS), EMPMD/SMD-Chemistry & Physics of Materials Committee

Program Organizer: Jeffrey J. Hoyt, Sandia National Laboratories, Materials & Process Modeling, Albuquerque, NM 87122 USA

Monday AM	Room:	202A		
March 15, 2004	Location	: Charlotte	e Convention	Center

Session Chair: TBA

#### 8:30 AM Invited

Asynchronous Parallelization of the n-Fold Way Algorithm for Simulation of Grain Growth in 2D: Anthony D. Rollett<sup>1</sup>; Priya A. Manohar<sup>1</sup>; <sup>1</sup>Carnegie Mellon University, Matls. Sci. & Engrg., 4315 Wean Hall, 5000 Forbes Ave., Pittsburgh, PA 15206 USA This work describes an implementation of the Potts model for simulation of grain growth in 2D on a distributed-memory parallel architecture. The simulation scheme utilizes continuous-time, asynchronous parallel version of the n-fold way algorithm. Each Processing Element (PE) carries a piece of the global simulation domain while the virtual topology of the PEs is in the form of a square grid in 2D and Torus in 3D. Different PEs have different local simulated times. Interprocessor communication is facilitated by the Message Passing Interface (MPI) routines. Sample results for grain growth simulation in 2D are presented for 840 x 840 global domain size distributed over 16 PEs. The grain growth kinetics obtained in the simulation of pure, isotropic systems demonstrates a close agreement with the analytical models. Grain size distribution obtained in the parallel simulation is well described by the expected lognormal distribution, thus validating the simulation procedure.

## 9:00 AM Invited

Grain Growth in Deformed Materials: Corbett C. Battaile<sup>1</sup>; <sup>1</sup>Sandia National Laboratories, Matls. & Process Modlg., PO Box 5800, MS 1411, Albuquerque, NM 87185-1411 USA

The thermomechanical processing of materials can induce deformation and modify microstructure. Both the deformation and the microstructure evolution affect the properties of the material, and are generally interdependent. Recrystallization from dislocation substructures can dramatically affect the microstructure, but whether or not recrystallization occurs, internal stresses and strains in a deformed material can drive grain boundaries to move abnormally. We will present coupled simulations of deformation and grain evolution in purelyelastic and elastic-plastic polycrystals. Finite element calculations provide the local mechanical state data necessary to model the spatially nonuniform interface pressures that drive grain boundary motion in a front tracking approach. The coupled simulation method will be described in detail, and results for elastic and plastic polycrystals presented. Particular attention will be paid to the role of nonuniform internal stresses in promoting irregular interface migration, and to the treatment of plastic deformation in an evolving microstructure.

#### 9:30 AM

Effect of Grain Boundaries on Spinodal Decomposition: Ramanarayan Hariharaputran<sup>1</sup>; Thennathur A. Abinandanan<sup>2</sup>; <sup>1</sup>Brown University, Div. of Engrg., Providence, RI 02906 USA; <sup>2</sup>Indian Institutute of Science, Dept. of Metall., Bangalore, Karnataka 560 012 India

Through our phase field study of polycrystalline alloys undergoing spinodal decomposition (SD), we describe a new grain boundary (GB) effect namely 'discontinuous SD'. Discontinuous SD is exhibited by systems in which both GB-enhanced atomic mobility and intrinsic GB mobility( $M_g$  and  $L_g$ , respectively) are high: transformation front is formed due to a fast decomposition along the GB.The migration of the transformation front results in alternating A-rich and B-rich lamellae behind the front. We formulate a phenomenological theory (for large ( $L_g / M_g$ ) regime) to explain the characteristics of front migration: lamellar spacing, front velocity and the degree of decomposition within the lamellae.

# 9:50 AM

Modeling Microstructure Evolution and Mechanical Properties of Alloys Based on First-Principles Energetics: *Jianwei Wang*<sup>1</sup>; Chris Wolverton<sup>2</sup>; Stefan Müller<sup>3</sup>; Zi-kui Liu<sup>1</sup>; Long-Qing Chen<sup>1</sup>; <sup>1</sup>Pennsylvania State University, Dept. of Matls. Sci. & Engrg., 106 Steidle Bldg., Univ. Park, State College, PA 16802 USA; <sup>2</sup>Ford Research Laboratory, MD 3028/SRL, Dearborn, MI 48121-2053 USA; <sup>3</sup>Universität Erlangen-Nürnberg, Lehrstuhl für Festkörperphysik, Staudtstrasse 7, Erlangen 91058 Germany

We demonstrate a coupling of state-of-the-art atomistic, statistical and continuum approaches aimed at predicting the microstructure evolution and mechanical properties of alloys. This integrated method includes (1) first-principles calculations of total energies of various configurations, (2) a mixed-space cluster expansion approach for the energetics of complex coherently constrained configurations, (3) a kinetic Monte Carlo technique, and (4) a mechanistic strengthening model. As a case study, first-principles total energies of Al-Cu configurations are fitted to a mixed-space cluster expansion, yielding an expression that can describe the energetics of complex ~250,000-atom coherently constrained configurations with the accuracy of first-principles calculations. Combining this expansion with a kinetic Monte Carlo approach as well as a strengthening model allows one to quantitatively predict the growth and coarsening kinetics of GP zones as well as the effect of the predicted GP zone morphologies on age hardening of Al-Cu alloys.

# 10:10 AM Break

# 10:20 AM Invited

Analysis and Application of a Subgrain Model for Strain-Free Grain Nucleation During Recrystallization: Elizabeth A. Holm<sup>1</sup>; Mark A. Miodownik<sup>2</sup>; <sup>1</sup>Sandia National Laboratories, Dept. 1834, PO Box 5800, MS 1411, Albuquerque, NM 87185-1411 USA; <sup>2</sup>King's College, Dept. of Mech. Engrg., Strand, London WC2R 2LS UK

During or after plastic deformation, dislocations may organize into compact structures such as cell walls in a process termed recovery. If sufficient stored energy remains, the material may recrystallize by nucleating and propagating dislocation-free grains. How a recovered dislocation structure generates growing, strain-free grains has been debated for decades. We suggest a subgrain growth model that incorporates subgrain topology, boundary distribution and boundary properties to predict a nucleation frequency and recrystallization texture. The nucleation event is the mobility-driven discontinuous growth of certain subgrains, and the crystallographic orientations of favored subgrains dictate the recrystallization texture. We test the model on subgrain structures in plastically deformed aluminum, obtaining excellent phenomenological agreement between the model and experiments. This nucleation model is also applied to larger-scale process models of recrystallization in steel and copper, which incorporate the nucleation model into a continuum mechanics framework.

# 10:50 AM Invited

Kinetics of 3-D Grain Growth: Martin E. Glicksman<sup>1</sup>; <sup>1</sup>Rensselaer Polytechnic Institute, Matls. Sci. & Engrg., CII-9111, 110 8th St., Troy, NY 12180-3590 USA

The kinetics of grain growth in 3-D isotropic polycrystals is predicted by representing grains with N neighbors, as "average N-hedra." Average N-hedra satisfy space-filling and thermodynamic equilibria at quadrajunctions and triple lines. The analysis, based on symmetry and space filling, yields growth laws for the volumetric and areal rates of change for grains as a function of N. The results extend to 3-D the half-century old von Neumann-Mullins topological grain growth law that provides the 'n - 6' relationship in 2-D. Analytic kinetic laws may prove useful for constructing more accurate kinetic models of grain growth, and help clarify several long-standing issues on microstructures. The availability of exact topological formulas could be used to provide benchmarks to test numerical simulations, to guide further quantitative experiments on network dynamics, and to assist in deriving important statistical measures for polycrystalline materials.

#### 11:20 AM

An Accurate Yet Simple von Neumann-Mullins Relation for Grain Growth in 3D: David T. Wu<sup>1</sup>; Carl E. Krill<sup>2</sup>; <sup>1</sup>Yale University, Dept. of Mech. Engrg., PO Box 208284, New Haven, CT 06520-8284 USA; <sup>2</sup>Universität des Saarlandes, FR 7.3 Technische Physik, Postfach 151150, Geb. 43, Saarbrücken D-66041 Germany

Von Neumann-Mullin's Law is central to our understanding of grain growth in 2D. Since the 1950's, efforts to extend this relation to 3D have been stymied by topological complexities. By treating the number of grain edges as the fundamental topological parameter characterizing a given grain, we have derived a simple statistical expression for the growth rate in any dimension. The exact result of von Neumann-Mullins is recovered in 2D, and excellent agreement is obtained with phase-field simulations in 3D.

#### 11:40 AM

Structure and Stability of Al-Mg-Si-(Cu) Precipitates: A First-Principles Study: Ravi Chinnappan<sup>1</sup>; Wolverton Christopher<sup>1</sup>; <sup>1</sup>Ford Motor Company, Phys. & Environml. Scis., Scientific Rsch. Lab., 2101 Village Rd., REC R, Rm. 1525, Dearborn, MI 48124 USA

Precipitation in Al-Mg-Si-(Cu) alloys has been extensively studied, since this quaternary forms the basis of a wide variety of commercial alloys (e.g., 6xxx series alloys). The observed precipitation sequence is complex and involves a wide variety of metastable phases (e.g., GP zones, beta", beta"). Calculations of metastable phase equilibria in these alloys are hampered by the lack of quantitative information on the thermodynamics of these precipitate phases. We have undertaken an extensive first-principles study of energetics of all the reported precipitate phases of Al-Mg-Si-(Cu) alloys, using both local density approximation (LDA) and generalized gradient approximation (GGA). Our calculations provide a clear and consistent picture of the energetics of the precipitate phases, and in certain cases, provide insight into the compositional changes of precipitates during aging. In addition to energetics, we also examine the relative volumes of the various phases, and find no significant deviations from that of the solid solution phases. Thus, we predict no significant dimensional stability issues should arise during aging of commercial Al-Mg-Si-(Cu) alloys. By combining our first-principles energetics with computational thermodynamics approaches, we provide predictions of metastable phase equilibriua and precipitate volume fractions in a variety of 6xxx series alloys.

# Cost-Affordable Titanium Symposium Dedicated to Prof. Harvey Flower: Overview and Innovative Processes

Sponsored by: Structural Materials Division, SMD-Titanium Committee

*Program Organizers:* M. Ashraf Imam, Naval Research Laboratory, Washington, DC 20375-5343 USA; Derek J. Fray, University of Cambridge, Department of Materials Science and Metallurgy, Cambridge CB2 3Q2 UK; F. H. (Sam) Froes, University of Idaho, Institute of Materials and Advanced Processes, Moscow, ID 83844-3026 USA

Monday AM	Room: 2	06B
March 15, 2004	Location:	Charlotte Convention Center

Session Chair: Derek J. Fray, University of Cambridge, Dept. of Matls. Sci. & Metall., Cambridge CB2 3Q2 UK

# 8:30 AM

**Cost Affordable Titanium** — Is it Possible?: *F. H. (Sam) Froes*<sup>1</sup>; M. Ashraf Imam<sup>2</sup>; Derek J. Fray<sup>3</sup>; <sup>1</sup>University of Idaho, Inst. for Matls. & Advd. Processes, McClure Bldg., Rm. 437, Moscow, ID 83844 USA; <sup>2</sup>Naval Research Laboratory, 4555 Overlook Ave. S.W., Washington, DC 20375-5343 USA; <sup>3</sup>University of Cambridge, Dept. of Matls. Sci. & Metall., Pembroke St., Cambridge CB2 3QZ UK

Titanium is the "wonder" metal, which makes sense as the material of choice for a wide variety of applications. However, because of its relatively high price - a result of extraction and processing costs - it is used basically only when it is the only choice with the caveat that titanium has a bright "image". This can lead to use even when the economics are unfavorable. This paper will overview the potential areas which are amenable to cost reduction for titanium products. This will emphasize all steps in component fabrication from extraction and processing to fabrication of final parts.

# 9:15 AM

Breakthrough Technologies in Titanium Refinement Methods: L. Christodoulou<sup>1</sup>; W. S. DeRosset<sup>2</sup>; J. Christodoulou<sup>3</sup>; P. L. Martin<sup>4</sup>; <sup>1</sup>DARPA/DSO, 3701 N. Fairfax Dr., Arlington, VA 22203 USA; <sup>2</sup>AMSRL-WM-MD, Aberdeen Proving Ground, MD 21005-5066 USA; <sup>3</sup>Office of Naval Research, Matls. Div., Code 332, 800 N. Quincy St., Arlington, VA 22217-5660 USA; <sup>4</sup>AFRL/MLLMD, Wright-Patterson AFB, OH 45433-7817 USA

Recent advances in novel processing approaches for the production of titanium metal have attracted worldwide interest. Affordable methods to replace the Kroll Process for the production of Ti sponge have been sought for decades. In the early 20th century, Al was transformed from a "precious metal" to a "commodity" through the development of an efficient electrochemical refinement process. If a similar breakthrough can be devised for Ti, it would find applications in many systems where specific properties are being recognized as enabling; for example advanced armored vehicles, corrosion resistant marine systems as well as the usual aerospace platforms. This presentation will provide an overview of the emerging chemical and moltensalt electrochemical methods being pursued under DARPA sponsorship. The objectives of these studies will be related to the potential benefits for structural applications in future defense systems.

#### 9:45 AM

#### Extraction of Titanium from Solid Titanium Dioxide in Molten Salts: Derek J. Fray<sup>1</sup>; George Z. Chen<sup>1</sup>; <sup>1</sup>University of Cambridge, Dept. of Matls. Sci. & Metall., Pembroke St., Cambridge CB2 3QZ UK

The search for a cheaper replacement of the Kroll Process has continued ever since titanium was first produced commercially. In 2000, the authors reported that it was possible to reduce titanium and other metal oxides directly to metals by making the oxide the cathode in a bath of molten calcium chloride. Since that time, our understanding of the process has increased and it has been found that it is possible to produce many alloys by the direct electro-deoxidation. This paper will review the understanding of the process and present the latest developments.

#### 10:15 AM

**Developing Applications for Titanium**: *F. H. (Sam) Froes*<sup>1</sup>; Oscar Yu<sup>2</sup>; Takashi Nishimura<sup>3</sup>; <sup>1</sup>University of Idaho, Inst. for Matls. &

Advd. Processes (IMAP), McClure Bldg., Rm. 437, Moscow, ID 83844 USA; <sup>2</sup>RMI Titanium Company, 1000 Warren Ave., Niles, OH 44446-0269 USA; <sup>3</sup>NTC Corporation, 4-15-11 Mikage-Ishimachi, Higashinada-Ku, Kobe 658-0045 Japan

One of the ways to make titanium products more cost affordable is to increase the number of applications for titanium. This paper will review near term and far term applications for titanium, with emphasis on activities in the USA and Japan; both parallel and contrasting efforts. Applications will include both expanding aerospace use and developing non-aerospace applications.

#### 10:45 AM

Economic Analysis of the Application of Emerging Reduction Technologies to Mill Products Production: Edwin H. Kraft<sup>1</sup>; <sup>1</sup>EHKTechnologies, 10917 SE Burlington Dr., Vancouver, WA 98664 USA

The search for lower cost manufacturing approaches has continued since the beginning of the titanium industry in the mid 20th century. Within the past few years, over a dozen new reduction technologies have emerged, with many proceeding to serious development. It is still unclear, however, whether many of these will be economically viable or actually provide product meeting technical requirements. These emerging reduction technologies will be briefly reviewed. Since commercial success would appear to require integration of such processes into the mill products production stream, the economics of current production and markets will be reviewed and analyzed. The Decisive Analysis methodology will then be applied to economic analysis of the production of mill products incorporating the new reduction processes. The methodology will be described and applied using assumed process routes, business factors and cost factor probability distributions. Resulting economic scenarios will be presented.

#### 11:15 AM

**P/M Titanium for Aeroengine Components**: *David Rugg*<sup>1</sup>; <sup>1</sup>Rolls Royce, Derby DE248BJ UK

The advent of new material production processes and improved control/prediction of powder consolidation offers the potential for reducing gas turbine life cycle costs. End user requirements in terms of product manufacture and certification will be reviewed with respect to requirements and potential for optimised raw material input morphology and cleanliness. Examples of components where nett shape or near nett shape technology could be applied will be reviewed along with current production and repair practice. This will include electrolytic deoxidation powder routes and metal addition processes for titanium alloys.

# Dislocations: Modeling and Simulation Fundamentals

Sponsored by: ASM International: Materials Science Critical Technology Sector, Electronic, Magnetic & Photonic Materials Division, Materials Processing & Manufacturing Division, Structural Materials Division, EMPMD/SMD-Chemistry & Physics of Materials Committee, MPMD-Computational Materials Science & Engineering-(Jt. ASM-MSCTS) *Program Organizers:* Elizabeth A. Holm, Sandia National Laboratories, Albuquerque, NM 87185-1411 USA; Richard A. LeSar, Los Alamos National Laboratory, Theoretical Division, Los Alamos, NM 87545 USA; Yunzhi Wang, The Ohio State University, Department of Materials Science and Engineering, Columbus, OH 43210 USA

Monday AM	Room:	201A		
March 15, 2004	Location	: Charlotte	Convention	Center

Session Chair: TBA

# 8:30 AM Invited

Level-Set Simulation of Dislocation Dynamics in the Presence of Particles: David J. Srolovitz<sup>1</sup>; Yang Xiang<sup>1</sup>; Li-Tien Cheng<sup>2</sup>; E. Weinan<sup>3</sup>; <sup>1</sup>Princeton University, Princeton Matls. Inst., 320 Bowen Hall, 70 Prospect Ave., Princeton, NJ 08540-5211 USA; <sup>2</sup>University of California, Dept. of Math., La Jolla, CA 92039 USA; <sup>3</sup>Princeton University, Dept. of Math., Princeton, NJ 08544 USA

We present a new method for modeling dislocation dynamics within a level-set framework. This method naturally accounts for dislocation topology change, glide and climb with arbitrary mobilities, cross-slip, and interactions with arbitrary microstructural elements. Examples applications include the expansion of dislocation loops by glide, climb and cross-slip, dislocation intersections, and the operation of a Freak-Read source. The method is applied to edges and screws bypassing arrays of particles (impenetrable or penetrable, misfitting or not) with a focus on understanding bypass mechanisms. In addition to classical particle cutting and the formation of Orowan loops, a wide variety of new bypass mechanisms are observed. Depending on dislocation type and the nature of the misfit, dislocation loops can be produced lying in the slip plane or perpendicular to it - in front of and/or behind the particle, on the sides of the particle, or around the particle (but orthogonal to an Orowan loop).

# 9:05 AM

# First Principles Evaluation of Re Solid-Solution Softening in BCC Mo: Christopher Woodward<sup>1</sup>; Satish Rao<sup>1</sup>; <sup>1</sup>Air Force Research Laboratory, Wright Patterson AFB, OH 45433-7817 USA

Solid solution softening observed in the group VA and group VIA transition metals has traditionally been attributed to either extrinsic or intrinsic effects. Extrinsic effects include the scavenging of interstitial impurities by substitutional solid-solutions while intrinsic effects assume a direct solute-dislocation interaction that lowers the Peierls barrier. We have applied first principles methods to evaluate possible intrinsic solid-solution-softening in the group VI BCC transition metals. First, we calculated the magnitude of size and modulus misfit parameters of several solid solutions in Mo as suggested by the work of Fleischer. Second, we calculated the change in the primary Peierls barrier when Re solid solutions are introduced along a straight a/ 2<111> screw dislocation in Mo. Here the local strain field associated with the dislocation core is self-consistently coupled to the long-range elastic field using the recently developed lattice Greens Function Boundary Condition method. The dislocation is contained in a very small simulation cell making it possible to directly simulate the solute-dislocation interaction. Results from these two methods will be contrasted and compared to available experimental results.

# 9:25 AM

Ab-Initio Based Classical Potential for Molydenum Predicts Line: *Richard G. Hennig*<sup>1</sup>; Thomas J. Lenosky<sup>2</sup>; Dallas R. Trinkle<sup>1</sup>; Sven P. Rudin<sup>3</sup>; Christopher F. Woodward<sup>4</sup>; John W. Wilkins<sup>1</sup>; <sup>1</sup>Ohio State University, Dept. of Physics, 174 W. 18th Ave., Columbus, OH 43210 USA; <sup>2</sup>Finisar Corporation, Sunnyvale, CA 94089 USA; <sup>3</sup>Los Alamos National Laboratory, Theoretical Div., Los Alamos, NM 87545 USA; <sup>4</sup>Air Force Research Laboratory, Matls. & Mfg. Direct., Wright Patterson AFB, Dayton, OH 45433 USA

A classical potential for molybdenum is developed which accurately predicts defect energies, phonon dispersion, melting point, surface energy, and ideal shear strength of the bcc phase. The potential form is given by the modified embedded atom method and the potential parameters are optimized using ab-initio energies, lattice parameters, forces and elastic constants. The classical potential determines the line energies, core structures and Peierls stresses of the screw and edge dislocations in bcc molybdenum.

# 9:45 AM

Atomistic Simulation of Dislocation Interactions: Brian D. Wirth<sup>1</sup>; Jennifer A. Young<sup>2</sup>; Jaime Marian<sup>2</sup>; Joshua Robach<sup>3</sup>; Ian M. Robertson<sup>3</sup>; <sup>1</sup>University of California, Dept. of Nucl. Engrg., MC 1730, Berkeley, CA 94720-1730 USA; <sup>2</sup>Lawrence Livermore National Laboratory, Chmst. & Matls. Sci. Direct., PO Box 808, Livermore, CA 94550 USA; <sup>3</sup>University of Illinois, Matls. Sci., IL USA

The mechanisms of dislocation motion and dislocation-obstacle interactions are of practical importance to developing quantitative structure-property relations, mechanistic understanding of plastic flow localization, predictive models of mechanical behavior in irradiated metals and the dynamic response of materials to shock loading. Molecular dynamics simulations directly account for core interactions through semi-empirical interatomic potentials and provide fundamental insight into dislocation migration and material deformation mechanisms. However, MD simulations are practically limited to interactions occuring at high-strain rate. In this presentation, we describe our recent results to investigate the motion of screw and edge dislocations and their interaction with a variety of obstacles, including radiation produced dislocation loops, stacking fault tetrahedra and helium bubbles, as well as nanometer coherent and incoherent precipitates. Finally, we will discuss the experimental validation of these results through comparisons to in-situ straining observations in transmission electron microscopy.

## 10:05 AM Break

# 10:20 AM Invited

Phase Field Microelasticity Theory and Model of Dislocations, and its Further Developments: Yu U. Wang<sup>1</sup>; Yongmei M. Jin<sup>1</sup>; Armen G. Khachaturyan<sup>1</sup>; <sup>1</sup>Rutgers University, Ceram. & Matls. Engrg., 607 Taylor Rd., Piscataway, NJ 08854 USA

The application of Phase Field method to dislocation modeling and its further advances are discussed. Phase Field method provides a natural mesoscale description of dislocation structures without explicitly tracking individual segments. The long-range elastic interactions between individual dislocations are numerically solved in Phase Field Microelasticity formalism. The "short-range" dislocation reactions, such as multiplication, annihilation and formation of various metastable configurations, are automatically taken into consideration through Landau-type "chemical" energy, gradient energy and elastic energy functional. No ad hoc assumptions are made on possible dislocation patterns during evolution. The model is extended to dislocation dynamics near free surfaces and in deposited thin films driven by relaxation of epitaxial stress. The effect of image forces on dislocation motions is consistently taken into account. Examples of 3D simulations are presented. The theory and model is further extended to multi-crack system. A further development to surface roughening of heteroepitaxial films is also made.

# 10:55 AM

Phase Field Modeling of Dislocation Networks and Dislocation Core Structures: Chen Shen<sup>1</sup>; Yunzhi Wang<sup>1</sup>; <sup>1</sup>Ohio State University, Dept. of Matls. Sci. & Engrg., 2041 College Rd., Columbus, OH 43210 USA

Phase field method has become an attractive alternative to study dislocations of arbitrary configurations and dislocation-precipitate interactions. Recently the model has been extended to describe dislocation nodal reactions and network formation, as well as dissociation of various dislocation configurations into Shockley partials. The extensions are necessary steps towards advanced applications of the phase field method to dislocation substructure formation and coarsening. By incorporating gamma surface data from ab initio calculations into the crystalline energy of the phase field model, quantitative analysis of dislocation core structures is made possible. We present various example applications of the method to dislocation-precipitate interaction (looping and shearing of ordered intermetallic precipitates).

## 11:15 AM

A Model for Simulating the Motion of Line Defects in Twin Boundaries in the HCP Metals: Anna Serra<sup>1</sup>; David J. Bacon<sup>2</sup>; Yuri N. Osetsky<sup>3</sup>; <sup>1</sup>Universitat Politecnica de Catalunya, Dept. de Matematica Aplicada III, Jordi Girona 1-3 modul C-2, Barcelona 08034 Spain; <sup>2</sup>The University of Liverpool, Matls. Sci. & Engrg.. Dept. of Engrg., Brownlow Hill, Liverpool L69 3GH UK; <sup>3</sup>Oak Ridge National Laboratory, Computer Sci. & Math. Div., PO Box 2008, Oak Ridge, TN 37831-6158 USA

In previous studies we have used computer simulation to investigate the atomic structure of twin boundaries and defects such as twinning dislocations in the HCP metals (e.g. Phil.Mag.A, 73 (1996) 333). The models employed used conventional periodic boundary conditions along the dislocation line and fixed conditions in the other two directions, so that extensive defect motion could not be considered. A method has now been developed to simulate a twin boundary containing a step with dislocation character, with full periodicity in the boundary plane. It may be used for investigating either the static or dynamic properties of such interfaces as the defects in them move over large distances. In the present work, we first demonstrate the nature of the method and apply the statics variant (T=0K) to determine the Peierls stress for motion of twinning dislocations in {10-12}, {11-21}, {10-11} and {11-12} boundaries. Except for the {11-21} twin, shuffles are required for dislocation glide and hence boundary movement. We also consider the dynamics of defect motion at T>0K.

# 11:35 AM

**Dynamical Scaling in a Simple 1D Model of Dislocation Activity**: *Jack Deslippe*<sup>1</sup>; Murray Daw<sup>1</sup>; Daryl Chrzan<sup>2</sup>; Mike J. Mills<sup>3</sup>; Neeraj Thirumalai<sup>4</sup>; <sup>1</sup>Clemson University, Physics & Astron., Clemson, SC 29634 USA; <sup>2</sup>University of California, Mat. Sci. & Engrg., Berkeley, CA USA; <sup>3</sup>Ohio State University, Matl. Sci. & Engrg., Columbus, OH USA; <sup>4</sup>OSU/Exxon USA

We study a simple 1D model of dislocation creation and motion. The dislocation source operates under a simple stress criterion. The dislocations move, overdamped, under an external force and mutual interactions with the other dislocations. The simple numerical simulations are examined for dynamical scaling, where the dislocation distribution function would obey the form  $n(x,t) = t^{\alpha} g(x/t^{\alpha})$ . The existence of scaling is confirmed by detailed analysis of the evolution equation and the (discrete) operation of the source. The analysis shows that b=1 and a approaches 0 from below, and that the dislocation

density asymptotically approaches a step function and decreases logarithmically in time. The approach to the asymptotic form is also logarithmic in time, which means that the numerical simulations only slowly converge to the asymptotic form.

#### 11:55 AM

Atomic-Level Study of Void Hardening in fcc Metals: Yury N. Osetsky<sup>1</sup>; David J. Bacon<sup>2</sup>; <sup>1</sup>Oak Ridge National Laboratory, Computer Scis. & Math., 4500 S. MS G138, Oak Ridge, TN 37831-6138 USA; <sup>2</sup>The University of Liverpool, Matls. Sci. & Engrg., Brownlow Hill, Liverpool L69 3GH UK

Voids are strong obstacles for moving dislocations and cause a significant hardening of metals subjected to irradiation with high energy particles at high temperatures. In this paper we present results of atomic-scale modelling of interaction between edge and screw dislocations and voids in Cu. Simulations were performed using a recently developed model based on a periodic array of dislocations. Interaction with voids of up to 4nm diameter was studied over the temperature range from 0 to 600K in crystals containing up to about 7 million atoms. Strong temperature dependence of the critical resolved shear stress and specific mechanisms related to dissociated dislocations were observed. The results obtained are compared with those obtained by dislocation dynamics at the continuum level.

# **General Abstracts: Session I**

#### Sponsored by: TMS

*Program Organizers:* Adrian C. Deneys, Praxair, Inc., Tarrytown, NY 10591-6717 USA; John J. Chen, University of Auckland, Department of Chemical & Materials Engineering, Auckland 00160 New Zealand; Eric M. Taleff, University of Texas, Mechanical Engineering Department, Austin, TX 78712-1063 USA

Monday AM	Room:	204		
March 15, 2004	Location	: Charlotte	Convention	Center

Session Chair: Joel Kapusta, Air Liquide Canada, Boucherville, QC J4B 1V6 Canada

#### 8:30 AM

On the Identification of Dislocation Types and Dislocation Morphorlogies in 316 LN Stainless Steel: Hongbo Tian<sup>1</sup>; Joseph A. Horton<sup>2</sup>; Peter K. Liaw<sup>1</sup>; Alexandru D. Stoica<sup>3</sup>; Xunli Wang<sup>3</sup>; Yandong Wang<sup>3</sup>; James W. Richardson<sup>4</sup>; <sup>1</sup>University of Tennessee, Matls. Sci. & Engrg., Knoxville, TN 37996 USA; <sup>2</sup>Oak Ridge National Laboratory, Metals & Ceram. Div., Oak Ridge, TN 37831 USA; <sup>3</sup>Oak Ridge National Laboratory, Spallation Neutron Source, Metals & Ceram. Div., Oak Ridge, TN 37831 USA; <sup>4</sup>Argonne National Laboratory, Intense Pulsed Neutron Source, Argonne, IL 60439 USA

Fatigue tests under fully reversed stresses were performed at 0.2 Hz, and microstructures of the specimens were carefully studied. Transmission-Electron Microscopy (TEM) was employed to analyze dislocations in Type 316 low-carbon nitrogen-added (LN) stainless steel (SS) samples with the intention to investigate the dislocation types, and change of dislocation structures with the fatigue process and grain orientation. The dislocations in 316 LN SS after fatigue at 0.2 Hz with a R ratio of -1 were found to be mostly edge type, which was also substantiated by studies using neutron diffraction.

#### 8:55 AM

Semi-Qualitative Relation Between Creep Curve and Metallurgical Observation During Creep of Ferritic Steel: Manabu Tamura<sup>1</sup>; Hideo Sakasegawa<sup>2</sup>; Akira Kohyama<sup>3</sup>; Kei Shinozuka<sup>1</sup>; Hisao Esaka<sup>1</sup>; <sup>1</sup>National Defense Academy, Dept. Matls. Sci. & Engrg., 1-10-20 Hashirimizu, Yokosuka 2398686 Japan; <sup>2</sup>Kyoto University, Grad. Sch. of Energy Sci., Gokasho, Uji, Kyoto 611-0011 Japan; <sup>3</sup>Kyoto University, Inst. of Advd. Energy, Gokasho, Uji, Kyoto 611-0011 Japan

Creep test was performed at around 650°C on three ferritic steels, iron, ultra low carbon steel containing small amount of TaN particles with 20nm in diameter and tempered martensitic steel, Fe-8%Cr-2%W-0.2%V-0.04%Ta steel. Hardness and integrated breadth of X-ray diffraction peak were measured for the crept specimens. The thin films were also observed under TEM. Two parameters, equivalent obstacle spacing (EOS) and dislocation density parameter (C) were calculated from only creep curves applying a dislocation model for creep deformation. Up to minimum creep, the above parameters are consistent with the metallurgical observations. In an accelerated creep range, the metallurgical observations of Fe and tempered martensitic steel correspond to the changes in EOS and/or C. However, in TaN particle hardening steel accelerated creep is observed, though there is little change in hardness and EOS. Absolute values of EOS are roughly equal to the TEM observations.

#### 9:20 AM

Flexure Strength and Shear Strength of Silicon Carbide Joints (SiC/SiC) Fabricated by a Molybdenum Diffusion Bonding Technique: Brian V. Cockeram<sup>1</sup>; <sup>1</sup>Bechtel Bettis Laboratory, PO Box 79, W. Mifflin, PA 15122-0079 USA

The capability to form robust SiC to SiC joints is needed to enable the fabrication of more complex SiC-based mechanical structures. In this work molybdenum foils are used to develop a diffusion bond with SiC during a vacuum heat treatment. Fracture strength data for SiC joined using a molybdenum foil diffusion bond are compared with results for monolithic Chemical Vapor Deposited (CVD) SiC using a standard 4-point flexural test method (ASTM C1161) from roomtemperature to 1100C. Shear Strength results obtained using a doublenotched specimen are also compared for the joined and monolithic specimens. The average shear strength values for the monolithic and joined specimens were typically lower than the flexural strength data, as observed for other ceramic materials. Differences in elastic properties and coefficient of thermal expansion between SiC and the phases that are produced in the molybdenum foil bond region result in the formation of slightly larger flaws in the SiC near the joint region. These flaws are shown to be fracture initiation sites that result in a lower range of flexural strength values for molybdenum bonded SiC (263 to 50 MPa) compared to monolithic SiC (443 to 197 MPa). However, the shear strength values for the molybdenum-joined SiC (264 to 61 MPa) are found to be within the data scatter of the monolithic material (397 to 31 MPa). These results indicate that a molybdenum diffusion bonding technique can be used to produce joints that have only slightly lower flexural strength than monolithic SiC, but the molybdenum diffusion bonds are as strong as monolithic SiC in shear.

#### 9:45 AM

Hardness and Electrical Resistivity of Molybdenum in the Post-Irradiated and Annealed Conditions: Brian V. Cockeram<sup>1</sup>; <sup>1</sup>Bechtel Bettis Laboratory, PO Box 79, W. Mifflin, PA 15122-0079 USA

Hardness and electrical resistivity are two indirect measures of the defect density of a metal. Hardness and electrical resistivity data were measured for sheet forms of Low Carbon Arc Cast (LCAC) molybdenum to provide a basic assessment of the influence of irradiation on the defect density. Irradiation of molybdenum in the High Flux Isotope Reactor (HFIR) at temperatures ranging from 270C to 1100C and to neutron fluence levels ranging from 10.5 to 64.4 X 10^20 n/  $cm^2$  (E > 0.1 MeV) was shown to result in a small increase in the electrical resistivity of molybdenum. Hardness was shown to be a more sensitive measure of the irradiated defect density than electrical resistivity, with increases in hardness on the order of 100% for irradiation at temperatures < 605C. Annealing was performed at temperatures between 300C and 1250C, and the kinetics for the recovery of the hardness and electrical resistivity were compared. Recovery of the initial hardness and electrical resistivity for LCAC molybdenum irradiated at 270C and 605C was observed at 970C and 1100C using 1-hour isochronel anneals. Irradiation at temperatures > 935C resulted in little change in hardness or electrical resistivity, and little change in these values was resolved after annealing to temperatures as high as 1250C

# 10:10 AM Break

#### 10:20 AM

A Comparison of the Properties of AA-6061 Processed by Different Methods of Severe Plastic Deformation (SPD): Bala Cherukuri<sup>1</sup>; Teodora Nedkova<sup>1</sup>; Raghavan Srinivasan<sup>1</sup>; <sup>1</sup>Wright State University, Mech. & Matls. Engrg., 3640 Col. Glenn Hwy., Dayton, OH 45435 USA

Severe Plastic Deformation (SPD) has been emerged as a promising approach to refine the grain size of a metal, increase strain rate sensitivity and formability at higher temperatures. This paper will present the results of a study on AA-6061-O, which was subject to SPD processing by Equal Channel Angular Extrusion (ECAE), Multi Axial Compression and Accumulative Roll Bonding (ARB) at room temperature. Over-aged samples of AA6061 were deformed to approximately the same accumulated strain. Results will include the as-processed microstructure, the stability of the microstructure at elevated temperatures, and the flow behavior of the different materials determined through tension and compression tests at different strain rates and temperatures. Hardness and Electrical Resistivity Measurement of Fe22.5Ni77.5 Permalloy as a Function of Annealing in a Magnetic Field: *A. Gali*<sup>1</sup>; C. J. Sparks<sup>2</sup>; R. K. Williams<sup>2</sup>; E. P. George<sup>2</sup>; <sup>1</sup>University of Tennessee, Matls. Sci. & Engrg., 434 Dougherty Engrg. Bldg., Knoxville, TN 37996 USA; <sup>2</sup>Oak Ridge National Laboratory, Metals & Ceram. Div., 1 Bethel Valley Rd., Oak Ridge, TN 37831 USA

We are interested in developing more rapid survey measurements of the effects of annealing on ferromagnetic alloys. Previous work has shown that both the electrical resistivity and hardness can be correlated with changes in the short range order. Diffuse X-ray scattering measurements have shown preference for Fe-Ni first neighbor pairs and their correlation lengths provides us with a better understanding of the effect of local atomic arrangements on these properties. The direction of the applied magnetic field was along [100], [110] and [111] crystallographic directions to determine orientation dependence of the applied field on the resistivity and hardness measurements. We will discuss the effects of the crystallographic dependence of the applied field on the measured properties of the Fe-Ni alloys. Also we plan to apply a tensile load to the Fe22.5Ni77.5 alloy below the elastic limit and anneal at temperature where diffusion can occur. This will provide us with information on the atomic pair alignments under stress.

## 11:10 AM

Surface Properties and Mechanical Behavior of Foam Electro Plasma Cleaned Steels: *Pankaj Gupta*<sup>1</sup>; Greg Tenhundfeld<sup>1</sup>; Edward O. Daigle<sup>1</sup>; <sup>1</sup>CAP Technologies, LLC, Louisiana Business & Tech. Ctr., S. Stadium Dr., Baton Rouge, LA 70803-6100 USA

Foam electro plasma process (FEPP) is a novel tool for cleaning and coating of conductive materials. FEPP is environmentally friendly exhibiting improved surface characteristics and corrosion resistance. This technology exhibits a great promise in various industrial applications. The present study involves cleaning of various grades of steels using FEPP. Microstructural analysis of cross-section of steel was analysed. Surface profile and morphology of the cleaned steel was studied by optical profilometer and SEM, respectively. The composition analysis and hydrogen profiling was performed by RBS and NRA, respectively. Surface analysis also described the level of cleaning. Microhardness studies were conducted to study the effect of process on hardness of the material. Microhardness tests were conducted on surface and cross section of the cleaned steel specimens. The results were compared to the steel cleaned by conventional industrial processes. An attempt has been made to develop an overall understanding of the processing-structure-property relationship of the cleaned steel.

# 11:35 AM

Effect of Boron and Carbon on the Mechanical Properties of Fe-Co-V Magnetic Alloys: Saurabh Kabra<sup>1</sup>; Easo P. George<sup>2</sup>; <sup>1</sup>University of Tennessee, Matls. Sci. & Engrg., Knoxville, TN 37996-2200 USA; <sup>2</sup>Oak Ridge National Laboratory, Metals & Ceram. Div., 1 Bethel Valley Rd., Oak Ridge, TN 37831-6093 USA

The Fe-Co system is well known for its excellent magnetic properties. But it exhibits brittle fracture both in the ordered and the disordered states. Vanadium additions (~2%) have been shown to improve ductility, more so in the disordered state than the ordered state. In an earlier study it was shown that small additions of boron and carbon can significantly improve the ductility of FeCo-2V. In this study, we have investigated the effects of higher levels of boron and carbon additions, and the role of changes in the vanadium concentration on the mechanical properties of ordered Fe-Co alloys. The effects of borides and carbides on slip refinement are investigated as well as the role of environment on ductility and fracture behavior. Research sponsored by the Division of Materials Sciences and Engineering, Office of Basic Energy Sciences, U. S. Department of Energy, under Contract DE-AC05-00OR22725 with UT-Battelle, LLC.

# General Pyrometallurgy: Session I

Sponsored by: Extraction & Processing Division, EPD-Pyrometallurgy Committee

Program Organizer: Thomas P. Battle, DuPont Titanium Technologies, Wilmington, DE 19880-0352 USA

Monday AM	Room: 202B
March 15, 2004	Location: Charlotte Convention Center

Session Chairs: Thomas P. Battle, DuPont Titanium Technologies, Wilmington, DE 19880-0352 USA; Florian Kongoli, FLOGEN Technologies Inc., Montreal H3S 2C3 Canada

# 8:30 AM

Study of Smelting Parameters in the Production of Silicomanganese from Denizli-Tavas Manganese Ores of Turkey: Ahmet Geveci<sup>1</sup>; Ender Keskinkilic<sup>1</sup>; <sup>1</sup>Middle East Technical University, Metallurgl. & Matls. Engrg. Dept., METU (ODTU), Ankara 06531 Turkey

Smelting of silicomanganese from Denizli-Tavas Mn ore (31%Mn) has been studied. Mixtures of calcined ore, active carbon, calcium oxide and quartz were smelted in graphite crucibles by using an electronically controlled muffle furnace. Temperature, time, charge basicity, active carbon/ore wt. ratio were determined as smelting parameters. Silicomanganese production necessitated higher temperatures compared to ferromanganese smelting since considerable amount of Si should be present in the final product. Oxides of iron and manganese were reduced faster, whereas sufficient time should be allowed for the system for desired reduction of SiO2. Determination of optimum charge basicity was crucial for silicomanganese production. Increase in quantity of active carbon led to increase in both Mn and Si recoveries. However, presence of excessive active carbon resulted in formation of carbides. Addition of high-manganese Brazilian sinter (53% Mn) to the domestic ore has also been studied in relation to both ferromanganese and silicomanganese smelting.

#### 8:55 AM

**Optimization, Control and Automation of Pyrometallurgical Processes:** *F. Kongoli*<sup>1</sup>; I. McBow<sup>1</sup>; S. Llubani<sup>1</sup>; <sup>1</sup>FLOGEN Technologies, Inc., 5757 Decelles Ave., Ste. 511, Montreal, Quebec H3S 2C3 Canada

The optimization of various non-ferrous smelting and converting processes as well as iron and steel making processes has been classically viewed and carried out in a classical static way. It has been always attempted to find the best unique set of conditions where the smelting, converting or iron and steel making processes could run smoothly. However this is associated with natural difficulties and some times has proven impossible due to the inherent characteristics of the raw materials and the new smelting technologies. In this work a new approach of the optimization of these processes has been exposed. This not only allows a continuous optimization of the smelting process but at the same time can serve as an adequate means of control and automation of any specific process. The advantages of this new approach have been discussed.

# 9:20 AM

**Modeling of Sulfide Capacities of Binary Titanate Slags**: *Bora C. Derin*<sup>1</sup>; Onuralp Yücel<sup>1</sup>; Ramana G. Reddy<sup>2</sup>; <sup>1</sup>Istanbul Technical University, Metallurgl. & Matls. Engrg. Dept., Maslak, Istanbul 34469 Turkey; <sup>2</sup>University of Alabama, Dept. of Metallurgl. & Matls. Engrg., Tuscaloosa, AL 35487-0202 USA

In this paper, the Reddy-Blander Model for sulfide capacity calculations has been applied to TiO2 containing binary slags. The sulfide capacities of FeO-TiO2 and MnO-TiO2 slag systems at 1500°C were calculated and compared with the experimental data. An excellent agreement between the model calculated Cs data and experimental data was observed.

# 9:45 AM

**Production of High-Grade Ferronickel from Low-Grade Oxide Nickel Ores:** V. M. Paretsky<sup>1</sup>; A. V. Tarasov<sup>1</sup>; I. D. Reznik<sup>1</sup>; <sup>1</sup>State Research Center of Russian Federation, State Rsch. Inst. of Nonferrous Metals, 13, Acad. Korolyov St., 129515 Moscow Russia

Production of commercial-grade nickel-containing products, and in particular ferronickel with a nickel content of at least 20% from low-grade oxide ores is a very important issue for Russia, because Russia has immense reserves of oxide nickel ores with a nickel content of less than 1.2%. In practice, the process of electric smelting with slags containing over 13% FeO inevitably results in uncontrolled frothing of the melt and its spillage from the furnace. A method has been developed in the Gintsvetmet Institute for production of high-grade ferronickel by oxidizing low-grade ferronickel with ore in an electric furnace; the gas emission and frothing are eliminated due to a low carbon content of the melt in this process. A flow diagram has been proposed with two parallel streams of ore treated in continuous mode in two electric smelting furnaces. To verify the proposed flowsheet, laboratory tests have been carried out, which have demonstrated the feasibility of production of commercial-grade ferronickel with a content of 26.6% Ni and 1.83% Co from ores containing 1.08-1.1% Ni, 0.08-0.12% Co and up to 30.7% Fe. This technology is now in the process of preparation for commercial introduction at the Buruktalsky nickel smelter (South Urals, Russia).

# 10:10 AM

# 10:20 AM

Intensification of Reduction of Oxide Nickel Ores: A. V. Tarasov<sup>1</sup>; P. A. Kovgan<sup>1</sup>; V. M. Paretsky<sup>1</sup>; <sup>1</sup>State Research Center of Russian Federation, State Rsch. Inst. of Nonferrous Metals, 13, Acad. Korolyov St., 129515 Moscow Russia

Laboratory studies into reduction of oxide nickel ores with cast iron in sparged melt were carried out in crucibles at 1500C. Argon blowing at a rate of 0.9 to 1.1 m3/m2s through a vertical lance submerged into the melt down to the iron/ore interface permitted production of discard slag with 0.03% to 0.05% Ni and 0.01 Co. Bench-scale investigations of metallothermic reduction of oxide nickel ores were carried out in a plasma-arc furnace in intermittent mode. Ore containing 1.0% Ni and 0.08% Co was fed to the furnace along with 15% of calcium oxide as fluxing agent. Coke fines were fed over the melt at a rate of 1% of the weight of the ore to reduce iron in the ore to wuestite and prevent "boiling-up" of the melt. The ferronickel obtained contained 15.2% Ni, 1.75% Co, 0.35% Si and 0.43% Cr. The nickel and cobalt contents in "discard" slags after blowing were on average 0.045 and 0.015%, respectively. The reduction process can be intensified by changing the position of the blowing lances in the bath and the depth of their submersion. The nickel and cobalt contents of ferronickel can be increased by periodical carbonization of cast iron.

#### 10:45 AM Cancelled

# Melting Zone Evaluation in New Hot Metal Processes – An Innovative Approach

#### 11:10 AM

Mineralogical Changes Occurring During the Roasting of Zinc Sulphide Concentrates: Tzong T. Chen<sup>1</sup>; *Yoo-Hyun Sung*<sup>2</sup>; John E. Dutrizac<sup>1</sup>; <sup>1</sup>CANMET, 555 Booth St., Ottawa, Ontario K1A 0G1 Canada; <sup>2</sup>Korea Resources Corporation, Tech. Rsch. Inst., 686-48, Shindaebang-dong, Dongjak-gu, Seoul 156-706 Korea

Zinc concentrates and fluid-bed roaster calcines from CEZinc were studied. The Zinc concentrates consist of sphalerite and minor to trace amounts of pyrite, chalcopyrite, anglesite, galena, pyrrhotite, ankerite, gysum and silicates. During roasting of the concentrates, the S in the sphalerite (Zn,Fe)S diffuses out of the particle, whereas the associated Zn and Fe react in situ to form (Zn,Fe)O. The Fe from the (Zn,Fe)O phase migrates towards the peripheries of the particles, forming ZnFe2O4. The resulting "ZnO+ZnFe2O4" particles further agglomerate to form large, porous, spherical masses. A relatively compact ZnO-rich shell subsequently develops on the surface of the agglomerates and the development continues inwards; eventually, the particles become compact. Rhythmic bands are often present in the agglomerated masses. However, a small number of the particles remain as tiny un-agglomerated grains. The calcines consist of spherically agglomerated particles, and fragments of agglomerated particles, of ZnO and ZnFe2O4, as well as traces of Zn2SiO4, Pb oxide/oxysulphate and silicates. The ZnO, ZnFe2O4, Zn2SiO4 and Pb oxide/oxysulphate often form intimate intergrowths in the rhythmic bands. The ZnO and Zn2SiO4 phases contain minor amounts of Fe; most of the Cu in the calcine is present in the ZnO and ZnFe2O4 phases.

#### 11:35 AM

**Decomposition Kinetics of Flash Smelting Flue Dust Sulphates:** *Elli Nurminen*<sup>1</sup>; Heikki Jalkanen<sup>2</sup>; Kim Fagerlund<sup>3</sup>; Tiina Ranki-Kilpinen<sup>4</sup>; <sup>1</sup>Helsinki University of Technology, Matls. Procg. & Powder Metall., Vuorimiehentie 2 K, Espoo FIN-02150 Finland; <sup>2</sup>Helsinki University of Technology, Metall., Vuorimiehentie 2 K, Espoo 02150 Finland; <sup>3</sup>Outokumpu Research, Pyrometall./Sulphide Smelting, PO Box 60, Pori FIN-28330 Finland; <sup>4</sup>Outokumpu Technology, PO Box 86, Espoo FIN-02201 Finland

Sulphate decomposition was studied in the conditions of a typical copper flash smelting heat recovery boiler. The aim was to determine

the kinetics of the copper sulphate decomposition reactions and to find out if they are likely to take place in the process conditions prevailing in an industrial HRB. The information is essential in CFDmodelling of the reactions taking place in the boiler and for optimising the process. Thermal decomposition of sulphates was studied by thermogravimetry. The experiments were conducted with a commercial copper sulphate, a partially sulphated copper oxide and an industrial process flue dust. The main variables studied were temperature and gas composition of a N2-O2-SO2-mixture. The samples were characterized with SEM, optical microscope and XRD. Temperature affected the decomposition rate strongly but the gas composition had a minor effect on the kinetics. The decomposition was fastest in the partly sulphated oxide and slowest in commercial copper sulphate.

# Hume Rothery Symposium: Structure and Diffusional Growth Mechanisms of Irrational Interphase Boundaries: Session I

Sponsored by: Electronic, Magnetic & Photonic Materials Division, Structural Materials Division, EMPMD/SMD-Alloy Phases Committee, MPMD-Phase Transformation Committee-(Jt. ASM-MSCTS)

*Program Organizer:* H. I. Aaronson, Carnegie Mellon University, Department of Materials Science and Engineering, Pittsburgh, PA 15213 USA

Monday AM	Room: 208A	
March 15, 2004	Location: Charlotte Convention	Center

Session Chair: Gary R. Purdy, McMaster University, Dept. of Matls. Sci. & Engrg., Hamilton, Ontario L8S 4L7 Canada

#### 8:30 AM Invited

Low Energy and Low Mobility Structures at Irrational Interphase Boundaries, and Compliance With Nucleation Theory: *Hubert I. Aaronson*<sup>1</sup>; <sup>1</sup>Carnegie Mellon University, Dept. of Matls. Sci. & Engrg., 5000 Forbes Ave., Wean Hall 2313, Pittsburgh, PA 15213-3890 USA

Nucleation theory has led to predictions that partially coherent interfacial structures should develop during diffusional growth even at irrational planar boundaries (ALK, 1968). This prediction is now tested in alloy systems that appear to be successively less metallic in character. In both a massively transformed Ag-26% Al alloy and during precipitation at grain boundaries in Ti-Cr and Ni-Cr, nearly all interphase boundaries are indeed partially coherent. However in the massive transformations in near-TiAl and in MnAl(+2% C) alloys partially coherent structures are largely absent (Vasudevan et al, Soffa et al., 2002). Nie and Muddle (NM, 2002) and Howe, Reynolds and Vasudevan (HRV, 2002) reported a preference for edge-to-edge (Kelly and Zhang, 1999) rather than plane-to-plane matching of certain low index planes in both lattices at facets in a Ti-46.54% alloy. Recently Reynolds et al (2003) have shown with 3-D, NCS modeling that planar facets whose highly irrational crystallography was accurately determined by NM and HRV correspond physically to dense parallel rows of atoms intermingled in no obvious sequence but perhaps displaceable only with Moire ledges. Li et al will report in this symposium planar ZrN:alpha Zr-N facets whose structures cannot be rationalized by edgeto-edge matching. This implies that other type(s) of irrational interfacial structure capable of impeding growth remain to be discovered. Al:Xe(solid) interfaces, at which {111}Al and {100}Al facets are present despite a misfit of ca. 50% (Howe), suggest shallow minima in the polar gamma-plot that affect only nucleation. This spectrum of observations indicates that a marked difference in bond strength and character in the matrix and the product phases can cause the two phases to play unequal roles in determining the crystallography and structure of low energy and low mobility boundaries.

# 9:10 AM Invited

Calculation of Alpha/Gamma Interfacial Energy in Iron in the Presence of Irrational Crystallography: Takatoshi Nagano<sup>1</sup>; *Masato Enomoto*<sup>1</sup>; <sup>1</sup>Ibaraki University, Dept. of Matls. Sci., 4-12-1, Nakanarusawa, Hitachi 316-8511 Japan

The interfacial energies between alpha and gamma iron crystals, not only K-S (or N-W), but also irrationally oriented, were calculated at various interface orientations using the EAM potential. Blocks of alpha and gamma iron  $(10x10x5 \text{ nm}^3)$  were joined and relaxed by Monte Carlo Method under the condition that atom positions are fixed at the outer surface of the blocks. Whereas the polar plot of

MONDAY AM

calculated interfacial energy exhibited a number of small and large cusps for K-S (or N-W) relationship, a smoother and irregular energy surface was obtained for irrational OR. The three-dimensional Wulff plot is made for equilibrium shape of intragranular ferrite idiomorphs that are K-S (or N-W) and irrationally oriented with the austenite matrix. The energy of austenite grain boundaries is calculated using the same potential. The equilibrium shape of grain boundary ferrite allotriomorphs will be calculated at some boundary misorientations.

# 9:50 AM Invited

Edge-to-Edge Matching as a Criterion for Interphase Interfaces of Low Energy: Gary R. Purdy<sup>1</sup>; <sup>1</sup>McMaster University, Dept. of Matls. Sci. & Engrg., 1280 Main St. W., Hamilton, Ontario L8S4L7 Canada

As demonstrated by Aaronson and his co-workers over some five decades, the structure, energy and dynamic response of interphase boundaries are strongly mutually correlated; it has also become clear that very few, if any, solid-solid transformation interfaces can seriously be considered "incoherent". In recent attempts to rationalize these observations, many descriptions of less-rational interphase boundaries have focused on considerations of matching between atomic planes, lying parallel to the interface in the parent and product crystals. After reviewing several simple boundaries, their structure, energetics and (in some cases) their migration mechanisms, the role of edge-to-edge matching is examined. It is noted that many cases of habit plane matching are also cases where other sets of densely populated atomic planes meet edgewise at the interface. Some recent observations of boundary faceting where edge-to-edge matching is not accompanied by facet plane matching are examined, and their significance is discussed.

# 10:30 AM Break

# 10:45 AM Invited

Crystallography and Growth Mechanisms of Interphase Boundaries: Jian-Feng Nie<sup>1</sup>; <sup>1</sup>Monash University, Sch. of Physics & Matls. Engrg., Victoria 3800 Australia

In this paper a Moire plane model is used to examine the orientation, structure and migration mechanism of irrational, planar interphase boundaries in phase transformations. In contrast to existing approaches of structural ledges, disconnections and invariant lines/ planes that are based essentially on matching of atoms or lattice sites within two parallel, or close to parallel, closely-packed planes in the two lattices, the present model involves consideration of matching of a pair of non-parallel, closely-packed lattice planes that are related by a correspondence. It will be demonstrated that irrationally-oriented, planar interphase boundaries are defined by the Moire plane resulting from the intersection of these two lattice planes, and that such boundaries migrate in their normal directions by successive nucleation and lateral movement, within the macroscopic interface planes, of interfacial defects that have the form of Moire ledges. A comparison will be provided between the Moire plane model and approaches of structural ledges, disconnections and invariant lines/planes.

#### 11:25 AM Invited

Structures in Irrational Singular Interfaces: Wen-Zheng Zhang<sup>1</sup>; Xiaopeng Yang<sup>1</sup>; <sup>1</sup>Tsinghua University, Dept. of Matls. Sci. & Engrg., Beijing 100084 China

Reproducible facets or habit planes in irrational orientations suggest that they should be singular interfaces associated with local energy minima. When it is singular with respect to the orientation relationship (OR) and the interface orientation (IO), an irrational interface usually contains periodical good matching regions, extended along an invariant line (or a quasi-invariant line when the lattice misfit is large) and alternated with dislocations. The corresponding OR can be described by parallelism of at least two measurable  $\Delta g$  vectors for a system of either small or larger lattice misfit. The singular irrational interface must lie along the common moiré planes normal to the  $\Delta g$ 's. The edge-to-edge matching can be realized in this interface for different sets of planes. An irrational interface singular with respect only to IO is normal to one  $\Delta g$ . The relationship between the  $\Delta g$  description and the interfacial structures is explained in the framework of the O-lattice/CSL/DSCL.

# Internal Stresses and Thermo-Mechanical Behavior in Multi-Component Materials Systems: Electronic Thin Films and Packaging Materials I

Sponsored by: Electronic, Magnetic & Photonic Materials Division, Structural Materials Division, EMPMD-Electronic Packaging and Interconnection Materials Committee, EMPMD-Thin Films & Interfaces Committee, SMD-Composite Materials Committee-Jt. ASM-MSCTS

*Program Organizers:* Indranath Dutta, Naval Postgraduate School, Department of Mechanical Engineering, Monterey, CA 93943 USA; Bhaskar S. Majumdar, New Mexico Tech, Department of Materials Science and Engineering, Socorro, NM 87801 USA; Mark A.M. Bourke, Los Alamos National Laboratory, Neutron Science Center, Los Alamos, NM 87545 USA; Darrel R. Frear, Motorola, Tempe, AZ 85284 USA; John E. Sanchez, Advanced Micro Devices, Sunnyvale, CA 94088 USA

Monday AM	Room:	209B
March 15, 2004	Location	: Charlotte Convention Center

Session Chairs: K. N. Subramanian, Michigan State University, E. Lansing, MI 488824 USA; John Sanchez, Unity Semiconductor, Matls. Sci., Santa Clara, CA 95050 USA; Vijay Sarihan, Motorola, Final Mfg. Tech. Ctr., Tempe, AZ 85284 USA

## 8:30 AM Keynote

**Stress Induced by Electromigration in VLSI Interconnects**: *King-Ning Tu*<sup>1</sup>; <sup>1</sup>University of California, Dept. of Matls. Sci. & Engrg., Los Angeles, CA 90095 USA

Multi-leveled thin film interconnects in microelectronic devices are 3-D in structure and are confined in a dielectric layer. Electromigration and the confinement produce mechanical stresses in the interconnect. The stress can enhance or retard electromigration. The 3-D structure also produces current crowding wherever the interconnect turns. The current crowding can lead to stress concentration and inhomogeneous stress distribution. The analysis of stress induced by electromigration will be presented. In the beginning of the talk, a brief introduction of the multi-leveled interconnect structure and memory devices based on field-effect transistors will be given.

#### 9:00 AM Invited

Role of Film Intrinsic Stress in Packaging of Multi-Layer Micro-Electronics and MEMS Structures: Vijay Sarihan<sup>1</sup>; <sup>1</sup>Motorola, Final Mfg. Tech. Ctr., 2100 E. Elliot Rd., MD EL725, Tempe, AZ 85284 USA

Internal stress due to material CTE and Young's modulus mismatch plays havoc in microelectronics and MEMS structures but is well understood and controllable. However the film intrinsic stress develops as a function of processing. The level of stress and how it changes with additional processing or environmental exposure is still not well understood. This stress is typically neglected in response prediction as value, behavior and response impact are not well known. Film intrinsic stress can play a substantial role in enhancing or degrading the response of multi-layer structures. Intrinsic stress can cause failures or can be mitigating to situations that would have otherwise resulted in disaster. Thin film intrinsic stress is processing related so, it can be controlled by modifying processing parameters provided we know what is the outcome of the process changes and the desired requirement. These requirements point to a need for a measurement capability and a response prediction capability. In addition to processing parameters there is also a size and thickness link. Thus the measurement capability should be capable of addressing the typical size and thickness seen in actual devices and MEMS structures. This paper will present the impact of intrinsic stress in response prediction of micro-electronic structures. Special emphasis will be given to the role of internal stress in packaging of micro-electronic devices and MEMS structures. A variety of examples delineating the impact of thermo-mechanical stress and intrinsic stress will be covered. This will include device interconnects, special via structures in compound semiconductor devices, wafer level packages and MEMS. It will also present innovative techniques for measuring intrinsic stress, techniques that take size into consideration and relate the measurements to the actual size of interconnects. Since the sample preparation follows the processing witnessed by the actual device the technique is also capable of accounting for the effect of microstructure change.

# 9:25 AM Invited

Cyclic Deformation and Fatigue in Thin Metal Films: O. Kraft<sup>1</sup>; R. Monig<sup>2</sup>; G. P. Zhang<sup>2</sup>; C. A. Volkert<sup>1</sup>; <sup>1</sup>Research Center and University of Karlsruhe Germany; <sup>2</sup>Max-Planck-Institute for Metals Research Stuttgart, Stuttgart Germany

Continuous and patterned metal thin films are widely used in microelectronic and micro-electro-mechanical systems (MEMS). In these applications, temperature changes of up to several  $100^{\circ}$ C may occur, and, as a result of thermal mismatch between film and substrate materials, large mechanical stresses arises, which have been the subject of many detailed studies in the last decade. However, only little attention has been paid to fatigue, i.e. the effect of repeated cyclic loading, on the integrity of thin films. We have found that fatigue failure of mechanically or thermomechanically strained thin films is associated with the formation of extrusions and voids. Details of the damage morphology have been observed to depend sensitively on film thickness and grain size. In particular, fatigue in metal films with thickness and/or grain size of less than approximately 500 nm appears to be controlled by diffusive rather than by dislocation mechanisms.

#### 9:50 AM Invited

Ultra High-Cycle Fatigue in Pure Al Thin Films and Line Structures: C. Eberl<sup>1</sup>; R. Spolenak<sup>2</sup>; O. Kraft<sup>3</sup>; F. Kubat<sup>4</sup>; A. Leidl<sup>3</sup>; W. Ruile<sup>3</sup>; E. Arzt<sup>1</sup>; <sup>1</sup>Institut für Metallkunde der Universität Stuttgart, Stuttgart Germany; <sup>2</sup>Max-Planck Institut für Metallforschung; <sup>3</sup>Forschungszentrum Karlsruhe Germany; <sup>4</sup>Clausthal University of Technology Germany

The requirements of mechanical devices (MEMS and Surface Acoustic Wave (SAW)) increase due to shrinking size, rising frequencies and driving power. We focus on novel fatigue mechanisms stemming from the combination of small dimensions (100 nm) and ultrahigh frequencies (GHz). Tailored SAW test devices have been developed for improved stress and temperature control. Quantitative post test analysis as a function of testing time, power density and temperature revealed a direct correlation between void/extrusion density and device performance. In-situ measurements of the characteristic damage formation revealed an extrusion mechanism that operates on a short time scale. We have developed sophisticated models relating the device power to the mechanical stress state. Combined with thermal stresses measured in the device, these allowed the complete stress tensor to be determined. This mechanistic insight provides the physical understanding for improved life-time models and lead to the development of high power durable metallizations.

#### 10:15 AM Invited

Internal Stresses on the Thermomechanical Behavior of Sn-Based Solder Joints: J. G. Lee<sup>1</sup>; H. Rhee<sup>1</sup>; K. N. Subramanian<sup>1</sup>; <sup>1</sup>Michigan State University, Dept. of Chem. Engrg. & Matls. Sci., E. Lansing, MI 48824-1226 USA

Solder joints consist of various entities such as in a typical multicomponent system. When such a joint is subjected to temperature excursions during service, large stresses can arise due to different coefficients of thermal expansion (CTE) of components that make up the joint. The magnitude of stresses that can develop not only depends on the temperature differences encountered, but also on rates at which such changes are imposed. Microstructural constituents present in the solder joint also play significant roles in the development of these stresses. Acknowledgement: Work supported by the National Science Foundation under grant NSF DMR-0081796.

#### 10:40 AM Invited

Assessment of Stress-Induced Mechanical Properties and Microstructural Changes in Pb-Free Solder-Joint Interconnects: James P. Lucas<sup>1</sup>; A. U. Telang<sup>1</sup>; J. G. Lee<sup>1</sup>; H. Rhee<sup>1</sup>; T. R. Bieler<sup>1</sup>; K. N. Subramanian<sup>1</sup>; <sup>1</sup>Michigan State University, Chem. Engrg. & Matl. Sci., 3526 Engrg. Bldg., E. Lansing, MI 48824-1226 USA

Solder joints represent multi-component materials systems that are subjected to rather complex stress states in operation. As a primary interconnect in microelectronic packaging not only must the solder joint function reliably as an electrical interconnect, it must perform mechanically as a structural unit, as well. Due to coefficient of thermal expansion (CTE) mismatch, stress and strain develop in the solder joint interconnect. Stresses and strains developed in the joint resulting from thermo-mechanical fatigue (TMF) cycling can be particular detrimental. Residual stress built up during TMF affects microstructure evolution in the joint long after TMF cycling ceases. Nanoindentation testing (NIT) along with scanning probe microscopy (SPM) will be used to investigate the mechanical properties and internal stress behavior in Sn-based eutectic and near-eutectic Pb-free solder joints. Orientation imaging microscopy (OIM) will also be used in the assessment of internal stress effects.

### 11:05 AM

Double Shear Thermomechanical Fatigue (TMF) Response of a Lead-Free Solder Reinforced with SMA Fiber: Z. X. Wang<sup>1</sup>; I. Dutta<sup>2</sup>; B. S. Majumdar<sup>1</sup>; <sup>1</sup>New Mexico Tech, Matls. Dept., Socorro, NM 87801 USA; <sup>2</sup>Naval Postgraduate School, Mech. Engrg. Dept., Monterey, CA 93943 USA

Failure of microelectronic solders usually occurs through accumulation and localization of large shear strain under TMF loading. Here we present results of a novel approach utilizing the active characteristics of shape memory alloy (SMA) reinforcements. The premise is that a reverse strain of the SMA associated with martensite (M) to austenite (A) transformation during heating would induce active backstress on the matrix. In order to test the feasibility of this approach, we have conducted double-shear tests of a long-fiber composite wire, composed of a Sn3Ag matrix reinforced with a NiTi wire. Under TMF at constant load, the composite wire exhibited a sudden decrease in the shear creep rate on reaching the transformation temperature. Correspondingly, a bare NiTi wire showed a reverse local displacement at the transformation temperature, consistent with an M to A transformation. Preliminary modeling of internal stresses will be presented. This research was supported by ARO.

# International Laterite Nickel Symposium - 2004: Economics and Project Assessment

Sponsored by: Extraction & Processing Division, EPD-Aqueous Processing Committee, EPD-Copper, Nickel, Cobalt Committee, EPD-Process Fundamentals Committee, EPD-Process Mineralogy Committee, EPD-Pyrometallurgy Committee, EPD-Waste Treatment & Minimization Committee *Program Organizer:* William P. Imrie, Bechtel Corporation, Mining and Metals, Englewood, CO 80111 USA

Monday AM	Room: 2	17B/C	
March 15, 2004	Location:	Charlotte	Convention Center

Session Chairs: Steve C.C. Barnett, VP HSEQC Stainless Steel Materials, BHP-Billiton, London SW1V 1BH UK; James A. Murray, Snr Principle Engineer, Bechtel Corp. Mining & Metals, San Francisco, CA 94119 USA

# 8:30 AM

Nickel Market Dynamics: Santo Ranieri<sup>1</sup>; <sup>1</sup>Noranda Inc./ Falconbridge Ltd., Mkt. Rsch., Queen's Quay Terminal, 207 Queen's Quay W., Ste. 800, Toronto, Ontario M5J 1A7 Canada

We will briefly review the nickel market in 2003 and look forward to the supply demand balance for the next few years focusing in on the key factors influencing future price dynamics. On the supply side, we will examine slated brownfield and greenfield expansions including the Norilsk factor and the small to mid-range 'supply creep'. We will also review the cost side of the industry and what to expect going forward. On the demand side, we will discuss the stainless steel and non-stainless demand, the China factor and the stainless steel scrap supply cycle. We will conclude by pinpointing where the market is on the current price cycle, and where we believe the mid-term direction is headed.

#### 9:00 AM

**Past and Future of Nickel Laterite Projects**: Ashok D. Dalvi<sup>1</sup>; *W. Gordon Bacon*<sup>1</sup>; Robert C. Osborne<sup>1</sup>; <sup>1</sup>Inco Limited, 2060 Flavelle Blvd., Sheridan Park, Mississauga, Ontario L6M 1V1 Canada

Production of nickel from laterite ores has occurred for over 100 years beginning with processing of garnieritic ores from New Caledonia. However, until now the world nickel supply has been predominantly from sulfide sources. Going forward, the authors project that the production of nickel from sulfide ores will remain more or less constant. Most of the expansion in nickel production capacity over the next ten years will come from processing of laterite ores. Thus the capital and operating costs of new laterite projects will have significant impact on the nickel supply and therefore price. The authors have reviewed the history and capital and operating costs of these projects and those "on the drawing board". The authors have also evaluated the risk associated with such projects. The paper will discuss the impact of this and the recent history on the future development of laterite nickel projects.

# 9:30 AM

Start Up and Reliability of Nickel Laterite Plants: Finlay Campbell<sup>1</sup>; Ed McConaghy<sup>1</sup>; William Vardill<sup>1</sup>; <sup>1</sup>Dynatec Corporation,

Metallurgl. Tech. Div., 8301 - 113 St., Ft. Saskatchewan, Alberta T8L 4K7 Canada

Nickel laterite pressure acid leach plants and reduction roast plants have had a chequered history in terms of engineering, construction, start-up and operational reliability. Many potential projects have been the subject of detailed studies over the last thirty to forty years. Four reduction roast plants are currently operating, an additional one was partially constructed but never completed and one more was started up in 1974 and shutdown after 12 years operation. Three acid leach plants have been built and commissioned in the last five years trying to follow the example of the Moa Nickel plant in Cuba. An additional acid leach project is currently on hold, following limited construction work, its future subject to review by the owner because of potential cost over-runs. The paper will discuss difficulties that may be encountered as a project is developed and will address factors which may affect production ramp-up schedule, long term production performance and overall project success. Comparisons are made with rampup performance at other large metallurgical plants that employ some comparable unit operations.

# 10:00 AM Break

# 10:10 AM

The Importance of Life-Cycle Assessment Approach to the Evaluation of Environmental Impacts Associated with the Pressure Acid Leach Treatment of Nickel Laterite Ores: *William James Middleton*<sup>1</sup>; Matthew Searles<sup>2</sup>; <sup>1</sup>Inco Limited, Corp., Gen. Engrg. Bldg. (ITSL Sec.), Copper Cliff, Ontario POM 1N0 Canada; <sup>2</sup>BHPBilliton Newcastle Technology

The life-cycle assessment (LCA) approach can be an important tool for the quantification and evaluation of environmental impacts associated with metal production systems. At the conceptual phase of a new metals development project, LCA can: · Aid project decision making by evaluating the environmental consequences of design decisions; · Support project permitting and reinforce site/process environmental impact assessment; · Allow environmental impact comparisons between alternate flow sheets. This paper discusses the life-cycle assessment methodology, and its application as a supportive tool for environmental decision-making in process design and for site environmental impact assessment and permitting. Selected examples from a recent LCA performed on the Pressure Acid Leach Process for treating nickel Laterite ores are employed to demonstrate the usefulness of the tool.

#### 10:40 AM

The Implications of Sustainability in Developing a Nickel Laterite Project: Denis J. Kemp<sup>1</sup>; Mark Wiseman<sup>1</sup>; <sup>1</sup>Noranda Inc-Falconbridge Limited, Queen's Quay Terminal, 207 Queen's Quay W., Ste. 800, Toronto, Ontario M5J 1A7 Canada

Laterite projects are found in the tropical and sub-tropical regions of the world. As a result severe meteorological situations accompany such projects, often in regions of high seismic activity and political uncertainty. Frequently, socio-economic development supported by political interest is a major driver for development, while environmental protection imposes numerous stresses on the project. This paper will review and examine the many social, environmental, technical and financial issues that a mining and extraction process is subject to during development. The options that must be evaluated will be discussed in the context of sustainable development. Issues of project standards and cultural impact through to long term issues such as greenhouse gasses and climate change will be assessed in redirecting project environmental norms. Although a rationale for sustainable project can be developed many long term uncertainties around issues remain.

#### 11:10 AM

Beating US\$10 Per Pound of Installed Capacity for a Laterite Nickel Plant: *David S. Dolan*<sup>1</sup>; Roger M. Nendick<sup>2</sup>; <sup>1</sup>Fluor Australia Pty Ltd., GPO Box 1320L, Melbourne, Victoria 3001 Australia; <sup>2</sup>Fluor Mining and Minerals, 1075 W. Georgia St, Ste. 700, Vancouver, BC V6E 4M7 Canada

To beat capital costs of US\$10 per pound of installed capacity has appeared as a major hurdle for the "third" generation laterite nickel plants. Forecast costs are escalating. Where can savings come from? Ore beneficiation can reduce the tonnage rate to be processed. High pressure acid leach options include use of indirect slurry heating and higher operating temperatures to reduce flow rates and residence time. Progress has been reported in atmospheric leaching. High counter current decantation circuit settling rates and high underflow densities reduce CCD costs. Metal recovery options include direct from leach solution to metal production as used by Bulong and espoused by Goro and indirect recovery as used by Moa Bay, Murrin Murrin and Cawse. Plant location impacts on the costs of tailings disposal. Finally nickel and cobalt metal production routes are electrowinning, hydrogen reduction or some innovative routes being proposed for Goro. This paper reviews the status in these developments, with particular reference to equipment and processes that offer lower capital costs.

#### 11:40 AM

An Alternative Nickel Laterite Project Development Model: David A. Neudorf<sup>1</sup>; David A. Huggins<sup>2</sup>; <sup>1</sup>Hatch Associates, 2800 Speakman Dr., Mississauga, Ontario L5K 2R7 Canada; <sup>2</sup>Consultant, 4 Steele Ave., Annapolis, MD 21401 USA

Known resources of nickel laterites considerably exceed nickel sulfide resources and there is a growing consensus that most new nickel production will be sourced from laterites. The development of nickel laterite projects is very capital intensive due to inherently low grades, inability to concentrate ore prior to processing, complex processing technology and typically large infrastructure requirements. This has resulted in most recently proposed projects being "mega-projects," to achieve economy of scale. However, this may result in unacceptable project risk in many cases. Furthermore, many known laterite resources are not large enough to support a mega-project. This paper describes an alternative model for nickel laterite project development that allows smaller scale and reduces capital exposure. The requirements of this model in terms of process technology, infrastructure and commercial innovation are described.

# Lead-Free Solders and Processing Issues Relevant to Microelectronic Packaging: Fundamentals, Phases, Wetting and Solidification

*Sponsored by:* Electronic, Magnetic & Photonic Materials Division, EMPMD-Electronic Packaging and Interconnection Materials Committee

Program Organizers: Laura J. Turbini, University of Toronto, Center for Microelectronic Assembly & Packaging, Toronto, ON MSS 3E4 Canada; Srinivas Chada, Jabil Circuit, Inc., FAR Lab/ Advanced Manufacturing Technology, St. Petersburg, FL 33716 USA; Sung K. Kang, IBM, T. J. Watson Research Center, Yorktown Heights, NY 10598 USA; Kwang-Lung Lin, National Cheng Kung University, Department of Materials Science and Engineering, Tainan 70101 Taiwan; Michael R. Notis, Lehigh University, Department of Materials Science and Engineering, Bethlehem, PA 18015 USA; Jin Yu, Korea Advanced Institute of Science and Technology, Center for Electronic Packaging Materials, Department of Materials Science & Engineering, Daejeon 305-701 Korea

Monday AM	Room: 219B	
March 15, 2004	Location: Charlotte Convention Center	

Session Chairs: Laura J. Turbini, University of Toronto, Ctr. for Microelect. Assembly & Pkgg., Toronto, Ontario M5S 3E4 Canada; Sung K. Kang, IBM, T. J. Watson Rsch. Ctr., Yorktown Heights, NY 10598 USA

# 8:30 AM Invited

**Controlling Ag3Sn Plate Formation in Near-Ternary-Eutectic Sn-Ag-Cu Solders by Minor Zn Alloying Addition**: *Sung K. Kang*<sup>1</sup>; Da-Yuan Shih<sup>1</sup>; Donovan Leonard<sup>1</sup>; Donald W. Henderson<sup>2</sup>; Timothy A. Gosselin<sup>2</sup>; Sungil Cho<sup>3</sup>; Won Kyoung Choi<sup>4</sup>; <sup>1</sup>IBM, T.J. Watson Rsch. Ctr., Yorktown Heights, NY 10598 USA; <sup>2</sup>IBM Microelectronics, Endicott, NY USA; <sup>3</sup>KAIST, Matls. Sci. & Engrg., Daejon Korea; <sup>4</sup>Samsung Advanced Institute of Technology, Suwon 440-600 Korea

As a result of extensive search, near-ternary-eutectic Sn-Ag-Cu alloys have been identified as the leading Pb-free solder candidate to replace Pb-bearing solders for microelectronic applications. However, recent studies on the processing behaviors and solder joints reliability assessment have revealed several potential reliability risk factors associated with the alloy system. The formation of large Ag3Sn plates in solder joints, especially solidified in a relatively slow cooling rate, is one issue of concern. In the previous studies, the implication of large Ag3Sn plates on solder joint performance has been reported in addition to several methods to control the formation of large Ag3Sn plates. In this study, the effects of minor Zn alloying addition are investigated to control the formation of large Ag3Sn plates. The minor Zn addition has found to reduce the amount of undercooling required for the solidification and thereby to suppress the formation of large Ag3Sn plates. The Zn addition has also caused the changes in the microstructure in bulk as well as the interfacial reaction. The interaction of Zn with other alloying elements in the solder has also been

investigated to understand the role of Zn during the solidification of the near-ternary-eutectic alloys.

# 8:55 AM

Contact Angle Measurements of Sn-Ag and Sn-Cu Lead-Free Solders on Copper Substrates: *Mario F. Arenas*<sup>1</sup>; Viola L. Acoff<sup>1</sup>; <sup>1</sup>The University of Alabama, Metallurgl. & Matls. Engrg., PO Box 870202, Tuscaloosa, AL 35487 USA

Due to environmental concerns, a variety of Pb-free solder alloys have been proposed to replace the conventional Pb-37Sn as a general use solder. Eutectic solders of compositions Sn-3.5Ag (wt%) and Sn-0.7Cu (wt%) are strong candidates for that purpose. Implementation of those solder alloys requires detailed knowledge of the wettability of the new alloys on copper substrates. Since wettability is generally described by the contact wetting angle, its determination is of particular interest. In this study, the contact angles of various lead-free solders, belonging to the eutectic systems mentioned above, were measured on copper substrates to investigate the wetting behavior. Measurements were performed using the sessile-drop method under constant temperature in combination with a photographic technique that produced precise results. The effects of the addition of Bi and Cu to the Sn-Ag alloy and the type of flux were also investigated. The microstructures obtained during the wetting process were analyzed by scanning electron microscopy with energy dispersive X-ray spectroscopy. Results were compared against the conventional Pb-Sn alloy.

#### 9:15 AM

Effect of Cu Concentration on Morphology of Sn-Ag-Cu Solders by Mechanical Alloying: *Szu Tsung Kao*<sup>1</sup>; Jenq Gong Duh<sup>1</sup>; <sup>1</sup>National Tsing Hua University, Dept. of Matls. Sci. & Engrg., 101, Sect. 2 Kuang Fu Rd., Hsinchu 300 Taiwan

Cu contents in the solder alloy have recently been found to affect the intermetallic compound (IMC) formation mechanism in Sn-Ag and Sn-Ag-Cu solder system when reacted with Ni under bump metallization (UBM) after reflow. In this study, the effect of Cu concentration in the ternary Sn-3.5Ag-xCu (x=0.2, 0.7, and 1) solder alloy by mechanical alloying (MA) was investigated. The (Cu, Sn) solid solution was precipitated as Cu6Sn5 IMC which distributed non-uniformly through the microstructure. The IMCs, which exists at high Cu composition, cause the as-milled MA particle to fracture to a smaller size. Appreciable distinction on morphology of as-milled MA powders with different Cu concentration was revealed. When the Cu concentration was low (x=0.2), MA particle aggregated to a spherical ingot with large particle size. For high Cu concentration (x=0.7 and x=1), MA particle turned to flakes with smaller particle size. In addition to morphological difference, the microstructure and thermal behavior with various milling time for Sn-Ag-Cu alloy was also evaluated.

#### 9:35 AM

Effect of Silver on the Grain Boundary Pinning and Grain Growth in Bulk Tin and Bulk Eutectic Tin Silver Solder: Adwait U. Telang<sup>1</sup>; Thomas R. Bieler<sup>1</sup>; K. N. Subramanian<sup>1</sup>; <sup>1</sup>Michigan State University, Chem. Engrg. & Matl. Sci., 2527 Engrg. Bldg., E. Lansing, MI 48824 USA

Bulk specimens using 99.99% pure tin and eutectic Sn-3.5wt.%Ag were cast into a ceramic crucible in air. The specimens were metallographically polished and the microstructure was characterized over a 1000x1000  $\mu$   $^{2}$  area using orientation imaging microscopy (OIM). The initial microstructure of the pure tin showed 100-200 µ polycrystalline grains with a wide variety of misorientations in the as cast condition. After aging at 150°C for 200 hours, grain growth occurred to 250-1000  $\mu$ , and there were only two highly preferred high angle misorientations. During heating, aging, and cooling, ledges developed at grain boundaries, marking the position of most of the grain boundaries at the beginning of aging, and at the end of aging. In contrast, the OIM investigation of the bulk eutectic specimen showed 10-20  $\mu$  tin cells in a dendritic microstructure having two dominant crystal orientations with strongly preferred misorientations of <10° and 60° in a similarly sized region. Aging did not alter the eutectic microtexture but some additional high angle misorientation peaks developed. There was no ledge formation after this isothermal aging treatment. Aging caused sharpening of low angle boundaries within tin cells, and some boundaries were evident within the Ag3Sn precipitation regions. The role of Ag<sub>3</sub>Sn precipitates and the anisotropy of the thermal expansion coefficient of tin on microstructural evolution, grain boundary sliding, and ledge development is discussed.

#### 9:55 AM

Development of New Lead-Free Solder Containing Nano Sized Particles: Keun-Soo Kim<sup>1</sup>; Katsuaki Suganuma<sup>1</sup>; Minoru Ueshima<sup>2</sup>; <sup>1</sup>Osaka University, ISIR, 8-1 Mihogaoka, Ibaraki, Osaka 567-0047 Japan; <sup>2</sup>Senju Metal, Hashido 23, Adachi, Tokyo 120-8555 Japan

Controlling solidification behavior becomes one of the key factors because the formation of solidification defects must be prevented in order to accomplish stable and reliable assembling. It is expected that the addition of some solidification nuclei for Sn-Ag-Cu solder can refine the solidification microstructure and will suppress undercooling. In this study, the effects of small addition, of the nano sized metal and ceramic particles, on solidification aspects, and solderabilities of Sn-3Ag-0.5Cu lead-free solder were investigated. The solidification process of solder fillets of Sn-3Ag-0.5Cu-X joint has been examined by using in situ observation system and the solidification simulation. The useful effects of preventing solidification defect and improving solder structure can be obtained by the addition of Ni, Co or ceramic nano particles. The addition of fourth elements to Sn-3Ag-0.5Cu alloy significantly reduced the solidification defect and suppressed undercooling by being nucleation sites for solidification.

# 10:15 AM Break

#### 10:25 AM Invited

Solidification Phenomenon in CSP Soldering with Sn-Ag-Cu Lead-Free Alloy Using In Situ Observation System with Computer Simulation: Katsuaki Suganuma<sup>1</sup>; Keun-Soo Kim<sup>1</sup>; Chi-Won Hwang<sup>1</sup>; <sup>1</sup>Osaka University, ISIR, 8-1 Mihogaoka, Ibaraki, Osaka 567-0047 Japan

The formation of solidification defects in lead-free solders is greatly influenced by material factors as well as a design of circuit assemblies. The sensitivity of Sn-Ag-Cu solder microstructure to various types of circuit assemblies must be understood systematically in order to establish sound joint structures. In the present study, the solidification process of solder balls on circuit boards with a chip scale package (CSP) soldered with Sn-3wt%Ag-0.5wt%Cu has been examined primarily by using in situ observation system and the solidification simulation. Microstructural observations were carried out on soldered joints by using metallography. The solidification of solder ball on a CSP propagated from the near top region to the base chip. The solidification rate of solder balls in CSP joint is inhomogeneous and locally time dependent. The solidification simulation of CSP joint showed the solidification sequence and predicted location of soldification defects. The experimental results correlated with the simulation.

#### 10:50 AM

A Study of Solidification and Microstructure Development in Reflow of Nickel-Reinforced Nano-Composite Lead-Free Solder Paste: D. C. Lin<sup>1</sup>; T. S. Srivatsan<sup>1</sup>; G.-X. Wang<sup>1</sup>; M. Petraroli<sup>2</sup>; <sup>1</sup>University of Akron, Mech. Engrg., 302 E. Buchtel Mall, Akron, OH 44325-3903 USA; <sup>2</sup>The Timken Company, Timken Rsch., 1835 S.W. Dueber Ave., Canton, OH 44706-0930 USA

The increasing use of electronic devices in automobile and spacerelated applications puts a stringent requirement on mechanical strength and fatigue endurance capabilities of solder joints. This engineered efforts for new and improved high-strength, lead-free solders. Recent developments in nano-technology have made available a spectrum of nano-sized particles. Potential attempts have been made to form nanocomposites by using nano-particles as the reinforcing agents. A series of recent experiments have convincingly demonstrated that addition of trace amounts of nano-sized particles does significantly improve properties of the material. In this study, the base material used was the eutectic Sn-3.5%Ag alloy, and the nanoparticle was pure nickel. Nanocomposite solder pastes mixed with varying percentages of nanoparticle have been developed. Reflow experiments were performed under various cooling conditions. It was observed that addition of trace amounts of nickel nano-particles does significantly alter the solidification kinetics of the solder while concurrently influencing the intrinsic microstructural features, i.e., microstructural development and phase formation in the solidified end product. The nano-composite solders revealed appreciable increase in microhardness, up to as high as 20%.

# 11:10 AM

Can Thermodynamic Data Help Us to Develop New Solder Materials?: *Sabine Knott*<sup>1</sup>; Adolf Mikula<sup>1</sup>; <sup>1</sup>University of Vienna, Inst. of Inorganic Chmst., Währingerstraße 42, Vienna 1090 Austria

In Europe lead containing solders must be replaced by July 2006 with lead free materials. Therefore an intensive research to develop some new solder to replace Pb-Sn is going on. For the development of these new materials information of the phase diagrams, the phase equilibria and the melting behaviour is necessary. Some of these properties, like the melting temperature, the solidification path and the surface properties, must be measured. To calculate some properties like wetting and surface tension, various models can be used. For all these calculations the knowledge of the thermodynamic properties is necessary. We will show how the thermodynamic properties of the Cu-In-Zn and the Al-Sn-Zn systems are determined and how we can calculate the wetting and surface tension of these new solder materials.

# 11:30 AM

Experimental Investigation and Thermodynamic Calculation of the Phase Equilibria in the Sn-Au-Ni System: Xing Jun Liu<sup>1</sup>; Makoto Kinaka<sup>1</sup>; Yoshikazu Takaku<sup>1</sup>; Ikuo Ohnuma<sup>1</sup>; Ryosuke Kainuma<sup>1</sup>; Kiyohito Ishida<sup>1</sup>; <sup>1</sup>Tohoku University, Dept. of Matls. Sci., Grad. Sch. of Engrg., Sendai, Miyagi 980-8579 Japan

The phase equilibria in the Sn-Au-Ni system are of importance for understanding interfacial reaction between Sn base solders and Cu substrate coated by Au and Ni. In the present work, the phase equilibria of the Sn-Au-Ni system were investigated by means of differential scanning calorimetry and metallography. Six isothermal section diagrams in the Sn-rich portion at 200-600C, as well as three vertical sections at Au:Ni=1:1, 50 wt.%Sn and 40 wt.%Sn were determined. Some experimental results were obtained as follows: (1) there exists a ternary compound, SnAuNi2, which is stable up to about 400C, (2) there are very large solubilities of Au in the Ni3Sn2 in the Sn-Ni system, and of Sn in the AuSn compound in the Au-Sn system, and (3) there exists the phase equilibrium between Ni3Sn2 and AuSn compounds at 400C, rather than the continuous phase region from Ni3Sn2 to AuSn phases reported previously. Thermodynamic assessment of the Sn-Au-Ni system was also carried out using the CALPHAD method, in which the Gibbs energies of the liquid, fcc and bcc phases are described by the subregular solution model and that of compounds, including a ternary compounds, are represented by the sublattice model. The thermodynamic parameters for describing the phase equilibria were optimized, and agreement between the calculated and experimental results was obtained.

### 11:50 AM

Wetting/Spreading in the Au-Sn System: *Timothy J. Singler*<sup>1</sup>; Liang Yin<sup>1</sup>; Stephan J. Meschter<sup>2</sup>; <sup>1</sup>SUNY Binghamton, Dept. of Mech. Engrg., Binghamton, NY 13902-6000 USA; <sup>2</sup>BAE System, Failure Analy. Lab., 600 Main St., Johnson City, NY 13790 USA

Sn drops spreading isothermally on Au substrates in a gaseous flux atmosphere were used to characterize wetting/spreading in the Au-Sn system. The narrow temperature range 250<T<430°C was explored and revealed a wide variation in dynamic liquid/solid phase behavior, including partial and complete solutal freezing and the appearance of an extremely short-lived (e.g., 350 ms) transient solid phase. Contact line mobility and the roles of dissolution and formation of specific intermetallic compounds ( $\eta$  (AuSn<sub>4</sub>),  $\varepsilon$  (AuSn<sub>2</sub>),  $\delta$  (AuSn),  $\zeta$ ) in wetting are discussed.

# Magnesium Technology 2004: Automotive Applications/Welding

Sponsored by: Light Metals Division, LMD-Magnesium Committee Program Organizer: Alan A. Luo, General Motors, Materials and Processes Laboratory, Warren, MI 48090-9055 USA

Monday AM	Room: 203B
March 15, 2004	Location: Charlotte Convention Center

Session Chairs: John E. Allison, Ford Motor Company, Dearborn, MI 48124-2053 USA; Allen Schultz, Hatch Associates, Mississauga, ON L5K 2R7 Canada

# 8:30 AM

The Magnesium Powertrain Cast Components Project: Part I -Accomplishments of Phase I and the Objectives and Plans for Testing the Magnesium Engine in Phase II: Bob R. Powell<sup>1</sup>; Larry J. Ouimet<sup>1</sup>; Joy A. Hines<sup>2</sup>; John E. Allison<sup>2</sup>; Randy S. Beals<sup>3</sup>; Lawrence Kopka<sup>3</sup>; Peter P. Ried<sup>4</sup>; <sup>1</sup>General Motors Corporation, Warren, MI 48090-9055 USA; <sup>2</sup>Ford Motor Company, Dearborn, MI USA; <sup>3</sup>DaimlerChrysler Corporation, Auburn Hills, MI USA; <sup>4</sup>Ried and Associates, Portage, MI USA

The US Automotive Materials Partnership (USAMP) and the US Department of Energy launched the Magnesium Powertrain Cast Components Project in 2001 to determine the feasibility and desirability of producing a magnesium-intensive engine; a V6 engine with a magnesium block, bedplate, and structural oil pan. The Project completed the first two of five project goals: (1) evaluation of the best available low-cost, creep-resistant magnesium alloys and (2) design of the engine components. The Phase II goals of the project are: (3) casting and dynamometer- or vehicle-testing the magnesium components in

assembled powertrains, (4) developing a powertrain magnesium alloy design database and common alloy specification for magnesium powertrain alloys, and (5) promoting the building of the scientific infrastructure for magnesium in North America to enable even more advanced powertrain applications in the future. This presentation provides an overview of the Project.

# 8:50 AM

The USAMP Magnesium Powertrain Cast Components Project: Part II - Properties of Several New Creep-Resistant Magnesium Alloys: Joy A. Hines<sup>1</sup>; Robert C. McCune<sup>1</sup>; John E. Allison<sup>1</sup>; Bob R. Powell<sup>2</sup>; Larry J. Ouimet<sup>2</sup>; Randy S. Beals<sup>4</sup>; Lawrence Kopka<sup>4</sup>; Peter P. Ried<sup>3</sup>; <sup>1</sup>Ford Motor Company, Dearborn, MI USA; <sup>2</sup>General Motors Corporation, Warren, MI USA; <sup>3</sup>Ried and Associates, Portage, MI USA; <sup>4</sup>DaimlerChrylser Corporation, Auburn Hills, MI USA

As automotive companies try to reduce weight in vehicles to improve fuel economy, magnesium alloys have increasingly become an attractive replacement material for many components. However, the lack of high temperature creep resistance in the established Mg alloys such as AZ91 or AM60 has precluded their use in powertrain applications such as engine blocks. Recently, a number of new alloys have been introduced to address the lack of creep resistance at a reasonable cost. USAMP is in the third year of a five year project aimed at determining the feasibility of several new Mg alloys for use in certain powertrain components including engine blocks, low crank cases, oil pans, and front covers. The Magnesium Powertrain Cast Components (MPCC) project has examined six die casting and three sand casting alloys for their mechanical properties, corrosion resistance and castability. This talk will present some of the preliminary results of this investigation.

# 9:10 AM

The USAMP Magnesium Powertrain Cast Components Project: Part III - Fundamental Scientific Needs for Magnesium Utilization in the Powertrain Environment: Randy S. Beals<sup>1</sup>; Lawrence Kopka<sup>1</sup>; Joy A. Hines<sup>2</sup>; Robert C. McCune<sup>2</sup>; John E. Allison<sup>2</sup>; Alan A. Luo<sup>3</sup>; Bob R. Powell<sup>3</sup>; Larry J. Ouimet<sup>3</sup>; Peter P. Ried<sup>4</sup>; <sup>1</sup>DaimlerChrysler Corporation, Auburn Hills, MI USA; <sup>2</sup>Ford Motor Company, Dearborn, MI USA; <sup>3</sup>General Motors Corporation, Warren, MI USA; <sup>4</sup>Ried and Associates, Portage, MI USA

The Magnesium Powertrain Cast Components Project is a jointly sponsored effort (by the US Department of Energy and the US Council for Automotive Research) to determine the feasibility and desirability of producing a magnesium-intensive engine. Through FEA design activities and extensive alloy testing, the Project seeks to determine the technical requirements of a V-engine and which of several newly developed, high temperature magnesium alloys meet those requirements. An additional objective of the Project is to identify the fundamental scientific challenges of using magnesium alloys and casting processes in powertrain components, both within the current Project and for more advanced powertrain components, including transmission cases. The areas thus identified, such as creep and fatigue deformation mechanisms of magnesium alloys, thermodynamic and phase equilibrium databases, and predictive models of casting, manufacturing, and performance behavior will be presented and discussed. The Project program to promote new, and strengthen existing, magnesium scientific research in the North America will be described.

# 9:30 AM

Friction Stir Welding of Magnesium AM60 Alloy: *Naiyi Li*<sup>1</sup>; Tsung-Yu Pan<sup>1</sup>; Ronald P. Cooper<sup>1</sup>; Dan Q. Houston<sup>1</sup>; Zhili Feng<sup>2</sup>; Michael L. Santella<sup>2</sup>; <sup>1</sup>Ford Motor Company, Mfg. & Processes, 2101 Village Rd. MD3135, Dearborn, MI 48124 USA; <sup>2</sup>Oak Ridge National Laboratory, Metals & Ceramics, PO Box 2008, Oak Ridge, TN 37831 USA

An investigation has been carried out on the friction stir welding of magnesium alloy, AM60. Casting samples of various thickness have each been welded and their mechanical properties were presented. The microstructure and defect formation were conducted by optical and scanning electron microscopes. More attention was paid to failure mode of welded pieces near joined area or so-called thermo-mechanical affected zone under tension and voids formed during friction stir welding. In addition, the effect of FSW processing parameters and casting thickness on the mechanical properties will be presented. At the end, a cost analysis using friction stir welding for magnesium application on the Ford GT vehicles will be presented.

# 9:50 AM Break

# 10:20 AM

Friction Stir Welding of Magnesium Die Castings: Jan Ivar Skar<sup>1</sup>; Haavard Gjestland<sup>2</sup>; Ljiljana Djapic Oosterkamp<sup>3</sup>; Darryl Albright<sup>4</sup>; <sup>1</sup>Norsk Hydro ASA, Corp. Rsch. Ctr., PO Box 2560, Porsgrunn N- 3907 Norway; <sup>2</sup>Hydro Aluminium, Magnesium Competence Ctr., PO Box 2560, Porsgrunn N-3907 Norway; <sup>3</sup>Hydro Aluminium, R&D Matls. Tech., Karmøy, Haavik N-4265 Norway; <sup>4</sup>Hydro Magnesium, Mkt. Dvlp., 39209 Six Mile Rd., Ste. 200, Livonia, MI 48152 USA

Friction stir welding (FSW), being a solid-state process, is an attractive method for joining magnesium die castings. In this study, FSW of AZ91D and AM50A plates was performed on the individual alloys and to join them together. The welds were sound and free from defects, except for small surface cracks in AM50A; a fine microstructure characterized the weld zones. The mechanical properties of specimens transverse to the weld zone were measured, as were the corrosion properties. The mechanical properties were somewhat lower than the base metal, with the largest percentage decrease found in the elongation of AM50A, perhaps due to the surface cracking. The corrosion resistance of the weld zone was relatively poor, most likely due to iron contamination from wearing of the tool. Further optimization of the FSW tool design and process parameters must take place to improve the reliability of FSW for magnesium die castings.

#### 10:40 AM

Fundamental Studies of the Friction-Stir Welding of Dissimilar Magnesium Alloys and Magnesium Alloys to 6061 Aluminum: Anand C. Somasekharan<sup>1</sup>; Lawrence E. Murr<sup>1</sup>; <sup>1</sup>University of Texas, Dept. of Metallurgl. & Matls. Engrg., 500 W. Univ. Ave., El Paso, TX 79968 USA

This study involved the friction-stir welding (FSW) of various dissimilar magnesium (Mg) alloys to themselves and to 6061 aluminum (Al). This paper describes the specificities of the process used for the FSW of the Mg alloys to themselves and to Al6061, as well as the analysis of the resultant welds. The various Mg alloys used were hotrolled alloy AZ31B-H24 and semi-solid-cast alloys AZ91D (primary solid fractions of ~3% and ~20%) and AM60 (primary solid fractions of ~3% and ~20%). Dissimilar Mg alloy systems included the FSW of AZ91D with AM60, and the FSW of AZ91D with AZ31B-H24. Both Mg AZ91D and AZ31B-H24 alloys were welded to Al 6061. Numerous welds were made with the Mg alloys and Al 6061 in the advancing and retreating sides. Optical metallography was used to observe and confirm the weld zone characteristics unique to dissimilar welds. Dynamic recrystallization was observed in the weld region as well as in the transition region (HAZ), with a clear decrease in the grain size from the base material through the transition zone and into the FSW zone. The welds were free of porosities. The dissimilar Mg alloy welds revealed a homogenous, equi-axed, fine-grain structure in the FSW zone, with complex intercalated microstructures in the FSW zone. Vickers microhardness testing on the dissimilar Mg alloy systems revealed no degradation of residual microhardness of the material in the FSW zone or the transition zone. The FSW zone in the welds of Mg alloys to Al6061 showed unique dissimilar-weld characteristics such as complex intercalated microstructures with bands of recrystallized Mg inside Al and vice versa. Elemental data analysis (EDAX) was performed on the weld region to gauge the distribution of either material. Bands with equal parts of Mg and Al, as well as unique recrystallized bands with predominance of either material were observed. Vickers microhardness testing was performed on the weld cross-sections to obtain microhardness profiles that revealed the compensation of the usual degradation of Al6061 in the HAZ. TEM studies were also undertaken to further the understanding of these welds.

#### 11:00 AM

Magnesium-Lithium Alloy Weldability: A Microstructural and Property Characterization: Garrett J. Atkins<sup>1</sup>; David L. Olson<sup>1</sup>; Dan Eliezer<sup>2</sup>; <sup>1</sup>Colorado School of Mines, Matls. & Metallurgl. Engrg., 1500 S. Illinois St., Hill Hall, Golden, CO 80401 USA; <sup>2</sup>Ben Gurion University of the Negev, Dept. of Matls. Engrg., Beer Sheva 84105 Israel

Magnesium with over 10-wt % Lithium alloy addition exhibits a BCC crystal structure. This situation often offers a significant improvement in formability when compared to HCP magnesium alloys. Magnesium is commonly used as a cast alloy. However, a magnesium alloy with acceptable weldability and improved formability offers an economical advantage by allowing the use of formed wrought material along with acceptable welding procedures to fabricate welded technical assemblies. In this research the weld microstructure and properties were characterized for two magnesium-lithium alloys. With 7.5-wt% Li the first alloy is an alpha+beta alloy. The other alloy contained 10.2-wt% Li making it a fully bcc (beta) alloy. These materials were welded using the GTAW process and specific microstructures were file and characterized. Corrosion susceptibility and hardness profiles were measured and compared to a traditional magnesium alloy.

# 11:20 AM

Laser Welding of AM60 Magnesium Alloy: A. Dasgupta<sup>1</sup>; J. Mazumder<sup>1</sup>; <sup>1</sup>University of Michigan, Ctr. for Laser Aided Intelligent Mfg., Ann Arbor, MI USA

Due to limited fossil fuel reserves and stringent emission regulations, automotive companies today are keen on finding out ways to reduce fuel consumption and emission of vehicles. As a result, there has been an increased focus on lighter metals like aluminum and magnesium for auto fabrication. While much research has been done on the use of aluminum, there are lots of unanswered questions as far as use of magnesium is concerned. In this paper we have discussed the feasibility of laser welding of die-cast magnesium alloy AM60 for automotive applications. Porosity, mechanical strength and material characteristics of welds are presented. Techniques for reducing porosity are also discussed.

# Materials by Design: Atoms to Applications: Materials Chemistry and Alloy Design

Sponsored by: Electronic, Magnetic & Photonic Materials Division, EMPMD/SMD-Chemistry & Physics of Materials Committee

*Program Organizers:* Krishna Rajan, Rensselaer Polytechnic Institute, Department of Materials Science and Engineering, Troy, NY 12180-3590 USA; Krishnan K. Sankaran, The Boeing Company, Phantom Works, St. Louis, MO 63166-0516 USA

Monday AM	Room: 210B
March 15, 2004	Location: Charlotte Convention Center

Session Chair: Krishna Rajan, Rensselaer Polytechnic Institute, Dept. of Matls. Sci. & Engrg., Troy, NY 12180-3590 USA

# 8:30 AM Symposium Introduction: K. Rajan and K. K. Sankaran 8:45 AM

First Principles Multi-Scale Materials Design: William A. Goddard, III<sup>1</sup>; <sup>1</sup>California Institute of Technology, Pasadena, CA 91125 USA

Advances in theory are making it practical to consider fully first principles (de novo) predictions of the performance of materials and functional devices for many important systems and processes. In order for such de novo atomistic simulations to fully impact industrial design applications, it is necessary to develop strategies for linking the time and length scales from electrons to manufacturing. We will describe some of the advances in the atomistic methods plus the strategies in developing mesoscale descriptions of that provide fully first principles (de novo) predictions of the fundamental properties and processes for such systems. Overlapping these levels allows a bottoms-up strategy for getting a first principles description at the continuum level. We will illustrate some of the recent progress in Multi Scale Materials Design with applications to various problems in materials ranging from metals and oxides to semiconductors and polymers to nucleic acids and proteins.

# 9:15 AM

Noburnium: A 1300C Cyberalloy: Gregory B. Olson<sup>1</sup>; <sup>1</sup>Northwestern University, Dept. of Matls. Sci. & Engrg., 2220 Campus Dr., Evanston, IL 60208 USA

Under the Air Force MEANS initiative, a multi-institutional, multidisciplinary project addresses optimal integration of computational design and efficient experimentation for the accelerated design and development of high performance materials using the example of Nb-based superalloys combining oxidation resistance, creep strength and ductility for aeroturbine applications operating at 1300C and above. Integrated within a systems engineering framework, the effort tests the limits of ab-initio quantum mechanical methods to accelerate assessment of thermodynamic and kinetic databases enabling comprehensive predictive design of multicomponent multiphase microstructures as dynamic systems. Based on established principles underlying Ni base superalloys, the central microstructural concept is a dispersion strengthened system in which coherent cubic aluminide phases provide both creep strengthening and a source of Al for Al2O3 passivation enabled by a Nb-based BCC alloy matrix with required transport and oxygen solubility behaviors.

#### 9:45 AM

Interfacing Ab Initio Results to Phenomenological Alloy Thermodynamics: Patrice E.A. Turchi<sup>1</sup>; Vaclav Drchal<sup>2</sup>; Josef Kudrnovsky<sup>2</sup>; Zi-Kui Liu<sup>3</sup>; Larry Kaufman<sup>4</sup>; <sup>1</sup>Lawrence Livermore National Laboratory, C.&M.S. (L-353), PO Box 808, Livermore, CA 94551 USA; <sup>2</sup>Institute of Physics, Acad. of Scis. of the Czech Republic, Na Slovance 2, Prague 8 CZ 182-21 Czech Republic; <sup>3</sup>Pennsylvania State University, Dept. of Matls. Sci. & Engrg., University Park, PA 16803 USA; <sup>4</sup>Massachusetts Institute of Technology, Dept. of Matls. Sci. & Engrg., Cambridge, MA 02139 USA

First-principles results of alloy energetics and phase diagrams can appropriately supplement thermodynamic databases that are used within the phenomenological CALPHAD approach for predicting the stability properties of complex multi-component alloys. Routine energy minimization of alloys stability within ab initio methodology provides input to CALPHAD in terms of heats of formation and transformation for alloys exhibiting various crystalline structures, and any chemical configuration. Additionally, ab initio energetics combined with a statistical treatment provide the necessary thermodynamic information for subsequent assessments similar to those performed with experimental data within CALPHAD. Following a brief overview of the firstprinciples and phenomenological methodologies, examples of both aspects of the interfacing will be presented with applications to multicomponent alloys. Finally, validity of this interfacing and its relevance to alloy design will be discus sed. Work performed under the auspices of the U.S. Department of Energy by the University of California Lawrence Livermore National Laboratory under Contract W-7405-ENG-48.

#### 10:15 AM Break

#### 10:30 AM

**Design of Electronic Materials**: Subhash Mahajan<sup>1</sup>; <sup>1</sup>Arizona State University, Chem. & Matls. Engrg., Tempe, AZ 85287 USA

Abstract not available.

# 11:00 AM

Materials-by-Design: Direct and Inverse Methods Using Multi-Objective Stochastic Optimization: George S. Dulikravich<sup>1</sup>; <sup>1</sup>Florida International University, Dept. of Mech. & Matls. Engrg., Miami, FL 33199 USA

Alloy design for critical aero engine components such as turbine blades and discs is a difficult, time-consuming and expensive process. We propose to use and adapt an advanced semi-stochastic algorithm for constrained multi-objective optimization and combine it with experimental testing and verification to determine optimum concentrations of alloying elements in heat-resistant and corrosion-resistant stainless steel alloys that will simultaneously maximize a number of alloy's mechanical properties. The proposed research will result in a rigorous and efficient tool for the design of high-strength heat-resistant and corrosion-resistant steels unattainable by any means existing at the present time. The proposed methodologies will be applicable for the optimization of the composition of arbitrary alloys tailored to several physical properties. Inversely, for a desired set of physical properties objectives this algorithm will be able to determinate a corresponding set of candidate alloy compositions that will be able to create these specified properties.

## 11:30 AM

Experimental Phase Relations and Thermodynamics of Ultra-High Temperature Metals and Alloys: Surendra Saxena<sup>1</sup>; <sup>1</sup>Florida International University, Ctr. for the Study of Matter Under Extreme Conditions, Miami, FL 33199 USA

We may conduct phase equilibrium experiments to temperatures reaching ~4000 K. For many binary systems, only calculated data are available at such high temperatures and at other temperatures the products are poorly characterized and in-situ characterization coupled with ex-situ studies of quenched systems (e.g. high resolution transmission electron microscopy and microanalysis of phase stability) is totally missing. A detailed experimental study of phase stability at a variety of length scales coupled to the characterization of the phase transformations using electron microscopy, X-ray and Raman should establish a comprehensive basis for the design of new material microstructures and chemistries. Examples of such systems are many: W with several other metals e.g. W-Cr (1500-3400 K), W- Mo (solidmelt relation from 2600 to 3500 K), and similar binary systems with rhenium, and hafnium-based materials, silicides and binary refractory oxides such as Bi2O3-Sc2O3. The techniques are quite suitable to explore the synthesis of new alloys and intermetallics at high temperatures and also involve pressure if need be. The experimental data will be coupled to computational studies based on the use of large-scale thermochemical and crystallographic databases for the calculation and prediction of phase stability.

# Materials Issues in Fuel Cells: State-of-the-Art

Sponsored by: TMS

*Program Organizers:* Brajendra Mishra, Colorado School of Mines, Kroll Institute for Extractive Metals, Golden, CO 80401-1887 USA; John M. Parsey, ATMI, Mesa, AZ 85210-6000 USA

Monday AM	Room: 207B/C
March 15, 2004	Location: Charlotte Convention Center

Session Chairs: Brajendra Mishra, Colorado School of Mines, Metallurgl. Engrg., Golden, CO 80401 USA; Z. Gary Yang, Pacific Northwest National Laboratory, Matls. Sci. Div., Richland, WA 99352 USA

#### 8:30 AM Keynote

The Hydrogen Economy: Opportunities of Materials and Nanomaterials to Address Some Grand Challenges: M. S. Dresselhaus<sup>1</sup>; <sup>1</sup>Massachusetts Institute of Technology, Depts. of Elect. Engrg. & Computer Sci., & Dept. of Physics, Cambridge, MA 02139 USA

One of the Grand Challenges of the 21st Century is to achieve a sustainable energy supply. The 20th Century has seen remarkable advances in Science and Technology, resulting in expectations for a higher standard of living. This has required large increases in per capita energy consumption. Projections of per capita energy needs for the 21st Century indicate that new technologies for sustainable energy production, storage, and use will need to be developed in the next 50 years. The so-called hydrogen economy is one such proposal that is presently being considered worldwide. In this talk the requirements of a hydrogen economy will be discussed in the context of the recent DOE report on "Basic Research Needs for the Hydrogen Economy". Hydrogen production, storage and utilization, will be discussed with emphasis given to the large gap between present science/technology knowhow and the requirements in efficiency/cost for a sustainable hydrogen economy. Opportunities for materials and nanomaterials to narrow this gap will be discussed.

# 9:10 AM Invited

Materials Issues in Fuel Cell Development and Manufacturing: Dennis W. Readey<sup>1</sup>; <sup>1</sup>Colorado School of Mines, Dept. of Metallurgl. & Matls. Engrg., 1500 Illinois St., Golden, CO 80401 USA

At present, there is considerable interest in making fuel cells commercially viable because of their promise of more efficient utilization of fuels and, in some cases, lower emissions. Fuel cells are conceptually simple but the range of applications, fuels, types, and system integration generate many materials issues. Fuel cells are currently being considered as large power sources for stationary power plants, as power sources requiring power and temperature cycling for automobiles and other vehicles, and as small energy sources to replace batteries in laptop computers and hand-held electronic devices. In addition, although there is a current emphasis on hydrogen as a fuel, there is a need to have fuel cells that can operate on hydrocarbons such as methane and renewable fuels such as methanol. Finally, there are different approaches to fuel cells depending on the nature of the ionconducting electrolyte with the current interest focused on hydrogen conducting polymer electrolytes and either oxygen or hydrogen conducting oxides. Materials issues range from the ionic conductivity of the electrolyte to the manufacturability of cell components. Critical materials issues for fuel cells are identified and their status and potential analyzed.

# 9:40 AM Invited

SOFC and PEM Materials Challenges and Development at Ford Motor Company: Alexander Bogicevic<sup>1</sup>; <sup>1</sup>Ford Motor Company, Rsch. & Advd. Engrg., 2101 Village Rd., Scientific Rsch. Labs., MD 3083, Dearborn, MI 48188 USA

Ford Motor Company is devoting significant research resources to the development of mobile and stationary fuel cell applications based on SOFC and PEM fuel cell technology. These include fuel cells for powertrain applications, auxiliary power units, and emissions abatement systems at automotive manufacturing plants. This presentation will focus on principal materials development challenges that underpin the technology progress in each of these applications. A broad perspective on how these are addressed within corporate, government, and university institutions will be given, and further development needs discussed.

10:10 AM Break

# 10:20 AM

**Thermodynamic Modeling of the LaCoO3-ä**: *Mei Yang*<sup>1</sup>; Zi-Kui Liu<sup>2</sup>; <sup>1</sup>Pennsylvania State University, Dept. Matls. Sci. & Engrg., 304 Steidle Bldg., University Park, State College, PA 16802 USA; <sup>2</sup>Pennsylvania State University, Dept. Matls. Sci. & Engrg., 209 Steidle Bldg., University Park, State College, PA 16802 USA

The perovskite-type binary oxide LaCoO3 has many possible applications in different fields, such as heterogeneous catalysis, oxygen sensors, solid oxide fuel cells and magnetic media. This oxide has a wide range of oxygen deficiency depending on temperature and oxygen partial pressure, which greatly affects its stability under service environment. It is thus desirable to establish a procedure to develop thermodynamic properties of this perovskite so its stability can be predicted. In the present work, the thermodynamic modeling and the first-principles calculations will be combined to obtain the Gibbs energy of LaCoO3-ä as a function of temperature and oxygen deficiency. As a solution phase, LaCoO3-ä was described by a three sublattice model (La)1(Co)1(O,Va)3. (La)1(Co)1(O)3 and (La)1(Co)1(Va)3 are two end-members of this LaCoO3-LaCoVa3 pseudo-binary system. The First-Principles calculations were performed using the computer code: VASP based on the pseudo-potentials and a plane wave basis set. The ground state total energies of the pure La, Co and O, and the both end-members of LaCoO3-ä were calculated at 0 K. The enthalpies of formation of the both end-members were obtained accordingly and used as a supplement in Thermo-Calc to evaluate the optimized Gibbs energy functions for LaCoO3-ä. Good agreement with experimental data is obtained by this combined Computational thermodynamics/ First-Principles calculations novel approach.

# 10:45 AM

Bismuth Substituted Dysprosium Iron Garnets for Magento-Optic Devices: *Pragati Mukhopadhyay*<sup>1</sup>; *Gautam Mukhopadhyay*<sup>2</sup>; <sup>1</sup>Indian Institute of Technology-Bombay, Advd. Ctr. for Rsch. in Elect., Powai, Mumbai, Maharashtra 400076 India; <sup>2</sup>Indian Institute of Technology-Bombay, Dept. of Physics, Powai, Mumbai, Maharashtra 400076 India

Bismuth substituted iron garnet (Bi DyIG) films are potential materials for magneto-optic devices. Efforts are being made world over to make films by various methods to enhance magneto-optic properties and make low cost viable devices. We have grown and reported many different rare earth substituted bismuth iron garnet films by LPE (Liquid Phase Epiptaxy) with enhanced magneto-optic properties but not of low cost. We report here the preparation and characterization of bismuth substituted dysprosium iron garnet films by an inexpensive sol gel method utilizing a modified chelating agent. By this method single phase garnet films can be grown with ease on larger surfaces on variety of substrates.

# 11:10 AM

Preparation of Ti-Fe-O Thin Films by Pulsed Laser Deposition: *Tsuneo Suzuki*<sup>1</sup>; Shuntaro Suzuki<sup>1</sup>; Satoko Ogata<sup>1</sup>; Makoto Hirai<sup>1</sup>; Hisayuki Suematsu<sup>1</sup>; Weihua Jiang<sup>1</sup>; Kiyoshi Yatsui<sup>1</sup>; <sup>1</sup>Nagaoka University of Technology, Extreme Energy-Density Rsch. Inst., 1603-1, Nagaoka, Niigata 940-2188 Japan

An intermetallic compound of TiFe is known as one of the reversible hydrogen storage alloys. Ti-Fe thin films have been prepared by Pulsed laser deposition. Although, the thin film prepared by the PLD method consisted of TiFe phase, the thin film contained the oxygen of 23 at. %. Although, the thin film prepared by the PLD method consisted of TiFe phase, the thin film contained the oxygen of 23 at. %. In previous work, by changing the titanium and iron contents in the Ti-Fe-O thin films, the thin films were observed to become from b-Ti phase dissolving iron atoms of 35% to TiFe one. In order to reveal the phase transition from b-Ti to TiFe phase in Ti-Fe-O thin film, we have changed the composition of the thin film by changing the surface area ratio of the targets (Ti and Fe plates).

# 11:35 AM

The Application of Planetary Ball Mill "Activator" for Fuel Cells Materials Synthesis in Industry Scale: Belyaev Eugene Yurievich<sup>1</sup>; <sup>1</sup>Activator Corporation, Musy Dzhalilya, 25, Novosibirsk, Novosibirsk reg 630055 Russia

The "Activator" mill predestinated for chemical synthesis under reactants intensive mechanical treatment. We were developing ones for synthesis nanostructures materials with the productivity 3-5 kg/h. The "Activator" advantages are: rotation speed 1200 rpm (balls acceleration up to 2000 m/sec2); smart balls moving by software control; active jars cooling by water; 4 or 6 jars (1 liter volume each). The process examples: preparing nanocomposite materials for solid oxide fuel cells (SOFC) - metal/YSZ or oxide/YSZ composites, solid state synthesis of perovskite structure materials (La1-XSrXMnO3, La1-XSrXFe1-YCoYO3). The mixing, preliminary annealing and grinding are the main part of ceramics technology. The mechanochemical advances are the steps diminishing and cost optimizing. The carbon nanostructures for fuel cells elements are easy produced by carbon treatment and controlled crystallization ones. By intensive milling, graphite structure was deformed and became amorphous. By recrystallization during annealing, the structure fragments is conversed to nanostructures - nanotubes or onion-like carbon. The advances are in low energy consumption and high productivity. We were optimizing chemical processes in jars by controls of balls moving and treatment regimes: impact (for grinding) - vortex (for mixing) - impact and shift (for synthesis). These regimes are programming by software because the central axis and planetary rotation separated by mechanics and controls by inverters.

# Materials Processing Fundamentals: Solidification and Casting

Sponsored by: Extraction & Processing Division, Materials Processing & Manufacturing Division, EPD-Process Fundamentals Committee, MPMD/EPD-Process Modeling Analysis & Control Committee

*Program Organizers:* Adam C. Powell, Massachusetts Institute of Technology, Department of Materials Science and Engineering, Cambridge, MA 02139-4307 USA; Princewill N. Anyalebechi, Grand Valley State University, L. V. Eberhard Center, Grand Rapids, MI 49504-6495 USA

Monday AM	Room: 2	12B		
March 15, 2004	Location:	Charlotte	Convention	Center

Session Chair: TBA

# 8:30 AM Invited

Technical Issues Impeding the Proliferation of Continuous Casting Processes in the Aluminum Industry: Prince N. Anyalebechi<sup>1</sup>; <sup>1</sup>Grand Valley State University, Padnos Sch. of Engrg., L. V. Eberhard Ctr., Ste. 718, Grand Rapids, MI 49504-6495 USA

In the past 35 years, the use of continuous casting in the Aluminum Industry has been mostly confined to "common alloy products" such as foils, electric conductor rods, building products, selected food packaging alloys, etc. Development of surface sensitive, high formability and drawability products, such as beverage can stock and automotive sheet continues to be technically challenging. This is ascribed to: (a) our insufficient understanding of the complex and dynamic phenomena that occur at the mold/metal interface during solidification and the constraints they place on productivity, product surface quality, range of "castable" aluminum alloy compositions, and cast microstructure; and (b) the lack of appropriate downstream process technology to take advantage of the unique metallurgical characteristics of continuously cast products. These and other reported technical problems encountered in the continuous casting of higher strength aluminum alloys and their attendant effects on the metallurgical characteristics of the final products are discussed.

# 9:00 AM

Effects of Alloying Elements on the Empirical Relationships Between Dendrite Arm Spacing and Solidification Processing Conditions in Aluminum Alloys: *Prince N. Anyalebechi*<sup>1</sup>; <sup>1</sup>Grand Valley State University, Padnos Sch. of Engrg., L. V. Eberhard Ctr., Ste. 718, Grand Rapids, MI 49504-6495 USA

Published and unpublished experimentally determined values of dendrite cell size and arm spacing in aluminum alloys as a function of solidification conditions and alloy composition have been critically reviewed and collated. Functional empirical models for predicting the effects of alloying elements, solidification rate, and local solidification time on dendrite arm spacing in binary and multicomponent aluminum alloys have been developed. Results of the study indicate that secondary dendrite arm spacing (or cell size) in aluminum alloys generally decrease with increase in solidification rate and by addition of titanium, copper, iron and silicon. Conversely, secondary dendrite arm spacing (or cell size) in cast aluminum products increases with increase in local solidification time and by addition of zinc. Magnesium, the most widely used alloying element in the aluminum industry, does not have any statistically significant effect on dendrite coarsening in commercial aluminum alloys.

# 9:20 AM Cancelled

Evaluation of the Reactivity of Gamma Titanium Aluminides with Multi-Layered, Yttria Face Coat, Investment Casting Shells

## 9:40 AM

**Control of a Die Casting Simulation Using an Industrial Adaptive Model-Based Predictive Controller**: *Richard Vetter*<sup>2</sup>; Daan M. Maijer<sup>1</sup>; Mihai Huzmezan<sup>2</sup>; Duncan Meade<sup>3</sup>; <sup>1</sup>University of British Columbia, Dept. of Metals & Matls. Engrg., 309 - 6350 Stores Rd., Vancouver, BC V6T 1Z4 Canada; <sup>2</sup>University of British Columbia, Dept. of Elect. & Compu. Engrg., 2356 Main Mall, Vancouver, BC V6T 1Z4 Canada; <sup>3</sup>Universal Dynamics Technologies Inc., 100-13700 International Place, Richmond, BC V6V 2X8 Canada

Mathematical modeling and simulation is a common technique to improve and optimize industrial processes. Complex models of casting processes are available to describe the evolution of process variables such as temperature and pressure, and can be used to reliably predict defect formation. Similarly, advances in control theory have lead to widespread use of online control for the majority of industrial processes. A multivariable control scheme has been developed to control a 2-D axisymmetric model of an industrial low-pressure wheel die casting process for use in assessing predictive control strategies to reduce defect formation. Temperatures at various locations within the die are controlled to predefined set points based on the cyclic steady state temperature profile. The volume flow rates of cooling media in multiple channels are used as control variables. The incoming molten aluminum temperature and die open time are used as a measured disturbance variables for the controller. The commercial adaptive predictive controller, BrainWave, which uses Laguerre basis functions to build its control models, has been used to control this virtual process.

#### 10:00 AM Break

#### 10:20 AM

Examination of Liquid-Tin Assisted Directional Solidification for Large Ni-Base Superalloy Castings: Andrew J. Elliott<sup>1</sup>; Graeme B. Karney<sup>2</sup>; Tresa M. Pollock<sup>1</sup>; Michael F.X. Gigliotti<sup>3</sup>; Warren T. King<sup>4</sup>; <sup>1</sup>University of Michigan, Matls. Sci. & Engrg., 2300 Hayward St., Ann Arbor, MI 48109-2136 USA; <sup>2</sup>Oxford University, Matls. Sci., Parks Rd., Oxford OX1 3PH UK; <sup>3</sup>GE, Corp. R&D, Niskayuna, NY 21309 USA; <sup>4</sup>GE, Power Sys., Greenville, SC 29602 USA

The liquid metal cooling (LMC) process has been used to directionally solidify large stepped cross-section Ni-base superalloy castings with significantly enhanced thermal gradients and increased withdrawal rates compared to the conventional radiation cooling process. The improved LMC process capabilities resulted in considerably enhanced cooling rates, refined microstructure, and reduced occurrence of casting defects, including elimination of freckle-type defects. Experiments designed to isolate individual process variables including withdrawal rate, superheat, and baffle thickness have been carried out in order to better understand the LMC process and how to optimize the casting process with particular emphasis on the solid-liquid interface location and shape. Relationships between process conditions and primary and secondary dendrite arm spacing are also investigated.

#### 10:50 AM

Columnar to Equiaxed Transition Analysis During Directional Solidification of Different Alloy Systems: Alicia Esther Ares<sup>2</sup>; Rubens Caram<sup>3</sup>; *Carlos Enrique Schvezov*<sup>1</sup>; <sup>1</sup>University of Misiones, 1552 Félix de Azara St., Posadas-Misiones 3300 Argentina; <sup>2</sup>CONICET, 1552 Félix de Azara St., Posadas-Misiones 3300 Argentina; <sup>3</sup>University of Campinas, CP 6122, Campinas-Sao Paulo CP 6122 Brazil

Experiments were carried out in which the conditions of columnar to equiaxed transition (CET) in directional solidification of dendritic alloys are known, in alloy systems such as Al-Cu, Al-Mg, Al-Zn, Al-Li, Al-Si, Al-Si-Cu, Cu-Zn, Pb-Sn, Sn-Pb and stainless steel. These experiments allow determine that two interfaces are defined, assumed to be macroscopically flat. The transition does not occur in abrupt form in the samples and is presented when the gradient in the liquid ahead of the columnar dendrites reaches critical and minimum values, being negative in most of cases. Finally, the own experimental results are compared with the reported in the literature by other authors, such as, Kisakurek in Pb-Sn alloys, Mahapatra and Weinberg in Sn-Pb alloys, Flood and Hunt, Ziv and Weinberg, Fredriksson and Olsson and Wang and Beckermann in Al-Cu alloys, Gandin in Al-Si alloys, and Poole and Weinberg in stainless steel.

#### 11:20 AM

Microstructure Analysis of ZA Alloy Rod Directionally Solidified by Heated Mold Continuous Casting: Ying Ma<sup>1</sup>; Yuan Hao<sup>1</sup>; Feng Yun Yan<sup>1</sup>; Hong Jun Liu<sup>1</sup>; <sup>1</sup>Lanzhou University of Science & Technology, State Key Lab of Advd. Non-Ferrous Matls., 85 Langongping Rd., Lanzhou, Gansu 730050 China

The as-cast and heat treatment microstructure of ZA alloy rod directionally solidified by continuous casting has been analyzed. The results show that the microstructure of the ZA alloy line is the parallel directional dendritic columnar crystal. Each dendritic crystal of eutectic alloy ZA5 is composed of many layer eutectic âandçphases. The microstructure of hyper eutectic ZA alloys is primary dendritic crystal and interdendritic eutectic structure. The primary phase of ZA8 and ZA12 is âphase, while the primary phase of ZA22 and ZA27 is á phase.

#### 11:40 AM

The Solidification of Ceramic-Reinforced Superalloy: *Rui Shao*<sup>1</sup>; Matthew J.M. Krane<sup>1</sup>; Kevin P. Trumble<sup>1</sup>; <sup>1</sup>Purdue University, Sch. of Matls. Engrg., 501 Northwestern Ave., W. Lafayette, IN 47907-2036 USA

Abrasive blade tips are sometimes used on turbine blades to increase turbine engine efficiency by decreasing gas leakage at the blade tips. This research studied a potential method for producing ABT in situ in the blade casting processing. A porous ceramic preform was infiltrated with liquid Ni-based superalloy under a gas pressure of about 1 atm, and then the alloy was solidified directionally at different rates through the preform, producing a metal-matrix composite. Single crystals were achieved at cooling rates  $\leq 15$  K/min. Laue X-ray diffraction showed that the orientation of the metallic grains were unaffected by the preform and no strange grains were nucleated there. Solidification and heat transfer were modeled using a commercial control-volume based code. The model predicted that the temperature gradient in the composite is higher than in the alloy without a preform, and so it is possible that the presence of the preform can suppress heterogeneous nucleation.

# Nanostructured Magnetic Materials: Recent Progress in Magnetic Nanostructures

Sponsored by: Electronic, Magnetic & Photonic Materials Division, EMPMD-Superconducting and Magnetic Materials Committee, EMPMD-Nanomaterials Committee Program Organizers: Ashutosh Tiwari, North Carolina State University, Department of Materials Science & Engineering, Raleigh, NC 27695-7916 USA; Rasmi R. Das, University of Wisconsin, Applied Superconductivity Center, Materials Science and Engineering Department, Madison, WI 53706-1609 USA; Ramamoorthy Ramesh, University of Maryland, Department of Materials and Nuclear Engineering, College Park, MD 20742 USA

londay AM	Room: 2	15
larch 15, 2004	Location:	Charlotte Convention Center

Session Chair: TBA

Μ

Μ

### 8:30 AM Introductory Remarks

#### 8:40 AM Invited

**Magnified Magnetocaloric Effects in Magnetic Nanocomposites:** *R. D. Shull*<sup>1</sup>; V. Provenzano<sup>1</sup>; <sup>1</sup>National Institute of Standards and Technology, Magnetic Matls. Grp., Gaithersburg, MD USA

Upon the removal of a magnetic field from a material, the resulting reduction in magnetic spin alignment represents an increase in the material's spin entropy ( $\Delta$  S). If the field reduction is performed adiabatically so that the total entropy change is zero, then the increased spin entropy is offset by an equal decrease in lattice entropy, as reflected by a decrease in the temperature of the material. This  $\Delta T$  is called the magnetocaloric effect, and it is a property of the material and its magnetic state. The magnetocaloric effect, upon which the technology of magnetic refrigeration depends, may be enhanced in certain field and temperature regimes by finely dividing and grouping a ferromagnetic species in a nonmagnetic or weakly magnetic matrix, as in a magnetic nanocomposite. Here the basis for this enhancement will be reviewed and experimental data measured on several magnetic nanocomposites will be presented in proof of the earlier predictions of this effect. In particular, experimental verification of cluster calculations will be provided by experimental data for a new magnetic nanocomposite,  $Gd_3Ga_{5-x}Fe_xO_{12}$  (GGIG), that is superparamagnetic and possesses magnetocaloric effects 3-4 times larger than those of the presently preferred low-temperature paramagnetic refrigerant, gadolinium gallium garnet (GGG). This new material possesses the potential for both increasing the operating temperature of magnetic refrigerators and lowering the magnetic fields required for their operation.

Magnetic refrigerators could then be substantially reduced in size, made much more efficient, and enable cooling to much higher temperatures.

# 9:10 AM Invited

# Understanding Nanomagnetism Via In-Situ Magnetization and Induction Mapping of Lithographically Patterned Arrays: Y. Zhu<sup>1</sup>; <sup>1</sup>Brookhaven National Laboratory, Upton, NY 11973 USA

Understanding spin dynamics, configuration and nano-scale magnetization process is crucial to the development of novel magnetic materials, especially for recording media and data storage applications. Here, modern electron microscopy plays an indispensable role in revealing time-resolved magnetic structural behavior. We report our in-situ studies of magnetic domain evolution of Ni, Co and permalloy islands and arrays on non-magnetic film matrix during magnetization and demagnetization process using electron holography and Lorentz phase microscopy. We develop quantitative procedures for phase retrieval in conjunction with preparing the assemblies that have well controlled geometry via electron beam lithography to separate magnetic potential from electrostatic potential. We focus our attention on the local induction distribution and magnetic interaction of the individual magnetic elements as a function of their size, shape and distance. Experimentally observed vortex-spin configurations are compared with calculations including micromagnetics simulation. Collaborations with V. Volkov, M. Schofield, M. Beleggia, J. Lau, M. De Graef and M. Malac are acknowledged. Work supported by US DOE, No. DE-AC02-98CH10886.

# 9:40 AM Invited

# Nanostructured Magnetic Materials for Electronic and Bio Applications: Sungho Jin<sup>1</sup>; <sup>1</sup>University of California, Dept. of Mech. & Aeros. Engrg., 9500 Gilman Dr., La Jolla, CA 92093-0411 USA

The properties and use of modern magnetic materials depend much on their nano-scale microstructure. In Fe-Cr-Co spinodal type permanent magnetic materials, the control of the dimension and shape of the microstructure is crucial. By making the (Fe, Co)-rich ferromagnetic phase elongated in nanoscale dimension within a matrix of Crrich non-magnetic phase, superior magnetic properties are achieved because of the shape anisotropy of the ferromagnetic phase introduced by microstructural control. Magnetic field heat treating process or deformation aging process can be utilized to produce desirable anisotropic two-phase microstructure. One examplary application of such a material is the magnetically tunable optical fiber grating device useful for telecom channel switching. In magnetically switchable materials such as phase-decomposed microduplex Fe-6% Ni alloys, the control of size, shape and twist of each of the phases can produce fast and abrupt magnetization reversal and voltage impulse signals which may be useful for sensor or actuator functions in electronic or bio applications.

# 10:10 AM Invited

# Field-Tuned Collapse of an Orbital Ordered and Spin-Polarized State: Colossal Magnetoresistance in Bilayered Ruthenate: G. Cao<sup>1</sup>; <sup>1</sup>University of Kentucky, Dept. of Physics & Astron., Lexington, KY 40506 USA

The bilayered  $Ca_3Ru_2O_7$  with a Mott-like transition at 48 K features different in-plane anisotropies of magnetization and magnetoresistance. Applying magnetic field along the magnetic easy-axis precipitates a spin-polarized state via a first-order metamagnetic transition, but does not lead to a full suppression of the Mott state, whereas applying magnetic field along the magnetic hard axis does, causing a resistivity reduction of three orders of magnitude. The novelty of this bilayered  $Ca_3Ru_2O_7$  is that the colossal magnetoresistivity is a result of the collapse of the orbital ordered state that is realized by demolishing the spin-polarized state. This new phenomenon is striking in that the spin-polarization, which is a fundamental driving force for all other magnetoresistive systems, is detrimental to the colossal magnetoresistence in this 4d-based electron system! Evidence for a density wave is also presented. This work was supported by a NSF grant DMR-0240813.

# 10:40 AM

# Magnetocaloric Effect in Nanoscale Ferromagnetic Composites: Alex Umantsev<sup>1</sup>; <sup>1</sup>University of North Carolina, Natural Scis., 1200 Murchison Rd., Lyons Scis. Bldg., Fayetteville, NC 28301 USA

Magnetic refrigeration is an efficient cooling technology due to the magnetocaloric effect of some materials. Upon the adiabatic removal of a magnetic field from the materials, increased spin entropy is offset by an equal decrease in lattice entropy, as reflected by a decrease in the temperature of the material. This temperature decrease is called the magnetocaloric effect, and it is a property of the material and its magnetic state. The crux of the problem presented here is that nanoscale particles stabilize unusual magnetic phases that are completely unstable in the bulk. I will present a theory of a refrigeration cycle that employs such unusual magnetic phases and discuss a possibility of using such cycles at room temperatures. Although there has been significant progress made recently in the area of magnetic refrigeration in nanoscale ferromagnetic composites, the effect that will be discussed here has not been address yet.

#### 11:00 AM

Enhancement of Ferromagnetism and Metallicity of the Ru Doped Two Dimensional Layered Manganite  $La_{1,2}Ba_{1,8}Mn_2$ ,  $_{x}Ru_{x}O_7$  (x = 0, 0.1, 0.5, and 1.0): Nori Sudhakar<sup>1</sup>; K. P. Rajeev<sup>1</sup>; A. K. Nigam<sup>2</sup>; <sup>1</sup>Indian Institute of Technology, Dept. of Physics, Kanpur, Uttar Pradesh 208016 India; <sup>2</sup>Tata Institute of Fundamental Research, Homi Bhabha Rd., Colaba, Mumbai, Maharashtra 400005 India

The electrical transport and magnetic studies of the Ru doped 2D layered manganite system  $La_{1,2}Ba_{1,8}Mn_{2,x}Ru_xO_7$  (x=0,0.1,0.5,1.0) have been carried out in the temperature range of 5 to 320 K and in the presence of magnetic fields up to 7 T in order to investigate the low temperature magnetic state of the system. The electrical resistivity ( $\rho$ ) curves show a peak at high temperatures and well defined minima at low temperatures akin to the colossal magnetoresistive (CMR) materials. Ru doping has increased the ferro-para transition temperature ( $T_c$ ), saturation magnetization and the hysteresis up to x=0.5. We expect that the mixed valency of Ru (Ru<sup>4+</sup>/ Ru<sup>5+</sup>) and Mn (Mn<sup>3+</sup>/ Mn<sup>4+</sup>) will lead to interesting results because of the possibility of Mn-O-Ru superexchange in addition to the usual Mn-O-Mn conduction channels already present in the system. We hitherto report rather high  $T_c$  values (> 310 K) obtained for the layered manganites.

#### 11:20 AM

A Novel MRAM Design Using Square Ring Elements for the Hard Layer: Dwarakanath N. Geerpuram<sup>1</sup>; Anand S. Mani<sup>1</sup>; <sup>1</sup>University of Illinois, Dept. of Elect. & Compu. Engrg., 851 S. Morgan M/C 154, Rm. 1020 SEO, Chicago, IL 60607 USA

Previous MRAM designs use structures where the switching phenomenon and the switching field strengths are constrained by the imperfections introduced in the fabrication process. We propose to use onion states in square rings for data storage in the MRAM. The onion state corresponds to each half of the square ring, on either side of the diagonal, having the same magnetization orientation and forming head-to-head and tail-to-tail domain walls. We have experimentally verified, for  $2\mu$ m permalloy rings, using Magnetic Force Microscopy that the onion state is stable at remanence. The switching between two onion states is nucleation free and occurs through the formation of a unique state called the horseshoe by domain wall movement. We have also verified that this unique switching mechanism is reproducible over an array of rings. Moreover, it is not affected by fabrication imperfections. In fact, switching can be controlled by specifically induced asymmetries in the rings.

#### 11:40 AM

Magnetic Interactions Between Nano Particles of Arbitrary Shape: A Fourier Space Approach: Shakul Tandon<sup>1</sup>; Marco Beleggia<sup>2</sup>; Yimei Zhu<sup>2</sup>; *Marc De Graef*<sup>1</sup>; <sup>1</sup>Carnegie Mellon University, Matls. Sci. & Engrg., 5000 Forbes Ave., Pittsburgh, PA 15213-3890 USA; <sup>2</sup>Brookhaven National Laboratory, Matls. Dept., Upton, NY 11973 USA

A new formalism has been developed to describe the demagnetization field around a particle of arbitrary shape and uniform or nonuniform magnetization state. The formalism relies on a Fourier Space description of particle shape, through the so-called shape amplitude. We will present examples of the computation of the demagnetization tensor field for several particle shapes, including the cylinder and facetted particles. We will introduce a formalism for the computation of the magnetostatic interaction energy between arbitrarily shaped particles. We will focus in particular on the interactions between cylindrical disks, and describe the interactions for in-plane and perpendicular magnetization states. Analytical computations are possible for systems with a small number of interacting disks, and we will show that the symmetric three-disk system undergoes a discontinuous phase transition from a regular vortex state with zero net magnetization to a dipolar ferromagnetic state described by a magnetic order parameter.

# Nanostructured Materials for Biomedical Applications: Session I

Sponsored by: Electronic, Magnetic & Photonic Materials Division, EMPMD-Thin Films & Interfaces Committee Program Organizers: Roger J. Narayan, Georgia Tech, School of Materials Science and Engineering, Atlanta, GA 30332-0245 USA; J. Michael Rigsbee, North Carolina State University, Department of Materials Science and Engineering, Raleigh, NC 27695-7907 USA; Xinghang Zhang, Los Alamos National Laboratory, Los Alamos, NM 87545 USA

Monday AM	Room: 2	219A
March 15, 2004	Location:	Charlotte Convention Center

Session Chairs: Buddy D. Ratner, University of Washington, Dept. of Bioengrg. & Chem. Engrg., Seattle, WA 98195-1720 USA; Sungho Jin, University of California, Mech. & Aeros. Engrg., La Jolla, CA 92093-0411 USA

# 8:30 AM Introductory Comments: Nanostructured Materials for Medical Applications

# 8:50 AM Invited

**Nanostructure Processing of Advanced Biomaterials**: *Jackie Y. Ying*<sup>1</sup>; <sup>1</sup>Institute of Bioengineering and Nanotechnology, 51 Sci. Park Rd. 01-01/10, The Aries, Science Park II, Singapore 117586 Singapore

Nanostructured materials are of interest for a variety of applications. This talk describes the synthesis and properties of nanostructured materials that are made up of crystallites or particles of ~10 nm. They may be generated by various physical and chemical approaches with ultrahigh surface reactivity. Through controlled synthesis in reverse microemulsions, my laboratory has achieved polymeric nanoparticles for the glucose-sensitive delivery of insulin. Through chemical precipitation and additive dispersion, we have also attained nanocomposite systems as highly selective and sensitive semiconductor sensors, bioactive ceramic orthopedic implants, and efficient gene delivery vectors.

# 9:20 AM Invited

Multiscale Materials Processing and Characterization for Tomorrow's Biomaterials: Adrian B. Mann<sup>1</sup>; Richard E. Riman<sup>1</sup>; <sup>1</sup>Rutgers University, Ceram. & Matls. Engrg., 607 Taylor Rd., Piscataway, NJ 08854-8065 USA

Materials research has recently directed its focus towards biomaterials. Our perspective on biomaterials design and processing relies heavily on an understanding of natural materials. Using dental enamel as an example of a hard tissue, we will review the multi-scale structure and mechanical properties of natural biomaterials, and the limitations that lead to their failure. These will be contrasted with the limitations of current biomaterials. Our observations of existing technologies have led us to envision future biomaterials with optimized physical and chemical characteristics for hard tissue replacement. Using the power of advanced materials processing and characterization, we are developing new replacement materials that closely mimic the properties of natural tissues. As an example, natural apatites are defective and non-stoichiometric, by mechanochemical-hydrothermal methods we can dope nanostructured hydroxyapatite with ions such as carbonate, sodium, magnesium and non-stoichiometric calcium to give a material closely resembling the composition of the surrounding hard tissue.

# 9:50 AM Invited

**Bio-Nanotechnology: The Use of Nanostructured Materials as Improved Tissue Engineering Materials**: *Thomas Jay Webster*<sup>1</sup>; <sup>1</sup>Purdue University, Biomed. Engrg., 1296 Potter Bldg., W. Lafayette, IN 47907-1296 USA

Although many advanced properties for materials with constituent particle sizes less than 100 nm have been observed for traditional engineering applications, few advantages for the use of these materials in tissue-engineering have been explored. However, nanophase materials may give researchers control over interactions with biological entities in ways previously unimaginable with conventional materials. This is because organs of the body are nanostructures and, thus, cells in the body are accustomed to interacting with materials that have nanostructured features. Work will be presented that provides evidence that nanophase materials can be designed to control interactions with proteins and subsequently mammalian cells for more efficient tissue regeneration. This has been demonstrated for a wide range of nanophase material chemistries including ceramics, polymers, composites thereof, and more recently metals. Such investigations are leading to the design of a number of more successful tissue-engineering materials for orthopedic/dental, vascular, neural, bladder, and cartilage applications.

# 10:20 AM Invited

Artificial Microvasculature: The Current and the Future: Yadong Wang<sup>1</sup>; <sup>1</sup>Massachusetts Institute of Technology, Chem. Engrg., E25-342, 45 Carleton St., Cambridge, MA 02142 USA

Vital organs are highly vascularized. One of the biggest challenges in tissue engineering (TE) is the vascularization of engineered organs. To fabricate metabolically demanding organs, engineered vasculature at the micron level has to be developed. Two general strategies are employed to meet the challenge: 1. induce neovascularization by growth factors or synthetic substances in vivo; 2. microfabricate polymer scaffolds in vitro. The advantages and disadvantages of both approaches will be illustrated. The focus of this talk will be on the microfabrication approach, and I will try to speculate the direction of research in this exciting field.

# 10:50 AM Invited

Atmospheric Plasma Treatment for Surface Adhesion– Nanostructure and Chemistry: Marian G. McCord<sup>1</sup>; Suzanne R. Matthews<sup>1</sup>; Megan A. Christie<sup>1</sup>; Mohamed Bourham<sup>1</sup>; Yoon J. Hwang<sup>1</sup>; <sup>1</sup>North Carolina State University, Biomed. Engrg. Dept., Box 8301, Raleigh, NC 27695-8301 USA

PET films were subjected to atmospheric plasma treatment with He and He/O<sub>2</sub> gas plasmas. The surface chemistry and morphology of the films were extensively characterized. XPS revealed that for short treatment durations (1 - 2 min. or less), plasma treatment resulted in a decrease in surface carbon content, with a concurrent increase in surface oxygen content, and small increment in surface nitrogen content. For longer treatment durations (>2 min.), the effect began to reverse. C<sub>1s</sub> deconvolution analysis showed that C-C bonds decreased up to 1 min. in the He/Air plasma and up to 2 min. for the O<sub>2</sub> plasma, then increased again corresponding to C<sub>1s</sub> results for both gases. This increase in C-C bonds is thought to be due to sub-surface cross-linking between benzene rings as a result of UV radiation during plasma treatment. This may be attributed to an abundance of UV radiation in plasma bulk when using helium. Chain scissions by active particles in the plasma bulk and subsequent chemical reactions between molecules and active species resulted in other changes in surface chemistry. AFM showed that surface nanoscale roughness increased after plasma treatment. The surface roughness increased up to 3 min. exposure time and then decreased again for both gases. This may be the result of a deposition of nanoparticles on the PET film surface.

Preliminary work shows porcine keratinocyte proliferation increases for the plasma treated films as compared to controls. The effect of surface chemical and structural modifications on the adhesion of keratinocytes is currently being investigated. Plasma treated films with increasing nanoscale roughness will be placed in tissue culture dishes and plated with porcine epithelial cells. Cell count, adhesion, and metabolic activity will be characterized immediately following plating via fluorescent assay and centrifugation, and then every day for one week, and will be correlated with surface chemical and nanostructural features as determined by XPS and AFM. Similar experiments will be performed with a series of ECM proteins, in order to determine the effects of surface nanostructure on protein binding.

# 11:20 AM Invited

Novel Laser Fabrication of Materials: Electronic Devices to Engineered Tissue Constructs: *Douglas B. Chrisey*<sup>1</sup>; <sup>1</sup>US Naval Research Laboratory, Code 6372, 4555 Overlook Ave., Washington, DC 20375-5345 USA

At the US Naval Research Laboratory (NRL), we have used pulsed lasers to process thin films and multilayers of almost all classes of materials from electronic ceramics for microwave devices to engineered tissue constructs. The novelty of processing materials this way starts with a fundamental understanding of the laser-material interaction and energy relaxation pathways and then exploiting the unique properties of lasers and materials to produce a vapor unobtainable by conventional physical or chemical methods. Recently, we have developed a new CAD/CAM technique for the soft laser forward transfer of a very large variety of materials called MAPLE DW for Matrix Assisted Pulsed Laser Evaporation Direct Write. The novelty in this approach is found in the laser-matrix interaction that results in a highly focused and soft material transfer. For electronic materials, this quality allows MAPLE DW to be able to transfer reproducible voxels of micron-size powders, nanoparticles, and organometallic precursors. The transfers take place at room temperature and in ambient air and we have demonstrated the mesoscopic scale (10 mm - 1 cm) fabrication of simple passive electronic devices (conductors, dielectrics, and resistors) and small sub-systems (x-band band pass filter) at low temperatures on plastic substrates (kapton). The electrical transport properties of all these component devices were comparable to more conventional thick film techniques such as screen-printing. Because of MAPLE DW's gentle nature this technique was also found to be successful in depositing patterns of viable biomaterials such as proteins, bacteria, and mammalian cells. When transferred as single layers, the cells spread out and multiply, but when deposited on top of one another they assemble and grow slowly together behaving more like natural tissue. The fabrication of three-dimensional tissue constructs that more closely replicates the heterogeneous structure of natural tissue may now be envisioned. This presentation will give an overview of the novel laser processing work being done at NRL and the fundamental science and engineering questions being answered as well as specific examples of technology being transferred to address next generation military and commercial applications.

# Phase Stability, Phase Transformation, and Reactive Phase Formation in Electronic Materials III: Session I

Sponsored by: Electronic, Magnetic & Photonic Materials Division, Structural Materials Division, EMPMD/SMD-Alloy Phases Committee

*Program Organizers:* C. Robert Kao, National Central University, Department of Chemical and Materials Engineering, Chungli City 32054 Taiwan; Sinn-Wen Chen, National Tsing-Hua University, Department of Chemical Engineering, Hsinchu 300 Taiwan; Hyuck Mo Lee, Korea Advanced Institute of Science & Technology, Department of Materials Science & Engineering, Taejon 305-701 Korea; Suzanne E. Mohney, Pennsylvania State University, Department of Materials Science & Engineering, University Park, PA 16802 USA; Michael R. Notis, Lehigh University, Department of Materials Science and Engineering, Bethlehem, PA 18015 USA; Douglas J. Swenson, Michigan Technological University, Department of Materials Science & Engineering, Houghton, MI 49931 USA

Monday AM	Room: 214
March 15, 2004	Location: Charlotte Convention Center

Session Chairs: C. Robert Kao, National Central University, Dept. of Chem. & Matls. Engrg., Chungli City Taiwan; Suzanne E. Mohney, Pennsylvania State University, Dept. of Matls. Sci. & Engrg., University Park, PA 16802 USA

# 8:30 AM Opening Remarks

#### 8:35 AM Invited

Instability of Immiscible Co/Cu Multilayered Thin-Film Structures: P. F. Ladwig<sup>1</sup>; J. D. Olson<sup>2</sup>; J. H. Bunton<sup>2</sup>; D. J. Larson<sup>3</sup>; R. M. Ulfig<sup>2</sup>; R. L. Martens<sup>2</sup>; E. Oltman<sup>2</sup>; M. C. Bonsager<sup>3</sup>; T. T. Gribb<sup>2</sup>; T. F. Kelly<sup>2</sup>; A. E. Schultz<sup>3</sup>; B. B. Pant<sup>3</sup>; Y. A. Chang<sup>1</sup>; <sup>1</sup>University of Wisconsin, Dept. of Matls. Sci. & Engrg., 1509 Univ. Ave., Madison, WI 53706 USA; <sup>2</sup>Imago Scientific Instruments Corp., Madison, WI USA; <sup>3</sup>Seagate Technology, Bloomington, MN USA

We will first present experimental evidence obtained by threedimensional atom probe (3DAP), TEM, x-ray diffraction, and DSC to show that multilayered thin-film structures of Cu/Co undergo intermixing when subjected to a thermal treatment from ambient to about 410°C. We will then provide a thermodynamic rationalization for the observed phenomena.

#### 9:00 AM Invited

Reliability Investigation and Interfacial Reaction on Lead-Free Sn-Cu/Ni BGA Package: *Seung-Boo Jung*<sup>1</sup>; Jeong-Won Yoon<sup>1</sup>; Sang-Won Kim<sup>1</sup>; <sup>1</sup>Sungkyunkwan University, Dept. of Advd. Matls. Engrg., 300 Chunchun-dong, Changan-gu, Suwon, Kyounggi-do 440-746 Korea

Among various Pb-free solders, Sn-Cu is one of the most promising Pb-free solders. Also, recent research on lead-free solders for flip-chip interconnection indicated that the Sn-0.7wt%Cu alloy had the best thermo-mechanical fatigue behavior among the lead-free alloys evaluated and could be the optimal solder alloy for such applications. The alternative materials and the possible risk of the reliability problems for the Pb-free products have been a major concern for the industries. In this paper, the growths kinetic of intermetallic compound layers

formed between Sn-3wt% Cu BGA solder and Au/Ni plated Cu substrate by solid-state isothermal aging were examined. Aging was performed for time periods of 1-100days and at temperatures of 70-170°. Also, ball shear strength values were measured to evaluate the effect of the interfacial IMC reactions on the mechanical reliability of solder bumps as a function of reflow numbers and aging. The Sn-0.7wt%Cu/Au/Ni/Cu couples provided the baseline.

# 9:25 AM Invited

Thermal and Electrical Instability of Ultra Fine Copper Interconnects Integrated with Low-k Dielectrics: Seung H. Kang<sup>1</sup>; <sup>1</sup>IC Device Technology, Agere Systems, 555 Union Blvd., Allentown, PA 18109 USA

As integrated-circuit technologies have scaled down to sub-100 nm range, its desirable circuit performance cannot be accomplished without incorporating reliable high-performance interconnects that utilize various types of metallic and dielectric films. Achieving sufficient reliability of these ultra-fine electronic interconnects has become increasingly challenging, primarily, due to revolutionary changes in materials (Cu/low-k system). Conventional electromigration and stress migration failure modes are still investigated as primary reliability issues. However, a relatively unfamiliar failure mode has emerged in relation to thermally and/or mechanically driven Cu diffusion into low-k, leading to a void in Cu (causing an open circuit) and a Cu extrusion or island in low-k (causing a short circuit). In general, this phenomenon is not observed for a silicon oxide based dielectric material. This paper investigates this failure mode at various electrical and thermal stress conditions. In particular, this paper attempts to separate this phenomenon from the conventional electromigration failure mechanism since electrical signals caused by Cu out-diffusion or extrusion to low-k may often be misunderstood as an indication of electromigration-induced damage. This paper also addresses that the integrity of Cu diffusion barrier and the microstructural quality of thin-film interfaces play a key role in the kinetics of this failure mode.

#### 9:45 AM

Compositional Shift of Alloy Semiconductors Beneath Contact Metallizations: Brett A. Hull<sup>1</sup>; Suzanne E. Mohney<sup>1</sup>; <sup>1</sup>Pennsylvania State University, Dept. of Matls. Sci. & Engrg., 206A Steidle Bldg., University Park, PA 16802 USA

Researchers have long recognized the opportunity to engineer contacts to compound semiconductors by annealing well-designed contact metallizations. For example, it is possible to exchange Ga for Al immediately beneath certain Al-bearing contacts to GaAs, leading to the formation of an alloy of AlAs and GaAs, along with an enhanced Schottky barrier height on the n-type semiconductor. We have recently found that when metal contacts are annealed on alloy semiconductors, similar compositional shifts can occur, even if no group III or V element is present in the contact metallization. Instead, preferential reaction of one component of the alloy semiconductor can take place, leaving an alloy semiconductor enriched in the other component. In this presentation, we discuss the results of experiments on this type of reaction as it occurs in late transition metal contacts to group III nitride semiconductor alloys.

#### 10:00 AM

Shallow Pd/W/Au Ohmic Contacts for Heterojunction Bipolar Transistors: Sammy H. Wang<sup>1</sup>; Eric M. Lysczek<sup>1</sup>; Joshua A. Robinson<sup>1</sup>; Suzanne E. Mohney<sup>1</sup>; <sup>1</sup>Pennsylvania State University, Dept. of Matls. Sci. & Engrg., 206A Steidle Bldg., University Park, PA 16803 USA

Very shallow ohmic contacts to p-InGa<sub>0.25</sub>Sb<sub>0.75</sub> and p-InAs base layers are required for low power heterojunction bipolar transistors under development today. We previously reported that a Pd/W/Au (5/ 50/145 nm) contact to p-InGaSb can exhibit a specific contact resistance less than 3 x 10<sup>-7</sup> Ohm cm<sup>2</sup>. Palladium makes intimate contact to the p-InGaSb, a W barrier protects the semiconductor from reaction with Au, and Au reduces the metal sheet resistance. In this presentation, we describe the long-term electrical and metallurgical stability of the contacts and the use of surface passivation to improve the performance of the shallowest contacts. For p-InAs, we have found that the Pd/W/Au contact provides a specific contact resistance approximately a factor of 2 lower than that of conventional Ti/Pt/Au contacts following very mild anneals. Materials characterization using TEM and AES will also be presented.

# 10:15 AM Break

10:30 AM Invited Improving the Barrier Integrity of Ultra-Thin Metallic Films by Tailoring Their Structure: The Case of Electroless Deposited Co-Based Alloys: Moshe Eizenberg<sup>1</sup>; Amit Kohn<sup>1</sup>; <sup>1</sup>Technion - Israel Institute of Technology, Dept. of Matls. Engrg., Technion City, Haifa 32000 Israel

The transition to copper metallization in ULSI devices requires ultra-thin conductive diffusion barriers. This research examines how the structure of metallic films can be modified in order to reduce copper diffusion via fast paths such as grain boundaries. A model system was chosen of electroless deposited cobalt-based films alloyed with phosphorus and tungsten. These elements have very limited solubility both in cobalt and copper. However, electroless deposition enables to incorporate them in the cobalt film at concentrations considerably larger than their equilibrium solubility. Following thermal annealing, the excess phosphorus and tungsten enrich the grain boundaries. We correlate between barrier integrity, structure, and copper diffusivity through the Co(P,W) films. Thus, we show that Co(P -8 at.%, W -2 at.%) and Co(P -10 at.%) films are effective barriers, considerably better than pure cobalt, because copper grain boundary diffusion is hindered due to occupation of boundary sites by the alloying elements.

#### 10:55 AM Invited

Reliability of Cu/Barrier Structure in Nanometer Interconnect Lines: Junichi Koike<sup>1</sup>; <sup>1</sup>Tohoku University, Matls. Sci., 02 Aoba, Aramaki, Aoba-ku, Sendai, Miyagi 980-8579 Japan

Interconnect lines in advanced integrated circuits has been reduced to a width of less than 100 nm. Further reduction is required in order to keep increasing device speed and cell density. The increased performance by decreasing the interconnect line width may become possible based on design-oriented expectations. However, there exist numerous material problems to meet the expectations. The major problems related to Cu/barrier interconnect lines include the reliability of an extremely thin barrier layer and the resistance to stress- and electromigration of Cu lines. These problems have thier origins to the Cu/ barrier interface properties. In the presentation, the current status of the reliability issues will be reviewed and the future direction will be presented based on our recent work on Cu/barrier interface adhesion strength and its relation to stress- and electro-migration resistance.

#### 11:15 AM

Semiconductor-to-Metallic Phase Transition of VO<sub>2</sub> by Laser Excitation: *Huimin Liu*<sup>1</sup>; Omar Vasquez<sup>1</sup>; Victor R. Santiago<sup>1</sup>; Luz Diaz<sup>1</sup>; Felix E. Fernandez<sup>1</sup>; <sup>1</sup>University of Puerto Rico, Physics, PO Box 5023, Mayaguez, PR 00681-5023 USA

VO<sub>2</sub> thin films deposited on fused quartz substrate were prepared by pulsed laser deposition technique. It shows phase transition (PT) from monoclinic semiconductor phase to a metallic tetragonal rutile structure when the sample temperature is above 68°C. The observed PT thermochromic effect was ultrafast and passive. Ultrafast PT was also observed when optically pumped by laser excitation. It was not thermally initiated in this case. An interest in understanding the mechanism was therefore motivated. In this paper we report the study of transient holography using degenerate-four-wave-mixing (DFWM) measurement to identify the PT mechanism. A Nd:YAG pulsed laser with pulse duration of 30 psec operating at 532 nm was employed as the coherent light source. It showed that the observed transient holography in VO2 thin film is associated with the excited state dynamical process which essentially causes the structural change, or so-called optically induced-PT. The observed extremely large polarizability is believed to relate with large offset in their potential well minimum between the ground state and excited state. Through an unidentified intermediate state the transient lattice distortion trigged to structural change.

#### 11:30 AM

The Relationship Between Phase Stability and High Temperature Thermoelectric Properties of La Filled IrSb3 Based Skutterudite Compounds: Sung Wng Kim<sup>1</sup>; Yoshisato Kimura<sup>1</sup>; Yoshinao Mishima<sup>1</sup>; <sup>1</sup>Tokyo Institute of Technology, Interdisplinary Grad. Sch. of Sci. & Engrg., Dept. Matls. Sci. & Engrg., 4259 Nagatsuta Midori-ku, Yokohama, Kanagawa 226-8502 Japan

We previously reported that IrSb<sub>3</sub> based ternary compounds have showed good electrical properties and the relatively high thermal conductivity prevented the enhancement of the efficiency of these compounds. Recently, we have investigated the high temperature thermoelectric properties of La filled IrSb<sub>3</sub> based skutterudite compounds from the viewpoint of decrease of lattice thermal conductivity. The relationship between phase stability and high temperature thermoelectric properties has been investigated for compounds which the adjustment of valence electron count (VEC) by Ge charge compensation in La filled compounds was conducted. It has been confirmed from the Rietveld analysis that the La atoms were placed in structural vacancies in Ge charge compensated  $La_x Ir_4 Ge_{3x} Sb_{12-3x}$  compounds and the amount was lower than purposed amount. Owing to the rattling effect of La atoms in vacancies, the Ge charge compensated  $La_xIr_4Ge_{3x}Sb_{12:3x}$  compounds exhibited the tremendously decreased lattice thermal conductivity, 1.8W/mK from 10.2W/mK of binary IrSb<sub>3</sub>.

#### 11:45 AM

**Controlling the Microstructure from the Gold-Tin Reactions**: J. Y. Tsai<sup>1</sup>; C. W. Chang<sup>1</sup>; W. C. Luo<sup>1</sup>; Y. C. Shieh<sup>1</sup>; C. Robert Kao<sup>1</sup>; <sup>1</sup>National Central University, Dept. of Chem. & Matls. Engrg., Chungli City 320 Taiwan

For bonding applications in microelectronic and optoelectronic packages, the Au-Sn alloys have the advantages of having higher thermal conductivities, lowest melting temperature, and better mechanical properties compared to the Au-Si and Au-Ge alloys. The Au-Sn eutectic alloy with the 80%Au-20%Sn (Au20Sn, wt.%) composition is one of the most important Au-Sn alloys for these applications. The microstructure of the Au-Sn bond inevitably has a major impact on the strength of the bonding. In this study, we show that the microstructure of the Au-Sn bond can be controlled by the bonding parameters.

# Recent Advances in Non-Ferrous Metals Processing: Reactive Metals

Sponsored by: Light Metals Division, LMD-Reactive Metals Committee, EPD-Waste Treatment & Minimization Committee Program Organizers: Brajendra Mishra, Colorado School of Mines, Kroll Institute for Extractive Metals, Golden, CO 80401-1887 USA; John N. Hryn, Argonne National Laboratory, Argonne, IL 60439-4815 USA; V. I. Lakshmanan, Ortech Corporation, Mississauga, Ontario L5K1B3k Canada; V. Ramachandran, Scottsdale, AZ 85262-1352 USA; Alton T. Tabereaux, Alcoa Inc., Process Technology, Muscle Shoals, AL 35661 USA

Monday AM	Room:	205		
March 15, 2004	Locatior	: Charlotte	Convention	Center

*Session Chairs:* Brajendra Mishra, Colorado School of Mines, Kroll Inst. for Extractive Metals, Golden, CO 80401-1887 USA; John N. Hryn, Argonne National Laboratory, Argonne, IL 60439-4815 USA

# 8:30 AM Opening Remarks

#### 8:35 AM

Understanding the Electro-Reduction of Metal Oxides in Molten Salts: George Zheng Chen<sup>1</sup>; Derek J. Fray<sup>2</sup>; <sup>1</sup>University of Nottingham, Sch. of Chem., Environmental & Mining Engrg., Univ. Park, Nottingham NG7 2RD UK; <sup>2</sup>University of Cambridge, Dept. of Matls. Sci. & Metall., Pembroke St., Cambridge CB2 3QZ UK

Recent work has demonstrated that solid metal oxides can be directly electro-reduced to the respective metals or alloys in molten salts. Typically, for the electrolysis of Cr2O3, less than 0.2 wt % oxygen could be achieved in the produced metal powder with the current efficiency and energy consumption being 75% and 5 kWh/kg, respectively. However, the electrolysis of TiO2 was found to be less efficient. Based on experimental observations and hypothetical models, this paper illustrates various possible steps of the reduction mechanism, including (1) separated electron and oxygen transfer at the three phase interline (boundary), (2) metal atom aggregation and oxide surface renewal, (3) consecutive metallisation of oxide particles, (4) three-phase interline propagation and oxide cathode surface metallisation, (5) intercalation of calcium into the metal oxide cathode, (6) oxygen transport in the solid and liquid phases, and (7) interactions between molten salt and cathode before and after reduction.

#### 9:05 AM Cancelled

Hot Consolidation of Cu-Li Powders Alloys: A First Approach to Characterization

# 9:35 AM

An Overview of the Effect of Quench Rate, Pre-Age Stretch, and Artificial Aging for the Al-Li-Cu-X AF/C-458 Alloy: Aladar A. Csontos<sup>1</sup>; Brian M. Gable<sup>2</sup>; Edgar A. Starke<sup>2</sup>; <sup>1</sup>U.S. Nuclear Regulatory Commission, Office of Nucl. Matl. Safety & Safeguards, Two White Flint N., MS T7F3, 11545 Rockville Pike, Rockville, MD 20852-2738 USA; <sup>2</sup>University of Virginia, Dept. of Matls. Sci. & Engrg., 116 Engineer's Way, PO Box 400745, Charlottesville, VA 22904-4745 USA

Many Al-Li-X alloys have been investigated, however, few have gained widespread implementation into commercial aerospace applications. The recent USAF development of an isotropic Al-Li-Cu-X

alloy designated AF/C-458 has renewed interest in these low-density alloys. This talk will provide an overview of our experimental results demonstrating the effect of quench rate, pre-age plastic deformation, and artificial aging time and temperature on the AF/C-458 microstructural evolution and mechanical properties. Cooling rates of 1.8°C/sec, 68°C/sec, and 290°C/sec were used from the solutionizing anneal while the amount of pre-age stretch ranged from a 0% non-stretched condition to 8% plastic deformation. The subsequent single, duplex, and triple near-peak aged heat treatments resulted in similar mechanical properties indicating a large processing window for this alloy.

10:05 AM Break

10:20 AM Cancelled

Kennecott Utah Copper Smelter Maintenance Initiative

# 10:50 AM

The Role of Slip Length on the Ductility and Fracture Behavior of Isotropic Al-Li-Cu-X Alloys: *Aladar A. Csontos*<sup>1</sup>; Edgar A. Starke<sup>2</sup>; <sup>1</sup>U.S. Nuclear Regulatory Commission, Office of Nucl. Matl. Safety & Safeguards, Two White Flint N., MS T7F3, 11545 Rockville Pike, Rockville, MD 20852-2738 USA; <sup>2</sup>University of Virginia, Dept. of Matls. Sci. & Engrg., 116 Engineer's Way, PO Box 400745, Charlottesville, VA 22904-4745 USA

Widespread implementation of Al-Li-Cu-X alloys for aerospace applications has been hindered due in part to their characteristic anisotropic mechanical and fracture behaviors. The USAF recently developed two isotropic Al-Li-X alloys designated AF/C-489 (2.1Li wt.%) and AF/C-458 (1.8Li wt.%) with  $\varepsilon_f$  of 5% and 10%, respectively. Our study examines the role of alloy composition, grain structure, and microstructure on the slip, deformation, and fracture behaviors of these alloys. Planar slip intensities were predicted through slip intensity calculations utilizing precipitate density measurements, dislocation-particle interactions, and grain boundary misorientation-slip continuity statistics. The slip intensity predictions were then correlated to AFM slip height measurements. Our results suggest that the low ductility and coarse intergranular fracture behavior of AF/C-489 in comparison to the higher ductility and transgranular fracture behavior of AF/C-458 is most strongly attributed to the ~3 times greater slip length and to a much lesser extent on the higher Li content for AF/C-489.

# **Recycling: General Recycling**

Sponsored by: Light Metals Division, Extraction & Processing Division, LMD/EPD-Recycling Committee *Program Organizer:* Gregory K. Krumdick, Argonne National Laboratory, Argonne, IL 60439 USA

Monday AM	Room: 2	17D
March 15, 2004	Location:	Charlotte Convention Center

Session Chairs: Gregory K. Krumdick, Argonne National Laboratory, Argonne, IL 60439 USA; John M. Rapkoch, Process Metallurgy Consultant, Western Springs, IL 60558 USA

# 8:30 AM

Calculation of Recycling Rates - Fable or Truth: Markus Andreas Reuter<sup>1</sup>; Antoinette Van Schaik<sup>1</sup>; <sup>1</sup>Delft University of Technology, 120 Mijnbouwstraat, Delft The Netherlands

This paper discussed the definition and calculation of recycling rates based on the combination of dynamic modeling and the modeling of recycling systems. It is demonstrated with suitable examples from the car recycling industry how recycling rates should be calculated taking into consideration all distributed properties of the product, design, life cycle, the metallurgy and physical processing, etc. This paper will therefore give a good indication how recycling rates are being and could be determined; and if recycling quotas can be reached or not. Especially important is the fact that recycling rate should be placed within a statistical framework i.e. a recycling rate should be eassociated with a standard deviation determined by all steps within the life cycle of a car. This paper discusses the recycling of cars, but the developed methods are equally valid for any modern consumer product.

#### 8:55 AM

Statistical Study of Mo Recovery from Molybdenum Waste Catalyst: Seham Nagib Tawfic<sup>1</sup>; <sup>1</sup>Academy of Specific Study, Tech. Dvlp. Dept., Worker University, El-Darrasa, El-Tarabishi St., Cairo Egypt

Dissolution of molybdenum from molybdenum waste catalyst (MWC) that contain wt %: 42.79 Mo, 9.54 Fe, 4.9 Al, 8.68 SiO2, 6

Na, and 1.5 Cr using different leaching agents such as H2SO4, HCl, and NaOH was carried out. It was found that, NaOH is the best leaching agent because it has the highest Mo recovery in combined with the lower Fe and Al dissolution than the HCl. Factorial design of experiments and application of statistical analysis on the results of leaching studies using NaOH were carried out. A regression equation for the dissolution of Mo was developed as a function of NaOH stoichiometric (S), L/S ratio (C, ml/g), and temperature (T, oC). All parameters were varied at two levels for designing experiments to estimate error.

## 9:20 AM

Quasi-Stationary Analysis on the Chlorination and Vaporization Reaction of Pb-Oxychloride in Ash and Dust Recycling: Nan Wang<sup>1</sup>; Yoshiki WaKimoto<sup>1</sup>; Yokiko Oyama<sup>1</sup>; Shu Yamaguchi<sup>1</sup>; <sup>1</sup>University of Tokyo, Dept. of Matls. Sci. & Engrg., Sch. of Engrg., 7-3-1 Hongo, Bunkyo Ward, Tokyo 113-8656 Japan

A quasi-stationary analysis on chlorination-vaporization reaction of Pb-oxychloride in pyrometallurgical processing of ash and dust has been made, with the goals of clarification of reaction mechanism, estimation of rate-limiting step and establishment of rate-controlling equation. A molten salt layer composed of PbO-PbCl2 was considered to be formed dependent on the relative magnitude of evaporation rate of PbCl2 to its formation one, and the corresponding bulk diffusion of components throughout the formed molten salt layer was estimated to be the rate-limiting step for the overall reactions. Based upon the theoretical treatment of phenomenological mass transport equations, simulation calculation for the relative chemical potential, molar fraction and mass flux of the related components throughout molten salt layer have been performed under quasi-steady state, which can be used to evaluate the effects of treatment temperature and Cl-potential in atmosphere on the chlorination-vaporization reaction. Furthermore, the possibility of the corresponding diffusion of combined oxygenion as rate-limiting step was also proposed.

#### 9:45 AM

**Slags from Secondary Lead Processing**: *A. V. Tarasov*<sup>1</sup>; A. D. Besser<sup>1</sup>; V. M. Paretsky<sup>1</sup>; <sup>1</sup>State Research Center of Russian Federation, State Rsch. Inst. of Nonferrous Metals, 13, Acad. Korolyov St., 129515 Moscow Russia

The technology developed in the Gintsvetmet Institute for treating battery scrap and other lead-containing wastes on the basis of electrothermal smelting permits production of secondary lead with minimum amounts of slag generated (by 3 to 5 times less than in case of conventional technologies) and a reduction in the process gas volumes by 2 to 3 times. The proposed technology permits to minimize the cost of off-gas treatment due to smaller volumes as well. Electric smelting slags contain after in-furnace cleaning about 1.0% to 1.7% of lead in insoluble compounds. Such slags are rated as Class IV of toxic substances and are acceptable for utilization, e.g., in road construction. It should be noted that when treating spent batteries, mechanized dismantling and separation of individual battery components into separate fractions minimizes the content of slag-forming constituents in the charge fed to electric smelting. In combination with the use of a low-ash reductant (coke fines) this makes it possible to operate the unit for an extended period of time without replacing the slag layer in the electric furnace. In practice, the excess of slag is discharged from a full-scale electric furnace once every 10 to 15 days.

#### 10:10 AM

The Cooling and Heat Releasing Behavior of Reductive Slag During its Oxidizing: *Yuanchi Dong*<sup>1</sup>; Liaosha Li<sup>1</sup>; Zhitong Sui<sup>2</sup>; <sup>1</sup>Anhui University of Technology, Anhui Key Lab. of Metallurgl. Engrg. & Resources Recycling, Ma an shan, An hui 243002 China; <sup>2</sup>Northeastern University, Metall. Dept., Shenyang, Liaoning 110006 China

The cooling behavior of melted slag of blast furnace with oxygen blowing was studied on the foundation of experiments. The results are as following: (1) A great deal of heat will be released during slag oxidizing that resulted in the slag temperature going up. Excepting for the heat compensation of radiation losing, the released heat could bring on 300 K increment of temperature. It means that the released heat is sufficient to meet the slag re-composition having no use for added fuel. (2) The cooling rate of slag will decreased as the increasing of slag amount obviously. The rate went down below 3 K/min with 1000 kg slag and below 2 K/min with 10000 kg slag. So that it is important to control proper temperature level being benefit of the precipitation and grain growing of minerals with reasonable oxygen blowing and slag amount.

# 10:45 AM

The Spent Consumer Battery Recycling Situation in Taiwan: Esher Hsu<sup>1</sup>; *Chen-Ming Kuo*<sup>2</sup>; <sup>1</sup>National Taipei University, Dept. of Statistics, 67 Sect. 3, Min-Sheng E. Rd., Taipei 104 Taiwan; <sup>2</sup>I-Shou University, Dept. of Mech. Engrg., 1, Sec. 1, Hsueh-Cheng Rd., Ta-Hsu, Kaohsiung 84008 Taiwan

On November 11, 1999, all spent consumer batteries are proclaimed to be collected in Taiwan. Under current recycling system, all producers and importers of consumer batteries have to pay a collection/recycling fee to the Recycling Management Fund (RMF) of EPA based upon the rate approved by EPA. Collectors and recycling plants receive subsidies from RMF according to the collected and treated amounts audited by an independent auditing organization. Collected spent consumer batteries only reached 700T per year equivalent to 7% of the total quantity since 2000. How to increase collection efficiency of used batteries becomes an important issue for EPA in Taiwan. The objective of this study is to explore current recycling system of spent consumer battery in increasing collection efficiency. Results provide some suggestions to Taiwan EPA regarding recycling route, recycling system, recycling rates, and recycling subsidies.

#### 11:10 AM

The Auditing Functions in Taiwan Recycling System: Esher Hsu<sup>1</sup>; Hung-Wen Shen<sup>1</sup>; Chen-Ming Kuo<sup>2</sup>; <sup>1</sup>National Taipei University, Dept. of Statistics, 67 Sect. 3, Min-Sheng E. Rd., Taipei 104 Taiwan; <sup>2</sup>I-Shou University, Dept. of Mech. Engrg., 1, Sec. 1, Hsueh-Cheng Rd., Ta-Hsu, Kaohsiung 84008 Taiwan

In 1997, Taiwanese Environmental Protection Administration (TEPA) established a new recycling system, which is managed by government directly. In the new system, manufacturers and importers have to pay recycling fees to the TEPA Recycling Management Fund (RMF), and TEPA uses this Fund as economic incentives to encourage involvements of private companies in public sorting and recycling activities. To prevent cheating problems, TEPA also entrusts auditing companies to check the sorting and recycling amounts and qualities, and based on the reports from auditing companies, TEPA available the TEPA trial and error experience in the past five years (from 1997-2003) on the auditing operations in plastic containers recycling. Based on this case, this paper also will discuss the advantages and problems in such auditing functions in a public managed recycling system.

# R.J. Arsenault Symposium on Materials Testing and Evaluation: Session I

Sponsored by: Structural Materials Division, SMD-Mechanical Behavior of Materials-(Jt. ASM-MSCTS), SMD-Nuclear Materials Committee-(Jt. ASM-MSCTS)

*Program Organizers:* Raj Vaidyanathan, University of Central Florida, AMPAC MMAE, Orlando, FL 32816-2455 USA; Peter K. Liaw, University of Tennessee, Department of Materials Science and Engineering, Knoxville, TN 37996-2200 USA; K. Linga Murty, North Carolina State University, Raleigh, NC 27695-7909 USA

Monday AM	Room: 2	211A
March 15, 2004	Location:	Charlotte Convention Center

Session Chairs: P. K. Liaw, University of Tennessee, Matls. Sci. & Engrg., Knoxville, TN 37996-2200 USA; K. Linga Murty, North Carolina State University, Coll. of Engrg., Raleigh, NC 27695-7909 USA

# 8:30 AM Invited

Constant Stress Component Contours for Mode III Crack in Power Law Hardening Solid: Johannes Weertman<sup>1</sup>; <sup>1</sup>Northwestern University, Matls. Sci., 2220 Campus Dr., Evanston, IL 60208 USA

We found earlier a solution for the mode III crack in a power law hardening solid for full scale yielding (J. Weertman, submitted for publication). The solution consists of determining for the mode III crack problem the appropriate "space" potential in stress space (the analogue of finding the stress potential in real space). From this solution for the space potential we obtained, in real space, constant stress magnitude  $\sigma$  contours plots for various values of the power law stress exponent m ( $0 < m \le 1$ ). Here  $\sigma^2 = \sigma^2_{yz} + \sigma^2_{zx}$  where  $\sigma_{yz}$  and  $\sigma_{zx}$  are the stress components. In this paper our solution is developed further by finding, in real space and for various values of m, constant stress contours for the individual stress components  $\sigma_{yz}$  and  $\sigma_{zx}$ .

# 9:00 AM Invited

Design of Ferromagnetic Shape Memory Alloy and Composites for Fast Responsive and Robust Actuators: *Minoru Taya*<sup>1</sup>; <sup>1</sup>University of Washington, Ctr. for Intelligent Matls. & Sys., Dept. of Mech. Engrg., Seattle, WA 98195-2600 USA

The large strains in ferromagnetic shape memory alloys (SMA) such as NiMnGa induced by the applied magnetic field are the results of rearrangement of martensite variants in the ferromagnetic SMA observed at temperature T≤M<sub>f</sub>. The flow stress level of the ferromagnetic SMA, NiMnGa is as low as several MPa. To design a robust yet compact actuator with large load bearing capacity at room temperature range, we proposed a new actuation mechanism for a ferromagnetic SMA, which provides a faster responsive yet powerful actuation, "hybrid mechanism", which is based on a sequence of chain reactions: First, applied magnetic field H or flux density B with large gradient, inducing large stress field in a ferromagnetic actuator material, prompting stress-induced martensite phase change (A to M phase), thus, the elastic properties change from stiff (austensite phase) to softer (martensite phase), resulting in larger displacement. This talk will discuss the design of such ferromagnetic SMA and its applications to several types of actuators.

#### 9:30 AM

Characterization of Laser-Driven Shocked NiAl Monocrystals and Bicrystals: Pedro D. Peralta<sup>1</sup>; Damian Swift<sup>2</sup>; Chyi-Hwang Lim<sup>1</sup>; Eric Loomis<sup>1</sup>; Ken J. McClellan<sup>3</sup>; <sup>1</sup>Arizona State University, Dept. of Mech. & Aeros. Engrg., Engrg. Ctr., G Wing, Rm. 346, Tempe, AZ 85287-6106 USA; <sup>2</sup>Los Alamos National Laboratory, Physics Div., P-24, MS E526, Los Alamos, NM 87545 USA; <sup>3</sup>Los Alamos National Laboratory, Matls. Sci. & Tech. Div., MST-8, MS G755, Los Alamos, NM 87545 USA

Disks of oriented single crystals and bicrystals of NiAl were tested under direct laser-driven shocks. Specimens were recovered and characterized to study cracking and slip behavior. In addition, the crystallographic orientation of the tested samples was studied using Orientation Imaging Microscopy. Results indicate that direct laser-driven shocks in monocrystals induce cracking on {110} planes, with a high crack density for <100> samples and a low crack density for <110> and <111> specimens. In one bicrystal, a Grain Boundary Affected Zone was observed close to the boundary in only one grain, where both cracking and slip were present. Specimens developed gradients of orientation due to bowing of the foil caused by the impact. Furthermore, changes in the speed of sound across the inclined interface correlated with the cracking mode, i.e., a shock propagating from a "slow" to a "fast" grain resulted in intergranular cracks, whereas the reverse resulted in transgranular cracks.

#### 9:50 AM Break

#### 10:30 AM

Comparison of Recrystallization During and After Hot Working in FCC Metals: *Hugh J. McQueen*<sup>1</sup>; John J. Jonas<sup>2</sup>; <sup>1</sup>Concordia University, Mech. Engrg., 1455 Maisonneuve Blvd. W., Montreal, Quebec H3G 1M8 Canada; <sup>2</sup>McGill University, Matls. Engrg., Montreal, Quebec H3A 2B2 Canada

The recrystallization responses of face-centered cubic (FCC) metals to hot deformation at similar strain rates 10-2 to 10+2 s-1 and homologous temperatures (>0.55T<sub>m</sub>) are strongly dependent on stacking fault energy (SFE). Discontinuous dynamic recrystallization occurs readily in all the metals, except Al, in which it is only observed at purities > 99.999% or when particle stimulated nucleation is taking place. After hot deformation, static recrystallization (SRX) occurs rapidly above 0.65 T<sub>m</sub>, even after low strains (20-50% rolling reduction) and is employed for grain refinement in the initial high temperature stages of industrial rolling. However in Al alloys, SRX is selectively induced by increasing the accumulated strain and the length of certain interpass intervals. The presence of solutes and particles, as well as the SFE, affect the recrystallization behavior through their influence on dynamic recovery, which controls the characteristics of the dislocation substructure; alloying also influences the grain boundary mobility through both solute drag and particle pinning effects.

#### 10:50 AM

Static Recrystallization of Tool Steels: *Clement A.C. Imbert*<sup>2</sup>; Hugh J. McQueen<sup>1</sup>; <sup>1</sup>Concordia University, Mech. Engrg., Montreal, Quebec H3G 1M 8 Canada; <sup>2</sup>University of the West Indies, Mech. Engrg., St. Augustine W1 Trinidad

Double-twist torsion tests were used to determine static softening in the hot working range of three tool steels: W1, a carbon steel (1.03% carbon plus 0.8% other elements), A2 and D2, a medium and a high alloy steel, containing 8.45% and 14.82% alloying elements respectively. The carbon steel, which was single-phase austenite in the hot-working range, experienced rapid static recrystalli-zation (SRX) due to increase in diffusion rate of iron, caused by carbon in hot austenite, very little alloying solute and no carbides. SRX of the alloy tool steels was compared with austenitic stainless steels, with similar strengths but much greater alloying content, and with microalloyed steels, as well as with the dynamic recrystallization kinetics. Carbides in alloy tool steels, which exist throughout the hot-working range, retard recrystallization but are responsible for enhancing initiation due to formation of nuclei at the strain concentration at the particle/ matrix interface.

#### 11:10 AM

Enhanced Mechanical Properties in Bulk Ultrafine-Grained Copper: S. Xie<sup>1</sup>; P. K. Liaw<sup>1</sup>; H. Choo<sup>1</sup>; D. E. Fielden<sup>1</sup>; G. Wang<sup>1</sup>; Y. Sun<sup>1</sup>; <sup>1</sup>University of Tennessee, Dept. of Matls. Sci. & Engrg., Knoxville, TN 37996 USA

Ultrafine-grained (UFG) pure copper has been prepared by rolling the commercial coarse-grained (CG) copper, with liquid nitrogen cooling of the samples between consecutive rolling passes. The microstructures of these materials have been characterized using x-ray diffraction (XRD) and transmission-electron microscopy (TEM). It is found that low-angle subgrain boundaries transform to high-angle grain boundaries, and the grain size is refined from 100  $\sim$  200 mm to 0.1  $\sim$ 0.5 mm following rolling at low temperatures. The yield strength and hardness have been measured by tensile tests and micro-hardness tests, respectively. The results show that the strength has been enhanced about two times and micro-hardness has been increased more than 100%, compared with the commercial CG copper. The mechanism leading to the significantly enhanced mechanical properties has been discussed. Furthermore, the cold-rolled UFG copper was annealed at elevated temperatures in an attempt to create a bimodal distribution in grain sizes. The mechanical behavior of the heat-treated UFG copper is compared to that of the as-rolled copper. The present work is supported by the NSF International Materials Institutes (IMI) Program under DMR-0231320, with Dr. Carmen Huber as the Program Director.

#### 11:30 AM

A Study of the Surface Nanocrystallization and Hardening Process for Improved Fatigue Resistance of C-2000: *W. Yuan*<sup>1</sup>; P. K. Liaw<sup>1</sup>; C. Stephens<sup>1</sup>; R. McDanice<sup>1</sup>; H. Tian<sup>1</sup>; D. E. Fielden<sup>1</sup>; J. C. Villegas<sup>2</sup>; L. L. Shaw<sup>2</sup>; D. L. Klarstion<sup>3</sup>; <sup>1</sup>University of Tennessee, Matls. Sci. & Engrg., Knoxville, TN 37996 USA; <sup>2</sup>University of Connecticut, Metall. & Matls. Engrg., Storrs, CT 06269 USA; <sup>3</sup>Haynes International, Inc., Kokomo, IN 46904 USA

The nanostructured layer on the surface has high resistance to the fatigue- crack initiation, and the coarse grain below the surface can retard the growth of fatigue cracks. By means of the surface nanocrystallization and hardening process (SNH), a nanostructured layer was formed on the surface of the Haynes C-2000 Superalloy disk, and the coarse grain below the surface was not changed. Microstructural features of cross section near and below the surface were investigated using X-ray diffraction (XRD), scanning-electron microscope (SEM), and transmission-electron microscopy (TEM). The microhardness of the cross section from the surface was measured by nanoindentation, and the residual stress was determined by XRD. A grain-size gradient from the nano-layer to coarse grain, the micro-hardness gradient, and the residual-stress distribution from the compressive stress to the tension stress were introduced through the cross section of a C-2000 disk. Four-point-bend tests were employed to study the fatigue behavior of the SNH-treated specimens, relative to the untreated specimens. When the surface defects introduced by the SNH treatment are removed, the fatigue life of the treated specimens can be improved. The present work is supported by National Science Foundation under DMR-0207729 with Dr. K. L. Murty as the contract monitor.

# Solidification Processes and Microstructures: A Symposium in Honor of Prof. W. Kurz: Processes

Sponsored by: Materials Processing & Manufacturing Division, MPMD-Solidification Committee

*Program Organizers:* Michel Rappaz, Ecole Polytechnique Fédérale de Lausanne, MXG, Lausanne Switzerland; Christoph Beckermann, University of Iowa, Department of Mechanical Engineering, Iowa City, IA 52242 USA; R. K. Trivedi, Iowa State University, Ames, IA 50011 USA

Monday AM	Room:	207D		
March 15, 2004	Location	: Charlotte	Convention	Center

Session Chair: Michel Rappaz, Ecole Polytechnique Federa, MXG, Lausanne Switzerland

# 8:30 AM Introduction and Welcome Michel Rappaz

#### 8:45 AM Invited

Semi-Solid Forming: Our Understanding Today and its Implication for Improved Processes: Merton C. Flemings<sup>1</sup>; James Yurko<sup>2</sup>; Raul A. Martinez<sup>1</sup>; <sup>1</sup>Massachusetts Institute of Technology, Dept. of Matls. Sci. & Engrg., Rm. 4-415, Cambridge, MA 02139 USA; <sup>2</sup>IdraPrince, New Product Dvlp., 670 Windcrest Dr., Holland, MI 49423 USA

During the careers of Professor Wilfried Kurtz and the senior author of this paper, a wide range of new processes have been developed for aluminum alloy casting. Some of these are designed primarily to achieve economic net shape parts. Others achieve improved cleanliness or freedom from dissolved gas. Still others are designed primarily to improve properties through microstructure control. Semi-solid forming of aluminum is finding its main niche today in its ability to 1) control metal viscosity and hence mold filling behavior, 2) reduce die casting cycle time, 3) improve die life, and 4) improve casting soundness. This paper will review the understanding of semi-solid forming achieved progressively over the last 30 years and focus on recent fundamental and applied developments. Recent studies have extended our knowledge of the viscosity behavior of semi-solid alloys up to the shear rates obtained in die casting and are elucidating the overriding importance of cooling rate and convection at precisely the time of first solid formation. Industrial developments include new processes designed to improve process economics and product quality.

#### 9:15 AM Invited

Contribution to the Knowledge of the Formation of the Skin in Continuous Casting of Steel: *G. Lesoult*<sup>1</sup>; L. Ladeuille<sup>2</sup>; C.-A. Gandin<sup>1</sup>; <sup>1</sup>Ecole des Mines, UMR-CNRS 7584, Nancy F-54042 France; <sup>2</sup>Thyssenkrupp, UGO-BP23, Isbergues F-62330 France

In several continuous casting processes, metal is extracted through a withdrawal-stop sequence instead of a constant withdrawal speed. In this case, the solid skin forms according to two modes of solidification, during two main steps. In the first step, the liquid metal coming into contact with the upper part of the mold wall, as the already solidified shell is extracted, solidifies as a fine continuous solid film. It adheres to the mold and is thus separated from the moving shell. Therefore, two phenomena have to be studied: the solidification of the "static shell"  $\mathbf{S}_{\mathrm{s}},$  as opposed to the solidification of the extracted "dynamic shell" S<sub>d</sub>. In the second step, when the speed of the dynamic shell with respect to the mold decreases, then becomes zero and reverses, the lips of the two shells enter into contact and become welded. When extraction starts again, the upper static shell is removed with the former dynamic shell, i.e., becomes dynamic, and a new static skin starts to form. The first hundreds of microns of the skin are likely formed during the first step. Therefore, there is a particular interest in studying the formation of microstructure and microsegregation during the solidification of the static shell. An experimental device has been built at the laboratory scale to reproduce the local thermal conditions of the initial solidification of the static shell. Droplets of liquid steel fall on a copper substrate instrumented with a Si-photodiode. Measurements performed with the photodiode are used to estimate the evolution of the thermal conditions (temperature gradient and growth rate) during the solidification of the first 500 µm in the droplets. The growth rate is of the order of 1 to 2 cm s<sup>-1</sup> at the very beginning; it decreases down to 3 mm s<sup>-1</sup> after about 200 ms. The temperature gradient in the solid varies from 106 to 2.105 Km<sup>-1</sup> in the same time. The temperature gradient in the liquid is much smaller (about 10<sup>4</sup> Km<sup>-</sup> 1); it may be negative in the very early stages if the nucleation undercooling is large enough. Two types of microstructures are observed: cells and dendrites. The comparison between predicted and calculated microstructures leads to conclusions related to nucleation conditions of the first shell and to its mechanical behavior.

# 9:45 AM Invited

Introducing Casting Simulation in Industry: The Steps Towards Success: Marco Gremaud<sup>1</sup>; <sup>1</sup>Calcom ESI, Parc Scientifique EPFL, Lausanne CH-1015 Switzerland

The industrial world is moving towards the "digital factory" - a prototype-less automated production environment based on virtual engineering. In terms of productivity, quality and innovation, the expected benefits of this transition are spectacular. In this "digital factory", manufacturers, their suppliers and partners simultaneously work on the same numerical prototype, allowing for continuous improvement in design and immediate decision-making. This "extended enterprise" marks a revolutionary departure from the time-consuming, costly trial and error processes of physical prototyping. Casting simulation is one small piece of that new technology. However, the introduction of a casting modeling package in a foundry is not a simple task and often the result is mitigated by the challenges of implemenation. The author will try to identify what are the key parameters ensuring success when introducing a casting simulation software in a foundry and why more than 90% of casting foundries are still not using simulation.

# 10:15 AM Break

# 10:45 AM

Simulation of Stress, Strain, and Shrinkage of Solidifying Steel Shells with Different Carbon Contents: Chunsheng Li<sup>1</sup>; Ya Meng<sup>1</sup>; *Brian G. Thomas*<sup>1</sup>; <sup>1</sup>University of Illinois, Mech. & Industrial Engrg., 138 Mech. Engrg. Bldg., 1206 W. Green St., Urbana, IL 61801 USA

Thermal-mechanical behavior of the solidifying shell is important for design of taper and understanding crack formation and other defects during continuous casting of steel. A two-dimensional finiteelement model, CON2D, has been developed to simulate the evolution of temperature, stress and strain in the solidifying shell during this process. The model features unified elastic-viscoplastic constitutive models for austenite, ferrite, mushy, and liquid steel. A simple microsegregation model is adopted to track the volume fractions of each phase. The model was validated by simulating an SSCT experiment similar to that of Kurz. CON2D was then applied to investigate the effect of steel grade on thermo-mechanical behavior of a slice domain under realistic heat flux conditions. The shrinkage predicted by CON2D was compared with simpler methods, such as that of Dippanaar. The simple methods are found to over-estimate the shrinkage of low carbon steels, where a substantial fraction of soft delta-ferrite exists, but matches reasonably for high carbon steel, containing strong austenite. Implications of the stress and strain profiles in the solidifying steel are also discussed.

#### 11:00 AM

A 3D-FEM Model Solving Thermomechanics and Macrosegregation in Binary Alloys Solidification: Michel Bellet<sup>1</sup>; Victor Daniel Fachinotti<sup>1</sup>; Sylvain Gouttebroze<sup>1</sup>; <sup>1</sup>Ecole des Mines de Paris, CEMEF, BP 207, Sophia Antipolis F-06904 France

The paper presents a three-dimensional coupled numerical solution of momentum, energy and solute conservation equations, for binary alloys solidification. The interdendritic flow in the mushy zone is assumed to obey the Darcy's law. Thermal and solutal buoyancy forces are taken into account by means of the Boussinesq's model. Microsegregation is governed either by lever rule or Scheil models, assuming local equilibrium at phase interfaces. The resulting solute transport equation is solved using the Streamline-Upwind Petrov/ Galerkin method. Momentum, energy and solute equations are discretised in space using tetrahedral finite elements and are coupled by a simple staggered scheme at each time step. The full algorithm was implemented the 3D code THERCAST. Two applications are given: a comparison with a 2D finite volume code in a 2D case (Fe-C alloy in a square cavity), and a comparison with experiment in a 3D case (Pb-Sn in a parallelepipedic cavity).

# 11:15 AM

Effect of Casting Speed on Structure Formation and Hot Tearing During Direct-Chill Casting of Al-Cu Alloys: X. Suyitno<sup>1</sup>; D. Eskin<sup>2</sup>; L. Katgerman<sup>1</sup>; <sup>1</sup>Delft University of Technology, Lab. of Matls., Rotterdamseweg 137, Delft 2628 AL The Netherlands; <sup>2</sup>Netherlands Institute for Metals Research, Rotterdamseweg 137, Delft 2628 AL The Netherlands

Professor W. Kurz recently suggested Solidification Structure-Processing Maps as a useful tool for controlling commercial solidification technologies. As a development of this idea we studied the effect of casting speed on the structure formation and hot tearing during directchill (DC) casting of binary Al-Cu alloys. Several binary alloys were cast in our laboratory scale DC casting that allowed an automatically controlled change of the casting speed during casting. The microstructure of billets was analyzed by optical microscope and computer image analysis, and hot tears were measured directly on the crack sites. Besides that a finite element simulation was performed. Hot tearing susceptibilities are computed using five different hot tearing criteria. Clear relationships between the structure parameters and hot tearing on one side and the casting speed and composition on the other side were found. The outcome of this research will be a Composition-Casting Speed-Hot Tearing process chart.

# 11:30 AM

Simulation of Solidification and Precipitation in Continuous Casting of Micro Alloyed Steels: *Mohammad Safi*<sup>1</sup>; Heikel Hamadou<sup>1</sup>; Dieter Senk<sup>1</sup>; <sup>1</sup>RWTH-Aachen University, IEHK, Intze Str., Aachen, NRW 52056 Germany

There is a large demand in industry to produce steel with particular mechanical properties, e.g. simultaneous high strength and high toughness. Two main possibilities to improve the final mechanical properties of steel semi products during production are control of chemical composition and micro-structure. To simulate solidification and developement of micro-structure during continuous casting, the temperature field of a strand shell was calculated. The results were used as a basis of other subprograms to calculate dendritic structure, micro-segregation and precipitation. Influences of casting flux on micro-structure and subsrface precipitations were experimentally examined. Micro-segregation and subsequent interdendritic precipitation of titanium nitride in subsurface regions during solidification are discussed.

## 11:45 AM

Stray Grain Formation in Nickel-Base Superalloy Single-Crystal Welds: John M. Vitek<sup>1</sup>; Suresh S. Babu<sup>1</sup>; Jin-Woo Park<sup>1</sup>; Stan A. David<sup>1</sup>; <sup>1</sup>Oak Ridge National Laboratory, Metals & Ceram. Div., PO Box 2008, MS 6096; Bldg. 4508, Oak Ridge, TN 37831-6096 USA

During the welding of nickel-base superalloys, it is desirable to maintain the single crystal nature of the base material in the weldments. Stray grain formation during solidification destroys the single crystal structure and compromises properties. In addition, weld cracks form more easily along stray grain boundaries. Kurz and Gaumann studied the stray grain formation tendencies in terms of the degree of constitutional supercooling ahead of the growing dendrites during weld solidification. Using the same ideas, the present work investigated the stray grain formation tendencies and cracking behavior in welds of Rene N5, a nickel-base single-crystal superalloy. The thermal behavior during welding was modeled and the extent of constitutional supercooling ahead of the growing interface was quantitatively evaluated. In addition, the dendrite orientation with respect to the moving solid-liquid interface was also taken into account. The results supported the mechanism proposed by Kurz for stray grain formation. The analysis provides insight into the conditions needed in order to minimize stray grain formation during welding of nickel superalloys. This research was sponsored by the Office of Fossil Energy, DOE National Energy Technology Laboratory, under contract DE-AC05-00OR22725 with UT-Battelle, LLC.

# 12:00 PM

New Features in Microstructure Control During E-LMF: Selim Mokadem<sup>1</sup>; Cyrille Bezençon<sup>1</sup>; Jean-Marie Drezet<sup>2</sup>; Alain Jacot<sup>2</sup>; Jean-Daniel Wagnière<sup>1</sup>; Wilfried Kurz<sup>1</sup>; <sup>1</sup>Ecole Polytechnique Fédérale de Lausanne, Matl. Sci. & Engrg. Inst., Lab. de simulation des matériaux, MXG, Ecublens, Lausanne, Vaud 1015 Switzerland; <sup>2</sup>Calcom ESI, Parc Scientifique - EPFL, Lausanne, Vaud 1015 Switzerland

The Laser Metal Forming (LMF) process where metal powder is injected into a molten pool formed by controlled laser heating is a near net shape process applied to rapid prototyping or repair engineering. The LMF process has been further developed and applied to the repair of SX HPT (single crystal High Pressure and Temperature) blades of gas turbines through the deposition of an epitaxial and SX layer onto SX superalloy substrates (Epitaxial-Laser Metal Forming : E-LMF). SX repair using E-LMF requires controlled solidification conditions such as to prevent the formation of stray crystals ahead of the columnar front i.e. to ensure epitaxial growth and to avoid the columnar to equiaxed transition (CET) during solidification. The aim of this work is to present the development of new strategies for microstructure control during Epitaxial Laser Metal Forming through the consideration of dendritic growth orientation, growth competition mechanism, loss of epitaxy related to branching mechanism and liquid convection in the melt pool. Control of these phenomena is of major importance for an effective industrial application of the E-LMF process. For this purpose modelling facilities have been developed and used in association with extended experimental observation to predict the expected solidification morphology for a given set of laser processing parameters. New microstructure features such as Oriented-to-Misoriented Transition (OMT) and Loss of Epitaxy in the critical branching zone are presented and measures to be taken for avoiding the formation of spurious grains within the repaired area are discussed.

# 12:15 PM

Microstructure and Mechanical Behavior of Liquid Metal Directionally Solidified GTD-444: Steve J. Balsone<sup>1</sup>; Ganjiang Feng<sup>1</sup>; Lance Peterson<sup>1</sup>; Jon C. Schaeffer<sup>1</sup>; <sup>1</sup>GE Power Systems, 300 Garlington Rd., Greenville, SC 29615 USA

GTD-444 is a precipitation-strengthened nickel-base superalloy developed and patented by GE for advanced large power generation gas turbine components. Most components are made by directional solidification (DS) investment casting. The increased firing temperature and the growing size of advanced turbine components creates a strong demand on manufacturing sound casting with homogeneous microstructure and improved mechanical properties. Extensive R&D in high gradient casting process shows that liquid metal cooling (LMC) directional solidification is one of the most promising technologies to produce high-performance castings. In the present study, microstructure and mechanical properties of LMC DS and conventional DS GTD-444 castings were compared. Microstructure features like dendrite arm spacing, phase segregation, carbide and gamma prime morphology were analyzed. The effect of the microstructure on mechanical behavior and fracture mode will be presented.

# Symposium on Microstructural Stability in Honor of Prof. Roger D. Doherty: Microstructural Stability: Recrystallization

Sponsored by: Aluminum Association, Materials Processing and Manufacturing Division, Structural Materials Division, MPMD-Solidification Committee, SMD-Physical Metallurgy Committee *Program Organizer:* Anthony D. Rollett, Carnegie Mellon University, Department of Materials Science & Engineering, Pittsburgh, PA 15213-3918 USA

Monday AM	Room: 2	216A
March 15, 2004	Location:	Charlotte Convention Center

Session Chair: Anthony D. Rollett, Carnegie Mellon University, Dept. of Matls. Sci. & Engrg., Pittsburgh, PA 15213-3918 USA

# 8:30 AM

Unsolved Problems in Physical Metallurgy of Structural Alloys: Roger D. Doherty<sup>1</sup>; <sup>1</sup>Drexel University, Dept. of Matls. Sci. & Engrg., Philadelphia, PA 19104 USA

For a symposium in my name that two of my colleagues have organized I feel that it might be of interest to give an outline of some of what I feel are important unsolved problems in the field in which I have spent my career. I would very much like to learn of solutions that might satisfy me and which I could use for students taking my classes at Drexel. In the area of microstructure development and stability the topics in which I know I do not understand include: abnormal grain coarsening seen in many, but not all cases, of normal grain coarsening pinned by a low volume fraction of particles. In the topic of precipitation the usual model for heterogeneous nucleation at grain boundaries and at dislocations seem to occur under conditions of low supersaturation in which the standard models predict that the sites do not have sufficient energy to act as catalysts. The problem of heterogeneous nucleation in solidification seems experimentally too difficult even to know if there is a problem or not. A further problem is the nucleation of growth ledges at the impingement point of plate like precipitates on different habit planes. Theories of coarsening, and many experiments, indicate that as the volume fraction of precipitates increases and the diffusion distance between particles becomes smaller, the coarsening rate accelerates. But in the Ni-Ni<sub>3</sub>Al system as Alan Ardell has clearly shown, there is, for some unexplained reason, no significant acceleration of coarsening in that alloy system. Somewhat further from my main area of research are some important problems that I do not understand, though that may reflect lack of knowledge of recent relevant studies. Amongst these topics are what is the mechanism and thus what determines the value of the proportionality constant, k<sub>v</sub>, in the Hall-Petch equation for grain size strengthening? Perhaps more surprising is the lack of our ability to predict the

strength of most Aluminum based precipitation hardened alloys even when the microstructure is fully characterized. Here the strengthening precipitate phases have a different crystal structures from the matrix and so they form plate or rod like precipitates. The text book account of peak strength - as occurring at the transition from underaged precipitates that are sheared by the dislocations to overaged precipitates that are by-passed works well for spherical GP zones but seems to fail for plate-like precipitates. The problems may be related as both concern the difficulty of dislocations passing from one crystal to another at an interface in which the slip plane and direction both change. In these two mechanical areas there is recently some work being done. However in the structural area that does not seem to be the case even when the precipitates may have nanometer sizes.

#### 9:05 AM

Static and Directional Recrystallization of Cold-Rolled Nickel: *I. Baker*<sup>1</sup>; J. Li<sup>1</sup>; H. J. Frost<sup>1</sup>; <sup>1</sup>Dartmouth College, Thayer Sch. of Engrg., 8000 Cummings Hall, Hanover, NH 03755 USA

The microstructures of both statically annealed and directionally recrystallized 90% cold-rolled polycrystalline nickel were investigated using both electron back-scattered patterns on a scanning electron microscope and optical microscopy. The statically annealed nickel showed a {100}<001> texture and small grains after primary recrystallization at low temperature (~700 K), but a {124}<21-1> texture and large grains after secondary recrystallization at higher temperatures (>1000 K). The effects of hot zone velocity during directional annealing at 1273 K were investigated. Some cold-rolled specimens were first statically recrystallized at 643 K prior to directional recrystallization at 1273K in order to examine whether directional recrystallization at 1273 K was by primary or secondary recrystallization. It was shown that directional recrystallization to columnar grains or, under optimum conditions, a single crystal was always by secondary recrystallization. Columnar grains could be produced over a wide range of hot zone velocities. Research supported by AFOSR grant F49620-00-1-0076 and NSF grants DMI 9976509 and DMI 0217565.

#### 9:35 AM

Increasing Grain Size in Electrical Steels by Light Reduction Followed by Annealing: *Fernando J.G. Landgraf*<sup>1</sup>; Taeko Yonamine<sup>1</sup>; Marcos Flavio de Campos<sup>2</sup>; Ivan G.S. Falleiros<sup>3</sup>; <sup>1</sup>IPT-Institute for Technological Research, Metall. Div., Av. Prof Almeida Prado 532, Sao Paulo, SP 05508-901 Brazil; <sup>2</sup>Universidade Federal Fluminense, EEIMVR, Volta Redonda, RJ Brazil; <sup>3</sup>Universidade de Sao Paulo, Depto. Engrg. Metalurgica e Materiais, Sao Paulo, SP 05508-901 Brazil

Approximately half of the annual 6 million tons of non-oriented electrical steels sheets attain the necessary large grain size (150µm) by light deformation (4 to 8% area reduction) followed by annealing at 760°C. This paper addresses the taxonomy debate (is it primary recrystallization or strain induced abnormal grain growth?), discusses the inhomogeneous microstructural evolution along the sheet and describes the texture evolution in some circumstances. Evidences will be shown in favour of the primary recrystallization concept, as it follows the Burke and Turnbull recrystallization rules: the grain size-deformation relationship is monotonic whether producing grain size refinement or increase, annealing temperature has no effect on the final grain size and the lower the deformation, the longer the incubation period and longer it takes to recrystallize. Partial recrystallization investigation indicates that recrystallization starts at the surface of the 0.5mm thick sheets, although there is very little hardness gradient. The extent of the inward growth varies along RD and TD, making very difficult for a recrystallization kinetics study. Texture evolution of samples with different histories will be compared, including a new process developed with Professor Doherty's help when visiting Brazil in 2002.

# 10:05 AM

Growth Aspects of Recrystallization: Dorte Juul Jensen<sup>1</sup>; Erik M. Lauridsen<sup>1</sup>; Soren Schmidt<sup>1</sup>; Roy A. Vandermeer<sup>1</sup>; <sup>1</sup>Riso National Laboratory, Ctr. for Fundamental Rsch., Metal Structures in 4-D, Roskilde Denmark

A much debated issue is if "oriented growth" is an important mechanism in recrystallization. This is adressed by presenting growt rate data obtained by EBSP measurements for both cold and hot deformed aluminium. It is shown that oriented growth is significant in several cold deformed samples while it is not for the hot deformed sample. This is discussed and possible mechanisms which may contribute to oriented growth are examined. The results reported in this first part of the talk refer to mean growth rates averaged over a large number of individual grains. In the second part, growth rates for individual grains obtained by 3 Dimensional X-Ray Diffraction using high energy synchrotron radiation are reported. It is shown that there is a very large variability between the grains even within texturecomponents, and simulations are finally presented which illustrate how such variability may affect the overall recrystallization kinetics.

# 10:40 AM

Effect of Annealing Temperature on the Development of Twin Boundaries: D. R. Waryoba<sup>1</sup>; P. N. Kalu<sup>1</sup>; <sup>1</sup>FAMU-FSU College of Engineering and National High Magnetic Field Laboratory, Tallahassee, FL 32310 USA

The development of twin boundaries has been monitored in heavily drawn oxygen free high conducting (OFHC) copper wires, which were subsequently annealed at different temperatures. Samples of the wires deformed to true strains of 1.69, 2.31 and 3.56, were isothermally annealed at temperatures between 150°C and 750°C for one-hour in an argon-filled environment, and characterized using Orientation Imaging Microscopy. Analyses of the microtexture results revealed that the densities (number/ $\mu$ m2) of the Sigma-3 and Sigma-9 twin boundaries peaked just prior to the onset of recrystallization, and most of the recrystallized grains were bounded by these twin boundaries. Secondary recrystallization occurred when the wires were annealed at high temperatures, and the twin boundaries were found to be largely associated with annealing twins, which developed under this condition. Higher order twin boundaries (Sigma-27a and Sigma-27b) were virtually negligible.

# 11:10 AM

The Critical Strain for Dynamic Recrystallization: John J. Jonas<sup>1</sup>; <sup>1</sup>McGill University, Metallurgl. Engrg., 3610 Univ. St., Wong Bldg., Montreal, Quebec H3A 2B2 Canada

Under conditions of dynamic recrystallization, an inflection point is observed in the plot of work hardening rate vs. flow stress. This is shown to be associated with the initiation of an additional dynamic softening mechanism, in this case the migration of high angle boundaries. A normalization procedure is introduced according to which such inflection points can be defined and predicted, even under conditions of decreasing temperature and increasing strain rate, as in hot strip mills. The data obtained on thirteen steels indicate that the ratio of the critical strain for the initiation of dynamic recrystallization to that of the peak strain falls in the range 0.5 to 0.6 and increases with the concentration of alloying elements present. An extension of the normalization technique is shown to apply to the softening that takes place between roll passes as well. Both of these methods are useful in modelling the loads developed and the microstructural changes taking place in rolling mills.

#### 11:40 AM

The 40°<111> Orientation Relationship in the Nucleation of Recrystallisation in Aluminium: *Erik Nes*<sup>1</sup>; <sup>1</sup>Norwegian University of Science and Technology (NTNU), Dept. of Matls. Tech., Trondheim N-7491 Norway

The 40° <111> orientation relationship has a central role in the discussion of recrystallisation textures. This orientation relationship has traditionally been associated with the oriented growth theory, but recent experimental observations clearly demonstrate a link also to oriented nucleation. In this presentation the importance and understanding of the 40° <111> orientation relationship in is discussed in terms of recrystallization after both hot and cold deformation of aluminium and aluminium alloys. Special attention will be focused on the effect of stored energy and finely dispersed particles on the nucleation.

# The Didier de Fontaine Symposium on the Thermodynamics of Alloys: Fundamentals of Alloy Theory

Sponsored by: Materials Processing and Manufacturing Division, MPMD-Computational Materials Science & Engineering-(Jt. ASM-MSCTS)

*Program Organizers:* Diana Farkas, Virginia Polytechnic Institute and State University, Department of Materials Science and Engineering, Blacksburg, VA 24061 USA; Mark D. Asta, Northwestern University, Department of Materials Science and Engineering, Evanston, IL 60208-3108 USA; Gerbrand Ceder, Massachusetts Institute of Technology, Department of Materials Science and Engineering, Cambridge, MA 02139 USA; Christopher Mark Wolverton, Ford Motor Company, Scientific Research Laboratory, Dearborn, MI 48121-2053 USA

Monday AM	Room: 2	216B		
March 15, 2004	Location:	Charlotte	Convention	Center

Session Chair: TBA

# 8:30 AM Keynote

**Reflections on "Alloy Theory"**: *Didier R. De Fontaine*<sup>1</sup>; <sup>1</sup>University of California, Matls. Sci., 210 Hearst Mining Bldg., Berkeley, CA 94720-1760 USA

Classical Gibbsian Thermodynamics is as close as one gets to a perfect theory, formally that is. Unfortunately, little practical work can be done with it without numerical knowledge of the parameters that enter its equations. In the past, parameters were determined empirically, but now, at least in principle, the required numerical values can be determined ab initio by quantum mechanical means. Hence, today's "Alloy Theory" combines statistical thermodynamics and quantum mechanics into one integrated whole for which computer code packages are in fact being developed. In this talk I shall briefly outline some of the important steps which led to the new approach of the old problem.

#### 9:00 AM Invited

Using Thermodynamic Equations for Checking Self-Consistency of Theories, Models, and Experiments: John W. Cahn<sup>1</sup>; <sup>1</sup>National Institute of Science and Technology, MSEL, Gaithersburg, MD 20899-8555 USA

Thermodynamics gives exact relations among quantities which are precisely defined and often independently measurable. Failures in the relations outside of experimental error, computational uncertainties, or with quantities derived from theoretical models are strong indications that something is wrong and should be investigated. The Gibbs adsorption equation will be used with models of various interfaces to illustrate discrepancies between calculated temperature dependences of interfacial free energies and interfacial entropies, and how some have been resolved. Earlier discrepancies have pointed to diffuse or rough interfaces. The temperature dependence of the energy of dislocation boundaries through the temperature coefficient of elastic constants and the magnitude of the Burgers vector is an interesting example.

#### 9:30 AM Invited

Reliable First-Principle Alloy Thermodynamic Via Truncated Cluster Expansions: Duane D. Johnson<sup>1</sup>; <sup>1</sup>University of Illinois, Matls. Sci. & Engrg., 1304 W. Green St., Urbana, IL USA

Many major developments and applications of the cluster expansion (CE) have originated from Prof. de Fontaine's group. As such, the CE is increasingly used to combine electronic-structure calculations and Monte Carlo methods to predict alloy thermodynamic properties. The CE is a basis set expansion in terms of lattice clusters and effective cluster interactions, but is tractable only if truncated from its exact (infinite) form. Yet until now there was no well-defined procedure that could guarantee a reliable truncated CE. We present a method for an optimal truncation of the CE basis set that provides reliable thermodyamics, and exemplify its importance in fcc Ni3V. The new truncation procedure now provides excellent agreement to a range of measured quantities for fcc Ni3V, where previous use of CE failed. The results show that T=0K DFT results are not always pertinent to characterization measurements.

# 10:00 AM Invited

A Data Mining Approach to Crystal Structure Prediction: Dane Morgan<sup>1</sup>; Stefano Curtarolo<sup>1</sup>; Gerbrand Ceder<sup>1</sup>; <sup>1</sup>Massachusetts Institute of Technology, Dept. of Matls. Sci., 77 Mass. Ave., 13-4061, Cambridge, MA 02139 USA

Predicting crystal structures for a new alloy is one of the most fundamental problems in materials science. Total energy ab initio approaches have proven a powerful tool for crystal structure prediction, but how to choose the best structures to calculate is still an open problem. Traditionally, researchers have used a combination of experimental results, model Hamiltonians, optimization methods, and hard-won intuition to find good candidate structures for a new alloy. In this paper a new approach is proposed, called Data Mining of Quantum Calculations (DMQC), which uses statistical and data mining methods to mine existing ab initio and/or experimental data to predict likely structures for new alloys. When faced with a new alloy, DMQC makes optimal use of existing data on other alloys. Key data mining techniques for DMQC will be described, compared to other approaches, and tested on a database of over 10,000 ab initio energies. DMQC is shown to dramatically decrease the time needed to identify stable crystal structures.

# 10:30 AM Break

# 10:40 AM Invited

Long Range Order and Diffraction: Denis Gratias<sup>1</sup>; <sup>1</sup>LEM-CNRS/ ONERA, 29, Av de la Division Leclerc, Chatillon 92322 France

Bragg diffraction is well known to characterize long range crystalline order. Dany Shechtman's discovery in 1984 of quasicrystals exhibiting sharp diffraction peaks with no periodic order has broken this paradigm and opened a more general question "What distribution of matter diffracts?". The present talk is a didactical attempt to summarize in an illustrative way some of the most important recent mathematical results on this apparently simple issue. It will shown through concrete examples and little mathematics that the problem is far from trivial and that Long Range Order is not necessarily associated to Bragg diffraction and vice versa.

# 11:10 AM Invited

Linking Structures Via Thermodynamics: Suzana G. Fries<sup>1</sup>; <sup>1</sup>AC-CESS e.V., RWTH-Aachen, Intzestrasse 5, Aachen D-52072 Germany

The combination of the knowledge about electronic, crystallographic, micro and macro structures of a material, using thermodynamics as media is a powerful approach. Some examples will be shown where pragmatic and theoretical methods are used in order to correlate that structures for real multicomponent materials.

#### 11:40 AM

Sources of Entropy in Solid-Solid Phase Transformations: Brent Fultz<sup>1</sup>; <sup>1</sup>California Institute of Technology, Matls. Sci., Mail 138-78, Pasadena, CA 91125 USA

Temperature drives the formation of antisite atoms, excitations of phonons, and excitations of electrons. In thermal equilibrium these configurational, vibrational, and electronic contributions to the entropy can be assessed if their energy spectra are known. Each of these phenomena can make significant and comparable contributions to the entropy of solid-state phase transformations. Their interactions at high temperature are another opportunity for future research. We have focused on inelastic neutron scattering experiments to measure the energy spectra of phonons, but we seek sources of entropy by combining results from other techniques. Some systematics are presented, such as the effect of solute mass and atomic size mismatch on phonon entropies of compound formation. Electronic entropy plays a big role in crystal structure transformations in cerium, uranium and plutonium. Overall, however, systematic correlations are at best semiquantitative. Understanding entropy in materials will require detailed analyses, rather than general rules of thumb.

# Third International Symposium on Ultrafine Grained Materials: Processing I: Fundamentals and Technology

Sponsored by: Materials Processing & Manufacturing Division, MPMD-Shaping and Forming Committee

Program Organizers: Yuntian Ted Zhu, Los Alamos National Laboratory, Materials Science and Technology Division, Los Alamos, NM 87545 USA; Terence G. Langdon, University of Southern California, Departments of Aerospace & Mechanical Engineering and Materials Engineering, Los Angeles, CA 90089-1453 USA; Terry C. Lowe, Metallicum, Santa Fe, NM 87501 USA; S. Lee Semiatin, Air Force Research Laboratory, Materials & Manufacturing Directorate, Wright Patterson AFB, OH 45433 USA; Dong H. Shin, Hanyang University, Department of Metallurgy and Material Science, Ansan, Kyunggi-Do 425-791 Korea; Ruslan Z. Valiev, Institute of Physics of Advanced Material, Ufa State Aviation Technology University, Ufa 450000 Russia

Monday AM	Room:	207A		
March 15, 2004	Location	: Charlotte	Convention	Center

Session Chairs: Ruslan Z. Valiev, Ufa State Aviation Technical University, Matls. Sci. & Tech. Div., Los Alamos, NM 87545 USA; Terry C. Lowe, Metallicum, Santa Fe, NM 87501 USA; Zenji Horita, Kyushu University, Dept. Matls. Sci. & Engrg., Fukuoka 812-8581 Japan

# 8:30 AM Introductory Remarks

#### 8:35 AM Invited

Application of Equal-Channel Angular Pressing for Grain Refinement of Plate Samples: Masakazu Kamachi<sup>1</sup>; Minoru Furukawa<sup>2</sup>; Zenji Horita<sup>1</sup>; Terence G. Langdon<sup>3</sup>; <sup>1</sup>Kyushu University, Fac. of Engrg., Dept. of Matls. Sci. & Engrg., 6-10-1 Hakozaki, Higashi-ku, Fukuoka, Fukuoka 812-8581 Japan; <sup>2</sup>Fukuoka University of Education, Dept. of Tech., Munakata, Fukuoka 811-4192 Japan; <sup>3</sup>University of Southern California, Depts. of Aeros. & Mech. Engrg. & Matls. Sci., Los Angeles, CA 90089-1453 USA

Equal-channel angular pressing (ECAP) was applied to plate samples of high-purity aluminum for grain refinement. The plate sample was rotated by 90° in the same sense about the plate normal between each pass, which was designated in this study route  $B_{\text{CZ}}$ . Samples were subjected to a total of 4 passes, equivalent to an imposed strain of ~4. The microstructures were examined using optical microscopy and transmission electron microscopy. It was found that the microstructure consisted of equiaxed grains and elongated grains with the former having area fractions of ~70 to 80%. The average grain size in the equiaxed grain area was ~0.9 µm. The Vickers microhardness was measured on the three orthogonal sections and there was no significant difference throughout each section and between the sections. Tensile tests were conducted at room temperature and the tensile behavior was found to be independent of the direction of the specimen gauge lengths which were taken parallel to the two orthogonal planes perpendicular to the plate normal.

#### 8:55 AM

Continuous ECAE (Conshearing) Process of Aluminum and Steel Strips: *Hiroshi Utsunomiya*<sup>1</sup>; Ken-ichi Hatsuda<sup>2</sup>; Yoshiaki Okamura<sup>2</sup>; Tetsuo Sakai<sup>2</sup>; Yoshihiro Saito<sup>3</sup>; <sup>1</sup>University of Cambridge, Dept. of Engrg., Trumpington St., Cambridge, Cambridgeshire CB2 1PZ UK; <sup>2</sup>Osaka University, Dept. of Matls. Sci. & Engrg., 2-1 Yamadaoka, Suita 565-0871 Japan; <sup>3</sup>Osaka University, 4-1-12-613, Yamadanishi, Suita, Osaka 565-0824 Japan

The authors developed the 'Conshearing' process as a continuous version of ECAE. In this study, the process was applied to 2mm-thick low carbon (0.044%C) steel and AA1100 aluminum alloy strips at room temperature. In the case of the low carbon steel, Goss {110}<001> orientation develops after 2 passes. In addition to Goss, {110}<112>, {111> and {112}<110> components are found after several passes. The tensile strength increases from 380MPa to 700MPa. Lamelar dislocation cells or subgrains are formed in grains. In the case of AA1100 strips, the <111>||ND shear texture showed maximum intensity after two passes, the mean thickness and the length of the grains are 0.42mm and 1.4mm, respectively. The obtained material shows a tensile strength of 170MPa and an elongation of 23%. The continuous ultra grain refinement of the aluminum strip coils is feasible at room temperature.

# 9:10 AM

Mechanical Properties and Microstructures of High-Purity Copper Processed by Equal Channel Angular Extrusion: David J. Alexander<sup>1</sup>; <sup>1</sup>Los Alamos National Laboratory, MST-6 G770, Los Alamos, NM 87545 USA

High-purity oxygen-free electronic copper (C10100) has been processed by equal channel angular extrusion with up to 16 passes at room temperature (90° tooling, route Bc). Small tensile specimens (gage section 1.3 by 2.5 by 5.1 mm) were sectioned along the length of the billet by electrodischarge machining, as well as compression cubes. The samples were tested in the as-processed condition, and also after various heat treatments. The microstructures and mechanical properties will be presented and discussed.

# 9:25 AM

Ausforming of NiTi Shape Memory Alloys Using Equal Channel Angular Extrusion: Ajay V. Kulkarni<sup>1</sup>; *Ibrahim Karaman*<sup>1</sup>; Zhiping Luo<sup>2</sup>; <sup>1</sup>Texas A&M University, Dept. of Mech. Engrg., MS 3123, College Sta., TX 77843 USA; <sup>2</sup>Texas A&M University, Microscopy & Imaging Ctr., College Sta., TX 77843 USA

In this study, thermomechanical properties of severely deformed Ti-50.8 at% Ni alloy using Equal Channel Angular Extrusion (ECAE) are investigated. Solutionized NiTi bars were deformed at different temperatures, i.e. room temperature which is above the austenite finish temperature (Af) and 450 C. The aim was to investigate the effects of ausforming (deformation above Af) on shape memory characteristics of NiTi such as superelasticity, transformation temperatures and fatigue properties. DSC was used to explore the effects of heat treatment temperature and time on the as-received, solutionized and asdeformed materials in terms of transformation temperatures, R-phase formation, and change in thermal hysteresis. TEM was utilized to reveal the changes in microstructure and formation of nanograins by in-situ heating and cooling experiment. Cyclic deformation tests are done on the as received, solutionized and as-deformed samples before and after some selected heat treatments. In this presentation improvement in thermal and mechanical properties with severe ausforming and subsequent annealing will be demonstrated. Stable cyclic response, pseudoelastic strain, change in transformation temperatures, formation of R-phase and nanograins, effects of precipitates will be rationalized with the observations on microstructures and possible deformation mechanisms.

# 9:40 AM Invited

# Fabrication of Bulk Nanostructured Materials by ARB (Accumulative Roll-Bonding) Process: Nobuhiro Tsuji<sup>1</sup>; <sup>1</sup>Osaka University, Dept. Adaptive Machine Sys., 2-1 Yamadaoka, Suit, Osaka 565-0871 Japan

Accumulative Roll-Bonding (ARB) is a severe plastic deformation (SPD) process applicable to bulky materials. In the ARB process, the rolled material is cut, stacked to be the initial dimension, and then rollbonded again. Because this procedure can be repeated limitlessly, huge amount of total plastic strain can be applied to materials. Ultrafine grained structures with mean grain sizes about 100 nm have successfully formed in various kinds of metallic materials after several cycles of ARB. Because bulky specimens with various ultrafine grain sizes can be fabricated by the ARB process followed by annealing, various properties of the ultrafine grained materials are systematically clarified. Furthermore, it would be possible to fabricate novel nanostructured materials, such as bulk amorphous sheet, in certain systems by SPD using the ARB. All these features of the ARB process, and structures and properties of the fabricated nanostructured materials will be introduced in the present paper.

# 10:00 AM

Large Scale Manufacturing of Ultrafine-Grained Materials: Kevin P. Trumble<sup>1</sup>; W. Dale Compton<sup>2</sup>; Srinivasan Chandrasekar<sup>2</sup>; Srinivasan Swaminathan<sup>2</sup>; Travis L. Brown<sup>2</sup>; <sup>1</sup>Purdue University, Sch. of Matls. Engrg., 501 Northwestern Ave., W. Lafayette, IN 47907-2036 USA; <sup>2</sup>Purdue University, Sch. of Industrial Engrg., 315 N. Grant St., W. Lafayette, IN 47907-2023 USA

It has been known for some time that ultrafine-grained materials have interesting mechanical properties making them attractive for use in the discrete products sector. It is shown here that by subjecting a material to large scale deformation using machining, very fine-grained structures can be produced in a variety of metals and alloys. The chips produced during lathe machining of pure metals, steels, and other alloys are shown to be ultrafine-grained with crystal sizes between 50 and 800 nm. The hardness of the chips is found to be significantly greater than that of the bulk material. The manufacture of ultrafinegrained metals by machining, when combined with powder and composite processing methods can be expected to lead to the development of a number of advanced materials and bulk forms having new and interesting combinations of properties. The possibility exists that this approach can overcome many of the limitations pertaining to cost and material types that are generally associated with the commonly used methods for making ultrafine-grained materials.

# 10:15 AM

Strain Accommodation in Pearlite Lamellae of a High Carbon Steel During Equal Channel Angular Pressing: Jingtao Wang<sup>1</sup>; Xiaofang Cao<sup>2</sup>; ZhongZe Du<sup>2</sup>; Zheng Zhang<sup>2</sup>; Xicheng Zhao<sup>2</sup>; <sup>1</sup>Nanjing University of Science and Technology, Dept. of Matls. Sci. & Engr., No. 200, Xiaolingwei, Nanjing 210094 China; <sup>2</sup>Xi'an University of Architecture and Technology, Sch. of Metallurgl. Engrg., Yanta Rd. No 13, Xi'an 710055 China

Equal channel angular pressing (ECAP) was successfully applied on pearlite lamellae structure of a high carbon steel 65Mn (Fe-0.65%C-0.90%Mn) at 650°C via route C up to 5 passes. Strain accommodation of lamellae structure and structure evolution were investigated. Intensive strain during ECAP was accommodated by the formation of quasi-regular bamboo structure, continuous wavy bending structure, regular sharp shear up to an true strain of 1.9, and shear cutting of the cement lamellae and ultra-refinement of the matrix ferrite was observed in the subsequent ECAP passes, and finally a homogeneous submicro-grained ferrite matrix with a grain size of 0.3 micrometers even dispersed by spheroidized ultra-fine cementite particles was achieved.

10:30 AM Break

# 10:40 AM Invited

Ultrafine Grained Aluminum Alloys Via Friction Stir Processing: *Rajiv S. Mishra*<sup>1</sup>; Indrajit Charit<sup>1</sup>; <sup>1</sup>University of Missouri, Dept. of Metallurgl. Engrg., 1870 Miner Cir., Rolla, MO 65409 USA

Friction stir processing is a new technique to refine grain size in metallic materials. In this paper, a brief overview of the state-of-theart of friction stir processing for obtaining ultrafine grained microstructure in aluminum alloys will be presented. The current trends indicate that bulk ultrafine grained aluminum alloys can be obtained via friction stir processing. Results will be also presented for direct conversion of cast material to ultrafine grained material in one pass. An attractive feature of this process is the ability to refine microstructure in commercially available high strength aluminum alloys.

# 11:00 AM Invited

Theoretical and Experimental Investigation of Texture and Microstructural Evolution During ECAE: Irene J. Beyerlein<sup>1</sup>; Carlos N. Tome<sup>1</sup>; David J. Alexander<sup>2</sup>; Donald W. Brown<sup>2</sup>; Sven C. Vogel<sup>2</sup>; Saiyi Li<sup>2</sup>; Mark A. Bourke<sup>2</sup>; <sup>1</sup>Los Alamos National Laboratory, Theoretl. Div., MS B216, Los Alamos, NM 87544 USA; <sup>2</sup>Los Alamos National Laboratory, Matls. Sci. Div., Los Alamos, NM 87544 USA

We will present our current progress on the development of a predictive simulation tool, called SPAIN (Simulating Polycrystals for the Advancement and Implementation of Nanomaterials) for advancing understanding and optimal design of Severe Plastic Deformation (SPD) technologies. SPAIN will be designed to predict two relationships: the microstructural evolution from conventional metals to nanometals during SPD processing and the mechanical properties of the resulting nano-structured materials. For this talk, we selected Equal Channel Angular Pressing (ECAP) as our focus SPD technology. Our approach to developing SPAIN integrates both theoretical and experimental efforts on several length scales. The foundation of our modeling effort is the Visco-plastic self-consistent (VPSC) polycrystalline model, incorporating results from both larger scale FEM simulations and smaller scale substructure evolution models. Our experimental efforts advocate the use of state-of-the-art neutron diffraction and Orientation Imaging Microscopy (OIM) instruments and SPD processing capabilities at Los Alamos. We will present results of our comparative analyses of texture and microstructure of both single phase face-centered cubic FCC (Cu, Ni, and Al) and hexagonal close packed HCP (Be) polycrystals processed under multiple passes of different ECAP routes.

# 11:20 AM

FEM Simulation of the Continuous Combined Drawing and Rolling Pressing in Equal Channel Angular (CCDR-ECAP): Carmelo J. Luis Pérez<sup>1</sup>; Javier Leon Iriarte<sup>1</sup>; Ignacio Puertas Arbizu<sup>1</sup>; Pedro A. Gonzalez Crespo<sup>1</sup>; <sup>1</sup>Public University of Navarre, Mech. & Matls. Engrg. Dept., Campus de Arrosadia s/n, Pamplona, Navarra 31006 Spain

Equal channel angular processes are innovative methods used with the aim of improving properties of materials by severe plastic deformation. Depending on the processing route, microstructural characteristics may differ from one route to another. In spite of the great advantages that ECAE processes allow us to obtain, from the point of view of improving mechanical properties in materials, low industrial applications have been developed, which is mainly caused by mechanical limitations (buckling of the punch) and the low velocity of the process. Because of the limitations, previously mentioned, low industrial applications have been developed and few patents dealing with ECAP have been developed. In this work a new method is shown termed Continuous Combined Drawing and Rolling Pressing in Equal Channel Angular (CCDR-ECAP) allowing us to develop a continuous ECAP. Finite element simulations are included in order to show the advantages of this technique in relationship with the previous methods.

# 11:35 AM

Effect of Cryogenic Rolling on the Formation of Ultra-Fine Grains in 5052 Al Alloy: *Won Jong Nam*<sup>1</sup>; Young Bum Lee<sup>1</sup>; *Dong Hyuk Shin*<sup>2</sup>; <sup>1</sup>Kookmin University, Dept. Matl. Sci. & Engrg., 861-1 Chongnung-Dong, Sungbuk-Ku, Seoul 136-702 Korea; <sup>2</sup>Hanyang University, Dept. Metall. & Matl. Sci., Ansan, Kyunggi-Do 425-791 Korea

It has been known that ultra-fine grains less than 1µm in diameter can be obtained by severe plastic straining. In the present work, we have applied cryogenic rolling process to 5052 aluminum alloy and have achieved ultra-fine grains with less than 1µm in diameter showing high strength. Cryogenic rolling of fully annealed 5052 Al alloy plates with 10mm in thickness was performed at various strains, in comparison with cold rolling. To investigate the effect of annealing temperature on recrystallization, the sheets received 88% reduction were annealed at the temperature range of  $150 \sim 300^{\circ}$ C for an hour. Annealing of Al alloy deformed 88%, at  $200^{\circ}$ C for an hour, results in the considerable increase of tensile elongation without the great loss of strength and the occurrence of new polygonal grains less than 300nm in diameter.

# 11:50 AM Invited

Measuring 3D Strain and Particle Distribution in Equal Channel Angular Pressing: Hans J. Roven<sup>1</sup>; <sup>1</sup>The Norwegian University of Science and Technology, Dept. of Matls. Tech., 7491 Trondheim Norway

Equal Channel Angular Pressing (ECAP) has been known to the international community since the former USSR patent presented by V.M. Segal (1977). ECAP is an efficient process for (i) creating ultrafine grained materials, (ii) systematic studies of the relationship between shear deformation and deformation history, (iii) large shear strain accumulations and (iv) thermo-mechanical studies of microstructure and texture development without changing the size and shape of the work-piece. The present work is part of an extensive program on SPD processing of Al alloys. The current knowledge on strain distributions in ECAP is primarily based on FE- simulations and real measurements are very scarce in the open literature. In order to fill some of this lacking knowledge, measurements in sectioned billets are used to map the quasi- 3D strain distribution in route A of a 6082 AlMgSi alloy. An automated strain analyses unit and a rectangular grid are used for this purpose. Details of the strain distribution in the shear zone and towards the edges and corners are also followed. Further, the overall plastic flow in 1-3 passes of route A are measured and compared for two different cases (full friction and minimum friction). Also, different heat treatment conditions of the alloy before deformation are characterized as to study the influence on strain distribution. Another strain and plastic flow related process in ECAP is the micrometer sized particle break-up and distribution. This is characterized for the same alloy in passes 1-8 in route A and route Bc. The experimental results give strong evidence that the classical recrystallization mechanism related to particle stimulated nucleation (PSN) is not operating in SPD at room temperature. The creation of ultrafine grains is mechanistically linked to the local plastic strain and the corresponding severe lattice rotations.

#### 12:10 PM

Strengthening Mechanisms of Surface Nanocrystallization and Hardening Process: Juan C. Villegas<sup>1</sup>; Kun Dai<sup>1</sup>; Zachary Stone<sup>1</sup>; *Leon L. Shaw*<sup>1</sup>; Peter K. Liaw<sup>2</sup>; <sup>1</sup>University of Connecticut, Metall. & Matls. Engrg., Storrs, CT 06269 USA; <sup>2</sup>University of Tennessee, Matls. Sci. & Engrg., Knoxville, TN 37996 USA

Surface nanocrystallization and hardening (SNH) process is a surface severe-plastic-deformation (SPD) process. The strengthening mechanism of this process has been investigated in this study. Three engineering materials, Ni C-2000, Ti-6Al-4V and Al 5052, have been utilized as model materials for this purpose. A hardness increase of the order of 150% with respect to untreated samples is achieved for Ni C-2000, whereas little hardening is observed for Ti-6Al-4V and Al 5052 exhibits an intermediate behavior. The different responses from different materials to the SNH process have been discussed in terms of their work hardening capacities, microstructural evolution, and formation of nanograins. The implications of this study on the efficacies of the SNH process are discussed. This research is supported under U.S. NSF grant DMR-0207729.

# 12:25 PM

Microstructure, Mechanical Properties and Anysotropy of Pure Ti Processed by Twist Extrusion and Cold Rolling: *Dmitry Orlov*<sup>1</sup>; Vladimir Stolyarov<sup>2</sup>; Hamit Salimgareyev<sup>2</sup>; E. P. Soshnikova<sup>2</sup>; Alexey Reshetov<sup>1</sup>; Yan Beygelzimer<sup>1</sup>; Sergey Synkov<sup>1</sup>; Victor Varyukhin<sup>1</sup>; <sup>1</sup>Donetsk Phys. & Tech. Inst. of the National Academy of Sciences of Ukraine, Physics of High Pressure & Advd. Tech., 72 R. Luxemburg St., Donetsk 83114 Ukraine; <sup>2</sup>Ufa State Aviation Technical University, Inst. of Physics of Advd. Matls., 12 K. Marx St., Ufa 450000 Russia

It's investigated UFG structure formation in CPTi bulks processed by SPD (cold Twist Extrusion(TE), true strain e~5.1, with the following Cold Rolling(CR), true strain e~0.7). Evolution of microstructure and tensile mechanical properties in the CPTi were investigated under room temperature. After the TE, in transversal section it is formed structure fragments with size less 1µm. Strength increased on 80%; elongation was 3.4%. Following low-temperature annealing (300°C, 1hour) leaded to increasing in both strength and ductility properties. In longitudinal section, specimens' strength properties increased slightly. Elongation was about 6%. The following low-temperature annealing practically did not influence on the strength but improved elongation to 7.2%. The additional CR leaded to forming severe deformed structure. Average size of fragments was 50-500nm. It was observed elimination of anisotropy and equalization of strength. In both directions ultimate tensile strength became about 780-800MPa and ductility properties remained the same as in the original.

# 5th Global Innovations Symposium: Trends in LIGA, Miniaturization, and Nano-Scale Materials, Devices and Technologies: Plenary: Trends: Past, Present, and Future

Sponsored by: Materials Processing & Manufacturing Division, MPMD-Powder Materials Committee, MPMD-Phase Transformations Committee-(Jt. ASM-MSCTS), MPMD-Computational Materials Science & Engineering-(Jt. ASM-MSCTS), MPMD/EPD-Process Modeling Analysis & Control Committee, MPMD-Surface Engineering Committee, MPMD-Shaping and Forming Committee, MPMD-Solidification Committee

*Program Organizers:* John E. Smugeresky, Sandia National Laboratories, Department 8724, Livermore, CA 94551-0969 USA; Steven H. Goods, Sandia National Laboratories, Livermore, CA 94551-0969 USA; Sean J. Hearne, Sandia National Laboratories, Albuquerque, NM 87185-1415 USA; Neville R. Moody, Sandia National Laboratories, Livermore, CA 94551-0969 USA

Monday PM	Room:	20	)2B		
March 15, 2004	Locatior	<b>1</b> :	Charlotte	Convention	Center

Session Chairs: John E. Smugeresky, Sandia National Laboratories, Livermore, CA 94551 USA; Neville R. Moody, Sandia National Laboratories, Livermore, CA 94551 USA

# 2:00 PM Opening Remarks John E. Smugeresky

# 2:10 PM

Perspectives on Nanosciences and Nanotechnology: M. S. Dresselhaus<sup>1</sup>; <sup>1</sup>Massachusetts Institute of Technology, Cambridge, MA 02139 USA

Nanoscience research is now entering a new phase where the structure and properties of materials can be investigated, characterized and controlled at the nanoscale. New physical phenomena appear at the nanoscale, giving rise to unexpected materials properties, thus bringing new excitement to this research field. In this talk, special emphasis will be given to one-dimensional nanowires and nanotubes because they, in particular, exhibit unusual physical properties, due to their reduced dimensionality and their enhanced surface/volume ratio. These unusual properties have attracted interest in their potential for applications in novel electronic, optical, magnetic and thermoelectric devices. Some examples of research accomplishments and opportunities at the nanoscale will be described, with a view toward new interdisciplinary research programs now under development in the field of nanoscience and nanotechnology worldwide.

#### 2:40 PM

# Nanoceramics, Nanotubes and Nanocomposites Paving the Way for Nanotechnology Revolution – A Review of the Industry and Markets: *Thomas Abraham*<sup>1</sup>; <sup>1</sup>Business Communications Co., 25 Van Zant St., Norwalk, CT 06855 USA

With large-scale current and potential use of nanostructured materials (and nanotubes) in applications such as chemical mechanical polishing (CMP), magnetic recording and ferrofluids, sunscreens, catalysts, biodetection/labeling, conductive coatings, optical fibers, FEDs, chips and nanocomposites, the nanotechnology industry is taking off with commercial markets. The presentation provides an overview of the technologies, applications, industry structure and markets.

# 3:10 PM

The Difficult Transition From Technology to Commercialization- Lessons Learned Over the Past 50 Years: Keith A. Blakely<sup>1</sup>; 'NanoDynamics, Inc., 901 Fuhrmann Blvd., Buffalo, NY 14203 USA Abstract not available.

#### 3:40 PM Break

# 4:00 PM Plenary

### Materials Processing and Manufacturing at the Nanoscale: Fundamental Research and Commercialization Opportunities: Haris Doumanidis<sup>1</sup>; <sup>1</sup>National Science Foundation

This presentation overviews the philosophy and current portfolio of the new Nanomanufacturing Program at NSF. This is placed in the context of the global competition in nanotechnology, the National Nanotechnology Initiative and its promised impacts to society and everyday life. The Nanomanufacturing Program was established in 2001 to promote fundamental research and education in manufacturing at the nanoscale, and to transfer developments in nanoscience and nanotechnology discoveries from the laboratory to industrial applications. This presentation emphasizes issues related to nanomanufacturing research for technology transfer and commercialization of nanotechnology products. It stresses on the need for materials processing for scale-up of nanotechnology and high rate production, reliability, robustness, yield, efficiency and cost issues for manufacturing products and services. Nanomanufacturing capitalizes on the special material properties and processing capabilities at the nanoscale, and promotes integration of nanostructures to functional microdevices and meso/macroscale architectures and systems, as well as the interfacing issues across dimensional scales. Research in nanomanufacturing machines covers interdisciplinary areas and entails multi-functionality across all energetic domains, including mechanical, thermal, fluidic, chemical, biochemical, electromagnetic, optical etc. Nanomanufacturing focuses on a systems approach, encompassing nanoscale materials and structures, fabrication and integration processes, production equipment and characterization instrumentation, theory/modeling/simulation and control tools, learning from nature and biomimetic design, integration of multi-scale functional systems, and industrial application. The NSF program places special emphasis in education and training of the workforce, involvement of socioeconomic sciences, addressing the health, safety and environmental implications, development of manufacturing infrastructure, as well as outreach and synergy of the academic, industrial, federal and international community. Current NSF funded research at universities and small businesses, as well as present research challenges and support opportunities are also reviewed.

## 4:30 PM Plenary

Nanoscale Integrated Circuits and Future Materials Challenges: C. Michael Garner<sup>1</sup>; <sup>1</sup>Intel Corporation, Matls. Tech. Operation, SC11-230, 2191 Laurelwood Rd., Santa Clara, CA 95054-1514 USA

Continued scaling of integrated circuits will require the development of many new materials with properties and structure controlled at the nanometer scale. Integrated circuits have had minimum feature sizes less than 100nm since 2000, and many new materials are being integrated with each generation. As scaling continues, the materials comprising the dielectrics and conductors in the transistors, and the interconnects must have controllable electronic, electrical, nano-structural, and mechanical properties. The electrical performance of the MOS transistor depends on the electrical properties of the gate dielectric, gate electrode and stress state of the silicon. Interconnect performance depends on the resistance of the metal and capacitance of the interlevel dielectrics (ILD). Much work is being done to reduce the dielectric constant of the ILD through fabrication of porous dielectrics, but significant challenges remain to do this while maintaining mechanical strength of the ILD. Furthermore, as copper interconnects are scaled to smaller feature sizes, the diffusion barrier layer must be reduced in thickness while maintaining an effective diffusion barrier for the copper. Finally, the electrical resistivity of the copper interconnects must not be reduced significantly even though there is significant scattering due to surface, interface roughness, and grain scattering. These challenges offer opportunities for nano-materials in processing, advanced structural applications and devices in the future, but significant progress must be made in characterizing their electronic, electrical and chemical and mechanical properties.

# 5:00 PM Plenary

Nanostructured Ceramics: Processing, Applications and Commercialization: B. H. Kear<sup>1</sup>; <sup>1</sup>Rutgers University, Ctr. for Nanomatls. Rsch., 607 Taylor Rd., Piscataway, NJ 08854-8065 USA

Two methods have been devised for the production of nanostructured ceramics: one for single phase or nanocrystalline ceramics and the other for multiphase or nanocomposite ceramics. The first method makes use of a metastable nano-scale powder as starting material and pressure-assisted sintering to develop a nanocrystalline product. The second method utilizes a metastable micro-scale powder as starting material and pressure-assisted sintering to develop a nanocomposite product. Both methods depend for their success on control of a pressure-induced phase transformation to promote rapid densification without causing significant grain growth. Several examples will be given to illustrate the versatility of the transformation-assisted consolidation process. In addition, progress in near-net shape superplastic-like forming of nancomposite ceramics will be described. Applications include engine components, machine tools, and household items. A methodology for commercializing the new technologies will also be discussed.

# Advanced Materials for Energy Conversion II: Metal Hydrides II

Sponsored by: Light Metals Division, LMD-Reactive Metals Committee

*Program Organizers:* Dhanesh Chandra, University of Nevada, Metallurgical & Materials Engineering, Reno, NV 89557 USA; Renato G. Bautista, University of Nevada, Metallurgical and Materials Engineering, Reno, NV 89557-0136 USA; Louis Schlapbach, EMPA Swiss Federal, Laboratory for Materials Testing and Research, Duebendorf CH-8600 Switzerland

Monday PM	Room: 203A	
March 15, 2004	Location: Charlotte Convention	Center

Session Chairs: Jim C.F. Wang, Sandia National Laboratories, Livermore, CA 94550 USA; Bruce Clemens, Stanford University, Matls. Sci., Stanford, CA 94305 USA; Jean-Marc Joubert, CNRS, Thais Cedex F94320 France

# 2:00 PM Plenary

Solid State and Surface Phenomena in Energy Transformation Materials: Louis Schlapbach<sup>1</sup>; <sup>1</sup>EMPA, Swiss Federal Lab for Matls. Testing & Rsch., CH-8600, Duebendorf Switzerland

Solid state and surface phenomenon in energy transformation materials will discussed. Environmental issues related to the energy conversion systems; mainly production of carbon dioxide is an important issue. Clean hydrogen energy will have a signifcant impact on global issues related to energy in both stationary as well as mobile power generators. Fundamental understanding of hydrogen interactions with materials will allow development of new light weight hydrogen storage materials/systems. The use of hydrogen in fuel cells and engines for automobiles will have to be fully explored for clean energy conversion. In addition, energy loss prevention by using quasicrystalline coatings on materials will reduce tribology (energy loss). Heat transfer issues in gas turbines need to be also evaluated. Other systems such as thermoelectrics, photovoltaics, and others will also be discussed.

## 2:30 PM Invited

Novel Hydrides with [Al-H] Bonding Synthsized by Hydrogenation of Intermetallic Compounds: Etsuo Akiba<sup>1</sup>; Qing An Zhang<sup>2</sup>; Yumiko Nakamura<sup>1</sup>; <sup>1</sup>National Institute of Advanced Science and Technology, Energy Elect. Inst., Tsukuba Central 5, 1-1-1, Higashi, Tsukuba, Ibaraki 305-8565 Japan; <sup>2</sup>Anhui University of Technology, Sch. of Metall. & Matl., Maanshan, Anhui 243002 China

We successfully prepared novel hydrides by hydrogenation of intermetallics compounds that consisted of alkali earth metal (Mg, Ca, Sr and Ba) and Al. Starting from SrAl<sub>2</sub> Zintl phase alloy, two novel hydrides such as SrAl<sub>2</sub>H<sub>2</sub> Zintl hydride and Sr<sub>2</sub>AlH<sub>7</sub> alanate were synthesized. Alanates of BaAlH<sub>5</sub> and Ba<sub>2</sub>AlH<sub>7</sub> were synthesized from Ba<sub>7</sub>Al<sub>13</sub> intermetallic compound. Crystal structures of these novel hydrides were refined using powder neutron diffraction. Phase relations of pseudo binary alloys of (Sr, X)Al<sub>2</sub> (X=Ca and Ba) and Sr(Al, Mg)<sub>2</sub> were also investigated.

# 2:55 PM Invited

Intermetallic Compounds for Hydrogen Gas Storage: Jean-Marc Joubert<sup>1</sup>; V. Iosub<sup>2</sup>; M. Latroche<sup>2</sup>; A. Percheron-Guégan<sup>2</sup>; <sup>1</sup>CNRS, Lab. de Chimie Métallurgique des Terres Rares, 2-8 rue H. Dunant, Thiais Cedex F-94320 France; <sup>2</sup>CNRS, Lab. de Chimie Métallurgique des Terres Rares, 2-8 rue Henri Dunant, F-94320 Thiais Cedex France

Hydrogen gas is expected to play an important role in the future as an energy career according to its zero emission behaviour when used as a fuel. Many intermetallic compounds (e.g. LaNi5- or ZrMn2-type) react reversibly with hydrogen near atmospheric pressure and ambient temperature to form metal hydrides giving rise to dense and safe hydrogen storage possibility. Possible modifications of the storage properties (such as capacity, hydrogen pressure, aging, kinetics) by composition changes in order to suit a given application represent one of the main features of those compounds. Advantages and drawbacks of metal hydrides are presented and compared with other storage media. An example of application as a storage unit for a stationary fuel cell supply will be detailed.

# 3:20 PM Break

# 3:35 PM Invited

Low and High Pressure Hydrogen Storage in V-0.5 at.%C Alloy: Dhanesh Chandra<sup>1</sup>; Archana Sharma<sup>1</sup>; Joseph R. Wermer<sup>4</sup>; Willliam K. Cathey<sup>1</sup>; Robert C. Bowman<sup>2</sup>; Franklin E. Lynch<sup>3</sup>; <sup>1</sup>University of Nevada, Metallurgl. & Matls. Engrg., Mackay Sch. of Mines, Reno, NV 89557 USA; <sup>2</sup>NASA Jet Propulsion Laboratory, MS 79-24, Pasadena, CA 91109 USA; <sup>3</sup>Hydrogen Consultants, 12400 Dumont Way, Littleton, CO 80125 USA; <sup>4</sup>Los Alamos National Laboratory, Tritium Sci. & Engrg. Grp., MS C-348, Los Alamos, NM 87545 USA

Low and high pressure hydrding of cold-worked V-0.5 at.%C alloy, cycling of hydrides, thermodynamic and structural parameter aspects were investigated. Thermal cycling between beta and gamma phase hydrides increased the hysteresis but the desorption pressure did not significantly change. Prestraining this alloy also increased the hysteresis but the desorption pressure decreased slightly as compared to that of the unstrained alloy. Microstrains, <exp2>1/2, in the beta phase of the thermally cycled hydrides decreased after >700 cycles, whereas the domain sizes increased. However in the gamma phase, both the microstrains and the domain sizes decreased after thermal cycling. The dehydrogenated alpha phase after >700 thermal cycles showed residual microstrains in the lattice, similar those observed for the intermetallic hydrides. Thermodynamic aspects of alpha to beta phase transitions at low pressures will also be presented. The effects of thermal cycling and cold-work on absorption and desorption pressures, H/ M ratio, microstrains, long range strains and domain sizes in the beta and gamma phase hydrides of V-0.5 at.%C alloy are presented.

# 4:00 PM Invited

Neutron Metrology for the Hydrogen Economy: Terrence J. Udovic<sup>1</sup>; Taner Yildirim<sup>1</sup>; Charles F. Majkrzak<sup>1</sup>; Muhammad Arif<sup>1</sup>; David L. Jacobson<sup>1</sup>; <sup>1</sup>National Institute of Standards & Technology, Ctr. for Neutron Rsch., 100 Bureau Dr., MS 8562, Gaithersburg, MD 20899-8562 USA

Neutron scattering, transmission, and analysis techniques are particularly well-suited for studying materials of relevance to fuel-cell and hydrogen-storage technologies. The unusually large neutron scattering cross section for hydrogen (and deuterium) as well as the neutron's great penetrating power are routinely exploited in order to probe the amount, location, bonding states, and dynamics of hydrogen (and water) in a variety of technologically interesting materials. Developments over the past decade at the NIST Center for Neutron Research and elsewhere have greatly increased the sensitivity and dynamic range of neutron methods. In this talk, we will provide a flavor of the capabilities of modern neutron instrumentation for the study of energy systems and materials important for the hydrogen economy, from micron-scale imaging of working fuel-cell stacks and hydrogenstorage beds to atomic-scale characterization of hydrogen location, bonding, and transport mechanisms in fuel-cell membranes and hydrogen storage materials.

#### 4:25 PM Invited

Sensing of Hydrogen in Advanced Ni-MH Battery Materials: Brajendra Mishra<sup>1</sup>; David L. Olson<sup>1</sup>; <sup>1</sup>Colorado School of Mines, Metallurgl. Engrg., 920 15th St., Golden, CO 80401 USA

The AB5 type alloys, such as LaNi5, are used as hydrogen storage materials. Absorbed hydrogen provides electrons to the conduction band and also creates the hydride bonding band. Consequently, electrons change the magnetic and thermoelectric power properties of the AB5 hydrogen storage. Additionally, the linear relationship between the magnetic and thermoelectric power properties is discovered. This phenomenon is due to the reduction of the magnetic moment in B site of AB5 alloys and the partial filling of electrons from hydrogen in the conduction band of the alloys. Effect of absorbed hydrogen on the Seebeck coefficient of the studied alloys shows the similar pattern as the pressure composition isotherm. This behavior shows that Seebeck coefficient is a potential parameter to be used as an indicator of micro-structure or phase of AB5 alloys. Consequently, the magnetic susceptibility measurement is an important tool to be developed as a phase indicator for AB5 alloys.

# Advances in Superplasticity and Superplastic Forming: Development of Advanced Superplastic Forming Processes

Sponsored by: Materials Processing and Manufacturing Division,
Structural Materials Division, MPMD-Shaping and Forming
Committee, SMD-Mechanical Behavior of Materials-(Jt. ASM-MSCTS),
SMD-Structural Materials Committee
Program Organizers: Eric M. Taleff, University of Texas,
Mechanical Engineering Department, Austin, TX 78712-1063 USA;
P. A. Friedman, Ford Motor Company, Dearborn, MI 48124 USA;
Amit K. Ghosh, University of Michigan, Department of Materials
Science and Engineering, Ann Arbor, MI 48109-2136 USA; P. E.
Krajewski, General Motors R&D Center; Rajiv S. Mishra, University of Missouri, Metallurgical Engineering, Rolla, MO 65409-0340
USA; J. G. Schroth, General Motors, R&D Center, Materials and Processes Laboratory, Warren, MI 48090-9055 USA

Monday PM	Room: 2	201B
March 15, 2004	Location:	Charlotte Convention Center

Session Chairs: Eric M. Taleff, University of Texas, Dept. of Mech. Engrg., Austin, TX 78712-0292 USA; Paul E. Krajewski, General Motors, R&D Ctr., Warren, MI 48090-9055 USA

# 2:00 PM

The History and Current State-of-the-Art in Airframe Manufacturing Using Superplastic Forming Technologies: Daniel G. Sanders<sup>1</sup>; <sup>1</sup>Boeing, MR&D & Phantom Works, PO Box 3707 MS 5K-63, Seattle, WA 98124-2207 USA

This paper examines the progression of SPF in aerospace from the early days of hot forming to the state-of-the-art in current fabrication technologies. In the past fifteen years there has been a remarkable evolution of the Superplastic Forming (SPF) as an aerospace manufacturing process. The original aerospace applications and development of SPF were heavily influenced by military aircraft requirements for bomber and fighter projects such as the B-1, B-2, F-15E, and the F/A-18. Parts for these USAF airframes were hand-built in small lot sizes of one to three parts. At Boeing, the natural progression of SPF and hot forming methodology turned towards commercial aviation in the 1990?s, during the design of the B-777 and B-737-NG. It was during this timeframe that SPF production rates increased from one or two parts per month on the military side of the business to several hundred per month required for passenger jetliner manufacturing. The SPF process was thrust into the mass production mode, whereby highly automated presses were developed and brought on-line. New tooling innovations and part trimming methods were co-developed. Along with the advancements in SPF automation, there have been a number of material inventions that have accelerated the proliferation of parts. New aluminum alloys like 5083-SPF and 2195 have allowed designers to create large monolithic panels to replace built-up assemblies that used to require hundreds of fasteners and eliminate dozens of detail parts. Several titanium alloys, such as SP-700, 6-2-2-2, 6-2-4-2 and 15-3-3-3 have opened-up a wider range of part families that are subjected to high stresses, sonic vibration, corrosive environments and high operating temperatures. SPF advances have been made possible by concurrent advances in many other enabling technologies. Through the application of new alloys and clever engineering design, SPF implementations at Boeing have resulted part consolidation, weight reduction, faster through-put, inventory reduction, elimination of tooling families, simplified assembly and substantial cost savings. As we move further into the twenty-first century, the teaming and partnering of government institutions, industry partners and the universities is vital. Teaming of these organizations will be an essential element as SPF manufacturing moves into the mainstream automotive and domestic goods markets.

# 2:25 PM

General Motors' Quick Plastic Forming Process: James G. Schroth<sup>1</sup>; <sup>1</sup>General Motors, R&D Ctr., Matls. & Proc. Lab., MC 480-106-212, 30500 Mound Rd., Warren, MI 48090-9055 USA

General Motors has used hot blow forming processes for the production of aluminum closure panels for specific automotive applications. In the initial manifestation of GM's "Quick Plastic Forming" process, automated forming cells were built around traditional heatedplaten superplastic forming presses. Automotive volumes demand fast forming cycles and reproducible dimensions in hot-formed aluminum panels. The initial implementation of hot blow forming technology leveraged fully automated handling systems, novel sealing geometries and panel extraction methods, and an optimized tool material/coating/ lubricant system in conjunction with specialized cooling fixtures to produce dimensionally correct panels directly out of the forming cell. GM has continued to evolve its forming technology to facilitate shorter forming times, more complex panel geometries, and improved panel dimensions. Representative panel geometries produced with the system are described.

# 2:50 PM

Heating Aluminum Sheet to Enable High-Strain Forming: John E. Carsley<sup>1</sup>; *Richard H. Hammar*<sup>1</sup>; <sup>1</sup>General Motors Corporation, R&D & Planning/Matls. & Proc. Lab., MC 480-106-212, 30500 Mound Rd., Warren, MI 48090-9055 USA

Several novel technologies for shaping aluminum sheet into complex geometries call for elevated temperatures to improve formability. Some of these technologies include warm stamping, superplastic forming and hot hydroforming. Production cycles should not be limited by the speed at which the aluminum blanks are heated to the required temperatures. Several methods of heating aluminum sheet have been investigated and modeled in terms of the primary modes of heat transfer including conduction, convection and radiation. The paper describes the advantages of each method relative to the specifications of attaining a uniform, stable temperature in minimal time while preserving Class-A surface quality. Examples of each method are compared with respect to a blank temperature of approximately 850°F to 900°F, as needed for superplastic forming of AA5083.

# 3:10 PM

Tooling Materials for Superplastic Forming Processes: *M. David* Hanna<sup>1</sup>; 'General Motors, R&D Ctr., Matls. & Proc. Lab., MC 480-106-212, 30500 Mound Rd., Warren, MI 48090-9055 USA

Different steels and cast iron tools used for superplastic and hot forming operate at temperatures as high as 500°C and could be used in service for as long as five years. Experiments were conducted to determine if such tool materials soften (temper) during long-term, hightemperature exposure. Extrapolation from short-term tempering data indicated that no appreciable softening was observed in nodular cast iron or three different tool steels after five years at 480°C.

# 3:30 PM Break

# 3:50 PM

Mass Production of a Spare Tire Housing for an Automobile: Kuniaki Osada<sup>1</sup>; <sup>1</sup>Nippon Yakin Kogyo Co., Ltd, Project Planning & Dvlp. Div., 1-5-8 Kyobashi, Chuou-Ku, Tokyo Japan

Mass production of a spare tire housing made of 5083 Al alloy by superplastic forming was achieved. The housing is composed of two parts with different 3D geometries. Monthly number of the parts was approaching 4,000. In production, multiple forming operations in a single tool set, semi-automatic application of lubricants, and an effective layout of the whole process were key contributions to achieving production goals. In the multiple forming operations, the two pieces of the housing were expanded with a characteristic forming gas inlet mechanism at once. Owing to the mechanism used, it turned out to be possible to form four parts in as short as fifteen minutes. Application of two lubricants onto areas that require specific friction coefficients effectively worked with advantage of resistance to scratches. Because outside appearance of the housing is considerably important in a consumer product, surface treatments were carried out before shipment. In the presentation, key factors that lead to successful production will be summarized.

# 4:15 PM

**Evaluation of Die Coatings for Superplastic Forming Processes:** *Arianna T. Morales*<sup>1</sup>; <sup>1</sup>General Motors, R&D Ctr., Matls. & Proc. Lab., MC 480-106-212, Warren, MI 48090 USA

Typically, superplastically formed parts are made from fine-grained aluminum sheets blow formed into a sculptured ferrous die, which is heated to the proper forming temperature. Intimate contact between the die and the work piece enables the action of interatomic forces (adhesion, friction), and solid lubricants have to be used to prevent sticking and bonding of the aluminum to the ferrous dies. The use of tool coatings tailored for this process may enable the reduction and possible elimination of solid lubricants. The tool coatings can provide an optimal surface configuration for the forming process and significantly increase tool life. This paper will present results obtained from experiments with different coatings and surface treatments on superplastic forming dies.

# 4:35 PM

Certain classes of automotive body panels, such as deck lid outer panels, are preferably formed in two stages. The first stage, called the pre-forming stage, creates the necessary length of line and the thickness distribution that are needed for the second and final forming operation to produce wrinkle-free panels without excessive thinning. The first-stage forming can be accomplished either by gas pressure, i.e. QPF, or by stamping. Double-action QPF tools are special tools that combine two forming stages into one compact tool geometry. Doubleaction QPF offers many advantages over its single-action counterpart in terms of attainable panel shape complexity, production cycle time, improved use of limited press space, etc. This paper describes alternate types of double-action tools: one based on punch pre-forming and one utilizing air-pressure pre-forming.

# 4:55 PM

**SSR Fender Tool Development**: *Chongmin Kim*<sup>1</sup>; Mark G. Konopnicki<sup>2</sup>; Frank G. Lee<sup>3</sup>; <sup>1</sup>General Motors, R&D Ctr., Matls. & Proc. Lab., MC 480-106-212, 30500 Mound Rd., Warren, MI 48090-9055 USA; <sup>2</sup>General Motors, MC 480-106-212, 30500 Mound Rd., Warren, MI 48090-9055 USA; <sup>3</sup>General Motors, GMNA Engrg., Pontiac, MI USA

Math-based technology was effectively used to design a tool set for hot blow forming of large SSR fender panels with complex curvatures. The surface geometries of the forming tool set, consisting of a preform tool and a final form tool, were optimized during the tool design phase with extensive use of finite-element analysis of the forming process. The forming tool set produced both right and left fenders from one blank, resulting in good productivity and high material utilization. The forming tool set was fabricated in less than 20 weeks. This tool development exercise and the immediate success of the forming trial set a benchmark for rapid production of complex body panels.

# Alumina and Bauxite: Process Modeling and Control

Sponsored by: Light Metals Division, LMD-Aluminum Committee Program Organizers: Travis Galloway, Century Aluminum, Hawesville, KY 42348 USA; David Kirkpatrick, Kaiser Aluminum & Chemical Group, Gramercy, LA 70052-3370 USA; Alton T. Tabereaux, Alcoa Inc., Process Technology, Muscle Shoals, AL 35661 USA

Monday PM	Room: 2	18A	
March 15, 2004	Location:	Charlotte C	onvention Center

Session Chair: Benoit Cristol, Aluminium Pechiney, Alumina Tech., Gardanne Cedex 13541 France

# 2:00 PM

Application and Benefits of Advanced Control to Alumina Refining: *Robert K. Jonas*<sup>1</sup>; <sup>1</sup>Honeywell Industrial Solutions, Mining, Metals, & Minerals, 2500 W. Union Hills Dr., Phoenix, AZ 85053 USA

Substantial returns to alumina refineries can be realized through the use of control technology that utilizes existing infrastructure and requires minimal support staff. The globalization of markets and the consolidation of producers have created a more competitive environment that drives the need for optimal production and performance in alumina refineries. Throughout the Bayer process, advanced control is becoming a preferred tool to deliver return on capital employed. Primarily, this is being done using the prevailing control technology, multivariable predictive control. This paper will discuss the applications and benefits of this technology in the alumina industry. Increases in production, yield, and quality are being realized in many areas of the Bayer cycle using multivariable predictive control, most notably in the control of the bauxite digestion area. New benefits are being achieved by applying this control technology to evaporation and heatinterchange units. The technology is also proving to be suited to grinding, precipitation, and calcination. Improvements in production or yield of up to 1/2 to 4% are realizable.

#### 2:25 PM

The Effects of Changes in Liquor Temperature and Caustic Concentration on Seed Balance Parameters in Alumina Refinery Seed Classification Systems: *Walter Mason Bounds*<sup>1</sup>; <sup>1</sup>2583 Woodland Ridge Blvd., Baton Rouge, LA 70816 USA An important consideration in controlling alumina refinery seed classification systems is ensuring that seed produced matches quantity and particle size distribution with seed charged. When this condition is not satisfied, the system may not be stable, resulting in changing seed inventory quantities and particle size distribution. Previous papers have described methods for evaluating operating parameters for individual classification systems. In this paper, information from previous papers is utilized to simulate a classification system and determine the effects of changes in liquor temperature and caustic concentration on seed balance parameters, including mass balance and particle size distribution. Temperature and caustic concentration effects on out-ofbalance cases are also established to aid in illustrating consequences.

#### 2:50 PM

Perfomance Stability Criteria and Expert Control System of Rotary Sintering Kiln at "Achinsk Alumina Plant" PSC: Alexander I. Berezin<sup>1</sup>; Oleg O. Rodnov<sup>1</sup>; Vladislav V. Blinov<sup>2</sup>; Pavel D. Stont<sup>2</sup>; Oleg A. Chashchin<sup>3</sup>; Peter Ya. Hohlov<sup>3</sup>; Anatoliy M. Skoptsov<sup>3</sup>; <sup>1</sup>RUSAL Engineering & Technology Center, Pogranichnikov st. 37, Krasnoyarsk 660111 Russia; <sup>2</sup>Mayak PKF Ltd., Bograda st. 108, Krasnoyarsk 660021 Russia; <sup>3</sup>"Achinsk Alumina Plant" PSC, Achinsk 662150 Russia

Sintering of the charge in a rotary kiln is a complex non-steady physical-chemical process specified by numerous internal and external disturbing factors and highly dynamic changes of energy and material flows. To describe it criteria of thermal-physical similarity based on the second theorem of similarity theory have been defined. Values of criteria calculated for time periods when the conditions were steady are applicable for analysis of conditions on analogous kilns, the criteria being those of conditions stability. These criteria are used in an expert system capable of automatically controlling the sintering conditions by the rules based on experience and knowledge of expert specialists. Current process parameters form the basis to calculate stability criteria to define and set such control parameter values that provide for stabilization of optimum conditions.

#### 3:15 PM

Design and Training Improvements Through the Use of Dynamic Simulation: Robert K. Jonas<sup>1</sup>; <sup>1</sup>Honeywell Industrial Solutions, Mining, Metals, & Minerals, 2500 W. Union Hills Dr., Phoenix, AZ 85053 USA

Extensive use of dynamic process simulators is becoming the norm for many greenfield facilities in metals and mining, especially among alumina refineries. Dynamic simulation provides a means to validate process design to a greater degree than possible with typical process design tools that cannot handle the complexities of refineries and their interactions with operators and control systems. Many leading companies are benefiting from the use of dynamic simulation for control upgrades and greenfield projects because of the complexity of controls in the Bayer cycle. Dynamic simulation of both process and control systems provides for enhanced control validation and operator training. This paper discusses the current practices and benefits of dynamic simulation in alumina refining. Interactive and accurate simulation provides the mechanism to validate and improve new process and control designs. These improvements have proven to minimize design shortfalls that would negatively impact throughput, quality, and comm issioning times. By using dynamic simulation for operator training, further benefits can be attained by improved availability (minimization of lost production), safety, and environmental and safety certification.

# Aluminum Reduction Technology: Cell Development and Operations

Sponsored by: Light Metals Division, LMD-Aluminum Committee Program Organizers: Tom Alcorn, Noranda Aluminum Inc., New Madrid, MO 63869 USA; Jay Bruggeman, Alcoa Inc., Alcoa Center, PA 15069 USA; Alton T. Tabereaux, Alcoa Inc., Process Technology, Muscle Shoals, AL 35661 USA

Monday PM	Room: 2	213D
March 15, 2004	Location	Charlotte Convention Center

Session Chair: Craig Taylor, Noranda Inc., St. Jude Industrial Park, New Madrid, MO 63869 USA

2:00 PM

The Impact of Anode Cover Control and Anode Assembly Design on Reduction Cell Performance: Mark P. Taylor<sup>1</sup>; Greg L.

Reduction line amperages have been increasing around the world in recent years as companies seek to increase the return from existing assets. A key part of a smelter's asset base is its fleet of anode rods, which were designed to take a particular current range, and to carry the anode of the day with an acceptable voltage drop, and robustly enough to prevent drop off or wide-spread cracking of the carbon. Similarly the anode cover on reduction lines has been optimised or at least designed primarily to prevent air access to the anode surface - still a key design criterion for the cell. However the increase in heat generation within the anode, and within the bath as well in many smelters, as amperage has increased, has eventually brought these cell components to their temperature limits or beyond. The anode assembly design criterion which is now most critical for the stability of the cell is the dissipation of sufficient heat from the assembly and the cover to maintain component temperature and overall cell heat balance. This paper builds on earlier work regarding the thermochemical stability of cover and crust [1] to discuss the operating practice and assembly design issues which must be addressed at a smelter to meet the amperage challenge. Simple modelling of the assembly heat flows and the impact of anode cover on them is combined with plant results to demonstrate how the above issues can be addressed.

# 2:25 PM

The Influence of the Thermo-Electrical Characteristics of the Coke Bed on the Preheating of an Aluminium Reduction Cell: Carl Laberge<sup>1</sup>; László I. Kiss<sup>1</sup>; Martin Desilets<sup>2</sup>; <sup>1</sup>Université du Québec, 555 boul. de l'Université, Chicoutimi, Québec G7H 2B1 Canada; <sup>2</sup>Alcan International Limitée, 1955 boul. Mellon, Jonquière, Québec G7S 4K8 Canada

Coke beds are frequently used for the electrical preheating of aluminium electrolysis cells. Their electrical and thermal resistances have a strong influence on the rate of heat generation and on the uniformity of the temperature distribution during the warming-up. Both the electric and thermal transport processes have a complex nature inside granular materials. Material properties, bed thickness, pressure, granulometry, temperature level - all have an effect on the electric resistance and equivalent thermal conductivity. An experimental study was completed in order to analyze the mechanism of the transport processes and to supply constitutive laws for the mathematical modelling of the electrical preheating of an aluminium reduction cell. Results are presented to represent the most important tendencies of the electrical resistance and equivalent thermal conductivity as functions of temperature and bed thickness.

#### 2:50 PM

# Autopsy Procedures and Results at Century West Virginia: Marilou McClung<sup>1</sup>; Ron Zerkle<sup>1</sup>; <sup>1</sup>Century Aluminum of West Virginia, Techl., PO Box 98, Ravenswood, WV 26164 USA

Extending pot life can be a significant cost savings for any Reduction facility. The first step in Century Aluminum of West Virginia's pot life improvement program was to observe pot failure modes and conduct autopsies on a wide variety of pots to determine failure causes and mechanisms. A set of procedures was developed to enable us to conduct comprehensive autopsies and to standardize the information collected on all cells. This paper includes information on ur four levels of autopsy procedures, autopsy results and steps taken from the information gathered to improve pot life. Several examples of autopsy results are discussed in detail.

# 3:15 PM

**Busbar Modification of the End Pots of Potline 1 of Albras**: *Guilherme Epifanio Mota*<sup>1</sup>; Gilvando Jose Andrade<sup>1</sup>; <sup>1</sup>Albras - Aluminio Brasileiro S/A, Area de Redução/Fundição, Estrada Pa 483 KM 21 Vila Murucupi, Bracarena, Para 68447-000 Brasil

In The Albras Potlines the end pots have always presented inferior performance compared to the midle pots, giving high instability and voltage oscillation resulting, in low current efficiency. Even after the magnetic compensation of all the pots, such difference between those pots still remained. So, in order to eliminate this situation, and based on electromagnetic model simulations, it was proposed busbars modification at the end of the potroom, to improve the magnetic configuration by reduction of intensity and better symmetry of the vertical magnetic field components inside the end pots. This modification consisted of increasing the distance between the end busbars and end pots, reducing magnetic influence. With this, pot voltage oscillation decreased and increasing current efficiency. In addition, we expect an increase in pot life. This paper presents the average results of the end pots for the 6 months following the modification and the involved costs.

# 3:40 PM Break

# 3:50 PM

CVG Venalum - Line VI and VII: Lenin Dario Berrueta<sup>1</sup>; <sup>1</sup>C.V.G. Venalum, Presidencia, AV. Fuerzas Armadas, Edif. Corporativo, Puerto Ordaz, Bolivar 8050 Venezuela

The short and medium expansion plans of Venalum consider the construction of two reduction lines. This plan has been scheduled into two stages, each reduction line to be constructed along with its carbon plant and cast shop required to operate the pots fully independent from the previous Venalum infrastructure. During construction of the first expansion, the actual port facilities will be enhanced to cover the two new lines material handling requirements. Engineering of this expansion is based on the use of our own reduction technology, The V-350 Cell, therefore, investment cost can be kept close to 600 million dollars for Line VI, and lower for Line VII. The annual production capacity of each line will be in the order of 210.000 tonnes, hence, total annual output of Venalum after completion of the two lines will be over 850.000 tonnes, and sales in excess of a thousand million american dollars.

# 4:15 PM

**Brazil 2001 Energy Crisis - The Albras Approach**: *Handerson Penna Dias*<sup>1</sup>; <sup>1</sup>Albras - Aluminio Brasileiro SA, Est. PA 483 Km 21, Vila de Murucupi, Barcarena, PA 68447000 Brazil

Due to many causes Brazil has suffered a major energy shortage during the year of 2001. The Aluminum Industry has been heavily hit and forced to reduce its energy consumption. The paper describes the approach adopted by Albras to deal with the crisis and to get a fast return to normal operation at the beginning of 2002. The results are discussed regarding the low energy input operation and the impact on cell life.

## 4:40 PM

Henan Hong Kong Longquan Aluminum Co. Ltd. — Growing Up: Haibo She<sup>1</sup>; Shichang Chen<sup>2</sup>; Juanzhang Zhang<sup>3</sup>; <sup>1</sup>Shenyang Aluminium & Magnesium Engineering & Research Institute (SAMI), R&D, 184 Hepingbei St., Shenyang, Liaoning 110001 China; <sup>2</sup>Henan Hong Kong Longquan Aluminium Co. Ltd, Yichuan County, Luoyang 471713 China; <sup>3</sup>Luoyang Tiansong Carbon Co. Ltd, Yichuan County, Luoyang, Henan 471312 China

Henan Hong Kong Longquan Aluminum Co. Ltd. (LQAL) and Luoyang Tiansong Carbon Co. Ltd. (TSC) are located in Yichuan County, Luoyang, Henan Province, China. These companies are separately engaged in aluminum reduction and prebaked anode block production respectively. They are both owned by Yichuan Electrical Group. The 300 kA potline in LQAL is the first 300 kA potline and with the largest capacity per potline in operation so far in China. LQAL(200kt/ a) took twelve months to complete the construction of the first 300 kA potline, five months to successfully start-up the 256 pots, and six months to reach the designed operating targets. TSC (120kt/a) took twenty months to complete the construction of the plant. The two projects both are praised as "miracle" in the aluminum industry construction of China.

# Automotive Alloys 2004: Session II

Sponsored by: Light Metals Division, LMD-Aluminum Committee Program Organizer: Subodh K. Das, Secat, Inc., Coldstream Research Campus, Lexington, KY 40511 USA

Monday PM	Room: 27	10A
March 15, 2004	Location:	Charlotte Convention Center

Session Chair: Subodh K. Das, Secat Inc., Coldstream Rsch. Campus, Lexington, KY 40511 USA

#### 2:00 PM

Flanging of Aluminum Panels: Sergey F. Golovashchenko<sup>1</sup>; Andrey V. Vlassov<sup>2</sup>; <sup>1</sup>Ford Motor Company, Ford Rsch. & Advd. Engrg., MD 3135, 2101 Village Rd., Dearborn, MI 48124 USA; <sup>2</sup>Bauman Moscow State Technical University, Mech. Engrg. Tech., 5 2nd Baumanskaya St., Moscow 107005 Russia

Implementation of aluminum alloys for the production of automotive skin panels may create problems due to their lack of formability. In flanging and hemming operations, it may result in splits on the Aclass surface. In order to produce high-quality exterior panels, new technologies of flanging and hemming have to be developed. Employment of elastic materials instead of regular steel allows reduce the cost of stamping dies because only one side of the die has to be machined. In addition, ductility of aluminum alloys in flanging and hemming operations can be improved by applying normal pressure to the outer surface of the blank, where stretching of the material takes place. Application of the external pressure through compression of elastic material shifts the stress state from tensile to tension-compression and increases the mean stress. Experimental and numerical results illustrating flat hemming and sharp flanging of 6111-T4 prestrained sheet will be presented.

#### 2:30 PM

# Incremental Forming of Aluminum Alloys: Sergey F. Golovashchenko<sup>1</sup>; *Al R. Krause*<sup>1</sup>; <sup>1</sup>Ford Motor Company, Ford Rsch. & Advd. Engrg., MD 3135, 2101 Village Rd., Dearborn, MI 48124 USA

The lack of formability found in aluminum alloys is often an issue in the manufacturing of body components, particularly for complex forming operations. Traditionally this problem was addressed by stamping separate panels and joining them by spot welding or riveting adding cost. For components that have geometries just beyond traditional forming capabilities another option may be possible. The objective of this research was to investigate the potential of an intermediate heat treatment to extend the range of deformation possible with aluminum alloys. Times and temperature ranges for typical automotive aluminum alloys were investigated and their effects on tensile behavior analyzed. The effect of pre-heat treatment deformation on heat-treat times were also investigated.

#### 3:00 PM

# Formability Studies on Al Alloy 5754 for Manufacture of a Specific Automotive Component: *Gyan Jha*<sup>1</sup>; <sup>1</sup>Arco Aluminum Inc., 9960 Corporate Campus Dr., Ste. 3000, Louisville, KY 40223-4032 USA

This paper attempts to present the work done by ARCO Aluminum in the manufacture of AA 5754 Al alloy sheet material using different thickness and final processing conditions for the manufacture of a specific automotive component. Mechanical properties were evaluated for the sheet at various thickness and formability studies were carried out for all the sheets to determine the behavior of the sheet during forming in all three dimensions. These results were integrated with the CAD/CAM design of the component applicable to a specific hydraulic manufacturing press into proprietary software Autoform to predict the possibility of forming 2 different components by comparing the stresses raised at various locations under actual production conductions with the mechanical properties. A clear view of the stresses at various locations during sheet forming is obtained and when compared with the mechanical properties it is possible to determine safe and highly stressed areas and using an acceptance criteria for safety it is possible to highlight area of criticality in the component. This permits modification of the tooling design and loading conditions without investment in expensive tooling costs. Where necessary this permits development of the alloy to the correct specifications and subsequent modeling trials without investment in expensive tooling and development efforts.

#### 3:25 PM

Abnormal Grain Growth in Friction Stir Welded and Post Thermal-Mechanical Treated Al-2195: *Stanley M. Howard*<sup>1</sup>; Anthony Barajas<sup>2</sup>; Richard Wellnitz<sup>1</sup>; Anand Kaligotla<sup>1</sup>; <sup>1</sup>South Dakota School of Mines and Technology, Dept. of Matls. & Metallurgl. Engrg., 501 E. St. Joseph St., Rapid City, SD 57701 USA; <sup>2</sup>Oglala Lakota College, Kyle, SD 57752 USA

Samples from a fully annealed friction stir welded Al-2195 plate (0.084x0.61x0.10 m) were subjected to selected thermo-mechanical treatments to determine the effect on abnormal grain growth. Aswelded samples exhibited typical fine grain nugget microstructure. Treatments consisted of cold rolling reductions of 6, 20, 25, and 30% and hot rolling reductions of 10, 20, 30, and 40%. Samples were cut and rolled transverse to the weld. Samples, including control samples, were heated to 950°F (783 K) for 5 minutes to initiate possible grain growth and water quenched. Also, a sample was step heated at 50° F/h (22 K/h) from 750 to 950°F (672 to 783 K). Metallographic examination showed that all samples, except the cold-rolled ones, showed marked abnormal grain growth. Less growth occurred in the 6% cold-worked sample, and none was observed in the more severely cold-worked samples.

#### 3:50 PM

Anelastic Deformation After Unloading: *Jianfeng Wang*<sup>1</sup>; Richard Boger<sup>1</sup>; Robert H. Wagoner<sup>1</sup>; <sup>1</sup>Ohio State University, Dept. of Matls. Sci. & Engrg., 2041 College Rd., Columbus, OH 43210 USA

Previous draw-bend experiments showed springback continued to change for at least 2 years after forming for various aluminum alloys:

2008-T4, 5182-O, 6022-T4 and 6111-T4. DQSK and HSLA steels tested under same conditions showed no time-dependent springback, even after 7 years. In order to investigate a possible role of anelasticity in the measured response, special compression-tension tests of 6022-T4 and DQSK steel were conducted. The materials exhibited similar anelastic behavior following monotonic and reversed strain paths, with rapidly decreasing strain rates within the first hour. The similarity of the behavior of the two alloys and other characteristics of the anelastic deformation suggest that it is not the dominant cause of the time-dependent springback of aluminum alloys. In order to understand the features of anelasticity, tension-compression-unloading tests were also conducted for pure aluminum 1100-O and pure zinc (Alloy 101).

#### 4:15 PM

**Constitutive Behaviour of A356 During the Quenching Operation**: *Christina Michelle Estey*<sup>1</sup>; Steve Cockcroft<sup>1</sup>; Chris Hermesmann<sup>2</sup>; <sup>1</sup>University of British Columbia, Metals & Matls. Engrg., 309-6350 Stores Rd., Vancouver, BC V6T 1Z4 Canada; <sup>2</sup>Canadian Autoparts Toyota Inc., 7233 Progress Way, Delta, BC V4G 1E7 Canada

A collaborative effort is underway between the University of British Columbia and Canadian Autoparts Toyota Inc. to develop a mathematical model to predict the formation of residual stress, and hence the deformation, in A356 cast aluminum wheels during the quenching operation. In order to produce an accurate thermal stress model of the quenching operation, a detailed description of the constitutive behaviour of A356 is required in the solutionized condition. Unfortunately, most published constitutive data for A356 focuses on the final heat treated T6 condition. Therefore, an investigation was performed to determine the constitutive behaviour of A356 in the solution condition, prior to quenching and artificial aging. Uniaxial compression tests were performed over a range of temperatures (up to 500°C) and strain-rates (from 10-3 s-1 to 1 s-1) that are commonly experienced during the quenching operation at the wheel manufacturing plant.

#### 4:40 PM

Effect of Precipitation of Nb on High Temperature Strength of Automotive Ferritic Stainless Steel: Jae Cheon Ahn<sup>1</sup>; Gyu Man Sim<sup>2</sup>; Seung Chan Hong<sup>2</sup>; Chan Young So<sup>1</sup>; Kyung Sub Lee<sup>2</sup>; <sup>1</sup>INI Steel Corporation, R&D Dept., 1, Song hyun-dong, Dong-Ku, Incheon 401-712 Korea; <sup>2</sup>Hanyang University, Matls. Sci. & Engrg., 17 Haeng Dang-Dong, Sung Dong-Ku, Seoul 133-791 Korea

The effect of precipitation of Nb (0.45wt%) on high temperature strength of ferritic stainless steel for automotive manifold was investigated. Hot tensile tests were carried out at 700C with different stroke rate ranging from 1mm/min to 10mm/min. The strength was enhanced as the amount of solute Nb increased. It was thought that the strengthening mechanism was not only the solid solution strengthening but also the dynamic precipitation strengthening by Fe2Nb, since the Fe2Nb precipitates with a size of 20nm, which were not found before the tensile test, were observed at sub-grain boundaries by TEM. Also, the amount of dynamically precipitated Fe2Nb increased as the stroke rate was reduced. Thus, increment of the strength by Nb addition increased as the stroke rate decreased. However, coarse Fe2Nb precipitated by pre-aging at 700C remarkably reduced the strength. Therefore, size control of Fe2Nb was important factor in high temperature strength of ferritic stainless steel.

# 5:05 PM

Characteristics of Closed Cell Al and Al Alloys Foam Made by Pot Foaming Process: *Bo-Young Hur*<sup>1</sup>; *Zhekui Quan*<sup>1</sup>; Arai Hiroshi<sup>1</sup>; Sang-Youl Kim<sup>1</sup>; <sup>1</sup>Gyeongsang National University, Div. of Matls. Engrg., Kajoadong 900#, Chinju 660-701 S. Korea

Metallic foams were made by the pot foaming process. The matrix chosen are pro-alloyed Al-Si alloy (Al-2Si, Al-4Si) to investigate the affection of its good casting properties on the foaming behaviors and Pure Al as the reference. During the process a few process parameters such as: viscosity; surface tension and mixing temperature that affect the structure and the morphology of the closed cell foam are investigated. Herein the proper viscosity is effective to decrease the effect of drainage. The mixing temperature affects mainly the solidification of Al foam.

# Beyond Nickel-Base Superalloys: Molybdenum Silicides I

Sponsored by: Structural Materials Division, SMD-Corrosion and Environmental Effects Committee-(Jt. ASM-MSCTS), SMD-High Temperature Alloys Committee, SMD-Mechanical Behavior of Materials-(Jt. ASM-MSCTS), SMD-Refractory Metals Committee *Program Organizers:* Joachim H. Schneibel, Oak Ridge National Laboratory, Oak Ridge, TN 37831-6115 USA; David A. Alven, Lockheed Martin - KAPL, Inc., Schenectady, NY 12301-1072 USA; David U. Furrer, Ladish Company, Cudahy, WI 53110 USA; Dallis A. Hardwick, Air Force Research Laboratory, AFTL/MLLM, Wright-Patterson AFB, OH 45433 USA; Martin Janousek, Plansee AG Technology Center, Reutte, Tyrol A-6600 France; Yoshinao Mishima, Tokyo Institute of Technology, Precision and Intelligence Laboratory, Yokohama, Kanagawa 226 Japan; John A. Shields, HC Stark, Cleveland, OH 44117 USA; Peter F. Tortorelli, Oak Ridge National Laboratory, Oak Ridge, TN 37831-6156 USA

Monday PM	Room: 2	11B		
March 15, 2004	Location:	Charlotte	Convention	Center

Session Chairs: Matthew J. Kramer, Iowa State University, Ames Lab., Ames, IA 50011-3020 USA; Kyosuke Yoshimi, Tohoku University, Inst. for Matls. Rsch., Sendai, Miyagi 980-8577 Japan

# 2:00 PM Invited

**Oxidation of High Temperature Structural Molybdenum Borosilicides:** S. Woodard<sup>1</sup>; S. Vega<sup>1</sup>; D. Berczik<sup>1</sup>; <sup>1</sup>Pratt and Whitney, 400 Main St., MS 114-51, E. Hartford, CT 06040 USA

Historically, as high temperature structural materials molybdenum and molybdenum-based alloys have been limited to non-oxidizing environments in an uncoated condition due to the volatility of the primary oxide that forms on these alloys. In the early-1990's molybdenum borosilicides were identified as a new class of alloys that potentially possess adequate oxidation resistance in combination with the necessary mechanical properties to be utilized as a high temperature structural material in an oxidizing environment. Superior oxidation resistance is realized in molybdenum borosilicides that possess a high volume fraction of intermetallic phases, while mechanical properties such as impact resistance and ductility are more readily achieved in a material with a molybdenum matrix and a small volume fraction of intermetallic. Alloys near Mo-3Si-1B(wt%) are promising because they approach a balance between these competing material requirements. The oxidation resistance of such alloys will be reviewed across the 25°F-2200°F-temperature range, accompanied by a discussion of some key mechanical properties.

#### 2:30 PM

Scale Development on Bcc-Mo Bearing Mo-Si-B Alloys in Synthetic Combustion Gas Atmospheres: Andrew J. Thom<sup>1</sup>; Pranab Mandal<sup>1</sup>; Vikas Behrani<sup>1</sup>; Matthew J. Kramer<sup>1</sup>; Mufit Akine<sup>1</sup>; <sup>1</sup>Iowa State University, Ames Lab. & Dept. of Matls. Sci. & Engrg., Matls. Chmst., Spedding Hall, Ames, IA 50011 USA

Previous work showed that Si-rich Mo-Si-B alloys form protective scales on exposure to dry air to at least 1600°C. Alloys containing bcc-Mo also show reasonable resistance to dry air to about 1400°C. Exposures to wet air and simulated combustion gas (SCG) promote growth of thicker scales on the bcc-Mo alloy at much lower temperatures. Iso-thermal TGA measurements reveal the alloy undergoes a slow linear mass loss on the order of 1 x 10-3 mg/cm2/hr. The present paper discusses the development of the scale in the presence of water and SCG. Scale evolution involves the simultaneous processes of borosilicate scale formation, subscale formation of Mo and MoO2, slow transport and evolution of MoOx through the borosilicate scale, and volatility of boron and Si(OH)x-containing species from the borosilicate glass. Oxidation kinetics and scale microstructural analyses will be discussed to construct a thermochemical treatment of the oxidation process.

# 2:45 PM

The Behavior of Multiphase Mo-Si-B Alloys in High-Temperature Oxidizing and Sulfidizing Environments: Peter F. Tortorelli<sup>1</sup>; Joachim H. Schneibel<sup>1</sup>; Karren L. More<sup>1</sup>; Michael P. Brady<sup>1</sup>; <sup>1</sup>Oak Ridge National Laboratory, PO Box 2008, Oak Ridge, TN 37831 USA

The high-temperature corrosion behavior of Mo-Si-B alloys under various environmental conditions is being studied for possible use in advanced energy systems based on fossil fuels. Alloys of Mo-Mo5SiB2-Mo3Si with different compositions and phase morphologies were isothermally and cyclically oxidized in dry air or exposed to an H-2-H2S- H2O-Ar environment. Effects of the multiphase nature (composition, morphology) of the Mo-Si-B system on environmental resistance under these conditions were evaluated. Microstructural characterization indicated that the oxidation reactions resulted in cooperative behavior among the different phases while preliminary analyses suggested that sulfide formation mimicked the starting alloy microstructure. Quite low corrosion rates under sulfidizing conditions were observed. Implications of these findings for alloy design for oxidation and/or sulfidation resistance will be discussed. Research sponsored by the Advanced Research Materials Program, Office of Fossil Energy, U.S. Department of Energy, under contract DE-AC05-000R22725 with UT-Battelle, LLC.

# 3:00 PM

**Oxidation Behavior of Multiphase Mo-Si-B Alloys**: Voramon Supatarawanich<sup>1</sup>; David R. Johnson<sup>1</sup>; M. A. Dayananda<sup>1</sup>; <sup>1</sup>Purdue University, Sch. of Matls. Engrg., 501 Northwestern Ave., W. Lafayette, IN 47907-2044 USA

In this study multiphase Mo-Mo5SiB2(T2)-Mo3Si alloys with different compositions were examined for microstructure and oxidation behavior. The alloys were prepared by powder metallurgy and casting techniques and contained up to 50 vol.% bcc Mo solid solution. Cyclic oxidation tests were conducted at temperatures ranging from 800 to 1500°C in air. Upon oxidation at 800°C, alloys containing mostly the T2 phase formed an amorphous, adherent, and oxidation resistant silicate scale. However, the scale was not protective at 1500°C. Conversely, alloys with ~50%Mo (by vol.) exhibited lower weight loss when tested at 1500°C compared to tests performed at 1300°C. The oxidation behavior will be discussed in terms of the differences in microstructure for the hot-pressed, cast and heat treated specimens.

# 3:15 PM

Phase Stability and Oxidation of the T<sub>2</sub>/Mo<sub>ss</sub> Eutectic Alloy Pack-Cemented in a Si-Base Pack Mixture: Kazuhiro Ito<sup>1</sup>; Masato Yokobayashi<sup>1</sup>; Taisuke Hayashi<sup>1</sup>; Masaharu Yamaguchi<sup>1</sup>; <sup>1</sup>Kyoto University, Matls. Sci. & Engrg., Sakyo-ku, Kyoto 606-8501 Japan

The  $T_2/Mo_{ss}$  eutectic alloy in the Mo-Si-B system was pack-cemented in a Si-base pack mixture (Si:NaF:Al<sub>2</sub>O<sub>3</sub>=5:1:44(wt.%)) and its oxidation behavior was examined. The deposited layer of as-cemented substrate consists of MoSi<sub>2</sub>. Upon heating to temperatures at and above 1773K, the deposited layer is transformed into B-doped Mo<sub>5</sub>Si<sub>3</sub> through a reaction between the deposited layer and the matrix containing B. The B-doped Mo<sub>5</sub>Si<sub>3</sub> coating layer consists of columnar grains with the [001] orientation perpendicular to the coating surface. Steady-state oxidation was observed at 1573-1773K and the steady-state oxidation rates at 1573 and 1773K are almost equal to those of MoSi<sub>2</sub>. After formation of the B-doped Mo<sub>5</sub>Si<sub>3</sub> coating layer, no significant weight change was observed during 26 cycles of short-term cyclic oxidation at 1773K (1h x 26). However, the coating layer was completely oxidized after 2 cycles of long-term cyclic oxidation at 1773K (50h x 2).

# 3:30 PM Break

4:00 PM

Influence of Alloying Element on the Stability of Molybdenum Silicides: A First Principles Study: Yan Song<sup>1</sup>; Zheng Xiao Guo<sup>1</sup>; <sup>1</sup>Queen Mary, University of London, Dept. of Matls., Mile End Rd., London E1 4NS UK

Molybdenum silicides exhibit an attractive potential for structural application at elevated temperature. Mo5Si3 has a high melting point (2180°C) and excellent high temperature strength, but its high temperature oxidation resistance is very poor. Recently, B-doped Mo5Si3 has been found to have much better oxidation resistance than Mo5Si3, which attributed to the formation of the adherent and passivating borosilicate layer on the surface of the T2 phase during exposure at high temperature in air. In the present paper, first principles calculations of Mo5Si3 and Mo5SiB2 were carried out to identify the characteristics of electronic structure of these alloys. The total energy and electronic structure were calculated using a full potential linearized augmented plane wave method with the GGA approximation. Bulk modulus and theoretical strength of these alloys were estimated through the calculation of the total energy. The influence of alloying element on the stability of molybdenum silicides was discussed based on the electronic structures.

# 4:15 PM

Alloy Design and Solidification Microstructures for Mo-Si-B Alloys: *Ridwan Sakidja*<sup>1</sup>; Jeff Werner<sup>1</sup>; Sungtae Kim<sup>1</sup>; John H. Perepezko<sup>1</sup>; <sup>1</sup>University of Wisconsin, Dept. of Matls. Sci. & Engrg., 1509 Univ. Ave., Madison, WI 53706 USA

Alloys in the Mo-Si-B system are attractive as high temperature structural materials. In the current study, the effect of transition metal additions (Group IV-VII B elements) on the phase stability in the

ternary system and the solidification microstructures has been examined. The Mo<sub>3</sub>Si (A15) phase has limited soubility with most of transition metals which accordingly limits the extension of the BCC+A15 two-phase field in the ternary and higher order systems. In contrast, with most of the transition metals examined the borosilicide ternary-based T<sub>2</sub> phase shows almost a complete solid solution extension. The critical factor for the phase stability appears to be the existence of a unique feature of BCC-like transition metal arrangements within the T<sub>2</sub> lattice. The stability of the BCC+T<sub>2</sub> two-phase field consequently facilitates a variety of new high-temperature solidification microstructures in combinations of other silicide phases. The support of AFOSR (F49620-03-1-0033) is gratefully acknowledged.

#### 4:30 PM

Phase Equilibria in the Mo-Si-Ti System: Experimental Measurements and Thermodynamic Modeling: *Ying Yang*<sup>1</sup>; Y. A. Chang<sup>1</sup>; <sup>1</sup>University of Wisconsin, Matls. Sci. & Engrg., 1509 Univ. Ave., Madison, WI 53706 USA

Microstructures and phase equilibria of the alloys in the Mo-Si-Ti system were studied in as-cast and long-term annealed conditions by imaging with back scattered electrons (BSE) in a scanning electron microscope (SEM), electron probe microanalysis (EPMA) and X-ray diffraction (XRD) analysis. Isothermal sections were established to describe the solid state phase equilibria at 1600 and 1425°C. Using the CALPHAD (CALculation of PHAse Diagram) approach, a thermodynamic data set of the Mo-Si-Ti system was optimized by considering both the present experimental results and reliable literature data. This thermodynamic modeling can satisfactorily account for the available experimental data. The liquidus surface near the metal-rich end of the Mo-Si-Ti system calculated from the present thermodynamic modeling is in good agreement with experimental observation. Two type-II invariant four-phase reactions were determined in the metal-rich region of the Mo-Si-Ti system. One is L + Mo(Ti)5Si3® Ti(Mo)5Si3 + Mo(Ti)3Si, and the other is L + Mo(Ti)3Si - Ti(Mo)5Si3 + ?(Mo,Si,Ti).

#### 4:45 PM

An Experimental Study of Alloying Behaviour in the Mo-Si-Al System: Aris Arvanitis<sup>1</sup>; Spyros Diplas<sup>1</sup>; *Panayiotis Tsakiropoulos*<sup>1</sup>; Mark Whiting<sup>1</sup>; <sup>1</sup>University of Surrey, Sch. of Engrg., Mech. & Aeros. Engrg., Metall. Rsch. Grp., Guildford, Surrey GU2 7XH England

High energy X-ray photoelectron spectroscopy was used to measure the Auger parameters and plasmon loss structures of Mo, Si and Al in MoSi2 and MoSi2 + xAl (x=10 to 40 at% Al) alloys, where the microstructure changes from C11b to C40 to C54 with the Al addition. The variations of the Auger parameters and charge redistribution calculations in MoSi2 indicated a charge transfer at the Si sites very close to zero; this means that Mo and Si bond covalently, in agreement with theoretical predictions from ab-initio calculations. On introduction of Al into the MoSi2 compound there is a minor charge transfer away from the Al sites which bond strongly with Mo. The plasmon loss structures of the Si 1s and Al 1s peaks showed reduced intensity in the alloys relative to the pure metals. This is attributed to more strongly bound valence electrons. The study explains the silicon substitution by aluminium in the {110} close packed planes and the crystal structure modification from tetragonal C11b to hexagonal C40.

# **Bulk Metallic Glasses: Processing II**

Sponsored by: Structural Materials Division, ASM International: Materials Science Critical Technology Sector, SMD-Mechanical Behavior of Materials-(Jt. ASM-MSCTS)

*Program Organizers:* Peter K. Liaw, University of Tennessee, Department of Materials Science and Engineering, Knoxville, TN 37996-2200 USA; Raymond A. Buchanan, University of Tennessee, Department of Materials Science and Engineering, Knoxville, TN 37996-2200 USA

Monday PM	Room: 2	09A
March 15, 2004	Location:	Charlotte Convention Center

Session Chairs: Peter K. Liaw, University of Tennessee, Matls. Sci. & Engrg., Knoxville, TN 37996-2200 USA; Takeshi Egami, University of Tennessee, Matls. Sci. & Engrg., Knoxville, TN 37996-2200 USA

#### 2:00 PM Invited

Recent Progress in Bulk Glassy Alloys in Late Transition Metal Base Systems: Akihisa Inoue<sup>1</sup>; <sup>1</sup>Tohoku University, Inst. for Matls. Rsch., Sendai 980-8577 Japan

Since 1988, a number of bulk glassy alloys in Mg-, Zr-, Ti-, Hf- and lanthanide metal-based systems have been developed. However, their alloy systems had been limited to simple metal-, early transition metal-, lanthanide metal- and noble metal-based components. Very recently, we have succeeded in fabricating a number of bulk glassy alloys in late transition metal (LTM) base systems containing Fe, Co, Ni and Cu elements as a main component. These new bulk glassy alloys also satisfied the following three component rules for stabilization of supercooled liquid, i.e., (1) multi-component consisting of more than three elements, (2) atomic size mismatches above 12% among main three components, and (3) negative heats of mixing among their elements. We have also reported that the alloys with the three rules have a new liquid structure with highly dense packing, new local atomic configurations and long-range homogeneity. The new configuration is the origin for the high glass-forming ability even for the LTM base alloys. The new bulk glassy alloys can be produced by various casting processes and exhibit various useful properties, e.g., soft magnetic properties with extremely low coercive force, high permeability and low core losses, high electrical resistivity and high strength for Febased glassy alloys, high-frequency permeability, extremely high strength and high corrosion resistance for Co-based glassy alloys, high tensile strength, high corrosion resistance and high permeation ability of hydrogen for Ni-based glassy alloys, and high tensile strength, good ductility and high corrosion resistance for Cu-based glassy alloys. The Fe-based bulk glassy alloys have been commercialized as power-inductors for various portable electrical equipments and as high-strength materials for shot peening balls. In addition, when the Cu-based bulk glassy alloys include special elements such as Nb, Ta, Pd or Au leading to the deviation from the three component rules, we have found the formation of nanocrystalline and nanoquasicrystal-dispersed bulk glassy alloys with higher strength and ductility. These data indicate that the LTM base bulk glassy alloys may develop as a new type of functional materials.

#### 2:25 PM Invited

Why Certain Metallic Alloys Form Bulk Glasses: Takeshi Egami<sup>1</sup>; <sup>1</sup>University of Tennessee/ORNL, MSE/Physics, 208 S. College, Knoxville, TN 37996-1508 USA

For a long time bulk glasses were found only in complex nonmetallic solids. But now bulk metallic glasses with various compositions are formed and tested for applications. We discuss why certain alloy systems form bulk metallic glasses based uponm our elastic theory of glass formation and atomic transport in liquids. In our view glasses are formed primarily because the crystals are unstable because of elastic interactions due to the atomic size mismatch. In addition the topological and chemical complexity of certain liquid alloys results in lower viscosity and slower crystallization kinetics, allowing bulk glasses to form. Molecular dynamics simulations of model systems to support our theory will be presented.

#### 2:50 PM Invited

Formation and Properties of Iron-Based Bulk Amorphous Metals: Joseph Poon<sup>1</sup>; Gary J. Shiflet<sup>2</sup>; <sup>1</sup>University of Virginia, Physics, PO Box 400714, Charlottesville, VA 22904-4714 USA; <sup>2</sup>University of Virginia, Matls. Sci. & Engrg., Charlottesville, VA 22904-4745 USA

Bulk-solidifying iron-based metallic glasses have been synthesized and investigated as amorphous steel alloys. The design strategy of these amorphous alloy systems including their microstructures will be discussed. One type of amorphous steel alloys contains manganese and boron as the principal alloying components, another type contains manganese, molybdenum, and carbon as the principal alloying components. The tensile yield strengths and Vickers hardness of the present alloys are about two to three times those known in high-strength steels, while the elastic moduli are comparable to those reported for super austenitic steels. Some good corrosion resistance features are also observed. Devitrification studies have been performed to characterize the phase regions near the bulk glass forming compositions. The crystallized products and microstructures have been investigated in detail. The high glass formability, which correlates with the enhancement in the stability of the glassy phases, will be discussed in light of current ideas of glass formation.

#### 3:15 PM Invited

Consolidation of Blended Powders by Severe Plastic Deformation to Form Amorphous Metal Matrix Composites: K. Ted Hartwig<sup>1</sup>; Ibrahim Karaman<sup>1</sup>; Suveen N. Mathaudhu<sup>1</sup>; <sup>1</sup>Texas A&M University, Mech. Engrg., 319 Engr. Phys. Bldg., College Station, TX 77845-3123 USA

Because bulk amorphous metal can fail by shear localization, it is a potential environmentally friendly substitute material for depleted uranium in kinetic energy penetrators (KEPs). However, a deficiency of bulk amorphous metal alloys for the KEP application is their low density. The purpose of the work reported here is to fabricate a dense amorphous metal matrix composite. Warm equal channel angular extrusion (ECAE) was used to consolidate blended powders of amorphous Vitreloy 106a (Zr58.5Cu15.6Ni12.8A110.3Nb2.8) and crystalline tungsten. Severe plastic deformation processing was performed at temperatures above the Tg (400C) but below the Tx (465C) of the V106a. The effects of tungsten volume fraction, extrusion temperature, number of extrusion passes were investigated by metallographic examination, DSC, XRD, hardness and mechanical testing. Results show good infiltration of the amorphous phase in between W particles, retention of amorphous character in the glassy phase and substantial W-Vit106a interphase bond strength. Experimental results are presented which indicate that ECAE is a viable process for the preparation of bulk amorphous metal matrix composites from particulate precursors.

#### 3:40 PM

**Formation of Metallic Glassy Ingots Based on Yttrium**: *Faqiang Guo*<sup>1</sup>; Joseph Poon<sup>1</sup>; Gary J. Shiflet<sup>2</sup>; <sup>1</sup>University of Virginia, Dept. of Physics, Charlottesville, VA 22903 USA; <sup>2</sup>University of Virginia, Dept. of Matls. Sci. & Engrg., Charlottesville, VA 22903 USA

We report a family of yttrium metallic alloys that are able to form glassy ingots directly from the liquid, as well as forming bulk-sized amorphous rods with diameters over 2 cm by water cooling of the alloy melt sealed in quartz tubes. It is apparent that, in addition to the strong chemical interaction among the components, the simultaneous occurrence of well-distributed atom sizes and a strongly depressed liquidus temperature in multicomponent metallic alloys is responsible for the formation of glassy ingots.

# 4:05 PM Invited

**Glass Forming Ranges of Al-Fe(Ni)-Gd(Y): Thermodynamic Analysis**: *Aiwu Zhu*<sup>1</sup>; Gary J. Shiflet<sup>1</sup>; <sup>1</sup>University of Virginia, Matls. Scis., 116 Engineer's Way, Charlottesville, VA 22904 USA

Based on CALPHAD models of Al-Fe-Gd, Al-Ni-Gd and Al-Ni-Y alloys, this work reports a thermodynamic analysis of the chemical short range order (CSRO) of the undercooled liquid employing a quasichemical approximation. The driving forces and associated kinetics are calculated for the polymorphous transformation to crystals and for the primary crystallization of the relevant FCC and inter-metallic phases from the undercooled liquid.

#### 4:30 PM Cancelled

Amorphous Alloys by Cold Rolling

#### 4:55 PM

Bulk Glass Formation in Cu-Ti-Zr-(Ag,Ni) Alloys: E. S. Park<sup>1</sup>; H. J. Chang<sup>1</sup>; W. T. Kim<sup>2</sup>; D. H. Kim<sup>1</sup>; <sup>1</sup>Yonsei University, Dept. of Metallurgl. Engrg., Ctr. for Non-Crystalline Matls., 134 Shinchon-Dong, Seodaemun-gu, Seoul 120-749 Korea; <sup>2</sup>Chongju University, Dept. of Physics, Chongju 360-764 Korea

In the present study, Cu-based bulk amorphous alloys were developed through a systematic alloy design in the alloy system Cu-Ti-Zr. TEM analysis indicated that the as-melt-spun microstructure of the ternary Cu60Ti40-xZrx (x=0, 10, 20) alloys consisted of a nanocrystalline phase embedded in an amorphous matrix. Based on the results from the ternary alloys, effect of the addition of the fourth alloying elements on the glass forming ability was investigated. Partial replacements of Cu by Ag or Ni significantly improved the glass forming ability. For example, a fully amorphous Cu45Ti10Zr30Ag15 alloy rod of 5 mm in diameter was fabricated by an injection casting method. To illustrate the improved glass forming ability, the crystallization behaviors of the ternary and quaternary alloys were examined in detail by XRD, TEM and DSC analyses.

#### 5:20 PM Invited

Carbon-Nanotube-Reinforced Zr-Based Bulk Metallic Glass Composites and Their Properties: *Wei Hua Wang*<sup>1</sup>; Zan Bian<sup>1</sup>; Ru Ju Wang<sup>1</sup>; M. X. Pan<sup>1</sup>; D. Q. Zhao<sup>1</sup>; <sup>1</sup>Chinese Academy of Science, Inst. of Physics, Beijing 100080 China

We report the preparation of Carbon-nano tube (CNT)-reinforced Zr-based BMG composites. Physical properties and mechanical properties of the composites were investigated. Compressive testing shows that the composites still display high fracture strength. Investigation also shows that the composites have strong ultrasonic attenuation characteristics and excellent wave absorption ability. The strong wave absorption ability implies that CNT-reinforced Zr-based BMG composites, besides their excellent mechanical properties, may also have significant potential of application in shielding acoustic sound or environmental noise.

# Carbon Technology: Anode Raw Materials

Sponsored by: Light Metals Division, LMD-Aluminum Committee Program Organizers: Markus Meier, R&D Carbon, Sierre CH 3960 Switzerland; Amir A. Mirchi, Alcan Inc., Arvida Research and Development Centre, Jonquiere, QC G7S 4K8 Canada; Alton T. Tabereaux, Alcoa Inc., Process Technology, Muscle Shoals, AL 35661 USA

Monday PM	Room: 2	13A
March 15, 2004	Location:	Charlotte Convention Center

Session Chair: Todd W. Dixon, Conocophillips, Lake Charles Calcining Plant, Lake Charles, LA 70602-3187 USA

# 2:00 PM

Performance of Blended and Unblended Green Cokes During Calcination: Ravindra Narayan Narvekar<sup>1</sup>; Ajit Sambhaji Sardesai<sup>1</sup>; <sup>1</sup>Goa Carbon Limited, Production, St. Jose De Areal, Margao, Goa 403709 India

As anode grade green cokes get scarcer in quantity and inferior in quality, calciners are finding it necessary to blend two or more cokes to obtain specifications desired by end-users, particularly aluminium smelters. Ideally green cokes should be calcined singly, as the operating parameters need to be changed in keeping with the characteristics of each quality of green coke, particularly volatile matter, density and granulometry. Pre-calcination blending is generally preferred to post calcination blending, supposedly for the homogeneity of the product. We decided to compare, ascertain and establish the performances of individual green cokes as against blends of the same cokes during calcination. GCL conducted trials for six cokes individually as well as with their blends under similar operating conditions. The properties of the calcined cokes resulting from using a blend were compared with those calcined individually.

#### 2:25 PM

A Preview of Anode Coke Quality in 2007: *Franz Vogt*<sup>1</sup>; Robert T. Tonti<sup>1</sup>; Maia Hunt<sup>1</sup>; Les Edwards<sup>1</sup>; <sup>1</sup>CII Carbon, L.L.C., 1615 E. Judge Perez Dr., PO Box 1306, Chalmette, LA 70044 USA

Demand for petroleum coke for aluminum smelting anodes has reached about 10.4 million metric tons in 2003. This has created a coke calciner demand of 13.8 million metric tons of green coke suitable for making anodes. The green coke demand will increase to about 16.5 million metric tons by 2007. Although the oil refining industry will produce ample green coke to meet this demand, the quality will be quite different from that used in the past. During the last few years, the calcining industry has started using green cokes of a quality that would not have been considered suitable for anode use ten years ago. This paper surveys the available quality of green cokes worldwide, and makes projections on the quality of anode coke by 2007. The calcined coke of the future will be higher in sulphur and vanadium, higher in porosity and more isotropic. The change in structure could eventually lead to higher thermal shock sensitivity of anodes. Smelters will need to adapt by making process changes and improvements.

#### 2:50 PM

Characterization of the Surface Properties of Anode Raw Materials: Angelique N. Adams<sup>1</sup>; Harold H. Schobert<sup>2</sup>; <sup>1</sup>Alcoa Technical Center, Hall Process Improvement, 100 Technical Dr., Alcoa Ctr., PA 15069 USA; <sup>2</sup>The Energy Institute, C211 Coal Utilization Bldg., Univ. Park, PA 16802 USA

The interaction between filler and binder in anode green mix is of significant importance to anode properties. A better understanding of the physical and chemical interactions taking place during mixing could facilitate raw materials and processing decisions that improve anode properties. The aim of this work was to characterize the surface properties of anode raw materials and relate them to pitch penetration behavior. The type and quantity of oxygen functional groups on the surface, and the estimated surface tension, of petroleum coke and recycled anode butt material were determined using selective neutralization and film flotation techniques. The extent of pitch penetration into these materials was evaluated by image analysis of green mix from bench-scale electrodes and thermal analysis of pitch penetrated particles. The results indicate that pitch penetration is affected by the extent of oxidation of the surface of filler materials and the presence of bath constituents.

# 3:15 PM

Anthracene Oil Synthetic Pitch: A Novel Approach to Hybrid Pitches: Juan Jose Fernandez<sup>1</sup>; Francisco Alonso<sup>1</sup>; <sup>1</sup>Industrial Quimica del Nalon, S.A., R&D, Avda. Galicia, 31 bajo, Oviedo, Asturias E-33005 Spain

Because of the coal tar supply shortage, the pitch market is becoming very tight due to an increasing demand powered by the aluminum industry. Anthracene oil is the heaviest fraction coming from coal tar distillation with a quality consistency and known chemical composition (metal and QI free), guaranteed by the distilling technology applied on its production. The primary anthracene oil major application is carbon black feedstock. The high aromatic content suggests the potential for other end uses with a higher added value. This paper reports Industrial Quimica del Nalon pilot plant experience in the manufacture of synthetic pitches from anthracene oil. Pitches so obtained shows excellent rheological and wetting properties with minimized environmental and health impact because of its low PAHs concentration and reduced volatility.

#### 3:40 PM Break

# 3:50 PM

Hydrogen Transfer During Carbonization of Binder Pitches: Stian Madshus<sup>1</sup>; Trygve Foosnaes<sup>1</sup>; Margaret M. Hyland<sup>2</sup>; Harald Øye<sup>1</sup>; <sup>1</sup>Norwegian University of Science and Technology, Dept. of Matls. Tech., Sem Saelands v 12, Trondheim 7491 Norway; <sup>2</sup>University of Auckland, Sch. of Engrg., Private Bag 92019, Auckland 1 New Zealand

The hydrogen transfer properties of five coal-tar pitches and four petroleum pitches have been estimated from their ability to donate hydrogen (HDa) to anthracene and abstract hydrogen (HAa) from tetralin at 400°C. The ratio of hydrogen donor ability to acceptor ability, HDa/HAa, was used as a parameter to describe the hydrogen transfer properties of the pitch. A correlation between this parameter and the percentage of volatile matter released during the critical stages of carbonization was found for the coal-tar pitches. The texture of cokes obtained from carbonization of pitches to 600°C, was studied by cross-polarized light microscopy using an automatic computerized image analysis method. Cokes were further carbonized to 1050°C and analyzed by X-ray diffraction. The hydrogen transfer properties could partly explain the development of optical texture and microstructure in the pitch coke. The QI content of the coal-tar pitches was found to influence the pitch coke structure to a significant extent, reducing the size of the optical domains and lowering the optical domain anisotropy.

# Cast Shop Technology: Modeling of Casting Processes

Sponsored by: Light Metals Division, LMD-Aluminum Committee Program Organizers: Corleen Chesonis, Alcoa Inc., Alcoa Technical Center, Alcoa Center, PA 15069 USA; Jean-Pierre Martin, Aluminum Technologies Centre, c/o Industrial Materials Institute, Boucherville, QC J4B 6Y4 Canada; Alton T. Tabereaux, Alcoa Inc., Process Technology, Muscle Shoals, AL 35661 USA

Monday PM	Room:	213B/C		
March 15, 2004	Location	: Charlotte	Convention	Center

Session Chairs: Brian G. Thomas, University of Illinois, Mech. & Industrial Engrg. Dept., Urbana, IL 61801 USA; Steve L. Cockcroft, University of British Columbia, Dept. of Metals & Matls. Engrg., Vancouver, BC V6T 1Z4 Canada

#### 2:00 PM

Temperature Measurements and Modeling of Heat Losses in Molten Metal Distribution Systems: Jonny Kastebo<sup>1</sup>; Torbjörn Carlberg<sup>1</sup>; <sup>1</sup>Mid Sweden University, Engrg., Physics & Math., Holmgatan 10, Sundsvall 85170 Sweden

During casting of aluminium ingots the molten metal have to be transported from the furnace to the moulds. During the transport heat is lost both to the atmosphere and to the refractory launder system itself. As different dimensions of the cast ingots necessitate different design of the system the difference between the furnace temperature and the temperature in the metal, which enters the mould, can vary significantly. It is therefore of importance to have a good knowledge of the heat fluxes in the launder system and of how the temperature decreases during metal flow. In this work thorough measurements of the temperature have been made in casting tables of different design during casting of different ingot dimensions. Based on the experimental results an analytic model has been derived. Good correlation between calculated and measured temperature losses was obtained.

#### 2:25 PM

FEM Modeling of the Compressibility of Partially Solidified Al-Cu Alloys: Comparison with a Drained Compression Test: J.-M. Drezet<sup>1</sup>; O. Ludwig<sup>2</sup>; C. Martin<sup>2</sup>; M. M'Hamdi<sup>3</sup>; H.-G. Fjaer<sup>4</sup>; <sup>1</sup>Ecole Polytechnique Federale de Lausanne, LSMX, CH-1015 Lausanne Switzerland; <sup>2</sup>Institut National Polytechnique de Grenoble, GPM2, F-38402 Saint Martin d'Heres France; <sup>3</sup>Sintef, N-0314 Oslo Norway; <sup>4</sup>Institute for Energy Technology, PO Box 40, N-2027 Kjeller, Oslo Norway

In order to tackle the problem of hot tearing in aluminium alloys, a good description of the rheological behaviour of the mushy zone is a prerequisite. Although rheological testing of partially solidified aluminium alloys presents some large difficulties, three different tests, corresponding to three different types of stress state, tension, shear and compression, were used to determine a new rheological model. This model is a compressible constitutive model, it uses two internal variables and it was implemented in both Abaqus and Tearsim2D. In this paper, attention is given to the drained compression (oedometric) test, for which an analytical solution of the stress development and of the evolution of the two internal variables exists. The results obtained by Abaqus and Tearsim2D are compared to the experimental results and validated against the analytical solution. Finally, the influence of the liquid pressure is discussed. This particular study was carried out within the framework of the VIR[CAST] project in which a general thermo-mechanical model is built in order to predict hot tearing in DC cast billets or slabs.

# 2:50 PM

**Mathematical Modeling of Ingot Caster Filling Systems**: John F. Grandfield<sup>1</sup>; Paul J. Cleary<sup>2</sup>; Mahesh Prakash<sup>2</sup>; M. Sinnott<sup>2</sup>; K. Oswald<sup>3</sup>; V. Nguyen<sup>1</sup>; <sup>1</sup>CAST, CSIRO Mfg. Sci. & Tech., cnr Albert & Raglan Sts., Preston, Vic. 3072 Australia; <sup>2</sup>CRC for Cast Metals Manufacturing (CAST), CSIRO Math. & Info. Sci., Clayton, Vic Australia; <sup>3</sup>o.d.t. Engineering, Dandenong, Victoria Australia

Operators of chain conveyor ingot casters are interested in reducing dross generated during filling. This problem becomes more acute when steps are taken to increase ingot caster production rate and filling times are reduced. Another performance measure of a filling system is the variation in ingot weight. In order to optimise the design and examine possible low dross generating designs for ingot casting machines, mathematical models of the existing pouring wheel filling system were developed. Ingot casting machine filling systems present challenges to conventional flow modelling packages. Difficulties include the handling of multiple moving surfaces (fluid and solid) and prediction of oxide generation. Smooth particle hydrodynamic (SPH) modelling has a number of advantages in this regard and was applied to this problem. A new filling system design tailored to 30 tonne per hour production has been developed based on the modelling work. This design was tested on a full scale system.

#### 3:15 PM

Heat Transfer Boundary Conditions for the Numerical Simulation of the DC Casting Process: Adrian S. Sabau<sup>1</sup>; Kazunori Kuwana<sup>2</sup>; Srinath Viswanathan<sup>3</sup>; Kozo Saito<sup>2</sup>; Lee J. Davis<sup>4</sup>; <sup>1</sup>Oak Ridge National Laboratory, Metals & Ceram. Div., Bldg. 4508, MS 6083, Oak Ridge, TN 37831 USA; <sup>2</sup>University of Kentucky, Dept. of Mech. Engrg., 513 CRMS Bldg., Lexington, KY 40506-0108 USA; <sup>3</sup>Sandia National Laboratories, MS 1134, Dept. 1835, Albuquerque, NM 87185-1134 USA; <sup>4</sup>Wagstaff, Inc., 3910 N. Flora Rd., Spokane, WA 99216-1720 USA

The temperature evolution during the start-up phase of the Direct Chill (DC) casting process is critical to the prediction of strain-stress evolution during solidification. The start-up phase of DC casting is complex, as heat is extracted by the mold, starting block, and cooling water, while process parameters are ramped up to their steady state values. The modeling of DC casting involves making assumptions on the various heat transfer mechanisms, such as (a) direct contact of liquid metal-mold, (b) air gap between mold and ingot, (c) water cooling on rolling and end faces of the ingot, (d) ingot contact with the starting block, and (e) water intrusion between the starting block and ingot. The boundary conditions for the heat transfer analysis during the startup are discussed in detail. Numerical simulation results are presented for a typical casting run, including variable casting speed, metal head, and water flow rate.

# 3:40 PM Break

# 3:50 PM

Modelling of Microstructure Development During DC Casting of AA3103 Ingots - Application of Vircast Project Developments: Gerd-Ulrich Gruen<sup>1</sup>; Werner E. Droste<sup>1</sup>; <sup>1</sup>Hydro Aluminium Deutschland GmbH, R&D, Georg-von-Boeselager-Str. 21, Bonn 53117 Germany

The microstructure of DC cast ingots is influencing the following processing steps as well as the material properties of final products and cast houses are increasingly asked to deliver with tighter specifications. In order to fulfil these requirements a correct prediction of the microstructure evolution during casting is an ongoing challenge. In the European funded joint research project VIRCAST a related modelling toolset for multi-component multi-phase alloys has been developed within the last four years. During the final stage of this project this toolset has been applied to full scale DC and laboratory casting experiments of AA3103 alloys, which have been extensively monitored and where the final microstructure of the cast material has been evaluated. Within this paper calculated key microstructure parameters are compared with the related measurements and critically discussed.

#### 4:15 PM

**Prediction of Hot Tears in DC-Cast Aluminum Ingots**: Andre Phillion<sup>1</sup>; Steve Cockcroft<sup>1</sup>; <sup>1</sup>University of British Columbia, Metals & Matls. Engrg., 309-6350 Stores Rd., Vancouver, BC V6T 1Z4 Canada

Hot tearing is a major quality issue during DC casting of aluminium alloys. Often, even small cracks on the surface of the ingot will cause the ingot to be scrapped because of the potential for defects during the later stages of the process. It is well known that aluminium ingots are susceptible to cracking along the centre of the rolling face during the start-up phase or at high casting speeds. Thus, these alloys must be cast at lower speeds, reducing productivity. The present work aims to incorporate hot tearing into a thermo-mechanical finite element (FE) model of aluminium DC ingot casting. Hot tearing models proposed in literature will be implemented into an FE model and comparisons to industrial and published data will be performed. The effect of process variables, such as cast velocity and water flow-rate on hot tearing will also be discussed.

#### 4:40 PM

Numerical Simulation of DC Casting: Interpreting the Results of a Thermo-Mechanical Model: *Wim Boender*<sup>1</sup>; Jan Rabenberg<sup>1</sup>; Erik Paul van Klaveren<sup>1</sup>; André Burghardt<sup>1</sup>; <sup>1</sup>Corus, RD&T, PO Box 10,000, Wenckebachstraat 1, IJmuiden 1970 CA The Netherlands

A few problems impede the efficiency of DC casting. Cold cracking, which occurs when thermally induced stresses locally exceed the tensile strength, is one of these problems. Especially, hard alloys like AA2000 and AA7000 alloys are prone to cold cracking. To gain insight into the mechanical behaviour of an ingot during casting, Corus RD&T developed a thermo-mechanical model. This numerical model simulates the evolution of temperatures, stresses, and strains inside the ingot as a result of the casting parameters, the cooling conditions, and the alloy's properties. A tri-axial state of stress is shown to develop almost everywhere in the solid ingot. Interpreting these results, two approaches are reciprocally used to estimate the likelihood that a cold crack will form. In one approach, the principal stresses are assessed, yielding insight into the locations and directions of cracks. The other approach is based on energy, i.e. on the fracture toughness KIc. It provides insight into possible ways to avoid cold cracks, e.g. by pointing out that internal defects, like inclusions or pores, should be smaller than the critical crack length. The findings will be illustrated with results for the DC casting of an Al - 4.5% Cu alloy.

#### 5:05 PM

Application of Mathematical Models to Optimization of Cast Start Practice for DC Cast Extrusion Billets: J. F. Grandfield<sup>1</sup>; L. Wang<sup>1</sup>; <sup>1</sup>CRC for Cast Metals Manufacturing (CAST), CSIRO Mfg. & Infrastructure Tech., Preston, Victoria Australia

Producers of DC casting billets are interested in reducing scrap caused by hot tearing at the start of casting. This is the subject of large ongoing research programs within the industry. Using a relatively simple thermal model, predictions of pool depth versus cast length are made. Results compare favorably with published pool depth data. We illustrate how a such a model and current know-how could be applied to improve the cast start practice in terms of starting speed and ramp-up or dome height for a given alloy and product diameter in order to reduce cracking tendency. This type of model can be also used to examine the effect of other cast start variables such as dummy design, fill time and hold time.

# CFD Modeling and Simulation of Engineering Processes: Remelt Processes

Sponsored by: Materials Processing & Manufacturing Division, ASM/MSCTS-Materials & Processing, MPMD/EPD-Process Modeling Analysis & Control Committee, MPMD-Solidification Committee, MPMD-Computational Materials Science & Engineering-(Jt. ASM-MSCTS)

*Program Organizers:* Laurentiu Nastac, Concurrent Technologies Corporation, Pittsburgh, PA 15219-1819 USA; Shekhar Bhansali, University of South Florida, Electrical Engineering, Tampa, FL 33620 USA; Adrian Vasile Catalina, BAE Systems, SD46 NASA-MSFC, Huntsville, AL 35812 USA

Monday PM	Room: 206A
March 15, 2004	Location: Charlotte Convention Center

*Session Chairs:* Ramesh S. Minisandram, Allvac, Monroe, NC 28111 USA; Srinath Viswanathan, Sandia National Laboratories, Albuquerque, NM 87185-1134 USA; Ashish D. Patel, Carpenter Technology Corporation, Reading, PA 19601 USA

#### 2:00 PM Opening Remarks - Ramesh Minisandram

#### 2:05 PM Invited

The Effect of Electromagnetic Stirring on the Turbulent Flow of Liquid Metal in a Vacuum Arc Remelted Ingot: *Alain Jardy*<sup>1</sup>; Thibaut Quatravaux<sup>1</sup>; Denis Ablitzer<sup>1</sup>; <sup>1</sup>Ecole des Mines de Nancy, LSG2M - UMR 7584, Parc de Saurupt, Nancy Cedex 54042 France

A numerical model of the Vacuum Arc Remelting process has been developed and applied to simulate remelting of various metallic materials, such as specialty steels, titanium, nickel-based superalloys and zirconium alloys. In practice, electromagnetic stirring is sometimes used, resulting in a complex 3D molten metal flow. After having validated the numerical model for different remelting conditions, we can use it to study the effect of applying a continuous or alternated magnetic field on the thermohydrodynamic behaviour of the melt pool, as well as dispersion of inclusions in the bath. The intensity of flow turbulence, computed with a classical k-epsilon model, is shown to depend strongly on the nature of electromagnetic stirring.

#### 2:40 PM

Modelling the Electroslag Remelting of Ni-8 Cr-25 Mo Alloy: Shawn A. Cefalu<sup>1</sup>; Kent J. VanEvery<sup>1</sup>; Matthew J.M. Krane<sup>1</sup>; <sup>1</sup>Purdue University, Sch. of Matls. Engrg., 501 Northwestern Ave., W. Lafayette, IN 47907 USA

Segregation during electroslag remelting (ESR) of a nickel-chromium-molybdenum alloy (Ni-8 wt% Cr-25 wt% Mo) has been modeled. Features of the model include species transport, AC electromagnetic effects and an adapting grid coupled with fluid flow, heat transfer, and solidification. The effect of varying processing conditions, including power, ingot diameter and slag thickness, on macrosegregation patterns, local solidification time, local phase fractions, and liquid pool profiles obtained from this model are demonstrated.

#### 3:10 PM Invited

Computational Analysis of Metal Spray in the Nucleated Casting Process: Kanchan M. Kelkar<sup>1</sup>; Ramesh S. Minisandram<sup>2</sup>; Suhas V. Patankar<sup>1</sup>; Robin M. Forbes Jones<sup>2</sup>; William T. Carter<sup>3</sup>; <sup>1</sup>Innovative Research Inc., 3025 Harbor Ln. N., Ste. 300, Plymouth, MN 55447 USA; <sup>2</sup>Allvac An Allegheny Technologies Company, R&D, 2020 Ashcraft Ave., PO Box 5030, Monroe, NC 28110 USA; <sup>3</sup>GE Corporate R&D, Schenectady, NY 12301 USA

The nucleated casting process currently under development has the potential for production of Ni-based superalloy preforms with microstructure that is superior to product made by conventional casting processes. In this process, electroslag remelted (ESR) clean molten metal is conveyed via a water-cooled copper Cold-walled Induction Guide (CIG) to a gas atomizer. The spray of clean metal is then directly cast into a water-cooled crucible for ingot production. The microstructure of the resulting ingot preform is a function of the thermal state of the incoming metal droplets. This, in turn, depends on particle size, flight time and heat exchange with the gas phase. In the present study, a computational model is developed for the analysis of the flow and heat transfer processes in gas-metal spray system under axisymmetric and steady-state conditions. The gas-phase flow is analyzed using an Eulerian framework and turbulent mixing within the gas phase is modeled using the two-equation k-e model. The dynamics of the metal particles is analyzed using a Lagrangian framework which

involves calculation of the trajectories of the metal droplets. Thus, the motion of the metal droplets is influenced by the fluid drag and the heat transfer from the metal particles is governed by convective and radiative cooling at the surface of the particles. A two-way coupling is considered whereby the flow and heat transfer in the gas phase is also influenced by the drag induced by and heat transfer from the metal droplets. The model enables prediction of the profiles of mass and enthalpy fluxes and the liquid fraction of the metal spray at the ingot surface. The paper demonstrates how such a model is useful for both process design & optimization.

3:40 PM Break

# 4:00 PM Invited

**CFD Modeling and Simulation Applications for PAM-Assisted Casting of Ti-6Al-4V Ingots and Slabs**: *Laurentiu Nastac*<sup>1</sup>; Frank Spadafora<sup>2</sup>; Ernie M. Crist<sup>2</sup>; <sup>1</sup>Concurrent Technologies Corporation, Product & Process Analysis, 425 6th Ave., Regional Enterprise Tower, 28th Floor, Pittsburgh, PA 15219 USA; <sup>2</sup>RMI Titanium Company, 1000 Warren Ave., Niles, OH 44446 USA

This paper describes the modeling techniques and the experimental and computer results for two casting processes that are under development and optimization. These processes are described as follows: 1) Electromagnetic stirring (EMS) during casting of Ti-6Al-4V round ingots using the plasma arc cold hearth melting (PAM) process: The purpose of EMS is to establish a single-melt PAM process capable of consistently producing as-cast ingots without helium porosity and also having no need for surface conditioning prior to secondary processing. The modeling approach is based on the numerical solution of Maxwell's equations, fluid flow, and heat transfer equations, and mesoscopic modeling of the grain structure. 2) Casting of Ti-6Al-4V slabs using the single-melt PAM process: The purpose of slab casting is to eliminate an intermediate blooming step for converting round ingots for yield increase. The modeling approach is based on the numerical solution of fluid flow and heat transfer equations. The effects of pouring and mold temperatures on the pool and temperature profiles were studied. Also, the torch effects (such as the torch standoff and its traversing path) on the pool and temperature profiles were investigated and the best-case scenario was used in the experiments. Evaluation results at RMI showed that the plates made from the slabs met the mechanical properties and microstructure requirements. Acknowledgment. This work was conducted by the National Center for Excellence in Metalworking Technology (NCEMT) operated by Concurrent Technologies Corporation (CTC) under contract No. N00014-00-C-0544 to the U.S. Navy as part of the U.S. Navy Manufacturing Technology Program. E. J. Fasiska, F. R. Dax, Y. Pang, and D. Winterscheidt from CTC and K. O. Yu from RMI are acknowledged for their contribution to this work.

#### 4:30 PM

**Modeling of Vacuum Arc Remelting Process**: Ashish D. Patel<sup>1</sup>; Ramesh S. Minisandram<sup>2</sup>; <sup>1</sup>Carpenter Technology Corporation, 101 W. Bern St., Reading, PA 19601 USA; <sup>2</sup>Allvac, 2020 Ashcraft Ave., Monroe, NC 28111 USA

Vacuum Arc Remelting (VAR) is the final, and hence very critical, melting step for the production of a sound segregation fee ingot. The Specialty Metal Processing Consortium (SMPC) has developed a mathematical model for the VAR process. The model predicts the temperature distribution in the solidifying ingot, the flow in the molten metal pool and the electromagnetic field in the ingot. These predictions are used to estimate key solidification parameters, which dictate the likely hood of defect formation. In this talk, typical simulation results from different stages of VAR for both Nickel base superalloys and Titanium alloys will be presented and differences in the melt cycles for these alloys will be highlighted. The effect of pool profile on melting parameters will also be presented.

#### 5:00 PM

Modeling of Single-Roll Strip Casting of an Aluminum Alloy: Correlation of Strip Thickness, Solidification Zone Length and Puddle Shape: Suyitno<sup>1</sup>; E. N. Straatsma<sup>1</sup>; L. Katgerman<sup>1</sup>; <sup>1</sup>Delft University of Technology, Lab. of Matls., Rotterdamseweg 137, Delft 2628 AL The Netherlands

Single-roll strip casting process is studied using computational fluid dynamics which takes into account fluid flow, heat transfer and solidification. The computational model is based on the conservation laws of momentum, energy and continuity. Correlation of strip thickness, solidification zone length, and puddle shape on single-roll strip casting of AA3004 is explored. Some parameters: feeding pressure, roll speed, melt temperature, slit breadth and heat transfer in the contact surface are investigated. The strip thickness slightly increases with pressure, similarly the length of solidification zone. The variations of strip thickness and solidification zone length with roll speed show a sharp decline for strip thickness and slight decline for the length of solidification zone with increasing roll speed. The other parameters show a minor effect on the strip thickness and solidification zone length. Severe turbulence is observed on the free-jet flow.

# Challenges in Advanced Thin Films: Microstructures, Interfaces, and Reactions: Microstructures, Properties, and Reliability of Microelectronic Devices

Sponsored by: Electronic, Magnetic & Photonic Materials Division, EMPMD-Thin Films & Interfaces Committee *Program Organizers:* N. M. (Ravi) Ravindra, New Jersey Institute of Technology, Department of Physics, Newark, NJ 07102 USA; Seung H. Kang, Agere Systems, Device and Module R&D, Allentown, PA 18109 USA; Choong-Un Kim, University of Texas, Materials Science and Engineering, Arlington, TX 76019 USA; Jud Ready, Georgia Tech Research Institute - EOEML, Atlanta, GA 30332-0826 USA; Anis Zribi, General Electric Global Research Center, Niskayuna, NY 12309 USA

Monday PM	Room: 21	18B
March 15, 2004	Location:	Charlotte Convention Center

Session Chairs: Seung H. Kang, Agere Systems, IC Device Tech., Allentown, PA 18109 USA; Choong-Un Kim, University of Texas, Matls. Sci. & Engrg, Arlington, TX 76109 USA; David P. Field, Washington State University, Sch. of Mech. & Matls. Engrg., Pullman, WA 76019 USA

#### 2:00 PM Invited

Growth and Characterization of Si/SiGe Epitaxial Layers for Heterojunction FET Applications: *Douglas A. Webb*<sup>1</sup>; <sup>1</sup>ATMI, Epitaxial Services, 550 W. Juanita Ave., Mesa, AZ 85210 USA

Strained silicon, and silicon-germanium, epitaxial layer structures on silicon substrates have attracted considerable interest due to substantial carrier mobility enhancements that have been observed in field-effect transistors. Several companies have publicly announced plans for incorporating such "strained silicon" technology in advanced CMOS devices. There are a number of materials challenges that must be addressed with this technology. Using LPCVD, we have demonstrated threading dislocation densities of < 1E05/cm2, and surface roughness of ~1 nm for strained silicon on relaxed, compositionally graded Si0.8Ge0.2 "virtual substrates." X-ray diffraction analysis of these films indicates that the SiGe layer is fully relaxed, and is tilted slightly from the substrate. The evolution of surface roughness during the growth of the relaxed SiGe virtual substrate has been evaluated by atomic-force microscopy. It is found that roughness of graded layers increases significantly at compositions greater than ~5 atomic percent germanium. The resulting surface texture may complicate lithographic patterning and other fab processes. It may also contribute to inhomogeneities in the strain of subsequently grown silicon and silicon-germanium layers. Silicon layers grown on the relaxed SiGe layers were characterized by x-ray diffraction and Raman spectroscopy. The results indicate that the silicon growth is fully pseudomorphic. Layers grown beyond the critical thickness for formation of misfit dislocations still exhibit substantial residual strain.

#### 2:25 PM

Advanced Materials and Processes for Sub-100 nm Metallizations: Daniel Josell<sup>1</sup>; Thomas P. Moffat<sup>1</sup>; Daniel Wheeler<sup>1</sup>; <sup>1</sup>NIST, Metall. Div., MS 8555, 100 Bureau Dr., Gaithersburg, MD 20899 USA

I will discuss several advances in metallizations for integrated circuits. These include new processes for superconformal deposition of copper, now the standard for high conductivity, high-speed metallizations. Advanced fabrication processes will also be presented for superconformal deposition of silver, the only metal with a higher bulk electrical conductivity than copper. The use of ruthenium barriers for "seedless" copper feature filling will also be presented. The Curvature Enhanced Accelerator Coverage mechanism behind the superconformal, bottom-up "superfilling" will be summarized.

#### 2:40 PM

Oxidation Characteristics of Si by Using High-Concentration Ozone: Kunihiko Koike<sup>1</sup>; Koichi Izumi<sup>1</sup>; Akira Kurokawa<sup>2</sup>; Shingo Ichimura<sup>2</sup>; <sup>1</sup>Iwatani International Corporation, 4-5-1 Katsube, Moriyama, Shiga 524-0041 Japan; <sup>2</sup>National Institute of Advanced Industrial Science and Technology, 1-1-4 Umezono, Tsukuba, Ibaraki 305-8568 Japan

We investigated ozone oxidation characteristics on Si substrate with high-concentration (>20vol%) ozone gas. High-concentration ozone gas was supplied by a specially designed ozone generator system with ozone condensation unit. In the oxidation by ozone with the concentration of 25vol% under the temperature range from 340 to 625°C at 8Torr (1.1kPa), the formed oxide film thickness increased with oxidation time in accordance with parabolic laws, which suggests diffusion-controlled step. Parabolic constant at 625°C in ozone oxidation was estimated at 0.19 nm2/min. That value is smaller than 18.3 nm2/min. under the dry oxidation at 800°C, which was proposed by Deal and Grove. As we confirmed the parabolic constants were dependent on temperature, the activation energy in ozone oxidation was determined at 0.52 eV. It is also small, compared to 1.2 eV of the activation energy reported in oxidation by oxygen. Those results indicate the species of reaction in ozone oxidation is different from that in oxygen oxidation. However, the activation energy of 0.52 eV in ozone oxidation under diffusion-controlled step is almost the same as that in plasma oxidation reported previously. Judging from the comparison of activation energies, it might be said even if O(1D) or O(1S) in excited state generates in plasma state, they would convert to O(3P) in graoud state during diffusing in oxide film due to short life. We concluded that the oxidation using high-concentration ozone is in no way inferior to plasma oxidation. Moreover, the quality of ozone oxidation film was evaluated by means of estimation of amount of suboxides (Si3++Si2++Si+) using XPS analysis and compressive stress using FT-IR. The both of results showed that the quality of ozone oxide film at 500°C is equal to that of pyrogenic oxidation at 750°C.

#### 2:55 PM

Phase Stabilities in the Hf-O-Si System: Dongwon Shin<sup>1</sup>; Kyuhwan Chang<sup>2</sup>; Jerzy Ruzyllo<sup>2</sup>; Zi-Kui Liu<sup>1</sup>; <sup>1</sup>Pennsylvania State University, Dept. of Matls. Sci. & Engrg., University Park, PA 16802 USA; <sup>2</sup>Pennsylvania State University, Dept. of Elect. Engrg., University Park, PA 16802 USA

The gate oxide (SiO<sub>2</sub>) thickness in advanced complementary metaloxide semiconductor (CMOS) integrated circuits is continuously decreasing and is about to reach the level (about 1 nm) beyond which no further thinning will be possible. In order to continue growth of CMOS technology SiO<sub>2</sub> gate oxide will have to be replaced at this time with dielectric featuring dielectric constant significantly higher than 3.9. Currently, hafnium oxide and/or hafnium silicate attracts a lot of attention due to their sufficiently high dielectric constants and perceived compatibility with the Si-O system. To better control the thin film processing, the thermodynamic stability of phases in the Hf-O-Si system is investigated through the CALPHAD (CALculation PHAse Diagram) approach assisted by the first-principles calculations. The ionic model is used in the Hf-O and Si-O binary systems. Combining with the thermodynamic parameters of the Hf-Si binary system, the thermodynamic description of the ternary Hf-O-Si system is obtained, and the stability diagrams pertinent to the thin film processing are calculated.

#### 3:10 PM

The Prediction of Critical Thickness in Epitaxial Thin Films: *Joshua Robbins*<sup>2</sup>; Tariq A. Khraishi<sup>1</sup>; <sup>1</sup>University of New Mexico, Mech. Engrg. Dept., MSC01-1150, Albuquerque, NM 87131 USA; <sup>2</sup>Sandia National Laboratories, Computational Physics R&D, PO Box 5800, MS0819, Albuquerque, NM 87185-0819 USA

The current work models the strains and stresses in thin films grown by epitaxial growth processes on finite-thickness compliant substrates. It rigorously examines how these elastic fields influence the prediction of the critical film thickness. Some of the issues or parameters considered include the free surface effects, the strain partitioning model, the relative epilayer to substrate thickness, and the lattice and elastic constants. The work modifies some existing models for strain partitioning and critical thickness. Comparison between the different models is provided.

#### 3:25 PM

#### Assessment of Seal Integrity for Porous Low-k Dielectric Materials: Dongmei Meng<sup>1</sup>; Nancy L. Michael<sup>1</sup>; Choong-Un Kim<sup>1</sup>; <sup>1</sup>University of Texas, Matls. Sci. & Engrg., Arlington, TX 76019 USA

A number of processing and reliability challenges have emerged with the incorporation of ultralow dielectric constant (ULK) materials into IC metallization. In particular, the long-term reliability of Cu/ ULK is of great concern because contaminants from ambient may penetrate the open pore structure of the ULK and affect both interconnect and dielectric integrity. In attempts to protect the metallization structure, various seal strategies have been developed to close the two primary infiltration paths, cut die edges and bond pads. In this study, the effectiveness of the edge seal and bond pad structure in several ULK materials is investigated using an optical microscopy technique. Results indicate that diagnostic probing can damage the fragile structure and open the bond pad to ambient infiltration. Furthermore, the as-manufactured side seal often does not provide a complete seal or is easily compromised by thermal cycling. The data gathered in this study clearly indicate that current side seal and bond-pad structures used for ULK are inadequate to prevent contaminants from reaching Cu lines in packaged samples.

3:40 PM Break

#### 3:55 PM

Texture Investigation of Copper Interconnects With a Different Line Width: Jae-Young Cho<sup>1</sup>; Karbir Mirpuri<sup>1</sup>; Dong Nyung Lee<sup>2</sup>; Joong Kyu Ahn<sup>2</sup>; Jerzy A. Szpunar<sup>1</sup>; <sup>1</sup>McGill University, Metals & Matls. Engrg., 3610 Univ. St., Montreal, Quebec H3A 2B2 Canada; <sup>2</sup>Seoul National University, Sch. of Matls. Sci. & Engrg., Seoul 151-744 Korea

In order to understand the effect of line width on textural and microstructural evolution of Cu damascene interconnects, three Cu interconnects samples which have a different line width are investigated. According to x-ray diffraction results, (111) texture is developed in all investigated lines. Scattered {111}<112> and {111}<110> texture component are present in 0.18 ?Ým width interconnect lines, and {111}<110> texture was developed in 2?Ým width interconnect lines. The directional changes of (111) plane orientation with increase of the line width were investigated by x-ray diffraction method. In addition, microstructure and GBCD (grain boundary character distribution) of Cu interconnects were measured using OIM (orientation imaging microscopy). This measurement demonstrated that bamboo-like microstructure is developed in the narrow line and polygranular structure is developed in the wider line. The percentage of ?Ã3 boundaries is increased as the line width increases but it decreases in the blanket film. New interpretation of textural and microstructural evolution with an increase of line width in damascene interconnects lines is suggested, based on the state of stress in different interconnect lines.

#### 4:10 PM

**Grain Growth and Texture Formation in Cu Damascene Lines:** *David P. Field*<sup>1</sup>; <sup>1</sup>Washington State University, Mech. & Matls. Engrg., Box 642920, Pullman, WA 99164-2920 USA

Copper interconnect lines manufactured by the in-laid, or damascene, processing technique have been shown to result in a wide variety of microstructures. These structures necessarily affect the material performance, such as stress voiding, during further processing and ultimately control the manufacturability of the lines. This study examines the microstructures of in-laid Cu lines as a function of line width and other processing parameters. It is shown that crystallographic texture, grain size, and twin boundary fractions are all directly related to line width for fixed chemistry and barrier layers. These results are discussed from the standpoint of controlling mechanisms.

#### 4:25 PM Invited

Thermo-Mechanical Modeling of Thin Films and Metal Interconnects: Y.-L. Shen<sup>1</sup>; <sup>1</sup>University of New Mexico, Dept. of Mech. Engrg., MSC01 1150, Albuquerque, NM 87131 USA

An overview of recent advances in thermo-mechanical modeling of metal thin films and interconnects will be given. Attention is devoted to the employment of appropriate constitutive material behavior and the proper application and interpretation of numerical data. New modeling results will be presented on the copper interconnect/low-k dielectric systems. Several geometric and material parameters are investigated. The evolution of stresses and deformation pattern in the dual-damascene copper, barrier layers, the dielectrics and their interfaces is seen to have prominent influences in the structural integrity and reliability of contemporary and future-generation devices. Aside from the continuum-based modeling techniques, atomistic simulations of some fundamental mechanical features of thin films and their implications will be presented.

#### 4:50 PM

**Thermal Failure Mechanism of Cu Interconnects in Porous Dielectric**: *Nancy L. Michael*<sup>1</sup>; Dongmei Meng<sup>1</sup>; Choong-Un Kim<sup>1</sup>; <sup>1</sup>University of Texas, Matls. Sci. & Engrg., Arlington, TX 76019 USA

The integration of ultralow-k dielectrics (ULK) into IC metallization is central to continued improvement in advanced electronic device performance. Because ULK materials are highly porous, they are fundamentally different from previously used materials and bring an array of new challenges. One challenge is that with their open pore structure, ULK dielectrics provide a location for process gases to be trapped and a path for ambient to infiltrate deep into the structure and create chemical or physical instabilities. In this study, the thermal stability of Cu/ULK (k~2.2) structures is investigated using 0.25im Cu lines with several diffusion barrier arrangements. Baking tests (185°C-325°C) are conducted in both air and nitrogen ambient with intermittent resistance measurements using minimal current. Results indicate that regardless of diffusion barrier or ambient, Cu interconnects degrade and fail readily, even at the low temperatures used here. Resistance data show that the degradation process begins almost immediately and that the overall failure kinetics are dependent on the diffusion barrier. SEM and TEM images reveal that Cu has diffused through the barrier and resides in the pores of the ULK in the form of Cu2O.

# 5:05 PM Invited

Tribo-Mechanical Characterization of Interconnect Materials for Integration in Cu-Damascene Process: Ashok Kumar<sup>1</sup>; P. Zantye<sup>1</sup>; A. K. Sikder<sup>1</sup>; <sup>1</sup>University of South Florida, Dept. of Mech. Engrg., Nanomatls. & Nanomfg. Rsch. Ctr., Tampa, FL 33620 USA

Chemical mechanical planarization (CMP) has emerged as the most preferred method for achieving excellent global and local planarity and, as the feature sizes shrink, understanding the basics of CMP will be critical for successful implementation of this process in sub 0.35micron technology. Also it is important to understand the effects of mechanical and tribological properties of the interlayer coatings on the CMP process in order to successful evaluation and implementation of these materials. The constant push towards sub-micron miniaturization of device dimensions, increased density of devices, and faster processing power has led to the development of new interconnect technologies that use Copper and ultra low-k (k<2.2) polymer based dielectrics. Here we presented the polishing behavior of different interconnect materials (SiO2, SiC, low-k, Ta and Cu) and discuss the correlation of their mechanical properties with the polishing behavior. Mechanical properties were evaluated by the nanoindentation technique. A CMP tester was used to study the fundamental aspects of CMP process. The coefficient of friction (COF) and acoustic emission (AE) signals were monitored and analyzed for defect analysis, endpoint detection and online process characterization. Delamination and other defect generated during the CMP process shall also be addressed.

# Computational Thermodynamics and Phase Transformations: Interfaces and Grain Boundaries

Sponsored by: ASM International: Materials Science Critical Technology Sector, Electronic, Magnetic & Photonic Materials Division, Materials Processing & Manufacturing Division, Structural Materials Division, MPMD-Computational Materials Science & Engineering-(Jt. ASM-MSCTS), EMPMD/SMD-Chemistry & Physics of Materials Committee

Program Organizer: Jeffrey J. Hoyt, Sandia National Laboratories, Materials & Process Modeling, Albuquerque, NM 87122 USA

Monday PM	Room:	202A
March 15, 2004	Location	: Charlotte Convention Center

Session Chair: TBA

#### 2:00 PM Invited

Phase Transitions and Dynamical Behavior in Ferroelectrics by Atomic-Level Simulation: Simon Robert Phillpot<sup>1</sup>; <sup>1</sup>Argonne National Laboratory, Matls. Sci. Div., 9700 S. Cass Ave., Bldg. 212, Argonne, IL 60439 USA

We use molecular-dynamics simulation to characterize the phase transitions and dynamical behavior in perovksite ferroelectric,s such as KNbO<sub>c3></sub> and BaTio<sub>3</sub>, and in LiNbO<sub>3</sub>. We also characterize the microscopic processes that take place during polarization reversal in the tetragonal orthorhombic and rhomobohedral phases of monodomain KNbO<sub>3</sub>, an order-disorder perovskite ferroelectric. In the tetragonal phase, the polarization of each unit cell reorients from an [001] orientation to an [00] orientation through intermediate states with polarization parallel to [011] and [01]. For low electric field and low temperature, chains of polarization reverse in a spatially coherent manner, resulting in macroscopic intermediate states with orthorhombic symmetry. At high electric field and high temperature the process is completely incoherent and there is no well-defined macroscopic intermediate state.

#### 2:30 PM Invited

Vacancy Interaction With Anti-Phase Boundaries in Ni3Al: Raymond Tedstrom<sup>1</sup>; Murray Daw<sup>1</sup>; <sup>1</sup>Clemson University, Physics & Astron., Clemson, SC 29634 USA

We have investigated the interaction of a vacancy with anti-phase boundaries (APBs) in Ni3Al. The dynamics are investigated using hyperdynamics. On-the-fly kinetic Monte Carlo is accomplished using the Dimer Method to find the saddlepoints exiting a valley. Energetics are calculated with the Embedded Atom Method. The effects of stoichiometry are included through the segregation of anti-site defects to the APB. We study the binding of vacancies and the migration in and around the APB. In particular, we look for processes which can translate the APB perpendicular to itself. The authors acknowledge support from NASA (Aeropropulsion Base Research and Technology).

#### 3:00 PM

**Modelling the Solid-Liquid Interfacial Structure of Al**: James R. Morris<sup>1</sup>; Mikhail I. Mendelev<sup>2</sup>; Seungwu Han<sup>2</sup>; David J. Srolovitz<sup>2</sup>; Graeme J. Ackland<sup>3</sup>; <sup>1</sup>Metals & Ceramics Sciences, Ames Lab., Ames, IA 50011-3020 USA; <sup>2</sup>Princeton University, Dept. of Mech. & Aeros. Engrg., Princeton Matls. Inst., Princeton, NJ USA; <sup>3</sup>University of Edinburgh, Dept. of Physics & Astron., Edinburgh EH9 3JZ, Scotland UK

We have developed a new Embedded Atom-type potential for aluminum, specifically to provide good crystal, defect and liquid phase properties, including the melting temperature. We have calculated the anisotropic solid-liquid interfacial free energy for this and several other Al potentials, all of which have similar melting points. The average interfacial free energy and its anisotropy depends strongly on the potential. We compare the results to experimental values for both of these properties, including data from nucleation, grain boundary groove, and equilibrium shape measurements.

#### 3:20 PM

Phase Transformations at Interfaces in NiAl: Juan Anthony Brown<sup>1</sup>; Yuri Mishin<sup>1</sup>; <sup>1</sup>George Mason University, Sch. of Computational Scis., 4400 Univ. Dr., MSN 5C3, Fairfax, VA 22030 USA

NiAl is a technologically important material whose grain boundaries and surfaces have a significant impact on the mechanical behavior, oxidation resistance and other properties. The chemical composition and structure of these interfaces are studied depending on the bulk composition, temperature, and geometry using grand-canonical Monte Carlo methods and other simulation techniques in conjunction with embedded-atom potentials. NiAl surfaces tend to become Ni-rich by local antisite disorder. Al-terminated surfaces are unstable and are often eliminated by development of a terrace structure with stoichiometric or Ni-rich facets, or by injection of an anti-phase boundary into the bulk. Correlations are studied between the equilibrium surface structure, its orientation, energy and surface stresses. Grain boundaries in NiAl also tend to be Ni-rich. At increased bulk Ni concentration, some grain boundaries undergo structural transformations to structures containing more Ni atoms. The possible impact of these interfacial phase transformations on NiAl properties is discussed.

#### 3:40 PM Break

#### 3:50 PM Invited

Effects of Fe on Grain Boundaries in Al: *Mikhail I. Mendelev*<sup>1</sup>; Seungwu Han<sup>1</sup>; David J. Srolovitz<sup>1</sup>; James R. Morris<sup>2</sup>; Graeme J. Ackland<sup>3</sup>; <sup>1</sup>Princeton University, Dept. of Mech. & Aeros. Engrg., Princeton, NJ 08544 USA; <sup>2</sup>Ames Laboratory, A524 Physics, Ames, IA 50011-3020 USA; <sup>3</sup>University of Edinburgh, Dept. of Physics & Astron., Edinburgh, Scotland EH9 3JZ UK

Fe impurities profoundly affect the mobility of grain boundaries in Al and, hence, strongly modify microstructural evolution in Al alloys. We investigate the role of Fe impurities on grain boundary migration in Al. We develop a new set of Al-Fe interatomic potentials and use them in MD simulations to determine the most important properties that affect grain boundary migration. The interatomic potentials are of the EAM-type and are fit to a wide range of crystal, liquid and defect properties in the pure metals and Al-Fe alloys (obtained from first principles calculations and experiment). MD simulations performed with these potentials are used to determine the diffusivity of Fe in Al (bulk and grain boundary), the heat of segregation and segregation isotherms for several grain boundaries over a range of temperature. These data are used as input to predict the effect of Fe impurities on grain boundary migration in Al.

#### 4:20 PM Invited

Multi Phase Field Simulation Study of the Effect of Particle -Grain Boundary Interaction on Particle Ripening in Solids: Ingo Steinbach<sup>1</sup>; Markus Apel<sup>1</sup>; <sup>1</sup>Access e.V., Intzestr.5, Aachen 52072 Germany

Particles of secondary precipitates in a solid matrix act as pinning centres for grain boundary movement. This is well described by the Zener pinning model, which considers the reduction of grain boundary energy due to the particle-grain boundary interaction. In technical alloys this effect is used for the stabilization of grain boundary networks by particle inclusions. Dependent on the conditions during thermal treatment, however, the particle distribution and thereby the pinning effect is subjected to the effects of growth/dissolution and ripening. In this study the ripening of particles, colocated in a grain boundary network, is investigated on the lengthscale of the individual particles using the Multi Phase Field method. The particles are treated near thermodynamic equilibrium with the matrix grains. Considering distributions with particles in the bulk grain, at grain boundaries and at triple junctions the effect of particle-grain boundary interaction on the ripening behaviour of the particles is studied. Effects of grain boundary diffusion and grain boundary anisotropy are discussed shortly.

#### 4:50 PM

Stress and Capillarity Driven Grain Boundary Migration: A Molecular Dynamics Study: *Hao Zhang*<sup>1</sup>; Mikhail I. Mendelev<sup>1</sup>; David J. Srolovitz<sup>1</sup>; <sup>1</sup>Princeton University, Dept. of Mech. & Aeros. Engrg., Princeton, NJ 08540 USA

Grain boundary migration is key to a wide range of materials processing strategies. Quantitative boundary mobility data is difficult to obtain, yet important for quantitative prediction of microstructural evolution and understanding defect migration fundamentals. We present the results of a series of 3-d molecular dynamics simulations of grain boundary migration as a function of temperature and bicrystallography. In one study, stored elastic energy was used to drive the migration of nominally flat <001> tilt grain boundaries. In another, boundary migration was driven using a half-loop geometry. The boundary velocity was found to be a linear function of driving force. Simulations performed at different temperatures were used to extract the activation energy for boundary migration. Activation energies obtained in both studies were in reasonable agreement, yet are substantially smaller than found in experiment. These data are used to analyze whether boundary mobilities depend on the nature of the driving force.

# 5:10 PM

A Study of Horns in Diffusion Paths: *Hongwei Yang*<sup>1</sup>; <sup>1</sup>University of Connecticut, Dept. of Metall. & Matls. Engrg., 97 N. Eagleville Rd., Unit 3136, Storrs, CT 06269 USA

Interdiffusion behavior of diffusion couple in the ?×+?Ò region of the Al-Cr-Ni system at 1200°C is simulated by DICTRA software which uses the finite difference method. DICTRA simulations show sharp deviation from linear zigzag behavior in the diffusion path. The deviation appears i§horns" pointing either inward or outward, which depends on the relative position between composition vector and eigenvectors. A hypothetical ternary system is built up to study the occurrence of i§horns" and the corresponding characteristics by the comparison between DICTRA simulation and phase filed calculations. It is shown that the i§kirkendall" effect may create horns in diffusion paths.

# Cost-Affordable Titanium Symposium Dedicated to Prof. Harvey Flower: Break Through Technologies

Sponsored by: Structural Materials Division, SMD-Titanium Committee

*Program Organizers:* M. Ashraf Imam, Naval Research Laboratory, Washington, DC 20375-5343 USA; Derek J. Fray, University of Cambridge, Department of Materials Science and Metallurgy, Cambridge CB2 3Q2 UK; F. H. (Sam) Froes, University of Idaho, Institute of Materials and Advanced Processes, Moscow, ID 83844-3026 USA

Monday PM	Room: 2	06B
March 15, 2004	Location:	Charlotte Convention Center

Session Chair: F. H. (Sam) Froes, University of Idaho, Inst. for Matls. & Advd. Processes (IMAP), Moscow, ID 83844-3026 USA

#### 2:00 PM

**Co-Reduction of Titanium-Refractory Element Mixed Oxides**: *Kevin F. Dring*<sup>1</sup>; Martin Jackson<sup>1</sup>; Richard J. Dashwood<sup>1</sup>; Harvey M. Flower<sup>1</sup>; <sup>1</sup>Imperial College London, Matls., Royal Sch. of Mines, Prince Consort Rd., London SW7 2AZ England

Binary alloys of titanium-tungsten and titanium-tantalum were prepared by electrochemical deoxidation of mixed oxide ceramics via the Fray-Farthing-Chen (FFC) process. Material exhibiting less than 1500ppm oxygen was obtained by electrochemical reduction in molten calcium chloride at 950°C for 70-100 hours. The distribution of the both constituents was studied in deoxidised binary alloys containing a range of heavy metal additions. Microstructural and chemical analyses were conducted using scanning electron microscopy and x-ray energy dispersive spectrometry. A comparison with conventional methods of producing refractory element bearing titanium alloys is discussed.

#### 2:30 PM

A Coupled Thermal and Microstructure Model for Laser Metal Deposition of Ti-6Al-4V: S. M. Kelly<sup>1</sup>; S. S. Babu<sup>2</sup>; S. A. David<sup>2</sup>; T. Zacharia<sup>3</sup>; S. L. Kampe<sup>4</sup>; <sup>1</sup>Oak Ridge National Laboratory, Jt. Inst. for Computational Scis., PO Box 2008, MS6096, Oak Ridge, TN 37831-6096 USA; <sup>2</sup>Oak Ridge National Laboratory, Metals & Ceram. Div., PO Box 2008, MS6096, Oak Ridge, TN 37831-6096 USA; <sup>3</sup>Oak Ridge National Laboratory, Computing & Computational Scis., PO Box 2008, MS6232, Oak Ridge, TN 37831-6232 USA; <sup>4</sup>Virginia Tech, Matls. Sci. & Engrg. Dept., 213 Holden Hall (0237), Blacksburg, VA 24061-0237 USA

Near-net shape processes, such as laser metal deposition (LMD), offer a unique combination of process flexibility, time savings, and reduced cost in producing titanium alloy components. The current challenge in processing titanium alloys using LMD methods is understanding the complex microstructure evolution as a part is fabricated layer by layer. The microstructure is effected by the repeated thermal cycling that occurs during the deposition process. The current work focuses on the thermal and microstructural modeling of multilayered Ti-6Al-4V deposits. Prior work with LMD-Ti-6Al-4V has shown that a complex microstructure evolves consisting of a two-phase alpha+beta structure. Depending on the location within the part, the Widmanstatten alpha morphology may be colony (layer band) or basketweave. A thermal model has been developed using finite difference techniques to predict the thermal history of LMD processes. The characteristics of a thermal cycle are used to semi-quantitatively map the evolution of equilibrium and nonequilibrium phases in the deposit. The results of the thermal and microstructure models will be discussed in relation to the as-deposited microstructure.

# 3:00 PM

**MEM Titanium Production: Possibilities for Cost Reduction:** Yaroslav Yurievich Kompan<sup>1</sup>; Igor Victorovich Protokovilov<sup>1</sup>; <sup>1</sup>The Paton Electric Welding Institute, 11 Bozhenko St., Kiev 03680 Ukraine

Key differences of magnetically controllable electroslag melting (MEM) from VAR, EBR and other means of titanium melting are intensive directed motion of metallurgical melt and purification of metal by halogen flux. Utilization of the MEM technology assures homogeneity, fineness and high purity of metal ingot. Intensive heat and mass transfer in metallurgical pool creates a uniform temperature field of melt (T=1700-2000°C) and distribution of alloying elements throughout ingot volume, at the same time avoiding their burn during the melting process of a consumable electrode. Among reserves for cost reduction under MEM production of titanium and its alloys are: utilization of lower grade titanium sponge, less repeated remeltings, absence of expensive alloying elements burn, reduced share of scrap, low cost and higher reliability of melting equipment. Economic effectiveness of the MEM technology increases along with increasing number of alloying components in multicomponent alloys.

#### 3:30 PM

**Titanium Extraction by Molten Oxide Electrolysis**: *Donald R. Sadoway*<sup>1</sup>; <sup>1</sup>Massachusetts Institute of Technology, Dept. of Matls. Sci. & Engrg., 77 Mass. Ave., Rm. 8-203, Cambridge, MA 02139-4307 USA

Molten oxide electrolysis (MOE) is an extreme form of molten salt electrolysis, a technology that has been producing tonnage metal for over 100 years: aluminum, magnesium, lithium, sodium, and the rare-earth metals are all produced in this manner. MOE is distinguished by the avoidance of halide electrolytes and carbon anodes which enables the production of oxygen gas instead of halogens or  $CO_2$ . The viability of adaptation of MOE for the extraction of titanium by the direct electrolysis of a multicomponent oxide melt containing dissolved TiO<sub>2</sub> to produce liquid titanium and oxygen gas is assessed.

#### 4:00 PM

Improving Wear Resistance of Ti-6Al-4V Alloy: *Ibrahim Ucok*<sup>1</sup>; Kevin L. Klug<sup>1</sup>; Mehmet N. Gungor<sup>1</sup>; Joseph R. Pickens<sup>1</sup>; <sup>1</sup>Concurrent Technologies Corporation, 100 CTC Dr., Johnstown, PA 15904 USA

An objective of the Combat Vehicle Research (CVR) Program at Concurrent Technologies Corporation is to facilitate extensive use of titanium alloys in combat vehicle applications to take advantage of their high specific strength and excellent corrosion resistance in both wrought and cast forms. These properties make Ti alloys very attractive for replacing steel components to reduce the weight of combat vehicles, thereby improving vehicle mobility and facilitating air transport. However, the inferior wear resistance of Ti alloys compared to steels may be a limiting factor in certain high wear applications, especially when Ti replaces surface-hardened steel. In this study, Ti-6Al-4V substrates were subjected to commercially available surface treatments such as plasma nitriding, electro-spark alloying, electroless plating and thermal spray coatings. The engineered surfaces were evaluated by wear testing, hardness measurements and metallography. Composite diamond and WC-Co coatings were found to have the highest wear resistance under the test conditions employed.

# 4:30 PM

A New Novel Electrolytic Process to Produce Titanium: Jim C. Withers<sup>1</sup>; R. O. Loutfy<sup>1</sup>; <sup>1</sup>MER Corporation, Tucson, AZ 85706 USA

Considerable past effort has been devoted to the electrolytic extraction of titanium without commercial success. A novel new process that combines thermal reduction and electrolytic reduction of titanium from its oxide contained in a composite the anode has been demonstrated. As no solubility of the reduced oxide in the electrolyte is required, there is a large diversity of electrolytes and bath operating parameters including low temperature that can be utilized to produce titanium in a morphology of powder, flake and solid. Not only can CP titanium be produced, but also it is possible to utilize other oxides in the anode and produce alloys such as Ti-6A1-4V and other alloys. Rutile can be used as a feed to produce a very low cost titanium in a less purity than aerospace grade. Powder geometry and size can be controlled based on electrolysis parameters and other operating conditions such that the powders can be utilized directly in powder metallurgy processing to produce titanium components. Economic projections suggest titanium powder can be produced at substantially lower cost than the Kroll or Hunter processes. History and recent results will be discussed.

#### 5:00 PM

**Titanium Biocomposites through Powder Metallurgy**: *M. Karanjai*<sup>1</sup>; R. Sundaresan<sup>1</sup>; T. R. Rama Mohan<sup>2</sup>; B. P. Kashyap<sup>2</sup>; <sup>1</sup>International Advanced Research Centre for Powder Metallurgy and New Materials, Hyderabad 500 005 India; <sup>2</sup>Indian Institute of Technology Bombay, Mumbai 400 076 India

Apart from its well known applications as structural material, titanium finds a niche use as a biomaterial because of its excellent biocompatibility. However, titanium is a bio-inert material, and in implantology it is desirable to make it bioactive by addition of materials like hydroxyapatite (HA) or tri-calcium phosphate (TCP). These bioactive additives are generally very expensive. Composites with bioactive additives like HA and TCP-like phases in Ti matrix have been developed by in-situ formation from inexpensive precursors through PM processing. The starting materials are titanium powder produced by H-DH process and appropriate salts containing calcium and phosphorous. Results confirming formation of bioactive phases and mechanical properties of the composites are reported.

# Dislocations: Simulation and Observation of Fundamental Mechanisms

Sponsored by: ASM International: Materials Science Critical Technology Sector, Electronic, Magnetic & Photonic Materials Division, Materials Processing & Manufacturing Division, Structural Materials Division, EMPMD/SMD-Chemistry & Physics of Materials Committee, MPMD-Computational Materials Science & Engineering-(Jt. ASM-MSCTS)

*Program Organizers:* Elizabeth A. Holm, Sandia National Laboratories, Albuquerque, NM 87185-1411 USA; Richard A. LeSar, Los Alamos National Laboratory, Theoretical Division, Los Alamos, NM 87545 USA; Yunzhi Wang, The Ohio State University, Department of Materials Science and Engineering, Columbus, OH 43210 USA

Monday PM	Room:	20	)1A		
March 15, 2004	Location	ו:	Charlotte	Convention	Center

Session Chair: TBA

2:00 PM

Models of the Ductile-Brittle Transition (DBT) in Single and Polycrystals: N. M. Ghoniem<sup>1</sup>; J. Huang<sup>1</sup>; S. Noronha<sup>1</sup>; <sup>1</sup>University of California, Mech. & Aeros. Engrg. Dept., Los Angeles, CA 90095-1597 USA

In bcc single and polycrystal metals, a transition from a state of ductility at high temperature is suddenly changed to a state of low ductility at low temperature. A critical transition temperature, Tc, defines this universal behavior, where the fracture toughness increases dramatically once the operating temperature is above Tc. Below Tc, the mode of fracture is characterized as brittle and energy is dissipated mainly in the cleavage of atomic planes, while fracture occurs by ductile tearing above Tc. Similar behavior is also observed in covalentlybonded crystals, such as Si and SiC. We present here a new methodology for representation of 3-D cracks of arbitrary shape with parametric dislocation loop pileups. The conditions of nucleation and emission of small dislocation loops from 3-D crack tips are investigated in single crystal bcc metals. It is shown that the stress state ahead of crack tips cannot be described by 2-D elasticity methods due to the 3-D nature of the interaction between emitted loops and the crack surface. The increase in fracture toughness is shown to result from dislocation shielding, once emitted dislocation loops interconnect and form a continuous configuration, while regions of shielding/ anti-shielding are shown to occur when emitted loops have not yet connected. Modeling DBT in polycrystals involves the interaction between a main crack, micro-cracks at fractured precipitates or other weak sites, and emitted dislocations from the main crack and micro-cracks. The increase in fracture toughness at temperatures above Tc is shown to be a result of two mechanisms: (1) shielding the crack tip by emitted dislocations; (2) dissipation of energy in the production of dislocations by multiplication and source generation mechanisms.

#### 2:35 PM

Slip Step Evolution Around Indentations: *Kevin A. Nibur*<sup>1</sup>; David F. Bahr<sup>1</sup>; Brian P. Somerday<sup>2</sup>; <sup>1</sup>Washington State University, Mech. & Matls. Engrg., PO Box 642920, Pullman, WA 99164-2920 USA; <sup>2</sup>Sandia National Laboratory, Matls. & Engrg. Sci., 7011 E. Ave., Livermore, CA 94551 USA

Microscopic analysis of the evolution of slip steps is used to study dislocation activity around indentations in FCC metals. Nanoindentation, atomic force microscopy and orientation imaging microscopy are used to extract fundamental material behavior and identify specific slip planes associated with each slip step. Alloys with lower SFE have smaller, straighter and more closely spaced slip steps, whereas high SFE metals display wavy steps with a range of heights. In a low SFE stainless steel, average slip step heights increased with indentation load up to 200 mN. Beyond this load, a constant average step height of 17 nm was maintained even though pile-up heights increased due to an increased number of steps. Deformation evolves by the creation of additional slip steps around the indentation and not by the extension of existing steps as the indentation proceeds. The method is able to probe both bulk and local properties.

#### 2:55 PM

**Dislocation Mechanisms in Grain Boundary Sliding**: Diana Farkas<sup>1</sup>; Brian Hyde<sup>1</sup>; <sup>1</sup>Virginia Polytechnic Institute and State University, Matls. Sci. & Engrg., 201-A Holden Hall, Blacksburg, VA 24061 USA

Atomistic computer simulations were performed to investigate the mechanisms of grain boundary sliding in BCC Fe using the embedded atom method. For this study we have chosen the  $\Sigma=5$  [001] (310) symmetrical tilt boundary under shear deformation. The response of the boundary to shear loading was studied by molecular statics and dynamics. Sliding was determined to be governed by dislocation activity. The dislocations that are active during grain boundary sliding belong to the DSC lattice. The results show that, at least for special boundaries, the sliding process occurs by the motion of grain boundary dislocations. In this process, the sliding of the boundary under shear is accompanied by migration of the boundary parallel to itself. In analogy to the deformation of bulk materials, the deformation of special boundaries occurs by dislocations at shear stress values much lower than the theoretical strength of the boundary. We also analyze in detail the role of partial DSC grain boundary dislocations as they change the grain boundary's structure. The implications for the sliding behavior of more general boundaries are discussed.

# 3:15 PM

Drag on Dislocation Motion Due to Glissile Interstitial Loops: Zhouwen Rong<sup>1</sup>; David J. Bacon<sup>1</sup>; Yuri N. Osetsky<sup>2</sup>; <sup>1</sup>University of Liverpool, Dept. of Engrg., Brownlow Hill, Liverpool L69 3GH UK; <sup>2</sup>Oak Ridge National Laboratory, Computer Scis. & Math., PO Box 2008, Oak Ridge, TN 37831-6158 USA

Computer simulation has shown that self-interstitial atoms form clusters of closely-packed crowdion defects during radiation damage in metals and, depending on the crystal structure, are equivalent to nanosized dislocation loops with perfect Burgers vector. They can execute fast, thermally-activated glide along the crowdion orientation. Their interaction with dislocations and subsequent effect on slip is expected to be important for radiation hardening and yield phenomena. We report atomic-scale computer simulations of the interaction of a gliding edge dislocation with interstitial loops near the glide plane and its influence on the dislocation dynamics. The drag due to a loop is determined as a function of temperature and Burgers vector orientation for both iron and copper. The results are interpreted in terms of the diffusivity of loops and general conditions under which drag or dislocation breakaway should occur are predicted.

#### 3:35 PM Break

#### 3:50 PM

Dislocation Dynamics as a Path to Parameter-Free Prediction of Crystal Strength: Vasily V. Bulatov<sup>1</sup>; <sup>1</sup>University of California, Lawrence Livermore Natl. Lab., Livermore, CA 94551 USA

Massively-parallel Dislocation Dynamics (DD) simulations are widely recognized as the most direct and rigorous way to connect crystal plasticity with the underlying physics of dislocation motion and interactions. There are two major issues to be addressed for the DD approach to deliver on its promise. The first relates to one's ability to identify and accurately quantify key mechanisms of dislocation behavior on the atomic level. High quality of the atomistic input (local rules, mobility functions) is a pre-requisite of high fidelity of the DD approach. Second, to make DD simulations truly predictable and representative of crystal plasticity, very large ensembles of interacting dislocations must be evolved over long time intervals. The ability to compute large enough and long enough, i.e. computability, is the second important issue to resolve. We will overview the progress being made in the LLNL group in the development and implementation of Dislocation Dynamics on massively parallel computers.

#### 4:25 PM

TEM In-Situ Straining Experiments of FeAl (B2) Oriented Single Crystals Containing Boron and/or Nickel: Anna Fraczkiewicz<sup>1</sup>; David Colas<sup>1</sup>; Olivier Calonne<sup>1</sup>; Francois H. Louchet<sup>2</sup>; <sup>1</sup>ENSMSE, URA CNRS 1884, 158 Cours Fauriel, St-Etienne 42100 France; <sup>2</sup>ENSEEG, LTPCM, BP 75, St-Martin d'Heres 38 054 France

B2-ordered FeAl alloys currently exhibit a yield stress anomaly (YSA) at intermediate temperatures. The origins of YSA in FeAl are not clearly established; two major phenomena are mentioned in literature: (i), superdislocation decomposition (<111> -> <100> + <110>); (ii) vacancy-induced dislocation locking. In this work, Fe-40 % Al-100 ppm B single crystals, containing or not 3.8 at. % Ni, were in situ strained (along a <110> direction) in a TEM, at temperatures ranging between 300 and 700°C. Dislocation dynamics was observed and recorded; their identification was completed by post-mortem analysis in CTEM. In this talk, we report crucial dynamic observations of dislocation mechanisms during TEM in situ straining. Experimental evidence of dislocation decomposition and the presence of mobile anisotropic <110> loops bands are given, along with direct observations of superdislocation locking by APB tubes created by thermal vacancies. These results suggest that both elementary mechanisms are involved in the YSA of FeAl.

#### 4:45 PM

Dynamic Dislocation Multiplication and Propagation in bcc Metals: Luke L. Hsiung<sup>1</sup>; <sup>1</sup>Lawrence Livermore National Laboratory, Chmst. & Matls. Sci., 7000 E. Ave., PO Box 808, L-352, Livermore, CA 94551-9900 USA

Initial dislocation structures in as-annealed Mo and Ta crystals, and dislocation structures developed within the crystals compressed under different strain rates have been investigated using transmission electron microscopy (TEM). The purpose of this study is to understand and elucidate underlying mechanisms for the formation of dipoles (debris), the development of cross-grid dislocation arrays and patterning, and the occurrence of {0-11} anomalous slip (i.e. the Schmid's law violation) in bcc metals. Novel mechanisms based upon dynamic dislocation multiplication and propagation are proposed for the formation of dipoles, cross-grid dislocation pairs, dislocation entanglement, and the occurrence of anomalous slip. This work was performed under the auspices of the U. S. Department of Energy by the University of California, Lawrence Livermore National Laboratory under Contract No. W-7405-Eng-48.

#### 5:05 PM

First-Principles Electronic Structure of Screw Dislocations in Alpha-Fe: Murray Daw<sup>1</sup>; Daryl Chrzan<sup>2</sup>; <sup>1</sup>Clemson University, Phys-

ics & Astron., Clemson, SC USA; <sup>2</sup>University of California, LBNL, Berkeley, CA USA

We have performed first-principles calculations of the electronic structure of screw dislocations in alpha-Fe. The calculations are performed within the spin-polarized Generalized Gradient Approximation (GGA), using the Projector Augmented-wave Method (PAW). The calculations have been performed using the ab-initio total-energy and molecular-dynamics program VASP (Vienna ab-initio simulation program) developed at the Institut fur Materialphysik of the Universitat Wien.<sup>1-3</sup> The periodic supercell contains 96 atoms, two (opposite) screws, and the periodic vectors are chosen to form a quadrupolar array of dislocations. Both easy-core and hard-core structures have been determined and compared. The effects of magnetization are examined. 1G. Kresse and J. Hafner, Phys. Rev. B47, 558 (1993); ibid. B49, 14 251 (1994). 2G. Kresse and J. Furthmuller, Comput. Mat. Sci. v6, 15 (1996); ibid. Phys. Rev. B54, 11 169 (1996). 3G. Kresse and D. Joubert, Phys. Rev. B59, 1758 (1999). Supported by DOE, DOE/ EPSCOR and NERSC.

#### 5:25 PM

**Dislocations in Laves Phases:** *Sharvan Kumar*<sup>1</sup>; Matthew F. Chisholm<sup>2</sup>; Peter M. Hazzledine<sup>3</sup>; <sup>1</sup>Brown University, Div. of Engrg., 182 Hope St., Box D, Providence, RI 02912 USA; <sup>2</sup>Oak Ridge National Laboratory, Solid State Div., 1 Bethel Valley Rd., Oak Ridge, TN 37831 USA; <sup>3</sup>UES, Inc, 4401 Dayton-Xenia Rd., Dayton, OH 45432 USA

Slip, twinning and polytypic transformations in Laves phases are thought to occur by synchroshear. While a geometric description of these processes through the motion of "synchro-shockley" dislocations exists, little is known about the core structure of these synchroshockley dislocations and the structure of the faults they bound. Experimental results on polytypic transformations of Cr-based Laves phases have shown that in general, the transformations are extremely sluggish, and in the one case where it is rapid, the transformation rate appears to depend on ternary substitution. Reasons for the sluggishness or this chemical dependence of kinetics are not known but are probably connected to the core structure of the dislocations. This paper describes some observations of fault and core structures by Z contrast HREM. They are discussed in relation to the kinetics of transformations and to ductility in Laves phases.

# **General Abstracts: Session II**

Sponsored by: TMS

*Program Organizers:* Adrian C. Deneys, Praxair, Inc., Tarrytown, NY 10591-6717 USA; John J. Chen, University of Auckland, Department of Chemical & Materials Engineering, Auckland 00160 New Zealand; Eric M. Taleff, University of Texas, Mechanical Engineering Department, Austin, TX 78712-1063 USA

Monday PM	Room:	204		
March 15, 2004	Location	h: Charlotte	Convention	Center

Session Chair: Joy A. Hines, Ford Motor Company, Dearborn, MI 48123 USA

#### 2:00 PM

Numerical Study of the Solidification of a Pure Metal in a Rectangular Cavity: Beth Anne V. Bennett<sup>1</sup>; Jason Hsueh<sup>1</sup>; David T. Wu<sup>1</sup>; <sup>1</sup>Yale University, Dept. of Mech. Engrg., PO Box 208284, New Haven, CT 06520-8284 USA

Solidification of pure aluminum or gallium within a rectangular cavity is modeled numerically, and results are compared with published data. The model includes latent heat release, convection, conduction (with temperature-dependent variation in viscosity during phase change), and buoyancy. Microstructural development is modeled via a crystal size distribution function (SDF), which can be expressed in terms of nucleation and growth rates. The governing partial differential equations consist of conservation equations for mass, momentum, and energy, and evolution equations for the zeroth through third moments of the SDF. At each time step, these coupled, nonlinear equations are solved simultaneously at all grid points using Newton's method within the local rectangular refinement (LRR) solution-adaptive gridding method. The fully implicit LRR method automatically generates unstructured adaptive grids and incorporates multiple-scale finite differences, producing considerable computational savings without loss of accuracy, as compared to similar solution techniques on structured grids

Computer Simulations of Stress Corrosion Behavior of ZA-27/ Quartz Metal Matrix Composites: P. V. Krupakara<sup>1</sup>; <sup>1</sup>R. V. College of Engineering, Dept. of Chmst., Mysore Rd., Bangalore 560059 India

The stress corrosion resistance of ZA-27/Quartz metal matrix composites (MMCs) in high temperature acidic media has been evaluated using autoclave. Liquidmelt metallurgy technique using vortex method was used to fabricate MMC. Quartz particulates of size 50-80micro meters in size are added as reinforcement. ZA-27 containing 2,4,6 weight percentage of quartz were prepared. Stress corrosion test were conducted by weight loss method for different exposure time, normality and temperature of the acidic medium. The corrosion rate of composites were lower to that of matrix ZA-27 alloy under all condition.

# 2:50 PM

Electrochemical Modeling of Corrosion Inhibition Using Surfactants: Michael L. Free<sup>1</sup>; <sup>1</sup>University of Utah, 135 S. 1460 E., Rm. 416, Salt Lake City, UT 84112 USA

Equilibrium adsorption equations can be used in connection with mixed potential theory to model corrosion inhibition using surfactant molecules. This modeling approach utilizes surfactant hydrocarbon chain length and solution ionic strength data along with electrochemical principles and functional group adsorption properties to predict the rate of corrosion under a variety of conditions.

#### 3:15 PM

Oxygen Distribution in Yttria-Stabilized Zirconia Sintered by Pulsed Current Sintering: *Kimihiro Ozaki*<sup>1</sup>; <sup>1</sup>National Institute of Advanced Industrial Science and Technology, Inst. for Structural & Engrg. Matls., Anagahora 2266-98 Shimoshidami, Moriyama, Nagoya 463-8560 Japan

Pulsed current sintering is a way of sintering powders at a high heating rate and a high cooling rate by flowing electrical current in powder directly. An YSZ shows ionic conductivity at a high temperature. When an YSZ powder is put in a carbon die and is sintered by the pulsed current sintering, electrical current flows in the carbon die at a low temperature and flows in both of the carbon die and the YSZ powder at a high temperature. In the YSZ sintered in a vacuum, an oxygen deficiency occurred, and the oxygen concentration of the anode side was different from it of the cathode side. The deficiency increased with increase of yttria content, and the YSZ became blacker.

# 3:40 PM Break

#### 3:50 PM

Effective Activation Enthalpy for a Periodic Reaction Sequence: Application of the Escher Ring: *David T. Wu*<sup>1</sup>; <sup>1</sup>Yale University, Dept. of Mech. Engrg., PO Box 208284, New Haven, CT 06520-8284 USA

Many driven processes that reach steady state (e.g., interface motion in crystallization or solid phase epitaxy; grain boundary motion; and crack propagation) may be modeled as periodic sequences of firstorder reactions. Kinetically such a reaction sequence is mathematically equivalent to a biased random walk on an "Escher Ring." The overall rate has a simple general solution, and an effective activation enthalpy can be identified, which is bigger than or equal to that obtained from the so-called rate-limiting step.

#### 4:15 PM

**Characterization of Environment-Induced Degradation in Type 422 Stainless Steel:** Ajit K. Roy<sup>1</sup>; *Ramprashad Prabhakaran*<sup>1</sup>; <sup>1</sup>University of Nevada, Dept. of Mech. Engrg., 4505 Maryland Pkwy., Las Vegas, NV 89154-4027 USA

Globally significant efforts are ongoing to reduce the half-lives of spent nuclear fuels by a process known as transmutation. Martensitic Type 422 Stainless Steel is a candidate structural material to contain a target material used in this application. Extensive work has been performed to characterize the environment-induced degradation such as stress corrosion cracking and localized corrosion (pitting and crevice) of this material in aqueous environments of different pH values at ambient and elevated temperatures. This paper is focused on elucidating the results of this study, in particular, the effect of metallurgical and environmental variables on the susceptibility of this alloy to these degradation modes. The metallurgical and fractographic evaluations of this material as determined by optical microscopy and scanning electron microscopy will also be summarized. In essence, a mechanistic understanding of these degradations, based on the analyses of the available results will be presented in this paper.

#### 4:40 PM

High-Temperature Corrosion of Iron Aluminides in O2/Cl2/Ar Atmosphere: Gilsoo Han<sup>1</sup>; Weol D. Cho<sup>1</sup>; <sup>1</sup>University of Utah,

Metallurgl. Engrg., 135 S. 1460 E., Rm. 412, Salt Lake City, UT 84112 USA

The high-temperature corrosion of iron aluminde (Fe3Al) in environments containing chlorine has been investigated at 700°C using thermogravimetric method. The corrosion experiments were performed in Ar/0.5%Cl2 mixtures containing various levels of oxygen from trace amounts to 20% at temperature of 700°C. In general, the corrosion rate decreases with increasing oxygen content in the gas mixture. Several kinetic modes during the corrosion were observed depending on oxygen content. The microstructure of the corrosion scale was analyzed by using several analytical tools to identify the corrosion mechanism. In addition, a quasi stability diagram was developed for the Fe-Al-Cl2-O2 system to explain the corrosion mechanism. The corrosion study was extended to the corrosion of Y-doped Fe3Al in the same corrosive environments to investigate the effect of yttrium on the corrosion. The beneficial effects of yttrium on the corrosion were analyzed by corrosion kinetics and the microstructure of the corrosion scale formed on Y-doped Fe3Al.

#### 5:05 PM

Atomic-Level Interaction of Edge and Screw Dislocations With Stacking Fault Tetrahedra in fcc Metals: Yury N. Osetsky<sup>1</sup>; David J. Bacon<sup>2</sup>; <sup>1</sup>Oak Ridge National Laboratory, Computer Scis. & Math., 4500 S. MS G138, Oak Ridge, TN 37831-6138 USA; <sup>2</sup>The University of Liverpool, Matls. Sci. & Engrg., Brownlow Hill, Liverpool L69 3GH UK

Interaction between moving edge and screw dislocations and stacking fault tetrahedra (SFTs) was studied at atomic scale via molecular dynamics and statics. A recently developed technique based on a periodic array of dislocations has been used together with the empirical many-body potential fitted to reproduce elastic properties and point defects energies in fcc Cu. SFTs of size from 2.5nm to 4nm containing from 45 to 136 vacancies were simulated over the temperature range from 0 to 450K. It was observed that the critical resolved shear stress depends strongly on the position of the dislocation glide plane relative to the SFT's face. It also depends on crystal temperature. A specific mechanism have been observed by which a sheared SFT may recover its regular configuration. The results are compared with the experimental observations in quenched and irradiated fcc metals with low stacking fault energy.

# **General Abstracts: Session III**

Sponsored by: TMS

*Program Organizers:* Adrian C. Deneys, Praxair, Inc., Tarrytown, NY 10591-6717 USA; John J. Chen, University of Auckland, Department of Chemical & Materials Engineering, Auckland 00160 New Zealand; Eric M. Taleff, University of Texas, Mechanical Engineering Department, Austin, TX 78712-1063 USA

Monday PM	Room: 2	12A		
March 15, 2004	Location:	Charlotte	Convention	Center

Session Chair: Aladar A. Csontos, US Nuclear Regulatory Commission, Washington, DC 20555 USA

#### 2:00 PM

**Enhancement of Bending Limits in Thick Plate AA 6061-T6**: *M. P. Miles*<sup>1</sup>; C. Fuller<sup>2</sup>; M. Mahoney<sup>2</sup>; <sup>1</sup>Brigham Young University, Mfg. Engrg. Tech., 265 CTB, Provo, UT 84602 USA; <sup>2</sup>Rockwell Science Center, 1049 Camino dos Rios, Thousand Oaks, CA 91360 USA

Friction Stir Processing (FSP) is used to modify the surface microstructure of one inch thick 6061-T6 plate in order to enhance bending performance. The plate is approximately 25 mm thick and is processed to depths of 5.4 mm and 3.0 mm on the pre-tensile surface. Plane-strain bending experiments were performed on an unprocessed plate and on the plates processed to 5.4 and 3.0 mm of depth until cracks began to form on the plate surface. Finite Element Analysis (FEA) was used to simulate the bending experiments. The Latham-Cockroft failure criterion was used to predict the onset of cracking and the resulting bending limit in each case.

#### 2:25 PM

The Four-Point-Bending Fatigue Behavior of Several Superalloys: *Robert L. McDaniels*<sup>1</sup>; John Michael Cunningham<sup>1</sup>; Wei Yuan<sup>1</sup>; Hongbo Tian<sup>1</sup>; Gongyao Wang<sup>1</sup>; Peter K. Liaw<sup>1</sup>; Dwaine L. Klarstrom<sup>2</sup>; <sup>1</sup>University of Tennessee, Matls. Sci. & Engrg., 434 Dougherty Hall, Knoxville, TN 37996 USA; <sup>2</sup>Haynes International, Inc, 1020 W. Park Ave., PO Box 9013, Kokomo, IN 46904-9013 USA The four-point-bending fatigue testing was conducted on several superalloys under stress-controlled conditions. The testing was performed at room temperature in laboratory air at a frequency of 10 Hz. All tests were run to failure. At regular intervals, the tests were suspended, and replicas of the gage length were made, and subjected to scanning electron microscopy to establish the small crack growth behavior of the alloys. Fractography and metallography examinations were performed on selected specimens from each alloy. A mechanistic understanding of fatigue crack initiation behavior is provided.

#### 2:50 PM

Mechanical Behavior of a Closed-Cell Octet Structure: Wynn Steven Sanders<sup>1</sup>; <sup>1</sup>Air Force Research Laboratory, AFRL/MLLMD, 2230 Tenth St., Bldg. 655, Rm. 025, Wright-Patterson AFB, OH 45433 USA

Lattice- and truss-based materials have been investigated as alternatives to low-density, stochastic metallic foams. These materials exhibit significantly improved properties compared to stochastic foams. However, these "ideal" truss materials are open-cell structures; there may be applications where a closed-cell structure is desired. A relatively simple technique has been developed to construct a closed-cell version of the octet-truss lattice. Initial finite element modeling has shown that the relative modulus and relative strength of the closedcell octet structure is about twice that compared to the open-cell octet-truss lattice for relative densities below ten percent. In fact, the modulus is within twenty percent of the Hashin-Shtrikman upper bound for an isotropic porous material. Additionally, this structure is nearly isotropic. The closed-cell octet structure, which can be envisioned as a "three-dimensional honeycomb," may be a beneficial alternative to existing low-density metallic materials.

# 3:15 PM Cancelled

Plastic Strain and Grain Size Effects in the Surface Roughening of Aluminum Alloys

#### 3:40 PM Break

#### 3:50 PM

Improvement in Damping Capacity of Sintered Aluminum Alloy by Ceramic Dispersion: *Takuya Sakaguchi*<sup>1</sup>; Katsuhiro Nishiyama<sup>2</sup>; <sup>1</sup>Toyota Motor Corporation, Matl. Engrg. Div. 3, Misyuku 1200, Susono, Shizuoka Japan; <sup>2</sup>Tokyo University of Science, Suwa, Chino, Nagano Japan

Conventional aluminum alloys are not available for damping materials due to their low damping capacity. For improving damping capacity of aluminum alloy, it is known to be an effective way to disperse graphite in the aluminum alloy. However, addition of a considerable amount of graphite reduces the rigidity of the aluminum alloy because the rigidity of graphite is very low. In the present study, we have tried to disperse fine particles of NdNbO4, which is known to be a high damping ceramic, in aluminum alloy by powder metallurgy in order to raise both damping capacity and rigidity of the alloy.

#### 4:15 PM

Plastic Instability of Aluminum-Magnesium Alloy 5052: Chen-Ming Kuo<sup>1</sup>; Chi-Ho Tso<sup>2</sup>; <sup>1</sup>I-Shou University, Dept. of Mech. Engrg., 1, Sec. 1, Hsueh-Cheng Rd., Ta-Hsu, Kaohsiung 84008 Taiwan; <sup>2</sup>I-Shou University, Dept. of Matls. Sci. & Engrg., 1, Sec. 1, Hsueh-Cheng Rd., Ta-Hsu, Kaohsiung 84008 Taiwan

Plastic instability is observed during stress rate change test of aluminum-magnesium alloy 5052 at room temperature. In the stress rate change tests, strain retardation and plastic deformation instability are observed. During the stress rate change test, plastic strain is insignificant until the plastic instability occurs. If there is no unstable phenomenon, the plastic strain rate would practically have no changes from beginning to end. The occurrence of plastic instability is related to the applied stress rate and retention time. By the argument of dynamic strain ageing effect, the plastic instability could be justified as the interaction between solid solution element, magnesium, and dislocations. In order to model the plastic deformation, thermally activated kinetic flow theory coupled with structural evolution law has been employed. By changing the values of suitable parameters to simulate the microstructure change of instability, plastic instability could be modeled by the use of numerical method.

### 4:40 PM

Processing of Aluminum (AA6061) for Continuous Severe Plastic Deformation Using ECAE Technique: Shravan Kumar Indrakanti<sup>1</sup>; Yogesh Bhambri<sup>1</sup>; Raghavan Srinivasan<sup>1</sup>; Qingyou Han<sup>2</sup>; <sup>1</sup>Wright State University, Mech. & Matls. Engrg., 209 Russ Engrg. Ctr., 3640 Col. Glenn Hwy., Dayton, OH 45435 USA; <sup>2</sup>Oak Ridge National Laboratory, Metals & Ceram., PO Box-2008, MS-6083, Oak Ridge, TN 37831-6083 USA Studies prove that Equal channel angular extrusion (ECAE) can be applied as a Severe Plastic Deformation (SPD) method to produce ultra fine-grained materials. However this technique is a multi-step batch process that produces small cross-section, short length stock, which severely limits its commercialization. To overcome the limitations of ECAE, a new technology known as Continuous Severe Plastic Deformation (CSPD) was conceptualized. CSPD will be able to produce continuous long lengths of bulk ultra fine-grained materials. In this study ECAE concept was used to impart plastic strain in to a long length of aluminum AA6061 bar having ½ inch square cross section. AA6061 bars at various conditions were subjected to CSPD through a 135° ECAE die at room temperature. The experiment was repeated for multiple passes. Initial results indicate that CSPD process can be used to refine grain sizes. Results will be compared with that of the ECAE of batch process.

#### 5:05 PM

Variation in Poisson's Ratio With Other Elastic Constants: An Attempt Towards Rationalization of Elastic Constants for Isotropic Solid Materials: Anish Kumar<sup>1</sup>; T. Jayakumar<sup>1</sup>; Baldev Raj<sup>1</sup>; K. K. Ray<sup>2</sup>; <sup>1</sup>Indira Gandhi Centre for Atomic Research, Metall. & Matls. Grp., Kalpakkam 603102 India; <sup>2</sup>Indian Institute of Technology, Kharagpur 721302 India

A low symmetry crystal may have as many as 21 independent elastic constants. However the polycrystalline isotropic materials can be characterized by only two independent elastic constants. Hence, identification of any new relationship between the two independent elastic constants for isotropic solid materials would reduce the number of required independent elastic constants to one. A number of researchers have given the empirical relationships to relate shear modulus (G), Young's modulus (E) and bulk modulus (B) for various elements. The correlation of E and G shows a linear behaviour with deviation for the elements having higher elastic moduli. Higher moduli elements always show higher values of G as compared to that predicted by the correlation. From the basic elastic constant interrelationships, it can be deduced that the higher values of G indicates that is lower for elements having higher elastic moduli. In this direction, an attempt has been made to study the variation of Poisson's ratio with other elastic constants using the experiment data generated by the authors and also that collected from the literature for various isotropic solid materials, such as pure elements, ceramics, polymers and intermetallics. The analysis revealed that Poisson's ratio decreases with increase in other elastic constants. A linear correlation has been obtained between Poisson's ratio and ultrasonic shear wave velocity with almost constant slope for any given alloy system with different microstructures associated with various heat treatments, alloying elements, grain size, temperature effect etc. This observation brings out the possibility for rationalization of elastic constants at least for a group of alloy systems with different microstructural conditions. It has also been shown mathematically using the basic relationships among the elastic constants that the decrease in the Poisson's ratio with the shear wave velocity indicates that the shear wave velocity is affected more than ultrasonic longitudinal wave velocity for any change in the material condition. As the shear wave velocity is affected more and the error in the measurement is also less (due to larger time of flight for the same thickness), it is also deduced that shear wave velocity is a better parameter for material/microstructural characterization as compared to longitudinal wave velocity.

# Hume Rothery Symposium: Structure and Diffusional Growth Mechanisms of Irrational Interphase Boundaries: Session II

Sponsored by: Electronic, Magnetic & Photonic Materials Division, Structural Materials Division, EMPMD/SMD-Alloy Phases Committee, MPMD-Phase Transformation Committee-(Jt. ASM-MSCTS)

*Program Organizer:* H. I. Aaronson, Carnegie Mellon University, Department of Materials Science and Engineering, Pittsburgh, PA 15213 USA

Monday PM	Room: 208A
March 15, 2004	Location: Charlotte Convention Center

Session Chair: J.-F. Nie, Monash University, Sch. of Physics & Matls. Engrg., Victoria 3800 Australia

# 2:00 PM Invited

**Edge-to-Edge Matching - The Fundamentals**: *Patrick Manning Kelly*<sup>1</sup>; Ming-Xing Zhang<sup>1</sup>; <sup>1</sup>University of Queensland, Div. of Matls., Sch. of Engrg., Brisbane, Queensland 4072 Australia

The basis of the present authors' 'edge-to-edge matching' model for understanding the crystallography of partially coherent precipitates is the minimisation of the energy of the interface between the two phases. For relatively simple crystal structures this energy minimisation occurs when close-packed, or relatively close-packed, rows of atoms match across the interface. Hence, the fundamental principle behind 'edge-to-edge matching' is that the directions in each phase that correspond to the 'edges' of the planes that meet in the interface should be close-packed, or relatively close-packed, rows of atoms. A few of the recently reported applications of 'edge-to-edge matching' appear to ignore this fundamental principle. By comparing theoretical predictions with experimental data, the paper will explore the validity of this critical atom row coincidence condition, in situations where the two phases have relatively simple crystal structures and in those where the precipitate has a more complex structure.

#### 2:40 PM Invited

An Energy Minimization Principle Applied to Irrational Interphase Boundaries: Jan H. van der Merwe<sup>1</sup>; *Max W.H. Braun*<sup>2</sup>; Gary J. Shiflet<sup>3</sup>; <sup>1</sup>University of South Africa, Physics Dept., Pretoria S. Africa; <sup>2</sup>University of Pretoria, Physics Dept., Pretoria S. Africa; <sup>3</sup>University of Virginia, Matls. Sci. & Engrg., Charlottesville, VA 22904-4745 USA

Interphase boundaries with irrational habit planes and orientational relationships between phases are thought to be of high mobility most notably in the massive, pearlite and cellular solid-state phase transformations. Growing crystalline phases are often enclosed by facets which have been reported to show periodic interfacial fine structure. This suggests that the boundary formation is orientationally driven by minimization of interfacial energies. An analytical formulation of interfacial energies is constructed and relevant parameters are quantified to assess their impact on boundary formation. It is shown that energy minimization is accomplished by edge-to-edge matching of close packed (CP) or near CP atomic planes in accordance with a row-matching principle.

#### 3:20 PM Invited

Irrational Interface Structures and Orientation Relationships of Precipitates in a Duplex Stainless Steel: *Robert C. Pond*<sup>1</sup>; Huisheng Jiao<sup>2</sup>; Mark Aindow<sup>3</sup>; <sup>1</sup>University of Liverpool, Engrg. (Matls. Sci. & Engrg.), Liverpool, Merseyside L69 3BX UK; <sup>2</sup>University of Birmingham, Sch. of Metall. & Matls., Birmingham B15 2TT UK; <sup>3</sup>University of Connecticut, Metall. & Matls. Engrg., Storrs, CT 06269-3136 USA

Precipitation in a commercial duplex stainless steel, Zeron-100, has been investigated using electron microscopy. Acicular fcc precipitates of Ni-rich gamma phase formed in the Cr-rich alpha matrix by suitable heat treatment. The orientation relationships between a large number of particles and the matrix were distributed in a range between the Kurdjumov-Sachs and Pitsch relationships. Two irrational facets bounded each particle, and it was deduced that their structures were based on distinct reference structures with different orientation relationships between the precipitate and matrix. This orientational incompatibility,  $5.76^{\circ}$  about [~1-11]a/[~101]g, was accommodated by networks of crystal dislocations superimposed on the facets. These acted as tilt walls, but, although their combined angular tilt was always

observed to equal about  $5.7^\circ$ , this was not partitioned in a unique manner between the two facets. Such differential partitioning offers a natural explanation for the observed variation in particle orientation.

# 4:00 PM Break

## 4:20 PM Invited

Orientation Relationships Associated with Austenite Formation from Ferrite in a Coarse Grained Duplex Stainless Steel: *E. F. Monlevade*<sup>1</sup>; I.G.S. Falleiros<sup>2</sup>; <sup>1</sup>Nokia Institute of Technology, Rodovia Torquato Tapajós, 7200, Km 12 Tarumã, 69048-660 - Manaus, AM Brazil; <sup>2</sup>Escola Politécnica de Universidade de São Paulo, Dept. Engrg. Metalúrgica e de Materiais, Av. Prof. Mello Moraes 2462, Sao Paulo, SP 05508-900 Brazil

Studies on the morphology and crystallography of austenite precipitated from ferrite were performed in an Fe-22.5% Cr- 4.7%Ni - 3% Mo- duplex stainless steel. Samples were solution treated at 1325°C (yielding a grain size of ca. 2 mm), water quenched and then aged at temperatures ranging from 700 to 1100°C for times ranging from 5000 to 20000 secs. The morphology of grain boundary precipitates depends on the grain boundary segment at which the precipitates are formed, and may be adequately described by the Dubé classification system. Orientation relationships between austenite and the ferritic matrix were determined with EBSD analysis, employing graphic and algebraic methods. Grain boundary precipitates exhibited Kurdjumov-Sachs or Nishyiama-Wassermann O-Rs with at least one of the adjacent grains, and in some cases relationships intermediate between K-S and N-W appeared. In approximately 60% of the cases examined, grain boundary precipitates show a K-S and/or a N-W orientation relationships with both grains forming a boundary, though with small deviations (up to 5°) from the exact relationships.

#### 5:00 PM Invited

Morphology and Interfacial Structure of Mg<sub>17</sub>Al<sub>12</sub> Precipitates in Mg-Al Alloys: *Jian-Feng Nie*<sup>1</sup>; <sup>1</sup>Monash University, Sch. of Physics & Matls. Engrg., Victoria 3800 Australia

The precipitation process in Mg-Al alloys, during isothermal ageing at 200°C, involves solely the formation of the equilibrium precipitate phase Mg<sub>17</sub>Al<sub>12</sub> (body-centred cubic). In the present study, the morphology and the interfacial structure of Mg<sub>17</sub>Al<sub>12</sub> precipitates have been characterised in detail using high-resolution transmission electron microscopy and electron diffraction. Our observations indicate that most Mg<sub>17</sub>Al<sub>12</sub> precipitates have an irrational orientation relationship that approximates to the Burgers relationship, and a faceted lath morphology with habit plane parallel to  $(0001)_{\alpha}$ . The crosssection of the lath, viewed along the direction normal to the habit plane, has a shape of parallelogram. Both the major and the minor facets of this parallelogram are irrational with respect to both phases but are parallel to Moire planes. These experimental observations will be analysed using the Moire plane model that has recently been developed for accounting for the crystallography and migration mechanisms of irrationally-oriented, planar interphase boundaries.

# Internal Stresses and Thermo-Mechanical Behavior in Multi-Component Materials Systems: Electronic Thin Films and Packagaing Materials II

Sponsored by: Electronic, Magnetic & Photonic Materials Division, Structural Materials Division, EMPMD-Electronic Packaging and Interconnection Materials Committee, EMPMD-Thin Films & Interfaces Committee, SMD-Composite Materials Committee-Jt. ASM-MSCTS

*Program Organizers:* Indranath Dutta, Naval Postgraduate School, Department of Mechanical Engineering, Monterey, CA 93943 USA; Bhaskar S. Majumdar, New Mexico Tech, Department of Materials Science and Engineering, Socorro, NM 87801 USA; Mark A.M. Bourke, Los Alamos National Laboratory, Neutron Science Center, Los Alamos, NM 87545 USA; Darrel R. Frear, Motorola, Tempe, AZ 85284 USA; John E. Sanchez, Advanced Micro Devices, Sunnyvale, CA 94088 USA

Monday PM	Room: 20	09B
March 15, 2004	Location:	Charlotte Convention Center

*Session Chairs:* Darrel R. Frear, Motorola, Final Mfg. Tech. Ctr., Tempe, AZ 85284 USA; Indranath Dutta, Naval Postgraduate School, Monterey, CA 93943 USA

# 2:00 PM Invited

Mechanical and Fracture Behavior of Thin-Film Structures for Device Technologies: *Reinhold H. Dauskardt*<sup>1</sup>; <sup>1</sup>Stanford University, Dept. of Matls. Sci. & Engrg., Stanford, CA 94305-2205 USA

The mechanical and fracture properties of thin-film structures for device technologies will be examined. Adhesion and time- or loadingcycle dependent delamination of interfaces that effect mechanical integrity particularly during processing and device packaging are well known. Significant challenges evident for the reliability of emerging device technologies involve the introduction of new materials and the effect of decreasing length scales. Materials are nearly always optimized for other desired properties (e.g. dielectric properties or barrier diffusion resistance) and the resulting deleterious effect on mechanical performance can be significant. Decreasing length scales in device structures frequently result in high stress gradients and mechanical properties that differ significantly from the bulk. The effects of salient interface parameters and thin-film composition will be considered. In the case of highly porous films produced through nanotemplating processes, it will be demonstrated that remarkable increases in fracture resistance can be obtained. These are described in terms of molecular byproducts of the pore-creating process itself, specifically, porogen residual provide molecular bridging mechanisms to markedly effect fracture resistance. Multi-scale models are developed to explain the effect of a range of interface and adjacent layer properties on debonding behavior. These include interface morphology and chemistry, ductile metal or dielectric layer thickness, elastic properties and thickness of the barrier layer, and loading mode. Finally, the effect of more complex patterned thin-film structures are examined where length scales are restricted in more than one dimension.

# 2:25 PM Invited

Linking Dislocation-Based Plasticity to the Thermomechanical Behavior of Thin Films: T. John Balk<sup>1</sup>; Linda Sauter<sup>1</sup>; Tobias Schmidt<sup>1</sup>; Gerhard Dehm<sup>1</sup>; Eduard Arzt<sup>1</sup>; <sup>1</sup>Max-Planck-Institut für Metallforschung, Heisenbergstr. 3, 70569 Stuttgart Germany

The geometry and interface chemistry of metal thin films govern dislocation mechanisms and the resulting stress state. This talk will relate in-situ transmission electron microscope observations of dislocation motion to thermomechanical measurements of Cu and Au films. In addition, the effect of interlayer materials (Ta, Ag, Ti) on the plasticity of Cu thin films will be discussed. In unpassivated Cu films 270 nm or thinner, dislocations glide parallel to and very near the film/substrate interface, even though no resolved shear stress should exist on such glide planes. In thicker Cu films, threading dislocations move on inclined planes and deposit interfacial segments that disappear at elevated temperatures. However, a Ta interlayer stabilizes them, even at 500°C. During thermal cycling, significantly higher stresses evolve in Cu films on Ta than in Cu on silicon nitride. Other connections between dislocations and the thermomechanical behavior of metal thin films will also be drawn.

# 2:50 PM

Effect of Internal Stresses on Thermo-Mechanical Stability of Back-End Interconnect Structures in Microelectronic Devices:

*Indranath Dutta*<sup>1</sup>; Deng Pan<sup>1</sup>; Robert A. Marks<sup>1</sup>; Chanman Park<sup>1</sup>; Joseph B. Vella<sup>2</sup>; <sup>1</sup>Naval Postgraduate School, Ctr. for Matls. Sci. & Engrg., Monterey, CA 93943 USA; <sup>2</sup>Motorola, Proc. Matls. Characterization Lab., Tempe, AZ 85284 USA

Interconnect structures at the back-end of microelectronic devices can undergo significant deformation due to internal stresses which are thermo-mechanically induced during processing, or during service as part of a microelectronic package. These effects can have a pronounced effect on component reliability. Here, we present results of atomic force microscopy (AFM) studies on Cu-low K dielectric (LKD) back-end interconnect structures (BEIS) to demonstrate these effects, which include creep/plasticity of interconnect lines, and diffusionally accommodated sliding at Cu-LKD interfaces. These effects may result in in-plane (IP) changes in Cu line dimensions, cause strain incompatibilities between Cu and LKD in the out-of-plane (OOP) direction, and cause Cu lines to migrate or crawl under far-field shear stresses imposed by the package. We then present a shear-lag based approach, which incorporates a constitutive interfacial sliding law developed by us previously, to model Cu line deformation and interfacial sliding during back-end processing as well as during service after the chip is packaged.

# 3:15 PM Invited

Intrinsic Stresses and Microstructural Stability of Multilayered Structures at Elevated Temperatures: *Daniel Josell*<sup>1</sup>; <sup>1</sup>NIST, Metall. Div., MS 8555, 100 Burea Dr., Gaithersburg, MD 20878 USA

I will discuss the origins of equilibrium stresses and strains in fine multilayered materials when they are brought to elevated temperatures, including discussions of both interface stresses and interface free energies. This will lead directly into discussion of the capillary forces that destabilize polycrystalline multilayered structures. The discussions will include descriptions of the types of experiments used to quantify the underlying interfacial thermodynamic quantities as well as quantitative analysis and application to several experimental systems.

#### 3:40 PM Invited

The Effect of Thermal and Mechanical Load History on the Damage Accumulation During TMF in Dual Shear Specimens: *Thomas R. Bieler*<sup>1</sup>; A. U. Telang<sup>1</sup>; <sup>1</sup>Michigan State University, Chem. Engrg. & Matl. Sci., 2527 Engrg. Bldg., E. Lansing, MI 48824 USA

The intrinsic anisotropy of tin can play a significant role in the damage accumulation in an unloaded single shear lap solder joint, as seen in prior studies. To investigate the effect of external loads arising from differential thermal expansion between a substrate and a surface mount component, specimens with a nickel simulated surface mount component on a copper substrate having a 1 mm<sup>2</sup> joint area and solder thickness of about 100µ were prepared to induce extrinsic shear in joints undergoing TMF cycling. In one specimen, the joints were not connected at the substrate during solidification and cool down to room temperature, so they were not stressed. In the other specimen, a continuous copper substrate caused these joints to be strained such that the component was put in compression during cool down. Then they were cycled at -15°C for 3.5 hr, followed by 20 minutes at 150°C. The first specimen was clamped to a copper block to cause a significant reversal in sign of the shear imposed on the solder joint. In the second specimen, the existing compressive strain in the component at room temperature was further increased with cooling, but it was nearly unstressed at 150°C. It is expected that more damage would develop in the second specimen, due to a larger imposed shear at -15°C. The effect of these two strain histories on evolution of surface damage and microstructure will be compared using SEM and Orientation Imaging Microscopy.

# 4:05 PM Invited

A Combined Experimental and Analytical Approach for Interface Fracture Parameters Between Dissimilar Materials in Electronic Packages: N. R. Kay<sup>1</sup>; S. Ghosh<sup>1</sup>; I. Guven<sup>1</sup>; *E. Madenci*<sup>1</sup>; <sup>1</sup>The University of Arizona, Aeros. & Mech. Engrg., Tucson, AZ 85721-0119 USA

This study concerns the development of a combined experimental and analytical technique to determine the critical values of fracture parameters for interfaces between dissimilar materials in electronic packages. Failure of materials and interfaces are commonly linked to the fracture parameters such as the stress intensity factors and the energy release rate. However, there exists no experimental procedure for the direct measurement of these fracture parameters. This paper reports on the development of a new technique to obtain these parameters by testing specimens created from post-production electronic packages. The results from the experimental testing are then used as the input for an analytical model, which returns the desired parameters. Multiple techniques were developed for the preparation of test specimens from electronic packages. These methods involve different procedures of encapsulation for sectioning and techniques for the introduction of the crack to the interface. Another contribution from this work is the development of an analytical model to accurately model the region near the junction of two dissimilar materials (elastic or viscoelastic). The mean value of the interfacial strength compares favorably to published results.

# 4:30 PM

Validation of Residual Stresses Encountered in Brazed Metal/ Ceramic Joints: John J. Stephens<sup>1</sup>; Steven N. Burchett<sup>1</sup>; Michael K. Neilsen<sup>1</sup>; Charles A. Walker<sup>1</sup>; Evan Dudley<sup>1</sup>; Gerald Stoker<sup>1</sup>; <sup>1</sup>Sandia National Laboratories, Dept. 1833, PO Box 5800, MS0889, Albuquerque, NM 87185-0889 USA

This talk describes an ASCII/MAVEN project at SNL/NM aimed at validating the creep/plasticity constitutive models currently used for prediction of residual stresses in metal/ceramic braze joints. The test vehicle represents a generic Kovar/alumina ceramic braze joint, which uses a geometry that is amenable to measuring the displacement of the Kovar flange thru a furnace viewport during the braze thermal process cycle. The braze filler metal of interest is the 98Ag-2Zr active braze alloy, and we will present the results of uniaxial compression creep and stress-strain tests used to develop the creep-plasticity correlation used for the validation calculations. We will also discuss the special surface requirements needed to maximize the displacement signal output during the cooldown from the braze process cycle to room temperature. The effect of furnace cooldown rate on minimizing residual stresses in the ceramic will also be discussed. This work was conducted at Sandia National Laboratories, a multiprogram laboratory operated by Sandia Corporation, a Lockheed Martin Company, for the United States Department of Energy's National Nuclear Security Administration under Contract DE-AC04-94AL85000.

# International Laterite Nickel Symposium - 2004: Mineralogy and Geometallurgy

Sponsored by: Extraction & Processing Division, EPD-Aqueous Processing Committee, EPD-Copper, Nickel, Cobalt Committee, EPD-Process Fundamentals Committee, EPD-Process Mineralogy Committee, EPD-Pyrometallurgy Committee, EPD-Waste Treatment & Minimization Committee

*Program Organizer:* William P. Imrie, Bechtel Corporation, Mining and Metals, Englewood, CO 80111 USA

Monday PM	Room: 217B/C
March 15, 2004	Location: Charlotte Convention Center

Session Chairs: Vanessa de Macedo Torres, Companhia Vale do Rio Doce, Base Metals Projects Dept., Santa Luzia, MG 33030-970 Brazil; Robert C. Osborne, Inco Technical Services, Mississauga, Ontario L5K 1Z9 Canada

#### 2:00 PM

Mineralogical Characterization of Nickel Laterites from New Caledonia and Indonesia: *Tzong T. Chen*<sup>1</sup>; John E. Dutrizac<sup>1</sup>; Eberhard Krause<sup>2</sup>; R. C. Osborne<sup>2</sup>; <sup>1</sup>CANMET, 555 Booth St., Ottawa, Ontario K1A 0G1 Canada; <sup>2</sup>Inco Technical Services Ltd., 2060 Flavelle Blvd., Mississauga, Ontario L5K 1Z9 Canada

This mineralogical study is based on samples from typical "wet" nickel laterites of humid rain forests. An in-situ nickel laterite sample from Goro and a transported laterite sample from Plaine des Lacs, New Caledonia, are predominantly limonitic. Two-thirds of the particles in the Goro sample are <10 µm in size; they consist of skeletal goethite and serpentine, as well as minor amounts of talc, gibbsite, chlorite, quartz and clay minerals. The coarser grains are mainly Cr-spinel, serpentine, gibbsite and Mn oxide. Nickel occurs mainly in goethite, serpentine and Mn oxide; cobalt occurs in goethite and Mn oxide. The Plaine des Lacs sample is finer-grained and contains more Al and CO3, but less Mg and Si than the Goro material. The sample contains more kaolinite, chlorite, siderite and feldspar, but less serpentine and gibbsite than the Goro material. Nickel is detected mainly in goethite, serpentine, Fe-Mg silicate and Fe-Mn oxide. The Indonesian ore from Sorowako, as sampled from the reduction kiln feed containing some reverts, is predominantly saprolitic, with apparent particle sizes ranging from <100 µm to >1 cm. The sample of reduction kiln feed is rich in Mg silicates, Mg-Fe silicates and goethite, and exhibits complex alteration textures. The nickel contents vary from particle to particle. Nickel is present mainly in serpentine, olivine, chlorite and amphibole, and in subordinate amounts in goethite and Mn oxide. Cobalt is detected in the Mn oxide.

#### 2:25 PM

Vermelho Nickel Laterite - Geological Modelling and Resource Estimation Developments: *Marcio B. Fonseca*<sup>1</sup>; Divino Fernando R. Fleury<sup>1</sup>; Walter Riehl<sup>1</sup>; Marcos Aurélio A. Ferreira<sup>1</sup>; Márcio Roberto S. Rocha<sup>1</sup>; Marcelo A.C. Albuquerque<sup>1</sup>; <sup>1</sup>Companhia Vale do Rio Doce, Mineral Dvlp. Dept., BR 262 - Km 296, Santa Luzia, MG 33030-970 Brazil

Nickel-cobalt laterite deposits have become the focus of attention for hydrometallurgical processing. Following the lessons of the second generation high pressure acid leach (HPAL) projects in Western Australia other Ni-Co laterite projects are now evaluating potential HPAL projects with a rigorous integrated approach that begins with geological modeling, resource estimation and metallurgical studies. The Vermelho nickel-cobalt laterite deposit has been under exploration and study for several years with investigations of various metallurgical processes. Recent HPAL studies have indicated that the nickel and cobalt laterite at this deposit is amenable to upgrading by silica rejection followed by pressure leaching. These studies have required a detailed geological investigation to generate a new resource model. The recent development of a sophisticated geological model integrated with a multi-element resource estimation for this complex tropical nickel laterite deposit in northern Brazil provides an example of the contribution of geology at the critical project stage where process technology decisions are made on relatively small samples of the total resource.

#### 2:50 PM

**Ore Variability Influence on the Metallurgical Process**: *Nolberto Moreno Borjas*<sup>1</sup>; <sup>1</sup>Grupo Empresarial del Niquel, Punta Gorda, Carretera Moa – Baracoa km 5, CP83330, Moa, Holguín Cuba

This paper outlines the detrimental impact that unblended ore can have on the Ni and Co recoveries and the ore slurry density with real data from the Caron low-pressure ammonia leaching process for the Punta Gorda ore. The author briefly discusses the reason for the decrease in slurry density that the process experiences. The lower metal recoveries in the process that are caused by the unblended ore chemical characteristics and variations are shown with a data base statistical analysis drawn from the results obtained from a pilot test, designed with different ore bypassed from the normal process flow and a similar ore from a similar metallurgical treatment.

# 3:15 PM Break

#### 3:25 PM

Ravensthorpe Nickel Project Beneficiation Prediction MLR and Interpretation of Results: *Geoffrey W. Miller*<sup>1</sup>; Darryl Sampson<sup>1</sup>; John Fleay<sup>2</sup>; Jerome Conway-Mortimer<sup>3</sup>; <sup>1</sup>Ravensthorpe Nickel Operations Pty Ltd, Tech., PO Box 7763, Cloisters Sq., Perth, Western Australia Australia; <sup>2</sup>Hatch Minproc Ravensthorpe Joint Venture, 144 Stirling St., Perth, Western Australia 6805 Australia; <sup>3</sup>Geostats, 68 Watkins St., White Gum Valley, Western Australia 6162 Australia

The Ravensthorpe Nickel Project (RNP) flow sheet provides for the upgrading of Ni & Co in a size based beneficiation process prior to leaching. The upgrading effect on Ni and Co makes the beneficiation process a powerful addition to the flow sheet. Multiple linear regression (MLR) analysis based on 351 individual batch tests, 52 large scale composites and 21 pilot plant tests has been used to successfully model beneficiation product grade, recovery, upgrade and mass recovery. Statistically, 83% and 96% of the variability in nickel recovery and nickel product grade respectively was accounted for. Algorithms have been developed for Ni, Co, Mg, Al and Fe, which represents the revenue and operating cost factors for the process. The algorithms have subsequently been applied to the resource model, allowing prediction of elemental grade and recovery for the development of the mine schedules based upon these parameters and not head grades alone. This has allowed optimisation of the mine schedule for improvement to the project's NPV.

#### 3:50 PM

Sechol Nickel - Cobalt Lateritic Project. A Major New Nickel Cobalt Province in Guatemala: *Ricardo A. Valls*<sup>1</sup>; T. John Magee<sup>1</sup>; Bryn Harris<sup>1</sup>; <sup>1</sup>Jaguar Nickel Inc., Exploration, 55 Univ. Ave., Ste. 910, Toronto, Ontario M5J 2H7 Canada

The Sechol Project is located in east-central Guatemala, 140 km northeast from Guatemala City. In situ resources in the immediate area contain 133 million tonnes of mineralization, grading 1.51% nickel. The deposit is conformed of several large lateritic pockets, delimited by tectonic faults and hosted by ultramafic rocks from an ophiolitic complex that intruded a continental plate during the Early Cenozoic Era. Metal recovery from the deposit will be based on a recently patented atmospheric chloride process, followed by solution purification, production of an intermediate nickel/cobalt hydroxide, and fi-

MONDAY PM

nally acid and magnesia recovery by standard spray roasting technology. The AAL process will allow the exploitation of the whole lateritic profile to produce 20,000 Mt of nickel hydroxide and 800 Mt of cobalt hydroxide per year. The laterite potential of the Izabal Ultramafic Intrusive in particular and of the Guatemalan Ophiolitic Belt in general has not been completely explored.

# International Laterite Nickel Symposium - 2004: Panel Discussion

Sponsored by: Extraction & Processing Division, EPD-Copper, Nickel, Cobalt Committee Program Organizer: William P. Imrie, Bechtel Corporation,

Mining and Metals, Englewood, CO 80111 USA

Monday PM	Room: 217B/C	
March 15, 2004	Location: Charlotte Convention Ce	nter

Session Chairs: Bruce McKean, Director, Environmental Affairs, Nickel Development Institute, Toronto M5J 2H7, Canada

# From Feasibility to Sustainability - Questions Society Will Ask Lateritic Nickel Producers

An open forum on the questions other stakeholders – governments, environmentalists, communities, shareholders – will be asking lateritic nickel producers about their processes, their products and their impacts on the environment and on society. Four presenters will offer high-level views on how nickel production from laterites and the value-chain of nickel can be seen from the optic of sustainability. Short presentations followed by discussion by all attendees.

# 4:30 PM Introduction

#### 4:35 PM

Sustainability Looks at Nickel – The Criteria by Which Lateritic Nickel Will Be Judged: Bruce McKean<sup>1</sup>; <sup>1</sup>Director, Environmental Affairs, Nickel Development Institute, Toronto M5J 2H7, Canada

The environmental drivers are introduced: future generations (availability, recyclability, recycling), impacts (on nature, human health, human society). The reputation-based environmental perceptions are introduced: reputation of nickel, of nickel producers, of the mining industry. Collectively these add up to attributes that will affect how nickel from laterites is viewed: a contributor or a hindrance to the achievement of sustainability.

# 4:55 PM

The Nickel Value Chain - Linking to the Sustainability Drivers: Steve C.C. Barnett<sup>1</sup>; <sup>1</sup>VP HSEC Stainless Steel Materials, BHP Billiton, London, UK

The nickel industry is looking downstream – currently just at the European Union but eventually the entire OECD – to learn more about how the nickel flows and how the nickel is used. Comments will be made on two basic observations: nickel adds a great deal of value along the way – including employment and tax revenues – but nickel is also a major component in the environmental burdens associated with nickel's main customer: stainless steel.

#### 5:05 PM

Can There Be Sustainability Without Profitability? - The Economics of Nickel Laterites: Ashok D. Dalvi<sup>1</sup>; <sup>1</sup>Director, Process Engineering and Strategic Studies, Inco Limited, Mississauga, Ontario, L6M 1V1, Canada

Laterites, representing 70% of the nickel resource base, contribute only 40% of nickel production. That will need to change if future nickel supply is going to be assured. But the environmental and sustainability yardsticks being applied to greenfield developments come at a price, a price that cannot be paid at historic price levels. "Sustainability" for the nickel industry will be based on appropriate technical choices but will also require a change in what society has been used to be paying for nickel.

# 5:15 PM

Sustainability and Closure - Policies and Practices for Operators: Denis J. Kemp<sup>1</sup>; <sup>1</sup>Director, Environmental Development, Noranda Inc.-Falconbridge Limited, Toronto, Ontario M5J 1A7, Canada

Operators properly focus on everything that will allow an operating permit to be granted and that will also reassure communities of interest that their concerns and issues are being considered. Considerations of sustainability, however, keep stretching the boundaries of what influences permitting. An issue faced by mining operations – laterites are no exception – is the question of "what happens when the mine closes?" Who is responsible for the "sustainability" of resource-dependent communities that grow up around the mines?

5:25 PM Open Discussion

# Lead-Free Solders and Processing Issues Relevant to Microelectronic Packaging: Environmental and Materials Issues for Lead-Free

*Sponsored by:* Electronic, Magnetic & Photonic Materials Division, EMPMD-Electronic Packaging and Interconnection Materials Committee

Program Organizers: Laura J. Turbini, University of Toronto, Center for Microelectronic Assembly & Packaging, Toronto, ON M5S 3E4 Canada; Srinivas Chada, Jabil Circuit, Inc., FAR Lab/ Advanced Manufacturing Technology, St. Petersburg, FL 33716 USA; Sung K. Kang, IBM, T. J. Watson Research Center, Yorktown Heights, NY 10598 USA; Kwang-Lung Lin, National Cheng Kung University, Department of Materials Science and Engineering, Tainan 70101 Taiwan; Michael R. Notis, Lehigh University, Department of Materials Science and Engineering, Bethlehem, PA 18015 USA; Jin Yu, Korea Advanced Institute of Science and Technology, Center for Electronic Packaging Materials, Department of Materials Science & Engineering, Daejeon 305-701 Korea

Monday PM	Room: 219B
March 15, 2004	Location: Charlotte Convention Center

Session Chairs: Srinivas Chada, Jabil Circuit Inc., FAR Lab/Advd. Mfg. Tech., St. Petersburg, FL 33716 USA; King-Ning Tu, University of California, Matls. Sci. & Engrg., Los Angeles, CA 90095 USA

# 2:00 PM Invited

COST 531 - A European Action on Lead-Free Soldering: Herbert Ipser<sup>1</sup>; <sup>1</sup>University of Vienna, Inst. f. Anorganische Chemie, Waehringerstr. 42, Wien A-1090 Austria

A European Research Action on lead-free soldering has been initiated in 2002. Its goal is the establishment of a database that contains the relevant knowledge on possible lead-free solder materials and to provide the expertise for selecting particular materials for specific soldering purposes. By July 2003, 19 European countries have signed the corresponding Memorandum of Understanding, in addition, one Canadian research organization has been accepted as non-European partner. The Action is structured into four Working Groups: WG1 is responsible for experimental data on phase equilibria and thermochemical properties of possible lead-free solder materials and systems of relevance for joints with various substrates. WG2 carries out the theoretical modeling of the corresponding phase diagrams. WG3/4 investigates physical and chemical properties of candidate alloys, and WG5/6 is responsible for reliability as well as for processing and packaging issues. Currently nine Group Projects are active involving scientists from 38 participating research institutions in 15 European countries.

# 2:25 PM

V-Grooved Optical Fiber Array Packaged by Lead-Free Solder: Shengquan Ou<sup>1</sup>; Gu Xu<sup>1</sup>; Yuhuan Xu<sup>1</sup>; King-Ning Tu<sup>1</sup>; <sup>1</sup>University of California, Matls. Sci. & Engrg., 405 Hilgard Ave., Los Angeles, CA 90095 USA

Etched V-grooves along the [110] direction on (001) surface of Si wafers have been used in high precision alignment between fibers in opto-electronic devices. Nevertheless, bonding the fibers to the chips has been a challenging issue. Currently, the positioning of fibers using epoxy-bonding lacks precision as well as long-term stability. We proposed and conducted the novel technology of using metallic solder packaging instead of the organic epoxy-bonding. The study is of scientific significance because of the fact that solder does not wet SiO2 surface. To circumvent this problem, electron beam evaporation is used to deposit the multi-layered metallic coatings on the surfaces of fibers and V-grooved chips. Three types of multi-layered metallic film coatings were adopted, and they are Ti/Au, Ti/Cu/Au, and Ti/Ni/Au. The metallic film coating on the fiber from infrared noise interference. We utilized a low melting point Pb-free solder - eutectic 43Sn57Bi (in wt. %) with a

melting point of 139°C to bond the array of fibers to V-grooved chips. The mechanical and optical tests illustrated that we can realize the precise alignment of fibers by the soldering method and the bonding structure is strong at room temperature. The metallic solder bonding can be hermetic and it can isolate the optical device from ambient environment.

# 2:45 PM

#### Nanoindentation Investigation of Au-Sn Solder for Optoelectronic Applications: *Richard R. Chromik*<sup>1</sup>; Laura Limata<sup>1</sup>; Dongning Wang<sup>1</sup>; Richard P. Vinci<sup>1</sup>; Michael R. Notis<sup>1</sup>; <sup>1</sup>Lehigh University, Dept. of Matls. Sci. & Engrg., 5 E. Packer Ave., Bethlehem, PA 18015 USA

The optoelectronics industry requires solder alloys with enhanced creep resistance and long term reliability. One such candidate is eutectic Au-Sn solder. To address reliability concerns, nanoindentation has been used to characterize the mechanical properties of intermetallic phases in this system. By solid state annealing of diffusion couples, continuous layers of intermetallics are formed that provide both reliable test volumes for nanoindentation and relevant length scales to real solder joints. Both the elastic modulus and hardness are measured for Au-Sn intermetallics with results compared to previous measurements in the Cu-Sn and Ag-Sn systems. Nanoindentation creep measurements are also underway to examine the effect of time and temperature on deformation within the solder matrix.

#### 3:05 PM

Assembly and Reliability of Isotropic Conductive Adhesives for Fine Pitch Flip-Chip Applications: Stoyan Stoyanov<sup>1</sup>; Chris Bailey<sup>1</sup>; Robert Kay<sup>3</sup>; Rajkumar Durairaj<sup>2</sup>; Mike Hendriksen<sup>4</sup>; Marc Desmuilliez<sup>3</sup>; Ndy Ekere<sup>2</sup>; <sup>1</sup>University of Greenwich, Computing & Math. Scis., Greenwich Maritime Campus, Park Row, Greenwich, London SE10 9LS UK; <sup>2</sup>University of Greenwich, Sch. of Engrg., Chatham Maritime, Chatham, Kent ME4 4TB UK; <sup>3</sup>Heriot Watt University, Microsys. Engrg. Ctr., Edinburgh Scotland; <sup>4</sup>Celestica Limited, West Ave., Kidsgrove, Stoke on Trent, Staffordshire UK

Isotropic conductive adhesives (ICAs) are suitable for low temperature assembly, and have the added advantage that they are also an alternative to lead-free solders. This paper will present results from a highly interdisciplinary project into the formation and subsequent reliability of ICAs interconnects or flip-chip assembly at very fine pitch. Experimental results will be discussed that detail the performance of novel stencils and how, together with the rheology of a particular ICA, these impact the printing behaviour at these fine dimensions. Reliability modelling will also be discussed. These models, based on finite element analysis, provide predictions of stress due to the thermal mismatch in the materials (i.e. silicon chip, polymer underfill, ICA, organic substrate, etc). Results from these models coupled with optimisation analysis have helped identify process conditions that lead to longer joint life.

#### 3:25 PM

A Study of On-Board Reliability for BT Substrate Base Green CSP (Chip Scale Package): Chung Cho Liang<sup>1</sup>; T. B. Lu<sup>2</sup>; <sup>1</sup>I-SHOU University, Matls. Sci. & Engrg. Dept., #1, Sect. 1, hsueh-cheng Rd., ta-hsu hsiang, Kaohsiung 84008 Taiwan

In this paper, the study on the on-board reliability relationship between green assembly material characteristic and reliability failure mechanism in both 63Sn/37Pb and lead-free solder were reported. The failure criterion is base on the temperature cycle test (TCT). Besides, the paper discusses the influences of IR-reflow profile parameters and how it affects the solder material properties. For instance, package block warpage induced by halogen-free compounds and transition point of flux decompose rate effects on the result of on-board reliability. The thermal decomposing behavior of the lead-free type fluxes were analyzed by differential scanning calorimetry (DSC) and thermo gravimetric analysis (TGA). Combined with the relative X-ray inspection was show in Figure 1. Examining the above results, they were the important references for the lead-free IR-reflow profile design to avoid voids forming and improve TCT reliability. On-board reliability specimens were sectioned and analyzed by scanning electron microscope (SEM) and X-ray. The evolution of package warpage of two kind halogen-free compounds, during IR-reflow process, were monitored by special designed thermal mechanic analysis (TMA) experiments. The stress distribution of solder joins within the on-board samples was examined during TCT reliability. Results shown that poor IR-reflow profile design induced voids forming within solder joins and halogenfree compound with lower glass transition temperature reveal larger block warpage change during TCT, respectively. These conduct poor performances in TCT reliability test.

# 3:45 PM Break

#### 3:55 PM Invited

A Dynamic System Model to Assess the Environmental Impact of the Use of Lead Free Solder in Electronic Goods: Markus Andreas Reuter<sup>1</sup>; <sup>1</sup>Delft University of Technology, 120 Mijnbouwstraat, Delft The Netherlands

A dynamic model that interconnects more than ten metals will demonstrate the environmental impact of the use of lead free solder in electronic goods. Various case studies will show that care should be taken when banning metals, due to the complex inteconnected nature of the base metallurgical industry. This paper will clearly show that removing lead from the metal cycle could have severe consequences for the metallurgical ecosystem.

#### 4:20 PM

Effects of Load and Thermal Conditions on Lead Free Solder Joint Reliability: *Jin Liang*<sup>1</sup>; Dongkai Shangguan<sup>2</sup>; Stuart Downes<sup>1</sup>; <sup>1</sup>EMC Corp, 176 South St., Hopkinton, MA 01748 USA; <sup>2</sup>Flextronics, 2090 Fortune Dr., San Jose USA

Reliability of lead-free solder joints has been a hot topic widely debated in the electronic industry long before the European Union passed lead-free legislations. A recent survey conducted in Europe indicated that only 6% companies perceive the change to lead-free soldering from Sn-Pb eutectic solder is for technology benefit (none for process reasons). Those who think lead-free soldering has merits beyond environmental benefit also believe lead-free solder joints will be more reliable than the current Sn-Pb eutectic solder joints. Although some published data supports this claim, others also indicate otherwise. This created a state of confusion in the industry about the actual reliability of lead-free solder joints compared to joints produced with tin-lead eutectic solder. In reality, many mechanical, metallurgical and thermal factors affect the service reliability of solder joints. This paper tries to shed some light on the effects of mechanical loading and thermal conditions on solder joint reliability. These conditions are determined not only by external environments, but also by the solder alloy itself and its shape and geometry. Analyses both with first principles and finite element modeling are carried out on both areal array and peripheral packages, both leaded and lead-less joints and BGA solder balls. A general life assessment methodology is presented by taking into consideration solder joint geometry, thermal and mechanical characteristics of components and substrate materials, as well as application conditions. The theory also helps explain why lead-free solder joints may not be more reliable in certain application conditions as expected.

# 4:40 PM

Ethyl Alcohol Based Flux for Sn-3 Ag-1 Zn Lead Free Solder: Shih-Chin Chang<sup>1</sup>; Hui-Sheng Chiang<sup>1</sup>; <sup>1</sup>National Tsing-Hua University, Dept. of Matls. Sci. & Engrg., HsinChu, Taiwan 30043 Taiwan

Ethyl alcohol based flux was applied for the soldering of Sn-3 Ag-1 Zn lead free solder and Fe-42 Ni alloy (alloy 42). Perfect bonding was observed by using different fluxes with a range of different concentrations. The fracture path in peel test was observed to propagate inside the solder material by a void formation and connection process.

# 5:00 PM

Effect of Corrosion on Physical and Mechanical Properties of SnZn and SnPb Solders and Joints: *Zhidong Xia*<sup>1</sup>; Yaowu Shi<sup>1</sup>; Yongping Lei<sup>1</sup>; <sup>1</sup>Beijing University of Technology, The Key Lab. of Advd. Functional Matls. Ministry of Educ., 100, Ping Leyuan, Chaoyang Dist., Beijing 100022 China

Electric conductivity and mechanical properties of SnZn-based, SnPb solders and their soldered joints were tested in tap water and in 3% NaCl solution at room temperature. Corrosion affects slightly on the electric conductivity of the solder and the joint. Low corrosion potential of SnZn solder alloy and thus smaller joint resistance make the corrosion current larger through the joint. Adding bismuth element in SnZn alloy can increase the resistance of the solder. Tensile experiment of the solder shows that the strength and elongation of the solder decrease as the soaked time increases. Creep life of SnZn joint shortens in 3%NaCl solution, while in tap water, the life elongates distinctly. Tested results also show that a little insoluble corrosive product has no harm on the creep-resistance of the joint. Analysis of fractograph of corroded joint by SEM finds out that corrosion occurs along the grain boundaries.

#### 5:20 PM

Effect of Surface Treatment on Ceramics Bonding with Solder Glass Frit: Zheng Sun<sup>1</sup>; Dayou Pan<sup>1</sup>; Jun Wei<sup>1</sup>; Chee Khuen Wong<sup>1</sup>; <sup>1</sup>Singapore Institute of Manufacturing Technology, 71 Nanyang Dr., Singapore 638075 Singapore

Bonding of ceramics is becoming an increasingly important technology and has found wide applications in different engineering and electronic applications. In the present paper, furnace brazing of ceramics using glass frit filler material was investigated with emphasis on effects of surface treatment and processing parameters. Alumina (Al2O3) sheets and Schottglas GL1 G017-393 solder glass frit were used as the base and brazing materials, respectively. The alumina substrates were chemically (or physically) treated using various acids, as well as air plasma arc, respectively. In addition, effects of brazing parameters such as temperature, time and load were investigated. Tensile test for the brazed joints was conducted to assess the joint strengths. The results show that both surface roughness and contact angle of the substrates decrease after the surface treatments. Results from both tensile and metallographical tests show that sound brazed (or sealed) joints can be produced if appropriate parameters applied. The results indicate that relatively high surface roughness facilitates the joint strength due probably to the enhanced mechanical interlocking. It appears that the appropriate combination of the substrate surface roughness and the glass frit particle size plays dominant role in the joint strength. Furthermore, the study demonstrated that the mechanism of ceramics bonding using solder glass frit is fundamentally different from that of conventional brazing or soldering process. Bonding strength is not only related to surface contact angle, but also surface roughness. It is shown that with appropriate bonding conditions, high quality ceramics bonding or sealing can be achieved.

# Magnesium Technology 2004: Wrought Magnesium Alloys I

Sponsored by: Light Metals Division, LMD-Magnesium Committee Program Organizer: Alan A. Luo, General Motors, Materials and Processes Laboratory, Warren, MI 48090-9055 USA

Monday PM	Room: 2	03B
March 15, 2004	Location:	Charlotte Convention Center

Session Chairs: Alan A. Luo, General Motors, Matls. & Processes Lab., Warren, MI 48090-9055 USA; Sean R. Agnew, University of Virginia, Dept. of Matls. Sci. & Engrg., Charlottesville, VA 22904 USA

#### 2:00 PM

Thermal Forming of Magnesium Alloys: Processing and Simulation: Suhui Wang<sup>1</sup>; Ramnath K. Krishnamurthy<sup>1</sup>; Xin Wu<sup>1</sup>; Wuhua Yang<sup>2</sup>; Michael Wenner<sup>2</sup>; <sup>1</sup>Wayne State University, Mech. Engrg., 5050 Anthony Wayne Dr., Detroit, MI 48202 USA; <sup>2</sup>General Motors, R&D Ctr., Mfg. Sys. Rsch. Lab., 30500 Mound Rd., MC 480-106-359, Warren, MI 48090-9055 USA

Under thermally activated deformation conditions magnesium alloys exhibit greatly enhanced formability. It is of great interest to investigate the possibility of deformation processing for high-efficiency and low-cost manufacturing. In this study the elevated temperature deformation behaviors of AZ31B were investigated, first to determine the window of processing temperature and strain rate suitable for net-shape forming processes. The formability was evaluated under a biaxial loading condition using tube specimens and with internal gas pressure and axial loading. Then, the gas forming of tubes was studied, and the forming mechanics was analyzed. It was found that the deformed parts showed a strong crystallographic texture and anisotropic properties. The texture evolution was analyzed with a strain rate dependent crystal plasticity method, and the results are in good agreement with the experimental observations. A combined process design and texture design for optimal post-forming performance is discussed.

#### 2:20 PM

Mechanical Response of AZ31B Magnesium as a Function of Temperature, Strain Rate, and Orientation: Carl M. Cady<sup>1</sup>; George T. Gray<sup>1</sup>; Benjamin L. Henrie<sup>1</sup>; Ellen K. Cerreta<sup>1</sup>; Laura B. Addessio<sup>1</sup>; Micheal F. Lopez<sup>1</sup>; Shuh-Rong Chen<sup>1</sup>; David F. Teter<sup>2</sup>; Clarissa A. Yablinsky<sup>3</sup>; <sup>1</sup>Los Alamos National Laboratory, MST-8, MS G-755, Los Alamos, NM 87544 USA; <sup>2</sup>Los Alamos National Laboratory, MST 6, Los Alamos, NM 87545 USA; <sup>3</sup>Carnegie Mellon University, Pittsburgh, PA 15213 USA

Constitutive property studies have been conducted on a commercial magnesium alloy as a function of temperature  $(-75 e^{a}C \text{ to } 200 e^{a}C)$ , strain rate (0.001 s-1 to 2500 s-1), orientation, and stress state. Minimal influence of strain rate on the yield and flow stress of this material was seen over the range of strain rates from 0.001 to 2500 s-1. HowMONDAY PM

ever, a large variation in the mechanical response was observed related to both orientation with respect to rolling direction and stress-state. The yield stress in the through-thickness orientation is twice that of the in-plane direction for all strain rates. The flow stress for the inplane orientation is initially lower than that seen in the through-thickness direction but it intersects at ~12% strain. Varying the temperature also influences the through-thickness flow stress behavior significantly more than the in-plane behavior. These differences can be attributed to the dominant deformation mechanism activated for each orientation.

#### 2:40 PM

TEM Investigation of the Dislocations Activated Within Magnesium Alloy AZ31B Under Various Loading Conditions: Ozgur Duygulu<sup>1</sup>; Sean R. Agnew<sup>1</sup>; <sup>1</sup>University of Virginia, Dept. of Matls. Sci. & Engrg., 116 Engineer's Way, Charlottesville, VA 22904 USA

Recent experimental and simulation-based studies of the deformation mechanisms of wrought magnesium alloy AZ31B have stressed the importance of non-basal slip of dislocations having Burger's vectors of <a> type, as well as <c+a> type for determining the overall plastic response of the alloy. These mechanisms have been invoked to explain the strong in-plane anisotropy typical of cold-rolled sheet as well as the improved formability at elevated temperatures, respectively. These conclusions are critically evaluated in light of transmission electron microscopy analyses of the dislocations present at various temperatures and under different loading conditions. By examining grains of various orientations within a given sample, an assessment of the population of various dislocations is possible. The results of this study have implications for both sheet alloy and process development, as well as warm forming process development.

#### 3:00 PM

Heated Hydro Mechanical Deep Drawing of Magnesium Sheet Metal: Gerrit Kurz<sup>1</sup>; <sup>1</sup>Institute for Metal Forming and Metal Machine Tools, Sheet Metal Forming, Welfengarten 1A, Hannover 30167 Germany

In order to reduce fuel consumption efforts have been made to decrease the weight of automobile constructions by increasing the use of lightweight materials. In this field of application magnesium alloys are important because of their low density. A promising alternative to large surfaced and thin die casting parts has been observed in construction parts that are manufactured by sheet metal forming of magnesium. Magnesium alloys show a limited forming ability at room temperature. A considerable improvement of formability can be reached by heating the material. Formability increases above a temperature of approximately  $T = 225^{\circ}C$ . This paper will give an overview about the heated hydro-mechanical deep drawing process of magnesium sheet metal. It will further show how the process parameters temperature and fluid pressure influence the deep drawing process. Results of these deep drawing tests lead to the conclusion that it is possible to replace conventional steel workpieces and aluminum sheet workpieces by magnesium sheet workpieces.

#### 3:20 PM

Dynamic Recrystallization of AZ31 Magnesium Alloy During Torsion Deformation at Elevated Temperatures: W. J. Liu<sup>1</sup>; V. Kao<sup>1</sup>; E. Essadiqi<sup>1</sup>; S. Yue<sup>2</sup>; V. Verma<sup>3</sup>; <sup>1</sup>Natural Resources Canada, Matls. Tech. Lab., CANMET, 568 Booth St., Ottawa, Ontario K1A 0G1 Canada; <sup>2</sup>McGill University, Dept. of Metals & Matls. Engrg., 3610 Univ. St., Montreal, Que. H3A 2B2 Canada; <sup>3</sup>General Motors, Matls. & Processes Lab., Warren, MI 48090-9055 USA

It is believed that dynamic recrystallization is the mechanism responsible for grain structure refinement of magnesium alloys during elevated temperature deformation. In this study, isothermal torsion tests were carried out on an AZ31 alloy under constant strain rate conditions. Two critical values that characterize the dynamic recrystallization kinetics, namely the critical strain for recrystallization start (es) and the critical strain for recrystallization finish (ef), were determined from the measured flow curves and verified metallographically based on quenching samples interrupted during deformation. A kinetic model is developed which is capable of predicting recrystallization fractions from usual processing and material parameters such as temperature, strain, strain rate and original grain size.

# 3:40 PM Break

#### 3:50 PM

Mechanical Properties, Formability and Microstructure of Magnesium Alloy Tubes: *Alan A. Luo*<sup>1</sup>; Anil K. Sachdev<sup>1</sup>; <sup>1</sup>General Motors Corporation, Warren, MI USA

Magnesium alloys are being increasingly used in automotive industry for weight reduction and fuel economy improvement. Extruded tubular sections provide further opportunities in mass-efficient designs for automotive structural and interior applications. In this paper, some fundamental aspects of structural design using magnesium alloy tubes are discussed. Furthermore, mechanical properties, formability and microstructure of magnesium alloy tubes are examined at room and elevated temperatures. Deformation mechanisms and their implications on formability of magnesium alloys are also discussed.

#### 4:10 PM

#### **Pneumatic Bulging of Magnesium AZ31 Tubes and Sheet Metal at Elevated Temperatures**: *K. Siegert*<sup>1</sup>; S. Jäger<sup>1</sup>; <sup>1</sup>Stuttgart University, Inst. for Metal Forming Tech. Germany

This paper deals with pneumatic bulging of Magnesium AZ31 tubes and AZ31 sheet metal at elevated temperatures. In the following, flow-stress curves for AZ31 tubes and AZ31 sheet metal are presented, determined by pneumatic bulging. In addition to that forming limit curves for Magnesium AZ31 tubes and AZ31 sheet metal at different forming temperatures are presented as well. It can be shown that magnesium AZ31 is quite good formable at temperatures in the range of 250°C to 350°C. Outgoing from these fundamental investigations, an auto body sheet metal component was formed by pneumatic bulging at a temperature of about 300°C. Furthermore, the strains over the component were measured with an automated grid analysis. This analysis shows a nearly equal distribution of the strains over the component.

# 4:30 PM

Microstructure and Mechanical Properties of Mg-Al-Zn Alloys Processed by Different-Speeds-Rolling: *Tsunemichi Imai*<sup>1</sup>; Shangli Dong<sup>2</sup>; Naobumi Saito<sup>1</sup>; Ichinori Shigemastu<sup>1</sup>; <sup>1</sup>National Institute of Advanced Industrial Science and Technology, Inst. of Structural & Engrg. Matls., Nagoya Japan; <sup>2</sup>Harbin Institute of Technology, Harbin China

Rolling is an important process for sheet production of metals and their alloys, and high performance sheet is essential to extending application of Magnesium (Mg) alloys. A different-speeds-rolling (DSR) processing was carried out on Mg-Al-Zn based alloys in current investigation, aimed at enhacing metallurgy quality and mechanical property of Mg-Al-Zn alloys. The speed ratio of the upper roll and lower one of the mill was selected as 1.364, while the rolls temperature changed from ambient temperature to 573K. Preheating temperature of the rolled sample could also be varied within a wide range in order to obtain Mg sheet free of crack with the final thickness of 1.1 mm. The influence of rolling conditions on microstructure and mechanical property of the rolled Mg-Al-Zn sheet were carefully studied by several techniques, and the benefits of DSR to produce Mg sheet would be indicated.

# 4:50 PM

Effect of Thermoplastic ECAP on Mechanical Properties and Microstructures of AZ61 Mg Alloy: Yan Yinbiao<sup>1</sup>; <sup>1</sup>Nanjing University of Science & Technology, Dept. of Matl. Sci. & Engrg., 200 XiaoLingWei, Nanjing, Jiangsu 210094 China

The commercial AZ61 Mg alloy and its solution treated have been deformed in the temperature from 250C to 450C by the equal channel angular pressing(ECAP) their microstructures are observed with the metallographic microscope and mechanical properties are determined with tensile testing by AGS-10KND Machine. The results show that the effect of primal microstructures of AZ61 Mg alloys on their mechanical properties after thermoplastic ECAP is very small; The grain significantly are refined. specific elongation and yield strength of AZ61 Mg alloy notablely increase, but no change of tensile strength after the thermoplastic ECAP, it may be result from fabricability formating while ECAP; the effect of the deformation temperature on grain sizes and specific elongation and yield strength is more intensive than that of tensile strength; the tensile strength of AZ61 Mg alloy could not be improved by the thermoplastic ECA.

# Materials by Design: Atoms to Applications: Materials Characterization and Microstructural Modeling

*Sponsored by:* Electronic, Magnetic & Photonic Materials Division, EMPMD/SMD-Chemistry & Physics of Materials Committee

*Program Organizers:* Krishna Rajan, Rensselaer Polytechnic Institute, Department of Materials Science and Engineering, Troy, NY 12180-3590 USA; Krishnan K. Sankaran, The Boeing Company, Phantom Works, St. Louis, MO 63166-0516 USA

Monday PM	Room: 210B
March 15, 2004	Location: Charlotte Convention Center

Session Chair: Mutsuhiro Shima, Renssselaer Polytechnic Institute, Matls. Sci. & Engrg., Troy, NY 12180 USA

#### 2:00 PM

Microstructures by Design: Simulations of Nonequilibrium Processing: Alan C. Lund<sup>1</sup>; *Christopher A. Schuh*<sup>1</sup>; <sup>1</sup>Massachusetts Institute of Technology, Matls. Sci. & Engrg., 77 Mass. Ave., Cambridge, MA 02139 USA

With the growing interest in advanced metallic materials such as metallic glasses and nanocomposites, nonequilibrium processing methods such as mechanical alloying and ion-beam mixing are gaining prominence. Using simplified atomic-level models, we simulate these nonequilibrium processes, treating the intrinsic thermodynamic parameters of the material as tailorable. For hypothetical binary alloys with many different compositions, radius mismatches, and heats of mixing, we explore the development of the structural phase-space under extrinsic driving. We provide guidelines for the development of both crystalline and amorphous solid solutions, chemically ordered crystals and glasses, as well as nanocomposite materials. Connection with nonequilibrium thermodynamic theory is also made.

#### 2:30 PM

Mesoscale Response of an Austenitic Stainless Steel: Part I -EBSD and Three-Dimensional Microstructural Characterization: A. C. Lewis<sup>1</sup>; J. F. Bingert<sup>2</sup>; A. B. Geltmacher<sup>3</sup>; G. Spanos<sup>3</sup>; <sup>1</sup>National Research Council/Naval Research Laboratory, Code 6352, 4555 Overlook Ave. SW, Washington, DC 20375 USA; <sup>2</sup>Los Alamos National Laboratory, Los Alamos, NM 87545 USA; <sup>3</sup>Naval Research Laboratory, 4555 Overlook Ave., Washington, DC 20375 USA

Alloy steels will continue to be one of the main structural materials in Navy ships and boats in the foreseeable future, due to their relatively low cost, their good combination of mechanical properties, and the existing infrastructure for processing and fabrication. The ultimate goal of a Naval Materials by Design program is to allow a design engineer to specify performance criteria for a specific Naval structure, such as eliminating magnetic signature, optimizing corrosion resistance, and maximizing material strength. The Materials by Design framework will then determine enhanced/optimized alloy compositions and processing procedures that meet the specified criteria in a timely manner. As a significant part of a multidisciplinary Materials by Design program, three-dimensional characterization techniques have been developed and utilized to provide guidance to first-principles and atomistic simulations and realistic input for image-based finite element models for material response on the mesoscale. Automated electron backscatter diffraction (EBSD) has been used to characterize AL-6XN, a super-austenitic stainless steel with high Ni and Cr content and relatively low C. This technique is used to provide orientation and misorientation statistical distributions, and identify dominant coincident site lattice boundary planes. The presence of second phases such as s will also be investigated in this steel. An experimental methodology has been developed to combine EBSD with standard serial sectioning and focused ion beam sectioning to construct 3D microstructure sets incorporating orientation data.

#### 3:00 PM

Thermography Detection of Low-Cycle Fatigue: *Bing Yang*<sup>1</sup>; Peter K. Liaw<sup>1</sup>; J. Y. Huang<sup>2</sup>; R. C. Kuo<sup>2</sup>; J. G. Huang<sup>3</sup>; D. E. Fielden<sup>1</sup>; <sup>1</sup>University of Tennessee, Dept of Matls. Sci. & Engrg., Knoxville, TN 37996 USA; <sup>2</sup>Institute of Nuclear Energy Research (INER), PO Box 3-14, 1000 Wenhua Rd., Chiaan Village, Lungtan 325 Taiwan; <sup>3</sup>Taiwan Power Company, Taipei Taiwan

Two-dimensional thermography is a new technology that in-situ obtains the target surface temperature. Since mechanical-damaging

processes are always accompanied by heat-dissipation processes, thermography provides a convenient method to in-situ monitor the fatigue-damage processes. In the current research, thermography was used to "watch" temperature evolutions of reactor pressure vessel (RPV) steels "cycle by cycle" during low-cycle fatigue. Numerical analyses integrating thermodynamics and heat-conduction theories have been formulated to quantify the observed temperature evolutions. Stress amplitude, strain amplitude, plastic work, fatigue life, and cyclic-softening behavior have been predicted directly from the observed temperature evolutions, which provides an innovative method to quantify and control the fatigue behaviors of RPV steels. Furthermore, only one or no experiment is needed to determine the required up wide applications of thermography in studying in-situ mechanical damage of materials and components.

#### 3:30 PM Break

## 3:45 PM

#### The Digital Material - An Environment for Collaborative Material Design: *Matthew P. Miller*<sup>1</sup>; Paul R. Dawson<sup>1</sup>; <sup>1</sup>Cornell University, Mech. & Aeros. Engrg., 194 Rhodes Hall, Ithaca, NY 14853 USA

In spite of the many recent advances that have been made in simulations, material design and selection processes continue to be expensive and time consuming. Opportunities for insertion of alternative materials is hampered by not having basic property data available when critical design decisions must be made. The main reason for the empirical nature of alloy design is the crucial role played by the actual form of the microstructure in dictating alloy properties and behavior. Important are the phases, their spatial distribution, and the defects within them, all of which can vary widely even for the same composition. While much research has focused on the response of metals on many of the relevant size scales, there is still a general lack of quantitative understanding about how these processes interact. How do structural features on one size scale dictate the response of the material on a larger scale and, more importantly, how can one accurately represent these structure - property relationships? This pertains to such basic properties as the elastic moduli and strength. The fundamental goal of the research described here is to develop an accelerated materials insertion methodology - a framework capable of encompassing many types of models from multiple size scales that we refer to as the Digital Material. The hallmarks of the Digital Material are its model independence; researchers from many areas can contribute to the description, and its hybrid nature; both simulated and physically measured data are employed in the representation. Iron/Copper alloys have been developed as prototype material systems using the framework. The processes for instantiating, loading and probing virtual and physical specimens are described in this talk.

#### 4:15 PM

Mesoscale Response of an Austenitic Stainless Steel: Part II -Image-Based Finite Element Modeling: A. C. Lewis<sup>1</sup>; J. F. Bingert<sup>2</sup>; A. B. Geltmacher<sup>3</sup>; <sup>1</sup>National Research Council/Naval Research Laboratory, Code 6352, 4555 Overlook Ave. SW, Washington, DC 20375 USA; <sup>2</sup>Los Alamos National Laboratory, Los Alamos, NM 87545 USA; <sup>3</sup>Naval Research Laboratory, 4555 Overlook Ave., Washington, DC 20375 USA

The goal of a Materials by Design program is to develop the framework for a future computationally-based materials design and selection system. A critical component of such a program is the combination of computational techniques, from atomistic to continuum length scales, used to design a material to meet specific property requirements. A significant part of this multidisciplinary Materials by Design program is the development of three-dimensional image-based computational techniques to examine the role of microstructure on the mesoscale response of materials. Experimental data of three-dimensional microstructures in a super-austenitic stainless steel are used to generate mesoscale finite element models based on actual grain orientations, grain boundaries and second-phase particle locations. The constitutive relationships in these models include anisotropic elasticity and crystalline plasticity. These mesoscale models are used to examine the generation of local stress and strain states that will potentially cause local phase transformations, plasticity, damage and ultimately failure.

#### 4:45 PM

On the Synergy Between Classification of Textures and Process Sequence Selection: Shankar Ganapathysubramanian<sup>1</sup>; Nicholas Zabaras<sup>1</sup>; <sup>1</sup>Cornell University, Matls. Proc. Design & Control Lab., Sibley Sch. of Mech. & Aeros. Engrg., 188 Frank H. T. Rhodes Hall, Ithaca, NY 14853-3801 USA

The state of art in computational materials processing is based on a multi-length scale analysis incorporating polycrystalline plasticity, grain size, grain shape effects and effects due to phase distribution and grain boundaries. Considering the computational complexity involved in such multi-length scale formulations, innovative algorithms are needed towards the development of fast and efficient design methodologies. Such developments are crucial for the basis of futuristic ideas of real time control of properties during material processing. Our earlier efforts have shown that reduced-order models of microstructure (texture in particular) are a simple approach towards the development of fast and reliable design/control algorithms. In addition to this, such approaches have the added advantage of their ability to extend easily towards classification problems. This process of classification of texture will be addressed through this presentation. Our analysis incorporates Support Vector Machines algorithms that have been used widely in statistical machine learning tasks. Application of such techniques in texture classification will be demonstrated through a series of examples. Further, we will describe ways to discern data/modes from experimental pole figures, including real time analysis through 'Machine vision', and to use such information in predicting the deformation paths and processes. Comments will also be made on the nonunique nature of such paths. Finally, we will describe and discuss how such developments play an integral role in the development of multilength scale design methodologies.

# Materials Issues in Fuel Cells: Materials Challenges Sponsored by: TMS

*Program Organizers:* Brajendra Mishra, Colorado School of Mines, Kroll Institute for Extractive Metals, Golden, CO 80401-1887 USA; John M. Parsey, ATMI, Mesa, AZ 85210-6000 USA

Monday PM	Room: 207B/C
March 15, 2004	Location: Charlotte Convention Center

Session Chairs: John Michael Parsey Jr., ATMI, Mesa, AZ 85210-6000 USA; Jeanne Pavio, Motorola Labs., Tempe, AZ 85284 USA

#### 2:00 PM Cancelled

# The Facts Behind the Headlines of the Hydrogen Economy

#### 2:40 PM Invited

Application of Oxidation/Heat Resistant Alloys for SOFC Interconnects: Status and Challenges: Z. Gary Yang<sup>1</sup>; John S. Hardy<sup>1</sup>; Dean M. Paxton<sup>1</sup>; Prabhakar Singh<sup>1</sup>; Jeff W. Stevenson<sup>1</sup>; Matt S. Walker<sup>1</sup>; K. Scott Weil<sup>1</sup>; Gordon Xia<sup>1</sup>; <sup>1</sup>Pacific Northwest National Laboratory, 902 Battelle Blvd., MB K2-44, Richland, WA 99352 USA

Over the past several years, advances in the design and fabrication of planar SOFCs have led to a steady reduction in the temperatures necessary for their operation. Consequently, it appears more realistic now to use low cost oxidation and heat resistant alloys for interconnects in the intermediate-temperature (650-800°C) SOFC stacks. There are a large number of compositions developed in the past for a variety of traditional applications and recently a few of new alloys have been added specifically for the SOFC interconnect applications. To help define the suitability of these alloys, PNNL has carried out a systematical screening study and evaluated numerous selected alloys against a set of properties relative to the SOFC interconnect applications. Recently we have also focused on modifying the bulk alloy interconnect composition and engineering its surface for an improved performance. This paper will address status and issues of alloy interconnects for SOFC applications and present the details of our development efforts.

#### 3:10 PM

Portable Methanol-Based Micro Fuel Cells: System Design, Tradeoffs and Results: Jeanne Pavio<sup>1</sup>; <sup>1</sup>Motorola Labs, 2100 E. Elliot Rd., Tempe, AZ 85284 USA

Methanol-based fuel cells, both direct methanol (DMFCs) and reformed methanol (RHFC), are a promising technology for compact power applications because they possess the potential for very high energy density. Motorola Lab's Fuel Cell team has demonstrated a number of prototype portable power systems ranging from 100mW to 2W for low power (<20W), compact electronic applications. Low power systems require not only small sized fuel cell stacks, but also miniature and low power peripheral components. Initial target applications, such as two-way radios and PDAs, require that the fuel cell system have an energy density as good as, or better than, current rechargeable battery technology. Consequently, system power density must be greater than 200 Wh/L. Developing a high energy density fuel cell system requires a high energy density fuel source such as pure methanol (4780Whr/L, 6043Wh/kg), it demands miniaturization of the system for good volumetric and weight effectivity, and it demands long-term reliable performance. Compact 1W and 2W power sources are described for wireless communications and portable computing systems. Motorola's approach to a 20W power system based on a small fuel processor that reforms methanol to hydrogen is also described. System considerations and electronic controls will be reviewed along with basic technology and performance characteristics. Performance of a 2W prototype system will be discussed, along with projections for the 20W system.

# 3:35 PM

#### Extrusion of Stabilized Zirconias for Solid Oxide Fuel Cell Electrolytes: Kevin M. Hurysz<sup>1</sup>; Joe K. Cochran<sup>1</sup>; <sup>1</sup>Georgia Institute of Technology, Matls. Sci. & Engrg., 771 Ferst Dr. NW, Atlanta, GA 30332-0245 USA

Stabilized zirconias, particularly scandia stabilized zirconia (ScSZ), have been proven to be good materials for use as Solid Oxide Fuel Cell (SOFC) electrolytes. This paper will discuss the formation of stabilized zirconia pastes for extrusion into SOFC electrolytes. Paste constituents are characterized using microscopy, particle size, and surface area measurements. Paste properties are modeled using mathematical methods which are compared to experimental property data. The pastes are extruded into a geometry consistent with an operational SOFC. A variety of drying methods are investigated to reduce deformation of the green ceramic. Finally, extrudate behavior on firing is described and fired microstructures presented. Effort toward incorporation of the structure into a SOFC will be discussed.

#### 4:00 PM Break

#### 4:10 PM

Y2Zr2O7 (YZ) - Pyrochlore Based Oxide as an Electrolyte Material for Intermediate Temperature Solid Oxide Fuel Cells (ITSOFCs) - Influence of Mn Addition on YZ: *Kumar Manickam*<sup>1</sup>; I. Arul Raj<sup>1</sup>; R. Pattabiraman<sup>1</sup>; <sup>1</sup>Central Electrochemical Research Institute, Batteries & Fuel Cell Div., karaikudi, Tamilnadu 630006 India

Compositions in the pyrochlore system Y2Zr2O7 (YZ) and Y2Zr2xMnxO7- (YZM) (where x = 0.025, 0.05, 0.075 and 0.10) were examined as possible alternatives to stabilized zirconia solid oxide electrolyte in Intermediate Temperature Solid Oxide Fuel Cells (ITSOFCs). Such materials were prepared by glycine-nitrate combustion process. The prepared compounds were characterized by X-Ray Diffraction, Particle size, density measurement, Fourier Transform infrared spectroscopy, and Thermal analysis. Circular pellets were fabricated and annealed at different temperatures ranging from 1000 to 1400°C. The sintering behavior of YZ and YZM were investigated to obtain information on the densification factor, relative percentage shrinkage/ expansion in volume after heat treatment and apparent porosity value. The small doping level of Mn (?T10.0 wt. %) resulted in increased conductivity values. The key features, which make the YZ and YZM systems attractive as a fuel cell component, are discussed.

#### 4:35 PM

The Anomalous Oxidation Behavior of Oxidation Resistant Alloys Under SOFC Interconnect Dual Exposure Conditions: Z. Gary Yang<sup>1</sup>; Gordon Xia<sup>1</sup>; Matt S. Walker<sup>1</sup>; Prabhakar Singh<sup>1</sup>; Jeff W. Stevenson<sup>1</sup>; <sup>1</sup>Pacific Northwest National Laboratory, 902 Battelle Blvd., Mail Box K2-44, Richland, WA 99352 USA

The oxidation behavior of oxidation resistant alloys under varied environments has been widely investigated for a number of traditional applications, and recently several works have also focused on SOFC interconnect applications. These studies, however, were carried out using single atmosphere exposure conditions and were presumably based on the implicit assumption that the oxidation behavior as measured in either an oxidizing or reducing environment will be essentially identical to that occurring on the air or fuel side of the material when it experiences the dual atmosphere exposure conditions characteristic of the SOFC interconnect environment. However, our recent investigation clearly indicates that under dual exposures, the oxidation behavior on the airside can differ significantly from the behavior observed when the steels are exposed to air only. This paper will present details of this finding and discuss the results from our study on a number of selected alloys under the SOFC operating conditions.

#### 5:00 PM

Mechanochemical Synthesis of PbMoO4 Compound Oxide: Aghasi Razmik Torosyan<sup>1</sup>; Svetlana Ashot Barseghyan<sup>1</sup>; <sup>1</sup>NAS RA, 10 Arghutyan, 2 District, Yerevan 375051 Armenia

The present work the synthesis of compound oxide PbMoO4 under mechanical alloying conditions were investigated. The experiments were carried out in vibration ball mill at vial amplitude of 4 mm and frequency of 25 Hz for up to 10h. PbO and MoO3 with molecular ratio 1:1 were used in experiments of mechanochemical synthesis. The maximal yield of PbMoO4 was 95%. Longer milling times of powder blends didn't result in increase of product yield. The obtained products and the yields of reaction were determined employing X-ray diffraction analysis. In addition to the compound oxides and residues of starting oxides a small quantity metallic iron was found being a result of contamination during milling.Refinement of synthesized PbMoO4 from impurities was carried out by sequential flushing of the powder starting with 25% solution of ammonia to remove MoO3, and then with diluted solution of acetic acid to remove PbO and Fe. Such method of refining allowed to obtain rather pure compound oxide applicable for growing of PbMoO4 crystals. PbMoO4 compound oxide has a number of practical applications as crystal. In most of the important applications very fine grain size in submicron-nanoscale range is important to obtain the best properties. Mechanochemical processing of compound oxides carried out at ambient temperature may be advantageous compared to synthesis methods at high temperatures.

# Materials Processing Fundamentals: Deformation Processing

Sponsored by: Extraction & Processing Division, Materials Processing & Manufacturing Division, EPD-Process Fundamentals Committee, MPMD/EPD-Process Modeling Analysis & Control Committee

*Program Organizers:* Adam C. Powell, Massachusetts Institute of Technology, Department of Materials Science and Engineering, Cambridge, MA 02139-4307 USA; Princewill N. Anyalebechi, Grand Valley State University, L. V. Eberhard Center, Grand Rapids, MI 49504-6495 USA

Monday PM	Room:	21	2B		
March 15, 2004	Locatior	n:	Charlotte	Convention	Center

Session Chair: TBA

Ν

#### 2:00 PM Invited

Differences in the Microstructures of Continuous Cast-Rolled and Conventional Wrought Aluminum Alloy Products: Prince N. Anyalebechi<sup>1</sup>; <sup>1</sup>Grand Valley State University, Padnos Sch. of Engr., L. V. Eberhard Ctr., Ste. 718, Grand Rapids, MI 49504-6495 USA

The differences in the microstructures of wrought aluminum alloy products produced via the continuous casting-rolling and the conventional ingot casting-rolling routes have been investigated. Irrespective of alloy composition, the microstructures of the products produced via the continuous casting route consist of bands of eutectic colonies elongated and strung out in the rolling direction surrounded by regions depleted in second phases. In contrast, the microstructures of conventional wrought products consist of a uniform distribution of comparatively coarser constituent phase particles. Most importantly, wrought aluminum alloy products produced via the continuous casting-rolling route do not contain the matrix-strengthening dispersoids. The differences in microstructure are attributed to the different prevailing solidification conditions in ingot and continuous casting processes. They appear to explain the differences in the response of the two types of wrought products to post-casting processes and attendant properties and performance.

#### 2:30 PM Invited

Atomic Mismatch and Coherency Issues in the Theory of Driven Alloys: *Alan C. Lund*<sup>1</sup>; Christopher A. Schuh<sup>1</sup>; <sup>1</sup>Massachusetts Institute of Technology, Matls. Sci. & Engrg., 77 Mass. Ave., Cambridge, MA 02139 USA

Driven alloys evolve under competition of an extrinsic forcing (e.g., irradiation or plastic straining) and intrinsic thermodynamic parameters (e.g., thermal equilibration). The theoretical framework for these systems has explained many interesting experimental findings in non-equilibrium processing by irradiation, ion-beam mixing, or ball milling of powders, but has largely focused on systems with perfect crystalline coherency. Here we use computer simulations of driven 2-D alloys to expand the discussion to systems with significant atomic level stresses owing to a radius mismatch. These simulations show a significant effect of incoherency that is manifested primarily at low processing temperatures.

#### 3:00 PM

Prediction of the Shape Changes and Microstructural Evolution: Hoon-Jae Park<sup>1</sup>; K.-H. Na<sup>1</sup>; Y.-S. Lee<sup>2</sup>; <sup>1</sup>KITECH, Microforming,

MONDAY PM

35-3, HongChonRi, IbJangMyon, ChonAnSi, Choonchung-nam-do 330815 S. Korea; <sup>2</sup>Kookmin University, Mech. Engrg., 861-1 Chungneung-Dong, Sungbuk-Gu, Seoul 136-702 S. Korea

Main objectives of the forming processes are to form the products having the shape and mechanical properties as designed. To effectively predict the shape changes in steady state forming processes, an Eulerian analysis supplemented with a free surface correction algorithm and a stream line technique is addressed. Since the mechanical properties are related directly to the microstructures of the work piece, the prediction of microstructural changes must be included in the process model. In this work, anisotropy from deformation texture and deterioration of mechanical properties due to growth of micro voids are directly coupled into the virtual work expressions for the mass and momentum balances. The anisotropy and accumulated damage in the rolled sheet could be predicted. Applications to hydrostatic clad extrusion as well as shape rolling are given and the results are discussed in detail.

# 3:30 PM

On the Development of a Three-Dimensional Deformation Process Design Simulator: Swagato Acharjee<sup>1</sup>; Nicholas Zabaras<sup>1</sup>; 'Cornell University, Matls. Proc. Design & Control Lab., Sibley Sch. of Mech. & Aeros. Engrg., 188 Frank H. T. Rhodes Hall, Ithaca, NY 14853-3801 USA

A mathematically rigorous continuum sensitivity method (CSM) is developed and incorporated in a gradient optimization framework for process optimization and control in three-dimensional metal forming applications. CSM involves differentiation of the governing field equations of the direct problem (constitutive, contact and kinematic problems) with respect to the design variables and development of the weak forms for the corresponding sensitivity equations. This work is an extension of our earlier work where the problems were restricted to 2D and axisymmetric cases. Extension to 3D involves a novel approach to the formulation of the contact sensitivity problem. A number of industrially relevant multi-stage design problems related to preform and die design for desired properties in the final product are considered highlighting the features of the metal forming design simulator developed in-house. While emphasis is given to phenomenological state-variable based constitutive models, extension of the design simulator to incorporate multi-length scale polycrystal plasticity based constitutive models will also be discussed.

#### 3:50 PM Break

#### 4:10 PM

Investigation of Microstructural Evolution of Cold Roll Bonded and Annealed TiAl-Sheets: *Kazim Serin*<sup>1</sup>; Gajanan Chaudhari<sup>1</sup>; Viola L. Acoff<sup>1</sup>; <sup>1</sup>University of Alabama, Dept. of Metallurgl. & Matls. Engrg., Box 870202, Tuscaloosa, AL 35487 USA

In this study, the kinetics of the interfacial layer thickness growth of cold roll bonded and annealed titanium and aluminum sheets is investigated. Interrupted annealing experiments were performed for alloys with defined reduction levels at different temperatures between 600°C and 1200°C. The final microstructure depends on the reduction level of the initial foils, annealing temperature, and annealing time. The layer thickness was investigated by quantitative microstructural measurements using scanning electron microscopy (SEM) and transmission electron microscopy (TEM). The appropriate treatment for processing of TiAl-sheet materials was defined.

#### 4:30 PM

High Temperature Flow Behavior of an Austenitic Stainless Steel, ISO 5832-9, Used for Orthopedic Applications: Enrico José Giordani<sup>1</sup>; Oscar Balancin<sup>1</sup>; <sup>1</sup>Universidade Federal de São Carlos, Depto. de Engenharia de Materiais, Rodovia Washington Luiz, km 235, São Carlos, São Paulo 13565-905 Brazil

Knowing how a particular type of steel behaves at high temperature is essential for adequate thermomechanical processing aimed at producing high-performance hot-worked products that combine high strength and toughness. These properties can be attained through a recrystallized microstructure composed of fine grains, provided secondary recrystallization does not occur. An investigation was made of the stress-strain behavior of an austenitic stainless steel used as a biomaterial, ISO 5832-9, based on isothermic torsion tests over a temperature range of 900°C to 1300°C, at strain rates of 0.5 to 5.0s-1. The flow stress generally rises to a maximum at the onset of straining, before dropping to a steady-state level. This behavior is characteristic of materials that soften by dynamic recrystallization. The material showed high values of deformation at the onset of the steady-state and the high value of apparent activation energy (Q=703 kJ/mol), indicating that the material underwent an intense strain-induced Z-Phase precipitation.

# 4:50 PM

Streamline of Microstructure Evolution During Plastic Deformation: *Dongsheng Li*<sup>1</sup>; Hamid Garmestani<sup>1</sup>; <sup>1</sup>Georgia Institute of Technology, Sch. of Matls. Sci. & Engrg., 771 Ferst Dr., NW, Atlanta, GA 30332 USA

Modeling the microstructure evolution during mechanical deformation is essential in finding out how to achieve the preferred microstructure. Texture coefficients were used as a descriptor of the microstructure. A linear model is proposed in this study to describe the evolution of microstructure during thermalmechanical processing. Using this linear model, processing path function and streamline function are derived. From these functions, using known texture at several deformation points, processing path and streamlines were calculated to simulate the microstructure evolution in a microstructure space which is composed of texture coefficients. From these streamlines, an optimized processing method will be found out to achieve the desired microstructure.

#### 5:10 PM

Microhardness Testing as a Method of Understanding Bauschinger Phenomena in Cold Formed 301 Austenitic Stainless Steel Sheet: Chirayu Garud<sup>1</sup>; Philip Nash<sup>1</sup>; Sheldon Mostovoy<sup>1</sup>; Joseph C. Benedyk<sup>1</sup>; <sup>1</sup>Thermal Processing Technology Center, IIT, Chicago, IL USA

Microhardness distributions gave an indication of Bauschinger phenomena in the forming of heavily cold rolled and tempered 301 austenitic stainless steel sheet. Stainless steel sheet samples from different lots were cut longitudinal and transverse to the cold rolling direction in the as-received and tempered conditions, then bent to varying radii, and microhardness distribution obtained throughout the thickness in the principal section of the bend. Microhardness differences between the sections of the bend that underwent tensile and compressive strains were significantly different, indicative of a strong Bauschinger effect. The degree of softening due to the Bauschinger effect varied with bend radius, direction of rolling, and tempering conditions. Correlations were made of the Bauschinger effect with microstructure and texture of the sheet. The microhardness distribution method was useful in ascertaining the bariation in the Bauschinger effect between the two lots of steel and potential problems noted in dimensional control during the manufacture of precision formed automotive gaskets.

# Nanostructured Magnetic Materials: Synthesis and Characterization of Nanostructured Magnetic Materials

Sponsored by: Electronic, Magnetic & Photonic Materials Division, EMPMD-Superconducting and Magnetic Materials Committee, EMPMD-Nanomaterials Committee Program Organizers: Ashutosh Tiwari, North Carolina State University, Department of Materials Science & Engineering, Raleigh, NC 27695-7916 USA; Rasmi R. Das, University of Wisconsin, Applied Superconductivity Center, Materials Science and Engineering Department, Madison, WI 53706-1609 USA; Ramamoorthy Ramesh, University of Maryland, Department of Materials and Nuclear Engineering, College Park, MD 20742 USA

Monday PM	Room: 2	15	
March 15, 2004	Location:	Charlotte Convention Center	

Session Chair: TBA

Ν

# 2:00 PM Invited

Magnetic Nanostructures by Templated Electrodeposition: Giovanni Zangari<sup>1</sup>; Jie Gong<sup>2</sup>; <sup>1</sup>University of Virginia, Dept. of Matls. Sci. & Engrg. & CESE, Charlottesville, VA 22904 USA; <sup>2</sup>University of Alabama, MINT Ctr., Tuscaloosa, AL 35487-0209 USA

Electrochemical deposition into self-assembled porous structures provides a convenient method for the fabrication of ordered arrays of metallic or semiconductive nanostructures. The availability of such systems opens a wide range of opportunities for the fabrication and study of the behavior of nanoparticle or nanowire assemblies and for the inexpensive and precise production of devices. Our work is focused on the fabrication of nanoparticle or nanowire arrays of magnetic materials, with the objective to study the magnetic and magnetotransport properties of nanostructures and their interactions. Ordered aluminum oxide porous templates are fabricated by multiple anodization of high-purity Al sheets or of Al films sputtered onto Si. Long range order of the pore array, up to about 100 ?Ým2 can be achieved. The period of the array (60 ¡V 600 nm) and the pore size (15 ¡V 500 nm) can be varied in a wide range by control of the anodization chemistry and/or the anodization voltage. Magnetic metals, alloys and multilayers were electrodeposited into the closed pores or into open pores plugged by metallic films by ac and pulse reverse electrodeposition. The latter method in particular is capable to achieve an unprecedented uniformity in the dimensions and microstructure of the elements. Metal nanoparticles are polycrystalline and the crystalline grains exhibit a random orientation when grown into the closed pores; as a consequence, magnetic anisotropy is mainly determined by particle shape. A transition from in-plane to perpendicular anisotropy is observed at an aspect ratio (height/diameter) of about 1. Interparticle interactions are extremely important in highly packed arrays, inducing strong demagnetization fields and skew in the hysteresis loops. Cobalt nanoparticles with size above 50 nm switch their magnetization by incoherent processes. Thermal stability of the magnetization of nanoparticle assemblies is investigated, showing that 50 nm diameter particles exhibit high magnetic stability against thermal demagnetization. High quality multilayers Cu/magnetic alloy have been grown into the pores and their magnetic properties in the current-perpendicular-to-plane configuration have been investigated. An outlook on the utilization of anodic templates for the synthesis of novel materials and the investigation of novel phenomena will be provided.

#### 2:30 PM Invited

Synthesis and Characterization of FeCo Based Nanomagnetic Alloys: *Raju V. Ramanujan*<sup>1</sup>; Huafang Li<sup>1</sup>; <sup>1</sup>Nanyang Technological University, Sch. of Matls. Engrg., Blk. N4.1, Singapore 639798 Singapore

FeCo based nanomagnetic materials exhibit several attractive soft magnetic properties and are being considered for several new applications in high magnetic induction and high temperature devices. Such materials have been produced by crystallization from melt spun amorphous precursors, mechanical alloying from elemental powders as well as by chemical synthesis techniques. DSC, electrical resistivity measurement, XRD, SEM, TEM and VSM have been used to characterize the samples prepared by these techniques. The crystallization behavior and microstructural evolution of melt spun FeCo based amorphous precursor is discussed. The alloying process and microstructure of mechanical alloyed FeCo based alloys will also be reported and a comparison of the properties of alloys processed by the three techniques is provided.

#### 3:00 PM Invited

#### Group IV Element-Based Magnetic Semiconductors: Frank Tsui<sup>1</sup>; <sup>1</sup>University of North Carolina, Dept. of Physics & Astron., Chapel Hill, NC 27599 USA

The prospect of integrating electron charge and spin degrees of freedom has invigorated the field of spin-polarized electronics, 'spintronics'. To date, most activities are focused on Mn doped compounds of group III-V and II-VI families, where high quality but low TC ferromagnetic epitaxial films have been grown. But there is considerable interest in higher TC materials, particularly group IV elementbased magnetic semiconductors, owing to their potential compatibility with current Si-based processing technology. In order to achieve this, doping levels in access of several at. % and relatively high processing temperature would be some of the basic requirements. However, they also have been the main obstacles for the synthesis, since they tend to promote phase separation of dopant rich compounds, resulting in disordered and inhomogeneous materials. We describe combinatorial MBE synthesis of stable epitaxial films of doped Si and Ge using two or more dopants, and the resulting characteristic properties of the systems. In-situ RHEED experiments, and ex-situ x-ray diffraction, x-ray fluorescence spectroscopy and cross-sectional high resolution transmission electron microscopy measurements show that the presence of several dopants alters the local energetics and kinetics so that the tendency to phase separate can be controlled during non-equilibrium synthesis. The magnetic and transport properties of the systems exhibit high TC, large magnetoresistance effects, and shallow level conduction with low-temperature behavior dominated by variable range hoping, all of which can be controlled systematically by the doping concentration. The viability of these materials for spintronics has been demonstrated in heterojunction diodes made from these materials exhibiting large magnetization-dependent rectification effects.<sup>1</sup> <sup>1</sup>F. Tsui, L. Ma, L. He, Appl. Phys. Lett. 83 (5), Aug. 4, 2003.

#### 3:30 PM

Role of Altering the Primary Solidification Field on Tailored Pr9Fe91-xBx Nanocomposites: Y. Q. Wu<sup>1</sup>; *M. J. Kramer*<sup>1</sup>; *Z.* Chen<sup>2</sup>; B. M. Ma<sup>2</sup>; <sup>1</sup>Iowa State University, Ames Lab., Dept. of Matls. Sci. & Engrg., 37 Wilhelm Hall, Ames, IA 50011 USA; <sup>2</sup>Magnequench Technology Center, Research Triangle Park, NC 27709 USA Altering the primary solidification field is one means of controlling the nanostructure in rapidly solidified alloys. We investigated the effect of the B:Fe on  $Pr_9Fe_{91-x}B_x$  (x=5-12) nanocomposites. This composition range moves the primary solidifying phases from  $R_2Fe_{14}B/\alpha$ -Fe to  $R_2Fe_{14}B/Fe3B$  with minor  $Pr_2Fe_{23}B_3$ . Increasing B:Fe increases coercivity (H<sub>ci</sub>) but decreases remanence (B<sub>r</sub>) and energy product (BH)<sub>max</sub>. For instance alloys of  $Pr_9Fe_{86}B_5$  and  $Pr_9Fe_{79}B_{12}$  are 9.54 kG, 6.5 kO<sub>e</sub>, 14.4 MGO<sub>e</sub> and 7.06 kG, 7.1 kO<sub>e</sub>, 6.5 MGO<sub>e</sub>, respectively. TEM observations show that the  $Pr_9Fe_{86}B_5$  alloy has smallest grain size distribution (~ 13 nm for soft phase, ~35 nm for hard phase). The grain size of hard phase significantly increases when increasing the B content, especially for the alloys with more than 10 at% B. Besides X-ray analyses, EDS analyses further confirmed the formation of  $Pr_2Fe_{23}B_3$  phase in higher B content alloys (B=8.5~10.5 at.%).

#### 3:50 PM

Plasma Deposition of Ultrathin Films on Nanoparticles/ Nanotubes for Novel Engineering Applications: Donglu Shi<sup>1</sup>; He Peng<sup>1</sup>; Mark Schulz<sup>2</sup>; David Mast<sup>2</sup>; Wim Van Ooij<sup>1</sup>; <sup>1</sup>University of Cincinnati, Dept. of Chem. & Matls. Engrg., Cincinnati, OH 45221 USA; <sup>2</sup>University of Cincinnati, Dept. of Mech. Engrg., Cincinnati, OH 45211 USA; <sup>3</sup>University of Cincinnati, Dept. of Physics, Cincinnati, OH 45221 USA

The development of surface nanostructures will be one of the key engines that drive our technological society in the 21-century. This rapidly growing area focuses on tailoring a nanoparticle surface structure for specific and unique properties. The "nano-scale" engineering has produced such materials as layered composite semiconductors for high speed electronic devices, blue lasers and diodes and vertical cavity lasers that read and write our CDs, and highly conductive, but low loss thin films for panel displays. The broad range of these properties due to nano surface structures can include electro-magnetic conductivities, uniformity, index of refraction, high reflectance, low absorption, stress, and the adhesion of the film structure to the substrate. In these applications, the nanostructure involves an ultrathin film on the nanoparticle surface that can also be tailored into multilayers by our unique plasma technique. Both the substrate nanoparticle and the ultrathin film serve certain functionalities for specific applications. In this presentation, critical issues in the plasma deposition of thin films on various nanoparticles including carbon nanotubes will be discussed. In particular, a novel application in biosensor area will be presented with recent results on coating of nano magnetic particles. With a thin layer of polymer functional group on the nanoparticle surface, special bio films can be attached for detecting specific virus in food, serving as an effective tool for instant food test.

#### 4:10 PM

Characterization of Mechanically-Milled Nanocrystalline Powders of NiFe and FeCo: *Ian Baker*<sup>1</sup>; Elizabeth Parrish<sup>1</sup>; Basavaraju Shashishekar<sup>1</sup>; <sup>1</sup>Dartmouth College, Thayer Sch. of Engrg., 8000 Cummings Hall, Hanover, NH 03755 USA

Nanocrystalline powders of both NiFe and FeCo were prepared by mechanically alloying of elemental powders using a high energy ball mill. The microstructural evolution was studied as a function of milling time and subsequent annealing using X-ray diffractometry, transmission electron microscopy, scanning electron microscopy and differential scanning calorimtery. The magnetic behavior of the specimens was characterized using both a vibrating sample magnetometer and a magnetic force microscope. A reduction in grain size coupled with an increase in coercivity was observed as function of milling time. Interestingly a decrease in the coercivity below a grain size of 50-100nm, as noted in a number of other soft magnetic alloys by Herzer (G. Herzer, J. Magn. Magn. Mat., 112 258-262, (1992)) was not observed. This research was funded by NIST grant 60NANB2D0120 and NSF grant DMR-0139085.

#### 4:30 PM

Chemical Vapor Synthesis of Iron and Iron Oxide Nanoparticles: Vijay K. Vasudevan<sup>1</sup>; James M. Vetrone<sup>2</sup>; G. R. Bai<sup>2</sup>; Loren J. Thompson<sup>2</sup>; U. Welp<sup>2</sup>; Jeffrey A. Eastman<sup>2</sup>; <sup>1</sup>University of Cincinnati, Chem. & Matls. Engrg., Cincinnati, OH 45221-0012 USA; <sup>2</sup>Argonne National Laboratory, Matls. Sci. Div., Argonne, IL 60439 USA

Iron and iron oxide nanoparticles were synthesized by chemical vapor decomposition of n-butylferrocene precursor gas in a hot-walled deposition system. The effects of variations in reactor chamber pressure, temperature, precursor flow-rate, and oxygen:-nitrogen supply gas ratio on the structure, composition, size and size distribution of the particles were studied. The nanoparticles produced in the reactor chamber were dispersed directly into ethylene glycol without exposure to air, and then characterized by x-ray and electron diffraction, nanoprobe energy-dispersive x-ray spectroscopy, and HRTEM. The results indicate that nanoparticles with diameters ranging from 3 to 40 nm can be produced controllably. Of the different processing variables studied, oxygen content in the flow gas was observed to have the most dominant effect on the structure, composition, and size of the particles. Without oxygen,  $\gamma$ -iron nanoparticles with an fcc structure and diameters of 3-10 nm were observed. The presence of even a small amount of oxygen in the flow gas led to the formation of fcc Fe<sub>3</sub>O<sub>4</sub> (magnetite) nanoparticles, together with core-shell structures consisting of a yiron metallic core surrounded by a shell of iron oxide. With increasing oxygen flow, the nanoparticles were observed to increase in size. Concomitantly, for larger particles the metallic core was found to exhibit the bcc  $\alpha$ -iron structure. At still higher oxygen concentrations, coarse particles of β-Fe<sub>2</sub>O<sub>3</sub> particles were observed, followed by α-Fe<sub>2</sub>O<sub>3</sub> particles. Magnetic properties of nanoparticles synthesized under different conditions were measured. The mechanisms of the synthesis of the nanoparticles and their structure, composition, and magnetic properties will be discussed, as will the potential for self-assembly of these particles into functional architectures.

# 4:50 PM

Dependance of GMR on Film Thickness in Electrodeposited Nanogranular Cu-Co Thin Films: Gyana R. Pattanaik<sup>1</sup>; Steffen Melcher<sup>2</sup>; Ulrich K. Rossler<sup>2</sup>; K. Nenkov<sup>2</sup>; K.-H. Muller<sup>2</sup>; Subhash C. Kashyap<sup>1</sup>; Dinesh K. Pandya<sup>1</sup>; <sup>1</sup>Indian Institute of Technology, Dept. of Physics, Hauz Khas, New Delhi 110016 India; <sup>2</sup>IFW Dresden, Dresden 01171 Germany

Giant magneto-resistance (GMR) in granular thin films is believed to be largely dependent on the spin dependent scattering at the magnetic particle-nonmagentic host interface. At low film thickness, comparable to the spin dependent mean free path, the surface scattering is expected to influence the GMR. In this work we present our attempt to study the GMR and magnetic properties of Cu-Co thin films as a function of film thickness. We have used electrochemical deposition to grow good quality Cu-Co thin films of suitable thickness for the present study. The films were deposited onto Cu-coated (~10 nm) alumina substrates from a single sulfate bath. The thickness of the film was measured by optical as well as stylus techniques and was calibrated with the deposition time. The films were annealed at 425 C for 30 min to optimize the GMR. A maximum GMR of ~15 % was found in thicker film (~ 1 µm) at 10 K. The GMR was found to decrease with the film thickness and the decrease was more rapid for thickness below 100 nm. The ZFC-FC curves indicate that the magnetic particles in the nanogranular films have a range of blocking temperatures (corresponding to a range of sizes) which extends at least to room temperature for films thicker than 100 nm. A combined effect of interparticle interactions and growing magnetic particle size seems to be more likely. The average magnetic particle size estimated from the superparamagnetic behavior (without considering the interaction effects) of the films below a thickness of 100nm was in the range of 8-12 nm and that calculated from XRD line-widths was in the range of 7-9 nm.

# 5:10 PM

Electrical and Magnetoresistance Properties of Hexaferrite FeCo/Fe Nanocomposites Prepared by In Situ Solid-Gas Reduction: *C. Sudakar*<sup>1</sup>; G. N. Subbanna<sup>1</sup>; T. R. Narayanan Kutty<sup>1</sup>; <sup>1</sup>Indian Institute of Science, Matls. Rsch. Ctr., Sir C.V. Raman St., Bangalore, Karnataka 560012 India

Nanocomposites containing Fe or FeCo dispersed in hexaferrites (M, W and Y-phase) are realized by the heterogeneous solid-gas reduction under H2+N2. TEM studies reveal that metal nanoparticles precipitate coherently as thin flakes along the 'a-b' planes of hexaferrite lattice above the characteristic reduction temperature, TR >375°C. complex permittivity and permeability are enhanced with alloy content upto ~50 and ~1.2, respectively, in the broad frequency range of 4-18 GHz and renders these composites useful as broadband electromagnetic microwave absorbers. The electrical resistivity measurements reveal that the charge transport mechanism in the composite is by tunneling, whereas samples having higher fractions of alloy particles show metallic behavior due to percolation. Controlled reduction at TR leads to apparent metal-insulator changeover in r vs. T plot. This changeover persists even in presence of high magnetic field (7T) and is ascribed to the percolation of metal particles due to the difference in the coefficient of thermal expansion between the constituents. Further in the insulator regime, negative magnetoresistance of ~5-6% is observed. These nanocomposites also exhibit non-linearity in the Current-Voltage (I-V) characteristics with a ranging from 1.2 to 1.4 at different temperatures.

# 5:30 PM

 Sudhakar<sup>1</sup>; K. P. Rajeev<sup>1</sup>; <sup>1</sup>Indian Institute of Technology, Dept. of Physics, Kanpur, Uttar Pradesh 208016 India

We report here the interesting results of magneto-transport and electrical resistivity ( $\rho$ ) in the temperature range of 4.2 to 320 K and in the presence of magnetic fields up to 10 T on Ru-doped bilayered manganite system La<sub>1.2</sub>Ca<sub>1.8</sub>Mn<sub>2.x</sub>Ru<sub>x</sub>O<sub>7</sub> (0≤ x≤ 1.0). We find that the Ru-doping is found to affect the magneto-transport properties considerably. The magnetoresistance (MR), defined as [ $\rho$ (B)- $\rho$ (0)]/ $\rho$ (0) has been found to increase with Ru doping from 58% to 64% up to x = 0.1 and decreases marginally to 45% for the x = 1.0 sample. The  $\rho$  (B, T) data were analyzed by fitting the data to the both power law equation  $\rho = \rho_0$  - AB<sup>n</sup> and also to the exponential variations. The isothermal MR versus B curves taken up to ±10 T are highly symmetrical about the y-axis and their curvature changes from concave upwards-like behaviour to that of a parabolic-like one as the temperature increases.

# Nanostructured Materials for Biomedical Applications: Session II

Sponsored by: Electronic, Magnetic & Photonic Materials Division, EMPMD-Thin Films & Interfaces Committee *Program Organizers:* Roger J. Narayan, Georgia Tech, School of Materials Science and Engineering, Atlanta, GA 30332-0245 USA; J. Michael Rigsbee, North Carolina State University, Department of Materials Science and Engineering, Raleigh, NC 27695-7907 USA; Xinghang Zhang, Los Alamos National Laboratory, Los Alamos, NM 87545 USA

Monday PM	Room: 219A
March 15, 2004	Location: Charlotte Convention Center

Session Chairs: Douglas B. Chrisey, Naval Research Laboratory, Plasma Procg. Sect., Washington, DC 20375-5345 USA; J. Michael Rigsbee, North Carolina State University, Dept. of Matls. Sci. & Engrg., Raleigh, NC 27695-7907 USA

#### 2:00 PM Invited

Engineering the Nanobiointerface: The Route to 21st Century Biomaterials: Buddy D. Ratner<sup>1</sup>; <sup>1</sup>University of Washington, UWEB, Dept. of Bioengrg. & Chem. Engrg., Washington Rsch. Foundation, Seattle, WA 98195 USA

Implantable medical devices, and the biomaterials that comprise them, are measured on macro scales (centimeters). Yet the biocompatibility of such devices may be dictated by phenomena best described at nanometer dimensions. Biomedical implants and the NSFfunded University of Washington Engineered Biomaterials (UWEB) Engineering Research Center will be introduced. The classical definition of biocompatibility will be contrasted to a newer definition embracing nanomolecular concepts. Biological data on the in vivo healing responses of mammals to matricellular proteins such as osteopontin, thrombospondin 2 and SPARC will be presented with an emphasis on exploiting the special reactivity of such proteins. First, non-specific protein adsorption must be inhibited. Strategies to achieve this design parameter will be presented. Then methods to deliver the specific protein signals will be addressed. An imprinting approach and a selfassembly approach will be described. Finally, speculation on how such materials that precisely control interfacial biological reactions will be used in medicine will complete this lecture. Modern surface analysis techniques that can address the complexity of a functional nanobiointerface will be highlighted to define nanostructures and probe for order and organization.

#### 2:40 PM Invited

**Complex Behavior of Metal Ions Near Biological Polyelectrolytes**: *Gerard C.L. Wong*<sup>1</sup>; <sup>1</sup>University of Illinois, Matls. Sci. & Engrg., 1304 W. Green St., Urbana, IL 61801 USA

Electrostatics in aqueous media is commonly understood in terms of screened Coulomb interactions, where like-charged objects, such as polyelectrolytes, always repel. These intuitive expectations are based on mean field theories, such as the Poisson-Boltzmann formalism, which are routinely employed in colloid science and computational biology. Like-charge attractions, however, have been experimentally observed in a wide variety of systems. Intense theoretical scrutiny over the last 30 years has suggested that counterions play a central role, but no consensus exists for the precise mechanism. We have examined the organization of multivalent ions on actin filaments (a well-defined biological polyelectrolyte) using synchrotron x-ray diffraction, and discovered a new collective counterion mechanism. We will also present recent results on the influence of counterion valence and dynamics on polyelectrolyte self-organization, and along a more general compass, the implications of entropically controlled electrostatics for problems in biomineralization and biomedical applications.

## 3:20 PM Invited

Nanoshells: Tunable Plasmon-Resonant Nanoparticles With Biomedical Applications: Naomi Halas<sup>1</sup>; <sup>1</sup>Rice University, Elect. & Computer Engrg., MS 366, Houston, TX 77005 USA

Nanoshells are dielectric core-metal shell nanoparticles with a strong resonant optical absorption that can be tuned systematically across the spectrum by varying the relative size of the nanoparticle's core and shell layers. For biophotonic applications, the optical absorption of nanoshells can be tuned to the near infrared "water window", making them extremely strong absorber/scatterers of infrared light in a wavelength region where remarkably few optically active materials are available. When the outer metal layer is made of gold, the nanoparticles become highly biocompatible, and ideal for a wide range of biomedical applications. Together with Rice bioengineering collaborator Jennifer West, we have recently demonstrated a variety of such applications of nanoshells, including a near-instantaneous whole blood immunoassay, a photothermally triggerable drug delivery device, and a highly localized photothermal cancer therapy, which will be described.

#### 4:00 PM Invited

#### **Molecular Simulation of Protein-Surface Interactions**: *Robert A. Latour*<sup>1</sup>; <sup>1</sup>Clemson University, Dept. of Bioengrg., 501 Rhodes Rsch. Ctr., Clemson, SC 29634 USA

The ability to simulate protein-surface interactions provides enormous potential for nanoscale biomaterial surface design. Because of the size of the systems involved, molecular modeling of protein adsorption behavior must be approached using force field-based methods. Force fields, however, are designed for specific applications and they are generally not transferable. Accordingly, a force field designed to represent protein behavior in solution may not accurately represent the adsorption of proteins to surfaces. As a further complication, when it comes to protein adsorption, it is still unclear what molecular behavior a properly tuned force field should even predict. In order to address these complex issues, we are developing complementary experimental and computational methods using model peptide-surface systems to assess existing force fields and modify them if necessary to accurately simulate protein adsorption behavior. An overview of the issues involved and our approach for force field development will be presented.

#### 4:40 PM Invited

Surface Engineering Strategies to Control Cell Adhesion and Function in Biomaterial Applications: *Andres J. Garcia*<sup>1</sup>; <sup>1</sup>Georgia Institute of Technology, Mech. Engrg., 315 Ferst Dr., Atlanta, GA 30332-0363 USA

Cell adhesion to adsorbed proteins or adhesive sequences engineered on surfaces is critical to biomedical and biotechnological applications. Cell adhesion is primarily mediated by integrin receptors. In addition to anchoring cells, supporting cell spreading and migration, integrins provide signals that direct cell survival, proliferation, and differentiation. We have developed two biomolecular strategies for the engineering of surfaces to control integrin binding and cell adhesion in order to direct cell function. The first approach focuses on surfaces presenting well-defined chemistries that control protein adsorption to modulate integrin binding in order to potentiate cell adhesion and bone cell differentiation. In a second approach, we have engineered bioinspired surfaces presenting controlled ligand densities that promote the binding of specific integrin receptors and direct cell adhesive interactions. These surface engineering strategies provide a basis for the rational design of robust surfaces that tailor adhesive interactions.

#### 5:20 PM Invited

Mechanical Behavior of Human Stratum Corneum Tissue: Implications for Transdermal Drug Delivery Technologies: *Reinhold Horst Dauskardt*<sup>1</sup>; Kenneth Wu<sup>1</sup>; Marc Taub<sup>1</sup>; <sup>1</sup>Stanford University, Dept. of Matls. Sci. & Engrg., Bldg. 550, Stanford, CA 94305-2205 USA

The mechanical and fracture behavior of soft tissues is often crucial to their function, with the underlying cellular and extracellular structures being optimized for the required properties. These structures contain microstructural features at length scales ranging from microns to nanometer that profoundly effect their properties. The outermost layer of skin, or stratum corneum (SC), provides mechanical protection and a controlled permeable barrier to the external environment. The mechanical behavior of SC is also important for a range of emerging transdermal drug delivery technologies. For effective drug delivery, good initial and long-term adhesion to SC, clean removability, and skin and drug compatibility are required. However, an understanding of the mechanics and chemical determinants of adhesion to the soft dermal layer, together with quantitative and reproducible test methods for measuring adhesion, are lacking. We present a mechanics approach to study the delamination resistance and mechanical behavior of human SC tissue. The debond energy and cohesive strength characteristics of human SC are described in terms of the underlying cellular and intercellular lipid structures. The effects of hydration, temperature, and lipid-extraction upon SC tissue were explored, and the highly anisotropic nature of SC mechanical and fracture behavior will be discussed with reference to the underlying cellular structure. Implications for emerging transdermal drug delivery technologies is considered.

# Phase Stability, Phase Transformation, and Reactive Phase Formation in Electronic Materials III: Session II

Sponsored by: Electronic, Magnetic & Photonic Materials Division, Structural Materials Division, EMPMD/SMD-Alloy Phases Committee

Program Organizers: C. Robert Kao, National Central University, Department of Chemical and Materials Engineering, Chungli City 32054 Taiwan; Sinn-Wen Chen, National Tsing-Hua University, Department of Chemical Engineering, Hsinchu 300 Taiwan; Hyuck Mo Lee, Korea Advanced Institute of Science & Technology, Department of Materials Science & Engineering, Taejon 305-701 Korea; Suzanne E. Mohney, Pennsylvania State University, Department of Materials Science & Engineering, University Park, PA 16802 USA; Michael R. Notis, Lehigh University, Department of Materials Science and Engineering, Bethlehem, PA 18015 USA; Douglas J. Swenson, Michigan Technological University, Department of Materials Science & Engineering, Houghton, MI 49931 USA

Monday PM	Room: 2	14		
March 15, 2004	Location:	Charlotte	Convention	Center

Session Chairs: Doug Swenson, Michigan Technological University, Dept. of Matls. Sci. & Engrg., Houghton, MI 49931 USA; Rainer Schmid-Fetzer, Technical University of Clausthal, Inst. of Metall., Clausthal-Zellerfeld D-38678 Germany

#### 2:00 PM Invited

Thermodynamic Stability of Nitride Semiconductors (GaN, InN): Rainer Schmid-Fetzer<sup>1</sup>; Jochen Unland<sup>1</sup>; Boguslaw Onderka<sup>2</sup>; <sup>1</sup>Technical University of Clausthal, Inst. of Metall., Robert-Koch-Str. 42, Clausthal-Zellerfeld D-38678 Germany; <sup>2</sup>Polish Academy of Sciences, Inst. of Metall. & Matls. Sci., Reymonta 25, Krakow 30-059 Poland

The comparison of the thermodynamic phase stability of GaN and InN is in the focus of this presentation. Distinct differences are pointed out for these two materials, which are otherwise very similar, both crystallize in their stable form in the wurtzite (hexagonal) structure with P63mc space group. The decomposition of GaN and InN powder was studied experimentally using two different customized thermogravimetric methods, dynamic oscillation TGA, and isothermal stepping TGA for a higher resolution of the decomposition start. A reproducible mass gain at slightly lower temperature is only found for GaN, it suggests the equilibrium temperature to be at  $1110 \pm 10$  K under 1 bar of nitrogen. By contrast, decomposition start of InN was found consistently at 773  $\pm$  5 K, which is considered to be substantially higher than the equilibrium temperature based on our CALPHAD type thermodynamic analysis of all available phase equilibrium and thermodynamic data. This analysis includes the determination of the absolute entropies of GaN and InN based on a Debye- and Einstein-analysis of the experimental data on the heat capacity. An explicit equation for the fugacity-pressure relation of nitrogen, f(P), is developed. This is crucial because f can be several orders of magnitude higher than P for the high pressures encountered during GaN and InN decomposition. Based on the consistent thermodynamic descriptions various T-P-x phase diagrams are calculated. They indicate a good overall agreement between the different types of experimental data (calorimetric, vapor pressure, phase equilibrium) for Ga-N but not for In-N. The highpressure part of the decomposition pressure of GaN is actually predicted from the thermodynamic model in good agreement with the experimental data.

#### 2:20 PM Invited

Interface Reaction Between Ni and Amorphous SiC: Sungtae Kim<sup>1</sup>; J. H. Perepezko<sup>1</sup>; Z. F. Dong<sup>2</sup>; A. S. Edelstein<sup>3</sup>; <sup>1</sup>University of Wisconsin, Dept. of Matls. Sci. & Engrg., 1509 Univ. Ave., Madison, WI 53706 USA; <sup>2</sup>University of Alberta, Dept. of Elect. Engrg., Edmonton, AB T6G 2V4 Canada; <sup>3</sup>US Army Research Laboratory, Sensor Integration Branch, AMSRL-SE-SS, 2800 Powder Mill Rd., Adelphi, MD 20783 USA

Multilayered Ni/amorphous(a)-SiC samples prepared by ion-beam deposition with equal thicknesses of the Ni and a-SiC layers and a wavelength of 100 nm, have been examined to identify the controlling kinetics for reactive diffusion between Ni and a-SiC. In the initial stage of the reaction, a distinct amorphous layer adjacent to the original Ni/ a-SiC interface forms under metastable conditions. The Ni diffusion into the a-SiC layer results in formation of the distinct amorphous layer growing with parabolic growth kinetics. The diffusion of Si and C from the a-SiC phase results in formation of the NiSi phase as an intermediate phase within the original Ni layer. The examination of the amorphous phase stability, by a thermodynamic model for supercooled liquids, reveals a Ni and a-SiC two phase equilibrium at low temperature. The support of ONR (N00014-02-1-0004) is gratefully acknowledged.

# 2:40 PM Invited

**UBM Diffusion and Integrity Studies on Copper/Low-k Dielectrics**: *Seung Wook Yoon*<sup>1</sup>; Vaidyanathan Kripesh<sup>1</sup>; Wenyu Gao<sup>1</sup>; Yong Jie Jeffrey Su<sup>1</sup>; Mahadevan Krishna Iyer<sup>1</sup>; <sup>1</sup>IME, Singapore Sci. Park II, Singapore 1176685 Singapore

As the semiconductor speed increases continuously, more usage of new polymeric low-k dielectric materials to enhance the performance in Cu chip has taken place in last few years. The objective of this study is to investigate the UBM characterization with low-k dielectric material used in damascene copper integrated circuits. This paper focuses on electroless Ni/Au, Cu/Ta/Cu, Cu post and Ti/Ni/Cu/Au UBM fabrication on 8 inch dual damascene Cu wafers and flip chip package reliability with Pb-bearing and Pb-free solders. Diffusion study and bump shear test was carried out to evaluate the bump bonding and interfacial microstructure. In order to investigate the thermal stability of UBM system with various solders, multiple reflow and HTSTwere performed and their each interface between solder and UBM was observed with optical and electron microscopy (SEM and TEM), respectively. Failures observed and mechanisms will be reported in the full paper.

#### 3:00 PM Cancelled

#### Interfacial Reaction of Ni(Ti)/Si0.8Ge0.2 Films

# 3:15 PM

Bulk and Thin Film Studies of the Ni/GaP System: Wai Can Chan<sup>1</sup>; *Douglas J. Swenson*<sup>1</sup>; <sup>1</sup>Michigan Technological University, Dept. of Matls. Sci. & Engrg., 1400 Townsend Dr., Houghton, MI 49931 USA

Gallium phosphide has received interest as a potential material for high temperature microelectronics. It is well known that contact metallizations have a tendency to interact chemically with III-V semiconductors during device processing. Several studies of phase equilibria and chemical reactions between near noble metals and GaP have been reported in the literature; however, to date no such study has been conducted for the common metallization material Ni. In the present study, bulk phase equilibria and reactive thin film phase formation have been investigated in the Ga-Ni-P system. Phase equilibria have been established at 700°C, using X-ray diffraction and electron probe microanalysis. Ni (50 nm) films deposited on GaP(001) substrates were characterized using transmission electron microscopy and Auger electron spectroscopy depth profiling, subsequent to reaction temperatures and times ranging from 25-700°C and 30 seconds to 2 days. respectively. Equilibrium conditions (formation of NiGa and Ni<sub>2</sub>P) are reached after annealing at 500°C for 30 s. Both equilibrium reaction products exhibit orientation relationships with respect to the GaP substrate that are similar to those observed between isostructural metal-III and metal-V compounds and the III-V semiconductors. The diffusion paths exhibited by the Ni/GaP thin film couples are rationalized in terms of diffusion theory and the newly established Ga-Ni-P phase diagram.

#### 3:30 PM

Preparation and Characterization of Sputtered Copper Films Containing Immisicible Tungsten Carbide: Jinn P. Chu<sup>1</sup>; Yung Yen Hsieh<sup>1</sup>; C. H. Lin<sup>2</sup>; T. Mahalingam<sup>3</sup>; <sup>1</sup>National Taiwan Ocean University, Inst. of Matls. Engrg., 2, Pei-Ning Rd., Keelung 202 Taiwan; <sup>2</sup>Chin-Min College, Dept. of Elect. Matls., 110, Syuefu Rd., Toufen Twp., Miaoli 351 Taiwan; <sup>3</sup>Alagappa University, Dept. of Physics, Karaikudi-630 003 India

Since Cu and WC are mutually immiscible, copper films containing tungsten carbide is likely to be a noble material for applications. In this study, Cu-WC, films are prepared by R.F. magnetron sputter deposition technique on glass substrate and then annealed at 200°C, 400°C, 530°C and 650°C for 1 hr. With careful control of processing conditions, the tungsten and carbon concentrations in Cu films can be up to 12.2 and 7.4 at.%, respectively. Nonequlibrium supersaturated solid solutions of WC, in Cu with nanocrystalline microstructures are observed in asdeposited Cu-WC<sub>x</sub> films. Variations in lattice parameters for as-deposited and as-annealed Cu-WCx films evidenced by XRD again indicate that solute tungsten and carbon atoms are in the solid solution with copper. XRD results of Cu-WCx films indicate that Bragg peaks of copper shift to low angle side with increasing tungsten and carbon content. Microstructures of both as-deposited and as-annealed Cu-WCx films are examined by SEM and TEM. Microstructure reveal that finer film grains go with tungsten carbide content. Ultra-microhardness results show an increase in hardness with tungsten and carbon contents for both as-deposited and as-annealed films. Electrical resistivity measurements reveal that resistivity of as-deposited Cu-WC, films increase with tungsten carbide content and decrease with annealing temperature.

#### 3:45 PM Break

#### 4:00 PM Invited

Line Width Dependence of Grain Structure and Stress in Damascene Cu Lines: Young-Chang Joo<sup>1</sup>; Jong-Min Paik<sup>1</sup>; Jung-Kyu Jung<sup>1</sup>; Hyun Park<sup>2</sup>; <sup>1</sup>Seoul National University, Sch. of Matls. Sci. & Engrg., Rm. # 30-503, Seoul 151-744 S. Korea; <sup>2</sup>Seoul National University, Ctr. for Microstructure Sci. of Matls., Rm. #30-503, Seoul 151-744 S. Korea

In damascene Cu lines complicated grain structures were observed because of the grains grown from the bottom as well as the sidewall of the trenches. Furthermore, grain growth in damascene Cu, which confined by dielectric materials, causes a stress due to the annihilation of grain boundaries. Grain structure and stress in 0.13 to 2  $\mu$  damascene lines were analyzed using TEM, EBSD and XRD. For the sub-micron lines, the grain size at the top of trenches was larger than that of inner. It is because the overburden layer affects the grain growth within the trenches and this effect was confirmed by the grain growth simulation using Monte Carlo method. The stress increase as the line width and it is indicated that the stress is related to the microstructure. Through comparing results from experiment and finite element analysis, relationship between microstructure and stress and its dependence on process condition were quantified.

# 4:20 PM Invited

Thermal Stability Study of Sputtered Cu Films with Various Insoluble Elements: J. P. Chu<sup>1</sup>; Chon-Hsin Lin<sup>2</sup>; T. Mahalingam<sup>3</sup>; Y. Y. Hsieh<sup>1</sup>; S. F. Wang<sup>4</sup>; <sup>1</sup>National Taiwan Ocean University, Inst. of Matls. Engrg., No. 2, Pei-Ning Rd., Keelung 202 Taiwan; <sup>2</sup>Chin-Min College, Dept. of Elect. Matls., No. 110, Shyue-Fun Rd., Tou-Fen, Miao-Li 351 Taiwan; <sup>3</sup>Alagappa University, Dept. of Physics, Karaikudi 630 003 India; <sup>4</sup>National Taipei University of Technology, Dept. of Matls. & Minerals Resources Engrg., Taipei 106 Taiwan

Copper is an attractive material for metallization in microelectronics, owing to its low resistivity and high reliability against electromigration compared with Al and its alloys. However, Cu diffuses readily into Si and SiO<sub>2</sub>, resulting in the formation of copper silicide compounds at low temperatures. Doping the Cu with immiscible elements has been investigated in the present study in order to develop new interconnect materials for advanced metallization. The thermal annealing behavior of the insoluble binary Cu-W, Cu-Mo, Cu-C and Cu-Nb alloy films was studied and compared with that of a pure sputtered Cu film. Magnetron co-sputtered copper films deposited on Si substrates with insoluble solute concentration compositions in the range of 2.0-11.3 at% were annealed in vacuum at 200, 400, 530 and 800°C for 1 hr. Twins are observed and they are investigated by means of focused ion beam (FIB) and transmission electron microscopy (TEM) techniques. Thus, according to the FIB and TEM images of as-deposited and 400°C-annealed pure Cu film confirm the existance of twins and the formation of these twins are attributed to the intrinsic low stacking fault energy. Twins existed in pure Cu film and formed during the initial stage of annealing period may provide an additional diffusion path for copper silicide formation. Thermal annealing of Cu-W, Cu-Mo and Cu-Nb alloy films increases the stacking fault energy and results in a low twin density whereas the Cu-C films have no apparent influence on reducing the twin density. The effects of W, Mo, Nb and C on the thermal stability of Cu film were analyzed by X-ray diffraction, secondary ion mass spectroscopy and differential scanning calorimetry and the results are discussed.

# 4:40 PM Invited

Development of Cu-Zn-Al Alloy Sheets with Low Thermal-Expansion Due to Martensitic Transformation and Cold-Rolling: Jijie Wang<sup>2</sup>; Toshio Ohmori<sup>1</sup>; Yuji Sutou<sup>1</sup>; *Ryosuke Kainuma*<sup>1</sup>; Kiyohito Ishida<sup>1</sup>; <sup>1</sup>Tohoku University, Dept. Matls. Sci., Aoba-yama 02, Sendai, Miyagi 980-8579 Japan; <sup>2</sup>Northeastern University, Sch. of Matls. & Metall., Shenyang 110004 China

Recently, we reported that the control of stress-induced (SI) martensitic transformation due to cold working of the Cu-Zn-Al polycrystalline alloy results in low thermal expansion (LTE). This new type of LTE material is easily fabricated by conventional cold-rolling, and the coefficient of thermal expansion (CTE) in the range from about 0 to 32\*10-6 K-1 can be obtained by controlling the reduction ratio. In this paper, the effects of grain size, volume fraction of the  $\alpha$ (fcc) phase in the  $\beta$ (bcc) matrix and thermal stability on LTE properties of Cu-Zn-Al shape memory (SM) alloys induced by cold-rolling were investigated by dilatometry, optical microscopy, differential scanning calorimetry and electric conductivity measurements. The alloys with the larger grains showed a superior two-way memory (TWM) effect, wider LTE temperature intervals with excellent thermal stability under 80°C, and reproducibility. The  $\alpha+\beta$  two-phase alloys also exhibited a good combination of cold-workability and LTEproperties.

# 5:00 PM

#### Bromine and Chloride Induced Degradation of Gold-Aluminum Bonds: Ker-Chang Hsieh<sup>1</sup>; Min-Hsien Lue<sup>1</sup>; Chen-Town Huang<sup>1</sup>; Sheng-Tzung Huang<sup>1</sup>; <sup>1</sup>National Sun Yat-sen University, Inst. of Matls. Sci. & Engrg., Kaohsiung Taiwan

The presence of bromine in flame retardant epoxies accelerates the degradation of gold-aluminum wire bonds. In this study, 5wt% 2,6dibromophenol added in regular molding compound applied in the test samples. The thermal aging treatment was held at 175C and 205C respectively in oven for up to 1008 hours. The intermetallic degrading microstructure examined at different aging period. In order to examine the detail degrading microstructure, bulk AuAl4 and Au5Al2 phases were prepared and reacted with molding compound at 250C. This could help the understanding of degradation mechanism. The analysis of intermetallic phases were examined by the Jeol Superprobe JXA-8900R under WDS mode. A similar chloride degrading study performed by adding Tetrachlorobisphenol A in regular molding compound. The results show that bromine attacked Au4Al phase first and then Au5Al2 phase. The chloride reacted with Au4Al phase only.

#### 5:15 PM

Crystallization and Failure Behaviors of Ta-Ni Nanostructured/ Amorphous Diffusion Barriers for Copper Metallization: Jau Shiung Fang<sup>1</sup>; Giin Shan Chen<sup>2</sup>; 'National Huwei Institute of Technology, Dept. of Matls. Sci. & Engrg., 64 Wunhua Rd., Huwei, Yunlin 632 Taiwan; <sup>2</sup>Feng Chia University, Dept. of Matl. Sci., Taichung 400 Taiwan

This work examines the thin-film properties and diffusion barrier behaviors of thin Ta-Ni films, aiming at depositing highly crystallization-resistant and highly conductive diffusion barriers for Cu metallization. Structure analyzing indicates that the deposited Ta-Ni films indeed have a glassy structure and are free from highly resistive intermetallic compounds, thus giving a low resisitivity of 15.9 mW-cm. Examining Si/Ta-Ni(50nm)/Cu stacked samples by using 4-point probes and XRD reveals that thermally induced failure of amorphous Ta-Ni barriers are triggered by the barrier's crystallization at temperatures around 500°C. The failure temperature for 50 nm Ta-Ni thin film was 650°, which is higher than that of crystallization temperature. The effectiveness of the nanostructure/amorphous Ta-Ni thin film thus can be substantially enhanced by effectively blocking diffusion of copper towards the underlying silicon.

# Processing, Microstructure and Properties of Powder-Based Materials: Session I

Sponsored by: Materials Processing and Manufacturing Division, MPMD-Powder Materials Committee

*Program Organizers:* K. B. Morsi, San Diego State University, Department of Mechanical Engineering, San Diego, CA 92182 USA; James C. Foley, Los Alamos National Laboratory, Los Alamos, NM 87545 USA; Karl P. Staudhammer, Los Alamos National Laboratory, Nuclear Materials Technology Division, Los Alamos, NM 87545 USA

Monday PM	Room: 208B
March 15, 2004	Location: Charlotte Convention Center

Session Chair: Khaled B. Morsi, San Diego State University, Dept. of Mech. Engrg., San Diego, CA 92182 USA

#### 2:00 PM Invited

Modeling of Sintering at Multiple Length Scales: Anisotropy Phenomena: Eugene A. Olevsky<sup>1</sup>; Boris Kushnarev<sup>1</sup>; Veena Tikare<sup>2</sup>; <sup>1</sup>San Diego State University, Mech. Engrg., 5500 Campanile Dr., San Diego, CA 92182-1323 USA; <sup>2</sup>Sandia National Laboratories, Albuquerque, NM USA

Two major approaches in modeling of real sintering processes: (i) microscopic, physically-based, and (ii) macroscopic, phenomenological are combined in order to predict the evolution of realistic microstructures coupled with technologically important macroscopic analysis. Constitutive models of sintering used in finite element computer codes are refined taking into consideration peculiarities of real grain structures. Using the newly developed multi-scale theory of sintering, a new model capable of describing an anisotropic shrinkage under sintering is put forward. The model is based on the consideration of an oriented grain-pore meso-structure. Both grain-boundary and surface diffusion mechanisms of the mass transport are taken into consideration. Based on the model assumptions, the expressions for the effective anisotropic sintering stress and the anisotropic generalized viscosity are derived as functions of material and structure parameters. The obtained multi-scale solutions are compared to the experimental data on sintering of oxide ceramics.

#### 2:20 PM

**Microstructural Evolution During Sintering Nano-Alumina**: Lia A. Stanciu<sup>1</sup>; *Joanna R. Groza*<sup>1</sup>; <sup>1</sup>University of California, Matls. Sci., One Shields Ave., Davis, CA 95616 USA

A laser-flash technique (TOM) was used to evaluate the diameter of the sintering necks formed during the first stage of the consolidation process. The thermal diffusivity of nano-alumina was measured in-situ by the TOM device, in a temperature range between 20 and 1300°C, with a heating rate of 10°C/min. The plot of shrinkage and thermal diffusivity versus temperature was calculated. The increase in thermal diffusivity corresponds to the formation of the sintering necks. Interrupted sintering experiments were performed by Conventional, Microwave and Field Activated Sintering (FAST), followed by measurements of the thermal diffusivity. The growth rate of the sintering neck radius is the largest for the sintering under an electrical field and does not depend on the heating rate, for the heating rates used in this work.

#### 2:40 PM

A Novel Approach to Fabricating Sample Containment Assemblies for Microgravity Materials Processing: Michael Fiske<sup>2</sup>; Ken G. Cooper<sup>1</sup>; Glenn A. Williams<sup>1</sup>; Amir Mobasher<sup>3</sup>; <sup>1</sup>NASA, Marshall Space Flight Ctr., MS ED34, Huntsville, AL 35812 USA; <sup>2</sup>Morgan Research Corporation, Marshall Space Flight Ctr., 4811 A Bradford Dr., Huntsville, AL 35805 USA; <sup>3</sup>Alabama A&M University, Mech. Engrg., PO Box 404, Normal, AL 35762 USA

Over the course of the next decade, NASA has planned the deployment of the Materials Science Research Rack (MSRR), a multi-experiment facility for the International Space Station (ISS). This rack will consist of multiple experiments dedicated to various aspects of materials processing. To date, no requirements for geometrical commonality have been imposed on these furnace systems. Therefore, each of these configurations will require the development of unique Sample Containment Assemblies (SCA). These SCA's can be required to operate at up to 1600°C in inert or vacuum environments. It is very difficult to manufacture refractory metal cartridges with the required length/diameter aspect ratios. Laser Engineered Net Shaping (LENS<sup>TM</sup>) is a unique manufacturing process. The process uses additive fabrication techniques to deposit metal powders and form a fully dense object

**MONDAY PM** 

directly from computer-generated drawings. MSFC has one of these LENS<sup>™</sup> systems, and this paper discusses the status of a project to demonstrate that hermetic (non-porous) Sample Containment Assemblies of refractory metal alloys can be fabricated using Laser Engineered Net Shaping at a substantial time or cost savings over the currently employed techniques of Chemical Vapor Deposition (CVD) and Vacuum Plasma Spray (VPS).

#### 3:00 PM

#### Investigation of Laser-Clad W-Cu Composite Coating: Sheng-Hui Wang<sup>1</sup>; Lijue Xue<sup>1</sup>; <sup>1</sup>National Research Council of Canada, Integrated Mfg. Tech. Inst., 800 Collip Cir., London, Ontario N6G 4X8 Canada

Tungsten-copper composite is widely used as heavy-duty electrical contactors and discharging electrodes. Typically, the whole component is fabricated by P/M methods, such as liquid phase sintering and infiltration of liquid copper into a porous-sintered tungsten skeleton. In practice, however, only the surface layer of the component is often subjected to harsh working condition and, therefore, W-Cu composite surface coating may be more effective and economical. In other cases, damaged electrodes may be easily repaired by local deposition of the composite. This opens up a potential application for laser cladding process. In this study, the feasibility of fabricating W-Cu composite overlay is examined by laser cladding with blown powder technique. Nickel addition is used to increase the wettability between tungsten powders and copper melt during the deposition and, thus, the interfacial binding between tungsten particles and the copper substrate. The microstructure and properties, in particular, the abrasion resistance, of the composite coating are investigated and discussed.

#### 3:20 PM

Study of Process Induced Residual Stresses in Laser Clad IN-625 Superalloy and P20 Tool Steel: J.-Y. Chen<sup>1</sup>; L. Xue<sup>1</sup>; <sup>1</sup>Integrated Manufacturing Technologies Institute, National Research Council Canada, 800 Collip Cir., London, Ontario N6G 4X8 Canada

A blown powder laser cladding technique was used to deposit IN-625 superalloy on wrought IN-625 substrate and P20 tool steel on wrought P20 substrate. The former had no solid-state phase transformation during the cooling down while the latter experienced a martensitic transformation instead. Due to thermal and/or mechanical incompatibility between the clad layer and the substrate, significant amount of residual stresses could be introduced into the clad part by the process, which may adversely affect its mechanical properties and dimensional stability. A series of stress-relief heat treatments were performed on both clad specimens in order to change their characteristics of the residual stresses, which were evaluated using a hole-drilling method. The microstructure evolution in the laser clad IN-625 and P20 specimens after the heat treatments was also examined using optical microscope, SEM/EDS and XRD techniques. Moreover, their implications on the mechanical properties of the clad parts will also be addressed.

# 3:40 PM Break

#### 3:50 PM

#### Increased Toughness of High Temperature Aluminum Alloys: William J. Golumbfskie<sup>1</sup>; <sup>1</sup>Pennsylvania State University, Dept. of Matls. Sci. & Engrg., University Park, PA 16802 USA

The tensile properties and fracture toughness of two spray formed Al-Y-Ni-Co alloys were measured and correlated with their resultant microstructures. Significant differences in mechanical properties were observed with respect to microstructural by altering the secondary processing parameters and/or composition. The microstructure of the spray formed alloys consists of a large volume fraction of intermetallic particles distributed in an aluminum matrix. The information of the structure-property relationship has been coupled with a computational thermodynamic modeling of quaternary alloy system in an attempt to better determine a specific composition range and set of processing conditions to produce an improved toughness at room temperature while retaining high temperature strength.

#### 4:10 PM

In Situ Processing of TiC/TiN-Fe (Ti) Nanocomposites by Thermal Plasma: Lirong Tong<sup>1</sup>; Ramana G. Reddy<sup>1</sup>; <sup>1</sup>University of Alabama, Dept. of Metallurgl. & Matls. Engrg., PO Box 870202, Tuscaloosa, AL 35487 USA

A novel in situ processing technique of nanocomposite powders of Titanium Carbide/Titanium Nitride Iron (Titanium) alloys by thermal plasma was developed to investigate vaporization of raw materials, synthesis of TiC/TiN and solidification of TiC/TiN-Fe(Ti) nanocomposites from supersaturating vapor. A basic understanding of thermodynamics of synthesis of TiC/TiN, temperature profile and velocity distribution within reactor and vapor saturation of TiC/TiN is essential for quantitative predictions of characteristics of in situ synthesized TiC/TiN-Fe (Ti) nanocomposites. The paper presents thermodynamic analysis for predicting conditions of synthesis and recovery ratio of TiC/TiN. A mathematic model was developed for describing temperature profile and velocity distribution within the reactor. The model is applied to predict feeding rate, design in situ processing system of TiC/TiN-Fe(Ti) nanocomposites and calculate the final size of TiC/TiN-Fe(Ti) nanocomposite powder. The model predictions were found to be in reasonable agreement with experimental data for this system.

#### 4:30 PM Cancelled

#### Microstructure, Properties and Switching Behavior of Silver/ Graphite Electrical Contact Material Fabricated by Applying Nanotechnology

#### 4:50 PM

Effect of Rare Earth Oxide Concentrates on Oxidation Behavioir of AISI 304L Stainless Steel: Lalgudi V. Ramanathan<sup>1</sup>; Marina Fusser Pillis<sup>1</sup>; Edival D. de Araujo<sup>1</sup>; <sup>1</sup>Instituto de Pesquisas Energeticas e Nucleares-IPEN, Matls. Sci. & Tech. Ctr., Av. Prof. Lineu Prestes 2242, Cidade Universitaria, São Paulo 05508-000 Brazil

Rare earths are often added to chromia forming alloys to improve high temperature oxidation resistance. Rare earths can also be added as oxide dispersions to alloys, to enhance oxidation resistance. Significant cost reductions are possible if rare earth concentrates can be used instead of pure rare earth oxides, the former being a stage earlier in the process to obtain pure rare earth oxides. In this study the effect of adding pure rare earth oxides and rare earth concentrates to AISI 304L on its oxidation behavior has been evaluated. AISI 304L stainless steel powder compacts containing 2vol% of high purity rare earth oxides or a concentrate with lanthanum and yttrium oxides were prepared by mixing the different powders in a vibratory mill followed by pressing. The compacts thus obtained were sintered in a vacuum furnace. Isothermal oxidation measurements were carried out in air for up to 200h at 900°C. The parabolic oxidation rate constants were calculated. The reaction products were examined using various techniques such as SEM, EDS and XRD. The compacts with high purity rare earth oxides and those with the mixed rare earth concentrates exhibited similar oxidation rates.

#### 5:10 PM

The Influences of RE (Rare Earths) Oxides on Microhardness and Microstructure of Laser Cladding Layer of Co Based Powder: Jianjun Ding<sup>1</sup>; Feiqun Li<sup>1</sup>; Mon-Yu Wei<sup>2</sup>; <sup>1</sup>Shanghai Jiao Tong University, Coll. of Matls. Sci. & Engrg., 1954 Huashan Rd., Shanghai 200030 China; <sup>2</sup>Ta Hwa Institute of Technology, 1,Ta Hwa Rd., Chiung-Lin, Hsin-Chu Taiwan, China

In order to tap ulteriorly the potential of laser cladding layer in microstructure and property, the RE oxides were adopted by mixing with Co based powder as an addition in cladding materials. The experimental results indicate that the microhardness of laser cladding layers of Co based powder with 5wt% RE oxide Yb2O3 has an obvious enhancement and the corresponding microstructures are more fine compared with that without RE oxide addition under same laser processing conditions. Based on the above advantages come from RE oxide additions, it may lead to improving the properties of laser cladding layer in wearability and corrosion resistance and to decreasing microcracking trend of to a degree.

# MONDAY PM

# Recent Advances in Non-Ferrous Metals Processing: Sustainable Development

Sponsored by: Light Metals Division, LMD-Reactive Metals Committee, EPD-Waste Treatment & Minimization Committee Program Organizers: Brajendra Mishra, Colorado School of Mines, Kroll Institute for Extractive Metals, Golden, CO 80401-1887 USA; John N. Hryn, Argonne National Laboratory, Argonne, IL 60439-4815 USA; V. I. Lakshmanan, Ortech Corporation, Mississauga, Ontario L5K1B3k Canada; V. Ramachandran, Scottsdale, AZ 85262-1352 USA; Alton T. Tabereaux, Alcoa Inc., Process Technology, Muscle Shoals, AL 35661 USA

Monday PMRoom: 205March 15, 2004Location: Charlotte Convention Center

Session Chair: V. I. Lakshmanan, Process Research ORTECH Inc., Mississauga, ON L5K 1B3 Canada

# 2:00 PM Opening Remarks

# 2:05 PM

**Developing Sustainable Resource Recovery and Recycling**: *Michael Clapham*<sup>1</sup>; <sup>1</sup>Natural Resources Canada, Resource Recovery & Recycling, Minerals & Metals Sector, 580 Booth St., Ottawa, Ontario K1A 0E4 Canada

This paper will explore issues to be addressed in the development of resource recovery and recycling initiatives, which lead to significant increases in the recovery of products and materials at end-of-life. Taking a life cycle approach the paper will explore how issues such as design for environment, consumption patterns, sustainable markets for recovered products, infrastructure, policy mechanisms and technology can influence recovery rates. The benefits of increased recovery, such as materials and energy efficiencies, reduced burdens to land-fill, green house gas emissions and social implications will be discussed. Examples of Canadian activities within the resource recovery and recycling sector will be provided.

# 2:35 PM

The Environmental and Human Health Risk Communication Theory and Practice: B. R. Conard<sup>1</sup>; <sup>1</sup>INCO Limited, Environml. & Health Scis., 145 King St. W., Ste. 1500, Toronto, Ontario L5H 4B7 Canada

The framework of risk assessment and risk management for inorganic substances is steadily gaining ground in its ability to cost – effectively deal with judging the health outcome severity and probability of exposure to a hazardous material. The issue of the safe use of metals and their compounds is important to workers in production and downstream customer occupations, to neighbors of industrial facilities, and to general population of consumers of products. A critical but often marginalized component of risk assessment is risk communication. Communication between humans is fraught with challenges in any area, but is even more difficult when the subject is health risks that are scientifically and medically complex. Discussion will focus on common mistakes in this area by large corporations in the past and with real examples, indicate directions that have been successful in closing the gap between industry's performance and society's expectation.

#### 3:05 PM

**Technological Cycles of Metals: Are They Sustainable?**: *R. B. Gordon*<sup>1</sup>; T. E. Graedel<sup>1</sup>; B. Reck<sup>1</sup>; <sup>1</sup>Yale University, Kline Geology Lab., PO Box 208109, New Haven, CT 06520-8109 USA

Rate of use of most of the industrial metals increased dramatically in the last quarter of the 21st century. This trend cannot be sustained indefinitely without the utilization of metals in discarded products. We have completed the characterization of technological cycles of copper, silver and zinc at country, region and planetary spatial levels. We have also completed a study of the copper cycle in N. America for the entire 20th century, including stocks in use and discard and recycling rates. All of this allows us to determine rates of recycling and reuse for various discard streams - electronics, vehicles, industrial products and so forth. Of these three metals, silver has the highest recycling rate, reflecting both its intrinsic value and its predominant use in photographic films. Copper is also effectively recovered, especially from electrical and electronic equipment and from end of life vehicles. The recycling of zinc, being predominantly used as a sacrificial coating for steel, is problematic. Results will demonstrate differences in the metal cycles in different world regions and in different epochs.

# 3:35 PM Break

#### 3:50 PM

Sustainable Development – The Role of Waste Minimization and Recyclables: V. I. Lakshmanan<sup>1</sup>; R. Sridhar<sup>1</sup>; R. Ramchandran<sup>2</sup>; <sup>1</sup>Process Research ORTECH Inc., 2395 Speakman Dr., Mississauga, ON L5K 1B3 Canada; <sup>2</sup>RAM Consultants, 9650 E. Peregrine Place, Scottsdale, AZ 85262 USA

Sustainable industries continuously seek to obtain aggressive economic advantages together with environmental and resource conservation benefits. As a major player in the global resource industries sector, Canadian mining and metallurgical industries, provide opportunities for technology transfer in process and product development to treat recyclables and minimize waste generation. Integrated process developments with recyclables contribute to green house gas emission reductions. The paper with selected examples will discuss synergy between major mining and metallurgical industries with end users in the building materials, automotive and electronic industries.

# 4:20 PM

**Demonstrating Corporate Social Responsibility**: *Bob White*<sup>1</sup>; <sup>1</sup>BRI International Inc., 2570 Matheson Blvd. E., Ste. 110, Mississauga, ON L4W 4Z3 Canada

This paper will provide an overview of Corporate Sustainability and Social Responsibility (CSR) in terms of: · What it is? · Who and why private and public sector organizations are moving toward CSR? · A framework that will allow an organization to demonstrate commitment to CSR. The paper starts by providing a broad definition of CSR and the difference between CSR and corporate governance. This definition will provide an opportunity to understand just how complex CSR is and how difficult it is to achieve and sustain a process for CSR. The paper will also introduce information on the drivers for CSR, the threats and opportunities. The threat associated with increasing demands to demonstrate CSR, by people that have a significant influence over the organization. The opportunities related to using a framework for CSR to contribute to achieving sustainable development and competitive advantage in the face of increasing globalization and trade liberalization. It will explore the link among sustainable economic, social and environmental development; and CSR. The important benefits of CSR, including the economic, financial, market share, environmental and social aspects. Finally, the paper will describe how an integrated management system based on the best practices defined in international management system standards and models can be used to demonstrate commitment and obtain the sustainable benefits of CSR.

# Recycling: Aluminum and Aluminum Dross Processing

Sponsored by: Light Metals Division, Extraction & Processing Division, LMD/EPD-Recycling Committee Program Organizer: Gregory K. Krumdick, Argonne National Laboratory, Argonne, IL 60439 USA

Monday PM	Room: 2	217D
March 15, 2004	Location:	Charlotte Convention Center

Session Chairs: Ray Peterson, IMCO Recycling, Rockwood, TN 37854 USA; Angela Withers, IMCO Recycling, Rockwood, TN 37854 USA

# 2:00 PM

Worldwide Aluminum Scrap Supply and Environmental Impact Model: Paul R. Bruggink<sup>1</sup>; Kenneth J. Martchek<sup>2</sup>; <sup>1</sup>Alcoa Inc., Alcoa Tech., 100 Technical Dr., Alcoa Ctr., PA 15069-0001 USA; <sup>2</sup>Alcoa Inc., EHS Services, 201 Isabella St., Pittsburgh, PA 15212-5858 USA

A quantitative tool has been developed for the Global Aluminium Recycling Committee of the International Aluminium Institute to better describe the past and to better characterize the future mix of primary and recycled global aluminum metal supply. The model provides a better understanding of worldwide aluminum recycling flows by comparing annual regional and global statistics on primary and recycled aluminum processing with anticipated annual recycled aluminum supply predicted on the basis of regional and market product net shipments, average product lives, collection and recovery rates. Furthermore, the model permits investigations of the sensitivities of changes in scrap collection, recovery rates, and product lifetimes on the worldwide supply system. The model has also been used to identify gaps in recycling data and areas of greatest potential for increased recycling and reduced environmental effects. As an example, the paper will highlight the model's use for examining the potential impact of aluminum recycling and product lifetime assumptions on the greenhouse gas implications of the global aluminum industry through year 2010.

# 2:25 PM

# Modeling the Impact of Recycling on the Total U.S. Aluminum Supply and on the Industry's Energy Requirements: *William T. Choate*<sup>1</sup>; John A.S. Green<sup>2</sup>; Brian J. Copeland<sup>1</sup>; <sup>1</sup>BCS, Incorporated, 5550 Sterrett Place #306, Columbia, MD 21044 USA; <sup>2</sup>Aluminum Industry Consultant, 3712 Tustin Rd., Ellicott City, MD 21042 USA

The future availability of aluminum scrap will have an impact on the supply of recycled metal and the energy intensity of the aluminum industry. Recycled aluminum now accounts for nearly a third of the U.S. metal supply. The growth of recycling is due not only to economics but in part to a greater awareness of the energy savings and emission reductions associated with recycling aluminum. A model of the scrap metal supply has been built by the authors using the past 40 years of statistical data for the major aluminum markets. The model assigns life cycles assumptions to each product and then is used to evaluate the recycling metal supply through 2020. This paper discusses future trends in metal supply (surplus or shortfall) in the light of the model assumptions and results.

#### 2:50 PM

**Process Modelling of Aluminium Scraps Melting**: Bo Zhou<sup>1</sup>; Yongxiang Yang<sup>1</sup>; *Markus A. Reuter*<sup>1</sup>; <sup>1</sup>Delft University of Technology, Applied Earth Scis., Mijnbouwstraat 120, Delft 2628 RX The Netherlands

In a secondary aluminium recovery, aluminium scraps are melted and refined often in a rotary melting furnace. The feed is normally a complex combination of aluminium scraps with different sizes, shapes, compositions, paintings and other contaminations. During the process, the scraps are charged into the rotary furnace, passing through a molten salt layer, and melting in a bottom aluminium bath. Efficient melting of the scraps in the molten melt is a critical issue in the secondary aluminium industry. To study the scrap melting behavior, a furnace model has been developed based on a Computational Fluiddynamics (CFD) framework, coupled with user developed aluminium melting sub-model. The furnace model consists of a gas region with turbulent flow and combustion as well as radiative heat transfer in the upper part of the furnace, and a solid-liquid region of salt and aluminium metal in the lower part of the furnace. The aluminium melting model was developed for a single particle in the molten salt and aluminium melt based on the experimental study and heat transfer theory. In the melting model, solid aluminium melting, salt shell formation and re-melting on the metal solids were included. To represent the distributed nature of the scrap feed, aluminium scraps were classified into several groups depending on their properties, e.g. size of the scraps. The melting sub-model was subsequently modified from the numerical model for a single aluminium particle to the multi-particle system. Aluminium melting behavior was calculated with the exchange of information between the melting sub-model and the CFD combustion space. Heat sink due to scrap melting, was calculated by the submodel and fed back to the CFD combustion space model. Gas flow and temperature distribution in the top combustion space of CFD model were used to calculate the melting rate of aluminium scrap in the submodel.

# 3:15 PM

**Developments in Automatic Sorting and Quality Control of Scrap Metals**: Marian-Bogdan Mesina<sup>1</sup>; Tako P.R. de Jong<sup>1</sup>; *Wijnand L. Dalmijn*<sup>2</sup>; <sup>1</sup>Delft University of Technology, Resource Engrg., Mijnbouwstraat 120, Delft 2628 RX The Netherlands; <sup>2</sup>Delft University of Technology, Faculty of Design, Engrg. & Production, Mekelweg 2, Delft 2628 CD The Netherlands

Despite the advantages of mechanical systems and hand picking, which until today are extensively used for scrap metal sorting, the quality of the product can be considerably improved when sensor based systems are used. Advanced data processing and the combination of different sensors are expected to gain in importance in future applications, and increase the automation of sorting. At Delft University of Technology new methods using sensors have been investigated for sorting and quality control of scrap non-ferrous metals. A prototype system was developed for the identification and separation of scrap metals using electromagnetic and dual energy X-ray sensors. Recently developed actuator design enables sorting into more than three fractions of particles that are randomly orientated on a flat conveyer belt. The main parts of the automatic system and the experimental results are reported. In addition, the possibilities to integrate such sensors into an industrial plant are discussed.

# 3:40 PM Break

# 3:55 PM

**DROSRITE Extensive On-Site Hot Dross Treatment Tests**: *Michel G. Drouet*<sup>1</sup>; <sup>1</sup>Pyrogenesis Inc., 2000 William St., Ste. 200, Montréal H3J 1R4 Canada

DROSRITE is a salt-free process for the recovery of metal from dross. In addition to producing a salt-free residue, it does not produce any CO2 or Nox gases. The process is highly energy efficient, extracting heat from energy in the residue and, thus, it does not require any external heat source such as a plasma torch, an electric arc or a gas or an oil burner. A DROSRITE pilot unit built by Pyrogenesis was used, in early 2003, for a two months extensive series of fifty tests on the site of a large aluminum smelter in Europe. All the different types of dross produced at the site were tested. Hot dross, charged into the DROSRITE furnace, was treated without any external heat input. Results of this extensive industrial trial will be presented together with analysis of both the input dross and the output residue. The economic analysis will also be presented.

#### 4:20 PM

Formalization of Concerts of the Processes Occurring in Melting Aluminum Rejects at Rotor Furnaces: A. G. Zholnin<sup>1</sup>; S. B. Novichkov<sup>2</sup>; A. G. Stroganov<sup>1</sup>; <sup>1</sup>MOPM, city of Voskresensk Russia; <sup>2</sup>Russkiy Aluminiy, Prokatniy Div., Moscow Russia

The experience of re-melting aluminum at the rotor inclined furnaces (RIF) showed that the current level of understanding is not sufficient to explain the observed effects and control them deliberately. Certain uncontrolled losses of metal result from that. The attempts to optimize the economic parameters (to reduce the melting time, reduce the amount of the used fluxing agent) from relatively rich aluminum raw materials (50 and more percent of metal) sometimes result in nothing. In the language of metallurgists it is called the 100% melting loss. It is implied that all the metal has burned out, i.e. has passed into an oxide state. In fact it was found out in the studies of the refused slag that the most part of the metal is left in slag in the form of small spherical drops covered with the oxide film. Such effects made it necessary to pay more attention to the processes, occurring in this situation. The presented work is an attempt of further development of the concepts of processes of melting at the RIF, w hich were published earlier.<sup>1,2</sup> The phenomenological model proposed for consideration is the result of generalization of visual observation of the processes of re-melting different types of aluminum raw materials at the rotor inclined furnaces and the analysis of the results of the laboratory researches of the initial raw materials, refused slag and dust in the exhaust gases. The stated fact is mainly related to melting different types of aluminum rejects in the mode of «dry» melting with lower amount of the fluxing agent when secondary dross is in the loose dispersed state. In the process of melting in the environment of permanently mixed furnace feed the solid aluminum can pass into different states and simultaneously be in an oxide form, small tailing, drops, mess and swamp and be removed with the exhaust gases in the form of dust and volatile compounds formed in the result of chemical interaction of aluminum with the fluxing agents. In the model are considered certain possible reactions of transition of the metal from some states to other ones at different stages of melting for different types of raw materials. The reactions determining the process of melting of different types of raw materials were tabulated. The qualitative description of the processes occurring in the furnace feed during the process of melting aluminum raw materials at the rotor furnaces is the first step in the way of development of the theory of re-melting aluminum raw materials. The next stage should be a mathematical description of each reaction of the transition. It will require theoretical investigation, as well as experimental researches for refinement of the parameters or examination of certain aspects. <sup>1</sup>A.G. Zholnin, Ñ.B. Novichkov. A model of the physicochemical processes occurring in melting aluminum rejects in the rotor furnaces. Collection of Proceedings of the VII International conference "Aluminum of Siberia -2001", 10-12 September, Krasnoyarsk, 2002, p. 225-228. <sup>2</sup>A.G. Zholnin, Ñ.B. Novichkov. Mechanism of transition of aluminum from slag to «swamp» in the process of re-melting aluminum rejects at the rotor furnaces. Non-ferrous metallurgy, Moscow, 2003, .11, p. 22-27.

#### 4:45 PM

Peculiarities of Melting Aluminum Slag in a Laboratory Inclined Rotor Furnace: A. G. Zholnin<sup>1</sup>; A. E. Zakharov<sup>1</sup>; S. B. Novichkov<sup>2</sup>; A. G. Stroganov<sup>1</sup>; <sup>1</sup>MOPM, city of Voskresensk Russia; <sup>2</sup>Russkiy Aluminiy, Prokatniy Div., Moscow Russia

In this work are presented the results of melting aluminous dross at a laboratory rotor inclined furnace (LRIF) described in the work.<sup>1</sup> It was studied the impact on the melting process of the amount of the added fluxing agent, the fluxing agent composition, the furnace speed of rotation, the temperature of pouring, the content of dust in the slag and the impact of moisture and time of storing on the metal output. As the output parameters of the process, the weight of the poured out metal, the weight of the refused dross and the breakup of beads left in dross after pouring out the metal were controlled. All the beads with the diameter over 1mm were picked up. The smaller particles of aluminum have been left beyond our control. The screening of aluminous dross with the maximum size of particles of 20 mm and the metal content about 50% was used as a raw material. The mixtures based on sodium and potassium chlorides with the cryolite admixture. 1.5-2 kg of dross was loaded into each melting. The speed of rotation in most cases, excluding those, which were specially stipulated, was 2.5 rpm. It was established that there is a minimum amount of the fluxing agent, below which the molten pools are not formed. The metal is left in the dross in the form of beads. The influence of the proportion of sodium and potassium chlorides on the metal output is weak. The cryolite admixtures are efficient only for small amounts of the fluxing agent. The increase of the furnace speed of rotation under high content of the fluxing agent facilitates coalescence, and under low content of the same it strengthens the effect of breaking the drops. The isothermal soaking of the furnace feed before pouring out renders an ambiguous effect. The increase of the content of dust fraction in dross in the process of melting in the «dry fluxing agent» mode facilitates breaking of the beads and the decrease of the metal output. The content of magnesium in the alloy depends on the dross consistence, its decrease may be an indicator of quality of melting. The performed researches showed the efficiency of using laboratory furnaces for finding out the mechanisms of melting aluminum raw materials in RIF. It is natural that the obtained results cannot be automatically extended to the large dimension industrial furnaces because of the existence of the scale factor.2 But the found out mechanisms of melting permit to give certain specific recommendations and may be useful for the development of the technology of melting dross at the rotor inclined furnaces. <sup>1</sup>D.Ì. Zakharenko, A.G. Zholnin, Ñ.B. Novichkov, A.G. Stroganov. A laboratory rotor inclined furnace for re-melting the secondary aluminum raw materials. Nonferrous metallurgy, Moscow, 2003, 12, p. 26-33. <sup>2</sup>A.G. Zholnin, Ñ.B. Novichkov. The role of the scale factor in the process of re-melting the secondary aluminum raw materials at the rotor inclined furnaces. Nonferrous metallurgy, Moscow, 2002, 111, p. 28-31.

# R.J. Arsenault Symposium on Materials Testing and Evaluation: Session II

Sponsored by: Structural Materials Division, SMD-Mechanical Behavior of Materials-(Jt. ASM-MSCTS), SMD-Nuclear Materials Committee-(Jt. ASM-MSCTS)

*Program Organizers:* Raj Vaidyanathan, University of Central Florida, AMPAC MMAE, Orlando, FL 32816-2455 USA; Peter K. Liaw, University of Tennessee, Department of Materials Science and Engineering, Knoxville, TN 37996-2200 USA; K. Linga Murty, North Carolina State University, Raleigh, NC 27695-7909 USA

Monday PM	Room: 2	11A
March 15, 2004	Location:	Charlotte Convention Center

Session Chairs: K. Linga Murty, North Carolina State University, Coll. of Engrg., Raleigh, NC 27695-7909 USA; Raul B. Rebak, Lawrence Livermore National Laboratory, Chmst. & Matls. Sci., Livermore, CA 94550 USA

#### 2:00 PM Invited

#### Use of Multiple Material Characterization Techniques to Study Precipitation Kinetics of Copper in HSLA Steel: Chandra Shekhar Pande<sup>1</sup>; <sup>1</sup>Naval Research Lab, Code 6325, Washington DC USA

Precipitation kinetic of copper in a high strength low carbon ferrous alloy has been studied in the past by field ion microscopy. These precipitates being initially coherent with the matrix are difficult to detect by convention transmission electron microscopy (TEM). We have therefore used TEM in conjunction with small angle neutron scattering (SANS) to study copper precipitation. Direct measurement from TEM micrographs and integral transform of the SANS data was used to calculate the size distribution for a variety of aging conditions. Possible role of another electron optical technique viz electron energy loss imaging was also explored.

## 2:30 PM

Thermal Aging Studies on Mechanical and Fracture Characteristics of 1Cr1M00.25V Steel Using Ball Indentation, Ultrasonic Attenuation and Electrical Resistivity Techniques: Chang-Sung Seok<sup>1</sup>; Jeong-Pyo Kim<sup>1</sup>; Bong-Kook Bae<sup>1</sup>; K. L. Murty<sup>2</sup>; <sup>1</sup>Sungkyunkwan University, Sch. of Mech. Engrg., 300 Chunchun-dong, Jangan-gu, Suwon, Kyonggi-do 440-746 Korea; <sup>2</sup>North Carolina State University, PO Box 7909, Raleigh, NC 27695-7909 USA

Effect of thermal aging on mechanical and fracture characteristics of 1Cr-1Mo-0.25V steel was investigated following heat treatment at 630C (903K) for varied times up to 1820 hours (~75 days). Tensile and fracture (K1C) tests were performed at ambient before and following thermal aging that indicated decreased strength and fracture toughness (KQ) with corresponding increase in ductility. Microstructure of the aged material revealed coarsening of carbides and precipitates. Yield and tensile strengths derived from ball indentation tests on the as-received and aged samples were in close agreement with the tensile data. In addition, the indentation energy to fracture (IEF) revealed similar trends as per the fracture toughness although no one-to-one correlation was noted. Electrical resistivity determined using 4-point DC potential drop method, decreased with thermal aging very similar to the strength and hardness. A linear correlation was observed between the resistivity and strength while a parabolic curve was noted when it was compared with fracture toughness. Ultrasonic tests yielded results on the attenuation coefficient and nonlinear parameter that increased with aging time. While the ultrasonic data correlated linearly with the uniform strain, an inverse relation was observed with fracture toughness. These studies reveal the usefulness of ball indentation technique to inquire into aging characteristics of the steel thereby indicating the possible application for on-line interrogation of the steel structures. Both the resistivity and ultrasonic methods are shown to be applicable for non-destructive characterization and condition monitoring of the structures fabricated with this steel.

#### 2:50 PM

**Corrosion Testing of Nickel and Titanium Alloys**: Kenneth J. Evans<sup>1</sup>; Lana L. Wong<sup>1</sup>; *Raúl B. Rebak*<sup>1</sup>; <sup>1</sup>Lawrence Livermore National Laboratory, Chmst. & Matls. Sci., 7000 East Ave., L-631, Livermore, CA 94550 USA

Titanium (Ti) and Nickel (Ni) alloys are highly resistant to corrosion and are therefore extensively used in industrial applications such as in the chemical process industry. Both families of alloys also find important applications in the nuclear power generation and in the nuclear waste disposal. When Ti and Ni alloys are exposed to aggressive conditions, they may fail by the three major mechanisms of general corrosion, localized corrosion and environmentally assisted cracking. To assess each type of failure mode, a number of testing methods may be used. This review will compare corrosion testing methods used to assess the corrosion behavior of several Ti and Ni alloys in different types of environments including solution composition, temperature and applied potential.

## 3:10 PM

Non-Destructive and Microstructural Characterization of Thermal Barrier Coatings: Vimal Desai<sup>1</sup>; Y. H. Sohn<sup>1</sup>; <sup>1</sup>University of Central Florida, AMPAC, Box 162455, Orlando, FL 32816-2455 USA

The durability and reliability of thermal barrier coatings (TBCs) play an important role in the service reliability and durability of hotsection components in advanced turbine engines. Electrochemical impedance spectroscopy (EIS) and photostimulated luminescence spectroscopy (PSLS) are being concurrently developed as a complimentary non-destructive evaluation (NDE) techniques for quality control and life-remain assessment of TBCs. This talk will overview the relative changes in the impedance and luminescence examined in terms of resistance (or capacitance) of TBC constituents, residual stress and phase constituents in thermally grown oxide scale. Results from NDE by EIS and PSLS will be discussed in the light of microstructural development during high temperature oxidation, using a variety of micro-scopic techniques including focused ion beam in-situ lift-out (FIB-INLO) and scanning transmission electron microscopy (STEM).

#### 3:30 PM Break

#### 3:50 PM

Scanning Pyrometry from Digital Color Imaging: Nathan Rolander<sup>1</sup>; Douglas M. Matson<sup>1</sup>; <sup>1</sup>Tufts University, Mech. Engrg., 025 Anderson Hall, 200 College Ave., Medford, MA 02155 USA

High-speed color digital images are formed using Bayer demosaicking schemes to interpolate color from an array of filtered sensors. By

suppressing this data smoothing protocol, individual sensors within the color filter array can be used as one-color pyrometers and a generate a thermal scan to obtain temperature as a function of position within the camera view. Differential channel amplification (red-greenblue) can provide greater thermal resolution. A calculation of signalto-noise for each channel is used to measure the responsivity as a function of wavelength. Analyses of resultant thermal histograms shows a precision of +/-3 degrees in the investigation of rapid solidification behavior of metal alloys.

#### 4:10 PM Cancelled

#### Thermography and X-Ray Detection on the Evolutions of Lüders Bands During Mechanical Testing

#### 4:30 PM

Watching Stress-Strain Evolutions During Low-Cycle Fatigue by Thermography: *Bing Yang*<sup>1</sup>; Peter K. Liaw<sup>1</sup>; J. Y. Huang<sup>2</sup>; R. C. Kuo<sup>2</sup>; J. G. Huang<sup>3</sup>; <sup>1</sup>University of Tennessee, Dept. of Matls. Sci. & Engrg., Knoxville, TN 37996 USA; <sup>2</sup>Institute of Nuclear Energy Research (INER), PO Box 3-14, 1,000 Wenhua Rd., Chiaan Village, Lungtan, Taiwan 325 China; <sup>3</sup>Taiwan Power Company, Taipei Taiwan

Both elastic and plastic deformations affect material temperatures, but in different fashions. Consequently, temperature patterns could serve as fingerprints for stress-strain behaviors. A high-speed and highsensitivity thermographic-infrared (IR)-imaging system has been used to watch the temperature evolution cycle by cycle during 0.5 Hz lowcycle fatigue experiments. Numerical analyses integrating thermodynamics and heat-conduction theories have been formulated to calculate the stress amplitude, strain amplitude, and plastic work from the observed temperature evolutions. Cyclic softening behavior has been observed by thermography. A theoretical model has been developed to predict fatigue lives from the observed specimen temperatures. Furthermore, constitutive equations have been formulated to in-situ predict stress-strain variations from the measured temperatures. Thus, a new method has been developed to in-situ 'watch' material stressstrain evolutions during cyclic-loading conditions, which can open up wide applications of thermography in studying in-situ mechanical damage of materials and components.

#### 4:50 PM

# Assessment of Thermal Characteristics of YSZ Coating: *Kyongjun An*<sup>1</sup>; M. K. Han<sup>1</sup>; Joon-Kyun Lee<sup>1</sup>; <sup>1</sup>Korea Institute of Industrial Technology, 35-3, HongChonRi, IbJangMyun, ChonAnSi Korea

The approach is based on an experimental set-up in which one surface of the coating is exposed to a high temperature environment and heat is extracted from the other side by flowing air. This arrangement could be set-up in a laboratory. By measuring the overall thermal resistances of coatings of various thicknesses, it has been shown that the thermal conductivity of a segment of the coating can be determined by the differences in thermal resistances of two specimens with varying coating thicknesses. The objective of the present work is to extract the thermal conductivity of the thermal barrier coatings under conditions that are nearly the same as the actual application. It is also of interest to see if the thermal conductivity of coating can be affected by applying different coating thicknesses.

#### 5:10 PM

Dislocation Structure Evolution in Copper Crystals Under Cyclic and High Speed Loading: S. X.  $Li^{1}$ ; <sup>1</sup>Shenyang National Laboratory for Materials Science, Inst. of Metal Rsch., Shenyang 110016 China

The dislocation structure evolution of persistent slip bands (PSBs) and deformation bands of copper single crystals under cyclic straining and the annihilation of PSBs during annealing were investigated by a electron channeling contrast (ECC) technique. The structure of shear bands of copper single crystals under high rate straining were also studied by ECC. The dislocation structure evolution of PSBs and its internal and external stress fields were also computer simulated using dislocation dynamics and finite element methods. The results may provide further understanding of the plastic deformation localization of metals under either cyclic or high speed loading.

# Solidification Processes and Microstructures: A Symposium in Honor of Prof. W. Kurz: Mushy Zone Dynamics

Sponsored by: Materials Processing & Manufacturing Division, MPMD-Solidification Committee

*Program Organizers:* Michel Rappaz, Ecole Polytechnique Fédérale de Lausanne, MXG, Lausanne Switzerland; Christoph Beckermann, University of Iowa, Department of Mechanical Engineering, Iowa City, IA 52242 USA; R. K. Trivedi, Iowa State University, Ames, IA 50011 USA

Monday PM	Room: 207D
March 15, 2004	Location: Charlotte Convention Center

Session Chair: Christoph Beckermann, University of Iowa, Dept. of Mech. Engrg., Iowa City, IA 52242 USA

#### 2:00 PM Invited

Alloy Melting: *William J. Boettinger*<sup>1</sup>; Daniel Josell<sup>1</sup>; Deb Basak<sup>1</sup>; Sam R. Coriell<sup>1</sup>; <sup>1</sup>NIST, Metall. Div., Gaithersburg, MD 20899 USA

For practical reasons, melting receives less research attention than solidification. Yet partial melting may occur during joining or during casting with mushy zone macrosegregation. The modeling of these processes requires knowledge of the interface conditions, specifically the validity of the local equilibrium assumption. Existing research on this subject will be reviewed. In particular, experiments are presented that measure the effect of heating rate and grain size on the melting of Nb-47 mass%Ti. The method uses resistive self-heating of wire specimens at rates between 10<sup>2</sup> and 10<sup>4</sup> K/s and simultaneous measurement of radiance temperature and normal spectral emissivity as functions of time. The interpretation of the shapes of the temperature-time curves is supported by a model that includes diffusion in the solid coupled with a heat balance during the melting process. There is no evidence of loss of local equilibrium at the melt front during melting in these experiments.

# 2:30 PM Invited

About the Interactions Between Thermo-Solutal Convection, Shrinkage Flow and Grain Sedimentation: Andreas Ludwig<sup>1</sup>; Menghuai Wu<sup>1</sup>; <sup>1</sup>University of Leoben, Dept. of Metall., Franz-Josef-Str. 18, Leoben 8700 Austria

Based on a two-phase volume averaging model for globular equiaxed solidification detailed simulation results on the formation of macrosegregations in Al-4wt.% Cu die casting are presented. The model considers nucleation and growth of equiaxed grains, motion and sedimentation of grains, solute transport by diffusion and convection, feeding flow and thermo-solutal buoyancy driven flow. Special attention is paid on the interactions between thermo-solutal convection, shrinkage flow and grain sedimentation and the impact of these interactions on the formation of macrosegregation.

#### 3:00 PM

Direct Observation of Controlled Melting and Re-Solidification of Succinonitrile Mixtures in a Microgravity Environment: *Richard N. Grugel*<sup>1</sup>; A. V. Anilkumar<sup>2</sup>; C. P. Lee<sup>3</sup>; <sup>1</sup>Marshall Space Flight Center, MS-SD46, Huntsville, AL 35812 USA; <sup>2</sup>Vanderbilt University, Mech. Engrg., Box 1592, Sta. B, Nashville, TN 37235 USA; <sup>3</sup>ESI, Marshall Space Flight Ctr., Huntsville, AL 35812 USA

In support of the Pore Formation and Mobility Investigation (PFMI) direct observation of experiments on the controlled melting and subsequent re-solidification of succinonitrile were conducted in the glovebox facility (GBX) of the International Space Station (ISS). Samples were prepared on ground by filling glass tubes, 1 cm ID and approximately 30 cm in length, with pure succinonitrile (SCN) and SCN-Water mixtures under 450 millibar of nitrogen. Experimental processing parameters of temperature gradient and translation speed, as well as camera settings, were remotely monitored and manipulated from the ground Telescience Center (TSC) at the Marshall Space Flight Center. Sample temperatures are monitored by six in situ thermocouples. Real time visualization during melt back revealed bubbles of different sizes initiating at the solid/liquid interface, their release, interactions, and movement into the temperature field ahead of them. Subsequent resolidification examined planar interface breakdown and the transition to steady-state dendritic growth. A preliminary analysis of the observed phenomena and its implication to future microgravity experiments is presented and discussed.

MONDAY PM

Kinetics of Dendritic Mushy Zones: Microgravity Experiments: Afina Lupulescu<sup>1</sup>; Martin E. Glicksman<sup>1</sup>; <sup>1</sup>Rensselaer Polytechnic Institute, Dept. of Matls. Sci. & Engrg., Troy, NY 12180 USA

Kinetics of melting pivalic acid dendrites was observed under convection-free conditions on STS-87 as part of USMP-4, flown on shuttle Columbia in 1997. At low Stefan numbers, St«1, dendrites melt and shrink steadily toward extinction. Individual fragments follow a characteristic time-dependence derived using quasi-static theory based on conduction-limited melting under shape-preserving conditions. Agreement between analytic theory and experiments is found when the melting process occurs under shape-preserving conditions, as measured by the C/A ratio of the needle-like crystal fragments, approximated as prolate spheroids. In experiments where C/A varies, a "sectorizing" approach may be employed that divides the melting process into a series of steps, each approximated by a constant value of C/A. The sectorized approach allows prediction of the dendritic melting process even when neighbor interactions and fragmentation occur. Fragmentation of the dendrites is observed at higher initial supercoolings where the dendritic crystals are initially finer.

#### 3:30 PM

# Coarsening of Dendritic Microstructures: R. Mendoza<sup>1</sup>; D. Kammer<sup>1</sup>; P. W. Voorhees<sup>1</sup>; <sup>1</sup>Northwestern University, Matls. Sci. & Engrg., 2225 N. Campus Dr., Cook Hall, Evanston, IL 60208 USA

Wilfried Kurz has had a longstanding interest in the factors controlling the size scale of dendritic microstructures. We investigate the evolution of these microstructures during coarsening using three-dimensional digital reconstructions. The reconstructions allow quantitative measures of the microstructure to be obtained that have heretofore been impossible. For example, we have determined the probability of finding a patch of interface with a certain mean and Gaussian curvature, and the genus of the microstructure, all as a function of time during coarsening. We find that the directional solidification process used to create the samples induces a strong microstructural anisotropy that plays a major role in the evolution of the microstructure during coarsening. The dynamics of coarsening as a function of the volume fraction of solid will also be discussed.

#### 3:45 PM Break

#### 4:15 PM

**Coherency, Hot Cracking and Wilfried Kurz**: *Jai A. Sekhar*<sup>1</sup>; <sup>1</sup>University of Cincinnati, Dept. of Chem. & Matls. Engrg., 496 Rhodes Hall, Cincinnati, OH 45221-0012 USA

Professor Wilfried Kurz has extended several important ideas about coherency and deformation in the semi-solid state encountered during solidification. An article by him with co-authors Ackermann and Heinemann which appeared in the J. Mater. Sci. Eng. Vol. 75, pg.79, 1985, led to new understanding of the role of deformation at various temperatures in the semi-solid range. Subsequently, we were able to publish several articles from my group on the solidification cracking tendency and deformation studies of IC396M and Rene 108 alloys in the equiaxed state and the directionally solidified state. These studies led to the discovery of a crack free processing window for such alloys, giving rise to improved fatigue life for IC396M rotors. These and other studies are reviewed for results regarding the critical variables which influence the solidification cracking tendency in equiaxed microstructures, directionally solidified microstructures and also in faceted microstructures.

#### 4:30 PM

#### In-Situ Observations of Phenomena Related to Solidification of Ferrous Alloys: *Alan W. Cramb*<sup>1</sup>; *Sridhar Seetharaman*<sup>1</sup>; <sup>1</sup>Carnegie Mellon University, Matls. Sci., 5000 Forbes Ave., Pittsburgh, PA 15217 USA

There have been significant advances in the field of modeling solidification of metals, alloys and molten oxides through computational methods such as cellular automata and phase field. The ability to experimentally verify the predictions has however lagged behind due to difficulties posed by the high temperatures involved, containment of reactive molten metals and problems with radiation from the metal surfaces. This paper reviews recent experimental results from the Center for Iron and Steelmaking Research at Carnegie Mellon University on elucidating phenomena related to solidification and casting of ferrous alloys through in-situ observations using Confocal Scanning Laser Microscopy, High temperature Optical Microscopy and X-ray fluoroscopy and radioscopy. The phenomena that will be discussed includes: inclusion evolution during steel solidification, peritectic transformation and crystallization of industrial slags and fluxes.

## 4:45 PM

A Simple Microsegregation Model for Application in Macro Scale Solidification Calculations: Vaughan R. Voller<sup>1</sup>; <sup>1</sup>University of Minnesota, Civil Engrg., 500 Pillsbury Dr. SE, Minneapolis, MN 55455 USA

A major problem in computational modeling of physical processes is developing computational approaches that are able to bridge across length and time scales. This is a central issue in developing solidification models where the macro scale nodal field variables need to be consistent with phenomena occurring at the sub grid length scale of the solid-liquid interface, in particular the thermodynamics and local scale mass transport (microsegregation). In this paper a relatively simple microsegregation model, on the scale of a dendrite secondary arm space, is developed. The key features in this model are (i) domain variables obtained directly form macro-scale conservation equations, (ii) a thermodynamic treatment, for a multi-component alloy, that only requires calls to equilibrium calculations (i.e., the lever rule), and (iii) an accurate accounting for back-diffusion and coarsening at each time step, based on the current solid solute profiles. The application of model is illustrated by comparing its predictive performance, for several limit cases, with full numerical microsegregation solutions.

#### 5:00 PM

Network Modelling of Liquid Metal Transport in Solidifying Aluminium Alloys: W. O. Dijkstra<sup>1</sup>; C. Vuik<sup>2</sup>; A. J. Dammers<sup>3</sup>; L. Katgerman<sup>4</sup>; <sup>1</sup>Delft University of Technology, Lab. of Matls., Rotterdamseweg 137, Delft 2628 AL Netherlands; <sup>2</sup>Delft University of Technology, Dept. of Appl. Math. Analy., Melkeweg 4, Delft 2628 CD Netherlands; <sup>3</sup>Netherlands Institute for Metals Research, Delft 2628 AL Delft Netherlands; <sup>4</sup>Delft University of Technology, Lab. of Matls., Rotterdamseweg 137, Delft 2628 AL Netherlands

Development of fluid flow within the mushy zone of a DC-casting is important for the optimal control of many properties of the final cast material. We present a new numerical model based on a channel network. It allows to study flow effects at low liquid fractions within the mushy zone on a mesoscopic scale. Simulation of solidification within the channels together with mixing rules on their junctions describe the behaviour of the microstructure. In order to reduce the computational costs, the channels have to be represented by simple geometric objects like tubes. The collective behaviour of many channels within the network indicate the macroscopic effects as they occur in a small region of the underlying solidification process. The results of calculations for Al-4.5wt.%Cu alloy with and without inclusion of solidification shrinkage are presented.

#### 5:15 PM

Modeling of Macrosegregation and Solidification Grain Structures with a Coupled Cellular Automaton - Finite Element Method: Gildas Guillemot<sup>1</sup>; Charles-Andre Gandin<sup>1</sup>; Herve Combeau<sup>1</sup>; <sup>1</sup>LSG2M, UMR CNRS-INPL-UHP 7584, Ecole des Mines, Parc de Saurupt, Nancy 54042 France

Extension of a coupled Cellular Automaton (CA) - Finite Element (FE) method is presented for the prediction of solidification grain structures and macrosegregation. Following the validation procedure proposed by Ahmad et al. [Metallurgical and Materials Transactions 29A (1998) 617-630], application of the model to the experiments conducted by Hebditch and Hunt is proposed [Metallurgical Transactions 5 (1974) 1557-1564]. The algorithm and the numerical implementation of the coupling between the CA and FE methods are first validated by considering a columnar grain structure that develops with almost no undercooling. Such a calculation retrieves the solution of a purely FE calculation in which the grain structure is not accounted for. Several applications of the model are then presented in order to quantify the combined effects of the grain structure on the final macrosegregation map. In particular, the effect of the undercooling of the columnar growth, the presence of equiaxed grains nucleated in an undercooled liquid, as well as the transport and sedimentation of the equiaxed grains are investigated. Several improvements of the predicted segregation maps are clearly revealed when comparing with the experimental results.

#### 5:30 PM

A Mushy Zone Rayleigh Number to Describe Interdendritic Convection During Directional Solidification of Hypoeutectic Pb-Sb and Pb-Sn Alloys: Surendra N. Tewari<sup>1</sup>; R. Tiwari<sup>1</sup>; G. Magadi<sup>2</sup>; <sup>1</sup>Cleveland State University, Chem. Engrg. Dept., SH 464, Cleveland, OH 44115 USA; <sup>2</sup>American Bureau of Shipping, ABS Plaza, 16855 Northchase Dr., Houston, TX 77060 USA

Based on measurements of specific dendrite surface area ( $S_v$ ), fraction interdendritic liquid ( $\phi$ ) and primary dendrite spacing ( $\lambda_1$ ) on

transverse sections in a range of directionally solidified hypoeutectic Pb-Sb and Pb-Sn alloys that were grown at thermal gradients varying from 10 to 197 Kcm<sup>-1</sup> and growth speeds ranging from 2 to 157 µm s<sup>-</sup> <sup>1</sup> it is observed that  $S_v = \lambda_1^{-1} S^{*-0.33}(3.38 - 3.29\phi + 8.85\phi^2)$ , where  $S^* =$  $D_1G_{eff}/[V m_1 \text{ Co } (k-1)/k]$ , with  $D_1$  being solutal diffusivity in the melt, G<sub>eff</sub>, the effective thermal gradient, V, the growth speed, m<sub>l</sub>, the liquidus slope, Co, the solute content of the melt, and k the solute partition coefficient. This relationship has been used to define a mushy-zone permeability which accounts for the role of side-branching; other permeability relationships assume that it depends only upon  $\phi$  and  $\lambda_1$ . Incorporation of this permeability allows us to develop a mushy-zone Rayleigh number that quantitatively explains the following three experimental observations related to interdendritic convection: 1) Increasing convection results in reduced primary dendrite spacing. 2) Extent of longitudinal macrosegregation increases with increased mushy-zone convection. 3) On-set of channel-segregate (freckle) formation.

#### 5:45 PM

**Dynamics of Particle-Solidification Front Interactions**: Justin Wayne Garvin<sup>1</sup>; Yi Yang<sup>1</sup>; H. S. Udaykumar<sup>1</sup>; <sup>1</sup>University of Iowa, Mech. Engrg., 3131 Seamans Ctr., Iowa City, IA 52242 USA

A particle interacting with an advancing solidification front is studied using numerical simulations to couple phase change with particle motion. The particle is set in motion through the forces that act across the gap between the particle and the solidifying interface. A sharp-interface method is used to track both the phase boundary and the particle. Previous force expressions used in past literature are carefully scrutinized and found to inadaquately describe the nature of the forces in the gap. The effect of a premelted layer between the particle and the solidification front on the interaction dynamics is also studied through the coupling procedure. It is determined that the use of a premelted layer in the coupled model greatly effects the dynamics of the particle-front interaction. Both stable interfaces as well as dendritic interfaces are used in this study.

# Symposium on Microstructural Stability in Honor of Prof. Roger D. Doherty: Microstructural Stability: Texture Development

Sponsored by: Aluminum Association, Materials Processing and Manufacturing Division, Structural Materials Division, MPMD-Solidification Committee, SMD-Physical Metallurgy Committee *Program Organizer:* Anthony D. Rollett, Carnegie Mellon University, Department of Materials Science & Engineering, Pittsburgh, PA 15213-3918 USA

Monday PM	Room:	21	6A		
March 15, 2004	Location	1:	Charlotte	Convention	Center

Session Chair: Robert E. Sanders, Alcoa Inc, Alcoa Tech. Ctr., Alcoa Ctr., PA 15069 USA

#### 2:00 PM

Simulation of Development of Annealing Texture: Jerzy A. Szpunar<sup>1</sup>; <sup>1</sup>McGill University, Dept. of Metals & Matls. Engrg., 3610 Univ. St., Montreal Canada

This presentation is an overview of our research on transformation of microstructure and texture during annealing operations A model is presented that allows simulating texture and microstructure development at various stages of the annealing process. The model incorporates a description of the initial texture and microstructure, the anisotropy of stored energy of deformation, condition of nucleation and and differences in mobility of different grain boundaries. Several examples are presented to illustrate various factors that influence texture transformation. In particular texture transformation in IF and low carbon steels, aluminum alloys, Fe-Si steels and nanocrystalline Ni is discussed.

#### 2:35 PM

Quantitative Analysis of Texture Evolution for Cold Rolled DC and CC AA5052 and AA5182 Aluminum Alloys During Isothermal Annealing: Yumin Zhao<sup>1</sup>; James G. Morris<sup>1</sup>; <sup>1</sup>University of Kentucky, Dept. of Matls. Sci. & Engrg., 177 Anderson Hall, Lexington, KY 40506 USA

The as-received Direct Chill Cast (DC) and Continuous Cast (CC) AA5052 and AA5182 hot bands were preheated at 454°C for 4 hours followed by cold rolling to 80% reduction in thickness. The cold rolled AA5052 and AA5182 aluminum alloys were isothermally annealed at

three temperatures. Texture evolution during isothermal annealing was investigated by X-ray diffraction using the Schulz technique and ODF procedure. After the volume fractions for the various texture components were calculated employing an improved integration method, texture evolution during isothermal annealing was quantitatively analyzed using an Avrami type equation. At the same time the differences in recryatllization behaviors between AA5052 and AA5182 aluminum alloys and between DC and CC materials were compared. It was found that the texture evolutions could be well expressed by Avrami type equations. The cube recrystallization texture component was strong for AA5052 aluminum alloys and annealing temperature had little influence on the recrystallization texture of the AA5052 aluminum alloys. The recrystallization textures of AA5182 alloys were weak and varied with annealing temperature. In addition, DC AA5052 and DC AA5182 materials possessed stronger cube recrystallization textures than the corresponding CC materials. Furthermore, the n value in the Avrami type equation possessed different values for AA5052 versus AA5182 aluminum alloys and for DC versus CC materials. For AA5052 alloys, the n values increased with increase in annealing temperature. On the other hand, the n values for AA5182 alloys remained constant for the different annealing temperatures.

#### 3:10 PM

Nucleation and Growth of Orientations from Cold Rolled OFE Copper: Carl T. Necker<sup>1</sup>; <sup>1</sup>Los Alamos National Laboratory, MST-6, MS G770, Los Alamos, NM 87545 USA

The macroscopic strains imposed during cold rolling yield dramatic changes in the initially equiaxed microstructure and nearly random texture. It is primarily the rolling process that predetermines the development of new microstructures and textures during static annealing treatments. Although the presence of retained rolling textures and the formation of very strong cube textures during recrystallization is well documented, the highly complex microstructures and graded textures from which these recrystallization textures arise are only partially understood and are still worth investigating. Orientation Imaging Microscopy is used to explore both the deformed microstructure and texture as well as the incipient strain free grains that foreshadow conditions in the fully recrystallized state.

#### 3:45 PM

Texture Evolution During Grain Growth: Effect of Boundary Properties and Initial Microstructure: Ning Ma<sup>1</sup>; Suliman A. Dregia<sup>1</sup>; Yunzhi Wang<sup>1</sup>; <sup>1</sup>Ohio State University, Matls. Sci. & Engrg., 2041 College Rd., Columbus, OH 43210 USA

We incorporate the dependence of grain boundary energy and mobility on misorientation in three-dimension into the phase field model to investigate orientation selection during grain growth in systems consisting of a single cube component embedded in a matrix of randomly oriented grains in the initial microstructure. Starting from various fractions and spatial distributions of the cube component, we show that the effect of energy anisotropy on texture development differs drastically from that of mobility anisotropy. In all cases the fraction of the cube component increases if boundary energy is anisotropic, and decreases if boundary mobility is anisotropic while energy is isotropic. Similar to previous studies, when boundary energy is anisotriopic the misorientation distribution is no longer time-invariant and grain growth kinetics deviates from the behavior of isotropic grain growth. However, mobility anisotropy could also alter misorientation distribution and hence affect grain growth kinetics, which is different from the results obtained previously for systems of either random or singlecomponent texture. The initial spatial distribution of the texture component plays an important role in determining the time-evolution of the misorientation distribution and hence affects the overall kinetics of texture evolution and grain growth.

#### 4:20 PM

Growth of the Cube Component in FCC Deformation Textures: Simulation and Theory: Anthony D. Rollett<sup>1</sup>; <sup>1</sup>Carnegie Mellon University, Matls. Sci. & Engrg., Wean Hall 4315, 5000 Forbes Ave., Pittsburgh, PA 15213 USA

Prof. Doherty has devoted a substantial fraction of his career to advancing our understanding of the stability or lack of stability of microstructures. A notable example of such an issue is the appearance of minority texture components during annealing of deformed metals. Many theories have been advanced to explain the origins, for example, the cube component,  $\{001\}<100>$ , in fcc metals. One such theory concerns "microselection" whereby the cube component is favored during the early stages of recrystallization where coarsening takes place in the subgrain structure formed during recovery. To address this possibility, Monte Carlo simulation of grain growth is used to study the behavior of the cube component during grain growth in a

polycrystal for which the dominant texture is representative of rolling textures in fcc metals. The cube component was treated as a special texture component, inserted into the microstructure by assigning nearcube orientations to particular grains. A sensitivity analysis varied such parameters as initial cube volume fraction, the grain boundary energy and mobility functions, spatial correlation of the special component, and rotations of the special component away from the exact cube position. The results indicate a strong tendency for the cube component to grow provided that a moderate level of anisotropy exists in the grain boundary energy and mobility.

### 4:55 PM

**3D Simulations of Zener Drag**: *Gael Couturier*<sup>1</sup>; Claire Maurice<sup>1</sup>; Roland Fortunier<sup>1</sup>; Roger Doherty<sup>2</sup>; Julian Driver<sup>1</sup>; <sup>1</sup>Ecole des Mines de Saint Etienne, Matls. Dept. France; <sup>2</sup>Drexel University, Dept. of Matls. Engrg., Philadelphia, PA USA

A 3D finite element model has been developed to simulate the interaction of a moving boundary with one or several second phase particles. The model is first applied to the case of curvature driven grain growth where a single boundary of varying dimension represents the average grain boundary radius during growth in a polycrystal containing particles. Compared with classical Zener predictions, it is shown that the restraining drag force exerted by each particle is less than expected but that an anchored boundary is in contact with 3 to 4 times the number of particles given by the rigid boundary assumption. Consequently the overall drag force is higher than derived from the basic Zener model and the limiting grain size is therefore smaller. Some preliminary results of Zener drag at a recrystallization boundary are also presented.

# The Didier de Fontaine Symposium on the Thermodynamics of Alloys: Experimental Techniques

Sponsored by: Materials Processing and Manufacturing Division, MPMD-Computational Materials Science & Engineering-(Jt. ASM-MSCTS)

*Program Organizers:* Diana Farkas, Virginia Polytechnic Institute and State University, Department of Materials Science and Engineering, Blacksburg, VA 24061 USA; Mark D. Asta, Northwestern University, Department of Materials Science and Engineering, Evanston, IL 60208-3108 USA; Gerbrand Ceder, Massachusetts Institute of Technology, Department of Materials Science and Engineering, Cambridge, MA 02139 USA; Christopher Mark Wolverton, Ford Motor Company, Scientific Research Laboratory, Dearborn, MI 48121-2053 USA

Monday PM	Room:	216B		
March 15, 2004	Location	: Charlott	e Convention	Center

Session Chair: TBA

### 2:00 PM Invited

Nanoscale Modulations in Optimally Doped YBa2Cu3O6.92: X-Ray Evidence for Atomic Displacements in Higher Order ORTHO Phases: Z. Islam<sup>2</sup>; J. C. Lang<sup>2</sup>; D. Haskel<sup>2</sup>; D. R. Lee<sup>2</sup>; G. Srajer<sup>2</sup>; D. R. Haeffner<sup>2</sup>; U. Welp<sup>3</sup>; S. K Sinha<sup>4</sup>; S. C. Moss<sup>1</sup>; P. Wochner<sup>5</sup>; <sup>1</sup>University of Houston, Dept. of Physics, Houston, TX USA; <sup>2</sup>Argonne National Laboratory, Advd. Photon Source USA; <sup>3</sup>Argonne National Laboratory, Matls. Sci. Div. USA; <sup>4</sup>University of California, Dept. of Physics, San Diego, CA USA; <sup>3</sup>Max-Planck Institute fuer Metallforschung, Stuttgart Germany

Diffuse, strain-induced, superlattice peaks have been observed using synchrotron x-rays in a single domain crystal of YBa2Cu3O6.92 along the a-axis, i.e. normal to the filled oxygen chains. These broad satellite peaks correspond to a 4-unit cell modulation of the structure which is poorly correlated along both x-and y-axes, indicating a kinetically (diffusion) limited formation of the ORTHO phase(s) predicted by De Fontaine and co-workers. In addition, the separate satellites show a pronounced modulation along the z-axis whose Fourier transform can be well fit by a set of atomic displacements within a unit cell along z which are not the same for all atoms in the cell; i.e. this is not simply a x-y planar modulation. At room temperature the diffuse scattering about a normal Bragg peak is dominated by the one-phonon thermal diffuse scattering (TDS) as calculated from the measured phonon dispersion curves. At low temperature, however, there can be seen a familiar "bow-tie" diffuse scattering in the H-K plane which peaks along the <110> directions, in a manner earlier observed for Al-doped YBCO, which could be attributed to disorder among the oxygen chainplane sites. In the present case, the disorder underlying this Huang diffuse scattering (HDS), presumably arises from the inherent disorder associated with the short-range nature of the locally modulated structure. These results will be discussed in terms of the tendency of YBCO to assume a range of ORTHO phases.

### 2:30 PM Invited

A Combined Kinetic Monte Carlo and Experimental Study of the Temporal: David N. Seidman<sup>1</sup>; <sup>1</sup>Northwestern University, Matls. Sci. & Engrg., Cook Hall, 2220 Campus Dr., Evanston, IL 60208-3108 USA

The temporal evolution of model Ni-Al-Cr superalloys is being studied, employing three-dimensional atom-probe (3DAP) and transmission electron microscopies, in parallel with kinetic Monte Carlo (KMC) simulations on the same alloys. The objectives are, employing these tools, to: (1) follow the kinetic pathways by which the gamma phase (fcc) decomposes into gamma (fcc) plus gamma-prime (L12 structure) phases; (2) to determine the chemistry of individual precipitates with subnanoscale resolution; (3) to distinguish between ordered gamma-prime precipitates and disordered ones; (4) to follow the temporal evolution of the concentration profiles of the precipitates; (5) to measure the time dependencies of the mean radius, number density and supersaturations of Al and Cr and to compare them with the Umantsev-Kuehmann-Voorhees model for coarsening of a ternary alloy; (6) to observe the process of coagulation of precipitates; (7) to examine the atomic mechanism of coarsening, that is, evaporationcondensation of single atoms versus the cluster-diffusion-coagulation mechanism.

### 3:00 PM Invited

Nucleation and Coarsening of  $\gamma$  (Ni-Al) Precipitates in a  $\gamma$ ' (Ni<sub>3</sub>Al) Matrix: Yong Ma<sup>1</sup>; *Alan J. Ardell*<sup>1</sup>; <sup>1</sup>University of California, Dept. of Matls. Sci. & Engrg., 6531 Boelter Hall, Los Angeles, CA 90095-1595 USA

The morphology, spatial correlations and kinetics of coarsening of Ni<sub>3</sub>Al ( $\gamma$ ') precipitates have been thoroughly investigated, while precipitation of the disordered Ni-Al ( $\gamma$ ) solid solution from supersaturated  $\gamma$ ' has received relatively little attention. Since the  $\gamma$ - $\gamma$ ' interfacial free energy, lattice mismatch and elastic-constant mismatch are entirely independent of the majority phase, precipitation of  $\gamma$  from supersaturated  $\gamma$ ' might be a mirror image of the precipitation of  $\gamma$ ' from  $\gamma$ . This conjecture is completely belied by our preliminary results. For example: Nucleation of  $\gamma$ ' from supersaturated  $\gamma$  is extremely fast while nucleation of  $\gamma$  from  $\gamma$ ' is very slow; The coarsening rates of  $\gamma$  in  $\gamma$ ' increase strongly with f;  $\gamma$ ' precipitates coalesce with difficulty during coarsening while  $\gamma$  precipitates coalesce in the context of thermodynamics and kinetic processes in Ni-Al alloys.

### 3:30 PM

Local Order or Local Decomposition in the Solid Solutions of Ni-Au and Pt-Rh?: *Bernd Schönfeld*<sup>1</sup>; Michael J. Portmann<sup>1</sup>; Christian Steiner<sup>1</sup>; Gernot Kostorz<sup>1</sup>; Felix Altorfer<sup>2</sup>; Joachim Kohlbrecher<sup>2</sup>; Angel Mazuelas<sup>3</sup>; Hartmut Metzger<sup>3</sup>; <sup>1</sup>ETH Zurich, Inst. of Appl. Physics, CH-8093 Zurich Switzerland; <sup>2</sup>PSI, CH-5232 Villigen Switzerland; <sup>3</sup>ESRF, F-38043 Grenoble France

For these two binary alloy systems exhibiting continuous solid solubility at elevated temperatures, there is an ongoing debate on the presence of short-range order and/or local clustering. Extensive measurements of diffuse scattering of neutrons and x-rays were thus performed to arrive at a conclusive characterization. Ni-Au single crystals containing 8.4 at.% and 60 at.% Au were studied in situ at temperatures above the miscibility gap, using small-angle and wide-angle neutron scattering. The incoherent scattering background was largely reduced by employing the Ni-58 isotope. An increase of coherent scattering towards small scattering vectors indicates local decomposition. A Pt-47 at.% Rh single crystal quenched from 920 K to room temperature, was investigated by laboratory X-rays, synchrotron radiation (enhanced scattering contrast at wavelengths close to the Rh K-edge) and neutrons. Weak maxima in diffuse scattering are found around 1 1/2 0 and 000, with local decomposition being more pronounced.

3:50 PM Break

## 4:00 PM Invited

Some Experimental Studies of Coherent Phase Separation in Binary Alloys: Gernot Kostorz<sup>1</sup>; <sup>1</sup>ETH Zurich, Appl. Physics, Zurich CH 8093 Switzerland On their way toward equilibrium, decomposing binary alloys often pass through intermediate, metastable states with coherent pre-precipitates. Small-angle scattering (of X-rays and neutrons) has been used to reveal microstructural features, especially early stages of decomposition in alloys, ideally studied as single crystals. Kinetic in-situ neutron scattering studies have been performed in newly developed high-temperature cells. A survey will be given on the early stages of phase separation in Ni-rich Ni-Ti where coherency strains and ordering of the precipitates affect the kinetics. A temporary slowing-down is observed in some cases. In Al-rich Al-Ag, coherency strains are small, but the decomposition also shows unexpectedly complex behavior. Here, the combined results of small-angle X-ray scattering, diffuse neutron scattering and high-resolution Z-contrast electron microscopy offer a consistent description of the microstructure starting with the very early stages of decomposition.

### 4:30 PM Invited

**Diffuse Scattering Methods - A Critical Testbed for Alloy Theory:** *Harald Reichert*<sup>1</sup>; <sup>1</sup>MPI für Metallforschung, Heisenbergstrasse 3, Stuttgart 70569 Germany

Recently developed diffuse x-ray scattering methods enable us to retrieve effective pair interactions in k-space with unprecedented resolution and accuracy. In parallel, we have combined first-principles calculations of the alloy energetics with reciprocal space methods for the interpretation of the experimentally determined diffuse scattering maps. We have used this method to separate chemical and straininduced components in the effective pair interactions. In this presentation we will directly compare results from first-principles calculations for a series of model alloys (Cu-Au, Au-Ni,Ti-V) with diffuse scattering data. In all cases we find new features in the scattering maps with profound consequences for mechanisms such as the screening in alloys or phase separation kinetics.

### 5:00 PM

Nanoscale Studies of the Temporal Evolution of the Early Stages of Decomposition and Coarsening in Model Ni-Al-Cr Superalloys: *Chantal K. Sudbrack*<sup>1</sup>; Kevin E. Yoon<sup>1</sup>; Jessica A. Weninger<sup>1</sup>; Ronald D. Noebe<sup>2</sup>; David N. Seidman<sup>1</sup>; <sup>1</sup>Northwestern University, Matls. Sci. & Engrg., 2220 Campus Dr., Evanston, IL 60208 USA; <sup>2</sup>NASA Glenn Research Center, 21000 Brookpark Rd., Cleveland, OH 44135 USA

Limited experimental data on decomposition pathways of ternary metallic alloys exists, and decomposition is not well understood due to complex interactions. We employ three-dimensional atom-probe (3DAP) and transmission electron microscopies to investigate gamma (fcc) to gamma (fcc) + gamma-prime (L1<sub>2</sub> structure) in Ni-5.2 Al-14.2 Cr and Ni-7.6 Al-8.6 Cr (at.%) aged at 600°C. For the times investigated (2 minutes to 1024 hours), these alloys exhibit a high number density ( $10^{24}$  m<sup>-3</sup>) of spheroidal precipitates, 0.5-10 nm in radius. The reaction is identified as nucleation, growth and coarsening by the presence of solute-rich precipitates, exhibiting short-range order in the asquenched state. Precipitate coagulation is present, and its influence on the power-law dependencies of the number density, mean radius, and supersaturations of Al and Cr, are discussed in light of parallel kinetic Monte Carlo simulations. This research is supported by the National Science Foundation and NASA Glenn HOTPC program.

### 5:20 PM

The Role of Re on the Temporal Evolution of the Nanostructure of a Model Ternary Ni-Cr-Al Superalloy: Kevin Eylhan Yoon<sup>1</sup>; Ronald D. Noebe<sup>2</sup>; David N. Seidman<sup>1</sup>; <sup>1</sup>Northwestern University, Matls. Sci. & Engrg., 2220 N. Campus Dr., Evanston, IL 60208 USA; <sup>2</sup>NASA Glenn Research Center, Cleveland, OH 44135 USA

The temporal evolution of  $\gamma'$  (L1<sub>2</sub>) precipitates in a quaternary  $\gamma$  (fcc) Ni-Cr-Al-Re alloy, aged at 1073 K from 0.25 to 264 hours, is investigated by transmission electron and three-dimensional atomprobe (3DAP) microscopies. Rhenium (2 at.%) was added to a model Ni-8.5 at.% Cr-10 at.% Al superalloy to study its effects on the temporal evolution. The number density, mean radius, and volume fraction of  $\gamma'$  precipitates are measured, as well as the supersaturations of alloying elements as functions of time. The morphology of  $\gamma'$  precipitates is spheroidal, even for extended aging times. Rhenium delays the coarsening of  $\gamma'$  precipitates and stabilizes their morphology, in comparison to a model Ni-Cr-Al superalloy, aged at 1073 K. The coarsening kinetics do not obey the time dependencies predicted by LSW theory. The coalescence of precipitates is suggested to be a factor. This research is supported by the NSF and NASA Glenn HOTPC program.

# Third International Symposium on Ultrafine Grained Materials: Processing II: Structural Evolution

Sponsored by: Materials Processing & Manufacturing Division, MPMD-Shaping and Forming Committee Program Organizers: Yuntian Ted Zhu, Los Alamos National

Laboratory, Materials Science and Technology Division, Los Alamos, NM 87545 USA; Terence G. Langdon, University of Southern California, Departments of Aerospace & Mechanical Engineering and Materials Engineering, Los Angeles, CA 90089-1453 USA; Terry C. Lowe, Metallicum, Santa Fe, NM 87501 USA; S. Lee Semiatin, Air Force Research Laboratory, Materials & Manufacturing Directorate, Wright Patterson AFB, OH 45433 USA; Dong H. Shin, Hanyang University, Department of Metallurgy and Material Science, Ansan, Kyunggi-Do 425-791 Korea; Ruslan Z. Valiev, Institute of Physics of Advanced Material, Ufa State Aviation Technology University, Ufa 450000 Russia

Monday PM	Room:	207A		
March 15, 2004	Location	: Charlotte	Convention	Center

Session Chairs: Dong H. Shin, Hanyang University, Dept. Metall. Matls. Sci., Ansan Korea; Yuri Estrin, Clausthal University of Technology Germany; Jingtao Wang, Nanjing University of Science & Technology, Sch. of Matls. Sci. & Engrg., Nanjing 210094 China

### 2:00 PM Invited

**Deformation Microstructures**: *Niels Hansen*<sup>1</sup>; Xiaoxu Huang<sup>1</sup>; Darcy A. Hughes<sup>2</sup>; <sup>1</sup>Risoe National Laboratory, Matls. Rsch. Dept., Ctr. for Fundamental Rsch., Metal Structures in 4-D, Roskilde DK-4000 Denmark; <sup>2</sup>Sandia National Laboratories, Ctr. for Matls. & Engrg. Scis., Livermore, CA 94550 USA

Microstructural characterisation and modelling have shown that a variety of metals deformed by different mechanical processes follow a general path of grain subdivision by dislocation boundaries and high angle boundaries. This general path has been demonstrated over length scales from the millimetre to the nanometre range by quantitative characterisation of microstructural parameters applying electron microscope techniques as transmission electron microscopy (TEM), Kikuchi pattern analysis and electron back scatter diffraction (EBSD). Studies on a finer scale by high resolution electron microscopy (HREM) have also been applied to characterise individual dislocations in the layers between boundaries. The microstructural characterisation has concentrated on metals as aluminium, copper, nickel and iron deformed by processes introducing strains up to about 5-10 (e.g., rolling, accumulative roll bonding and equal channel angular extrusion) and processes introducing strains of 100 or more (e.g., cyclic extrusion compression, high pressure torsion and friction). The structural parameters over many length scales have been analysed applying physical principles and mathematical procedures including scaling. This has led to improved understanding of the subdivision process and the relationships between processing and microstructure, and between microstructure and properties.

### 2:20 PM

Principles of High-Pressure Torsion and Equal-Channel Angular Pressing: A Comparison of Microstructural Characteristics: Alexandre P. Zhilyaev<sup>1</sup>; Minoru Furukawa<sup>2</sup>; Zenji Horita<sup>3</sup>; *Terence G. Langdon*<sup>4</sup>; <sup>1</sup>Universitat Autonoma de Barcelona, Dept. de Fisica, Bellaterra 08193 Spain; <sup>2</sup>Fukuoka University of Education, Dept. of Tech., Munakata, Fukuoka 811-4192 Japan; <sup>3</sup>Kyushu University, Matls. Sci. & Engrg., Fac. of Engrg., Fukuoka 812-8581 Japan; <sup>4</sup>University of Southern California, Aeros. & Mech. Engrg. & Matls. Sci., Los Angeles, CA 90089-1453 USA

Two major procedures are currently in use for the production of ultrafine-grained materials: high-pressure torsion (HPT) in which a sample is subjected to a high pressure with concomitant torsional straining and equal-channel angular pressing (ECAP) where a sample is pressed through a die constrained within a channel that is bent through an abrupt angle. Both of these procedures lead to the imposition of a large imposed strain without any reduction in the cross-sectional dimensions of the work-piece. This paper examines these two procedures with special reference to the factors influencing the microstructural characteristics.

# MONDAY PM

### 2:35 PM

**Evolution in Microstructural Parameters During High Pressure Torsion of Nickel**: *Xiaoxu Huang*<sup>1</sup>; A. Vorhauer<sup>2</sup>; Grethe Winther<sup>1</sup>; Niels Hansen<sup>1</sup>; R. Pippan<sup>2</sup>; M. Zehetbauer<sup>3</sup>; <sup>1</sup>Risoe National Laboratory, Matls. Rsch. Dept., Ctr. for Fundamental Rsch., Metal Structures in 4-D, Roskilde DK-4000 Denmark; <sup>2</sup>Austrian Academy of Sciences, Erich Schmid Institute Austria; <sup>3</sup>University of Vienna, Inst. of Matls. Physics Austria

High pressure torsion (HPT) is a well-developed deformation process which allows metal samples to be deformed to extremely high strains. In this work we apply HPT to deform nickel samples to strains above 10. At such high strains, the microstructural evolution has not been well understood. In this work, the microstructural evolution is characterized by transmission electron microscopy (TEM), with emphasis on the characterization of misorientation angles and their distribution. A semiautomatic TEM method is employed for orientation measurement to get a good statistics. The results showed that low misorientation angles dominate at low strains and that the fraction of low angle boundaries decreases with increasing strain. However, even at an effective strain of 34, there is still quite a large fraction of low angle dislocation boundaries existing in the structure that leads to a deviation of the misorientation distribution from that for a polycrystal with random orientations of grains.

### 2:50 PM Invited

**Development of Microstructure During Equi-Channel Angular Pressing of Pure Aluminum**: *Terry R. McNelley*<sup>1</sup>; Douglas L. Swisher<sup>1</sup>; Keiichiro Oh-ishi<sup>1</sup>; <sup>1</sup>Naval Postgraduate School, Dept. of Mech. Engrg., 700 Dyer Rd., Monterey, CA 93943-5146 USA

The evolution of microstructure and microtexture during repetitive equi-channel angular pressing (ECAP) of high-purity Al was examined by orientation imaging microscopy (OIM) and convergent beam electron diffraction (CBED) methods in transmission electron microscopy (TEM). Shear textures are apparent after an initial pressing pass but are very inhomogeneous. The texture and microstructure become more homogeneous and a highly refined, equiaxed deformation-induced microstructure evolves during repetive pressing operations. Nevertheless, after four ECAP passes a band-like arrangement may be resolved in both the OIM and TEM data. The bands align with shear plane and the interfaces between the bands are high-angle boundaries. Low angle boundaries separate equiaxed cells within the bands. After 12 ECAP passes the bands have become increasingly elongated such that there are only one or two cells across each band and the fraction of high-angle boundaries is increased. The mechanism of microstructure transformation will be discussed.

### 3:10 PM Invited

Severe Plastic Deformation of Al: Effect of Strain Path: Ayman A. Salem<sup>1</sup>; S. L. Semiatin<sup>2</sup>; <sup>1</sup>Universal Technology Corporation, Dayton, OH 45432 USA; <sup>2</sup>Air Force Research Laboratory, Matls. & Mfg. Direct., Wright-Patterson AFB, OH 45433 USA

Microstructure evolution during severe plastic deformation of unalloyed aluminum (high purity and commercial-purity) was investigated to establish the effect of processing route and purity level on grain refinement and subgrain formation. Two lots of unalloyed aluminum with different purity levels (99.99%Al and 99%Al) were subjected to large plastic strains at room temperature. Four different deformation processes were used: equal channel angular extrusion, conventional conical-die extrusion, sheet rolling, and uniaxial compression. Orientation imaging microscopy was employed to characterize the developed microstructures. The various deformation routes yielded an ultrafine microstructure with a ~1.5 µm grain size in commercialpurity aluminum. For high-purity aluminum, however, the minimum grain size produced after the various deformation routes was  $\sim 20 \ \mu m$ , and there were indications of recrystallization. The high fraction of high-angle grain boundaries and the absence of subgrains/deformation bands in the final microstructure confirmed the occurrence of recrystallization of high-purity aluminum at large plastic strains.

### 3:30 PM Invited

Formation of Defects During Equal Channel Angular Extrusion: *Rimma Lapovok*<sup>1</sup>; P. McKenzie<sup>1</sup>; <sup>1</sup>Monash University, Sch. of Physics & Matls. Engrg., Clayton, Vic 3800 Australia

The theoretical definition of damage imparted to a material by it's processing method, which is proportional to plastic deformation, unites several types of defects; such as that of grain-boundary voids and micro cavities formed by decochesion of hard particles from the surrounding matrix. As Equal Channel Angular Extrusion (ECAE) is a process of severe plastic deformation, the damage accumulated during processing of a material is significant. The intensity of damage accumulation depends on the route of extrusion taken and back-pressure

applied. In this paper, the damage accumulation-recovery model introduced in our previous works is proven experimentally. The initial distribution of cavities, the distribution in intermediate passes and after processing, and the development of defects due to plastic deformation during ECAE processing was studied by high resolution Field Emission Gun (FEG) Scanning Electron Microscopy (SEM) for different processing routes. It is shown, that Route A is the most favorable route for defect formation. Increasing the back-pressure was found to change the character of fracture in samples produced, because the decohesion of particles within the matrix and brittle fracture of hard particles is suppressed. The source of formation of voids during ECAE is therefore reduced.

### 3:50 PM Break

### 4:00 PM Invited

Microstructure and Texture Development in Cu and Al Under ECAP: New Experimental Results and Modeling: Yuri Estrin<sup>1</sup>; *Ralph Hellmig*<sup>1</sup>; Seung Chul Baik<sup>1</sup>; Hyoung Seop Kim<sup>2</sup>; Hans-Günter Brokmeier<sup>1</sup>; Aikaterini Zi<sup>1</sup>; <sup>1</sup>Clausthal University of Technology, Matls. Engrg. & Tech., Agricolastrasse 6, Clausthal-Zellerfeld 38678 Germany; <sup>2</sup>Chungnam National University, Dept. of Metallurgl. Engrg., Daejeon 305-764 Korea

Aluminum and copper were processed by equal channel angular pressing (ECAP) following the four standard routes. The effect of the ECAP route and the number of passes on strength and ductility as well as on the dislocation cell structure and texture was studied for both materials. To investigate the stress distribution in ECAP deformed workpieces, hardness maps with small imprint spacing were produced for various sections of the workpieces. The experimental results were compared with the simulations based on a phase-mixture model that combines a dislocation density evolution approach with crystal plasticity considerations. A good predictive capability of the model was confirmed.

### 4:20 PM

**On the Mechanism of Grain Subdivision During Severe Plastic Deformation**: *A. E. Romanov*<sup>1</sup>; T. S. Orlova<sup>1</sup>; N. A. Enikeev<sup>2</sup>; A. A. Nazarov<sup>2</sup>; I. V. Alexandrov<sup>2</sup>; R. Z. Valiev<sup>2</sup>; <sup>1</sup>Ioffe Physico-Technical Institute, 26 Polytechnicheskaya, St. Petersburg 194021 Russia; <sup>2</sup>Ufa State Aviation Technology University, 12 K. Marx St., Ufa 450000 Russia

The problem of theoretical description of microstructure evolution at severe plastic deformation (SPD) is addressed. An energetic consideration for grain subdivision is developed in terms of disclination theory. The model assumes that larger grains split into a number of substructure elements in order to reduce the total latent energy stored in the material due to plastic deformation inhomogenities. The stored energy of a probe grain, which is constrained to a specific crystallographic orientation, is calculated using the disclination description. The grain is believed to be divided into a number of subgrains if the split configuration possessed lower energy than the initial one. Resulting structures are treated as disclination dipole and quadrupole configurations. The developed model demonstrates the typical features of substructure evolution at SPD: transformation of substructure into high angle grain boundaries and grain size refinement.

### 4:35 PM

**Microstructures of Ferritic Warm Rolled Plain Carbon Steels**: *Gwenola Herman*<sup>1</sup>; Benoît Lechevalier<sup>2</sup>; Frank Montheillet<sup>2</sup>; Tarcisio Oliveira<sup>3</sup>; <sup>1</sup>Arcelor, R&D, CRDM, rue du comte Jean, Grande-Synthe BP2508, Dunkerque cedex 1 59381 France; <sup>2</sup>Ecole Nationale Supérieure des Mines de Saint-Etienne, CNRS URA 1884, Saint Etienne France; <sup>3</sup>ACESITA, Centro de Pesquisas, Praça 1° de Maio, 9, Timoteo - MG 35180-000 Brazil

Little work has been performed on ferritic warm deformation of plain carbon steels. By contrast, work on ferritic stainless steels has shown that intense hot deformation could lead to a fully dynamically recrystallised structure. This suggests that warm deformation in the ferritic region of steels could also lead to such microstructure, and therefore interesting prospects for the improvement of properties through grain size refinement. That is why the present prospective work focuses on warm rolling of plain carbon steels. Low carbon microalloyed steels (C<0.1%, 0.5%<Mn<1.5%, Si<0.4% + V) were intensively warm rolled (400-700°C) in the ferritic region after austenitic hot rolling on a laboratory rolling mill. This study shows that warm deformation in the ferritic region of plain carbon steels is indeed able to induce fragmentation of grains, although fragmentation remains partial. The EBSD analyses of microstructures suggest that in our case warm rolling induces continuous dynamic recrystallisation, although heterogeneous.

# 4:50 PM

Nano-Grained Steels Produced by Various Sever Plastic Deformation Processes: *Minoru Umemoto*<sup>1</sup>; *Yoshikazu Todaka*<sup>1</sup>; Koichi Tsuchiya<sup>1</sup>; <sup>1</sup>Toyohashi University of Technology, Production Sys. Engrg., 1-1 Hibarigaoka, Tempaku-cho, Toyohashi, Aichi 441-8580 Japan

The formation of nanocrystalline structure (NS) in steels by various severe plastic deformation processes, such as ball milling, a ball drop test, particle impact deformation and air blast shot peening are studied. Layered or equiaxed nanograined region appeared near the specimen surface and dislocated cell structured region appeared interior of specimens. The deformation induced nanograined regions have the following common specific characteristics: 1) with grains smaller than 100 nm and low dislocation density interior of grains, 2) extremely high hardness, 3) dissolution of cementite when it exist and 4) no recrystallization and slow grain growth by annealing. The deformation conditions to produce NS was discussed based on the available data in literatures. It was suggested that the most important condition is to impose a strain larger than about 7. High strain rates, low deformation temperature, multidirectional deformation, hydrostatic pressure are considered to be favorable conditions to produce NS.

### 5:05 PM

Investigation Into the Effect on Grain Refinement of Developing a Strong Texture in an UFG Al-0.13% Mg Alloy Severely Deformed by ECAE: Christopher Paul Heason<sup>1</sup>; Philip B. Prangnell<sup>1</sup>; <sup>1</sup>UMIST, Manchester Matls. Sci. Ctr., Grosvenor St., Manchester M1 7HS UK

Much work has been done over the years in studying the production of UFG materials using equal channel angular extrusion (ECAE). Such materials are known to exhibit weak textures as a consequence of the repeated shear deformation. However, to date no investigation has been made into the effect of changing the deformation mode on such material. In this current study, a single phase Al-0.13% Mg alloy was severely deformed to a strain of ~10 at room temperature by ECAE, producing a submicron grain structure (>70% HAGB) and weak texture. Deformed billets were subsequently deformed by both conventional rolling and accumulative roll-bonding (ARB), producing sheet material with strong rolling textures and, in the case of ARB, an additional shear {001}<110> texture. It was found that, although initially the grain size decreased and HAGB fraction increased, as the rolling texture strengthened the HAGB fraction decreased to below 70% leading to an increase in grain size. This was associated with the appearance of coarse, unrefined banded regions, which were found to have very strong textures.

### 5:20 PM

Structural Transformations in Metallic Multilayers During Intense Deformation: *Rainer J. Hebert*<sup>1</sup>; John H. Perepezko<sup>1</sup>; <sup>1</sup>University of Wisconsin, Dept. of Matls. Sci. & Engrg., 1509 Univ. Ave., Madison, WI 53706 USA

During repeated rolling and folding of metallic multilayers structural transformations occur that can include a refinement of the grainsize and the layer thickness to a nanometer level as well as atomicscale mixing and alloying reactions at the layer interfaces. The layer refinement is analyzed for Al-Pt and Al-Hf multilayers as a function of strain in terms of the relative specific interface area, the layer thickness distribution and the compass dimension of the layers. The analysis reveals a difference in the average layer thickness and the relative specific interface area between Al-Pt and Al-Hf multilayers that is approximately two orders of magnitude. The amorphization reaction at the Al-Pt interfaces during rolling is examined based on a TEM analysis. The results demonstrate the significance of the layer refinement for structural transformations in multi-phase materials during severe plastic deformation. The support of the ARO is gratefully acknowledged (DAAD 19-01-1-0486).

### 5:35 PM

Structure Evolution During High Pressure Torsion of Ti-Ni-Based Shape Memory Alloys: Sergey Dmitriy Prokoshkin<sup>1</sup>; Irina Borisovna Trubitsyna<sup>1</sup>; Irina Yuriy Khemelevskaya<sup>1</sup>; Sergey Vladimir Dobatkin<sup>2</sup>; Evgeniy Vasiliy Tatyanin<sup>2</sup>; <sup>1</sup>Moscow State Steel and Alloys Institute, Leninsky prospekt 4, Moscow 119049 Russia; <sup>2</sup>Russian Academy of Science, Baikov Inst. of Metall. & Matl. Sci., Dept. of Phys.-Mech. Problems of Bulk Nanomatls., Leninsky prospekt 49, Moscow 119991 Russia

Ti-50.0at.%Ni (Ms = 68°C after quenching), Ti-50.7at.%Ni (Ms = -20°C) and Ti-47at.%Ni-3at.%Fe (Ms = -127°C) shape memory alloys subjected to a severe plastic deformation by high pressure torsion (HPT) have been studied using transmission electron microscopy, X  $_i$ V ray diffractometry and microhardness tests. True torsion strains var-

ied from 0 to 6.6, deformation temperatures from -196 to 200°C, and pressure from 4 to 8 GPa. A general sequence of structure formation with strain is from a strain-hardened dislocation substructure to a nanocrystalline structure and ultimately to an amorphized structure in all alloys studied. The tendency to form an amorphized structure is different for different alloys and depends on relative positions of the deformation temperature and starting point of the martensitic transformation Ms. Increasing of a pressure suppresses the tendency to form an amorphized structure as a consequence of the Ms lowering.

# Third International Symposium on Ultrafine Grained Materials: Posters

Sponsored by: Materials Processing & Manufacturing Division, MPMD-Shaping and Forming Committee
Program Organizers: Yuntian Ted Zhu, Los Alamos National Laboratory, Materials Science and Technology Division, Los
Alamos, NM 87545 USA; Terence G. Langdon, University of
Southern California, Departments of Aerospace & Mechanical
Engineering and Materials Engineering, Los Angeles, CA 90089-1453 USA; Terry C. Lowe, Metallicum, Santa Fe, NM 87501 USA;
S. Lee Semiatin, Air Force Research Laboratory, Materials & Manufacturing Directorate, Wright Patterson AFB, OH 45433 USA;
Dong H. Shin, Hanyang University, Department of Metallurgy and
Material Science, Ansan, Kyunggi-Do 425-791 Korea; Ruslan Z.
Valiev, Institute of Physics of Advanced Material, Ufa State Aviation Technology University, Ufa 450000 Russia

Mon PM/Tue/Wed	Room:	207A		
March 15-17, 2004	Location	n: Charlotte	Convention	Center

**Production of Fine-Grained Beryllium-6 wt% Copper for Fusion Ignition Capsules**: *David J. Alexander*<sup>1</sup>; Jason C. Cooley<sup>1</sup>; Dan J. Thoma<sup>2</sup>; Arthur Nobile<sup>3</sup>; <sup>1</sup>Los Alamos National Laboratory, MST-6 G770, Los Alamos, NM 87545 USA; <sup>2</sup>Los Alamos National Laboratory, ADWEM F654, Los Alamos, NM 87545 USA; <sup>3</sup>Los Alamos National Laboratory, MST-7, E549, Los Alamos, NM 87545 USA

Beryllium doped with 6 weight % copper is the material of choice for fabrication of target capsules for the National Ignition Facility because of its combination of attractive neutronic, physical, and mechanical properties. The target capsules are very small (2 mm in diameter) and thin-walled (150 microns) and must meet demanding dimensional specifications. The material must be fine-grained and of low inclusion content. Arc-melted Be-Cu is being produced to eliminate the oxide content that is inevitably present in conventional powder-metallurgy materials. Equal channel angular extrusion (ECAE) is being used to refine the as-cast grain structure. Be rods produced by the arc-melting process (5 mm in diameter by 30 mm in length) are enclosed in nickel cans with electron-beam welded plugs. The Be-in-Ni billets (9.5 mm in diameter by 45 mm in length) have been processed by ECAE at temperatures from 500 to 750°C. The resultant microstructures will be presented.

High Strain Rate Deformation Behavior of Ultra-Fine Grain Aluminum Produced by Equal Channel Angular Pressing: *Hiroyuki Miyamoto*<sup>1</sup>; <sup>1</sup>Doshisha University, Dept. of Mech. Engrg., 1-3 Miyakodani Tatara, Kyotanabe, Kyoto 610-0321 Japan

Deformation behavior of ultra-fine grained aluminum at high strain rates were investigated by impact tensile test, using Split Hopkinson Pressure Bar method. Ultra fine grained aluminum of commercial purity were produced by equal channel angular pressing by eight passes. Both the ultra-fine grained aluminum and polycrystalline aluminum of conventional grain size were deformed by the impact tensile tests and normal tensile test at the strai rate of 1200 1/s and 10-3 1-s, respectively under room temperature. It was found that ultra-fine grained aluminum show lower flow stress than that deformed at normal tensile stess while polycrystalline aluminum showed relatively similar stress in impact and tensile test. Microstructure after the tests were examined by transmission electron microscopy, and resuls were discussed in terms of dislocation dynamics.

**Computer Simulation of SPD Processes:** Alexander V. Spuskanyuk<sup>1</sup>; <sup>1</sup>Donetsk Physical & Technical Institute, 72 R. Luxemburg St., Donetsk 83114 Ukraine

New SPD processes Twist Extrusion and Equal Channel Multi-Angular Extrusion (ECMAE) have been studies by means of computer simulations. During twist extrusion a workpiece is extruded through the helical die with prismatic input and calibrating output channels localizing the twisting deformation in the beginning and in the end of helical die. ECMAE is performed by extruding a workpiece through constant cross-section channel with several changes of metal flowing direction. Computer simulation of the deformation and structure forming has been performed by combined use of mechanical FEM modeling for detailed study of the stressed-strained state evolution and original micromechanical multiscale model of polycrystalline aggregate to study the microstructure modification with emphasis on grain refinement. Correct correspondence of the simulation results with the experimental data for number of materials has allowed predicting of material structure and properties' evolution during processing, which made it possible to control and enhance these technologies.

Evolution of Grain Boundary Character Distribution in ECA-Pressed Pure Ti: Seng-Ho Yu<sup>1</sup>; *Sun-Keun Hwang*<sup>1</sup>; Dong-Hyuk Shin<sup>2</sup>; <sup>1</sup>Inha University, Sch. of Matls. Sci. & Engrg., #253, Yonghyun-Dong, Nam-Ku, Inchon 402-751 Korea; <sup>2</sup>Hanyang University, Dept. of Metall. & Matls. Sci., Kyunggi-Do, Ansan 425-791 Korea

Evolution of the grain shape, texture and grain boundary misorientation angle of commercially pure Ti during equal channel angular (ECA) pressing were studied with the use of microscopy, X-ray diffraction and electron back scattered diffraction. The grain size refinement was about a factor of 100 although the high angle boundaries were only realized with more than 4 passes using the route BC at various temperatures (250 to 550°C). Evolution of the texture during ECA pressing was derived from the complex combined activation of slip systems and twin systems, which was confirmed by texture prediction modeling based on visco-plastic self-consistent theory. Grain growth phenomena were studied with a Monte-Carlo computer simulation technique using a direct mapping concept. Overall the grain growth was characterized as a normal growth in the microstructure with stable random boundaries. The texture was found to be tenacious during subsequent heat treatment after ECA pressing.

Structural Changes of Severely Plastic Deformed Rail Steel: *Florian Wetscher*<sup>1</sup>; Richard Stock<sup>2</sup>; Baohui Tian<sup>1</sup>; Reinhard Pippan<sup>1</sup>; <sup>1</sup>Erich-Schmid Institute of Materials Science, Jahnstraße 12, Leoben 8700 Austria; <sup>2</sup>voestalpine Schienen GmbH, Tech./R&D, Kerpelystrasse 199, Leoben 8700 Austria

Severe Plastic Deformation (SPD) has been applied to ARMCOiron and the pearlitic rail steel S900A by means of High Pressure Torsion (HPT). In this study the evolution of the microstructure was investigated by different x-ray diffraction techniques and by transmission electron microscopy (TEM). The texture development in ARMCOiron and the rail steel as well as the obtained size of the structural elements will be compared. For the pearlitic steel the special features of microstructural evolution at larger strains, fragmentation of cementite lamellae, solution of carbon, etc. are described and discussed.

Processing of Aluminum Nickelides by Equal-Channel Angular Extrusion: Laszlo J. Kecskes<sup>1</sup>; Hyo Y. Kim<sup>1</sup>; Robert H. Woodman<sup>1</sup>; <sup>1</sup>US Army Research Laboratory, AMSRL-WM-MD, Deer Creek Loop, Aberdeen Proving Ground, MD 21005-5069 USA

Two series of nickel-coated aluminum (Al Ni) powder compositions were consolidated to full or near-full density by an equal channel engular extrusion technique. Mixtures of 78Al 22Ni at.% (63Al 37Ni wt.%) or 39Al 61Ni at.% (23Al 77Ni wt. %) were placed in squareshaped copper blocks, sealed, preheated to a range of temperatures from ambient to 700°C, and, once at a uniform temperature, dropped into a ECAE die and extruded. It was found that the preheating temperature affected the transformation of the initial Al Ni composition into aluminum nickelide (Al Ni) intermetallics. Scanning electron microscopy, energy dispersive x-ray spectroscopy, x-ray diffraction, and microhardness measurements were used to examine the nature of the resultant intermetallics. The onset and nature of the transformation from the precursors into the products were further studied by differential thermal analysis. These results and the role of ECAE on the transformation are discussed.

Generation of Sub-Micrometer Structures During Orthogonal Cutting of 1100Al: Mustafa Elmadagli<sup>1</sup>; Hai Ni<sup>1</sup>; Hai Ni<sup>1</sup>; Ahmet T. Alpas<sup>1</sup>; <sup>1</sup>University of Windsor, NSERC/GM of Canada Industrial Rsch. Chair, Mech., Auto. & Matls. Engrg., 401 Sunset Blvd., Windsor, Ontario N9B 3P4 Canada

Sub-micrometer structures developed in the material ahead of the tool tip in commercial purity 1100 Al samples (with an initial grain size of 4.6 mm and microhardness of 45 kg/mm2) that were subjected to an orthogonal cutting process were investigated using TEM. The microstructure of the primary deformation zone, where stains of the order of 1.5 were measured, was characterized by the formation of elongated dislocation cell structures of 370 nm in thickness, 725 nm in length that were composed of heavily tangled dislocation walls. Further grain refinement occurred in the chip as a result of dynamic

recrystallization and subdivision of the elongated cells into smaller equiaxed sub-micron size (300 nm diameter) grains. This was accompanied with a hardness increase to 80 kg/mm2. In this region strains were as high as 2.2. The strengthening arising from grain refinement is discussed using the Hall-Petch equation.

Microstructural Development in Interstitial Free Steel Processed by Equal Channel Angular Extrusion: Azdiar A. Gazder<sup>1</sup>; Elena V. Pereloma<sup>1</sup>; <sup>1</sup>Monash University, Sch. of Physics & Matls. Engrg., Bldg. 69, Monash Univ., Victoria 3800 Australia

Considerable grain refinement in bulk materials is achievable through the application of severe plastic deformation. In particular, equal channel angular extrusion could be utilized for this purpose. In current work, samples of interstitial free steel were pressed in air at room temperature. The tests were performed with the angle between channels of the die of 90 and 120° and up to 2 and 4 passes, respectively. The specimens were characterized using transmission electron microscopy and texture analysis. Effect of accumulated strain on the: (i) formation of systems of parallel microbands, delineated by planar boundaries, (ii) development of dislocation cells substructure, (iii) formation of shear bands and (iv) texture was evaluated.

**Response of Mechanical Properties Along the Workpiece Section to ECA-Pressing**: *Alexander I. Korshunov*<sup>1</sup>; <sup>1</sup>RFNC-VNIIEF, Tech. Div., Mira St., Bldg. 37, Sarov, Nizhny Novgorod Region 607190 Russia

Nonuniformity of mechanical properties along the workpiece section depending on the number of ECA-pressing operations was studied using annealed M1 Cu (min. Cu content 99.9%) as a sample material. The samples under examination had a square section with a side length of 8 mm and were cut out from an 8-mm thick sheet along the rolling direction. Microhardness distribution along the sample section was determined. Mechanical properties at drawing (conventional yield strength, ultimate strength, relative elongation and contraction) were determined at 9 points along the section using microsamples with a diameter of 1.5 mm cut out along the pressing direction. Strain diagrams were drawn. The investigations were carried out after 1, 2 and 4 pressing operations along the BC and C routes.

Structural Models of High-Energy Nanostructures in Metals and Intermetallic Materials Under Severe Plastic Deformation: Alexander Nikolaevich Tyumentsev<sup>1</sup>; Alexander Dmitrievich Korotaev<sup>2</sup>; 'Russian Academy of Science, Inst. of Strength Physics & Matls. Tech., Lab. of Struct. Transformations, 2/1, Academicheskii pr., Tomsk 634055 Russia; <sup>2</sup>Siberian Physicotechnical Institute, Tomsk 634050 Russia

Electron microscopy was used to investigate the features of the highly nonequilibrium structural states occurring in nanostructural metals and intermetallic compounds after severe plastic deformation caused by equichannel angular pressing, torsion in Bridgemen anvils, and cold rolling. A model has been proposed that treats nanostructural states as states with a high continual density of defects (dislocations and disclinations) in the bulk of submicrograins and a high density of partial disclinations) in the bulk of submicrograins and a high density of partial disclinations at their boundaries. Based on this model, methods for electron microscopic examination of local internal stress fields on the submicron scale have been developed. It has been shown that on the characteristic scale about 0.1 micrometer, these stresses reach values (~ E/30) close to the theoretical strength of the crystal and are responsible for the high stress gradients (moments), constituting the driving force of the collective rotational mode of deformation and reorientation of microvolumes.

Microstructure, Texture and Enhanced GB Energy in UFG Nickel: Alexandre P. Zhilyaev<sup>1</sup>; Jerzy A. Szpunar<sup>2</sup>; Maria Dolors Baró<sup>1</sup>; Terence G. Langdon<sup>3</sup>; <sup>1</sup>Universitat Autònoma de Barcelona, Dept. of Physics, Bellaterra, BCN 08193 Spain; <sup>2</sup>McGill University, Dept. of Metals & Matl. Engrg., 3610 Univ. St., Montreal H3A 2B2 Canada; <sup>3</sup>University of Southern California, Dept. Aeros. & Mech. Engrg., Los Angeles, CA 90089-1453 USA

Ultrafine-grained materials are expected to have higher strength and toughness comparing to their coarse-grained counterparts. Generally, grain refinement has been accomplished by using various thermomechanical processing treatments involving both heat treatments and mechanical working. But these procedures have the disadvantage that new and often complex procedures must be developed for each individual alloy. An alternative procedure is to use processes involving severe plastic deformation (SPD): equal channel angular pressing (ECAP) and high-pressure torsion (HPT). Thorough investigation of microstructure, texture and grain boundary statistics has been carried out in pure nickel samples fabricated by means of ECAP, HPT and their combination. It was accomplished that combination of ECAP and HPT leads to a deeper refinement of nickel samples possessing homogeneous and equiaxed microstructures. A difference between the released enthalpy in DSC experiments and the elastic energy evaluated by high-resolution x-ray diffractometry is attributed to the decrease in total surface energy during grain growth in ultrafine-grained nickel. The grain boundary (GB) surface energy of high angle boundaries was also evaluated.

**Destabilization of FCC Stable Materials at SPD Under High Pressure**: Boris M. Efros<sup>1</sup>; Yan Beygelzimer<sup>1</sup>; Anatoly Deryagin<sup>2</sup>; Natalia Efros<sup>1</sup>; Vitaliy Pilyugin<sup>2</sup>; *Dmitry Orlov*<sup>1</sup>; <sup>1</sup>University of the National Academy of Science, Donetsk Phys. & Tech. Inst., Physics of High Pressure & Advd. Tech. Dept., 72 R. Luxemburg St., Donetsk 83114 Ukraine; <sup>2</sup>Russian Academy of Science, Inst. of Metal Physics, Ekaterinburg 620219 Russia

It was shown that of a fine  $\alpha$ -phase was formed in the Hadfield steel a cold plastic deformation to  $\varepsilon = 50\%$ . Nuclei of the  $\alpha$ -phase of deformed samples reduced the decomposition start temperature of the austenite by 180C. Fine crystals of an  $\alpha$ -phase nearly 30 nm in size, whose concentration was as high as ~2.3%, were detected in a steel Fe79.55Mn17A13C0.45 after a SPD to  $\varepsilon = 92\%$ . A steel Fe61.2Cr18Mn20N0.7C0.1 contained fine crystals of a strain-induced  $\alpha$ -phase 20 nm in size after a low temperature plastic deformation. The  $\alpha$ -phase, which was formed under the given conditions, had an extremely low Curie temperature T<sub>c</sub> = 400C. When the steel was strongly deformed (e ~ 8) by SPD a strain-induced  $\alpha$ -phase have a normal Curie temperature T<sub>c</sub> = 600C. Thus, the obtained results indicate that SPD can result in a considerable destabilization of stable austenitic steels.

### Fatigue Strength for Iron Based Nano-Composite: Chitoshi Masuda<sup>1</sup>; <sup>1</sup>Waseda University, Kagami-Memorial Lab. for Matls. Sci. & Tech., 2-8-26, Nishiwaseda, Sinjuku, Tokyo Japan

For electric refined iron having fine grain size the fatigue strength was about 300 MPa at the number cycles to failure of 107. This value is higher than that for a S25C carbon steels. It is suggested that the fatigue strength for iron and steels would be improved to be higher by the grain size or nano-structures. It has been reported that the iron having a nano-structures had a very high tensile strength up to about 1500 MPa, while the fatigue strength was not discussed yet. In this study, the fatigue strength and fatigue fracture mechanisms are discussed for iron having nano-structures. The iron powders of average size less than 45 mm were mixed by high energy ball mill and canning into the low carbon steel tube. The tube was welded for both sides and vacuumed at high temperature. After that the material was hot rolled and finally cold drawn in 5mm in diameter. The fatigue specimen was machined in order to remove the outer low carbon steel. The fatigue strength is about 500 MPa at the number cycles to failure of 107. The average fatigue strengths for S35C(12 Heats), S45C(11 Heats) and S55C(11 Heats) carbon steels quenched and tempered at 600°C are about 385, 437 and 463 MPa, respectively. The result obtained in this study is very higher than that for S35C, S45C and S55C carbon steels tempered at 600°C. Moreover, the fatigue strength for electric refined iron having the average grain size of 3mm was about 300 MPa at the number of cycles to failure reported. The fatigue strength for nanostructured iron was also 200 MPa higher than that for a iron having a fine grain size. Nano structured iron have a very fine grain size. It is more fine for nano-structured iron than electric refined iron cold drawn. The difference of fatigue strength beteen nano-structured iron and cold drawing electric refined iron would be caused by the decrease of the grain size and the dispersing the Fe2O3 nano-particles in iron matrix. Finally the fatigue strength and fatigue fracture mechanism for nano-structured composite will be compared with the material fabricated by powder iron, being the same as nano-composite, canning and drawing at room temperature.

### **Developments in Equal Channel Angular Extrusion Technol**ogy: *David J. Alexander*<sup>1</sup>; <sup>1</sup>Los Alamos National Laboratory, MST-6 G770, Los Alamos, NM 87545 USA

Equal channel angular extrusion (ECAE) is the most developed method of severe deformation processing. Several extensions of the original ECAE technology have been developed at Los Alamos National Laboratory. These include: processing of long billets; processing of flat plate samples; continuous roll-fed ECAE; and dual-axis and triple-axis ECAE. These developments will be described and discussed.

### Grain Refinement of Electron-Beam Melted Crystal Bar Zirconium by Equal Channel Angular Extrusion: David J. Alexander<sup>1</sup>; David A. Korzekwa<sup>1</sup>; <sup>1</sup>Los Alamos National Laboratory, MST-6 G770, Los Alamos, NM 87545 USA

Electron-beam melted crystal bar zirconium results in a very low oxygen content (approximately 100 ppm by weight), but a coarse grain structure (10s of mm) that must be refined. Cylindrical rods were sectioned by electrodischarge machining, and enclosed in seamless nickel tubing (1.2 mm wall thickness) by electron beam welding plugs in each end to make a final billet 9.5 mm in diameter by 60 mm in length. The billet was deformed by equal channel angular extrusion (ECAE) at room temperature in 120° tooling. After extrusion for 4 passes via route Bc the material was annealed in vacuum for 1 h at 550°C. Because of the low oxygen content, the Zr could be successfully deformed by ECAE to high strains at room temperature. The ascast grains were extensively subdivided by the processing. A fine uniform grain size of approximately 2 microns was achieved after the anneal.

Development of Crystallographic Texture During ECAPing of Beryllium: A Neutron Diffraction and Polycrystalline-Plasticity Modeling Study: Donald W. Brown<sup>1</sup>; David J. Alexander<sup>2</sup>; Irene J. Beyerlein<sup>3</sup>; Mark A.M. Bourke<sup>1</sup>; Carlos N. Tome<sup>1</sup>; Sven C. Vogel<sup>4</sup>; <sup>1</sup>Los Alamos National Laboratory, MST-8, MS-H805, Los Alamos, NM 87545 USA; <sup>2</sup>Los Alamos National Laboratory, MST-6, MS-G770, Los Alamos, NM 87545 USA; <sup>3</sup>Los Alamos National Laboratory, T-3, MS-B216, Los Alamos, NM 87545 USA; <sup>4</sup>Los Alamos National Laboratory, LANSCE-12, MS-H805, Los Alamos, NM 87545 USA

Beryllium samples were extruded from 1 to 4 passes through a 120° bend at 425°C following route Bc. In parallel, samples were also deformed under uniaxial compression at comparable strain rates and at 425°C. The crystallographic texture of each sample was determined using time-of-flight neutron diffraction techniques on the High Pressure Preferred Orientation (HIPPO) Diffractometer at LANSCE. A visco-plastic self-consistent (VPSC) model was developed to simulate the texture development during both deformation processes. Comparison of the model predictions of texture and flow strength to the simple uniaxial tests defined input parameters for the model, such as critical resolved shear stresses and hardening rates. These parameters were then used in an attempt to predict the more complicated deformation associated with ECAP'ing. A critical comparison of the observed and calculated texture development of the ECAP'ed samples will be given.

Mechanical Properties and Evolution of the Grain Structure of an Ultra-Fine Grained Cu-Al-O Alloy During Deformation: *Eduard V. Kozlov*<sup>1</sup>; Yurii F. Ivanov<sup>1</sup>; Anatolii N. Zhdanov<sup>2</sup>; Nina A. Koneva<sup>1</sup>; <sup>1</sup>Tomsk State University of Architecture and Building, Dept. of Physics, Solyanaya sq. 2, Tomsk 634003 Russia; <sup>2</sup>Altai State Technical University, Lenin Str., 46, Barnaul 656099 Russia

A dispersion strengthened Cu-Al-O alloy prepared by high-temperature extrusion was studied in this work. The samples with different average grain sizes in the range between 0.2 and 0.3 micron were studied. Deformation of the samples was performed in compression at room temperature. The structure of the alloys in the as-prepared state and after deformation was studied using TEM. A high yield stress and the stages III and V of work hardening were observed. Hall-Petch relationship was valid near the yield stress and at stress levels that correspond to developed plastic deformation. The analysis of the structure showed different behavior of grains with different sizes in a polycrystalline aggregate. During the deformation process, grain size distribution function, fraction of dislocation-free grains and their critical sizes are changing. The behavior of other parameters of the dislocation structure and the strengthening phases during deformation was also analyzed.

**Equal Channel Angular Pressing as an Efficient Technique for Grain Refiniment**: *Farid Z. Utyashev*<sup>1</sup>; Georgy I. Raab<sup>1</sup>; Ruslan Z. Valiev<sup>1</sup>; <sup>1</sup>Ufa State Aviation Technical University, Inst. of Physics of Advd. Matls., 12 K. Marx St., Ufa 450000 Russia

In the paper we compare various techniques for introducing large advanced strains leading to formation of fine grains and subgrains. Structural and mechanical analysis performed on the basis of experimental and theoretical data substantiates the need for formation of a homogeneous UFG structure refined down to the limit in materials of spatially non-monotone billet deformation in controlled thermomechanical conditions. Different examples of such deformation implementation are considered, including modified ECA pressing schemes, as well as microstructures and mechanical properties of a number of materials processed by severe plastic deformation, including hard-to-deform alloys.

**Processing Ultrafine Grained Composites of Elemental Titanium and Aluminum by Severe Plastic Deformation**: *Gajanan Chaudhari*<sup>1</sup>; Kazim Serin<sup>1</sup>; Viola L. Acoff<sup>1</sup>; <sup>1</sup>University of Alabama, Metallurgl. & Matls. Engrg., Box 870202, 126, 7th Ave., Tuscaloosa, AL USA

Ultrafine grained composite sheets of elemental titanium and aluminum foils were processed using the roll bonding process. These sheets were severely deformed by repeated cold rolling with interspersed folding of the sheets. The titanium layer was observed to neck and break down producing a finely dispersed intermixture of Ti-Al binary. The structural evolution of the resulting material was investigated using transmission electron microscopy (TEM). It revealed the formation of nano-scale grains in the composite. X-ray diffraction, differential scanning calorimetry (DSC) and scanning electron microscopy were also utilized to characterize the composites. Tensile testing, microhardness testing and nanoindentation were used to evaluate the mechanical properties of the resulting composite.

**Manufacturing of Long Specimens by ECAP**: *Gyorgy Krallics*<sup>1</sup>; Dmitry Malgin<sup>2</sup>; Georgy I. Raab<sup>3</sup>; Igor V. Alexandrov<sup>3</sup>; <sup>1</sup>Budapest University of Technology and Economics, Dept. of Matls. Sci. & Engrg., 7 Bertalan L., Budapest 1111 Hungary; <sup>2</sup>Drehsden Ltd., Budapest Hungary; <sup>3</sup>Ufa State Aviation Technical University, Inst. of Physics of Advd. Matls., 12 K. Marx St., Ufa, Bashkortostan 450000 Russia; <sup>3</sup>Ufa State Aviation Technical University, Inst. of Physics of Advd. Matls., 12 K. Marx St., Ufa, Bashkortostan 450000 Russia

ECAP is the most wide-spread technique for producing ultra-fine grained materials. Due to the cyclic nature of the process, it is difficult to produce specimens with a high length to diameter ratio. Ratios of 6-7 have been reported in the literature to date. Longer specimens, however, are useful since the homogenous part is larger and the relative size of end effects are smaller. Two methods were developed to obtain length to diameter ratios as high as 10. These methods allow using all routes (A, B, C) in the manufacturing process. This new technique was developed using the finite element computer simulation. The thermo-mechanical material tests before and after ECAP (1, 4 and 8 pass) are presented in this paper in order to show the influence of the process on mechanical properties of material (Al alloy 6082).

Use of Back Pressure During ECAP as a Means to Enhance the Deformability of Materials and Efficiently Refine the Structure: Georgy I. Raab<sup>1</sup>; Nickolay A. Krasilnikov<sup>2</sup>; Ruslan Z. Valiev<sup>1</sup>; <sup>1</sup>Ufa State Aviation Technical University, Inst. of Physics of Advd. Matls., 12 K. Marx st., Ufa 450000 Russia; <sup>2</sup>Ulyanovsk State University, 42 L. Tolstoy str., Ulyanovsk 432700 Russia

Equal channel angular pressing (ECAP) is an efficient technique for refinement of structure in bulk materials. However, fabrication by ECAP of samples out of low-ductile materials with a homogeneous ultrafine-grained structure without visible surface cracks and defects presents a problem. One of the techniques that enables to accomplish this task is use of back pressure in the process of ECAP allowing to control the stress strain in the strain center. By the example of copper (99.9%) and CP Ti it is shown that use of back pressure during ECAP leads to an increase in the number of passes before failure of the billet. Another advantage of ECAP with back pressure is formation of a more homogeneous structure with smaller grain size. The physical reasons and the role of back pressure for enhancement of strength and ductility in materials after ECAP are discussed in the present paper.

From Macro- to Meso-Level of Plastic Deformation During Equal-Channel-Angular Processing: Grigoreta Mihaela Stoica<sup>1</sup>; S. R. Agnew<sup>2</sup>; E. A. Payzant<sup>3</sup>; D. A. Carpenter<sup>4</sup>; P. K. Liaw<sup>1</sup>; <sup>1</sup>University of Tennessee, Matl. Sci. & Engrg., 323 Dougherty Bldg., Knoxville, TN 37996-2200 USA; <sup>2</sup>University of Virginia, Matls. Sci. & Engrg., Charlottesville, VA 22904 USA; <sup>3</sup>Oak Ridge National Laboratory, Metals & Ceram. Div., Oak Ridge, TN 37831 USA; <sup>4</sup>Y-12 National Security Complex, Oak Ridge, TN 37831 USA

Mg-alloy, ZK60, was subjected to Equal-Channel-Angular Processing (ECAP) using different strain paths: route A, B, and C. Optical microscopy, X-ray diffraction (XRD), and orientation-imaging microscopy (OIM) analyses are used for structural characterization at macro- and meso-levels of plastic deformation. The grain refinement, texture evolution, and elastic microstrain are determined, and correlated with the initiation of dynamic recrystallization during severe plastic deformation of ZK 60.

Influence of Experimental Parameters on the Plastic Flow Curve Obtained by Ball Indentation Testing: Gopinath R. Trichy<sup>1</sup>; Ronald O. Scattergood<sup>1</sup>; Kishore Ramaswamy<sup>1</sup>; Carl C. Koch<sup>1</sup>; K. L. Murty<sup>1</sup>; <sup>1</sup>North Carolina State University, Matls. Sci. & Engrg., Stinson Dr., Riddick Bldg., Raleigh, NC 27695-7907 USA

The techniques for material characterization need to be modified such that reliable data is obtained for the small samples typically produced for nanocrystalline materials. The ball indentation (BI) test is one such technique. BI tests were performed on steels, aluminum alloys and pure zinc (conventional and nanocrystalline) using a computer-controlled screw driven UTM. True stress and plastic strain were evaluated by changing the fixture compliance and indenter ball size. The plastic diameter of the impression was obtained by partial unloading, complete unloading, and optical measurement. BI tests were compared to conventional tensile tests and the influence of the experimental parameters on the flow curve is discussed. The theoretical background necessary for the BI methodology is also discussed.

An Evaluation of Cavity Development in the Tensile Testing of Ultrafine-Grained Iron Processed by ECAP: *Hsuankai Lin*<sup>1</sup>; Cheng Xu<sup>1</sup>; Bing Q. Han<sup>2</sup>; Enrique J. Lavernia<sup>2</sup>; Terence G. Langdon<sup>1</sup>; <sup>1</sup>University of Southern California, Aeros. & Mech. Engrg. & Matls. Sci., Los Angeles, CA 90089-1453 USA; <sup>2</sup>University of California, Chem. Engrg. & Matls. Sci., Davis, CA 95616-5294 USA

Iron of commercial purity was subjected to Equal-Channel Angular Pressing (ECAP) to reduce the grain size from an annealed value of ~200  $\mu$ m to a final value of ~0.2 - 0.4  $\mu$ m. Following ECAP, tensile samples were cut from the as-pressed billets with their tensile axes lying along the pressing direction. These samples were pulled to failure over a range of elevated temperatures using an initial strain rate of 1 x 10<sup>-3</sup> s<sup>-1</sup>. After fracture, samples were sectioned, polished and then examined carefully in an optical microscope equipped with a video camera and a facility for recording quantitative information on the size and shape of any internal cavities. Measurements were taken to record the average cavity area, the cavity shape in terms of the roundness coefficient and the orientation of the long axis of each cavity with respect to the tensile axis.

**Computer Simulation Analysis of Texture Formation Processes at ECAP**: *Igor V. Alexandrov*<sup>1</sup>; Andrey V. Shcherbakov<sup>1</sup>; Marina Zhilina<sup>1</sup>; Irene J. Beyerlein<sup>2</sup>; <sup>1</sup>Ufa State Aviation Technical University, Inst. of Physics of Advd. Matls., 12 K. Marx St., Ufa, Bashkortostan 450000 Russia; <sup>2</sup>Los Alamos National Laboratory, Theoretical Div., T-3, MS B216, Los Alamos, NM 87545 USA

Recent investigations have successfully demonstrated that the process of equal-channel angular pressing (ECAP) is accompanied by an intensive texture formation. However, the mechanisms of texture evolution are still not totally understood due to a complexity of the stress- strain state imposed on the sample by different routes of ECAP. In this work we represent the results of investigation of texture formation in pure copper using three types of polycrystalline models: the full constraints Taylor model, Sachs' model, and the visco-plastic selfconsistent model. Their predictive capability is compared for different ECAP routes and number of passes. The obtained simulation results are also compared with the available experimental measurements of texture in pure copper using X-ray diffraction. Conclusions about the influence of the mentioned simulation parameters on the character of the texture formation processes at ECAP are made.

**FEM Investigations of Equal-Channel Angular Pressing**: *Igor N. Budilov*<sup>1</sup>; Igor V. Alexandrov<sup>1</sup>; Yuriy V. Lukashchuk<sup>1</sup>; Irene J. Beyerlein<sup>2</sup>; Vladimir S. Zhernakov<sup>1</sup>; <sup>1</sup>Ufa State Aviation Technical University, 12 K. Marx St., Ufa, Bashkortostan 450000 Russia; <sup>2</sup>Los Alamos National Laboratory, Theoretical Div., T-3, MS B216, Los Alamos, NM 87545 USA

Realization of equal-channel angular pressing (ECAP) and as a result processing of bulk nanostructured billets possessing attractive exploitation properties represents a hard-to-perform task and is a many-factor experiment. In this connection application of computer simulation is very perspective. In the current report one may observe the results of the analysis of processes, which take place at ECAP of a copper billet applying the finite-elements method (FEM) by LS-DYNA and Superform codes. 3D analysis has revealed that in the area of contact interaction between the billet and the die-set a formation of areas with a considerable heterogeneity of plastic deformation fields takes place. There has been conducted an investigation of the influence of principal parameters of the technological process on the obtained results. There have been elaborated recommendations on the die-set construction's optimization for ECAP of copper billets with a square cross section.

Features of the Localization of Plastic Deformation of Ultrafine-Grained Copper: *Ivan Alexandrovich Ditenberg*<sup>1</sup>; Alexander Nikolaevich Tyumentsev<sup>2</sup>; <sup>1</sup>Siberian Physicotechnical Institute, Tomsk 634050 Russia; <sup>2</sup>Russian Academy of Science, Inst. of Strength Physics & Matls. Tech., Tomsk 634055 Russia

Electron microscopy was used to investigate the evolution of the microstructure of samples of ultrafine-grained (UFG) copper subjected to active tension at room temperature. It has been revealed that under these conditions, from the very beginning of the deformation process, a major mechanism for plastic flow is the formation of strain localization mesobands through quasi-periodic events of formation and relaxation of stress mesoconcentrators at the front of propagation of the mesobands. Mechanisms for the plastic relaxation of mesoconcentrators at the front of propagation of mesobands have been revealed and discussed, such as dynamic recrystallization, mechanical twinning, collective dislocation-disclination mechanisms for the deformation and

reorientation of the lattice in the zones where the local stresses of mesoconcentrators are maximum and inside deformation microtwins.

Microstructure Evolution and Mechanical Behavior of Bulk Copper Obtained by Consolidation of Micro and Nano Powders: Mohammed Haouaoui<sup>1</sup>; *Ibrahim Karaman*<sup>1</sup>; Hans J. Maier<sup>2</sup>; <sup>1</sup>Texas A&M University, Dept. of Mech. Engrg., MS 3123, College Sta., TX 77843 USA; <sup>2</sup>University of Paderborn, Lehrstuhl f. Werkstoffkunde, Paderborn 33095 Germany

Consolidation of micro and nano copper particles (-325 mesh, 130 nm, and 100 nm) was performed using room temperature equal channel angular extrusion (ECAE). The evolution of the microstructure and the mechanical behavior of the consolidates were investigated and related to the processing route. Possible deformation mechanisms are proposed and compared to those in ECAE processed bulk Cu. The effects of extrusion parameters for consolidation such as ECAE route, number of passes and extrusion rate are evaluated. Two extrusion passes were sufficient for obtaining full density. Combined high ultimate tensile stress (490 MPa) and ductility (~20% tensile fracture strain) with near elasto-plastic behavior was observed in consolidated -325 mesh Cu powder. On the other hand, early plastic instability took place leading to a continuous softening in flow stress of bulk ECAEd copper. Increase in both strength and ductility was evident with increasing number of passes in the bulk samples. Compressive strengths as high as 760 MPa were achieved in consolidated 130 nm copper powder. The average grain size of the consolidated 130 nm powder was about 90 nm. The simultaneous increase in strength and ductility in extruded bulk Cu observed in a microstructure with an average grain size of 300-500 nm appears to be inconsistent with grain boundary moderated deformation mechanisms as proposed before. Instead, the increase of ductility is attributed to dynamic recovery and local recrystallization forming bimodal microstructures. Near-perfect elastoplasticity was encountered in consolidated -325 mesh Cu powder. This effect is explained by a combined effect of strain hardening accommodated by large grains in the bimodal structure and softening caused by a recovery mechanism such as trapping of dislocations at grain boundaries. The present study shows that ECAE consolidation of nanoparticles opens a new possibility for the study of deformation mechanisms and mechanical behavior of bulk nanocrystalline materials as well as offering a new class of bulk materials for practical engineering applications. This work was supported by the National Science Foundation contract CMS 01-34554, Solid Mechanics and Materials Engineering Program, Directorate of Engineering, Arlington, Virginia and Deutsche Forschungsgemeinschaft.

Grain Refinement and Deformation Twinning in Severely Deformed AISI 316L Stainless Steel at High Temperatures (0.4 Tm - 0.65 Tm): G. Guven Yapici<sup>1</sup>; Yang Cao<sup>1</sup>; Ibrahim Karaman<sup>1</sup>; Zhiping Luo<sup>2</sup>; <sup>1</sup>Texas A&M University, Dept. of Mech. Engrg., MS 3123, College Sta., TX 77843 USA; <sup>2</sup>Texas A&M University, Microscopy & Imaging Ctr., College Sta., TX 77843 USA

The present work focuses on the grain refinement and deformation twinning of AISI 316L austenitic type stainless steel. Bulk stainless steel bars are processed using equal channel angular extrusion (ECAE) with a 90° tool angle. Microstructure and mechanical properties of successfully extruded billets are reported through light microscopy, electron microscopy, and mechanical experiments. X-ray analysis is conducted to report macro-texture evolution. Results are compared for different extrusion conditions including variations in temperature (450°C, 550°C, 600°C, 700°C and 800°C) and processing routes (one pass or two passes). Higher tensile and compressive strengths are obtained after ECAE compared to that of initial materials in relation with the grain refinement and deformation twinning. One pass extrusion at 700°C resulted in flow strength values more than 1000 MPa. Observed tension/compression asymmetry in the yield strength values and strain hardening was attributed to the deformation induced directional back stress, texture produced after ECAE and different deformation mechanisms under tension and compression. The goal is to produce desired end microstructures where deformation twinning is stabilized at high temperatures forming nanostructured AISI 316L stainless steel, leading to improved mechanical properties.

Peculiarities of the Reorientation of the Crystal Lattice During the Formation of Nanocrystals and Submicrocrystals of High-Nitrogen Austenitic Steel: *Igor Litovchenko*<sup>1</sup>; Alexander Nikolaevich Tyumentsev<sup>1</sup>; <sup>1</sup>Russian Academy of Science, Inst. of Strength Physics & Matls. Tech., Tomsk 634055 Russia

Transmission electron microscopy was used to study the evolution of the defect structure of a high-nitrogen austenitic steel in the process of its cold rolling. For profound strains of over 0.9 the crystal lattice of gamma-austenite is observed to disperse into nanocrystals with large-angle and small-angle disorientations. It has been revealed that the fragmentation of the crystal lattice into nanostructural states occurs with the participation of several mechanisms: the disclination mechanism for reorientation through collective rearrangements of substructures with a continual disclination density into nonequilibrium boundaries with high densities of grain-boundary disclinations; the prevailing mechanism for the formation of large-angle boundaries is mechanical twinning; a new mechanism for the deformation and reorientation of the lattice has been discovered which involves direct and reverse (over alternative systems) martensitic transformations in high local stress fields, leading to the formation of large-angle boundaries with reorientation vectors about 60°.

Microstructural Features and Mechanical Behavior of UFG Ti-6AI-4V Eli Alloy: Irina P. Semenova<sup>1</sup>; Yuntian Theodore Zhu<sup>2</sup>; Terry C. Lowe<sup>2</sup>; Georgy I. Raab<sup>1</sup>; Ruslan Z. Valiev<sup>1</sup>; <sup>1</sup>Ufa State Aviation Technical University, Inst. of Physics of Advd. Matls., 12 K. Marx St., Ufa, Bashkortostan 450000 Russia; <sup>2</sup>Los Alamos National Laboratory, Matls. Sci. & Tech. Div., MS G755, STC, Los Alamos, NM 87545 USA

This paper presents the research results of two-phase (a+b)Ti-6Al-4V Eli alloy, aimed at the formation of homogeneous ultra-fine grained (UFG) structure using severe plastic deformation (SPD) by means of ECAP and additional thermo-mechanical treatment. The mechanical behavior of the alloy during tensile tests at room teperature and their failure behavior were investigated. The study of structure formation and phase morphology features during deformation was carried out. It was found that SPD of Ti-6Al-4V Eli resulted in considerable enhancing of mechanical properties due to grain refinement and high internal stresses. For example, yield stress in processed samples increased by 30% in comparison with the initial state, preserving sufficient ductility. There were found some regularities in structure formation and properties of the alloy depending on the regimes of treatment. It was established that the combination of deformation and metastable phases' decomposition during SPD enabled to control microstructure and phase composition of the alloy and, correspondingly, its strength and ductility.

Structural Evolution by ECAP Processing of Copper and Tantalum: James M. O'Brien<sup>1</sup>; Joel W. House<sup>2</sup>; William F. Hosford<sup>4</sup>; Robert J. De Angelis<sup>3</sup>; <sup>1</sup>O'Brien and Associates, 406 S. Lane St., Blissfield, MI 49228 USA; <sup>2</sup>Air Force Reseach Laboratory, MNMW, 101 W. Eglin Blvd., Ste. 125, Eglin AFB, FL 32542-6810 USA; <sup>3</sup>University of Florida/ GERC, Shalimar, FL USA; <sup>4</sup>University of Michigan, Ann Arbor, MI 48109-4788 USA

Equal angular channel pressing (ECAP) provides practical advantages for material processing since the final geometry is unchanged from the initial geometry of the work piece. This attribute can be exploited in manufacturing environments where a) existing processing lines for specific part geometries are well established, or b) the part geometry dictates a specific processing route. If the in-service application of the part can utilize the unique properties attributable to ultra-fine grain structure than ECAP processing is a viable technology to be studied. In this investigation, tantalum and copper rods were processed by ECAP. A series of 2.5 inch diameter, 5 inch long cylinders of copper and tantalum were pushed through a 135° channel die. The cylinders were strained to a magnitude of 4 and 8 using Route B processing. Specimens of the materials were annealed after ECAP processing. The mechanical properties of the materials were characterized by hardness and tensile test measurements. The structural properties were characterized by grain size and grain orientation, via texture analysis. Results of the data analysis indicate the level of grain size reduction, uniformity and texture evolution that can be achieved by ECAP processing of copper and tantalum.

An Investigation on the Effect of Different Routes of Equal Channel Angular Pressing on Structure Evolution in a Commercial Low Carbon Steel: *Jingtao Wang*<sup>1</sup>; Junxia Huang<sup>2</sup>; ZhongZe Du<sup>2</sup>; Zheng Zhang<sup>2</sup>; Xicheng Zhao<sup>2</sup>; <sup>1</sup>Nanjing University of Science and Technology, Dept. of Matls. Sci. & Engrg., XiaoLingWei 200#, Nanjing 210094 China; <sup>2</sup>Xi'an University of Architecture and Technology, Sch. of Metallurgl. Engrg., Yanta Rd. No 13, Xi'an 710055 China

Structure evolution in a commercial low carbon steel (Fe-0.15%C-0.52%Mn) during equal channel angular pressing (ECAP) at room temperature was investigated comparatively via route C and Bc. Although in both cases the SAD pattern changes in a similar way, from a single crystal pattern with increasing azimuth spreading of the spots at low ECAP passes, to a discontinuous ring pattern with extensive azimuth spreading at high ECAP passes, indicating the formation of highly non-equilibrium structure with high grain boundary misorientations; with route C, nearly parallel bands of elongated substructures pertains in the ferrite microstructure after ECAP from 1 to 11 passes, with a slight decrease of the band width from 0.3-0.4 to 0.20.3 micrometers, while with route Bc, equiaxed grain structure with a grain size of about 0.25 micrometers forms at after 4 passes of ECAP. It is concluded in this investigation that ECAP route is critical to the formation of equiaxed grain structure in low carbon steel at room temperature.

Microstructure Evolution in a Lamellae Al-33%Cu Eutectic Alloy During Equal Channel Angular Pressing: *Jingtao Wang*<sup>1</sup>; Suk-Bong Kang<sup>2</sup>; Hyung-Wook Kim<sup>2</sup>; 'Nanjing University of Science and Technology, Dept. of Matls. Sci. & Engrg., XiaoLingWei 200#, Nanjing 210094 China; <sup>2</sup>Korea Institute of Machinery and Materials, Dept. of Matls. Engrg., Changwon 641-010 Korea

Strain driven transformation of lamellae structure in an eutectic Al-33%Cu alloy into a homogeneous equiaxed micro-duplex structure was investigated in equal channel angular pressing(ECAP) at 400°C via route Bc. Intensive strain during ECAP is accommodated by periodic bending, periodic shear banding, parallel shearing, and shear cutting of the lamellae in the eutectic. The transformation follows the stages of subdivision of the colonies into smaller lamellae blocks; the separation of these lamellae blocks into isolated islands, and finally the shrinkage to disappear of these islands, through the breaking down of the lamellae at near the lamellae block-equiaxed region boundaries. The kinetics of this strain driven microstructure transformation process, described by the dependence of relative lamellae area fraction on accumulated ECAP equivalent true strain, physiognomically resembles that of thermal activated transformation process.

Effect of Hard Cyclic Viscoplastic Deformation on Hardening/ Softening of SPD Copper: Lembit Kommel<sup>1</sup>; <sup>1</sup>Tallinn Technical University, Dept. of Matls. Engrg., Ehitajate tee 5, 19086, Tallinn Estonia

Detailed studies of ultrafine grained copper were performed on hard cyclic viscoplastic hardening/softening behavior. The hysteresis loops and axial stress amplitude analysis were made in the total deformation range 1%, 2% and 1+2+1% at 30 cycles accordingly. Special attention was paid to the role of structure condition depending on severe plastic deformation (SPD) passes number or grain sizes and heat treatment regimes of specimens. The results of this study show, that the ultrafine grained copper after SPD had a maximal axial stress, up to 435 MPa, the three times higher then annealed coarse grained copper after deformation hardening during viscoplastic deformation. In especially high cyclic hardening was measured of annealed at 400°C by low heating rate at 1°C/min of nanocrystalline copper but nanocrystalline copper, annealed at 200°C has minimal hardening/softening behavior and constant stress amplitudes during hard cyclic viscoplastic deformation. These behaviors are discussed in the terms of developing structures

An Examination of Cavity Development in an Aluminum-6061 Metal Matrix Composite Processed by Equal-Channel Angular Pressing: Megumi Kawasaki<sup>1</sup>; Yi Huang<sup>1</sup>; Cheng Xu<sup>1</sup>; Minoru Furukawa<sup>2</sup>; Zenji Horita<sup>3</sup>; Terence G. Langdon<sup>1</sup>; <sup>1</sup>University of Southern California, Aeros. & Mech. Engrg. & Matls. Sci., Los Angeles, CA 90089-1453 USA; <sup>2</sup>Fukuoka University of Education, Dept. of Tech., Munakata, Fukuoka 811-4192 Japan; <sup>3</sup>Kyushu University, Matls. Sci. & Engrg., Fac. of Engrg., Fukuoka 812-8581 Japan

An Al-6061 metal matrix composite, reinforced with 10 vol% of very fine Al2O3 particulates, was subjected to equal-channel angular pressing (ECAP). Inspection showed the grain size of the composite was reduced to the submicrometer level through processing by ECAP. The mechanical properties of the material were investigated using tensile testing at high temperatures over a range of strain rates. A detailed examination was conducted to evaluate the extent of cavitation in the samples pulled to failure and the results were recorded quantitatively using an appropriate analytical technique. This paper describes the development of cavities in the composite during tensile testing after ECAP and presents representative plots that summarize the cavity characteristics.

**On the Forces Generated During Friction Stir Processing of Aluminum 5052 Sheets**: Rajeswari R. Itharaju<sup>1</sup>; *Marwan K. Khraisheh*<sup>1</sup>; <sup>1</sup>University of Kentucky, Ctr. for Mfg., Mech. Engrg. Dept., 210 CRMS Bldg., Lexington, KY 40506-0108 USA

Friction Stir Processing (FSP) is a new advanced processing technique used to refine and homogenize the microstructure of alloy sheets. FSP has several advantages over traditional processing techniques including single step process, non-consumable and inexpensive tool, environmentally friendly, and easy to implement. Several studies have been conducted to optimize the process and relate various process parameters like rotational and translation speeds to the resulting microstructure. However, there is little data reported on the relation between forces generated during processing and the resulting microstructure. In this work, we discuss the relationship between the processing forces, the process parameters and the resulting microstructure of AA 5052. Sheets of 1/8 inch thickness were stir processed using a CNC HAAS vertical milling machine at different combinations of rotational and translational speeds. The forces were measured using a 3-component piezoelectric KISTLER dynamometer. The results indicate that the processing forces are sensitive to the process parameters and can be used to control and optimize the process.

On the Description of Intergranular Boundaries Misorientation During Severe Plastic Deformation: Nariman A. Enikeev<sup>1</sup>; Igor V. Alexandrov<sup>1</sup>; Ruslan Z. Valiev<sup>1</sup>; Tatiana S. Orlova<sup>2</sup>; Alexei E. Romanov<sup>2</sup>; <sup>1</sup>Ufa State Aviation Technical University, Inst. of Physics of Advd. Matls., ul. K.Marxa, 12, Ufa 450000 Russia; <sup>2</sup>Ioffe Physico-Technical Instutite, Polytechnicheskaya, 26, St. Petersburg 194021 Russia

There are numerous evidences that during severe plasctic deformation (SPD) mean misorientation evolution takes place and nanostructures with high angle grain bounaries are formed. In the given publication a theoretical description of transormation of low angle grain boundaries to high angle ones is discussed. A physical approach to this description connected with accumulating of sessile dislocations during deformation is considered. The interaction of interface boundaries with lattice dislocations is described and contribution of resulting defect structures to mean misorientation evolution is estimated. The obtained results are compared to experimental data available in literature.

**Evolution of the Structure of an Ultra-Fine Grained Cu During Plastic Deformation**: *Nina A. Koneva*<sup>1</sup>; Nataliya A. Popova<sup>1</sup>; Anatolii N. Zhdanov<sup>2</sup>; Lina N. Ignatenko<sup>1</sup>; Eduard V. Kozlov<sup>1</sup>; <sup>1</sup>Tomsk State University of Architecture and Building, Dept. of Physics, Solyanaya sq. 2, Tomsk 634003 Russia; <sup>2</sup>Altai State Technical University, Lenin Str., 46, Barnaul 656099 Russia

This paper is devoted to the study of plastic deformation and evolution of the structure of the ultra-fine grained Cu with the average grain size of 0.21 micron during compression at room temperature. The compression experiments revealed changes in the Cu substructure in the strain range between 0 and 90%. TEM of thin films and replicas was used to study the structure. The quantitative analysis of the substructure evolution during deformation was performed. The following parameters of the Cu structure were studied as a function of strain: grain size, density of boundaries of different types, scalar and excess dislocation densities, curvature-torsion of the crystal lattice, the amount of the dislocation slip within grains and grain boundary sliding. The chosen grain size ensured manifestation of the stages III and V of work hardening. The stage V was related to the oscillating behavior of most parameters of the dislocation structure with deformation.

Grain Refinement Mechanisms Operating During Severe Deformation of Aluminium Alloys Containing Second-Phase Particles: *Pete Apps*<sup>1</sup>; Philip B. Prangnell<sup>1</sup>; <sup>1</sup>UMIST, Manchester Matls. Sci. Ctr., Grosvenor St., Manchester M1 7HS UK

The effects of coarse second-phase particles (Al<sub>13</sub>Fe<sub>4</sub>), and fine coherent dispersoids (Al<sub>3</sub>Sc), on the evolution of ultra-fine grained structures have been examined in simple model aluminium alloys deformed by ECAE. The microstructural evolution has been studied using high-resolution EBSD and compared to previous work on single-phase alloys. It is shown that the presence of coarse particles dramatically increases the rate of grain refinement, and allows a uniform fine grain structure to be developed at a strain of ~5. In contrast, the presence of fine dispersoids appears to inhibit the formation of high-angle grain boundaries at low strain and, hence, retard the formation of a fine grain structure after severe deformation ( $\epsilon$ ~10). The microstructural mechanisms operating in each case are discussed.

Processing and FEM Simulation of a 5083 Aluminium Alloy at Room Temperature: Pedro A. Gonzalez Crespo<sup>1</sup>; Ignacio Puertas Arbizu<sup>1</sup>; Carmelo J. Luis Pérez<sup>1</sup>; <sup>1</sup>Public University of Navarre, Mech. & Matls. Engrg. Dept., Campus de Arrosadía s/n, Pamplona, Navarra 31006 Spain

The enhanced mechanical properties of crystalline materials is linked to very small grain sizes. ECAP is a technique for developing an ultrafine grained microstructure by introducing a severe plastic deformation in bulk materials by simple shear with no changes in their cross-section. The AA5083, an Al-Mg-Mn commercial alloy, is known for its superplastic behaviour. The room temperature mechanical properties of the extruded alloy were investigated through hardness measurements and tensile tests. Mechanical properties evolution during annealing is also considered. SEM-EBSD observations have been made in order to discuss the microstructural characteristics of the deformed alloy. Finite Element Modelling is used to predict the ECAE behaviour in different extrusions conditions and compared with experimental processes carried out in similar conditions.

Computer Simulation of Material Deformation Under Intense Plastic Strain During Equal-Channel Angular Pressing: Petr N. Nizovtsev<sup>1</sup>; <sup>1</sup>RFNC-VNIIEF, Teoretical Div., Mira St., Bldg. 37, Sarov, Nizhny Novgorod Region 607190 Russia

The analysis of behavior of material subjected to intense plastic strain (IPS) under the conditions of equal-channel angular pressing (ECAP) is an involved problem. When solving this problem, computer simulation of deformation processes at different scale levels plays an important role. At the macro-level, the material behavior can be described with a given scheme of deformation in accordance with its parameters. At the meso-level, which implies the study of grain and sub-grain structure and texture parameter evolution during the deformation, information about interrelation of the forming structure and properties of materials obtained can be acquired. The micro-level studies addressing elementary reactions of the atom-crystal defect interactions reveal the physical nature of the features of the processes that proceed. The paper presents the results of the first phase of the studies, i.e. macro-level material behavior simulation for one-pass ECAP with using a simple isotropic model of material (copper).

**Product Yield of ECAE Processed Material**: *Robert E. Barber*<sup>1</sup>; Tami Dudo<sup>1</sup>; Phillip B. Yasskin<sup>2</sup>; K. Ted Hartwig<sup>1</sup>; <sup>1</sup>Texas A&M University, Mech. Engrg., College Sta., TX 77843-3123 USA; <sup>2</sup>Texas A&M University, Math., College Sta., TX 77843-3368 USA

The growing study of ECAE has produced ever-increasing work on microstructural changes imparted to processed material. Little work, however, has been devoted to examining the resulting fully worked material volume in a given billet. In this paper, various processing schedules (routes) are studied, and the fully worked volume fraction and the billet region shapes reported. Each route is examined through at least eight passes, with billet aspect ratios ranging from 3:1 to 20:1. Volumes were calculated using Maple® math software and solid model techniques to verify the findings. This research will aid technology transfer to industry, since the useful volume fraction could greatly influence production efficiency and the final geometric shapes can influence the practicality of trimming operations, further reducing the useful material produced. The results to be reported are both surprising and interesting; route B ( $B_A$ ) for instance, was found to be far more efficient than route A.

Ultrafine Grained Steel After Heavy Warm Deformation of Ferritic - Pearlitic C-Mn Steels: Rongjie Song<sup>1</sup>; *Dirk Ponge*<sup>1</sup>; Radko Kaspar<sup>1</sup>; Dierk Raabe<sup>1</sup>; <sup>1</sup>Max-Planck-Institut für Eisenforschung, Max-Planck-Str. 1, 40237 Düsseldorf, Germany

In order to produce ultrafine ferrite in plain C-Mn steels with 0.15-0.3%C, the effect of heavy warm deformation with subsequent coiling on a ferritic-pearlitic structure was studied. It is shown that the resulting microstructure consists of ultrafine ferrite ( $\alpha$ ) grains (0.80-0.95 µm) and a homogeneously distributed cementite ( $\Theta$ ). Based on the results of Electron Back-Scattered Diffraction (EBSD), the fraction of highangle grain boundaries (> 15°) was in the range of 60% to 65%. Due to this refined microstructure, even these unalloyed steels exhibited excellent combinations of mechanical properties.

Microstructure and Mechanical Properties of Ultrafine Grained Low Carbon Steel Fabricated by Conventional Cold-Rolling and Annealing of Martensite: *Rintaro Ueji*<sup>1</sup>; Nobuhiro Tsuji<sup>1</sup>; Yoritoshi Minamino<sup>1</sup>; Yuichiro Koizumi<sup>1</sup>; <sup>1</sup>Osaka University, Dept. of Adaptive Machine Sys., 2-1, Yamadaoka, Suita, Osaka 565-0871 Japan

A new thermomechanical processing named the martensite process which can easily fabricate the ultrafine grained steels without severe plastic deformation was developed. In this process, martensite is used as the starting structure. The martensite starting structure was conventionally cold-rolled by various reductions and then annealed at various temperatures. The cold-rolled martensite mainly exhibited lamellar structure, which is typical in severely deformed materials. The area fraction of the lamellar structure increased and the mean spacing of the lamellar boundaries decreased with increasing the rolling reduction, accompanying significant strengthening. After subsequent annealing at warm temperatures, the lamellar structure turned to equiaxed ultrafine ferrite grains with carbides precipitated uniformly, and at higher temperatures conventional recrystallization occurred to form coarse grained structure. The recrystallization temperature became lower with increasing the rolling reduction. The specimen rolled to intermediate reduction (50%) performed the largest ductility keeping high strength around 900MPa after warm-temperature annealing.

The Effect of Rolling Strain on the Development of Ultrafine Grained Ti-Al-Nb Intermetallics: *Rengang Zhang*<sup>1</sup>; Viola L. Acoff<sup>1</sup>; Gajanan Chaudhari<sup>1</sup>; <sup>1</sup>University of Alabama, Dept. of Metallurgl. & Matls. Engrg., Box 870202, Tuscaloosa AL35487 USA

Ultrafine grained Ti-Al-Nb intermetallics were processed by cold rolling and reaction annealing of elemental Ti, Al and Nb foils to produce Ti-46Al-9Nb(at%) alloy. The microstructure and phase development during cold rolling and reaction annealing were characterized by XRD, SEM/EDS and TEM analysis. With increasing reduction in thickness, more Ti3Al and Nb3Al phases are expected to occur at the Ti/Al and Nb/Al interfaces. This study will characterize the effect of rolling strain on development of these phases. After two-stage reaction annealing, the microstructure is complex due to the presence of several phases. XRD pattern shows that mainly g-TiAl and a2-Ti3Al are present, but small amounts of a-Ti and AlNb3 can also be identified. The element Nb is mostly dissolved in the g phase where it replaces the Ti. The reactive phase formation sequence of the multilayer foils after annealing was studied for different reduction rates using DSC.

Novel Equal Channel Angular Extrusion Processing Schedules for Microstructural Refinement: Suveen N. Mathaudhu<sup>1</sup>; Jae-Taek Im<sup>1</sup>; Robert E. Barber<sup>1</sup>; K. Ted Hartwig<sup>1</sup>; <sup>1</sup>Texas A&M University, Mech. Engrg., Spence St., College Sta., TX 77842-3123 USA

Multipass equal channel angular extrusion (ECAE) has been utilized extensively for the purpose of grain refinement and for inducing or eliminating texture in a variety of materials. But reports have been conflicting and often contradictory as to what number of extrusions with which route produces the best results. In addition, the process yield (percentage of fully processed material) for these processing schedules has not been reported. In this paper, the recrystallized microstructures of a FCC material (Cu), a BCC material (Ta) and an intermetallic compound (Bi2Te3) processed by a novel processing schedule (route E) in 90° tooling are compared with the same materials processed using conventional ECAE processing routes. Grain size, microstructural uniformity and process yield are compared for each case. It is seen that route E effectively refines the microstructure of a variety of materials while retaining a higher level of process yield when compared to the conventional ECAE routes.

**Microstructure Refinement in Pure Metals by Machining**: *Travis* L. Brown<sup>1</sup>; Srinivasan Swaminathan<sup>1</sup>; Srinivasan Chandrasekar<sup>1</sup>; W. Dale Compton<sup>1</sup>; Kevin P. Trumble<sup>2</sup>; Alexander H. King<sup>2</sup>; <sup>1</sup>Purdue University, Sch. of Industrial Engrg., 315 N. Grant St., W. Lafayette, IN 47907-2023 USA; <sup>2</sup>Purdue University, Sch. of Matls. Engrg., 501 Northwestern Ave., W. Lafayette, IN 47907-2036 USA

A study has been made of microstructure and mechanical properties of machining chips created from commercially pure metals. Significant microstructure refinement has been observed, the resulting chip being composed entirely of ultrafine-grained structures. While the formation of these structures is a consequence of very large strain deformation imposed by the tool, characteristics of the microstructure are seen to be influenced by machining parameters, e.g. strain. Large plastic strains, typically between two and fifteen, are shown to be created in the chip in a single stage of deformation. The relationship between the strain, microstructure, and mechanical properties of the chip has been characterized. The results have provided unique insights into microstructure evolution and refinement during very large strain deformation. The viability of machining as a technique for studying the formation of ultrafine-grained pure metals, and extensions of the work to solid solutions and dispersion-strengthened metals will be discussed.

Enhanced Properties of Titanium and Titanium Alloys: Vladimir V. Latysh<sup>1</sup>; Ruslan Z. Valiev<sup>2</sup>; Terry C. Lowe<sup>3</sup>; Robert Asaro<sup>3</sup>; Yuntian Theodore Zhu<sup>4</sup>; <sup>1</sup>Scientific Engineering and Design Office "ISKRA", 81 Pushkin St., Ufa 450025 Russia; <sup>2</sup>Ufa State Aviation Technical University, Inst. of Physics of Advd. Matls., 12 K. Marx St., Ufa 450000 Russia; <sup>3</sup>Metallicum LLC, 1207 Callejon Arias, Santa Fe, NM 87501 USA; <sup>4</sup>Los Alamos National Laboratory, Matls. Sci. & Tech. Div., MS G755, STC, Los Alamos, NM 87545 USA

Severe plastic deformation (SPD) can modify the microstructures of metals to improve their mechanical properties. However, the variants of SPD methods that produce the best properties are best suited for the synthesis of small quantities and small volumes of metal. Recent work using a proprietary SPD process has demonstrated that exceptional properties can be achieved in billets of commercial purity (CP) titanium and Ti-6Al-4V ELI with diameters between 6.5 and 13 mm and lengths between 0.3 and 1 m. The increases in mechanical properties achieved in CP titanium over the as-received material include 102% increase in fatigue strength and 196% increase in yield strength. For Ti-6Al-4V ELI the increases are less, but still significant with 45% increase in fatigue strength and 66% increase in yield strength. These materials are promising for application in medical device, aerospace and automotive applications.

Nanostructures and Phase Transformations in Shape Memory TiNi-Based Alloys Subjected to Severe Plastic Deformation: Vladimir G. Pushin<sup>1</sup>; Ruslan Z. Valiev<sup>2</sup>; Dmitry V. Gunderov<sup>2</sup>; Nickolay I. Kourov<sup>1</sup>; Ludmila I. Yurchenko<sup>1</sup>; Terry C. Lowe<sup>3</sup>; Yuntian Theodore Zhu<sup>3</sup>; <sup>1</sup>Ural Division of Russian Academy of Sciences, Inst. of Metal Physics, 18 S. Kovalevskaya St., Ekaterinburg 620219 Russia; <sup>2</sup>Ufa State Aviation Technical University, Inst. of Physics of Advd. Matls., 12 K.Marx St., Ufa 450000 Russia; <sup>3</sup>Los Alamos National Laboratory, Matls. Sci. & Tech. Div., MS G755, STC, Los Alamos, NM 87545 USA

Using severe plastic deformation processing by HPT and ECAP we could produce nanostructured shape memory TiNi-based alloys with grain size near 100 mn and less. The paper presents the results of the first studies of phase and structure transformations in nanostructured SPD-processed TiNi-based alloys during cooling and heating using measurements of  $\rho(T)$  and  $\chi(T)$ , as well as the methods of TEM and X-ray diffraction. New mechanisms of thermoelastic martensitic transformations in the given alloys are revealed and their critical temperatures are determined. It is shown that use of SPD allows to vary essentially the temperatures and consecution of martensitic transformations in B2 TiNi-based alloys, their mechanical properties and shape memory effect. Above all, SPD ensures high reactive stress of SME which is necessary for application of high-strength nanostructured shape memory alloys for diminutive load-bearing units and elements.

Influence of High Pressure on 301 Stainless Steel Hardening Under Large Deformations in Diamond Anvil Apparatus: Victor Varyukhin<sup>1</sup>; Boris M. Efros<sup>1</sup>; Yan Beygelzimer<sup>1</sup>; Dmitry Orlov<sup>1</sup>; <sup>1</sup>National Academy of Science of Ukraine, Donetsk Phys. & Tech. Inst., 72 R. Luxemburg St., Donetsk 83114 Ukraine

The behaviour of metal gaskets between diamond anvils in a high pressure apparatus has been studied. Along with a basic function of pressure generation a gasket supports the anvils' working planes' peripheral area. The elastic-plastic deformation mechanics of a 301 stainless steel gasket was investigated while generating pressure up to 65 GPa on the gasket axis. It is showed deformation under high pressure leads to more larger hardening of the 301 stainless steel in comparison with the same deformation under normal conditions.

Influence of Outer Arc Angle on Mechanical Properties of Bulk Ultrafine Grained Pure Copper: Wei Wei<sup>1</sup>; Guang Chen<sup>1</sup>; *Jingtao Wang*<sup>1</sup>; <sup>1</sup>Nanjing University of Science and Technology, Matls. Sci. & Engrg., Xiao Lingwei Rd. 200, Nanjing, Jiangsu 210094 China

Equal channel angular pressing?iECAP?jis applied to 12mm?~12mm?~80mm billet of pure copper (99.98%) at room temperature. The effects of ECAP passes and the outer arc angle of the die on the hardness (HBS) and tensile properties of processed copper are studied. Optical microscopy is used to examine the shear deformation characteristics. The results of tensile test suggest that the outer arc angle close to 22??is in favor of improving the ductility of ECAPed specimens. Simultaneously the hardness value at =22??is higher than that of the other three outer arc angles beyond four passes. Two distinct stages representing different hardening characteristics were also observed at fourth pass.

**Grain Refinement at SPD: View of Metal Forming Engineer**: *Yan Beygelzimer*<sup>1</sup>; <sup>1</sup>National Academy of Sciences of Ukraine, Donetsk Phys. & Tech. Inst., High Pressure, Donetsk 83050 Ukraine

We offer and try to validate the following hypotheses. Every metal (under given thermo-speed conditions of deformation and a given value of hydrostatic pressure) possesses a certain stationary microstructure (SM), which is attained at sufficiently large quasi-monotonous deformations. SM is characterized by a certain size of fragments, and it guarantees for the metal its ideal plasticity under pressure in the sense that the deformation is fracture- and hardening- free. The SM of a given metal is formed faster by those processes that lead to a larger decrease of plasticity of this metal (under the same level of hydrostatic pressure in the center of deformation). In order to obtain UFG structures, it is necessary to carry out these processes under high hydrostatic pressure in the center of deformation. In this case, the relaxation of internal stress happens along the direction of crystalline refinement, not the direction of microvoid formation.

Equal Channel Angular Pressing as a Means of Improving the Hydrogen Absorption/Desorption Properties of Alloy ZK60: Vladimir Skripnyuk<sup>2</sup>; Eugen Rabkin<sup>2</sup>; Yuri Estrin<sup>1</sup>; *Rimma Lapovok*<sup>3</sup>; <sup>1</sup>Clausthal University of Technology, Matls. Engrg. & Tech., Agricolastrasse 6, Clausthal-Zellerfeld 38678 Germany; <sup>2</sup>Technion, Matls. Engrg., Haifa 32000 Israel; <sup>3</sup>Monash University, Sch. of Physics & Matls. Engrg., Clayton, Victoria 3800 Australia

Magnesium alloys are popular candidate materials for hydrogen storage in automotive applications. However, their hydrogen desorption kinetics are too slow for the purpose. An enhancement of the desoprtion rate is commonly achieved through microstructure refinement by means of high energy ball milling (HEBM). In the present work, an attempt was undertaken to reach the same goal by using equal channel angular pressing (ECAP). The object of the study was the commercial magnesium alloy ZK60 (Mg-4.95 wt.%Zn-0.71 wt. % Zr). ECAP was shown to have a significant accelerating effect on the hydrogen absorption/desorption kinetics, comparable with or even exceeding that of HEBM. An interesting feature associated with combined ECAP/HEBM processing is the disappearance of pressure hysteresis with regard to hydrogen absorption/desorption. This hydrogenation behavior is explained in terms of the microstructure of bulk samples and the morphology of dehydrogenated powders as observed by TEM and by high resolution scanning electron microscopy.

Effect of Microstructure on the Sliding Wear Performance of Ultrafine-Grained Aluminum Alloys by ARB: Yong-Suk Kim<sup>1</sup>; Jong Soo Ha<sup>1</sup>; Dong Hyuk Shin<sup>2</sup>; <sup>1</sup>Kookmin University, Advd. Matls. Engrg., 861-1 Chongnung-dong Songbuk-ku, Seoul 136-702 S. Korea; <sup>2</sup>Hanyang University, Dept. of Metall. & Matls. Sci., 1271 Sa 1-dong, Ansan, Kyunggi-Do 425-791 S. Korea

Dry sliding wear behavior of ultrafine-grained 5052 and 5083 Al alloys and commercial purity Al (1100) by an accumulative roll bonding (ARB) process was investigated. Pin-on-disk wear tests of the ultrafine-grained Al alloys were carried out under various applied load conditions using hardened bearing steel as a counterpart material. Wear resistance of the Al alloys was not increased by the grain refinement, though their strength (hardness) increased nearly two times after the ARB process. Wear rate of the ultrafine-grained Al alloys rather increased with the increase of the accumulative plastic strain (the number of ARB cycles). Worn surfaces and cross-sections of the worn specimens were examined with SEM and TEM to investigate the wear mechanism and to explain the rather unexpected wear behavior of the ultrafine-grained Al alloys. The high wear rate of the ultrafine-grained Al alloys was discussed with emphasis on the unstable and non-equilibrium microstructure of the Al alloys.

# Index

# A

Aaronson, H I		186,	228,
			415
Abadias, G			429
Abbaschian, R 3	15	 277	
			420
Abe, E			295
Abe, T			420
Abedrabbo, S		180,	321
Abiko, T			366
Abinandanan, T A			181
Ablitzer, D			219
Abraham, T			209
Abu-Dheir, N M			450
Abu-Farha, F K			398
Acharjee, S			237
Ackland, G J			222
Acoff, V L 1	90.	237.	255,
			456
Adachi, H			
			314
Adam, G			406
Adamini, P			329
Adams, A N			217
Adams, B L		347,	390,
			451
1			394
			329
Adams, D P			
Adams, D P Adams, M			
Adams, D P Adams, M Adams, T M			321
Adams, D P Adams, M Adams, T M Addessio, L B		453,	
Adams, D P Adams, M Adams, T M Addessio, L B 2 Afshar, S	233,	453,	321
Adams, D P Adams, M Adams, T M Addessio, L B 2 Afshar, S Agarwal, A	233,	453, 301,	321 454
Adams, D P Adams, M Adams, T M Addessio, L B 2 Afshar, S Agarwal, A	233,	453, 301,	321 454 177 346,
Adams, D P Adams, M Adams, T M Addessio, L B 2 Afshar, S Agarwal, A	233,	453, 301, 428,	321 454 177 346, 450
Adams, D P Adams, M Adams, T M Addessio, L B 2 Afshar, S Agarwal, A	233,	453, 301, 428,	321 454 177 346, 450 264
Adams, D P Adams, M Adams, T M Addessio, L B 2 Afshar, S Agarwal, A Agarwal, S Aghion, E	233,	453, 301, 428, 333,	321 454 177 346, 450 264 375
Adams, D P Adams, M Adams, T M Addessio, L B 2 Afshar, S Agarwal, A Agarwal, S Aghion, E Agia, M	233,	453, 301, 428, 333,	321 454 177 346, 450 264 375 331
Adams, D P Adams, M Adams, T M Addessio, L B 2 Afshar, S Agarwal, A Agarwal, A Aghion, E Agia, M Agnew, S R 2	233,	453, 301, 428, 333, 256,	321 454 177 346, 450 264 375 331 287,
Adams, D P Adams, M Adams, T M Addessio, L B 2 Afshar, S Agarwal, A	233,  88,  233, 39,	453, 301, 428, 333, 256, 392,	321 454 177 346, 450 264 375 331
Adams, D P Adams, M Adams, T M Addessio, L B 2 Afshar, S Agarwal, A	233,  88,  233, 39,	453, 301, 428, 333, 256, 392,	321 454 177 346, 450 264 375 331 287,
Adams, D P Adams, M Adams, T M Addessio, L B 2 Afshar, S Agarwal, A	233,  88,  233, 39,	453, 301, 428, 333, 256, 392,	321 454 177 346, 450 264 375 331 287, 410 173
Adams, D P Adams, M Adams, T M Addessio, L B 2 Afshar, S Agarwal, A	233,  88,  233, 39,	453, 301, 428, 333, 256, 392,	321 454 177 346, 450 264 375 331 287, 410 173 437
Adams, D PAdams, MAdams, T MAdams, T MAdams, T MAddessio, L B2 Afshar, SAgarwal, A	233,  888, 233, 39,	453, 301, 428, 333, 256, 392,	321 454 177 346, 450 264 375 331 287, 410 173 437 349
Adams, D P Adams, M Adams, T M Addessio, L B		453, 301, 428, 333, 256, 392,	321 454 177 346, 450 264 375 331 287, 410 173 437 349 214
Adams, D P Adams, M Adams, T M Addessio, L B 2 Afshar, S Agarwal, A		453, 301, 428, 333, 256, 392, 426,	321 454 177 346, 450 264 375 331 287, 410 173 437 349 214 448
Adams, D PAdams, MAdams, MAdams, T MAdams, T MAdams, T MAdaesio, L B2 Afshar, SAgarwal, A		453, 301, 428, 333, 256, 392, 426,	321 454 177 346, 450 264 375 331 287, 410 173 437 349 214 448 221
Adams, D P Adams, M Adams, T M Addessio, L B 2 Afshar, S Agarwal, A		453, 301, 428, 333, 256, 392, 426,	321 454 177 346, 450 264 375 331 287, 410 173 437 349 214 448
Adams, D PAdams, MAdams, MAdams, T MAdams, T MAdams, T MAdaesio, L B2 Afshar, SAgarwal, A	233, 	453, 301, 428, 333, 256, 392, 426, 426, 453,	321 454 177 346, 450 264 375 331 287, 410 173 437 349 214 448 221
Adams, D P         Adams, M         Adams, T M         Adams, T M         Addessio, L B         Addessio, L B         Agarwal, S         Adams, B         Ahmed, F M         Ahn, J         Ahn, J         Ahn, J         Ahn, S         Ain, S		453, 301, 428, 333, 256, 392, 426, 453,	321 454 177 346, 450 264 375 331 287, 410 173 437 349 214 422 448 221 454 276
Adams, D PAdams, MAdams, T MAdams, T MAdams, T MAdams, T MAdams, T MAdams, T MAdams, SAgarwal, A		453, 301, 428, 333, 256, 392, 426, 453,	321 454 177 346, 450 264 375 331 287, 410 173 437 349 214 448 221 454 221 454 228
Adams, D P         Adams, M         Adams, T M         Agarwal, S	233, 888, 233, 39,	453, 301, 428, 333, 256, 392, 426, 453,	321 454 177 346, 450 264 375 331 287, 410 173 437 349 214 448 221 454 228 381
Adams, D PAdams, MAdams, T MAdams, T MAdams, T MAdams, T MAdams, T MAdams, T MAdams, SAgarwal, A	233, 	453, 301, 428, 333, 256, 392, 426, 453, 380,	321 454 177 346, 450 264 375 331 287, 410 173 437 349 214 448 221 454 228 381 441
Adams, D PAdams, MAdams, T MAdams, T MAdams, T MAdams, T MAdams, T MAdams, T MAdams, SAgarwal, A	233, 	453, 301, 428, 333, 256, 392, 426, 453, 380,	321 454 177 346, 450 264 375 331 287, 410 173 437 349 214 454 221 454 228 381 441 437
Adams, D PAdams, MAdams, T MAdams, T MAdams, T MAdams, T MAdams, T MAdams, T MAdams, SAgarwal, A	233, 888, 233, 39,	453, 301, 428, 333, 256, 392, 426, 453, 380,	321 454 177 346, 450 264 375 331 287, 410 173 437 349 214 448 221 454 228 381 441
Adams, D PAdams, MAdams, T MAdams, T MAdams, T MAdams, T MAdams, T MAdams, T MAdams, SAgarwal, A	233, 888, 233, 39,	453, 301, 428, 333, 256, 392, 426, 453, 380,	321 454 177 346, 450 264 375 331 287, 410 173 437 349 214 454 221 454 228 381 441 437
Adams, D PAdams, MAdams, T MAgarwal, A	233,  233, 39, 	453, 301, 428, 333, 256, 392, 426, 453, 380, 210,	321 454 177 346, 450 264 375 331 287, 410 173 437 349 214 454 221 454 228 381 441 437 360
Adams, D PAdams, MAdams, T MAdams, SAgarwal, AAgarwal, AAgarawal, SAgarawal, SAgaraw	233, 	453, 301, 428, 333, 256, 392, 426, 453, 380, 210, 175,	321 454 177 346, 450 264 375 331 287, 410 173 437 349 214 448 221 454 228 381 441 437 360 353 215
Adams, D PAdams, MAdams, T MAdams, T MAdams, T MAdams, T MAdams, T MAddessio, L B2 Afshar, SAgarwal, A	233, 	453, 301, 428, 333, 256, 392, 426, 453, 380, 210, 175,	321 454 177 346, 450 264 375 331 287, 410 173 437 349 214 448 221 454 276 228 381 441 437 360 353 215 180
Adams, D PAdams, MAdams, T MAdams, T MAdams, T MAdams, T MAdams, T MAddessio, L B2 Afshar, SAgarwal, A	233, 	453, 301, 428, 333, 256, 392, 426, 453, 380, 210, 175, 	321 454 177 346, 450 264 375 331 287, 410 173 437 349 214 448 221 454 276 228 381 441 437 360 353 215 180 317
Adams, D PAdams, MAdams, MAdams, T MAdams, T MAdams, T MAdams, T MAdams, T MAdams, T MAgarwal, SAgarwal, A	233, 	453, 301, 428, 333, 256, 392, 426, 453, 453, 380, 210, 175, 	321 454 177 346, 450 264 375 331 287, 410 173 437 349 214 448 221 454 276 228 381 441 437 360 353 215 180 317 342
Adams, D PAdams, MAdams, T MAdams, T MAdams, T MAdams, T MAdams, T MAddessio, L B2 Afshar, SAgarwal, A	233, 	453, 301, 428, 333, 256, 392, 426, 453, 380, 210, 175, 	321 454 177 346, 450 264 375 331 287, 410 173 437 349 214 448 221 454 228 381 441 437 360 353 215 180 317 342 431
Adams, D PAdams, MAdams, T MAdams, T MAddessio, L B2Afshar, SAgarwal, A	233, 	453, 301, 428, 333, 256, 392, 426, 453, 453, 210, 175, 380, 375,	321 454 177 346, 450 264 375 331 287, 410 173 437 349 214 448 221 454 276 228 381 441 437 360 353 215 180 317 342 431 444
Adams, D PAdams, MAdams, T MAdams, T MAddessio, L B2Afshar, SAgarwal, A	233, 	453, 301, 428, 333, 256, 392, 426, 453, 453, 210, 175, 380,  3375, 	321 454 177 346, 450 264 375 331 287, 410 173 437 349 214 448 221 454 228 381 441 437 360 353 215 180 317 342 431
Adams, D PAdams, MAdams, T MAdams, T MAddessio, L B2Afshar, SAgarwal, A	233, 	453, 301, 428, 333, 256, 392, 426, 453, 453, 210, 175, 380, 210, 175, 375, 212,	321 454 177 346, 450 264 375 331 287, 410 173 437 349 214 448 221 454 276 228 381 441 437 360 353 215 180 317 342 431 444
Adams, D PAdams, MAdams, T MAdams, T MAdams, T MAdams, T MAdams, T MAdams, T MAdams, SAgarwal, A	233, 	453, 301, 428, 333, 256, 392, 426, 453, 453, 210, 175, 380, 210, 175, 375, 212,	321 454 177 346, 450 264 375 331 287, 410 173 437 349 214 448 221 454 276 228 381 441 437 360 353 215 180 317 342 431 444 230

Alex, T C		171
Alexander, D J	207.	253,
·		434
Alexandrov IV	255,	
Alexandrov, I V	252,	256,
	258,	306
Alfantazi, A M	280,	325,
	409,	444
Algoso, P R		345
Ali, M T		360
	177	
Allaire, C	1//,	178
Allaire, J		177
Allameh, S		308
Allen, S M		420
Allison, J E		375
Allocca, C M		414
Alman, D E		440
Almer, J D	272,	283
Alonso, F		218
Alpas A T	254	413
Alpas, A T Alpay, S P	201,	426
Alpay, 51		
Alsem, D		309
Altenhof, W		313
Altorfer, F		250
Alur, A P		316
Alven, D A		215,
	257	
	357,	400
Aly, I H		403
Amaranti, J		329
Amweg, M L		447
An, K		247
Anand, S		336
Andersen, F B		400
Anderson, A J		341
Anderson, I E	287,	295,
	377.	
	377,	420
	377,	420 408
	377,	420 408 364
	377,	420 408 364 411
	377,	420 408 364 411
	377,	420 408 364 411 213
	377,	420 408 364 411 213 212
	377,	420 408 364 411 213 212 436
	377,	420 408 364 411 213 212 436 271
	377,	420 408 364 411 213 212 436 271 329
	377,	420 408 364 411 213 212 436 271 329
	377,	420 408 364 411 213 212 436 271 329
	377,	420 408 364 411 213 212 436 271 329 247
	377, 	420 408 364 411 213 212 436 271 329 247 296 445
	377, 	420 408 364 411 213 212 436 271 329 247 296 445 449
	377, 	420 408 364 411 213 212 436 271 329 247 296 445 449 361
	377, 	420 408 364 411 213 212 436 271 329 247 296 445 449 361 317
	377, 	420 408 364 411 213 212 436 271 329 247 296 445 449 361 317 236,
	377, 	420 408 364 411 213 212 436 271 329 247 296 445 449 361 317 236,
	377, 295, 422, 427, 194, 378,	420 408 364 411 213 212 436 271 329 247 296 445 449 361 317 236, 420
	377, 295, 422, 427, 194, 378,	420 408 364 411 213 212 436 271 329 247 296 445 449 361 317 236, 420 397
	377, 295, 422, 427, 194, 378,	420 408 364 411 213 212 436 271 329 247 296 445 449 361 317 236, 420 397 359
	377, 295, 422, 427, 194, 378,	420 408 364 411 213 212 436 271 329 247 296 445 449 361 317 236, 420 397 359 222
	377, 295, 422, 427, 194, 378, 369,	420 408 364 411 213 212 436 271 329 247 296 445 449 361 317 236, 420 397 359
	377, 295, 422, 427, 194, 378, 369,	420 408 364 411 213 212 436 271 329 247 296 445 449 361 317 236, 420 397 359 222
	377, 295, 422, 427, 194, 378, 369,	420 408 364 411 213 212 436 271 329 247 296 445 449 361 317 236, 420 397 359 222 414
	377, 295, 422, 427, 194, 378, 369,	420 408 364 411 213 212 436 271 329 247 296 445 449 361 317 236, 420 397 359 222 414 290 258
	377, 295, 422, 427, 194, 378, 369,	420 408 364 411 213 212 436 271 329 247 296 445 449 361 317 236, 420 397 359 222 414 290 258 317
	377, 295, 422, 427, 194, 378, 369, 180,	420 408 364 411 213 212 436 271 329 247 296 445 449 361 317 236, 420 397 359 222 414 290 258 317 321
	377, 295, 422, 427, 194, 378, 369, 180,	420 408 364 411 213 212 436 271 329 247 296 445 449 361 317 236, 420 397 359 222 414 290 258 317 321 453
	377, 295, 422, 427, 194, 378, 369, 180,	420 408 364 411 213 212 436 271 329 247 296 445 449 361 317 236, 420 397 359 222 414 290 258 317 321
	377, 295, 422, 427, 194, 378, 369, 180,	420 408 364 411 213 212 436 271 329 247 296 445 449 361 317 236, 420 397 359 222 414 290 258 317 321 453
	377, 295, 422, 427, 194, 378, 369, 180,	420 408 364 411 213 212 436 271 329 247 296 445 449 361 317 236, 420 397 359 222 414 290 258 317 321 453 243
	377, 295, 422, 427, 194, 378, 369, 180,	420 408 364 411 213 212 436 271 329 247 296 445 449 361 317 236, 420 397 359 222 414 290 258 317 321 453 243 274 314
	377, 295, 422, 427, 194, 378, 369, 180, 250,	420 408 364 411 213 212 436 271 329 247 296 445 449 361 317 236, 420 397 359 222 414 290 258 317 321 453 243 274 314 322
	377, 295, 422, 427, 194, 378, 369, 180, 180, 250, 190.	420 408 364 411 213 212 436 271 329 247 296 445 449 361 317 236, 420 397 359 222 414 290 258 317 321 453 243 274 314 322 362
	377, 295, 422, 427, 194, 378, 369, 180, 180, 250, 190, 344,	420 408 364 411 213 212 436 271 329 247 296 445 449 361 317 236, 420 397 359 222 414 290 258 317 321 453 243 274 314 322 362 440
	377, 295, 422, 427, 194, 378, 369, 180, 180, 250, 190, 344,	420 408 364 411 213 212 436 271 329 247 296 445 449 361 317 236, 420 397 359 222 414 290 258 317 321 453 243 274 314 322 362 440

Argyropoulos, S A 379,	423,
	447
Arif, M	210
Ariza, M P	365
Arjunan, V	397
Arkhipov, G V	438
Arlyuk, B	313
Arroyave, R	363
Artemev, A 334,	384
Arvanitis, A	216
Arya, A	274
Arzt, E	188
Arzt, E 229,	383
Asaro, R	259
Ashida, T	399
Asta, M D 205, 250,	304,
115tu, 111 D 200, 200,	504,
	430 430
	430
	430 386
	430 386 192
	430 386 192 316
	430 386 192 316 172
	430 386 192 316 172 429
	430 386 192 316 172 429 361
	430 386 192 316 172 429 361 403 411
	430 386 192 316 172 429 361 403 411
	430 386 192 316 172 429 361 403 411 .444
	430 386 192 316 172 429 361 403 411 .444 176

# B

Babu, S S	203.	223.	345
Bacchi, D P			319
Backerud, L			403
Backhouse, N			172
Bacon, D J			184.
	224,	226,	425
Bacon, W G			188
Bae, B			246
Bae, D H		287,	438
Bae, J			. 382
Baek, C			352
Baerhold, F			329
Baghbanan, M			308
Bahr, D 224, 262,	275,	394,	435
Bai, G R			238
Bai, J G			428
Baik, S			252
Bailey, C	232,	362,	416
Bailey, R			376
Bainbridge, I	272,	281,	439
Baker, I			281
Baker, J D			436
Bakhtiyarov, S I		375,	450
Bakke, P			444
Balancin, O			237
Balascuta, S			337
Balema, V P			263
Balk, T J			229
Balogh, M P			264
Balooch, M			310
Balsone, S J			204
Bamberger, M			444
Ban, Z			426
Banerjee, D K			319
Bang, J J			395

Bang, W		
	283,	383
Bannuru, T	,	352
Daminuru, 1		
Banovic, S W		418
Barabash, R 279,	324,	394
Barajas, A		214
Barber, M		312
Barber, R E		259
Barbour, J C		352
Barca, B J		399
Bark, C		441
Barmak, K		455
Barnes, A J		264
Barnett, M R		340
Barnett, R S		385
Barnett, S		231,
		443
Baró, M		254
Barrabes, S A		433
Barrie, R L		340
Barron, M F		266
Barseghyan, S A		236
Bartelo, J		416
Bartos, S C		333
Basak, D		247
Baskes, M I 279, 282,	306,	324
Bastaweesy, A		403
Bastawros, A		317
Bates, C E		428
Battaile, C C		452
Battle, T		368
Bautista, R G 169, 210,	202,	309,
		436
Bayuzick, R J		345
Beals, R S		191
Beckermann, C 202,	247,	299,
	423,	446
Behrani, V	175,	215
Bei, H 357,	372,	
	<i>c</i> , <i>-</i> ,	401
Beleggia, M		401 196
Bell, B F	381,	196 451
Bell, B F Bellam, H C	381,	196 451 350
Bell, B F Bellam, H C Bellet, M	381, 203,	196 451 350 404
Bell, B F Bellam, H C Bellet, M 178, Belt, C K	381, 203,	196 451 350 404 177
Bell, B F           Bellam, H C           Bellet, M           Bellet, C K           Ben-Eliyahu, Y	381, 203,	196 451 350 404 177 395
Bell, B F Bellam, H C Bellet, M 178, Belt, C K Ben-Eliyahu, Y Benedikt, B	381, 203,	196 451 350 404 177 395 371
Bell, B F Bellam, H C Bellet, M 178, Belt, C K Ben-Eliyahu, Y Benedikt, B Benedyk, J C	381, 203,	196 451 350 404 177 395 371 237
Bell, B F Bellam, H C Bellet, M 178, Belt, C K Ben-Eliyahu, Y Benedikt, B Benedyk, J C Bennett, B V	381, 203,	196 451 350 404 177 395 371
Bell, B F Bellam, H C Bellet, M 178, Belt, C K Ben-Eliyahu, Y Benedikt, B Benedyk, J C	381, 203,	196 451 350 404 177 395 371 237
Bell, B F Bellam, H C Bellet, M 178, Belt, C K Ben-Eliyahu, Y Benedikt, B Benedyk, J C Bennett, B V	381, 203,  297,	196 451 350 404 177 395 371 237 225
Bell, B FBellam, H CBellet, M178,Belt, C KBen-Eliyahu, YBenedikt, BBenedyk, J CBennett, B VBenson, M L271,Benum, S	381, 203, 297,	196 451 350 404 177 395 371 237 225 411
Bell, B FBellam, H CBellet, M178,Belt, C KBen-Eliyahu, YBenedikt, BBenedyk, J CBennett, B VBenson, M L271,Benzio, M	381, 203, 	196 451 350 404 177 395 371 237 225 411 385 417
Bell, B FBellam, H CBellet, M178,Belt, C KBen-Eliyahu, YBenedikt, BBenedyk, J CBennett, B VBenson, M L271,Benzio, MBerberoglu, H	381, 203, 297,	196 451 350 404 177 395 371 237 225 411 385 417 173
Bell, B FBellam, H CBellet, MBelt, C KBen-Eliyahu, YBenedikt, BBenedyk, J CBennett, B VBenson, M L271,Benzio, MBerberoglu, HBerczik, D	381, 203, 297,	196 451 350 404 177 395 371 237 225 411 385 417 173 215
Bell, B FBellam, H CBellet, MBelt, C KBen-Eliyahu, YBenedikt, BBenedyk, J CBennett, B VBenson, M L271,Benzio, MBerberoglu, HBerczik, DBerezin, A I	381, 203, 297, 212,	196 451 350 404 177 395 371 237 225 411 385 417 173 215 267
Bell, B FBellam, H CBellet, MBelt, C KBen-Eliyahu, YBenedikt, BBenedyk, J CBennett, B VBenson, M L271,Benzio, MBerberoglu, HBerczik, DBerezin, A IBerezowsky, R M	381, 203, 297, 297, 212, 284,	196 451 350 404 177 395 371 237 225 411 385 417 173 215 267 443
Bell, B FBellam, H CBellam, H CBellt, M178,Belt, C KBenedikt, BBenedikt, BBenedyk, J CBennett, B VBenson, M L271,Benzio, MBerberoglu, HBerczik, DBerezin, A IBergman, C	381, 203, 297, 297, 212, 284,	196 451 350 404 177 395 371 237 225 411 385 417 173 215 267 443 414
Bell, B FBellam, H CBellam, H CBellt, M178,Belt, C KBeneEliyahu, YBenedikt, BBenedyk, J CBennett, B VBenson, M L271,Benzio, MBerberoglu, HBerczik, DBerezin, A IBergman, CBergoint, D	381, 203, 297, 212, 284,	196 451 350 404 177 395 371 237 225 411 385 417 173 215 267 443 414 365
Bell, B FBellam, H CBellam, H CBellt, MI78,Belt, C KBenedikt, BBenedikt, BBenedyk, J CBennett, B VBenson, M L271,Benzio, MBerberoglu, HBerczik, DBerezin, A IBergman, CBergoint, DBernard, D	381, 203, 297, 212, 284, 273,	196 451 350 404 177 395 371 237 225 411 385 417 173 215 267 443 414 365 361
Bell, B F Bellam, H C Bellam, H C Bellet, M	381, 203, 297, 212, 284, 273,	196 451 350 404 177 395 371 237 225 411 385 417 173 215 267 443 414 365
Bell, B F Bellam, H C Bellam, H C Bellet, M	381, 203, 297, 212, 284, 273,	196 451 350 404 177 395 371 237 225 411 385 417 173 215 267 443 414 365 361 213 200
Bell, B F Bellam, H C Bellam, H C Bellet, M	381, 203, 297, 212, 284, 273,	196 451 350 404 177 395 371 237 225 411 385 417 173 215 267 443 414 365 361 213
Bell, B F Bellam, H C Bellam, H C Bellet, M	203, 203, 297, 212, 284, 273, 296,	196 451 350 404 177 395 371 237 225 411 385 417 173 215 267 443 414 365 361 213 200
Bell, B FBellam, H CBellam, H CBellt, M178,Belt, C KBen-Eliyahu, YBenedikt, BBenedikt, BBenedyk, J CBennett, B VBenson, M L271,Benzio, MBerberoglu, HBerczik, DBerezowsky, R MBergman, CBergoint, DBernard, DBernueta, L DBesser, A DBesterci, MBewlay, B	381, 203, 297, 212, 284, 273, 296,	196 451 350 404 177 395 371 237 225 411 385 417 173 215 267 443 414 365 361 213 200 311
Bell, B FBellam, H CBellam, H CBellt, M178,Belt, C KBen-Eliyahu, YBenedikt, BBenedikt, BBenedyk, J CBennett, B VBenson, M L271,Benzio, MBerberoglu, HBerczik, DBerezowsky, R MBergman, CBergoint, DBernard, DBernueta, L DBesser, A DBesterci, MBewlay, B	381, 203, 297, 212, 284, 273, 296,	196 451 350 404 177 395 371 237 225 411 385 417 173 215 267 443 414 365 361 213 200 311 358 434
Bell, B FBellam, H CBellam, H CBellt, MBellt, MBen-Eliyahu, YBenedikt, BBenedikt, BBenedyk, J CBennett, B VBenson, M L271,Benzio, MBerberoglu, HBerczik, DBerezowsky, R MBergman, CBernard, DBernard, DBesser, A DBesterci, MBesterci, MBeyerlein, I J208,	381, 203, 297, 212, 284, 273, 296, 256, 255,	196 451 350 404 177 395 371 237 225 411 385 417 173 215 267 443 414 365 361 213 200 311 358 434 260
Bell, B F Bellam, H C Bellam, H C Bellet, M	381, 203, 297, 212, 284, 273, 296, 255,	196 451 350 404 177 395 371 237 225 411 385 417 173 215 267 443 414 365 361 213 200 311 358 434 260 203
Bell, B F Bellam, H C Bellam, H C Bellet, M	381, 203, 297, 212, 284, 273, 296, 255, 255,	196 451 350 404 177 395 371 237 225 411 385 417 173 215 267 443 414 365 361 213 200 311 358 434 260 203 445
Bell, B F Bellam, H C Bellam, H C Bellet, M	381, 203, 297, 212, 284, 273, 296, 255, 255,	196 451 350 404 177 395 371 237 225 411 385 417 173 215 267 443 414 365 361 213 200 311 358 434 260 203 445 445
Bell, B F Bellam, H C Bellam, H C Bellet, M	381, 203, 297, 212, 284, 273, 296, 255, 255,	196 451 350 404 177 395 371 237 225 411 385 417 173 215 267 443 414 365 361 213 200 311 358 434 260 203 445

Bhansali, S       178, 219, 273,		
$\begin{array}{cccccccccccccccccccccccccccccccccccc$	Bhansali, S 178, 219,	273,
Bhattacharya, P       291         Bhethanabotla, V R       455         Bi, S       265         Bian, Z       217         Biancaniello, F S       372         Bickert, C       177         Bicler, T R       188, 190, 229, 286,		455
Bhethanabotla, V R       455         Bi, S       265         Bian, Z       217         Biancaniello, F S       372         Bickert, C       177         Bieler, T R       188, 190, 229, 286,		
Bi, S       265         Bian, Z       217         Biancaniello, F S       372         Bickert, C       177         Bieler, T R       188, 190, 229, 286,	Bhattacharya, P	
Bian, Z       217         Biancaniello, F S       372         Bickert, C       177         Bieler, T R       188, 190, 229, 286,		
Biancaniello, F S       372         Bickert, C       177         Bieler, T R       188, 190, 229, 286,		
Bickert, C       177         Bieler, T R       188, 190, 229, 286,		
Bieler, T R       188, 190, 229, 286,		
Bilello, J C       176         Bilodeau, J       361         Biloni, H       300, 450         Biner, S B       317, 365         Bing, X       289         Bingert, J F       234, 235, 445         Birdsell, S A       353         Birol, Y       173         Bisen, K B       362         Bittencourt, E       377         Bizos, R       381         Bjerke, W       399         Blakely, K A       209         Blanchard, D       353         Blanchard, P J       287         Blander, A J       356         Blandin, J       417, 438         Blasques, J       M         Blavert, C       445         Bletry, M       438         Blinov, V V       212         Biznyukov, S       440         Blobaum, K J       431         Bloch, J       395         Bloomfield, MO       423         Blue, C A       287, 411         Blum, W       303         Blut, J W       411         Boehlert, C J       391, 445         Boenting, M       358         Boettinger, W J       247, 276, <td></td> <td></td>		
Biloni, H       300, 450         Biner, S B       317, 365         Bing, X       289         Bingert, J F       234, 235, 445         Birdsell, S A       353         Birol, Y       173         Bisen, K B       362         Bittencourt, E       377         Bizios, R       381         Bjerke, W       399         Blakely, K A       209         Blanchard, D       353         Blanchard, P J       287         Blander, A J       356         Blandin, J       417, 438         Blasques, J       M         Blowert, C       445         Bletry, M       438         Bloov, V V       212         Blizonyukov, S       440         Blobaum, K J       431         Bloch, J       395         Bloomfield, M O       423         Blue, C A       287, 411         Blum, W       383         Blust, J W       411         Boehlert, C J       391, 445         Boender, W       219         Boening, M       358         Boettcher, H       403         Boettinger, W J       247, 276,<		
Biner, S B       317, 365         Bing, X       289         Bingert, J F       234, 235, 445         Birdsell, S A       353         Birol, Y       173         Bisen, K B       362         Bittencourt, E       377         Bizios, R       381         Bjerke, W       399         Blakely, K A       209         Blanchard, D       353         Blanchard, P J       287         Blander, A J       356         Blandin, J       417, 438         Blasques, J       M         Blawert, C       445         Bletry, M       438         Blinov, V V       212         Bliznyukov, S       440         Blobaum, K J       431         Bloch, J       395         Bloomfield, M O       423         Blue, C A       287, 411         Blum, W       383         Blust, J W       411         Boehlert, C J       391, 445         Boender, W       219         Boening, M       358         Boettcher, H       403         Boettinger, W J       247, 276,	Bilodeau, J	361
Bing, X       289         Bingert, J F       234, 235, 445         Birdsell, S A       353         Birol, Y       173         Bisen, K B       362         Bittencourt, E       377         Bizios, R       381         Bjerke, W       399         Blakely, K A       209         Blanchard, D       353         Blanchard, P J       287         Blander, A J       356         Blandin, J       417, 438         Blasques, J       M         Blewert, C       445         Bletry, M       438         Blinov, V V       212         Bliznyukov, S       440         Blobaum, K J       431         Bloch, J       395         Bloomfield, M O       423         Blue, C A       287, 411         Bum, V       304         Blum, W       383         Blust, J W       411         Boehert, C J       391, 445         Boettinger, W J       222, 344         Boger, R       214, 314         Bogicevic, A       193         Boileau, J       328         Bojarevics, V       437	Biloni, H 300,	450
Bingert, J F       234, 235, 445         Birdsell, S A       353         Birol, Y       173         Bisen, K B       362         Bittencourt, E       377         Bizios, R       381         Bjerke, W       399         Blakely, K A       209         Blanchard, D       353         Blanchard, P J       287         Blander, A J       356         Blandin, J       417, 438         Blasques, J       M         Blewett, C       445         Bletry, M       438         Blinov, V V       212         Bliznyukov, S       440         Blobaum, K J       431         Bloch, J       395         Bloomfield, M O       423         Blue, C A       287, 411         Bum, V       304         Blum, W       383         Blust, J W       411         Boehert, C J       391, 445         Boettinger, W J       222, 344         Boger, R       214, 314         Bogicevic, A       193         Boileau, J       328         Bojarevics, V       437         Boland, M       415		
Birdsell, S A       353         Birol, Y       173         Bisen, K B       362         Bittencourt, E       377         Bizios, R       381         Bjerke, W       399         Blakely, K A       209         Blanchard, D       353         Blanchard, P J       287         Blander, A J       356         Blandin, J       417, 438         Blasques, J       M         Bletry, M       433         Blinov, V V       212         Bliznyukov, S       440         Blobaum, K J       431         Bloch, J       395         Bloomfield, M O       423         Blue, C A       287, 411         Blum, V       304         Blum, W       383         Blust, J W       411         Boehlert, C J       391, 445         Boender, W       219         Boenting, M       358         Boettcher, H       403         Boettinger, W J       247, 276,		
Birol, Y       173         Bisen, K B       362         Bittencourt, E       377         Bizios, R       381         Bjerke, W       399         Blakely, K A       209         Blanchard, D       353         Blanchard, P J       287         Blander, A J       356         Blandin, J       417, 438         Blasques, J       M         Blawert, C       445         Bletry, M       438         Blinov, V V       212         Bliznyukov, S       440         Blobaum, K J       431         Bloch, J       395         Bloomfield, M O       423         Blue, C A       287, 411         Blum, V       304         Blum, W       383         Blust, J W       411         Boehlert, C J       391, 445         Boender, W       219         Boenting, M       358         Boettcher, H       403         Boettinger, W J       247, 276,		
Bisen, K B       362         Bittencourt, E       377         Bizios, R       381         Bjerke, W       399         Blakely, K A       209         Blanchard, D       353         Blanchard, P J       287         Blander, A J       356         Blandin, J       417, 438         Blasques, J       M         Blawert, C       445         Bletry, M       438         Blinov, V V       212         Bliznyukov, S       440         Blobaum, K J       431         Bloch, J       395         Bloomfield, M O       423         Blue, C A       287, 411         Blum, V       304         Blum, W       383         Blust, J W       411         Boehert, C J       391, 445         Boettinger, W J       247, 276,		
Bittencourt, E       377         Bizios, R       381         Bjerke, W       399         Blakely, K A       209         Blanchard, D       353         Blanchard, P J       287         Blander, A J       356         Blander, A J       356         Blander, A J       417, 438         Blasques, J       M 172         Blawert, C       445         Bletry, M       438         Blinov, V V       212         Bliznyukov, S       440         Blobaum, K J       431         Bloch, J       395         Bloomfield, M O       423         Bluw, V       304         Blum, W       383         Blust, J W       411         Boehert, C J       391, 445         Boettcher, H       403         Boettinger, W J       247, 276,		
Bizios, R       381         Bjerke, W       399         Blakely, K A       209         Blanchard, D       353         Blanchard, P J       287         Blanchard, P J       287         Blanchard, P J       287         Blanchard, P J       287         Blanchard, P J       356         Blandin, J       417, 438         Blasques, J       M         Blawert, C       445         Bletry, M       438         Blinov, V V       212         Bliznyukov, S       440         Blobaum, K J       431         Bloch, J       395         Bloomfield, M O       423         Blue, C A       287, 411         Blum, W       383         Blust, J W       411         Boehlert, C J       391, 445         Boender, W       219         Boening, M       358         Boettcher, H       403         Boettinger, W J       247, 276,		
Bjerke, W       399         Blakely, K A       209         Blanchard, D       353         Blanchard, P J       287         Blander, A J       356         Blandin, J       417, 438         Blasques, J       M         Blawert, C       445         Bletry, M       438         Blinov, V V       212         Bliznyukov, S       440         Blobaum, K J       431         Bloch, J       395         Bloomfield, M O       423         Blue, C A       287, 411         Blum, V       304         Blum, W       383         Blust, J W       411         Boehlert, C J       391, 445         Boender, W       219         Boening, M       358         Boettcher, H       403         Boettinger, W J       247, 276,		
Blakely, K A       209         Blanchard, D       353         Blanchard, P J       287         Blander, A J       356         Blandin, J       417, 438         Blasques, J       M         Blawert, C       445         Bletry, M       438         Blinov, V V       212         Bliznyukov, S       440         Blobaum, K J       431         Bloch, J       395         Bloomfield, M O       423         Blue, C A       287, 411         Blum, V       304         Blum, W       383         Blust, J W       411         Boehlert, C J       391, 445         Boender, W       219         Boening, M       358         Boettcher, H       403         Boettinger, W J       247, 276,		
Blanchard, D       353         Blanchard, P J       287         Blander, A J       356         Blandin, J       417, 438         Blasques, J       M         Blawert, C       445         Bletry, M       438         Blinov, V V       212         Bliznyukov, S       440         Blobaum, K J       431         Bloch, J       395         Bloomfield, M O       423         Blue, C A       287, 411         Blum, V       304         Blum, W       383         Blust, J W       411         Boehlert, C J       391, 445         Boender, W       219         Boening, M       358         Boettcher, H       403         Boettinger, W J       247, 276,		
Blander, A J       356         Blandin, J       417, 438         Blasques, J       M         Blawert, C       445         Bletry, M       438         Blinov, V V       212         Bliznyukov, S       440         Blobaum, K J       431         Bloch, J       395         Bloomfield, M O       423         Blue, C A       287, 411         Blum, V       304         Blum, W       383         Blust, J W       411         Boehlert, C J       391, 445         Boender, W       219         Boening, M       358         Boettcher, H       403         Boettinger, W J       247, 276,	Blanchard, D	353
Blandin, J	Blanchard, P J	287
Blasques, J		
Blawert, C.       445         Bletry, M.       438         Blinov, V V.       212         Bliznyukov, S.       440         Blobaum, K J.       431         Bloch, J.       395         Bloomfield, M O.       423         Blue, C A.       287, 411         Blum, V.       304         Blum, W.       383         Blust, J W.       411         Boehlert, C J.       391, 445         Boender, W.       219         Boening, M.       358         Boetther, H.       403         Boettinger, W J.       247, 276,		
Bletry, M       438         Blinov, V V       212         Bliznyukov, S       440         Blobaum, K J       431         Bloch, J       395         Bloomfield, M O       423         Blue, C A       287, 411         Blum, V       304         Blum, V       304         Blum, W       383         Blust, J W       411         Boehlert, C J       391, 445         Boender, W       219         Boening, M       358         Boettcher, H       403         Boettinger, W J       247, 276,		
Blinov, V V       212         Bliznyukov, S       440         Blobaum, K J       431         Bloch, J       395         Bloomfield, M O       423         Blue, C A       287, 411         Blum, V       304         Blum, W       383         Blust, J W       411         Boehlert, C J       391, 445         Boender, W       219         Boening, M       358         Boettcher, H       403         Boettinger, W J       247, 276,		
Bliznyukov, S       440         Blobaum, K J       431         Bloch, J       395         Bloomfield, M O       423         Blue, C A       287, 411         Blum, V       304         Blum, W       383         Blust, J W       411         Boehlert, C J       391, 445         Boender, W       219         Boening, M       358         Boettcher, H       403         Boettinger, W J       247, 276,		
Blobaum, K J       431         Bloch, J       395         Bloomfield, M O       423         Blue, C A       287, 411         Blum, V       304         Blum, W       383         Blust, J W       411         Boehlert, C J       391, 445         Boender, W       219         Boening, M       358         Boettcher, H       403         Boettinger, W J       247, 276,		
Bloch, J		
Bloomfield, M O       423         Blue, C A       287, 411         Blum, V       304         Blum, W       383         Blust, J W       411         Boehlert, C J       391, 445         Boender, W       219         Boening, M       358         Boettcher, H       403         Boettinger, W J       247, 276,		
Blue, C A       287, 411         Blum, V       304         Blum, W       383         Blust, J W       411         Boehlert, C J       391, 445         Boender, W       219         Boening, M       358         Boettcher, H       403         Boettinger, W J       247, 276,		
Blum, W       383         Blust, J W       411         Boehlert, C J       391, 445         Boender, W       219         Boening, M       358         Boettcher, H       403         Boettinger, W J       247, 276,		
Blust, J W       411         Boehlert, C J       391, 445         Boender, W       219         Boening, M       358         Boettcher, H       403         Boettinger, W J       247, 276,	Blum, V	304
Boehlert, C J       391, 445         Boender, W       219         Boening, M       358         Boettcher, H       403         Boettinger, W J       247, 276,		383
Boender, W       219         Boening, M       358         Boettcher, H       403         Boettinger, WJ       247, 276,		
Boening, M       358         Boettcher, H       403         Boettinger, W J       247, 276,		
Boettcher, H       403         Boettinger, W J       247, 276,		
Boettinger, W J       247, 276, 322, 344         Boger, R       214, 314         Bogicevic, A       193         Boileau, J       328         Bojarevics, V       437         Boland, M       415         Bonacuse, P J       340         Bonsager, M C       198         Bortha, S       281         Borge, G       361         Borjas, N M       230         Bossuyt, S       316         Bottani, C E       429         Bouchet, J       431         Boulianne, R       171         Bourbay, W M       212         Bourham, M       197         Bourgeois, L       295         Bourke, M A       187, 207, 229, 255,		
Boger, R       214, 314         Bogicevic, A       193         Boileau, J       328         Bojarevics, V       437         Boland, M       415         Bonacuse, P J       340         Bonsager, M C       198         Bontha, S       281         Borge, G       361         Borjas, N M       230         Bossuyt, S       316         Bottani, C E       429         Bouchet, J       431         Boulianne, R       171         Bourds, W M       212         Bourham, M       197         Bourgeois, L       295         Bourke, M A       187, 207, 229, 255,	-	
Bogicevic, A       193         Boileau, J       328         Bojarevics, V       437         Boland, M       415         Bonacuse, P J       340         Bonsager, M C       198         Bontha, S       281         Borge, G       361         Borjas, N M       230         Bossuyt, S       316         Bottani, C E       429         Bouchet, J       431         Boulianne, R       171         Bourds, W M       212         Bourham, M       197         Bourgeois, L       295         Bourke, M A       187, 207, 229, 255,		
Boileau, J       328         Bojarevics, V       437         Boland, M       415         Bonacuse, P J       340         Bonsager, M C       198         Bontha, S       281         Borge, G       361         Borjas, N M       230         Bossuyt, S       316         Bottani, C E       429         Bouchet, J       431         Boulianne, R       171         Bourks, W M       212         Bourham, M       197         Bourgeois, L       295         Bourke, M A       187, 207, 229, 255,		
Bojarevics, V       437         Boland, M       415         Bonacuse, P J       340         Bonsager, M C       198         Bontha, S       281         Borge, G       361         Borjas, N M       230         Bossuyt, S       316         Bottani, C E       429         Bouchet, J       431         Boulianne, R       171         Bourds, W M       212         Bourham, M       197         Bourgeois, L       295         Bourke, M A       187, 207, 229, 255,		328
Bonacuse, P J       340         Bonsager, M C       198         Bontha, S       281         Borge, G       361         Borjas, N M       230         Bossuyt, S       316         Bottani, C E       429         Bouchet, J       431         Boulianne, R       171         Bourds, W M       212         Bourham, M       197         Bourgeois, L       295         Bourke, M A       187, 207, 229, 255,		
Bonsager, M C       198         Bontha, S       281         Borge, G       361         Borjas, N M       230         Bossuyt, S       316         Bottani, C E       429         Bouchet, J       431         Boulianne, R       171         Bourds, W M       212         Bourham, M       197         Bourgeois, L       295         Bourke, M A       187, 207, 229, 255,		415
Bontha, S       281         Borge, G       361         Borjas, N M       230         Bossuyt, S       316         Bottani, C E       429         Bouchet, J       431         Boulianne, R       171         Bourds, W M       212         Bourham, M       197         Bourgeois, L       295         Bourke, M A       187, 207, 229, 255,	Bonacuse, P J	
Borge, G       361         Borjas, N M       230         Bossuyt, S       316         Bottani, C E       429         Bouchet, J       431         Boulianne, R       171         Bounds, W M       212         Bourham, M       197         Bourgeois, L       295         Bourke, M A       187, 207, 229, 255,		
Borjas, N M       230         Bossuyt, S       316         Bottani, C E       429         Bouchet, J       431         Boulianne, R       171         Bounds, W M       212         Bourham, M       197         Bourgeois, L       295         Bourke, M A       187, 207, 229, 255,		
Bossuyt, S       316         Bottani, C E       429         Bouchet, J       431         Boulianne, R       171         Bounds, W M       212         Bourham, M       197         Bourgeois, L       295         Bourke, M A       187, 207, 229, 255,		
Bottani, C E       429         Bouchet, J       431         Boulianne, R       171         Bounds, W M       212         Bourham, M       197         Bourgeois, L       295         Bourke, M A       187, 207, 229, 255,		
Bouchet, J       431         Boulianne, R       171         Bounds, W M       212         Bourham, M       197         Bourgeois, L       295         Bourke, M A       187, 207, 229, 255,		
Boulianne, R       171         Bounds, W M       212         Bourham, M       197         Bourgeois, L       295         Bourke, M A       187, 207, 229, 255,		
Bounds, W M       212         Bourham, M       197         Bourgeois, L       295         Bourke, M A       187, 207, 229, 255,		
Bourham, M       197         Bourgeois, L       295         Bourke, M A       187, 207, 229, 255,		
Bourgeois, L         295           Bourke, M A         187, 207, 229, 255,		
Bourke, M A 187, 207, 229, 255, 	Bourgeois, L	295
	Bourke, M A 187, 207, 229,	255,
Bourret, R H 370		
	Bourret, R H	570

Boutorabi, S M	439
Bowden, D M	419
Bowles, A L	445
Bowman, B	. 286
Bowman, R C	210
Boyapati, K	431
Boyce, B L 261, 308,	342
Boydon, J F	264
Boylstein, R E	318
	265
Bradley, J R 264,	
Bradshaw, R C	438
Brady, M P	215
Brady, S	263
Braginsky, M V	452
Brandstaetter, W	404
Bratkovsky, A M	425
Braun, M J	178
Braun, M W 228,	327
Bravman, J C	394
Bray, G	410
Brechet, Y 307,	438
Bretz, G T	287
Briant, C L 264, 347, 418,	419
Brill, M	395
Brinks, H W	353
Brokmeier, H	252
Bronchart, Q	390
Bronfin, B	333
Brooks, C R	271
Brown, D W 207, 255, 283,	296,
	434
Brown, J A	222
Brown, T L 207,	259
Brown, W L	352
Browning, J 172,	399
Browning, P F	411
Brubaker, C	417
Brueck, S R	
	394
Bruggeman, J 212, 267,	394 312,
Bruggeman, J 212, 267,	394 312, 437
Bruggeman, J 212, 267, 	394 312, 437 244
Bruggeman, J 212, 267, 	394 312, 437 244 284
Bruggeman, J	394 312, 437 244 284 270,
Bruggeman, J	394 312, 437 244 284 270, 438
Bruggeman, J	394 312, 437 244 284 270, 438 308,
Bruggeman, J	394 312, 437 244 284 270, 438 308, 452
Bruggeman, J	394 312, 437 244 284 270, 438 308,
Bruggeman, J	394 312, 437 244 284 270, 438 308, 452
Bruggeman, J       212, 267,	394 312, 437 244 284 270, 438 308, 452 256 296 411
Bruggeman, J	394 312, 437 244 284 270, 438 308, 452 256 296 411
Bruggeman, J       212, 267,	394 312, 437 244 284 270, 438 308, 452 256 296 411
Bruggeman, J       212, 267,	394 312, 437 244 284 270, 438 308, 452 256 296 411 .172
Bruggeman, J       212, 267,	394 312, 437 244 284 270, 438 308, 452 256 296 411 .172 318
Bruggeman, J       212, 267,	394 312, 437 244 284 270, 438 308, 452 256 296 411 .172 318 225
Bruggeman, J	394 312, 437 244 284 270, 438 308, 452 256 296 411 .172 318 225 198 346
Bruggeman, J	394 312, 437 244 284 270, 438 308, 452 256 296 411 .172 318 225 198 346 230
Bruggeman, J	394 312, 437 244 284 270, 438 308, 452 256 296 411 .172 318 225 198 346 230 170
Bruggeman, J	394 312, 437 244 284 270, 438 308, 452 256 296 411 .172 318 225 198 346 230 170 219
Bruggeman, J	394 312, 437 244 284 270, 438 308, 452 256 296 411 .172 318 225 198 346 230 170 219 433
Bruggeman, J	394 312, 437 244 284 270, 438 308, 452 256 296 411 .172 318 225 198 346 230 170 219 433 304
Bruggeman, J	394 312, 437 244 284 270, 438 308, 452 256 296 411 .172 318 225 198 346 230 170 219 433 304 262
Bruggeman, J	394 312, 437 244 284 270, 438 308, 452 256 296 411 .172 318 225 198 346 230 170 219 433 304

# С

Cabibbo, M	351
Cady, C M	233
Cahn, J W 205,	384

Calata, J N	428	Chang,
Cale, T S		Chang,
Callahan, P		Chani, V
Calonne, O		Chapell
Campbell, F		Charette
Candy, I		Charit, l
Cantor, B		Chase, I
Cao, F		Chashch
Cao, G		Chatterj
Cao, X		Chaubal
Cao, Y		Chaudh
	257	Chaudh
Capps, J	450	Chawla
Caram, R 195, 344,	440	Chawla.
Caraveo, V		
Carbonneau, A	177	Chen, C
Carlberg, T 218,	298	Chen, C
Carleton, E	354	Chen, C
Carlisle, J A	429	Chen, G
Carlisle, K B	343	Chen, H
Carmo, O A	329	Chen, H
Caro, A	348	Chen, J
Caro, M	348	Chen, J
Caron, Y	273	Chen, J
Carpenter, D A		3
	339	Chen, L
Carsley, J E 211,	265	Chen, L
Carte, S	399	
Carter, E A	274	
Carter, J T 386,	450	Chen, L
Carter, W T 219,	414	Chen, L
Castro, M	273	Chen, L
Castro-Cedeno, M H	273	Chen, L
Caswell, K K	395	Chen, N
Catalina, A V 178, 179,	219,	Chen, P
	404	Chen, Q
Cathey, W K		Chen, Q
Ceder, G 205, 250,		Chen, S
		Chen, S
Cefalu, S A	219	Chen, S
Celanovic, I		Chen, S
Cerreta, E K 233, 303, 453,	454	Chen, S
Cha, P		Chen, T
Chada, S 189,		Chen, T
		Chen, W
Chadha, G	375	Chen, X
Chan, H W		Chen, X
Chan, K S 365,		Chen, Y
Chan, W		Chen, Y
Chandler, R C		Chen, Z
Chandra, D 169, 210, 262,		Chen, Z
	396,	Cheng,
		Cheng,
Chandrasekar, S 207,		Cheng,
Chang, A		Chenmi
Chang, C		Cheong
Chang, C		Cheruku
Chang, C W 199,		Chesoni
Chang, H		
Chang, H		Chiang,
Chang, H J		Chiang,
Chang, I T		Chiang,
Chang, J		Chiang,
Chang, K		Chien, V
Chang, L J		Chiew,
Chang, M S		Childs,
Chang, S 232,	5//	Chin, B

Chang, T	285
Chang, Y A 198,	216
Chani, V	342
Chapelle, P	
Charette, A	423
Charit, I 207,	311
Chase, R	399
Chashchin, O A	212
Chatterjee, A 175,	400
Chaubal, M V	265
Chaudhari, G 237, 255,	259
Chaudhury, P	281
Chawla, K K 293,	343
Chawla, N 286, 293,	331,
	446
	382
Chen, G 260, Chen, G S	439 242
Chen, G Z 182, 199,	242
Chen, H	269
Chen, H	409
Chen, J	243
Chen, J	407
Chen, J J 184, 225, 226,	281.
	441
Chen, L	
Chen, L 181, 277, 294,	305,
	363,
	426
Chen, L J	294
Chen, L J	392
Chen, L J	411
Chen, L Q	277
Chen, L Q	277 374
Chen, M Chen, P	
Chen, M Chen, P Chen, Q 410,	374 409 411
Chen, M Chen, P Chen, Q 410, Chen, Q	374 409 411 312
Chen, M Chen, P Chen, Q	374 409 411 312 382
Chen, M Chen, P Chen, Q	<ul> <li>374</li> <li>409</li> <li>411</li> <li>312</li> <li>382</li> <li>213</li> </ul>
Chen, M Chen, P Chen, Q	<ul> <li>374</li> <li>409</li> <li>411</li> <li>312</li> <li>382</li> <li>213</li> <li>298</li> </ul>
Chen, M	<ul> <li>374</li> <li>409</li> <li>411</li> <li>312</li> <li>382</li> <li>213</li> <li>298</li> <li>330</li> </ul>
Chen, M         Chen, P         Chen, Q         Marcological Action         Chen, S         Chen, S <t< td=""><td><ul> <li>374</li> <li>409</li> <li>411</li> <li>312</li> <li>382</li> <li>213</li> <li>298</li> <li>330</li> <li>367</li> </ul></td></t<>	<ul> <li>374</li> <li>409</li> <li>411</li> <li>312</li> <li>382</li> <li>213</li> <li>298</li> <li>330</li> <li>367</li> </ul>
Chen, M         Chen, P         Chen, Q         410,         Chen, Q         Chen, S         233,         Chen, T	<ul> <li>374</li> <li>409</li> <li>411</li> <li>312</li> <li>382</li> <li>213</li> <li>298</li> <li>330</li> <li>367</li> <li>374</li> </ul>
Chen, M	<ul> <li>374</li> <li>409</li> <li>411</li> <li>312</li> <li>382</li> <li>213</li> <li>298</li> <li>330</li> <li>367</li> <li>374</li> <li>230</li> </ul>
Chen, M       Chen, P         Chen, Q       410,         Chen, Q       410,         Chen, S       198, 240, 293, 338,         Chen, S       Chen, S         Chen, S       Chen, S         Chen, S       233,         Chen, S       233,         Chen, T       186,         Chen, W       186,	<ul> <li>374</li> <li>409</li> <li>411</li> <li>312</li> <li>382</li> <li>213</li> <li>298</li> <li>330</li> <li>367</li> <li>374</li> <li>230</li> <li>383</li> </ul>
Chen, M         Chen, P         Chen, Q         410,         Chen, Q         Chen, S         Chen, T         Chen, T         Chen, T         Chen, W         Chen, X	<ul> <li>374</li> <li>409</li> <li>411</li> <li>312</li> <li>382</li> <li>213</li> <li>298</li> <li>330</li> <li>367</li> <li>374</li> <li>230</li> <li>383</li> <li>292</li> </ul>
Chen, M         Chen, P         Chen, Q         410,         Chen, Q         Chen, S         Chen, T         Chen, T         Chen, T         Chen, X         Chen, X G	<ul> <li>374</li> <li>409</li> <li>411</li> <li>312</li> <li>382</li> <li>213</li> <li>298</li> <li>330</li> <li>367</li> <li>374</li> <li>230</li> <li>383</li> <li>292</li> <li>439</li> </ul>
Chen, M         Chen, P         Chen, Q         410,         Chen, Q         Chen, S         Then, S         Chen, T         Chen, T         Chen, T         Chen, T         Chen, X         Chen, X G         Chen, Y	<ul> <li>374</li> <li>409</li> <li>411</li> <li>312</li> <li>382</li> <li>213</li> <li>298</li> <li>330</li> <li>367</li> <li>374</li> <li>230</li> <li>383</li> <li>292</li> <li>439</li> <li>389</li> </ul>
Chen, M         Chen, P         Chen, Q         410,         Chen, Q         Chen, S         Chen, T         Chen, T         Chen, T         Chen, T         Chen, X         Chen, X G         Chen, Y	<ul> <li>374</li> <li>409</li> <li>411</li> <li>312</li> <li>382</li> <li>213</li> <li>298</li> <li>330</li> <li>367</li> <li>374</li> <li>230</li> <li>383</li> <li>292</li> <li>439</li> <li>389</li> <li>326</li> </ul>
Chen, M         Chen, P         Chen, Q         410,         Chen, Q         Chen, S         Chen, T         Chen, T         Chen, T         Chen, T         Chen, X         Chen, X G         Chen, Y         304,         Chen, Z	<ul> <li>374</li> <li>409</li> <li>411</li> <li>312</li> <li>382</li> <li>213</li> <li>298</li> <li>330</li> <li>367</li> <li>374</li> <li>230</li> <li>383</li> <li>292</li> <li>439</li> <li>389</li> <li>326</li> <li>238</li> </ul>
Chen, M         Chen, P         Chen, Q         410,         Chen, Q         Chen, S         Chen, T         Chen, T         Chen, T         Chen, T         Chen, X         Chen, X G         Chen, Y         Sold,         Chen, Z	<ul> <li>374</li> <li>409</li> <li>411</li> <li>312</li> <li>382</li> <li>213</li> <li>298</li> <li>330</li> <li>367</li> <li>374</li> <li>230</li> <li>383</li> <li>292</li> <li>439</li> <li>389</li> <li>326</li> <li>238</li> <li>373</li> </ul>
Chen, M         Chen, P         Chen, Q         410,         Chen, Q         Chen, S         Chen, T         Chen, T         Chen, T         Chen, T         Chen, X         Chen, X G         Chen, Y         Sold,         Chen, Z         Chen, Z         Chen, Z	<ul> <li>374</li> <li>409</li> <li>411</li> <li>312</li> <li>382</li> <li>213</li> <li>298</li> <li>330</li> <li>367</li> <li>374</li> <li>230</li> <li>383</li> <li>292</li> <li>439</li> <li>389</li> <li>326</li> <li>238</li> <li>373</li> <li>443</li> </ul>
Chen, M         Chen, P         Chen, Q         410,         Chen, Q         Chen, S         Chen, T         Chen, T         Chen, T         Chen, T         Chen, X         Chen, X G         Chen, Y         Slow, Chen, Z         Chen, L	<ul> <li>374</li> <li>409</li> <li>411</li> <li>312</li> <li>382</li> <li>213</li> <li>298</li> <li>330</li> <li>367</li> <li>374</li> <li>230</li> <li>383</li> <li>292</li> <li>439</li> <li>389</li> <li>326</li> <li>238</li> <li>373</li> </ul>
Chen, M         Chen, P         Chen, Q         410,         Chen, Q         Chen, S         Chen, T         Chen, T         Chen, T         Chen, T         Chen, X         Chen, X G         Chen, Y         Sold,         Chen, Z         Chen, Z         Chen, Z	<ul> <li>374</li> <li>409</li> <li>411</li> <li>312</li> <li>382</li> <li>213</li> <li>298</li> <li>330</li> <li>367</li> <li>374</li> <li>230</li> <li>383</li> <li>292</li> <li>439</li> <li>389</li> <li>326</li> <li>238</li> <li>373</li> <li>443</li> <li>182</li> </ul>
Chen, M	<ul> <li>374</li> <li>409</li> <li>411</li> <li>312</li> <li>382</li> <li>213</li> <li>298</li> <li>330</li> <li>367</li> <li>374</li> <li>230</li> <li>383</li> <li>292</li> <li>439</li> <li>389</li> <li>326</li> <li>238</li> <li>373</li> <li>443</li> <li>182</li> <li>413</li> </ul>
Chen, M	<ul> <li>374</li> <li>409</li> <li>411</li> <li>312</li> <li>382</li> <li>213</li> <li>298</li> <li>330</li> <li>367</li> <li>374</li> <li>230</li> <li>383</li> <li>292</li> <li>439</li> <li>389</li> <li>326</li> <li>238</li> <li>373</li> <li>443</li> <li>182</li> <li>413</li> <li>455</li> <li>454</li> <li>184</li> </ul>
Chen, M	<ul> <li>374</li> <li>409</li> <li>411</li> <li>312</li> <li>382</li> <li>213</li> <li>298</li> <li>330</li> <li>367</li> <li>374</li> <li>230</li> <li>383</li> <li>292</li> <li>439</li> <li>389</li> <li>326</li> <li>238</li> <li>373</li> <li>443</li> <li>182</li> <li>413</li> <li>455</li> <li>454</li> </ul>
Chen, M	<ul> <li>374</li> <li>409</li> <li>411</li> <li>312</li> <li>382</li> <li>213</li> <li>298</li> <li>330</li> <li>367</li> <li>374</li> <li>230</li> <li>383</li> <li>292</li> <li>439</li> <li>389</li> <li>326</li> <li>238</li> <li>373</li> <li>443</li> <li>182</li> <li>413</li> <li>455</li> <li>454</li> <li>184</li> </ul>
Chen, M	<ul> <li>374</li> <li>409</li> <li>411</li> <li>312</li> <li>382</li> <li>213</li> <li>298</li> <li>330</li> <li>367</li> <li>374</li> <li>230</li> <li>383</li> <li>292</li> <li>439</li> <li>389</li> <li>326</li> <li>238</li> <li>373</li> <li>443</li> <li>182</li> <li>413</li> <li>455</li> <li>454</li> <li>184</li> <li>272,</li> </ul>
Chen, M Chen, P Chen, Q Chen, Q Chen, Q Chen, S Chen, S Chen, S Chen, S Chen, S Chen, S Chen, T Chen, T Chen, T Chen, T Chen, T Chen, T Chen, X Chen, X Chen, X Chen, X Chen, X Chen, Y Chen, Z Chen, Z Cheng, C Cheng, C Cheng, X Cheng, X Cheng, X Cheng, X Cheng, X Cheng, X Cheng, Y Cheng, X Cheng, Y Cheng, X Cheng, Y Cheng, C Cheng, C C	<ul> <li>374</li> <li>409</li> <li>411</li> <li>312</li> <li>382</li> <li>213</li> <li>298</li> <li>330</li> <li>367</li> <li>374</li> <li>230</li> <li>383</li> <li>292</li> <li>439</li> <li>389</li> <li>326</li> <li>238</li> <li>373</li> <li>443</li> <li>182</li> <li>413</li> <li>455</li> <li>454</li> <li>184</li> <li>272,</li> <li>439</li> <li>438</li> <li>377</li> </ul>
Chen, M Chen, P Chen, Q Chen, Q Chen, S Chen, S Chen, S Chen, S Chen, S Chen, S Chen, S Chen, T Chen, T Chen, T Chen, T Chen, T Chen, T Chen, X Chen, X Chen, X Chen, X Chen, X Chen, Y Chen, Z Chen, Z Cheng, C Cheng, C Cheng, X Cheng, X Cheng, X Cheng, X Cheng, X Cheng, Y Cheng, X Cheng, Y Cheng, X Cheng, Y Cheng, X Cheng, C Cheng, C C	<ul> <li>374</li> <li>409</li> <li>411</li> <li>312</li> <li>382</li> <li>213</li> <li>298</li> <li>330</li> <li>367</li> <li>374</li> <li>230</li> <li>383</li> <li>292</li> <li>439</li> <li>326</li> <li>238</li> <li>373</li> <li>443</li> <li>182</li> <li>413</li> <li>455</li> <li>454</li> <li>184</li> <li>272,</li> <li>439</li> <li>438</li> <li>377</li> <li>374</li> </ul>
Chen, M	<ul> <li>374</li> <li>409</li> <li>411</li> <li>312</li> <li>382</li> <li>213</li> <li>298</li> <li>330</li> <li>367</li> <li>374</li> <li>230</li> <li>383</li> <li>292</li> <li>439</li> <li>326</li> <li>238</li> <li>373</li> <li>443</li> <li>182</li> <li>413</li> <li>455</li> <li>454</li> <li>184</li> <li>272,</li> <li>439</li> <li>438</li> <li>377</li> <li>374</li> <li>232</li> </ul>
Chen, M	<ul> <li>374</li> <li>409</li> <li>411</li> <li>312</li> <li>382</li> <li>213</li> <li>298</li> <li>330</li> <li>367</li> <li>374</li> <li>230</li> <li>383</li> <li>292</li> <li>439</li> <li>326</li> <li>238</li> <li>373</li> <li>443</li> <li>373</li> <li>443</li> <li>182</li> <li>413</li> <li>455</li> <li>454</li> <li>184</li> <li>272,</li> <li>439</li> <li>438</li> <li>377</li> <li>374</li> <li>232</li> <li>436</li> </ul>
Chen, M Chen, P Chen, Q Chen, Q Chen, S Chen, T Chen, T Chen, T Chen, T Chen, T Chen, X Chen, X Chen, X Chen, X Chen, X Chen, X Chen, Y Chen, Z Chen, Z Cheng, C Cheng, X Chenming, X Cheong, Y Cherukuri, B Chesonis, C 177, 218, 	<ul> <li>374</li> <li>409</li> <li>411</li> <li>312</li> <li>382</li> <li>213</li> <li>298</li> <li>330</li> <li>367</li> <li>374</li> <li>230</li> <li>383</li> <li>292</li> <li>439</li> <li>326</li> <li>238</li> <li>373</li> <li>443</li> <li>373</li> <li>443</li> <li>182</li> <li>413</li> <li>455</li> <li>454</li> <li>184</li> <li>272,</li> <li>439</li> <li>438</li> <li>377</li> <li>374</li> <li>232</li> <li>436</li> <li>294</li> </ul>
Chen, M	<ul> <li>374</li> <li>409</li> <li>411</li> <li>312</li> <li>382</li> <li>213</li> <li>298</li> <li>330</li> <li>367</li> <li>374</li> <li>230</li> <li>383</li> <li>292</li> <li>439</li> <li>326</li> <li>238</li> <li>373</li> <li>443</li> <li>373</li> <li>443</li> <li>182</li> <li>413</li> <li>455</li> <li>454</li> <li>184</li> <li>272,</li> <li>439</li> <li>438</li> <li>377</li> <li>374</li> <li>232</li> <li>436</li> </ul>

Chin, J		443
Chin, L A		311
Chinnappan, R		181
Chipara, M		337
Chisholm, M F		225
Chiti, F		318
Chitre, K 2		321
Cho, G		376
Cho, H S		349
Cho, J		221
Cho, J		448
Cho, J		339
Cho, J 2		321
Cho, K H		362
Cho, S		453
Cho, S		189
Cho, W D 2	26,	368
Choate, W T 2	245,	313
Choe, H		356
Choi, B		413
Choi, D		381
Choi, G 4		454
Choi, W K		189
Choi, Y		334
Choi, Y		455
Choksi, R		425
Chao II 202 206 2		
Choo, H 202, 296, 2	.97,	372
Choudhury, S		426
Chown, L H		270
Choy, K		322
Chrisey, D B 1	97,	239
Christakis, N		404
Christie, M A		197
Christodoulou, J		182
Christodoulou, L 1		422
Christopher, W		181
		352
Chromik, R R 2 Chrzan, D 1	.83,	225
Chu, J P 241, 3		438
Cnu, J P 241. 3		4 <del>3</del> X
	00	
Chu, M G 2		343,
Chu, M G 2 	27,	343, 449
Chu, M G 2	27,	343,
Chu, M G 2 	27, 55,	343, 449
Chu, M G	27, 55, 802,	343, 449 456
Chu, M G	27, 55, 802,	343, 449 456 442
Chu, M G	27, 55, 802,	343, 449 456 442 314 433
Chu, M G	27, 55, 802, 	343, 449 456 442 314 433 422
Chu, M G	-27, -55, 802, 	343, 449 456 442 314 433 422 296
Chu, M G	-27, -55, 	<ul> <li>343,</li> <li>449</li> <li>456</li> <li>442</li> <li>314</li> <li>433</li> <li>422</li> <li>296</li> <li>321</li> </ul>
Chu, M G	27, 55, 802, 	<ul> <li>343,</li> <li>449</li> <li>456</li> <li>442</li> <li>314</li> <li>433</li> <li>422</li> <li>296</li> <li>321</li> <li>271</li> </ul>
Chu, M G2	27, 55, 802,     	<ul> <li>343,</li> <li>449</li> <li>456</li> <li>442</li> <li>314</li> <li>433</li> <li>422</li> <li>296</li> <li>321</li> <li>271</li> <li>445</li> </ul>
Chu, M G	27, 55, 002,      	343, 449 456 442 314 433 422 296 321 271 445 456
Chu, M G	-27, -55,       	343, 449 456 442 314 433 422 296 321 271 445 456 244
Chu, M G	.27, 55, 602,    	343, 449 456 442 314 433 422 296 321 271 445 456 244 283
Chu, M G	227, 555, 602,  391, 	343, 449 456 442 314 433 422 296 321 271 445 456 244
Chu, M G	227, 555, 602,  391, 	343, 449 456 442 314 433 422 296 321 271 445 456 244 283
Chu, M G       2	27, 55, 802,       	<ul> <li>343,</li> <li>449</li> <li>456</li> <li>442</li> <li>314</li> <li>433</li> <li>422</li> <li>296</li> <li>321</li> <li>271</li> <li>445</li> <li>456</li> <li>244</li> <li>283</li> <li>171</li> </ul>
Chu, M G	227, 1555, 302,  391,  284, 771,	<ul> <li>343,</li> <li>449</li> <li>456</li> <li>442</li> <li>314</li> <li>433</li> <li>422</li> <li>296</li> <li>321</li> <li>271</li> <li>445</li> <li>244</li> <li>283</li> <li>171</li> <li>296,</li> </ul>
Chu, M G	227, 1555, 302,  391,  1884, 771, 	343, 449 456 442 314 433 422 296 321 271 445 456 244 283 171 296, 434 218
Chu, M G	227, 155, 155, 1002,  1002,	343, 449 456 442 314 433 422 296 321 271 445 456 244 283 171 296, 434 218 210
Chu, M G	227, 555, 602,  	343, 449 456 442 314 433 422 296 321 271 445 456 244 283 171 296, 434 218 210 170
Chu, M G	227, 555, 302,  391,  284, 771, 	343, 449 456 442 314 433 422 296 321 271 445 456 244 283 171 296, 434 218 210 170 310
Chu, M G	227, 555, 302,  391,  284, .71, 	343, 449 456 442 314 433 422 296 321 271 445 456 244 283 171 296, 434 218 210 170 310 236
Chu, M G	227, 555, 602,       	343, 449 456 442 314 433 422 296 321 271 445 456 244 283 171 296, 434 218 210 170 310 236 304
Chu, M G	227, 555, 602,       	343, 449 456 442 314 433 422 296 321 271 445 456 244 283 171 296, 434 218 210 170 310 236 304 386
Chu, M G	227, 555, 602,  591,  284, 771,  284, 219, 84,	343, 449 456 442 314 433 422 296 321 271 445 456 244 283 171 296, 434 218 210 170 310 236 304 386 315
Chu, M G	227, 555, 602,  591,  284, 771,  284,  219, 84, 	343, 449 456 442 314 433 422 296 321 271 445 456 244 283 171 296, 434 218 210 170 310 236 304 386
Chu, M G	227, 555, 602,  591,  284, 771,  284,  219, 84, 	343, 449 456 442 314 433 422 296 321 271 445 456 244 283 171 296, 434 218 210 170 310 236 304 386 315

~	10.5
Coleman, M A	436
Colley, L J	386
Collins, P C	358
Collins, T L	319
Collins, T	
Colton, F	329
Colvin, J 406,	431
Combeau, H	248
Compton, C C	
Compton, C.C	303
Compton, W D 207,	259
Conard, B R	244
Conlon, K T	371
Conrad, H 380,	392
Conradi, M	263
Conway-Mortimer, J	230
Cook, B A	287
Cook, R	341
Cooley, J C	253
Cooper, K G	242
Cooper, K P 394,	435
Cooper, R P	191
Copeland, B J	245
Corby, C P	376
Cordes, R	369
Cordill, M J	262
Coriell, S R	247
Cormier, D	197
Cornish, L	270
Correa, O V	429
Corson, R P 396,	397
Costa, M L	329
Cotts, E J 382,	416
Counts, W A	452
Couper, M J	299
Coupez, T	178
Courtenay, J 361,	403
Couturier, G	250
Covert, C	266
Cramb, A W	248
Crimp, M A 324,	
Crist, E M	220
Cristol, B 170, 171,	
Cross, M	
Cruz, E S	
Csontos, A A 199, 200,	226
Cuitino, A M	365
Cunningham, J M	226
Curlook, W 285,	443
Curran, M	316
Curry, M	262
Curtarolo, S 205,	
Czerny, C	329
<i>CL</i> 01111y, C	527

# D

da Cruz, V F	320
Dahle, A 272,	299,
	411
Dahotre, N B 301,	346,
	450
Dai, K	208
Daigle, E O	185
Daimer, J	177
Dalmijn, W L 173,	245
Dalton, R	172
Dalvi, A D 188,	231
Dammers, A J	248

D ( ))D	
Dando, N R 267,	399
Dan'ko, V A	180
Dantzig, J A	386
Dariavach, N	339
Darmawan, F	448
Das, R P	336
Das, R R 195,	237,
	336
Das, S K 172,	213,
	385
Dasari, A	302
Dasgupta, A	192
Dashwood, R J 223,	323
Date, M	294
Dattelbaum, A M	447
Dauskardt, R H 229, 240,	270
David, S A 203, 223,	345
Davies, R W	268
Davis, B R	357
Davis, L J	218
Daw, M 183, 222,	225
Dawson, P R	235
Dax, B 379, 423,	446
Dax, R F	319
Daya, Z A	417
Dayan, D	287
Dayananda, M A 215,	315
Daymond, M R 297, 328,	372
De Angelis, R J	257
de Campos, M F	204
De Fontaine, D R	205
De Graef, M 196,	422
de Groot, J D	273
De Hosson, J T	275
de Jong, R A	362
de Jong, T P 173,	245
de Lima, N B	429
De Messemaeker, J	392
de Napole Gregolin, E	440
de Vasconcelos, P D	172
de Vries, A J	360
Decker, R F	418
Deevi, S C	413
Defendi, G A	320
Dehm, G	229
Dehoff, R R	358
Dejmek, M	387
Del Corso, G	414
Delaire, O	405
Delos-Reyes, M A	279
Demonstration C D 279	
Demopoulos, G P 378,	426
Deneys, A C 184, 225, 226,	281,
	441
Deng, X 286, 293, 331, 341,	416
Denning, J W 276,	332
Dennis, K	296
Derev'yanko, O V	381
Derin, B C	185
Derlet, P M	
Dernedde, E	נער
	305 398
	398
DeRosset, W S	398 182
DeRosset, W S Deryagin, A	398 182 255
DeRosset, W S Deryagin, A Desai, V	398 182 255 410
DeRosset, W S Deryagin, A Desai, V 246, Deshmukh, P V	398 182 255
DeRosset, W S Deryagin, A Desai, V	398 182 255 410
DeRosset, W S Deryagin, A Desai, V 246, Deshmukh, P V	<ul> <li>398</li> <li>182</li> <li>255</li> <li>410</li> <li>398</li> <li>213</li> <li>183</li> </ul>
DeRosset, W S Deryagin, A Desai, V	<ul> <li>398</li> <li>182</li> <li>255</li> <li>410</li> <li>398</li> <li>213</li> </ul>
DeRosset, W S Deryagin, A Desai, V	<ul> <li>398</li> <li>182</li> <li>255</li> <li>410</li> <li>398</li> <li>213</li> <li>183</li> </ul>

Detavernier, C	370
Deveaux, E	415
Deveaux, M	361
	278
Devincre, B	
DeYoung, D H 273,	361
Dias, H P	213
Diaz, L 199,	321
Díaz, R J	171
Dickerson, M B	291
Dickerson, R 342,	411
Dickmann, D	391
Diepers, H	386
Dijkstra, W O	248
Dimiduk, D M 309,	357
Dinda, G	351
Ding, J	243
Ding, R	280
Ding, W	325
Ding, W	288
Dinh, L N	310
Diplas, S	216
Ditenberg, I A	256
Dixon, T W	217
Djambazov, G S	362
Dahadain Q.V. 252 422	
Dobatkin, S V 253, 432,	433
Dogan, N	273
Dogan, O N	401
Doherty, R 204, 250, 302,	303
Dolan, D S	189
Donaldson, A	369
Donaldson, D J	285
Dong, H 278,	406
Dong, S	234
Dong, Y	200
Dong, Z F	241
Dorsam, G	400
Dou, S X	354
Douglas, E	377
Doumanidis, H	209
Dow, J D	276
Downes, S 232,	339
Doyle, C	415
Doyle, F M 280,	448
Drawin, S	358
Drchal, V 192,	304
Dregia, S A	249
Dresler, W	444
Dresselhaus, M S 193,	209
Dreyfus, J	177
Dreysse, H C	348
Drezet, J 203, 218, 385,	450
Dring, K F 223,	323
Driver, J	250
Droste, W E	219
Drouet, M G	245
Drummond, B G	173
Druschitz, A P	442
Druschitz, E A	442
Du, Q 323, 387,	406
Du, T 410,	448
Du, Z 207,	257
Duda, S	373
Dudley, E	230
Dudo, T	259
Dufour, G	171
Dugger, M T	309
1-46601, 141 1	509

460

Duh, J G				332, 447
Dulikravich, G S			193,	288
Dunand, D C	327,	328,	340,	356
Dündar, M			273,	450
Dunham, S N				381
Dunn, J				365
Dunstan, D				262
Duomo, Z				378
Dupuis, M				437
Duquette, D J				413
Durairaj, R			232,	416
Duterque, J				329
Dutrizac, J E		186,	230,	231
Dutta, I	187,	188,	229,	283,
	286,	327,	342,	371
Duval, H				319
Duxbury, P M				391
Duygulu, O				233
Duz, V A	278,	364,	365,	440
Dybkov, V I				455
Dyck, C				394
Dye, D				371
Dyer, T		•••••		370

# E

Earthman, J C	326
Eastman, J A	238
Easton, M 344,	403
Eaton, S	263
Eberl, C	188
Eckert, C E	370
Edelstein, A S	241
Edrisy, A	413
Edwards, B J	317
Edwards, L	217
Efros, B M 255,	260
Efros, N	255
Egami, T	216
Ege, E S	286
Egry, I	380
Eidet, T	272
Eisinger, N 391,	445
Eizenberg, M	198
Ekenes, J M	272
Ekere, N 232,	416
El-Kaddah, N 362,	428
Elder, K R	322
Eliezer, D	192
Elliott, A J	195
Elliott, A L 281,	282
Elmadagli, M	254
Elmer, J W	345
Embury, D 339,	408
Embury, J D 261, 302,	303
Emelander, D	417
Emerson, J A	394
Emura, S	337
Engh, T A	266
England, L G 300,	343
Enikeev, N A 252,	258
Enomoto, M	186
Erasmus, L	330
Erb, A	276
	270 308
Erb, U Erickson, K L	308 338
EIICKSUII, K L	330

Erlebacher, J D	379
Ernst, W	364
Erol, A	290
Esaka, H 184,	301
Escobedo, J	361
Escudero, R	378
Eskin, D	203
Espinoza-Nava, L	399
Esquivel, E V 279, 395,	441
Essadiqi, E	233
Estey, C M	214
Estrin, Y 251, 252,	260
Evangelista, E	351
Evans, G A	292
Evans, J W 280,	319,
	448
Evans, K J	246
Evelin, S S	329
Ewing, W	448
-	

# F

Fabina, L	
Fachinotti, V D	
Fagerlund, K	
Faivre, G P	
Faizan, M	374
Fallahi, A 30	3, 431
Falleiros, I G 20	
Faller, K	
Falticeanu, L C	341
Fan, J	380
Fan, P	368
Fan, W	394
Fang, J S	242
Fang, Q T	318
Farkas, D 205, 224, 25	
	0, 451
Favet, S	
Fazeli, F	
Fecht, H	
Feigl, K	
Feng, F	
Feng, G	
Feng, J C	392
Feng, Q 27	
Feng, Z	-,
Fenton, C	
Fergus, J W	
Fernandes, F	
Fernandes, S M	
Fernandez, F E 19	
Fernandez, J	
Fernández-Flores, R	
Fernández-Serrano, R	
Ferreira, I	
Ferreira, M A	
Ferres, L	
Ferron, C J	
Ferry, M	433
Field, D P 22	
222 279, 320, 34	
	- ) -
Field, R D	
Fielden, D E 202, 23	
Fields, R J	
Finel, A	- )
Fiory, A 180, 27	6, 321

Fiot, L	172
Fischer, B	270
Fischer, C C	348
Fischer, F D	405
Fischer, W K	
	360
Fishman, S G	315
Fiske, M	242
Fiterman, M J	267
Fittock, J E 373,	443
Fitz-Gerald, J	321
Fjaer, H 218,	385
Fjeld, A	319
Fleay, J	230
Fleming, C A	284
Flemings, M C 202, 296,	369
Fleury, D R	230
Flisakowski, P J	361
Florando, J N	309
Flores, A	361
Flores, K H	316
Flores, K M	316
Floro, J A	394
Flower, H M 173, 223,	323
Foecke, T J	268
Foiles, S M	347
Fok, I	285
Folch, R	387
Foley, J C 242, 295,	340
-	
Folz, H	442
Fonseca, M B	230
Foosnaes, T	218
Forbes Jones, R M 219,	414
Fornaro, O	300
Forrest, S	
	180
Forslund, K G	176
Forté, G 170,	311
Fortier, M	439
Fortunier, R	250
Fox, S P 278,	406
Fraczkiewicz, A	225
Franetovic, V 386,	450
Frank, R A	361
Frankel, J I 298,	421
Franklin, J S	296
Frary, M	451
Fraser, H L 309,	358
Fray, D J 182, 199, 223,	
	278,
	440
Frazier, W E 419,	420
Frear, D R 187,	229,
	371
Frederick, M J	422
Free, M L 226, 369,	413
Freels, M	271
Freeman, A J 270,	430
Freibergs, J	437
Frias, J	415
Friedman, L H	408
Friedman, P A 211,	264,
310, 355, 397,	398
Friedrich, H	365
Fries, S G	206
Frisk, K	363
Froes, F H 182, 223,	278,
	440
Frost, H J	204
Frost, M T	
	• ± /

Fu, E K	350
Fu, X	390
Fuentes-Cabrera, M	431
Fujii, H	323
Fujii, H	354
Fujikura, M	315
Fujita, A	396
Fujiyoshi, M	294
Fukamichi, K	396
Fuller, C	226
Fultz, B 206, 354,	405
Furrer, D U 174,	215,
	400
Furu, E	172
Furuhara, T 282,	327
Furukawa, M 206,	251,
	433
Furuno, K	433
Furuya, K	301
Fushen, L	325

# G

Gabb, T P	340
Gable, B M 199,	376
Gabrielyan, T N	312
Gaddis, C S	291
Gagne, J	171
Galarraga, R A	171
Gali, A	185
Galloway, T 170, 212, 265,	311
Gamsjäger, E	405
Ganapathysubramanian, S	235
Gandin, C 202,	248
Ganesan, P G	422
Gang, F	261
Gangloff, R P	410
Gangopadhyay, A K	438
Gao, B	400
Gao, H	395
Gao, J	177
Gao, M C 363,	442
Gao, W	413
Gao, W	241
Gao, X	445
Gao, Y	173
Gararia, S N	312
Garbellini, O B	450
Garcia, A J 240,	291
Gariepy, B	266
Garmestani, H	237
Garner, C M	209
Garratt, M	410
Garud, C	237
Garvin, J W	249
Gatty, D G	399
Gazder, A A	254
Geerpuram, D N	196
Geiss, E	451
Geltmacher, A B 234,	235
Gemeinböck, G	392
Genau, A L	345
Geng, J	359
Gentz, M	371
George, E P 185, 269, 372,	401
George, S	261
Gerberich, W W	261

Gerdemann, S J	
	440
Gerogiorgis, D I	356
Gerritsen, T 330,	331
Gesing, A J 172,	173
Geveci, A	185
Geyrhofer, W	
	336
Ghomashchi, M R	423
Ghomashchi, R	439
	224
Ghoniem, N M	
Ghorbani, H R	331
Ghosh, A K 211, 264,	310,
	419
Ghosh, G 294, 304,	358
Ghosh, S	229
Ghosh, S	328
Giannuzzi, L A	432
Gibala, R 379,	430
Gibson, R	399
Gigliotti, M F	195
Gillaspie, J	443
Gilmer, G	431
	237
Giordani, E J	
Girgin, S	426
Girin, O B 280,	447
Gjestland, H	191
Gladysz, G M	343
Glaner, L	270
Glatzel, U	270
Glavicic, M G	324
Gleeson, B 295, 455,	456
Glicksman, M E 181,	248,
299,	
	409
Gnäupel-Herold, T 268,	372
Go, J	268
Goddard, III, W A	192
Godfrey, A B	407
Goff, A	295
Goldsmith, C	416
	435
Gole, J L 170,	
Golovashchenko, S F 213,	214
Golovashchenko, S F 213,	
Golovashchenko, S F 213, Golumbfskie, W J	243
Golovashchenko, S F 213, Golumbfskie, W J Gomes, A S	243 272
Golovashchenko, S F 213, Golumbfskie, W J Gomes, A S Gomez-Cordobes, J	243 272 412
Golovashchenko, S F 213, Golumbfskie, W J Gomes, A S Gomez-Cordobes, J	243 272 412
Golovashchenko, S F 213, Golumbfskie, W J Gomes, A S Gomez-Cordobes, J Gong, J	243 272 412 237
Golovashchenko, S F 213, Golumbfskie, W J Gomes, A S Gomez-Cordobes, J Gong, J Gonzalez, C	243 272 412 237 449
Golovashchenko, S F 213, Golumbfskie, W J Gomes, A S Gomez-Cordobes, J Gong, J Gonzalez, C Gonzalez Crespo, P A 207,	243 272 412 237 449 258
Golovashchenko, S F 213, Golumbfskie, W J Gomes, A S Gomez-Cordobes, J Gong, J Gonzalez, C	243 272 412 237 449
Golovashchenko, S F 213, Golumbfskie, W J Gomes, A S Gomez-Cordobes, J Gong, J Gonzalez, C Gonzalez Crespo, P A 207, González, M A	243 272 412 237 449 258 361
Golovashchenko, S F 213, Golumbfskie, W J Gomes, A S Gomez-Cordobes, J Gong, J Gonzalez, C Gonzalez Crespo, P A 207, González, M A González-Doncel, G	243 272 412 237 449 258 361 361
Golovashchenko, S F 213, Golumbfskie, W J Gomes, A S Gomez-Cordobes, J Gong, J Gonzalez, C Gonzalez Crespo, P A 207, González, M A González-Doncel, G Goods, S H 209,	243 272 412 237 449 258 361 361 261,
Golovashchenko, S F 213, Golumbfskie, W J Gomes, A S Gomez-Cordobes, J Gong, J Gonzalez, C Gonzalez Crespo, P A 207, González, M A González-Doncel, G	243 272 412 237 449 258 361 361
Golovashchenko, S F 213, Golumbfskie, W J Gomes, A S Gomez-Cordobes, J Gong, J Gonzalez, C Gonzalez, C González, M A González-Doncel, G Goods, S H	243 272 412 237 449 258 361 361 261,
Golovashchenko, S F 213, Golumbfskie, W J Gomes, A S Gong, J Gonzalez, C Gonzalez, C González, M A González-Doncel, G Goods, S H 209, 	243 272 412 237 449 258 361 361 261, 418 244
Golovashchenko, S F 213, Golumbfskie, W J Gomes, A S Gong, J Gonzalez, C Gonzalez, C González, M A González-Doncel, G Goods, S H	243 272 412 237 449 258 361 361 261, 418 244 444
Golovashchenko, S F 213, Golumbfskie, W J Gomes, A S Gomez-Cordobes, J Gonzalez, C Gonzalez, C González, M A González-Doncel, G Goods, S H 209, 	243 272 412 237 449 258 361 361 261, 418 244
Golovashchenko, S F 213, Golumbfskie, W J Gomes, A S Gomez-Cordobes, J Gonzalez, C Gonzalez, C González, M A González-Doncel, G Goods, S H 209, 	243 272 412 237 449 258 361 361 261, 418 244 444
Golovashchenko, S F 213, Golumbfskie, W J Gomes, A S Gomez-Cordobes, J Gonzalez, C Gonzalez, C González, M A González-Doncel, G Goods, S H 209, 	243 272 412 237 449 258 361 361 261, 418 244 444 288 270
Golovashchenko, S F 213, Golumbfskie, W J Gomes, A S Gomez-Cordobes, J Gonzalez, C Gonzalez, C González, M A González-Doncel, G Goods, S H	243 272 412 237 449 258 361 361 261, 418 244 444 288 270 425
Golovashchenko, S F213,Golumbfskie, W JGomes, A SGomez-Cordobes, JGonzalez, CGonzalez, CGonzalez, CGonzález, M A207,González-Doncel, G209,	243 272 412 237 449 258 361 361 261, 418 244 444 288 270 425 416
Golovashchenko, S F 213, Golumbfskie, W J Gomes, A S Gomez-Cordobes, J Gonzalez, C Gonzalez, C González, M A González-Doncel, G Goods, S H	243 272 412 237 449 258 361 361 261, 418 244 444 288 270 425
Golovashchenko, S F213,Golumbfskie, W JGomes, A SGomez-Cordobes, JGonzalez, CGonzalez, CGonzalez, C207,González, M A207,González-Doncel, G209,	243 272 412 237 449 258 361 361 261, 418 244 444 288 270 425 416 395
Golovashchenko, S F213,Golumbfskie, W JGomes, A SGomez-Cordobes, JGong, JGonzalez, CGonzalez, CGonzález, M A207,González-Doncel, G209,	243 272 412 237 449 258 361 361 261, 418 244 444 288 270 425 416 395 266
Golovashchenko, S F213,Golumbfskie, W JGomes, A SGomez-Cordobes, JGonzalez, CGonzalez, CGonzalez, C207,González, M AGonzález-Doncel, GGoods, S H	243 272 412 237 449 258 361 361 261, 418 244 444 288 270 425 416 395 266 203
Golovashchenko, S F213,Golumbfskie, W JGomes, A SGomez-Cordobes, JGong, JGonzalez, CGonzalez, CGonzález, M A207,González-Doncel, G209,	243 272 412 237 449 258 361 361 261, 418 244 444 288 270 425 416 395 266
Golovashchenko, S F213,Golumbfskie, W JGomes, A SGomez-Cordobes, JGong, JGonzalez, CGonzalez, CGonzález, M A207,González-Doncel, GGonzález-Doncel, GGoods, S H	243 272 412 237 449 258 361 361 261, 418 244 444 288 270 425 416 395 266 203 244
Golovashchenko, S F 213, Golumbfskie, W J Gomes, A S Gomez-Cordobes, J Gonzalez, C Gonzalez, C González, M A González-Doncel, G Goods, S H Goods, S H Goren-Muginstein, G R Gornostyrev, Y N	243 272 412 237 449 258 361 361 261, 418 244 444 288 270 425 416 395 266 203 244 354
Golovashchenko, S F213,Golumbfskie, W JGomes, A SGomez-Cordobes, JGong, JGonzalez, CGonzalez, CGonzález, M AGonzález-Doncel, GGoods, S H	243 272 412 237 449 258 361 361 261, 418 244 444 288 270 425 416 395 266 203 244 354 354
Golovashchenko, S F 213, Golumbfskie, W J Gomes, A S Gomez-Cordobes, J Gonzalez, C Gonzalez, C González, M A González-Doncel, G Goods, S H Goods, S H Goren-Muginstein, G R Gornostyrev, Y N Gornostyrev, Y N	243 272 412 237 449 258 361 361 261, 418 244 444 288 270 425 416 395 266 203 244 354
Golovashchenko, S F213,Golumbfskie, W JGomes, A SGomez-Cordobes, JGong, JGonzalez, CGonzalez, CGonzález, M AGonzález-Doncel, GGoods, S H	243 272 412 237 449 258 361 361 261, 418 244 444 288 270 425 416 395 266 203 244 354 354
Golovashchenko, S F213,Golumbfskie, W JGomes, A SGomez-Cordobes, JGong, JGonzalez, CGonzalez, CGonzález, M AGonzález-Doncel, GGoods, S H209,	243 272 412 237 449 258 361 361 261, 418 244 444 288 270 425 416 395 266 203 244 354 354 442 386
Golovashchenko, S F213,Golumbfskie, W JGomes, A SGomez-Cordobes, JGong, JGonzalez, CGonzalez, CGonzález, M AGonzález-Doncel, GGoods, S H209,	243 272 412 237 449 258 361 361 261, 418 244 444 288 270 425 416 395 266 203 244 354 354 442 386 219
Golovashchenko, S F213,Golumbfskie, W JGomes, A SGomez-Cordobes, JGong, JGonzalez, CGonzalez, CGonzález, M AGonzález-Doncel, GGoods, S H209,	243 272 412 237 449 258 361 361 261, 418 244 444 288 270 425 416 395 266 203 244 354 354 442 386 219
Golovashchenko, S F213,Golumbfskie, W JGomes, A SGomez-Cordobes, JGong, JGonzalez, CGonzalez, CGonzález, M AGonzález-Doncel, GGoods, S H	243 272 412 237 449 258 361 361 261, 418 244 444 288 270 425 416 395 266 203 244 354 354 442 386 219

Grant, G J 268,	314
Grasso, P 385,	450
Gratias, D	206
Gray, G T 233,	303,
	454
Grazier, J M	331
Green, B	359
Green, J A	245
Green, W P	264
Greer, A J	276
Greer, A L 298, 316, 344,	403
Greer, J R	261
Gregori, F	366
Gremaud, M	203
Gribb, T T	198
Griese, R 276,	332
Griffin, J V	273
Griffith, M	370
Grimm, T L	303
Grindstaff, Q G	396
Grosjean, E	417
Gross, K J 262,	310
Groza, J R	242
Gruen, G	219
Grugel, R N	247
Grund, G	330
Gschneidner, K A	396
Gu, S	171
Gu, Y 269,	270
Guangjun, Z	455
Guclu, M	365
Guduru, R	393
Guertsman, V	355
Guillemot, G	248
Guillot, J	319
Guinta, R K	394
Guldhav, A	272
Gundakaram, R C	391
Gunderov, D V	260
Gungor, M N 223,	323
Gunnewiek, L 362,	424
Guo, D	447
Guo, F	217
Guo, G	323
Guo, H	282
Guo, T 178,	387
Guo, X	288
Guo, Z X	215
Guozhi, Z	325
Gupta, A K	399
Gupta, M	262
Gupta, P	185
Gurupira, T Z	414
Guruswamy, S 396,	397
Gusev, A	437
Gustafson, T W	173
Guthrie, R I	417
Guven, I	229
Guyer, J E	276
Guyot, P	438
п	

# H

Ha, D	453
На, Ј	260
Haataja, M	276
Haberling, C	383



Hackenberg, R E	•••••	442
Haeffner, D R		272
Haggett, R		420
Hagiwara, M		337
Hagman, A		436
Hagni, A M		295
Hahn, H W		306
Hakik, M		342
Hakonsen, A		318
Halali, M		369
Halas, N		240
Haldenwanger, H		383
Halikia, I		330
Hall, M G		282
Hallbom, D J		443
Hamadou, H		203
Hamawi, D		395
Hamipikian, J		381
Hammar, R H		211
Hammon, D L		261
Hampikian, J		388
Han, B Q 256, 352,		392
Han, C		448
Han, E		412
Han, G		226
Han, J 301,		388
Han, J		454
Han, K		407
Han, K		392
Han, K		448
Han, L		311
Han, M K		247
Han, Q 227, 266, 281,	298,	299,
		449
Han, S Han, S Y		222 433
Hanada, S		455 315
Hanagan, M J		319
Handtrack, D		315
Hanna, M D		211
Hanrahan, R J		396
Hansen, B L		453
Hansen, J		436
Hansen, N 251, 252,	302	346
Hanson, R		404
Нао, Ү		195
Haouaoui, M	257,	341
Haouaoui, M Harada, H 174,	257, 269,	
Harada, H 174,	269,	341
Harada, H 174, Hardwick, D A	269, 174,	341 270
Harada, H 174, Hardwick, D A 269, 315,	269, 174, 357,	341 270 215,
Harada, H 174, Hardwick, D A	269, 174, 357,	341 270 215, 400
Harada, H 174, Hardwick, D A 269, 315,	269, 174, 357, 	341 270 215, 400 235
Harada, H 174, Hardwick, D A 269, 315, Hardy, J S Hariharaputran, R	269, 174, 357, 	341 270 215, 400 235 181
Harada, H 174, Hardwick, D A	269, 174, 357, 	341 270 215, 400 235 181 287
Harada, H 174, Hardwick, D A 269, 315, Hardy, J S Hariharaputran, R Harringa, J L Harris, B	269, 174, 357, 	341 270 215, 400 235 181 287 230
Harada, H 174, Hardwick, D A	269, 174, 357, 	341 270 215, 400 235 181 287 230 329
Harada, H 174, Hardwick, D A	269, 174, 357, 	341 270 215, 400 235 181 287 230 329 333
Harada, H 174, Hardwick, D A	269, 174, 357, 	341 270 215, 400 235 181 287 230 329 333 328 397 197
Harada, H 174, Hardwick, D A	269, 174, 357,	341 270 215, 400 235 181 287 230 329 333 328 397
Harada, H 174, Hardwick, D A	269, 174, 357, 	341 270 215, 400 235 181 287 230 329 333 328 397 197 276 349
Harada, H 174, Hardwick, D A	269, 174, 357, 	341 270 215, 400 235 181 287 230 329 333 328 397 197 276 349 295
Harada, H 174, Hardwick, D A	269, 174, 357,   288,	341 270 215, 400 235 181 287 230 329 333 328 397 197 276 349 295 324
Harada, H 174, Hardwick, D A	269, 174, 357,	341 270 215, 400 235 181 287 230 329 333 328 397 197 276 349 295 324 435
Harada, H 174, Hardwick, D A	269, 174, 357,	341 270 215, 400 235 181 287 230 329 333 328 397 197 276 349 295 324 435 413
Harada, H 174, Hardwick, D A	269, 174, 357,	341 270 215, 400 235 181 287 230 329 333 328 397 197 276 349 295 324 435

Hashimoto, S		338
Haskel, D		250
Hasnaoui, A		305
Hassan, H		372
Hassan, M I		385
Hata, S		390
Hatch, C		323
Hatsuda, K		206
Hauback, B C		353 318
Haugen, T Hawk, J A	•••••	401
Hayashi, T 215,	315	401
Hayashi, Y		435
Hayes, P C		330
Haywood, R		362
Hazzledine, P M		225
He, G		337
Не, М		373
Heamot, N		426
Hearne, S J		261,
		418
Heason, C P		253
Hebert, R J		253
Hedjazi, J Heilmaier, M		439 355
Hellmig, R		252
Hemker, K J		283
Henager, C H		355
Henderson, D W		286,
		417
Hendriksen, M	232,	416
Henein, H 379,		446
Hennig, R G	183,	431
Henrie, B L	233.	202
		303,
	451,	453
	451,	453 428
	451, 	453 428 441
Henry, D M	451,  344,	453 428 441 380
Henry, D M	451,  344,	453 428 441 380 252
Henry, D M Henry, P J Herlach, D M Herman, G Hermesmann, C	451,  344, 	453 428 441 380 252 214
Henry, D M	451,  344,  408,	453 428 441 380 252
Henry, D M Henry, P J Herlach, D M Herman, G Hermesmann, C Hernández-Morales, J B	451,  344,  408,	453 428 441 380 252 214 409
	451,  344,  408,  340,	<ul> <li>453</li> <li>428</li> <li>441</li> <li>380</li> <li>252</li> <li>214</li> <li>409</li> <li>353</li> </ul>
	451,  344,  408,  340, 	453 428 441 380 252 214 409 353 270 356 390
	451,  344,  408,  340, 	453 428 441 380 252 214 409 353 270 356 390 291
	451,  344,  408,  340, 	<ul> <li>453</li> <li>428</li> <li>441</li> <li>380</li> <li>252</li> <li>214</li> <li>409</li> <li>353</li> <li>270</li> <li>356</li> <li>390</li> <li>291</li> <li>417</li> </ul>
	451,  344,  408,  340, 	453 428 441 380 252 214 409 353 270 356 390 291 417 324
	451,  344,  408,  340, 	453 428 441 380 252 214 409 353 270 356 390 291 417 324 287
	451, 	453 428 441 380 252 214 409 353 270 356 390 291 417 324 287 177
	451, 	453 428 441 380 252 214 409 353 270 356 390 291 417 324 287 177 225
	451,  344,  408,  340,  191, 	453 428 441 380 252 214 409 353 270 356 390 291 417 324 287 177 225 175
	451, 	453 428 441 380 252 214 409 353 270 356 390 291 417 324 287 177 225
	451, 344,  408,  340,  191, 	453 428 441 380 252 214 409 353 270 356 390 291 417 324 287 177 225 175 194
	451, 	453 428 441 380 252 214 409 353 270 356 390 291 417 324 287 177 225 175 194 323
	451, 	453 428 441 380 252 214 409 353 270 356 390 291 417 324 287 175 194 323 453
	451, 	453 428 441 380 252 214 409 353 270 356 390 291 417 324 287 175 194 323 453 269 408 453
	451, 344,  340,  340,  191,  191,  404, 	453 428 441 380 252 214 409 353 270 356 390 291 417 324 287 177 225 175 194 323 453 269 408 453 355
	451, 	453 428 441 380 252 214 409 353 270 356 390 291 417 324 287 175 175 175 175 194 323 453 269 408 453 355 408
	451, 	453 428 441 380 252 214 409 353 270 356 390 291 417 324 287 175 175 175 175 194 323 453 269 408 453 355 408 278
	451,  344,  408,  340,  191,  191,  191,  191,  191,  191,  191, 	453 428 441 380 252 214 409 353 270 356 390 291 417 324 287 175 194 323 453 269 408 453 355 408 278 311
	451, 	453 428 441 380 252 214 409 353 270 356 390 291 417 324 287 177 225 175 194 323 453 269 408 453 355 408 278 311 261
	451, 	453 428 441 380 252 214 409 353 270 356 390 291 417 324 287 177 225 175 194 323 453 269 408 453 355 408 278 311 261 370
	451, 	<ul> <li>453</li> <li>428</li> <li>441</li> <li>380</li> <li>252</li> <li>214</li> <li>409</li> <li>353</li> <li>270</li> <li>356</li> <li>390</li> <li>291</li> <li>417</li> <li>324</li> <li>287</li> <li>177</li> <li>225</li> <li>175</li> <li>194</li> <li>323</li> <li>453</li> <li>269</li> <li>408</li> <li>453</li> <li>355</li> <li>408</li> <li>278</li> <li>311</li> <li>261</li> <li>370</li> <li>178</li> </ul>
	451, 	453 428 441 380 252 214 409 353 270 356 390 291 417 324 287 177 225 175 194 323 453 269 408 453 355 408 278 311 261 370

Holloway, P H	377
110110 way, 1 11	
Holm, E A 181, 182,	224,
Holm, E A 181, 182,	407
Holmsen, A	398
Holtkamp, D B	303
Homentcovschi, D	417
Hon, M	374
Hong, D	377
Hong, F	417
Hong, J	321
Hong, K	293
6	
Hong, S 214,	350
Hongming, G	455
Hoo, N	416
Hopkins, P L	338
Horita, Z 206,	251,
	433
	356
Horstemeyer, M	
Hort, N	445
Horton, D J	297
Horton, J A 184, 287,	359
Horton, J A 104, 207,	
Horton, W S	286
Hosford, W F	257
Hosking, F M	368
	443
Houchin, M	
House, J W	257
Houston, D Q	191
Howard, D W	395
Howard, S M 214,	314
Howe, J M 371,	384
Howell, S W	441
Hoyt, J J 180,	222,
Hoyt, J J 180,	
	405
Hryn, J 199, 244, 357, 417,	100
$111 \text{ y}_{11}, \text{ J}_{}, 199, 2++, 337, +17,$	429
Hsieh, K	242
Hsieh, K Hsieh, Y Y	242 241
Hsieh, K Hsieh, Y Y Hsiung, L L	242
Hsieh, K Hsieh, Y Y Hsiung, L L	242 241
Hsieh, K Hsieh, Y Y Hsiung, L L Hsu, E	242 241 225 201
Hsieh, K Hsieh, Y Y Hsiung, L L Hsu, E Hsu, S C	242 241 225 201 294
Hsieh, K Hsieh, Y Y Hsiung, L L Hsu, E Hsu, S C Hsu, Y	<ul> <li>242</li> <li>241</li> <li>225</li> <li>201</li> <li>294</li> <li>382</li> </ul>
Hsieh, K Hsieh, Y Y Hsiung, L L Hsu, E Hsu, S C	242 241 225 201 294
Hsieh, K Hsieh, Y Y Hsiung, L L Hsu, E Hsu, S C Hsu, Y	<ul> <li>242</li> <li>241</li> <li>225</li> <li>201</li> <li>294</li> <li>382</li> <li>225</li> </ul>
Hsieh, K Hsieh, Y Y Hsiung, L L Hsu, E Hsu, S C Hsu, Y Hsueh, J Hu, H	<ul> <li>242</li> <li>241</li> <li>225</li> <li>201</li> <li>294</li> <li>382</li> <li>225</li> <li>447</li> </ul>
Hsieh, K Hsieh, Y Y Hsiung, L L Hsu, E Hsu, S C Hsu, Y Hsueh, J Hu, H 311, 313, 376, Hu, S 277,	<ul> <li>242</li> <li>241</li> <li>225</li> <li>201</li> <li>294</li> <li>382</li> <li>225</li> <li>447</li> <li>408</li> </ul>
Hsieh, K         Hsieh, Y Y         Hsiung, L L         Hsu, E         Hsu, S C         Hsu, Y         Hsueh, J         Hu, H         311, 313, 376,         Hu, S         277,         Hu, Y C	<ul> <li>242</li> <li>241</li> <li>225</li> <li>201</li> <li>294</li> <li>382</li> <li>225</li> <li>447</li> <li>408</li> <li>338</li> </ul>
Hsieh, K Hsieh, Y Y Hsiung, L L Hsu, E Hsu, S C Hsu, Y Hsueh, J Hu, H 311, 313, 376, Hu, S 277,	<ul> <li>242</li> <li>241</li> <li>225</li> <li>201</li> <li>294</li> <li>382</li> <li>225</li> <li>447</li> <li>408</li> </ul>
Hsieh, K         Hsieh, Y Y         Hsiung, L L         Hsu, E         Hsu, S C         Hsu, Y         Hsueh, J         Hu, H         Y         Hu, S         Hu, S         Hu, S         Y         Hu, S         Y         Hu, S         Y         <	242 241 225 201 294 382 225 447 408 338 331
Hsieh, K         Hsieh, Y Y         Hsiung, L L         Hsu, E         Hsu, S C         Hsu, Y         Hsueh, J         Hu, H         Mu, S         Hu, H         Mu, S         Hu, S         Hu, S         Hu, S         Hu, S         Hu, S         Hu, Y C         332,         Huag, C	242 241 225 201 294 382 225 447 408 338 331 269
Hsieh, K         Hsieh, Y Y         Hsiung, L L         Hsu, E         Hsu, S C         Hsu, Y         Hsueh, J         Hu, H         Mu, S         Hu, H         Mu, S         Hu, S         Hu, S         Hu, S         Hu, S         Huag, C         Huang, C	<ul> <li>242</li> <li>241</li> <li>225</li> <li>201</li> <li>294</li> <li>382</li> <li>225</li> <li>447</li> <li>408</li> <li>338</li> <li>331</li> <li>269</li> <li>242</li> </ul>
Hsieh, K         Hsieh, Y Y         Hsiung, L L         Hsu, E         Hsu, S C         Hsu, Y         Hsueh, J         Hu, H         Mu, S         Hu, H         Mu, S         Hu, S         Hu, G         Hu, S         Huag, C         Huang, C S         Muang, C S	<ul> <li>242</li> <li>241</li> <li>225</li> <li>201</li> <li>294</li> <li>382</li> <li>225</li> <li>447</li> <li>408</li> <li>338</li> <li>331</li> <li>269</li> <li>242</li> <li>339</li> </ul>
Hsieh, K         Hsieh, Y Y         Hsiung, L L         Hsu, E         Hsu, S C         Hsu, Y         Hsueh, J         Hu, H         Mu, S         Hu, H         Mu, S         Hu, S         Hu, G         Hu, S         Huag, C         Huang, C S         Muang, C S	<ul> <li>242</li> <li>241</li> <li>225</li> <li>201</li> <li>294</li> <li>382</li> <li>225</li> <li>447</li> <li>408</li> <li>338</li> <li>331</li> <li>269</li> <li>242</li> </ul>
Hsieh, K         Hsieh, Y Y         Hsiung, L L         Hsu, E         Hsu, S C         Hsu, Y         Hsu, Y         Hsueh, J         Hu, H         Mu, S         Hu, Y         Mu, S         Hu, F         294,         Huang, C         Huang, J	242 241 225 201 294 382 225 447 408 338 331 269 242 339 224
Hsieh, K         Hsieh, Y Y         Hsiung, L L         Hsu, E         Hsu, S C         Hsu, Y         Hsueh, J         Hu, H         Mu, S C         Hu, G         Mu, H         Mu, S         Hu, Y C         Mu, Y C         Mu, Y C         Huang, C         Huang, C S         Huang, J	242 241 225 201 294 382 225 447 408 338 331 269 242 339 224 257
Hsieh, K         Hsieh, Y Y         Hsiung, L L         Hsu, S C         Hsu, Y         Hsueh, J         Hu, H         Mu, S C         Hu, G         Hu, H         Mu, S         Hu, S         Hu, S         Hu, Y C         Mu, S         Huang, C         Huang, C S         Huang, J         Huang, J G         Huang, J G	242 241 225 201 294 382 225 447 408 338 331 269 242 339 224 257 247
Hsieh, K         Hsieh, Y Y         Hsiung, L L         Hsu, E         Hsu, S C         Hsu, Y         Hsueh, J         Hu, H         Mu, S C         Hu, G         Mu, H         Mu, S         Hu, Y C         Mu, Y C         Mu, Y C         Huang, C         Huang, C S         Huang, J	242 241 225 201 294 382 225 447 408 338 331 269 242 339 224 257
Hsieh, K         Hsieh, Y Y         Hsiung, L L         Hsu, S C         Hsu, Y         Hsu, Y         Hsueh, J         Hu, H         Mu, Y C         Mu, Y C         Mu, F         Huang, C         Huang, C S         Huang, J         Huang, J G         232,         Huang, J Y	242 241 225 201 294 382 225 447 408 338 331 269 242 339 224 257 247
Hsieh, K         Hsieh, Y Y         Hsiung, L L         Hsu, S C         Hsu, Y         Hsu, Y         Hsueh, J         Hu, H         Mu, S         Hu, S         YC         Huang, C         Huang, C S         Huang, J         Huang, J G         Yang, J Y         Yang, J Y	242 241 225 201 294 382 225 447 408 338 331 269 242 339 224 257 247 247 306
Hsieh, K         Hsieh, Y Y         Hsiung, L L         Hsu, S C         Hsu, Y         Hsu, Y         Hsu, Y         Hsu, Y         Mu, H         Mu, S         YC         Huang, C         Huang, C S         Huang, J         Huang, J G         Huang, J Y         Huang, J Y	242 241 225 201 294 382 225 447 408 338 331 269 242 339 224 257 247 247 306 271
Hsieh, K         Hsieh, Y Y         Hsiung, L L         Hsu, S C         Hsu, Y         Hsu, Y         Hsu, Y         Hsu, Y         Hueh, J         Hu, S         YC         Huang, C         Huang, C         Huang, J         Huang, J G         Huang, J Y         Huang, J Y         Huang, J Y         Huang, M	242 241 225 201 294 382 225 447 408 338 331 269 242 339 224 257 247 247 306
Hsieh, K         Hsieh, Y Y         Hsiung, L L         Hsu, S C         Hsu, Y         Hsu, Y         Hsueh, J         Hu, H         Mu, Y C         Mu, F         Poly         Huang, C         Huang, J         Huang, J G         Huang, J Y         Huang, J Y         Huang, J Y         Huang, J S	242 241 225 201 294 382 225 447 408 338 331 269 242 339 224 257 247 247 306 271
Hsieh, K         Hsieh, Y Y         Hsiung, L L         Hsu, S C         Hsu, Y         Hsu, Y         Hsueh, J         Hu, H         Mu, Y C         Mu, F         Poly         Huang, C         Huang, J         Huang, J G         Huang, J Y         Huang, J Y         Huang, J Y         Huang, J S	242 241 225 201 294 382 225 447 408 338 331 269 242 2339 224 257 247 247 306 271 271
Hsieh, K         Hsieh, Y Y         Hsiung, L L         Hsu, S C         Hsu, Y         Hsu, Y         Hsu, Y         Hsueh, J         Hu, H         Mu, S         YC         Huang, C         Huang, C S         Huang, J         Huang, J Y         Huang, J Y         Huang, J Y         Huang, J Y         Huang, J T         Huang, J Y         Huang, J T	242 241 225 201 294 382 225 447 408 338 331 269 242 339 224 257 247 247 306 271 271 242 439
Hsieh, K         Hsieh, Y Y         Hsiung, L L         Hsu, S C         Hsu, Y         Hsu, Y         Hsu, Y         Huang, J         Huang, J G         Huang, J Y         Huang, J G         Huang, J Y         Huang, J T         Huang, J T         Huang, J S         Huang, J T         Huang, J Y         Huang,	242 241 225 201 294 382 225 447 408 338 331 269 242 2339 224 257 247 247 306 271 271 242 439 302
Hsieh, K         Hsieh, Y Y         Hsiung, L L         Hsu, S C         Hsu, Y         Hsu, Y         Hsu, Y         Huang, J         Huang, J G         Huang, J Y         Huang, J G         Huang, J Y         Huang, J F         Huang, J Y         Huang,	242 241 225 201 294 382 225 447 408 338 331 269 242 2339 224 257 247 247 306 271 271 242 439 302 261
Hsieh, K         Hsieh, Y Y         Hsiung, L L         Hsu, S C         Hsu, Y         Hsu, Y         Hsu, Y         Huang, J         Huang, J G         Huang, J Y         Huang, J G         Huang, J Y         Huang, J F         Huang, J Y         Huang,	242 241 225 201 294 382 225 447 408 338 331 269 242 2339 224 257 247 247 306 271 271 242 439 302
Hsieh, K         Hsieh, Y Y         Hsiung, L L         Hsu, S C         Hsu, Y         Hsu, Y         Hsu, Y         Mu, H         311, 313, 376,         Hu, S         Y         Hu, H         311, 313, 376,         Hu, S         Y         Huang, Y         Huang, C         Huang, C         Huang, C         Huang, J         Huang, J         Huang, J G         Huang, J Y         Huang, Y	242 241 225 201 294 382 225 447 408 338 331 269 242 339 224 257 247 247 247 247 306 271 247 247 306 271 247 247 247 247 247 247 267 247 247 247 247 247 247 247 247 247 24
Hsieh, K         Hsieh, Y Y         Hsiung, L L         Hsu, S C         Hsu, Y         Hsu, Y         Hsu, Y         Huang, J         Huang, C         Huang, C         Huang, J         Huang, Y         Huang, Y          Huang, Y	242 241 225 201 294 382 225 447 408 338 331 269 242 339 224 257 247 247 247 247 306 271 247 247 306 271 242 439 302 261 251
Hsieh, K         Hsieh, Y Y         Hsiung, L L         Hsu, S C         Hsu, Y         Hsu, Y         Hsu, Y         Huang, J         Huang, C         Huang, C         Huang, J         Huang, Y         Huang, Y         Huang, Y	242 241 225 201 294 382 225 447 408 338 331 269 242 339 224 257 247 247 247 247 306 271 271 242 439 302 261 258 374
Hsieh, K         Hsieh, Y Y         Hsiung, L L         Hsu, S C         Hsu, Y         Hsu, Y         Hsu, Y         Mu, H         311, 313, 376,         Hu, Y         Hu, H         311, 313, 376,         Hu, S         Y         Huang, Y         Huang, C         Huang, C S         Huang, C S         Huang, J         Huang, J G         Huang, J G         Huang, J Y         Huang, J Y         Huang, J Y         Huang, S         Huang, T F         Huang, X         251, 252,         Huang, Y         Huang, Y	242 241 225 201 294 382 225 447 408 338 331 269 242 339 224 257 247 247 247 247 247 306 271 271 242 439 302 261 258 374 402
Hsieh, K         Hsieh, Y Y         Hsiung, L L         Hsu, S C         Hsu, Y         Hsu, Y         Hsu, Y         Mu, H         311, 313, 376,         Hu, Y         Hu, H         311, 313, 376,         Hu, S         Y         Huang, Y         Huang, C         Huang, C S         Huang, C S         Huang, J         Huang, J G         Huang, J G         Huang, J Y         Huang, J Y         Huang, J Y         Huang, S         Huang, T F         Huang, X         251, 252,         Huang, Y         Huang, Y	242 241 225 201 294 382 225 447 408 338 331 269 242 339 224 257 247 247 247 247 247 306 271 271 242 439 302 261 258 374 402
Hsieh, K         Hsieh, Y Y         Hsiung, L L         Hsu, S C         Hsu, Y         Hsu, Y         Hsueh, J         Hu, H         311, 313, 376,         Hu, Y         Huaeh, J         Huang, C         Huang, C S         Huang, J         Huang, J Y         Huang, J Y         Huang, J Y         Huang, S         Huang, T F         Huang, X         251, 252,         Huang, Y         Huang, Y         Huang, Y         Huang, Y         Huang, Y         Huang, Y	242 241 225 201 294 382 225 447 408 338 331 269 242 339 224 257 247 247 306 271 271 242 439 302 261 261 258 374 402 189
Hsieh, K         Hsieh, Y Y         Hsiung, L L         Hsu, S C         Hsu, Y       332,         Hsueh, J       311, 313, 376,         Hu, H       311, 313, 376,         Hu, H       311, 313, 376,         Hu, S       277,         Hu, Y C       332,         Huar, S       277,         Hu, Y C       332,         Huar, S       274,         Huang, C       332,         Huang, J       294,         Huang, J       234,         Huang, J Y       234,         Huang, J Y       234,         Huang, J Y       234,         Huang, J Y       234,         Huang, S       Huang, T F         Huang, X       251, 252,         Huang, X       251, 252,         Huang, Y       Huang, Y         Huang, Y       Huang, Y         Huang, Y       271	242 241 225 201 294 382 225 447 408 338 331 269 242 339 224 257 247 247 306 271 271 242 439 302 261 258 374 402 189 346
Hsieh, K         Hsieh, Y Y         Hsiung, L L         Hsu, S C         Hsu, Y         Hsu, Y         Hsueh, J         Hu, H         311, 313, 376,         Hu, Y         Huaeh, J         Huan, F         Huang, C         Huang, C S         Huang, J         Huang, J G         Huang, J Y         Huang, J Y         Huang, S         Huang, T F         Huang, Y         Huang, D A         Huang, Y         Huang, Y         Huang, Y         Huang, Y         Huang, D A	242 241 225 201 294 382 225 447 408 338 331 269 242 339 224 257 247 247 247 247 306 271 271 242 439 302 261 258 374 402 189 346 384
Hsieh, K         Hsieh, Y Y         Hsiung, L L         Hsu, S C         Hsu, Y       332,         Hsueh, J       311, 313, 376,         Hu, H       311, 313, 376,         Hu, H       311, 313, 376,         Hu, S       277,         Hu, Y C       332,         Huar, S       277,         Hu, Y C       332,         Huar, S       274,         Huang, C       332,         Huang, J       294,         Huang, J       234,         Huang, J Y       234,         Huang, J Y       234,         Huang, J Y       234,         Huang, J Y       234,         Huang, S       Huang, T F         Huang, X       251, 252,         Huang, X       251, 252,         Huang, Y       Huang, Y         Huang, Y       Huang, Y         Huang, Y       271	242 241 225 201 294 382 225 447 408 338 331 269 242 339 224 257 247 247 306 271 271 242 439 302 261 258 374 402 189 346

Hultman, L	429
Hults, W L	283
Hung, C M	375
Hünsche, I	401
Hunt, M	217
Huo, Y	380
Hur, B 214, 404,	453
Hurysz, K M	236
Hutchinson, C R	425
Huzmezan, M	195
Hwang, C 190,	338
Hwang, S	254
Hwang, W	285
Hwang, Y J	197
Hyde, B 224,	
Hyde, J R	441
Hyers, R W 289, 299,	438
Hyland, M 218, 265, 399,	412

# Ι

Ice, G E	279,	324,	394
Ichikawa, T			354
Ichimura, S			220
Ignatenko, L N			258
Ikeda, M			324
Ilegbusi, O J			448
Ilyoukha, N			369
Im, J	259,	341,	435
Im, Y H			423
Imai, T			234
Imam, A			278
Imam, M	182,	223,	278,
			440
			441
Imbert, C A Imrie, W P 188	, 230,	231,	284,
	372,	415,	443
Indrakanti, S K		227,	281
Indutnyy, I Z			180
Inel, C			173
Inman, D			323
Inoue, A		216,	271
Inoue, H			401
Inspektor, A			421
Ionescu, A			173
Iosub, V			210
Ipser, H		231,	382
Irvine, S			441
Isac, M			417
Ishida, K		191,	242
Ishikawa, K			397
Islam, Z	•••••		250
Itakura, M			390
Itharaju, R R			258
Ito, K 215	315,	357,	401
Ivan, J			296
Ivanisenko, Y			307
Ivanov, Y F	•••••		255
Iwata, S			304
Iyer, M K			241
Izumi, K	•••••		220

# J

Jablokov, V R		173
Jackson, G		416
Jackson, M	223,	323

Jackson, M R	358
Jackson, S M	413
Jacobsen, L	364
Jacobson, D L	210
Jacot, A 203, 385,	387
Jäger, S	234
Jahnsen, E J	330
Jak, E	330
Jakobsson, A	409
Jalkanen, H	186
Jamey, C	172
Jang, G Y 293,	332
Jang, S J	439
Jankowski, A	406
Janousek, M 174,	215,
	400
Janzen, J 330,	331
Jaouen, O	178
Jaradeh, M	298
Jardy, A 219,	404
Jarry, P P	298
Jayakumar, T	227
Jayaraj, B	410
Jayasekera, S	329
Jeannette, J	417
Jéhanno, P 315,	358
Jensen, C M 263,	353
Jeong, H	438
Jeong, S	286
Jerman, G	
Jha, G	
Jha, M K	171
Jian, X 299,	318
Jiang, C 349,	364
Jiang, F 379,	446
Jiang, H	
Jiang, W	
Jiang, W	316
Jiang, Y T	439
Jiao, H Jiao, W L	228 290
Jiao, w L	
Jin, C	
Jili, M	213
Jin, S 196, 197, Jin, Y M 183, 277,	384
Jin, Z 349,	350
Jo, H	
Jog, J	
Johnson, C	
Johnson, D D	
Johnson, D R 215,	269.
270, 315,	
Johnson, G L	212
Johnson, J A 284,	318
Johnson, J R	353
Johnson, W C 277,	
Johnson, W L 316,	
Jolly, M R	
JUILV, IVI IX	369
	369 318
Jonas, J J 201,	369 318 205
Jonas, J J 201, Jonas, R K	369 318 205 212
Jonas, J J 201, Jonas, R K Jones, C L	369 318 205 212 414
Jonas, J J 201, Jonas, R K Jones, C L Jones, H 298,	369 318 205 212 414
Jonas, J J 201, Jonas, R K Jones, C L Jones, H 298, Jones, H N 392,	<ul> <li>369</li> <li>318</li> <li>205</li> <li>212</li> <li>414</li> <li>301</li> </ul>
Jonas, J J	369 318 205 212 414 301 435 418
Jonas, J J	<ul> <li>369</li> <li>318</li> <li>205</li> <li>212</li> <li>414</li> <li>301</li> <li>435</li> <li>418</li> <li>420</li> </ul>
Jonas, J J	<ul> <li>369</li> <li>318</li> <li>205</li> <li>212</li> <li>414</li> <li>301</li> <li>435</li> <li>418</li> <li>420</li> <li>170</li> </ul>

Joo, Y		293
Jörgl, H P		336
Josell, D	220,	229,
	280,	409
Joubert, J		210
Juarez, J A		449
Jung, C		300
Jung, J		383
Jung, J		241
Jung, K	380,	392
Jung, S 198, 338,	374,	455
Jung, Y		362
Jungk, J	261,	308
Juul Jensen, D	204,	390

# K

Kabansky, A E	169
Kabra, S	185
Kaczorowski, J	266
Kad, B 366, 371,	383
Kadolkar, P B	411
Kai, H	378
Kaibyshev, R O	311
Kaikake, A	415
Kainer, K U 418,	445
Kainuma, R 191,	242
Kakegawa, K	296
Kakihira, T	366
Kalantar, D H	366
Kalidindi, S R	303
Kaligotla, A	214
Kalu, P 205,	407
Kamachi, M	206
Kamavaram, V	325
Kammer, D	248
Kamp, N	411
Kampe, S L 223, 295,	296
Kane, J	413
Kaneno, Y 174,	401
Kanert, O	297
Kang, S	258
	198.
Kang, S H 179, 220, 274,	320
Kang, S K 189,	231,
285, 331, 373,	416
Kang, T	382
Kang, Y	309
Kantzos, P T	340
Kao, C R 198, 199, 240,	293,
Kao, C.K 198, 199, 240, 	
	382
Kao, H R	375
Kao, S T	190
Kao, V	233
Kaplan, D I	364
Kaplan, H	332
Kapusta, C	
Kapusta, J	184
Karabasevic, D	180
Karabelchtchikova, O P	421
Karaca, H	442
Karaman, I 207, 216,	257,
	442
Karanjai, M	224
Karma, A S	386
Karner, W	
Karney, G B	195



Kasapoglu, Z	315
Kaschner, G C	451
Kashani-Nejad, S	333
Kashyap, B	224
Kashyap, S C	239
Kaspar, R 259,	350
Kassner, M E 279,	433
Kastebo, J	218
Katgerman, L 203, 220, 248,	385
Katiyar, R S	291
Katsman, A	444
Kaufman, L	192
Kawagoishi, N 410,	411
Kawakami, A	323
Kawamura, Y 295,	438
Kawano, Y	449
Kawasaki, M	258
Kawazoe, Y	390
Kay, N R	229
Kay, R	232
Ke, L	294
Ke, W	288
Kear, B H	209
Kecskes, L J	254
Keen, L	377
Keist, J	414
Keles, Ö 273,	450
Kelkar, K 219,	362
Keller, J	396
Keller, R	399
Kelly, J J	308
Kelly, P M	228
Kelly, S M	223
Kelly, T F	198
Kelton, K F 289,	438
Kemp, D J 189,	231
Kempshall, B W	432
Kendig, K	175
Kennedy, M S	275
Kenney, M 378,	420
Kepes, A Kerdouss, F	330 361
Kerns, R	
	441
Kerr, M Kerstiens, B	331 330
Kertý, B 273, Kertz Yurko, J E	450 299
Keskinkilic, E	185
Kestler, H	315
Khachaturyan, A 183,	277,
353,	384
Khan, Z H	171
Khemelevskaya, I Y	253
Khor, K	411
Khraisheh, M K 258, 398,	450
Khraishi, T 221, 356,	451
Kiese, J	365
Kift, J R	415
Kikuchi, E	449
Kikuchi, K	314
Kikuchi, M	407
Kilmametov, A R	306
Kimanetov, AR	180
Kim, C	212
Kim, C 179,	220,
	339
Kim, C	442

Kim, D	374
Kim, D H 217,	438
Kim, D S	287
Kim, H	442
Kim, H 453,	454
Kim, H	448
Kim, H	339
Kim, H	389
Kim, H	448
Kim, H	258
Kim, H J	411
Kim, H S Kim, H Y	252 254
Kim, I J	287
Kim, I S	412
Kim, J	246
Kim, J	175
Kim, J	389
Kim, J	352
Kim, J	455
Kim, J	416
Kim, J 453, 454,	455
Kim, J H	433
Kim, J H 286,	294
Kim, J S	417
Kim, K Kim, K	190 281
Kim, K	309
Kim, N	382
Kim, N J	287
Kim, S 198,	338
Kim, S 214,	453
Kim, S	451
Kim, S	455
Kim, S	264
Kim, S	454
Kim, S 215, Kim, S G	241 387
Kim, S H	387 454
Kim, S K	376
Kim, S S	412
Kim, S W 199,	435
Kim, T	374
Kim, W 321,	358
Kim, W T 217, 387,	438
Kim, Y	287
Kim, Y	352
Kim, Y Kim, Y	260 455
Kim, Y Kim, Y	455 309
Kim, Y H	374
Kim, Y S 412,	454
Kim, Y S 412, Kimura, T Kimura, T	
Kim, Y S 412, Kimura, T Kimura, T	454 351
Kim, Y S 412,	454 351 384
Kim, Y S       412,         Kimura, T	454 351 384 435
Kim, Y S       412,         Kimura, T	454 351 384 435 191 367 259
Kim, Y S       412,         Kimura, T	454 351 384 435 191 367 259 416
Kim, Y S       412,         Kimura, T	454 351 384 435 191 367 259 416 406
Kim, Y S       412,         Kimura, T	454 351 384 435 191 367 259 416 406 195
Kim, Y S       412,         Kimura, T	454 351 384 435 191 367 259 416 406 195 416
Kim, Y S       412,         Kimura, T	454 351 384 435 191 367 259 416 406 195 416 272
Kim, Y S       412,         Kimura, T	454 351 384 435 191 367 259 416 406 195 416 272 353
Kim, Y S       412,         Kimura, T	454 351 384 435 191 367 259 416 406 195 416 272 353 268
Kim, Y S       412,         Kimura, T	454 351 384 435 191 367 259 416 406 195 416 272 353 268 311

Kiss, L I 213,	
Kissane, J	
Kitahara, H	
Kiyobayashi, T	26
Klarstion, D L	20
Klarstrom, D L 226, 297,	41
Kleber, S	35
Klein, B	44
Kleinschrodt, H	43
Kletsky, S V	27
Klingbeil, D	36
Klingbeil, N W	28
Klingensmith, M A	31
Klinger, C	36
Klug, K L 223,	32
Klushin, S D	33
Kluthe, C	35
Kmiotek, D S	34
Knabl, W	40
Knapp, J A	26
Knott, S	19
Ko, Y G	43
Kobade, R	33
Kobayashi, K Kobayashi, T	32 27
	17
Kobbeltvedt, O	
Koch, C C 256, 391,	42
Kogut, D	36
Kohlbrecher, J	25
Kohn, A	19
Kohn, R V	42
Kohyama, A	18
Koike, J 199, 340, 384,	42
Koike, K	22
Koike, M	40
Koizumi, Y 259, 351,	38
Kolbe, M	38
Kolobov, Y R	30
Koltun, P	33
Komandur, K	41
Komatsu, S	32
Kommel, L	25
Kompan, Y Y	22
Kondoh, K	41
Kondoh, M	44
Koneva, N A 255,	25
Kongoli, F	18
Konopnicki, M G	21
Konstantinov, K K	35
Kontsevoi, O Y	27
Коо, Н	32
Коо, Ј	45
Коо, Ү	44
Kooistra, G W	32
Kool, P	38
Koopman, M C 293,	34
	41
NUDL O N	19
Kopf, S R	- 1 2
Kopka, L	30
Kopka, L Korb, G	
Kopka, L Korb, G Korhonen, M A	41
Kopka, L Korb, G Korhonen, M A 286, Korhonen, T K	41 28
Kopka, L Korb, G Korhonen, M A 286, Korhonen, T K Korhonen, T M	41 28 41
Kopka, L Korb, G Korhonen, M A	41 28 41 25
Kopka, L Korb, G Korhonen, M A	41 28 41 25 25
Kopka, L Korb, G Korhonen, M A	41 28 41 25 25 25
Kopka, L Korb, G Korhonen, M A 286, Korhonen, T K Korhonen, T M Korotaev, A D Korshunov, A I	

Kossler, W J	. 276
Koster, E	
Kostika, I	
Kostorz, G	250
Kourov, N I	
Kovar, D	
Kovgan, P A	
Kozeschnik, E	. 405
Kozlov, E V 255	
Kraft, E H	
Kraft, O 188	
Krajewski, P E 211	, 264,
Kral, M V 327	
Krallics, G	
Kramer, M J 175, 215, 238	, 296
Kramer-White, J	419
Vrono M I 105 210 297	400
Krane, M J 195, 219, 387	, 408
Krasilnikov, N A 256	
Krause, A R	214
Krause, E 230	, 231
Krill, C E	
Krioukovsky, V	
Kripesh, V	241
Krishnamurthy, R K	233
<b>2</b>	
Krishnan, A	
Kroupa, A	. 382
Kruger, G A	. 212
Krumdick, G K 200, 244	
Krupakara, P V	226
Kruzic, J J 315	, 316
Krylov, L	. 437
Kuba, M	
Kubat, F	
Kubin, L	
Kudrnovsky, J 192	, 304
Kudrnovsky, J 192 Kulas, M	, 304 . 264
Kudrnovsky, J 192 Kulas, M Kulkarni, A V	, 304 . 264 . 207
Kudrnovsky, J 192 Kulas, M	, 304 . 264 . 207
Kudrnovsky, J 192 Kulas, M Kulkarni, A V Kumar, A	, 304 . 264 . 207 . 227
Kudrnovsky, J 192 Kulas, M Kulkarni, A V Kumar, A Kumar, A	, 304 . 264 . 207 . 227 . 222
Kudrnovsky, J 192 Kulas, M Kulkarni, A V Kumar, A Kumar, A Kumar, D	, 304 . 264 . 207 . 227 . 222 . 336
Kudrnovsky, J 192 Kulas, M Kulkarni, A V Kumar, A Kumar, A	, 304 . 264 . 207 . 227 . 222 . 336 , 431
Kudrnovsky, J 192 Kulas, M Kulkarni, A V Kumar, A Kumar, A Kumar, D Kumar, M 390, 406 Kumar, R	, 304 . 264 . 207 . 227 . 222 . 336 , 431 . 171
Kudrnovsky, J 192 Kulas, M Kulkarni, A V Kumar, A Kumar, A Kumar, D Kumar, M 390, 406 Kumar, R	, 304 . 264 . 207 . 227 . 222 . 336 , 431 . 171
Kudrnovsky, J 192 Kulas, M Kulkarni, A V Kumar, A Kumar, A Kumar, D Kumar, M	, 304 . 264 . 207 . 227 . 222 . 336 , 431 . 171 , 360
Kudrnovsky, J       192         Kulas, M       Kulkarni, A V         Kumar, A       Kumar, A         Kumar, D       Sumar, B         Kumar, R       390, 406         Kumar, S       225, 316         Kumosa, M       225, 316	, 304 . 264 207 . 227 . 222 336 , 431 . 171 , 360 371
Kudrnovsky, J       192         Kulas, M       Kulkarni, A V         Kumar, A       Kumar, A         Kumar, D       Sumar, B         Kumar, R       390, 406         Kumar, S       225, 316         Kumosa, M       Kumta, P	, 304 . 264 207 . 227 . 222 . 336 , 431 . 171 , 360 . 371 . 424
Kudrnovsky, J       192         Kulas, M       Kulkarni, A V         Kumar, A       Kumar, A         Kumar, D       Sumar, B         Kumar, R       390, 406         Kumar, S       225, 316         Kumosa, M       225, 316	, 304 . 264 207 . 227 . 222 . 336 , 431 . 171 , 360 . 371 . 424
Kudrnovsky, J       192         Kulas, M       Kulkarni, A V         Kumar, A       Kumar, A         Kumar, D       Kumar, M         Kumar, R       390, 406         Kumar, S       225, 316         Kumosa, M       Kumta, P         Kumat, P N       Sumar, P	, 304 . 264 207 . 227 . 222 336 , 431 . 171 , 360 371 . 424 . 381
Kudrnovsky, J       192         Kulas, M       Kulkarni, A V         Kumar, A       Kumar, A         Kumar, D       Kumar, M         Kumar, R       390, 406         Kumar, S       225, 316         Kumata, P       Kumta, P         Kumata, C       Kumata, C         Kumar, S       225, 316         Kumata, C       Kumata, C         Kumata, C       Kumata, C         Kumata, C       T	, 304 . 264 207 . 227 . 222 336 , 431 . 171 , 360 371 . 424 . 381 429
Kudrnovsky, J       192         Kulas, M       Kulkarni, A V         Kumar, A       Kumar, A         Kumar, D       Sumar, A         Kumar, M       390, 406         Kumar, R       Sumar, B         Kumar, S       225, 316         Kumta, P       Kumta, P         Kumta, P N       Kunioshi, C T         Kuo, C       201, 227	<ul> <li>, 304</li> <li>, 264</li> <li>207</li> <li>, 227</li> <li>, 336</li> <li>, 431</li> <li>, 171</li> <li>, 360</li> <li>, 371</li> <li>, 424</li> <li>, 381</li> <li>, 429</li> <li>, 280</li> </ul>
Kudrnovsky, J       192         Kulas, M       Kulkarni, A V         Kumar, A       Kumar, A         Kumar, D       Kumar, M         Kumar, R       390, 406         Kumar, S       225, 316         Kumosa, M       Kumta, P         Kumat, P N       Kunioshi, C T         Kuo, C       201, 227         Kuo, R C       234	<ul> <li>, 304</li> <li>, 264</li> <li>, 207</li> <li>, 222</li> <li>, 336</li> <li>, 431</li> <li>, 171</li> <li>, 360</li> <li>, 371</li> <li>, 424</li> <li>, 381</li> <li>, 429</li> <li>, 280</li> <li>, 247</li> </ul>
Kudrnovsky, J       192         Kulas, M       Kulkarni, A V         Kumar, A       Kumar, A         Kumar, D       Kumar, M         Kumar, R       390, 406         Kumar, S       225, 316         Kumosa, M       Kumta, P         Kumat, P N       Kunioshi, C T         Kuo, C       201, 227         Kuo, R C       234	<ul> <li>, 304</li> <li>, 264</li> <li>, 207</li> <li>, 222</li> <li>, 336</li> <li>, 431</li> <li>, 171</li> <li>, 360</li> <li>, 371</li> <li>, 424</li> <li>, 381</li> <li>, 429</li> <li>, 280</li> <li>, 247</li> </ul>
Kudrnovsky, J       192         Kulas, M       Kulkarni, A V         Kumar, A       Kumar, A         Kumar, D       Kumar, B         Kumar, R       390, 406         Kumar, R       225, 316         Kumas, S       225, 316         Kumta, P       Kumta, P         Kunioshi, C T       201, 227         Kuo, R C       234         Kuriyama, N       Sumar, N	<ul> <li>, 304</li> <li>, 264</li> <li>207</li> <li>, 227</li> <li>, 336</li> <li>, 431</li> <li>, 171</li> <li>, 360</li> <li>, 371</li> <li>, 424</li> <li>, 381</li> <li>, 429</li> <li>, 280</li> <li>, 247</li> <li>, 263</li> </ul>
Kudrnovsky, J       192         Kulas, M       Kulkarni, A V         Kumar, A       Kumar, A         Kumar, D       Kumar, B         Kumar, R       390, 406         Kumar, R       225, 316         Kumas, M       225, 316         Kumat, P       Kumas, M         Kumat, P N       Kunioshi, C T         Kuo, C       201, 227         Kuo, R C       234         Kuriyama, N       Kurokawa, A	<ul> <li>, 304</li> <li>, 264</li> <li>, 207</li> <li>, 222</li> <li>, 336</li> <li>, 431</li> <li>, 171</li> <li>, 360</li> <li>, 371</li> <li>, 424</li> <li>, 381</li> <li>, 429</li> <li>, 280</li> <li>, 247</li> <li>, 263</li> <li>, 220</li> </ul>
Kudrnovsky, J       192         Kulas, M       Kulkarni, A V         Kumar, A       Kumar, A         Kumar, D       Kumar, B         Kumar, R       390, 406         Kumar, R       225, 316         Kumas, S       225, 316         Kumat, P       Kumat, P         Kumat, P N       Kunioshi, C T         Kuo, C       201, 227         Kuo, R C       234         Kuriyama, N       Kurokawa, A         Kurtz, R J       Sumation of the second of	<ul> <li>, 304</li> <li>, 264</li> <li>, 207</li> <li>, 222</li> <li>, 336</li> <li>, 431</li> <li>, 171</li> <li>, 360</li> <li>, 371</li> <li>, 424</li> <li>, 381</li> <li>, 429</li> <li>, 280</li> <li>, 247</li> <li>, 263</li> <li>, 220</li> <li>, 355</li> </ul>
Kudrnovsky, J       192         Kulas, M       Kulkarni, A V         Kumar, A       Kumar, A         Kumar, D       Kumar, B         Kumar, R       225, 316         Kumas, M       225, 316         Kuma, P       Kumar, B         Kuma, P N       Kunioshi, C T         Kuo, C       201, 227         Kuo, R C       234         Kuriyama, N       Kurokawa, A         Kurz, R J       Kurz, G	, 304 . 264 207 . 227 . 222 336 , 431 . 171 , 360 371 . 424 . 381 429 , 280 , 247 . 263 220 355 233
Kudrnovsky, J       192         Kulas, M       Kulkarni, A V         Kumar, A       Kumar, A         Kumar, D       Kumar, B         Kumar, R       225, 316         Kumas, M       225, 316         Kuma, P       Kumar, B         Kuma, P N       Kunioshi, C T         Kuo, C       201, 227         Kuo, R C       234         Kuriyama, N       Kurokawa, A         Kurz, R J       Kurz, G	, 304 . 264 207 . 227 . 222 336 , 431 . 171 , 360 371 . 424 . 381 429 , 280 , 247 . 263 220 355 233
Kudrnovsky, J       192         Kulas, M       Kulkarni, A V         Kulkarni, A V       Kumar, A         Kumar, A       Sumar, A         Kumar, D       Sumar, B         Kumar, R       390, 406         Kumar, R       225, 316         Kumar, S       225, 316         Kumar, P       Kumosa, M         Kumia, P N       Kunioshi, C T         Kuo, C       201, 227         Kuo, R C       234         Kuriyama, N       Kurokawa, A         Kurz, R J       Kurz, G         Kurz, W       203	<ul> <li>, 304</li> <li>, 264</li> <li>, 207</li> <li>, 222</li> <li>, 336</li> <li>, 431</li> <li>, 171</li> <li>, 360</li> <li>, 371</li> <li>, 424</li> <li>, 381</li> <li>, 429</li> <li>, 280</li> <li>, 247</li> <li>, 263</li> <li>, 220</li> <li>, 355</li> <li>, 233</li> <li>, 345</li> </ul>
Kudrnovsky, J       192         Kulas, M       Kulkarni, A V         Kulkarni, A V       Kumar, A         Kumar, A       Sumar, A         Kumar, D       Sumar, B         Kumar, R       390, 406         Kumar, R       225, 316         Kumar, S       225, 316         Kumar, P       Kumosa, M         Kumia, P N       Kunioshi, C T         Kuo, C       201, 227         Kuo, R C       234         Kuriyama, N       Kurokawa, A         Kurz, R J       Kurz, W         Kuz, W       203         Kushida, A       Sushida, A	<ul> <li>, 304</li> <li>, 264</li> <li>, 207</li> <li>, 222</li> <li>, 336</li> <li>, 431</li> <li>, 171</li> <li>, 360</li> <li>, 371</li> <li>, 424</li> <li>, 381</li> <li>, 429</li> <li>, 280</li> <li>, 247</li> <li>, 263</li> <li>, 220</li> <li>, 355</li> <li>, 233</li> <li>, 345</li> <li>, 426</li> </ul>
Kudrnovsky, J       192         Kulas, M       Kulkarni, A V         Kulkarni, A V       Kumar, A         Kumar, A       Sumar, B         Kumar, R       390, 406         Kumar, R       225, 316         Kumar, S       225, 316         Kumar, P       Kumar, B         Kumta, P       201, 227         Kuo, C       201, 227         Kuo, R C       234         Kuriyama, N       Kurokawa, A         Kurz, R J       Kurz, G         Kurz, W       203         Kushida, A       Kushnarev, B	<ul> <li>, 304</li> <li>, 264</li> <li>, 207</li> <li>, 222</li> <li>, 336</li> <li>, 431</li> <li>, 171</li> <li>, 360</li> <li>, 371</li> <li>, 424</li> <li>, 381</li> <li>, 429</li> <li>, 280</li> <li>, 247</li> <li>, 263</li> <li>, 220</li> <li>, 355</li> <li>, 233</li> <li>, 345</li> <li>, 426</li> <li>, 242</li> </ul>
Kudrnovsky, J       192         Kulas, M       Kulkarni, A V         Kulkarni, A V       Kumar, A         Kumar, A       Sumar, A         Kumar, D       Sumar, B         Kumar, R       390, 406         Kumar, R       225, 316         Kumar, S       225, 316         Kumar, S       225, 316         Kumar, P       Kumosa, M         Kumta, P       Kunioshi, C T         Kuo, C       201, 227         Kuo, R C       234         Kuriyama, N       Kurokawa, A         Kurz, R J       Kuz, G         Kuz, W       203         Kushida, A       Kushnarev, B         Kusui, J       Sushida, A	<ul> <li>, 304</li> <li>, 264</li> <li>, 207</li> <li>, 222</li> <li>, 336</li> <li>, 431</li> <li>, 171</li> <li>, 360</li> <li>, 371</li> <li>, 424</li> <li>, 381</li> <li>, 429</li> <li>, 280</li> <li>, 247</li> <li>, 263</li> <li>, 220</li> <li>, 355</li> <li>, 233</li> <li>, 345</li> <li>, 426</li> <li>, 242</li> <li>, 314</li> </ul>
Kudrnovsky, J       192         Kulas, M       Kulkarni, A V         Kulkarni, A V       Kumar, A         Kumar, A       Sumar, A         Kumar, D       Sumar, B         Kumar, R       390, 406         Kumar, R       225, 316         Kumar, S       225, 316         Kumar, S       225, 316         Kumar, P       Kumosa, M         Kumta, P       Kunioshi, C T         Kuo, C       201, 227         Kuo, R C       234         Kuriyama, N       Kurokawa, A         Kurz, R J       Kuz, G         Kuz, W       203         Kushida, A       Kushnarev, B         Kusui, J       Sushida, A	<ul> <li>, 304</li> <li>, 264</li> <li>, 207</li> <li>, 222</li> <li>, 336</li> <li>, 431</li> <li>, 171</li> <li>, 360</li> <li>, 371</li> <li>, 424</li> <li>, 381</li> <li>, 429</li> <li>, 280</li> <li>, 247</li> <li>, 263</li> <li>, 220</li> <li>, 355</li> <li>, 233</li> <li>, 345</li> <li>, 426</li> <li>, 242</li> <li>, 314</li> </ul>
Kudrnovsky, J       192         Kulas, M       Kulkarni, A V         Kulkarni, A V       Kumar, A         Kumar, A       Sumar, B         Kumar, M       390, 406         Kumar, R       Sumar, B         Kumar, S       225, 316         Kumosa, M       Kumosa, M         Kumta, P       Kumosa, M         Kunioshi, C T       201, 227         Kuo, R C       204, 227         Kuo, R C       234         Kuriyama, N       Kurokawa, A         Kurz, R J       Kuz, W         Kuz, W       203         Kushida, A       Kushida, A         Kusui, J       Kutty, M G	<ul> <li>, 304</li> <li>, 264</li> <li>, 207</li> <li>, 222</li> <li>, 336</li> <li>, 431</li> <li>, 171</li> <li>, 360</li> <li>, 371</li> <li>, 424</li> <li>, 381</li> <li>, 429</li> <li>, 280</li> <li>, 247</li> <li>, 263</li> <li>, 220</li> <li>, 355</li> <li>, 233</li> <li>, 345</li> <li>, 426</li> <li>, 242</li> <li>, 314</li> <li>, 445</li> </ul>
Kudrnovsky, J       192         Kulas, M       Kulkarni, A V         Kulkarni, A V       Kumar, A         Kumar, A       Sumar, B         Kumar, R       390, 406         Kumar, R       Sumar, B         Kumar, S       225, 316         Kumosa, M       Kumosa, M         Kumta, P       Sumosa, M         Kunioshi, C T       201, 227         Kuo, R C       204, 227         Kuo, R C       201, 227         Kuo, R C       2034         Kuriyama, N       Kurokawa, A         Kurz, R J       Kurz, G         Kurz, W       203         Kushida, A       Kushida, A         Kusui, J       Kutty, M G         Kutty, M G       Kutty, T N	<ul> <li>, 304</li> <li>, 264</li> <li>, 207</li> <li>, 222</li> <li>, 336</li> <li>, 431</li> <li>, 171</li> <li>, 360</li> <li>, 371</li> <li>, 424</li> <li>, 381</li> <li>, 429</li> <li>, 280</li> <li>, 247</li> <li>, 263</li> <li>, 220</li> <li>, 355</li> <li>, 233</li> <li>, 345</li> <li>, 426</li> <li>, 242</li> <li>, 314</li> <li>, 445</li> <li>, 239</li> </ul>
Kudrnovsky, J       192         Kulas, M       Kulkarni, A V         Kulkarni, A V       Kumar, A         Kumar, A       Sumar, A         Kumar, D       Sumar, B         Kumar, S       225, 316         Kumar, S       225, 316         Kumar, S       225, 316         Kumar, S       225, 316         Kumosa, M       Kumosa, M         Kumta, P       Kumosa, M         Kunioshi, C T       Sunoshi, C T         Kuo, C       201, 227         Kuo, R C       234         Kuriyama, N       Kurokawa, A         Kurz, R J       Kurz, G         Kurz, W       203         Kushida, A       Kushida, A         Kusui, J       Kutty, M G         Kutty, T N       Kuwana, K	<ul> <li>, 304</li> <li>, 264</li> <li>, 207</li> <li>, 222</li> <li>, 336</li> <li>, 431</li> <li>, 171</li> <li>, 360</li> <li>, 371</li> <li>, 424</li> <li>, 381</li> <li>, 429</li> <li>, 280</li> <li>, 247</li> <li>, 263</li> <li>, 220</li> <li>, 355</li> <li>, 233</li> <li>, 345</li> <li>, 426</li> <li>, 242</li> <li>, 314</li> <li>, 445</li> <li>, 239</li> <li>, 218</li> </ul>
Kudrnovsky, J       192         Kulas, M       Kulkarni, A V         Kulkarni, A V       Kumar, A         Kumar, A       Sumar, A         Kumar, D       Sumar, B         Kumar, R       390, 406         Kumar, S       225, 316         Kumosa, M       Kumar, S         Kumar, S       225, 316         Kumosa, M       Kumosa, M         Kumta, P       Kumosa, M         Kunioshi, C T       201, 227         Kuo, R C       201, 227         Kuo, R C       234         Kuriyama, N       Kurokawa, A         Kurz, R J       Kurz, G         Kurz, W       203         Kushida, A       Kushida, A         Kusui, J       Kutty, M G         Kutty, M G       Kuwana, K         Kuwano, N       Kuwano, N	<ul> <li>, 304</li> <li>, 264</li> <li>, 207</li> <li>, 227</li> <li>, 322</li> <li>, 336</li> <li>, 431</li> <li>, 171</li> <li>, 360</li> <li>, 371</li> <li>, 424</li> <li>, 381</li> <li>, 429</li> <li>, 280</li> <li>, 247</li> <li>, 263</li> <li>, 220</li> <li>, 355</li> <li>, 233</li> <li>, 345</li> <li>, 426</li> <li>, 242</li> <li>, 314</li> <li>, 445</li> <li>, 239</li> <li>, 218</li> <li>, 390</li> </ul>
Kudrnovsky, J       192         Kulas, M       Kulkarni, A V         Kulkarni, A V       Kumar, A         Kumar, A       Sumar, A         Kumar, D       Sumar, B         Kumar, R       390, 406         Kumar, S       225, 316         Kumosa, M       Kumar, S         Kumar, S       225, 316         Kumosa, M       Kumosa, M         Kumta, P       Kumosa, M         Kunioshi, C T       201, 227         Kuo, R C       201, 227         Kuo, R C       234         Kuriyama, N       Kurokawa, A         Kurz, R J       Kurz, G         Kurz, W       203         Kushida, A       Kushida, A         Kusui, J       Kutty, M G         Kutty, M G       Kuwana, K         Kuwano, N       Kuwano, N	<ul> <li>, 304</li> <li>, 264</li> <li>, 207</li> <li>, 227</li> <li>, 322</li> <li>, 336</li> <li>, 431</li> <li>, 171</li> <li>, 360</li> <li>, 371</li> <li>, 424</li> <li>, 381</li> <li>, 429</li> <li>, 280</li> <li>, 247</li> <li>, 263</li> <li>, 220</li> <li>, 355</li> <li>, 233</li> <li>, 345</li> <li>, 426</li> <li>, 242</li> <li>, 314</li> <li>, 445</li> <li>, 239</li> <li>, 218</li> <li>, 390</li> </ul>
Kudrnovsky, J       192         Kulas, M       Kumar, A         Kumar, A       Kumar, A         Kumar, D       Sumar, B         Kumar, M       390, 406         Kumar, R       Sumar, S         Kumar, S       225, 316         Kumosa, M       Kumosa, M         Kumita, P       Kumosa, M         Kunosa, M       Kumosa, M         Kumta, P       201, 227         Kuo, C       201, 227         Kuo, R C       234         Kuriyama, N       Kurz, RJ         Kurz, G       Kurz, G         Kuz, W       203         Kushida, A       Kusui, J         Kusui, J       Kusui, J         Kutty, M G       Kutty, M G         Kutty, T N       Kuwana, K         Kuwano, N       Kvande, H	<ul> <li>, 304</li> <li>, 264</li> <li>, 207</li> <li>, 222</li> <li>, 336</li> <li>, 431</li> <li>, 171</li> <li>, 360</li> <li>, 371</li> <li>, 424</li> <li>, 381</li> <li>, 429</li> <li>, 280</li> <li>, 247</li> <li>, 263</li> <li>, 220</li> <li>, 355</li> <li>, 233</li> <li>, 345</li> <li>, 426</li> <li>, 242</li> <li>, 314</li> <li>, 445</li> <li>, 239</li> <li>, 218</li> <li>, 390</li> <li>, 356</li> </ul>
Kudrnovsky, J       192         Kulas, M       Kumar, A         Kumar, A       Kumar, A         Kumar, D       Sumar, B         Kumar, M       390, 406         Kumar, R       Sumar, S         Kumar, S       225, 316         Kumosa, M       Kumosa, M         Kumita, P       Sumosa, M         Kunosa, M       Kumosa, M         Kumta, P       Sumar, S         Kunosa, M       Sumar, S         Kurat, P       Sumar, S         Kurata, P       Sumar, S         Kuriyama, N       Sumar, S         Kurz, G       Sumar, S         Kurz, G       Sushida, A         Kusui, J       Sumar, S         Kusui, J       Sumar, S         Kutty, M G       Sumar, S         Kutty, T N       Suwana, K         Kuwano, N       Sumar, S         Kvande, H       Sumar, S	<ul> <li>, 304</li> <li>, 264</li> <li>, 207</li> <li>, 222</li> <li>, 336</li> <li>, 431</li> <li>, 171</li> <li>, 360</li> <li>, 371</li> <li>, 424</li> <li>, 381</li> <li>, 429</li> <li>, 280</li> <li>, 247</li> <li>, 263</li> <li>, 220</li> <li>, 355</li> <li>, 233</li> <li>, 345</li> <li>, 426</li> <li>, 242</li> <li>, 314</li> <li>, 445</li> <li>, 239</li> <li>, 218</li> <li>, 390</li> <li>, 356</li> <li>, 266</li> </ul>
Kudrnovsky, J       192         Kulas, M       Kumar, A         Kumar, A       Kumar, A         Kumar, D       Sumar, B         Kumar, M       390, 406         Kumar, R       Sumar, S         Kumar, S       225, 316         Kumosa, M       Kumosa, M         Kumita, P       Kumosa, M         Kunosa, M       Kumosa, M         Kumta, P       201, 227         Kuo, C       201, 227         Kuo, R C       234         Kuriyama, N       Kurz, RJ         Kurz, G       Kurz, G         Kuz, W       203         Kushida, A       Kusui, J         Kusui, J       Kusui, J         Kutty, M G       Kutty, M G         Kutty, T N       Kuwana, K         Kuwano, N       Kvande, H	<ul> <li>, 304</li> <li>, 264</li> <li>, 207</li> <li>, 222</li> <li>, 336</li> <li>, 431</li> <li>, 171</li> <li>, 360</li> <li>, 371</li> <li>, 424</li> <li>, 381</li> <li>, 429</li> <li>, 280</li> <li>, 247</li> <li>, 263</li> <li>, 220</li> <li>, 355</li> <li>, 233</li> <li>, 345</li> <li>, 426</li> <li>, 242</li> <li>, 314</li> <li>, 445</li> <li>, 239</li> <li>, 218</li> <li>, 390</li> <li>, 356</li> <li>, 266</li> </ul>

# L

Laberge, C	213
LaCombe, J	395
Lacroix, S	177
Ladeuille, L	202
Ladwig, P F	198
Laha, T	388
Lai, Y	357
Lakshmanan, VI 199, 244,	329
LaLonde, A	417
Lamb, J H	397
Lamérant, J	265
Lamperti, A	429
Landgraf, F J	204
Landis, C	328
Lane, J F	410
Lang, J C	250
Langdon, T G 206, 251, 253,	254,
	340,
	433
Langer, S A	406
Langlais, J	273
Lapovok, R 252, 260, 269,	333
Larocque, J E	311
Larouche, A	273
Larson, C	417
Larson, D J	198
Larson, E J	436
Lashkari, O	423
Latapie, A	301
Latour, R A	240
Latroche, M	210
Latysh, V V	259
Laughlin, D E	371
Lauridsen, E M	204
Lauro, P	416
Laux, H 179,	423
Lavernia, E J 256, 306,	352,
	449
Lavoie, C	370
Laxminarayana, P Lazarz, K A	412 287
Le Bouar, Y M 349,	
Le Boual, 1 M	390 361
Lech-Grega, M	403
Lechevalier, B	252
Lee, C	374
Lee, C P	247
Lee, C S 368,	411
Lee, C S	433
Lee, D 221, 346,	350
Lee, D L	368
Lee, D R	250
Lee, F G	212
Lee, G W	438
Lee, H 325,	442
Lee, H	389
Lee, H	454
Lee, H C	287
Lee, H M 198, 240,	286,
	200.
	280, 382
	382
Lee, I	382 382
Lee, I	382 382 416
Lee, J 382, Lee, J	382 382 416 383

Lee, J	339
Lee, J	247
Lee, J	301
Lee, J	454
Lee, J 293, 409,	447
Lee, J C	374
Lee, J G 188, 285, 286,	293
Lee, J G	287
Lee, J K	277
Lee, J W	293
Lee, K	309
Lee, K	455
Lee, K	453
Lee, K	376 350
Lee, K J 214,	350
Lee, M 214,	438
Lee, M G	438 314
Lee, P D	173
Lee, S	309
Lee, S 271, 272,	360
Lee, S	293
Lee, S	442
Lee, W	455
Lee, W 453,	454
Lee, Y	309
Lee, Y 236,	438
Lee, Y B	208
Legault-Seguin, E N	444
Lehman, L P 286, 382,	416
Lei, Y	232
Leidl, A	188
LeMay, J D	310
Lenosky, T J	183
Leo, P H	277
Leon Iriarte, J	207
Leonard, D	189
Leonard, F	276
LeSar, R A 182,	224, 407
Lesoult, G	202
Levanyuk, A P	425
Levi-Setti, R	429
Levine, L E	279
Lewandowski, J J 359,	360,
	372
Lewis, A C 234,	235
Lewis, C	443
Lewis, M	371
Lherbier, L	414
Li, B 276, 289,	414
	414 379,
Li, B	379,
Li, B Li, C	379, 446 265 432
Li, B Li, C Li, C	379, 446 265 432 203
Li, B Li, C Li, C Li, D	379, 446 265 432 203 312
Li, B Li, C Li, C Li, D Li, D	379, 446 265 432 203 312 336
Li, B Li, C Li, C Li, D Li, D Li, D	379, 446 265 432 203 312 336 237
Li, B Li, C Li, C Li, D Li, D Li, D Li, F	379, 446 265 432 203 312 336 237 243
Li, B Li, C Li, C Li, D Li, D Li, D Li, F Li, H	379, 446 265 432 203 312 336 237 243 .178
Li, B Li, C Li, C Li, D Li, D Li, D Li, F Li, H	379, 446 265 432 203 312 336 237 243 .178 .238
Li, B Li, C Li, C Li, D Li, D Li, D Li, H Li, H Li, H	379, 446 265 432 203 312 336 237 243 .178 .238 .452
Li, B Li, C Li, C Li, D Li, D Li, D Li, H Li, H Li, H Li, H Li, J	379, 446 265 432 203 312 336 237 243 .178 .238 .452 204
Li, B Li, C Li, C Li, D Li, D Li, D Li, F Li, H Li, H Li, H Li, H Li, J	379, 446 265 432 203 312 336 237 243 .178 .238 .452 204 319
Li, B Li, C Li, C Li, D Li, D Li, D Li, F Li, H Li, H Li, H Li, J Li, J	379, 446 265 432 203 312 336 237 243 .178 .238 .452 204 319 357
Li, B Li, C Li, C Li, D Li, D Li, D Li, F Li, H Li, H Li, H Li, H Li, J	379, 446 265 432 203 312 336 237 243 .178 .238 .452 204 319 357 384



Li, J		334
Li, J C 283,		342
Li, L		368
Li, M Li, N 191, 313,		288 447
Li, N 191, 515, Li, P		
Li, Q		357
Li, S		434
Li, S		374
Li, S X		247
Li, W		312
Li, W		424
Li, X		395
Li, X		262
Li, Y		402
Li, Y		383
Li, Y L	324,	426
Li, Z		268
Liang, B		332
Liang, C C		232
Liang, J		339
Liang, J		413
Liang, R		449
Liang, Y		332
Liang, Z		319
Liao, C		383 350
Liao, X		
Liaw, P K 175, 184, 208, 216, 226,	201,	202, 246,
	234, 271,	240, 296,
	342,	290, 359,
		438
Liedl, G L		377
Liedtke, A		447
Lienert, U 272,		372
Lifen, L		325
Lightle, C	172,	399
Lilleodden, E T		275
Lim, C		201
Lim, K		454
Lim, S		
Limata, L		
Lin, A		291
Lin, C		
Lin, C C		326
Lin, C H		
Lin, C		
Lin, D C		
Lin, H		
Lin, K 189,		
Lin, Q		
Lin, T	326,	337
Lin, W		455
Lin, Y		449
Lin, Y H	332,	338
Lin, Y L		338
Lincoln, J D		326
Lindley, T C		173
Ling, Y		
Lisovskyy, I P		180
Litovchenko, I		257
Little, A L		297
Littleton, H E		428
Liu, B		319 372
L10, C		514

Liu, C T 175, 269, 271,	402
Liu, C Y 294, 332,	375
Liu, H	345
Liu, H	284
Liu, H	443
Liu, H 199,	321
Liu, H J	195
Liu, H K	354
Liu, J	374
Liu, J	292
Liu, N	416
Liu, S	446
Liu, S 299,	300
Liu, S	379
Liu, S	319
Liu, T	374
Liu, W 279,	324
Liu, W J	233
Liu, X J	191
Liu, Y	428
Liu, Y	268
Liu, Y	357
Liu, Y H	421
	269
Liu, Z 181, 192, 194, 221, 277, 294, 305, 322,	349
	445
Liu, Z	304
Liu, Z	313
Liu, Z	421
Livneh, T	395
Lloyd, D J	303
Llubani, S	
Lo, C	
Lo, C C	
Lo, T	337
Loan, M 171,	311
Lofland, S E	291
Loiseau, A	
Lokshin, R G	267
Lomas, R	
Longo, F G	
-	
Looij, J	
Loomis, E	
Lopasso, E	348
Lopez, M F	233
Lorimer, G W 294,	295
Lou, J 261, 308,	377
	225
Louchet, F H	278
Louchet, F H 224,	200
Louchet, F H	399
Louchet, F H 224, Loutfy, R O 224, Love, R	257
Louchet, F H	
Louchet, F H 224, Loutfy, R O 224, Love, R	257 432
Louchet, F H	257 432 441
Louchet, F H	257 432 441 288
Louchet, F H	257 432 441 288 294
Louchet, F H	257 432 441 288 294 428
Louchet, F H	257 432 441 288 294 428 416
Louchet, F H Loutfy, R O	257 432 441 288 294 428 416 411
Louchet, F H Loutfy, R O	257 432 441 288 294 428 416
Louchet, F H Loutfy, R O	257 432 441 288 294 428 416 411
Louchet, F H Loutfy, R O	257 432 441 288 294 428 416 411 332 343
Louchet, F H Loutfy, R O	257 432 441 288 294 428 416 411 332 343 232
Louchet, F H Loutfy, R O	257 432 441 288 294 428 416 411 332 343 232 440
Louchet, F H	257 432 441 288 294 428 416 411 332 343 232 440 409
Louchet, F H Loutfy, R O	257 432 441 288 294 428 416 411 332 343 232 440 409 411
Louchet, F H	257 432 441 288 294 428 416 411 332 343 232 440 409 411 265
Louchet, F H	257 432 441 288 294 428 416 411 332 343 232 440 409 411 265 175
Louchet, F H	257 432 441 288 294 428 416 411 332 343 232 440 409 411 265 175

Lubarda, V A Lubecka, M	366 321
Lucadamo, G A 308,	347
Lucas, J P 188,	285,
	394
Luckey, S G 397,	398
Ludwig, A 178, 247, 386,	423
Ludwig, L	395
Ludwig, O	218
Ludwig, W	411
Lue, M	242
Lui, T 332,	337
Luis Pérez, C J 207,	258
Lukac, P D	425
Lukashchuk, Y V	256
Lukyanov, I V	312
Lund, A C 234, 236,	317
Luo, A A 191, 233,	287,
	444
Luo, W C 199,	374
Luo, Z 207, 257,	350
Lupulescu, A 248,	409
Lynch, F E	210
Lynn, K	380
Lyon, P	445
Lysczek, E M	198
•	

# Μ

Ma, B M	238
Ma, D	345
Ma, E 176, 305,	391
Ma, H	176
Ma, N	249
Ma, P X	292
Ma, R 313,	332
Ma, S 279,	283
Ma, T	331
Ma, Y	195
Ma, Y	250
Ma, Z Y	311
MacDonald, B	446
MacKay, R A 322,	364
Mackenzie, J M	444
Mackowiak, V	447
MacLaren, I	307
Madenci, E	229
Madshus, S	218
Maeland, A J	353
Magadi, G	248
Magee, T J 230,	329
Magnusson, J H	361
Mahajan, S	193
Mahalingam, T	241
Mahapatra, S P 171,	368
Mahato, C	428
Mahoney, M	226
Maier, H J 257, 302, Maijer, D M 173, 195,	341
Maijer, D M 173, 195,	386
Majetich, S	336
Majkrzak, C F	210
Majumdar, B S 187, 188,	229,
	371
Majzoub, E H 263, 430,	436
Makhlouf, M M 343, 376,	409
Maki, T	282
Maksymowicz, L J	321

Maksyutov, A F	270
Maland, G	318
Malgin, D	256
Mallick, P K	288
Mandal, P	215
Mani, A S	196
Manias, E Manickam, K	424
Maniruzzaman, M 404,	236
Mann, A B	423 197
Mann, V C	267
Manning, C	366
Mannweiler, U	360
Manohar, P A	180
Mantese, J V	426
Mara, N A 317,	432
Marcus, H L	451
Margulies, L 302,	372
Marian, J	183
Marks, J	399
Marks, R A 229,	342
Marshall, D	284
Martchek, K 244,	398
Martens, R L	
Martin, C	
Martin, C	
Martin, E S	266
Martin, G	
Martin, J 177, 218,	272,
	439
Martin, J J	338
Martin, P L 182,	357
Martinent, V	265
Martinez, H	326
Martinez, J V	435
Martinez, R A	202
Martocci, A	436
Maruyama, K	384
Marvin, J	328
Marzari, N	304
Mason, D E	431
Mason, P G 328,	443
Mason, T A 303,	451
Massalski, T B	371
Mast, D	238
Masuda, C 255,	393
Masumura, R A	302
Mathaudhu, S N 216, 259,	341
Mathier, V	
Mathis, A	361
Mathisen, S T	172
Matson, D M 246, 289,	299
Matsuda, T	397
Matsumoto, A	326
Matsuoka, R	449
Matthews, S R	
Matyas, A	330
Maurice, C	250
Maxey, E	297
Mayer, R	411
Mayer, T M	
Mayeaux, B	
Maziarz, W	321
Mazuelas, A	250
Mazumder, J	192
Mazunov, D O	180
Mazzei, Â C	368

McBow, I	185
McCabe, R J 306,	324
McCall, L	441
McCallum, W	296
McClellan, K J	201
McClung, M 213,	399
McComas, E	370
McConaghy, E	
McCord, M G 197, McCoy, R A	447 374
McCrabb, L C	443
McCune, R C 191,	288
McDanels, S	
McDanice, R	202
McDaniels, R L	226
McDonald, M	420
McDonald, N J	300
McDonald, R G	284
McDonald, S D	343
McDougall, J L McDowell, D L	367 289
McFadden, G B 276,	322
McGarrity, E	391
McIntyre, H R	343
McKamey, C G	269
МсКау, В Ј	344
McKay, J	378
McKean, B	
McKenzie, P	
McKillip, J L	381
McLean, A McLean, W	417 310
McNelley, T R 252, 264,	349
10101 (cilcy, 1 it 252, 20-,	
McNerny, C	421 302
	421
McNerny, C	421 302
McNerny, C	421 302 195 300 347
McNerny, C           McQueen, H J         201,           Meade, D	421 302 195 300 347 318
McNerny, C         201,           McQueen, H J         201,           Meade, D	421 302 195 300 347 318 341
McNerny, C         201,           McQueen, H J         201,           Meade, D	421 302 195 300 347 318 341 437
McNerny, C         201,           McQueen, H J         201,           Meade, D	421 302 195 300 347 318 341 437 377
McNerny, C           McQueen, H J         201,           Meade, D	421 302 195 300 347 318 341 437 377 421
McNerny, C           McQueen, H J         201,           Meade, D         201,           Meco, H         308,           Medlin, D L         308,           Meek, T T         299,           Meeks, H S         400,           Mehl, M J         400,           Mehrotra, P         400,           Meier, M         176,	421 302 195 300 347 318 341 437 377
McNerny, C           McQueen, H J         201,           Meade, D	421 302 195 300 347 318 341 437 377 421 217,
McNerny, C         McQueen, H J       201,         Meade, D       201,         Meco, H       308,         Medk, T T       299,         Meeks, H S       299,         Meehl, M J       Mehl, M J         Mehrotra, P       176,         Meier, M H       272, 317,         Meinke, J H       Melcher, S	421 302 195 300 347 318 341 437 377 421 217, 360
McNerny, C         McQueen, H J       201,         Meade, D       201,         Medo, H       308,         Medin, D L       308,         Meek, T T       299,         Meeks, H S       299,         Mehl, M J       100,         Mehrotra, P       176,         Meier, M       176,         Melcher, S       176,         Melssari, B       100,	421 302 195 300 347 318 341 437 377 421 217, 360 391
McNerny, C         McQueen, H J       201,         Meade, D	421 302 195 300 347 318 341 437 377 421 217, 360 391 239 447 317
McNerny, C         McQueen, H J       201,         Meade, D	421 302 195 300 347 318 341 437 377 421 217, 360 391 239 447 317 223
McNerny, C         McQueen, H J       201,         Meade, D	421 302 195 300 347 318 341 437 377 421 217, 360 391 239 447 317 223 357
McNerny, C         McQueen, H J       201,         Meade, D	421 302 195 300 347 318 341 437 377 421 217, 360 391 239 447 317 223 357 322
McNerny, C         McQueen, H J       201,         Meade, D	421 302 195 300 347 318 341 437 377 421 217, 360 391 239 447 317 223 357 322 221
McNerny, C         McQueen, H J       201,         Meade, D	421 302 195 300 347 318 341 437 377 421 217, 360 391 239 447 317 223 357 322 221 203
McNerny, C         McQueen, H J       201,         Meade, D	421 302 195 300 347 318 341 437 377 421 217, 360 391 239 447 317 223 357 322 221
McNerny, C         McQueen, H J       201,         Meade, D	421 302 195 300 347 318 341 437 377 421 217, 360 391 239 447 317 223 357 322 221 203 436
McNerny, C         McQueen, H J       201,         Meade, D	421 302 195 300 347 318 341 437 377 421 217, 360 391 239 447 317 223 357 322 221 203 436 357
McNerny, C         McQueen, H J       201,         Meade, D	421 302 195 300 347 318 341 437 377 421 217, 360 391 239 447 317 223 357 322 221 203 436 357 270 271 180
McNerny, C         McQueen, H J       201,         Meade, D	421 302 195 300 347 318 341 437 377 421 217, 360 391 239 447 317 223 357 322 221 203 436 357 270 271 180 191
McNerny, C         McQueen, H J       201,         Meade, D	421 302 195 300 347 318 341 437 377 421 217, 360 391 239 447 317 223 357 322 221 203 436 357 270 271 180 191 245
McNerny, C         McQueen, H J       201,         Meade, D	421 302 195 300 347 318 341 437 377 421 217, 360 391 239 447 317 223 357 322 221 203 436 357 270 271 180 191 245 424
McNerny, C         McQueen, H J       201,         Meade, D       308,         Medin, D L       308,         Meek, T T       299,         Meeks, H S       Megahed, M M         Mehl, M J       Mehrotra, P         Meier, M       176,         272, 317,       Meiker, S         Melher, S       Meloher, S         Mello, J M       222,         Mendiratta, M G       174,         Meng, D       Meng, 248,         Meng, J       Menon, S K         Menon, S K       174,         Menzel, B       Mercer, C         Merfeld, D       Messersmith, P B         Messersmith, P B       265,	421 302 195 300 347 318 341 437 377 421 217, 360 391 239 447 317 223 357 322 221 203 436 357 270 271 180 191 245 424 399
McNerny, C         McQueen, H J       201,         Meade, D       308,         Medin, D L       308,         Meek, T T       299,         Meeks, H S       99,         Meehl, M J       90,         Mehrotra, P       90,         Meier, M       176,         272, 317,       91,         Melcher, S       90,         Melissari, B       91,         Mello, J M       222,         Mendiratta, M G       174,         Mendoza, R       248,         Meng, D       90,         Meng, J       90,         Mengel, J       90,         Menon, S K       174,         Menzel, B       90,         Merfeld, D       90,         Mesina, M       90,         Messersmith, P B       90,         Metson, J B       265, <td>421 302 195 300 347 318 341 437 377 421 217, 360 391 239 447 317 223 357 322 221 203 436 357 270 271 180 191 245 424 399 250</td>	421 302 195 300 347 318 341 437 377 421 217, 360 391 239 447 317 223 357 322 221 203 436 357 270 271 180 191 245 424 399 250
McNerny, C         McQueen, H J       201,         Meade, D	421 302 195 300 347 318 341 437 377 421 217, 360 391 239 447 317 223 357 322 221 203 436 357 270 271 180 191 245 424 399 250 381
McNerny, C         McQueen, H J       201,         Meade, D       308,         Medin, D L       308,         Meek, T T       299,         Meeks, H S       99,         Meehl, M J       90,         Mehrotra, P       90,         Meier, M       176,         272, 317,       91,         Melcher, S       90,         Melissari, B       91,         Mello, J M       222,         Mendiratta, M G       174,         Mendoza, R       248,         Meng, D       90,         Meng, J       90,         Mengel, J       90,         Menon, S K       174,         Menzel, B       90,         Merfeld, D       90,         Mesina, M       90,         Messersmith, P B       90,         Metson, J B       265, <td>421 302 195 300 347 318 341 437 377 421 217, 360 391 239 447 317 223 357 322 221 203 436 357 270 271 180 191 245 424 399 250 381 385</td>	421 302 195 300 347 318 341 437 377 421 217, 360 391 239 447 317 223 357 322 221 203 436 357 270 271 180 191 245 424 399 250 381 385

Michael, N L	221
Middleton, W J	189
Migchielsen, J	
Mihalkovic, M	431
Mikula, A	
Miles, M P	
Militzer, M 268,	405
Miller, G	443
Miller, G 329,	230
Miller, M	329
Miller, M K 402,	408
Miller, M P	235
Mills, M J 183,	309,
	407
Minamino, Y 259, 351,	388
Mineta, K	449
Minisandram, R S 219,	220
Minor, A 275,	352
Minor, A M	
Mintz, M H	
Miodownik, M A	181
Miracle, D 175,	402
Mirchi, A A 176,	217,
	360
Mirpuri, K	
Mishima, Y 174, 199, 215,	269,
	435
Mishin, Y 222, 346,	377
Mishra, B 193,	199,
	244
Mishra, C R	
Mishra, N C	
Mishra, R K 207, 211,	347 264,
MISHTA, K S 207, 211,	264
210 211 255	
	397
Misra, A 261, 302, 324,	397 408
Misra, A 261, 302, 324, Misra, D K	397 408 302
Misra, A 261, 302, 324, Misra, D K Mistree, F	397 408 302 289
Misra, A	<ul><li>397</li><li>408</li><li>302</li><li>289</li><li>408</li></ul>
Misra, A	<ul> <li>397</li> <li>408</li> <li>302</li> <li>289</li> <li>408</li> <li>408</li> </ul>
Misra, A	<ul> <li>397</li> <li>408</li> <li>302</li> <li>289</li> <li>408</li> <li>408</li> <li>359</li> </ul>
Misra, A	<ul> <li>397</li> <li>408</li> <li>302</li> <li>289</li> <li>408</li> <li>408</li> <li>359</li> <li>424</li> </ul>
Misra, A       261, 302, 324,         Misra, D K	397 408 302 289 408 408 359 424 340
Misra, A       261, 302, 324,         Misra, D K	<ul> <li>397</li> <li>408</li> <li>302</li> <li>289</li> <li>408</li> <li>408</li> <li>359</li> <li>424</li> <li>340</li> <li>253</li> </ul>
Misra, A       261, 302, 324,         Misra, D K       Mistree, F         Mitchell, T E       324,         Mitlin, D       Miura, S         Miura, S       Miura, Y         Miyahara, Y       Miyamoto, H         Mizutani, Y       Mizutani, Y	<ul> <li>397</li> <li>408</li> <li>302</li> <li>289</li> <li>408</li> <li>408</li> <li>359</li> <li>424</li> <li>340</li> <li>253</li> <li>300</li> </ul>
Misra, A       261, 302, 324,         Misra, D K	<ul> <li>397</li> <li>408</li> <li>302</li> <li>289</li> <li>408</li> <li>408</li> <li>359</li> <li>424</li> <li>340</li> <li>253</li> <li>300</li> <li>385</li> </ul>
Misra, A       261, 302, 324,         Misra, D K	<ul> <li>397</li> <li>408</li> <li>302</li> <li>289</li> <li>408</li> <li>408</li> <li>359</li> <li>424</li> <li>340</li> <li>253</li> <li>300</li> <li>385</li> <li>242</li> </ul>
Misra, A       261, 302, 324,         Misra, D K	<ul> <li>397</li> <li>408</li> <li>302</li> <li>289</li> <li>408</li> <li>408</li> <li>359</li> <li>424</li> <li>340</li> <li>253</li> <li>300</li> <li>385</li> <li>242</li> <li>280</li> </ul>
Misra, A       261, 302, 324,         Misra, D K       Mistree, F         Mitchell, T E       324,         Mitlin, D       Miura, S         Miura, S       Miura, Y         Miyahara, Y       Miyamoto, H         Mizutani, Y       Mo, A         Mobasher, A       Moffat, T P         Mohamed, F A       391,	<ul> <li>397</li> <li>408</li> <li>302</li> <li>289</li> <li>408</li> <li>408</li> <li>359</li> <li>424</li> <li>340</li> <li>253</li> <li>300</li> <li>385</li> <li>242</li> <li>280</li> <li>392</li> </ul>
Misra, A	<ul> <li>397</li> <li>408</li> <li>302</li> <li>289</li> <li>408</li> <li>408</li> <li>359</li> <li>424</li> <li>340</li> <li>253</li> <li>300</li> <li>385</li> <li>242</li> <li>280</li> <li>392</li> <li>437</li> </ul>
Misra, A       261, 302, 324,         Misra, D K       Mistree, F         Mitchell, T E       324,         Mitlin, D       Miura, S         Miura, S       Miura, Y         Miyahara, Y       Miyamoto, H         Mizutani, Y       Mobasher, A         Moffat, T P       220,         Mohamed, F A       391,         Mohanty, P S       S	<ul> <li>397</li> <li>408</li> <li>302</li> <li>289</li> <li>408</li> <li>408</li> <li>359</li> <li>424</li> <li>340</li> <li>253</li> <li>300</li> <li>385</li> <li>242</li> <li>280</li> <li>392</li> <li>437</li> <li>288</li> </ul>
Misra, A       261, 302, 324,         Misra, D K       Mistree, F         Mitchell, T E       324,         Mitlin, D       Miura, S         Miura, S       Miura, Y         Miyahara, Y       Miyamoto, H         Mizutani, Y       Mobasher, A         Moffat, T P       220,         Mohamed, F A       391,         Mohanty, P S       198,	397 408 302 289 408 408 359 424 340 253 300 385 242 280 392 437 288 240,
Misra, A       261, 302, 324,         Misra, D K       Mistree, F         Mitchell, T E       324,         Mitlin, D       Miura, S         Miura, S       Miura, Y         Miyahara, Y       Miyamoto, H         Mobasher, A       Moffat, T P         Mohamed, F A       391,         Mohamed, S A       Mohanty, P S         Mohney, S E       198,	397 408 302 289 408 408 359 424 340 253 300 385 242 280 392 437 288 240, 382
Misra, A       261, 302, 324,         Misra, D K       Mistree, F         Mitchell, T E       324,         Mitlin, D       Miura, S         Miura, S       Miura, Y         Miyahara, Y       Miyamoto, H         Mobasher, A       Moffat, T P         Mohamed, F A       391,         Mohamed, S A       Mohanty, P S         Mohney, S E       198,	397 408 302 289 408 408 359 424 340 253 300 385 242 280 392 437 288 240, 382 431
Misra, A       261, 302, 324,         Misra, D K       Mistree, F         Mitchell, T E       324,         Mitlin, D       Miura, S         Miura, S       Miura, Y         Miyahara, Y       Miyamoto, H         Mizutani, Y       Mobasher, A         Moffat, T P       220,         Mohamed, F A       391,         Mohamed, S A       Mohanty, P S         Mohney, S E       198,	397 408 302 289 408 408 359 424 340 253 300 385 242 280 392 437 288 240, 382 431
Misra, A	397 408 302 289 408 408 359 424 340 253 300 385 242 280 392 437 288 240, 382 431 203
Misra, A	397 408 302 289 408 359 424 340 253 300 385 242 280 392 437 288 240, 382 431 203 290
Misra, A	397 408 302 289 408 408 359 424 340 253 300 385 242 280 392 437 288 240, 382 431 203 290 188 228
Misra, A	397 408 302 289 408 408 359 424 340 253 300 385 242 280 392 437 288 240, 382 431 203 290 188 228 197
Misra, A	397 408 302 289 408 408 359 424 340 253 300 385 242 280 392 437 288 240, 382 431 203 290 188 228 197
Misra, A	<ul> <li>397</li> <li>408</li> <li>302</li> <li>289</li> <li>408</li> <li>359</li> <li>424</li> <li>340</li> <li>253</li> <li>300</li> <li>385</li> <li>242</li> <li>280</li> <li>392</li> <li>437</li> <li>288</li> <li>240,</li> <li>382</li> <li>431</li> <li>203</li> <li>290</li> <li>188</li> <li>228</li> <li>197</li> <li>454</li> </ul>
Misra, A	397 408 302 289 408 408 359 424 340 253 300 385 242 280 392 437 288 240, 382 431 203 290 188 228 197 454 398
Misra, A	397 408 302 289 408 408 359 424 340 253 300 385 242 280 392 437 288 240, 382 431 203 290 188 228 197 454 398 364,
Misra, A       261, 302, 324,         Misra, D K       Mistree, F         Mitchell, T E       324,         Mitlin, D       Miura, S         Miura, S       Miura, Y         Miyahara, Y       Miyamoto, H         Mizutani, Y       Mobasher, A         Moffat, T P       220,         Mohamed, F A       391,         Mohaned, S A       391,         Mohaned, S A       293, 338,         Mohri, T       304, 359, 389,         Mokadem, S       Monlevade, E F         Monteiro-Riviere, N       Montejano, S         Montgomery, G P       397,         Montgomery, J S       278,	397 408 302 289 408 408 359 424 340 253 300 385 242 280 392 437 288 240, 382 431 203 290 188 228 197 454 398 364, 440
Misra, A	397 408 302 289 408 359 424 340 253 300 385 242 280 392 437 288 240, 382 431 203 290 188 228 197 454 398 364, 440 252 262,
Misra, A       261, 302, 324,         Misra, D K       Mistree, F         Mitchell, T E       324,         Mitlin, D       Miura, S         Miura, S       Miura, Y         Miyahara, Y       Miyamoto, H         Mizutani, Y       Mo, A         Moffat, T P       220,         Mohamed, F A       391,         Mohamed, S A       391,         Mohaney, S E       198,	397 408 302 289 408 359 424 340 253 300 385 242 280 392 437 288 240, 382 431 203 290 188 228 197 454 398 364, 440 252 262, 418

Moore, J F	429
Morales, A T	211
Morando, C N	450
Moraru, A 173,	437
Mordike, B	383
More, K L	215
Morgan, D 205,	289
Morgan, J K	441
Mori, H	301
Mori, T	
Morin, G	
Morishita, M	427
Moriyama, K	
Morral, J E 174,	322
Morris, J G 249,	314
Morris, J R 222, 316, 317,	365
Morris, J W 275, 283,	331
Morrison, M L 271,	359
Morrow, A	415
Morsi, K B 242, 295,	340
Mortensen, D	
Mosher, J	
Moss, S C	250
Mostovoy, S	237
Mota, G E 172,	213
Motahari, S	328
Motoyasu, G	
Moura, R R	
Mourou, G	345
Moxson, V 278, 364, 365,	440
Mucciardi, F 278, 304, 305,	
	380
Muddle, B 371,	415
Mueller-Krumbhaar, H	
Muhlstein, C L	
Muir, D M	284
Mukherjee, A 317, 355,	432
Mukhopadhyay, A 362,	404
Mukhopadhyay, G	194
Mukhopadhyay, P	194
	346,
Mukhopadhyay, S M 301,	450
Mulholland, M	356
Muller, K	
Müller, S	181
Muncy, M	
Mungsantisuk, P 396,	397
Munitz, A 287,	418
Murali, K	397
Murayama, N 426,	427
Murphy, C J	395
Murphy, K	
Murr, L E 192, 279, 395,	
Murray, J	441
	441
Murray, J A	277
	277 188
Murti, V S	277 188 413
Murty, K L 201, 246,	277 188 413 256,
Murty, K L 201, 246,	277 188 413 256, 379
Murty, K L 201, 246, 	277 188 413 256, 379 311
Murty, K L 201, 246,	277 188 413 256, 379 311
Murty, K L 201, 246, 	277 188 413 256, 379 311

# Ν

Na, K	236
Nafisi, S 423,	439
Nagano, T	186
Nagasawa, Y	390
Nah, J	294

Naik, R R	291
Nakagawa, Y	401
Nakamori, Y	263
Nakamura, H	401
Nakamura, N	384
Nakamura, Y	210
Nakano, T	390
Nakano, T	300
Nakayama, K	427
Nam, S	281
Nam, W J	208
Nandy, T	270
Napolitano, R 300, 343, Narayan, J 291, 334,	427
Narayan, J 291, 334,	336
Narayan, R J 197, 239, 291,	337,
	451
Nardi, P	352
Narita, H	449
Narvekar, R N	217
Nash, P 237,	314
Nastac, L 178, 219,	220,
	404
Nastasi, M 302,	408
Navarra, P	380
Nayak, S	334
Nazarov, A A	252
Necker, C T	249
Nedkova, T	184
Needleman, A	377
Neelameggham, R	332
Neilsen, M K	230
Neitzel, G P	404
Nendick, R M	189
Nenkov, K	239
Nerikar, P	302
Nes, E	351
Neudorf, D A 189,	443
Neuschutz, D Ng, K W	404 333
Ngoh, S L	
Nguyen, V	
Ni, H	254
Nibur, K A	224
Nicholson, B K	406
Nicholson, D 359,	431
Nicol, M J	443
Nie, J 187, 228, 294,	295,
	445
Nieh, T G	438
Nielsen, M C	179
Niemczura, W	263
Nienow, A W	318
Nieves, J	291
Nigam, A K	196
Nikandrov, K P	267
Nikoloski, A N	
Nishimura, T	
Nishio, T	
Nishiyama, K	227
Nix, W D 261,	309
Nizovtsev, P N	259
Noakes, R	
Nobile, A	253
Noebe, R D	
Nogita, K	
Noguez, M E	
Norfleet, D M	352

Noronha, S	224
Northwood, D	
Notis, M R 189, 198, 231,	232,
	331,
	416
Novichkov, S B	245
Novotnak, D	414
Nowak, R	177
Noyan, I C	416
Ntakaburimvo, N	178
Nunomura, Y	174
Nurminen, E	186
Nyberg, E	287

# 

O'Brien, J M	257
O'Callaghan, J F	373
Ochoa, F A	331
Oda, T	
	323
Oda, Y	407
Oertel, C	
Ogata, S	
Oh, B	337
Oh, K	383
Oh, K H	283
Oh, S	382
Oh-ishi, K 252, 264,	433
Ohkubo, C	407
Ohkubo, K	359
Ohmori, T	242
Ohnaka, I	
Ohno, M 389,	431
Ohnuma, I	
Okabe, T 366, 407,	449
Okamura, Y	206
Okane, T	299
Okazaki, K	434
Okuno, O	407
Olevsky, E A	242
Olivares, R	440
Oliveira, T	252
Oliver, E C	
Oliver, S R 275,	321
Oliver, W C	308
Olson, D L 192, Olson, G B 192,	210
	358,
	425
Olson, J D	198
Olsvik, A	272
Oltman, E	
Omanovic, S	280
Omran, A M	403
Onderka, B	240
Ooij, W V	238
Oona, H	436
Oosterkamp, L D	191
Oppenheimer, S M	340
Opsahl, T	398
Orimo, S	396
Orlov, D 208, 255,	
Orlova, T S 208, 253, 252,	260
	258
Orth, A	330
Ortiz, A L	346
Ortiz, M	365
Osada, K	211
Osamura, K	314

Osborne, G E	421
Osborne, R C 188, 230,	231
Osetsky, Y N 183, 184, 224,	226
Oshinowo, L 285, 362,	424
Ossi, P M	429
Österle, W	367
Oswald, K	218
Otto, F	425
Ou, S	
Ouimet, L J	191
Ovcharenko, V I	280
Overfelt, R A 375,	450
Oyama, Y	200
Øye, H 176,	218
Oygard, A	318
Ozaki, K 226,	326
Ozcan, A	370
Ozolins, V 263, 305,	430

# P

Padhi, B	368
Paglieri, S N 353,	436
Paik, J	241
Paik, K 294,	339
Pal, U B 280, 325, 366,	409
Palacio, H A 300,	450
Palenik, B P	291
Palumbo, G	308
Pan, D	232
Pan, D 229, 286,	342
Pan, M X	217
Pan, T	191
Panaitescu, A 173,	437
Panaitescu, I 173,	437
Pande, C S 246, 302,	435
Pandya, D K	239
Pang, J H 286, 338,	339
Pang, J W 279,	324
Pang, Y 278,	406
Panov, A V	312
Pant, B B	198
Pao, P S	392
Papaconstantopoulos, D A	377
Papadimitrakopoulos, F	451
Papangelakis, V G	284
Parent, L	361
Paretsky, V M 185,	186,
	449
Parikh, A N	447
Parish, C	395
Parisi, A	387
Park, C	455
Park, C	229
Park, E S	217
Park, H	236
Park, H	241
Park, J	339
Park, J	203
Park, J	452
Park, J I	442
	454
Park, J S 453.	
Park, J S 453, Park, J S	411
Park, J S	411
Park, J S	
Park, J S Park, K S Park, K T	368 349
Park, J S	

Park, S	453
Park, S	455
Park, S S	287
Park, Y	
Parkes, R C	286
Parkin, S	290
Paromova, I V	312
Parrish, E	238
Parsell, D E	359
Parsey, J M 193,	235
Parthasarathy, T A 174,	357
Paserin, V	355
Pasturel, A	390
Patankar, S V	
Patel, A D 219,	220
Patel, J	394
Patel, M K 362,	404
Patino, E	378
Pattabiraman, R	236
Pattanaik, G R 239,	291
Patterson, E	399
Patti, A	380
Patzelt, N	330
Paulsen, K	172
Pavio, J	235
Pawaskar, D N	406
Pawlek, R P	313
Paxton, D M	235
Payzant, E A 176, 256,	392
Pecharsky, V K 263,	396
Pedersen, R	272
Peker, A 271,	359
Pekguleryuz, M O	444
Pelletier, J	438
Pellin, M J	429
Pena, J S	320
Peng, H	238
	434
Peng, L	
Peralta, P D 201, 342,	411
Percheron-Guégan, A 210,	262
Pereloma, E V	254
	254
Perenezko I.H. 215 241 253	
Perepezko, J H 215, 241, 253,	344
Perez-Prado, M	344 433
Perez-Prado, M Perruchoud, R C	344 433 360
Perez-Prado, M	344 433
Perez-Prado, M Perruchoud, R C Perry, T	344 433 360 413
Perez-Prado, M Perruchoud, R C Perry, T Peter, W	344 433 360 413 359
Perez-Prado, M Perruchoud, R C Perry, T Peter, W 271, Peterson, L	344 433 360 413 359 204
Perez-Prado, M Perruchoud, R C Perry, T Peter, W 271, Peterson, L Peterson, R 244,	<ul> <li>344</li> <li>433</li> <li>360</li> <li>413</li> <li>359</li> <li>204</li> <li>266</li> </ul>
Perez-Prado, M           Perruchoud, R C           Perry, T           Peter, W           271,           Peterson, L           Peterson, R           244,           Petit, P	<ul> <li>344</li> <li>433</li> <li>360</li> <li>413</li> <li>359</li> <li>204</li> <li>266</li> <li>358</li> </ul>
Perez-Prado, M Perruchoud, R C Perry, T Peter, W 271, Peterson, L Peterson, R 244, Petit, P Petraroli, M	<ul> <li>344</li> <li>433</li> <li>360</li> <li>413</li> <li>359</li> <li>204</li> <li>266</li> </ul>
Perez-Prado, M           Perruchoud, R C           Perry, T           Peter, W           271,           Peterson, L           Peterson, R           244,           Petit, P	<ul> <li>344</li> <li>433</li> <li>360</li> <li>413</li> <li>359</li> <li>204</li> <li>266</li> <li>358</li> </ul>
Perez-Prado, M Perruchoud, R C Perry, T Peter, W 271, Peterson, L Peterson, R 244, Petit, P Petraroli, M Petricca, S	<ul> <li>344</li> <li>433</li> <li>360</li> <li>413</li> <li>359</li> <li>204</li> <li>266</li> <li>358</li> <li>190</li> <li>381</li> </ul>
Perez-Prado, M Perruchoud, R C Perry, T Peter, W	<ul> <li>344</li> <li>433</li> <li>360</li> <li>413</li> <li>359</li> <li>204</li> <li>266</li> <li>358</li> <li>190</li> <li>381</li> <li>275</li> </ul>
Perez-Prado, M Perruchoud, R C Perry, T Peter, W	344 433 360 413 359 204 266 358 190 381 275 264
Perez-Prado, M Perruchoud, R C Perry, T Peter, W	<ul> <li>344</li> <li>433</li> <li>360</li> <li>413</li> <li>359</li> <li>204</li> <li>266</li> <li>358</li> <li>190</li> <li>381</li> <li>275</li> <li>264</li> <li>444</li> </ul>
Perez-Prado, M Perruchoud, R C Perry, T Peter, W	344 433 360 413 359 204 266 358 190 381 275 264
Perez-Prado, M Perruchoud, R C Perry, T Peter, W	<ul> <li>344</li> <li>433</li> <li>360</li> <li>413</li> <li>359</li> <li>204</li> <li>266</li> <li>358</li> <li>190</li> <li>381</li> <li>275</li> <li>264</li> <li>444</li> </ul>
Perez-Prado, M Perruchoud, R C Petry, T Peter, W	<ul> <li>344</li> <li>433</li> <li>360</li> <li>413</li> <li>359</li> <li>204</li> <li>266</li> <li>358</li> <li>190</li> <li>381</li> <li>275</li> <li>264</li> <li>444</li> <li>348</li> <li>401</li> </ul>
Perez-Prado, M Perruchoud, R C Petry, T Peter, W	<ul> <li>344</li> <li>433</li> <li>360</li> <li>413</li> <li>359</li> <li>204</li> <li>266</li> <li>358</li> <li>190</li> <li>381</li> <li>275</li> <li>264</li> <li>444</li> <li>348</li> <li>401</li> <li>219</li> </ul>
Perez-Prado, M Perruchoud, R C Petry, T Peter, W	<ul> <li>344</li> <li>433</li> <li>360</li> <li>413</li> <li>359</li> <li>204</li> <li>266</li> <li>358</li> <li>190</li> <li>381</li> <li>275</li> <li>264</li> <li>444</li> <li>348</li> <li>401</li> <li>219</li> <li>171</li> </ul>
Perez-Prado, M Perruchoud, R C Perry, T Peter, W	<ul> <li>344</li> <li>433</li> <li>360</li> <li>413</li> <li>359</li> <li>204</li> <li>266</li> <li>358</li> <li>190</li> <li>381</li> <li>275</li> <li>264</li> <li>444</li> <li>348</li> <li>401</li> <li>219</li> <li>171</li> <li>222</li> </ul>
Perez-Prado, M Perruchoud, R C Petry, T Peter, W	<ul> <li>344</li> <li>433</li> <li>360</li> <li>413</li> <li>359</li> <li>204</li> <li>266</li> <li>358</li> <li>190</li> <li>381</li> <li>275</li> <li>264</li> <li>444</li> <li>348</li> <li>401</li> <li>219</li> <li>171</li> <li>222</li> </ul>
Perez-Prado, M Perruchoud, R C Perry, T Peter, W	<ul> <li>344</li> <li>433</li> <li>360</li> <li>413</li> <li>359</li> <li>204</li> <li>266</li> <li>358</li> <li>190</li> <li>381</li> <li>275</li> <li>264</li> <li>444</li> <li>348</li> <li>401</li> <li>219</li> <li>171</li> <li>222</li> </ul>
Perez-Prado, M Perruchoud, R C Perry, T Peter, W	<ul> <li>344</li> <li>433</li> <li>360</li> <li>413</li> <li>359</li> <li>204</li> <li>266</li> <li>358</li> <li>190</li> <li>381</li> <li>275</li> <li>264</li> <li>444</li> <li>348</li> <li>401</li> <li>219</li> <li>171</li> <li>222</li> <li>418</li> <li>345</li> </ul>
Perez-Prado, MPerruchoud, R CPerry, TPeter, W271,Peterson, LPeterson, R244,Petir, PPetraroli, MPetrova, R SPetrova, R SPettengill, E CPettersen, KPettifor, D GPharr, G M372,Phillion, APhillips, E CPhillpot, S RPiascik, RPickens, J R223,	<ul> <li>344</li> <li>433</li> <li>360</li> <li>413</li> <li>359</li> <li>204</li> <li>266</li> <li>358</li> <li>190</li> <li>381</li> <li>275</li> <li>264</li> <li>444</li> <li>348</li> <li>401</li> <li>219</li> <li>171</li> <li>222</li> <li>418</li> <li>345</li> <li>365</li> </ul>
Perez-Prado, MPerruchoud, R CPerry, TPeter, W271,Peterson, LPeterson, R244,Petir, PPetraroli, MPetrova, R SPetrova, R SPettengill, E CPettersen, KPettifor, D GPharr, G M372,Phillion, APhillipot, S RPiascik, RPicard, Y NPickens, J R223,Pickering, H W	<ul> <li>344</li> <li>433</li> <li>360</li> <li>413</li> <li>359</li> <li>204</li> <li>266</li> <li>358</li> <li>190</li> <li>381</li> <li>275</li> <li>264</li> <li>444</li> <li>348</li> <li>401</li> <li>219</li> <li>171</li> <li>222</li> <li>418</li> <li>345</li> <li>365</li> <li>409</li> </ul>
Perez-Prado, M Perruchoud, R C Perry, T Peter, W	<ul> <li>344</li> <li>433</li> <li>360</li> <li>413</li> <li>359</li> <li>204</li> <li>266</li> <li>358</li> <li>190</li> <li>381</li> <li>275</li> <li>264</li> <li>444</li> <li>348</li> <li>401</li> <li>219</li> <li>171</li> <li>222</li> <li>418</li> <li>345</li> <li>365</li> <li>409</li> <li>399</li> </ul>
Perez-Prado, M         Perruchoud, R C         Perry, T         Peter, W         271,         Peter, W         Peterson, L         Peterson, R         Petraroli, M         Petraroli, M         Petrova, R S         Petrova, R S         Pettengill, E C         Pettersen, K         Pettifor, D G         Pharr, G M         Phillips, E C         Phillpot, S R         Piascik, R         Picard, Y N         Pickens, J R         Pillai, V C         Pillis, M F	<ul> <li>344</li> <li>433</li> <li>360</li> <li>413</li> <li>359</li> <li>204</li> <li>266</li> <li>358</li> <li>190</li> <li>381</li> <li>275</li> <li>264</li> <li>444</li> <li>348</li> <li>401</li> <li>219</li> <li>171</li> <li>222</li> <li>418</li> <li>345</li> <li>365</li> <li>409</li> </ul>
Perez-Prado, M         Perruchoud, R C         Perry, T         Peter, W         271,         Peter, W         Peterson, L         Peterson, R         Petraroli, M         Petraroli, M         Petrova, R S         Petrova, R S         Pettengill, E C         Pettersen, K         Pettifor, D G         Pharr, G M         Phillips, E C         Phillpot, S R         Piascik, R         Picard, Y N         Pickens, J R         Pillai, V C         Pillis, M F	<ul> <li>344</li> <li>433</li> <li>360</li> <li>413</li> <li>359</li> <li>204</li> <li>266</li> <li>358</li> <li>190</li> <li>381</li> <li>275</li> <li>264</li> <li>444</li> <li>348</li> <li>401</li> <li>219</li> <li>171</li> <li>222</li> <li>418</li> <li>345</li> <li>365</li> <li>409</li> <li>399</li> </ul>
Perez-Prado, MPerruchoud, R CPerry, TPeter, W271,Peterson, LPeterson, R244,Petirson, RPetraroli, MPetraroli, MPetrova, R SPetrova, R SPettengill, E CPettersen, KPettifor, D GPharr, G M372,Phillion, APhillipot, S RPiascik, RPicard, Y NPickens, J RPillai, V CPillis, M FPilon, L	<ul> <li>344</li> <li>433</li> <li>360</li> <li>413</li> <li>359</li> <li>204</li> <li>266</li> <li>358</li> <li>190</li> <li>381</li> <li>275</li> <li>264</li> <li>444</li> <li>348</li> <li>401</li> <li>219</li> <li>171</li> <li>222</li> <li>418</li> <li>345</li> <li>365</li> <li>409</li> <li>399</li> <li>243</li> <li>173</li> </ul>
Perez-Prado, M         Perruchoud, R C         Perry, T         Peter, W         271,         Peter, W         Peterson, L         Peterson, R         Petraroli, M         Petraroli, M         Petrova, R S         Petrova, R S         Pettengill, E C         Pettersen, K         Pettifor, D G         Pharr, G M         Phillips, E C         Phillpot, S R         Piascik, R         Picard, Y N         Pickens, J R         Pillai, V C         Pillis, M F	<ul> <li>344</li> <li>433</li> <li>360</li> <li>413</li> <li>359</li> <li>204</li> <li>266</li> <li>358</li> <li>190</li> <li>381</li> <li>275</li> <li>264</li> <li>444</li> <li>348</li> <li>401</li> <li>219</li> <li>171</li> <li>222</li> <li>418</li> <li>345</li> <li>365</li> <li>409</li> <li>399</li> <li>243</li> </ul>

Pineault, J	
	177
Pinoncely, A 272,	399
Pint, B A	174
Piotrowski, G B	341
Pippan, R 252, 254,	350
$D_{1}^{2} = 1^{2} + T_{1}^{2} + T_{2}^{2} + T_{1}^{2} + T_{2}^{2} + T_{2}^{2} + T_{1}^{2} + T_{2}^{2} + T_{2}^{2$	
Pisarkiewicz, T	321
Piskajova, T V	267
Pitchure, D	287
Plapp, M	387
Platek, P	268
Platonov, V	437
Plikas, T	424
Pluth, M J 301,	388
Podey, L	318
Pohar, P	378
Poirier, D R 385,	428
Polasik, S J	309
Poliakov, P V	267
Pollock, T M 195, 270,	345
Pomrenke, G S	179
Pomykala, J A	357
Poncsák, S	447
Pond, R C 228,	425
Ponge, D 259,	350
Pongsaksawad, W	367
Poole, W J 268, 303,	307
Poon, J 216,	217
Popescu, G	290
Popov, V P	381
Popova, N A	258
Portella, P D	367
Porter, W 176, 298,	421
Portmann, M J	250
Posada, T	361
Potens, B	388
	000
Potluri, K	274
Potluri, K	274
Potocnik, V	274 437
Potocnik, V Potzies, C	274 437 418
Potocnik, V	274 437 418
Potocnik, V Potzies, C Poulsen, H	274 437 .418 372
Potocnik, V Potzies, C Poulsen, H	274 437 418 372 431
Potocnik, V Potzies, C Poulsen, H	274 437 418 372 431 289,
Potocnik, V Potzies, C Poulsen, H	274 437 418 372 431
Potocnik, V Potzies, C Poulsen, H	274 437 418 372 431 289, 366,
Potocnik, V Potzies, C	274 437 .418 372 431 289, 366, 420
Potocnik, V Potzies, C Poulsen, H	274 437 .418 372 431 289, 366, 420 444
Potocnik, V Potzies, C Poulsen, H	274 437 .418 372 431 289, 366, 420
Potocnik, V Potzies, C Poulsen, H	274 437 .418 372 431 289, 366, 420 444
Potocnik, V Potzies, C Poulsen, H	274 437 418 372 431 289, 366, 420 444 396 226
Potocnik, V Potzies, C Poulsen, H	274 437 418 372 431 289, 366, 420 444 396 226 372
Potocnik, V Potzies, C Poulsen, H	274 437 418 372 431 289, 366, 420 444 396 226 372 372
Potocnik, V Potzies, C Poulsen, H	274 437 418 372 431 289, 366, 420 444 396 226 372
Potocnik, V Potzies, C Poulsen, H	274 437 418 372 431 289, 366, 420 444 396 226 372 372
Potocnik, V         Potzies, C         Poulsen, H       302,         Pourboghrat, F         Powell, A C       194, 236, 280,	274 437 418 372 431 289, 366, 420 444 396 226 372 372 218 258
Potocnik, V         Potzies, C         Poulsen, H       302,         Pourboghrat, F         Powell, A C       194, 236, 280,	274 437 418 372 431 289, 366, 420 444 396 226 372 218 258 372
Potocnik, V         Potzies, C         Poulsen, H       302,         Pourboghrat, F         Powell, A C       194, 236, 280,	274 437 418 372 431 289, 366, 420 444 396 226 372 372 218 258
Potocnik, V         Potzies, C         Poulsen, H       302,         Pourboghrat, F         Powell, A C       194, 236, 280,	274 437 418 372 431 289, 366, 420 444 396 226 372 218 258 372 218 258 372 371
Potocnik, V         Potzies, C         Poulsen, H       302,         Pourboghrat, F         Powell, A C       194, 236, 280,	274 437 418 372 431 289, 366, 420 444 396 226 372 218 258 372 218 371 340
Potocnik, V         Potzies, C         Poulsen, H       302,         Pourboghrat, F         Powell, A C       194, 236, 280,	274 437 418 372 431 289, 366, 420 444 396 372 218 258 372 218 258 372 371 340 436
Potocnik, V         Potzies, C         Poulsen, H       302,         Pourboghrat, F         Powell, A C       194, 236, 280,	274 437 418 372 431 289, 366, 420 444 396 226 372 218 258 372 218 371 340
Potocnik, V         Potzies, C         Poulsen, H       302,         Pourboghrat, F         Powell, A C       194, 236, 280,	274 437 418 372 431 289, 366, 420 444 396 372 218 258 372 218 258 372 371 340 436
Potocnik, V         Potzies, C         Poulsen, H       302,         Pourboghrat, F         Powell, A C       194, 236, 280,	274 437 418 372 431 289, 366, 420 444 396 226 372 218 258 372 218 258 372 371 340 436 378 269
Potocnik, V         Potzies, C         Poulsen, H       302,         Pourboghrat, F         Powell, A C       194, 236, 280,	274 437 418 372 431 289, 366, 420 444 396 226 372 218 258 372 218 258 372 371 340 436 378 269 360
Potocnik, V         Potzies, C         Poulsen, H       302,         Pourboghrat, F         Powell, A C       194, 236, 280,	274 437 418 372 431 289, 366, 420 444 396 372 218 258 372 218 258 372 371 340 436 378 269 360 253
Potocnik, V         Potzies, C         Poulsen, H       302,         Pourboghrat, F         Powell, A C       194, 236, 280,	274 437 418 372 431 289, 366, 420 444 396 226 372 218 258 372 218 258 372 371 340 436 378 269 360
Potocnik, V         Potzies, C         Poulsen, H       302,         Pourboghrat, F         Powell, A C       194, 236, 280,	274 437 418 372 431 289, 366, 420 444 396 226 372 218 258 372 218 258 372 371 340 436 378 269 360 253 223
Potocnik, V         Potzies, C         Poulsen, H       302,         Pourboghrat, F       302,         Powell, A C       194, 236, 280,	274 437 418 372 431 289, 366, 420 444 396 226 372 218 258 372 218 258 372 371 340 436 378 269 360 253 223 361
Potocnik, V         Potzies, C         Poulsen, H       302,         Pourboghrat, F       302,         Powell, A C       194, 236, 280,	274 437 418 372 431 289, 366, 420 444 396 226 372 218 258 372 218 258 372 371 340 436 378 269 360 253 223 361 195
Potocnik, V         Potzies, C         Poulsen, H       302,         Pourboghrat, F       302,         Powell, A C       194, 236, 280,	274 437 418 372 431 289, 366, 420 444 396 226 372 218 258 372 218 258 372 371 340 436 378 269 360 253 223 361
Potocnik, V         Potzies, C         Poulsen, H       302,         Pourboghrat, F       302,         Powell, A C       194, 236, 280,	274 437 418 372 431 289, 366, 420 444 396 226 372 218 258 372 218 258 372 371 340 436 378 269 360 253 223 361 195 263
Potocnik, V         Potzies, C         Poulsen, H       302,         Pourboghrat, F       302,         Powell, A C       194, 236, 280,	274 437 418 372 431 289, 366, 420 444 396 226 372 218 258 372 218 258 372 218 258 372 371 340 436 378 263 253 223 361 195 263 258
Potocnik, V         Potzies, C         Poulsen, H       302,         Pourboghrat, F       302,         Powell, A C       194, 236, 280,	274 437 418 372 431 289, 366, 420 444 396 226 372 218 258 372 218 258 372 218 258 372 371 340 436 378 263 253 223 361 195 263 258 339
Potocnik, V         Potzies, C         Poulsen, H       302,         Pourboghrat, F       302,         Powell, A C       194, 236, 280,	274 437 418 372 431 289, 366, 420 444 396 226 372 218 258 372 218 258 372 218 258 372 371 340 436 378 263 253 223 361 195 263 258 339
Potocnik, V         Potzies, C         Poulsen, H       302,         Pourboghrat, F	274 437 418 372 431 289, 366, 420 444 396 226 372 218 258 372 218 258 372 218 258 372 371 340 436 378 269 360 253 223 361 195 263 258 339 353
Potocnik, V         Potzies, C         Poulsen, H       302,         Pourboghrat, F	274 437 418 372 431 289, 366, 420 444 396 226 372 218 258 372 218 258 372 218 258 372 371 340 436 378 269 360 253 361 195 263 258 339 353 282
Potocnik, V         Potzies, C         Poulsen, H       302,         Pourboghrat, F	274 437 418 372 431 289, 366, 420 444 396 226 372 218 258 372 218 258 372 218 258 372 371 340 436 378 269 360 253 361 195 263 258 339 353 282

470

Puttlitz, K J ..... 286, 416

# Q

Qi, G	373
Qi, Y	331
Qian, M 294, 376,	417
Qin, Q	357
Qiu, Z 357,	400
Quan, Z	214
Quatravaux, T	219
Quested, T E	298
Quiroga, A S	300

# R

Raab, G I	255,	256,	257
Raabe, D		259,	350
Rabba, S A			360
Rabeeh, R			308
Rabenberg, J			219
Rabiei, A			447
Rabkin, E			260
Rack, H			446
Rack, H J			350
Rackaitis, M			424
Radmilovic, V			408
Raghavan, P			406
Raghavan, S			387
Rahman, M M			274
Raj, B			227
Raj, I A			236
Rajagopalan, B			288
Rajagopalan, S			342
Rajan, K	192.	234.	288.
	334.	376.	419
Rajeev, K P			239
Rama Mohan, T R			224
Ramachandran, V			244
Ramakrishnan, S			333
Ramanath, G			422
Ramanathan, L V			429
Ramanujan, R V		273,	424
Ramaswamy, K		250,	256
Ramchandran, R			230
Ramesh, N N			412
Ramesh, R 195,	227	200	336
Ramirez, A G	237,	290,	453
Ramirez, J			4 <i>33</i> 86
Ramírez, J			454
Ramovic, R			180
Ramsey, L		202	371
Rangaswamy, P Ranieri, S	•••••	203,	188
Ranki-Kilpinen, T			186
Rao, S			
Rao, V N			412
Rapkoch, J M			200
Rappaz, M	202	247	200
	202,	247,	299, 450
Ratchev, I			
Rath, B B	169,	334,	446
Rath, C			
Rathod, C R			
Rathz, T J			
Ratke, L			
Ratner, B D		197,	239

Raty, M 171,	
I(aly, W = 1/1, 1/1)	311
Ravinder Reddy, N	
Ravindra, N M 179,	
Rawn, C J	400
Ray, K K	227
Ray, L D	
Raychenko, O I	
Readey, D W	193
Ready, J 179, 220, 274,	320
Rebak, R B	. 246
Reck, B	
	413
Reddy, M R	
Reddy, R G 185, 243,	268,
	357
Redl, C	404
Reed, B 406,	431
Reichert, H	251
Reichman, S H	278
Reid, J G 372,	373
Reilly, E K	354
Reilly, J J	353
Rejaee, M	333
Rejent, J A	331
Remhof, A	395
Remington, B A	366
Renaudier, S	437
Reny, P	
Reshetov, A	208
Reuter, M A 200, 232, 245,	362
Reutzel, S	380
Reynier, Y	
	. 554
Reynolds, T	
Reynolds, W T 282,	371
Rez, P	354
Reznik, I D	185
Rhee, H 188, 285,	286
Rhee, K H	269
Richards, C D 275,	435
Richards, R F 275,	435 435
Richards, R F 275, Richardson, J W 184, 297,	435 435 372
Richards, R F 275, Richardson, J W 184, 297, Ricker, R	435 435 372 287
Richards, R F 275, Richardson, J W 184, 297, Ricker, R Ricketts, N J	435 435 372 287 376
Richards, R F 275, Richardson, J W 184, 297, Ricker, R Ricketts, N J Rickkets, M S	435 435 372 287
Richards, R F 275, Richardson, J W 184, 297, Ricker, R Ricketts, N J	435 435 372 287 376
Richards, R F 275, Richardson, J W 184, 297, Ricker, R Ricketts, N J Rickkets, M S Riddle, R K	435 435 372 287 376 288 330
Richards, R F       275,         Richardson, J W       184, 297,         Ricker, R       Rickets,         Rickkets, M J       Rickkets,         Riddle, R K       343, 347,	435 435 372 287 376 288 330 376
Richards, R F       275,         Richardson, J W       184, 297,         Ricker, R       Rickets, N J         Ricketts, N J       Rickets,         Riddle, R K       Riddle, R K         Riddle, Y W       343, 347,         Ried, P P       P	435 435 372 287 376 288 330 376 191
Richards, R F       275,         Richardson, J W       184, 297,         Ricker, R       Rickets, N J         Rickkets, M S       Riddle, R K         Riddle, R K       343, 347,         Rieger, L E       Rieger, L E	435 435 372 287 376 288 330 376 191 326
Richards, R F       275,         Richardson, J W       184, 297,         Ricker, R       Rickets, N J         Rickkets, M S       Riddle, R K         Riddle, R K       343, 347,         Rieger, L E       Riehl, W	435 435 372 287 376 288 330 376 191 326 230
Richards, R F       275,         Richardson, J W       184, 297,         Ricker, R       Rickets, N J         Rickkets, M S       Riddle, R K         Riddle, R K       343, 347,         Rieger, L E       Riehl, W         Rietz, W       Rietz, W	435 435 372 287 376 288 330 376 191 326 230 417
Richards, R F       275,         Richardson, J W       184, 297,         Ricker, R       Rickets, N J         Rickkets, M S       Riddle, R K         Riddle, R K       343, 347,         Rieger, L E       Riehl, W         Rietz, W       Rietz, W	435 435 372 287 376 288 330 376 191 326 230 417
Richards, R F	<ul> <li>435</li> <li>435</li> <li>372</li> <li>287</li> <li>376</li> <li>288</li> <li>330</li> <li>376</li> <li>191</li> <li>326</li> <li>230</li> <li>417</li> <li>453</li> </ul>
Richards, R F	<ul> <li>435</li> <li>435</li> <li>372</li> <li>287</li> <li>376</li> <li>288</li> <li>330</li> <li>376</li> <li>191</li> <li>326</li> <li>230</li> <li>417</li> <li>453</li> <li>330</li> </ul>
Richards, R F       275,         Richardson, J W       184, 297,         Ricker, R       184, 297,         Rickets, N J       Rickets,         Rickkets, M S       Riddle, R K         Riddle, R K       343, 347,         Rieder, L E       Riehl, W         Rietz, W       Rietz, W         Rigg, P A       Rigopoulos, E         Rigsbee, J M       197, 239, 291,	435 435 372 287 376 288 330 376 191 326 230 417 453 330 326,
Richards, R F       275,         Richardson, J W       184, 297,         Ricker, R       184, 297,         Rickets, N J       184, 297,         Rickets, M S       184, 297,         Rickets, M S       184, 297,         Riddle, R K       184, 347,         Riddle, Y W       343, 347,         Riede, P P       184, 347,         Rieger, L E       184, 100, 100, 100, 100, 100, 100, 100, 10	<ul> <li>435</li> <li>435</li> <li>372</li> <li>287</li> <li>376</li> <li>288</li> <li>330</li> <li>376</li> <li>191</li> <li>326</li> <li>230</li> <li>417</li> <li>453</li> <li>330</li> </ul>
Richards, R F       275,         Richardson, J W       184, 297,         Ricker, R       184, 297,         Rickets, N J       Rickets,         Rickkets, M S       Riddle, R K         Riddle, R K       343, 347,         Rieder, L E       Riehl, W         Rietz, W       Rietz, W         Rigg, P A       Rigopoulos, E         Rigsbee, J M       197, 239, 291,	435 435 372 287 376 288 330 376 191 326 230 417 453 330 326,
Richards, R F       275,         Richardson, J W       184, 297,         Ricker, R       184, 297,         Rickets, N J       Rickets, M S         Rickkets, M S       Riddle, R K         Riddle, R K       343, 347,         Ried, P P       343, 347,         Ried, P P       Rieger, L E         Riehl, W       Rietz, W         Rigg, P A       Rigopoulos, E         Rigsbee, J M       197, 239, 291,	435 435 372 287 376 288 330 376 191 326 230 417 453 330 326, 447
Richards, R F       275,         Richardson, J W       184, 297,         Ricker, R       184, 297,         Rickets, N J       184, 297,         Rickets, N J       184, 297,         Rickets, M S       184, 297,         Rickets, M S       184, 297,         Riddle, R K       184, 347,         Riddle, Y W       343, 347,         Riede, P P       343, 347,         Rieger, L E       184, 100, 100, 100, 100, 100, 100, 100, 10	435 435 372 287 376 288 330 376 191 326 230 417 453 330 326, 447 263 197
Richards, R F       275,         Richardson, J W       184, 297,         Ricker, R       184, 297,         Rickets, N J       184, 297,         Rickets, N J       184, 297,         Rickets, M S       184, 297,         Rickets, M S       184, 297,         Riddle, R K       184, 343, 347,         Riddle, R K       343, 347,         Riede, P P       343, 347,         Rieger, L E       Riehl, W         Rietz, W       Rig, P A         Rigg, P A       197, 239, 291,	<ul> <li>435</li> <li>435</li> <li>372</li> <li>287</li> <li>376</li> <li>288</li> <li>330</li> <li>376</li> <li>191</li> <li>326</li> <li>230</li> <li>417</li> <li>453</li> <li>330</li> <li>326,</li> <li>447</li> <li>263</li> <li>197</li> <li>419</li> </ul>
Richards, R F       275,         Richardson, J W       184, 297,         Ricker, R       Rickets, M J         Ricketts, M S       Riddle, R K         Riddle, R K       343, 347,         Riede, P P       343, 347,         Ried, P P       Rieger, L E         Rietz, W       Riegy, P A         Rigopoulos, E       Rigsbee, J M         Rigsbee, J M       197, 239, 291,	435 435 372 287 376 288 330 376 191 326 230 417 453 330 326, 447 263 197 419 316
Richards, R F       275,         Richardson, J W       184, 297,         Ricker, R       Rickets, M S         Ricketts, M S       Riddle, R K         Riddle, R K       343, 347,         Riede, P W       343, 347,         Riede, P P       Rieger, L E         Rietz, W       Rieg, P A         Rigg, P A       197, 239, 291,	435 435 372 287 376 288 330 376 191 326 230 417 453 330 326, 447 263 197 419 316 341
Richards, R F       275,         Richardson, J W       184, 297,         Ricker, R       Rickets, M J         Ricketts, M S       Riddle, R K         Riddle, R K       343, 347,         Riede, P P       343, 347,         Ried, P P       Rieger, L E         Rietz, W       Riegy, P A         Rigopoulos, E       Rigsbee, J M         Rigsbee, J M       197, 239, 291,	435 435 372 287 376 288 330 376 191 326 230 417 453 330 326, 447 263 197 419 316 341
Richards, R F	435 435 372 287 376 288 330 376 191 326 230 417 453 330 326, 447 263 197 419 316 341 266
Richards, R F	435 435 372 287 376 288 330 376 191 326 230 417 453 330 326, 447 263 197 419 316 341 266 421
Richards, R F       275,         Richardson, J W       184, 297,         Ricker, R       184, 297,         Rickets, N J       Rickets, M S         Rickkets, M S       Riddle, R K         Riddle, R K       343, 347,         Riddle, Y W       343, 347,         Rieger, L E       Rieger, L E         Rieg, P A       Rigopoulos, E         Rigsbee, J M       197, 239, 291,	<ul> <li>435</li> <li>435</li> <li>372</li> <li>287</li> <li>376</li> <li>288</li> <li>330</li> <li>376</li> <li>191</li> <li>326</li> <li>230</li> <li>417</li> <li>453</li> <li>330</li> <li>326,</li> <li>447</li> <li>263</li> <li>197</li> <li>419</li> <li>316</li> <li>341</li> <li>266</li> <li>421</li> <li>319</li> </ul>
Richards, R F	<ul> <li>435</li> <li>435</li> <li>372</li> <li>287</li> <li>376</li> <li>288</li> <li>330</li> <li>376</li> <li>191</li> <li>326</li> <li>230</li> <li>417</li> <li>453</li> <li>330</li> <li>326,</li> <li>447</li> <li>263</li> <li>197</li> <li>419</li> <li>316</li> <li>341</li> <li>266</li> <li>421</li> <li>319</li> <li>177</li> </ul>
Richards, R F       275,         Richardson, J W       184, 297,         Ricker, R       184, 297,         Rickets, N J       Rickets, M S         Rickkets, M S       Riddle, R K         Riddle, R K       343, 347,         Riddle, Y W       343, 347,         Rieger, L F       Rieger, L E         Rieg, P A       Rigopoulos, E         Rigsbee, J M       197, 239, 291,	<ul> <li>435</li> <li>435</li> <li>372</li> <li>287</li> <li>376</li> <li>288</li> <li>330</li> <li>376</li> <li>191</li> <li>326</li> <li>230</li> <li>417</li> <li>453</li> <li>330</li> <li>326,</li> <li>447</li> <li>263</li> <li>197</li> <li>419</li> <li>316</li> <li>341</li> <li>266</li> <li>421</li> <li>319</li> <li>177</li> <li>270</li> </ul>
Richards, R F	<ul> <li>435</li> <li>435</li> <li>372</li> <li>287</li> <li>376</li> <li>288</li> <li>330</li> <li>376</li> <li>191</li> <li>326</li> <li>230</li> <li>417</li> <li>453</li> <li>330</li> <li>326,</li> <li>447</li> <li>263</li> <li>197</li> <li>419</li> <li>316</li> <li>341</li> <li>266</li> <li>421</li> <li>319</li> <li>177</li> <li>270</li> </ul>
Richards, R F	<ul> <li>435</li> <li>435</li> <li>372</li> <li>287</li> <li>376</li> <li>288</li> <li>330</li> <li>376</li> <li>191</li> <li>326</li> <li>230</li> <li>417</li> <li>453</li> <li>330</li> <li>326,</li> <li>447</li> <li>263</li> <li>197</li> <li>419</li> <li>316</li> <li>341</li> <li>266</li> <li>421</li> <li>319</li> <li>177</li> <li>270</li> <li>410</li> </ul>
Richards, R F       275,         Richardson, J W       184, 297,         Ricker, R       184, 297,         Ricketts, N J       Ricketts, M S         Rickkets, M S       Riddle, R K         Riddle, R K       343, 347,         Riddle, Y W       343, 347,         Rieger, L F       Rieger, L E         Rieg, P A       Rigopoulos, E         Rigsbee, J M       197, 239, 291,	<ul> <li>435</li> <li>435</li> <li>372</li> <li>287</li> <li>376</li> <li>288</li> <li>330</li> <li>376</li> <li>191</li> <li>326</li> <li>230</li> <li>417</li> <li>453</li> <li>330</li> <li>326,</li> <li>447</li> <li>263</li> <li>197</li> <li>419</li> <li>316</li> <li>341</li> <li>266</li> <li>421</li> <li>319</li> <li>177</li> <li>270</li> <li>410</li> <li>183</li> </ul>

Robertson, I M	183
Robinson, J A	198
Robinson, M C	275
Robinson, T P	313
Rocha, M S	230
Rodnov, O O 212,	267
Rodrigues, R L	329
Rodriguez Gan, R	373
Rodriguez, P	415
Roesner, H 346,	351
Ruesliel, H	
Rogan, R	372
Rogers, J R 289,	438
Rohrer, G 390,	391
Rolander, N	246
Rolland, K	172
Rollett, A D 180, 204,	249,
	451
Romanov, A E 252,	258
Rong, Z	224
Rosales, I	326
Rosales, P I	175
Rösner, H	307
Ross, C A	420
Rossler, U K	239
	171
Rousseaux, J	
Roven, H J	208
Roy, A	357
Roy, A K	226
Roytburd, A L 322, 334, 384,	425
Rozin, A V	318
Ruban, A V	405
Rubinovich, Z	333
Rubisov, D	284
Ruckebusch, H	173
Ruda, M	451
Rudd, T J	301
Rudin, S P 183,	282
Rudko, G Y	180
Rugg, D 182,	
Rühle, M	
Ruile, W	
Runt, J P	424
Russell, R	436
Russell, R 418,	419
Ruuskanen, P R	412
Ruzyllo, J	221
Ryan, L	415
Ryu, D	413
Ryu, H 453,	454
Ryu, J	442

# S

Saatci, A		265
Sabau, A S 218, 2	298,	362,
	123,	446
Sachdev, A K	233,	347
Sachenko, P		432
Sadananda, K	348,	366
Sadigh, B	406,	431
Sadler, B A		360
Sadoway, D R 223, 325, 3	366,	420
Saeki, Y		
Saez, E		178
Safi, M		203
Sahling, M		398
Saito, K 2	218,	450

Saito, N		234
Saito, T		440
Saito, Y		206
Sakaguchi, T		227
Sakai, T		206
Sakamoto, H		449
Sakamoto, M		175
Sakasegawa, H		184
Sakidja, R		400
Salami, T O	215, 275	321
Salas, G		454
Saleh, T A		297
Salem, A A		303
Salimgareyev, H		208
Samanta, D		
Sambandam, S N		455
Sampson, D		230
Samson, S		
Sanchez, J E		229,
		371
Sanders, D G		211
Sanders, R E		249
Sanders, T H	296,	404
Sanders, W S 175,	227,	402
Sandhage, K H		337
Sandoz, D		415
Sandrock, G		170
Sankar, J		337
Sankaran, K K		234,
		419
Santella, M		436
	191, 199,	
		321
Sardesai, A S		217
Sarihan, V		
Sarikaya, M		337
Socter D H		
Sastry, D H		432
Sato, K		432 294
Sato, K Sato, M		432 294 388
Sato, K Sato, M Saunders, T		432 294 388 172
Sato, K Sato, M Saunders, T Sauter, L		432 294 388 172 229
Sato, K Sato, M Saunders, T Sauter, L Sauvage, X		432 294 388 172 229
Sato, K Sato, M Saunders, T Sauter, L		432 294 388 172 229
Sato, K Sato, M Saunders, T Sauter, L Sauvage, X		432 294 388 172 229 306
Sato, K Sato, M Saunders, T Saunders, T Sauvage, X Sauvage, M F		432 294 388 172 229 306 352
Sato, K Sato, M Saunders, T Sauter, L Sauvage, X Savage, M F Savin, I		<ul> <li>432</li> <li>294</li> <li>388</li> <li>172</li> <li>229</li> <li>306</li> <li>352</li> <li>322</li> <li>288</li> </ul>
Sato, K Sato, M Saunders, T Sauter, L Sauvage, X Savage, M F Savin, I Saxena, S Sayed, H S	193,	<ul> <li>432</li> <li>294</li> <li>388</li> <li>172</li> <li>229</li> <li>306</li> <li>352</li> <li>322</li> <li>288</li> </ul>
Sato, K Sato, M Saunders, T Sauter, L Sauvage, X Savage, M F Savin, I Saxena, S Sayed, H S Saylor, D M	193,	<ul> <li>432</li> <li>294</li> <li>388</li> <li>172</li> <li>229</li> <li>306</li> <li>352</li> <li>322</li> <li>288</li> <li>437</li> </ul>
Sato, K Sato, M Saunders, T Sauter, L Sauvage, X Savage, M F Savin, I Saxena, S Sayed, H S Saylor, D M Saytaeva, K	193,	<ul> <li>432</li> <li>294</li> <li>388</li> <li>172</li> <li>229</li> <li>306</li> <li>352</li> <li>322</li> <li>288</li> <li>437</li> <li>391</li> <li>311</li> </ul>
Sato, K Sato, M Saunders, T Sauter, L Sauvage, X Savage, M F Savin, I Saxena, S Sayed, H S Saylor, D M Saytaeva, K Scarber, P	193,	<ul> <li>432</li> <li>294</li> <li>388</li> <li>172</li> <li>229</li> <li>306</li> <li>352</li> <li>322</li> <li>288</li> <li>437</li> <li>391</li> <li>311</li> <li>320</li> </ul>
Sato, K Sato, M Saunders, T Sauter, L Sauvage, X Savage, M F Savin, I Saxena, S Sayed, H S Saylor, D M Saytaeva, K Scarber, P Scattergood, R O		<ul> <li>432</li> <li>294</li> <li>388</li> <li>172</li> <li>229</li> <li>306</li> <li>352</li> <li>322</li> <li>288</li> <li>437</li> <li>391</li> <li>311</li> <li>320</li> <li>393</li> </ul>
Sato, K Sato, M Saunders, T Sauter, L Sauvage, X Savage, M F Savin, I Saxena, S Sayed, H S Saylor, D M Saytaeva, K Scarber, P Scattergood, R O Schadler, L S	193, 256,	<ul> <li>432</li> <li>294</li> <li>388</li> <li>172</li> <li>229</li> <li>306</li> <li>352</li> <li>322</li> <li>288</li> <li>437</li> <li>391</li> <li>311</li> <li>320</li> <li>393</li> <li>381</li> </ul>
Sato, K Sato, K Sauders, T Sauter, L Sauvage, X Savage, M F Savin, I Saxena, S Sayed, H S Saylor, D M Saytaeva, K Scarber, P Scattergood, R O Schadler, L S Schaeffer, J C	193, 256,	<ul> <li>432</li> <li>294</li> <li>388</li> <li>172</li> <li>229</li> <li>306</li> <li>352</li> <li>322</li> <li>288</li> <li>437</li> <li>391</li> <li>311</li> <li>320</li> <li>393</li> <li>381</li> <li>204</li> </ul>
Sato, K Sato, M Saunders, T Sauter, L Savage, M F Savage, M F Savena, S Sayed, H S Saylor, D M Saytaeva, K Scarber, P Scattergood, R O Schadler, L S Schaeffer, J C Schaffer, P L	193, 256,	432 .294 388 172 229 306 352 322 288 437 391 311 320 393 381 204 403
Sato, K Sato, M Saunders, T Sauter, L Savage, M F Savage, M F Savena, S Sayed, H S Saylor, D M Saytaeva, K Scarber, P Scattergood, R O Schadler, L S Schaeffer, J C Schaper, M	193,	432 .294 388 172 229 306 352 322 288 437 391 311 320 393 381 204 403 315
Sato, K	193,	<ul> <li>432</li> <li>294</li> <li>388</li> <li>172</li> <li>229</li> <li>306</li> <li>352</li> <li>322</li> <li>288</li> <li>437</li> <li>391</li> <li>311</li> <li>320</li> <li>393</li> <li>381</li> <li>204</li> <li>403</li> <li>315</li> <li>310</li> </ul>
Sato, K Sato, M Saunders, T Sauter, L Savage, M F Savage, M F Savena, S Sayed, H S Saylor, D M Saylor, D M Saytaeva, K Scarber, P Scattergood, R O Schadler, L S Schaeffer, J C Schaeffer, P L Schaper, M Schildbach, M A Schlapbach, L 169, 210,	193, 256, 262,	432 .294 388 172 229 306 352 322 288 437 391 311 320 393 381 204 403 315 310 309,
Sato, K Sato, M Saunders, T Sauter, L Sauvage, X Savage, M F Savin, I Saxena, S Sayed, H S Saylor, D M Saytaeva, K Scarber, P Scattergood, R O Schadler, L S Schaeffer, J C Schaffer, P L Schaper, M Schildbach, M A Schlapbach, L 169, 210, 	193, 256, 262, 435,	432 .294 388 172 229 306 352 322 288 437 391 311 320 393 381 204 403 315 310 309, 436
Sato, K Sato, M Saunders, T Sauter, L Sauvage, X Savage, M F Savin, I Saxena, S Sayed, H S Saylor, D M Saytaeva, K Scarber, P Scattergood, R O Schadler, L S Schaeffer, J C Schaeffer, P L Schaper, M Schildbach, M A Schlapbach, L 169, 210, 	193, 256, 262, 435,	432 .294 388 172 229 306 352 322 288 437 391 311 320 393 381 204 403 315 310 309, 436 240
Sato, K Sato, K Sato, M Saunders, T Sauter, L Sauvage, X Savage, M F Savin, I Saxena, S Sayed, H S Saylor, D M Saytaeva, K Scarber, P Scattergood, R O Schadler, L S Schaeffer, J C Schaeffer, J C Schaffer, P L Schaper, M Schildbach, M A Schlapbach, L 169, 210, 	193, 256, 262, 435,	432 .294 388 172 229 306 352 322 288 437 391 311 320 393 381 204 403 315 310 309, 436 240 265
Sato, K Sato, M Saunders, T Sauter, L Sauvage, X Savage, M F Savin, I Saxena, S Sayed, H S Saylor, D M Saytaeva, K Scarber, P Scattergood, R O Schadler, L S Schaeffer, J C Schaeffer, J C Schaffer, P L Schaper, M Schildbach, M A Schildbach, M A Schlapbach, L 169, 210, 	193, 256, 262, 435, 204,	<ul> <li>432</li> <li>294</li> <li>388</li> <li>172</li> <li>229</li> <li>306</li> <li>352</li> <li>322</li> <li>288</li> <li>437</li> <li>391</li> <li>311</li> <li>320</li> <li>393</li> <li>381</li> <li>204</li> <li>403</li> <li>315</li> <li>310</li> <li>309,</li> <li>436</li> <li>240</li> <li>265</li> <li>390</li> </ul>
Sato, K Sato, K Sato, M Saunders, T Sauter, L Sauvage, X Savage, M F Savin, I Saxena, S Sayed, H S Saylor, D M Saytaeva, K Scarber, P Scattergood, R O Schadler, L S Schaeffer, J C Schaffer, P L Schaper, M Schildbach, M A Schlapbach, L Schaider, E Schaider, E Schaider, H W Schmidt, S Schmidt, S Schmidt, T	193, 256, 262, 435, 204,	<ul> <li>432</li> <li>294</li> <li>388</li> <li>172</li> <li>229</li> <li>306</li> <li>352</li> <li>322</li> <li>288</li> <li>437</li> <li>391</li> <li>311</li> <li>320</li> <li>393</li> <li>381</li> <li>204</li> <li>403</li> <li>315</li> <li>310</li> <li>309,</li> <li>436</li> <li>240</li> <li>265</li> <li>390</li> <li>229</li> </ul>
Sato, K Sato, K Sato, M Saunders, T Sauter, L Sauvage, X Savage, M F Savin, I Saxena, S Sayed, H S Sayed, H S Saylor, D M Saytaeva, K Scarber, P Scattergood, R O Schadler, L S Schaeffer, J C Schaffer, P L Schaper, M Schildbach, M A Schildbach, M A Schlapbach, L Schaid-Fetzer, R Schmidt, Fetzer, R Schmidt, S Schmidt, T Schmidt, T Schmitz, T	193, 256, 262, 435, 204,	<ul> <li>432</li> <li>294</li> <li>388</li> <li>172</li> <li>229</li> <li>306</li> <li>352</li> <li>322</li> <li>288</li> <li>437</li> <li>391</li> <li>311</li> <li>320</li> <li>393</li> <li>381</li> <li>204</li> <li>403</li> <li>315</li> <li>310</li> <li>309,</li> <li>436</li> <li>240</li> <li>265</li> <li>390</li> <li>229</li> <li>330</li> </ul>
Sato, K Sato, K Sato, M Saunders, T Sauter, L Sauvage, X Savage, M F Savin, I Saxena, S Sayed, H S Saylor, D M Saytaeva, K Scarber, P Scattergood, R O Schadler, L S Schaeffer, J C Schaeffer, J C Schaeffer, J C Schaffer, P L Schaper, M Schildbach, M A Schildbach, M A Schildbach, L 169, 210, 	193, 256, 262, 435, 204, 204,	432 .294 388 172 229 306 352 322 288 437 391 311 320 393 381 204 403 315 310 309, 436 240 265 390 229 330 269,
Sato, K	193, 256, 262, 435, 204, 215, 401,	<ul> <li>432</li> <li>294</li> <li>388</li> <li>172</li> <li>229</li> <li>306</li> <li>352</li> <li>322</li> <li>288</li> <li>437</li> <li>391</li> <li>311</li> <li>320</li> <li>393</li> <li>381</li> <li>204</li> <li>403</li> <li>315</li> <li>310</li> <li>309,</li> <li>436</li> <li>240</li> <li>265</li> <li>390</li> <li>229</li> <li>330</li> <li>269,</li> <li>432</li> </ul>
Sato, K	193, 256, 262, 435, 204, 215, 401,	<ul> <li>432</li> <li>294</li> <li>388</li> <li>172</li> <li>229</li> <li>306</li> <li>352</li> <li>322</li> <li>288</li> <li>437</li> <li>391</li> <li>311</li> <li>320</li> <li>393</li> <li>381</li> <li>204</li> <li>403</li> <li>315</li> <li>310</li> <li>309,</li> <li>436</li> <li>240</li> <li>265</li> <li>390</li> <li>229</li> <li>330</li> <li>269,</li> <li>432</li> <li>366</li> </ul>
Sato, K	193, 256, 262, 435, 204, 215, 401,	<ul> <li>432</li> <li>294</li> <li>388</li> <li>172</li> <li>229</li> <li>306</li> <li>352</li> <li>322</li> <li>288</li> <li>437</li> <li>391</li> <li>311</li> <li>320</li> <li>393</li> <li>381</li> <li>204</li> <li>403</li> <li>315</li> <li>310</li> <li>309,</li> <li>436</li> <li>240</li> <li>265</li> <li>390</li> <li>229</li> <li>330</li> <li>269,</li> <li>432</li> </ul>
Sato, K	193, 256, 262, 435, 204, 215, 401,	<ul> <li>432</li> <li>294</li> <li>388</li> <li>172</li> <li>229</li> <li>306</li> <li>352</li> <li>322</li> <li>288</li> <li>437</li> <li>391</li> <li>311</li> <li>320</li> <li>393</li> <li>381</li> <li>204</li> <li>403</li> <li>315</li> <li>310</li> <li>309,</li> <li>436</li> <li>240</li> <li>265</li> <li>390</li> <li>229</li> <li>330</li> <li>269,</li> <li>432</li> <li>366</li> <li>217</li> </ul>
Sato, K Sato, K Sato, M Saunders, T Sauter, L Sauvage, X Savage, M F Savin, I Saxena, S Sayed, H S Sayed, H S Sayed, H S Saylor, D M Saytaeva, K Scarber, P Scattergood, R O Schadler, L S Schaeffer, J C Schaeffer, J C Schaffer, P L Schaper, M Schildbach, M A Schlapbach, L Schailer, E Schmidt, Fetzer, R Schmidt, H W Schmidt, S Schmidt, T Schmidt, S Schmidt, T Schneibel, J H Schieler, M S Schobert, H H	193, 256, 262, 435, 204, 215, 401, 330,	<ul> <li>432</li> <li>294</li> <li>388</li> <li>172</li> <li>229</li> <li>306</li> <li>352</li> <li>322</li> <li>288</li> <li>437</li> <li>391</li> <li>311</li> <li>320</li> <li>393</li> <li>381</li> <li>204</li> <li>403</li> <li>315</li> <li>310</li> <li>309,</li> <li>436</li> <li>240</li> <li>265</li> <li>390</li> <li>229</li> <li>330</li> <li>269,</li> <li>432</li> <li>366</li> <li>217</li> <li>415</li> </ul>

Schönfeld, B	2	250
Schroth, J G 2	211, 2	212,
	55, 3	97
Schuh, C A 2		36.
		51
Schultz, A		91
Schultz, A E		98
Schulz, M		38
Schulze, R K		02
Schumacher, P		344
Schvezov, C E 195, 3		40
Schwandt, C		280
Schwartz, C L		68
Schwarz, R B		53
Schwarz, S M		32
Sciammarella, F M		14
Seal, S 3		46.
		-50
Searles, M		89
Sears, J 341, 4		40
Sedighy, M		31
Seekely, M J		609
Seel, S C		94
Seeley, L 284, 3	28, 4	43
Seetharaman, S 2	80, 4	-09
Seetharaman, S 2	48, 3	00
Segal, A	4	41
Sehitoglu, H	3	02
Seidman, D N 2		251
Sekhar, J A 248, 3		88
Sekido, N	3	58
Semenova, I P	2	257
	50 0	
Semiatin, S L 206, 251, 2		253,
	32, 4	.53, .33
	32, 4 3	33 00
	32, 4 3 3	33 00 66
	32, 4 3 3 1	33 00 66 79
	32, 4 3 3 1 3	33 00 66 79 20
	32, 4 3 1 3 2	33 00 666 79 20 203
	32, 4 3 1 3 2 75, 4	<ul> <li>33</li> <li>00</li> <li>66</li> <li>79</li> <li>20</li> <li>203</li> <li>02</li> </ul>
	32, 4 3 1 2 75, 4 4	-33 600 666 79 620 203 602 602
	32, 4 3 1 3 2 75, 4 4 3	<ul> <li>33</li> <li>00</li> <li>66</li> <li>79</li> <li>20</li> &lt;</ul>
	32, 4 3 3 1 3 2 75, 4 3 3 3 3	-33 600 666 79 620 803 602 602 650 846
	32, 4 3 1 3 2 75, 4 4 3 2 2 2	.33 600 666 79 620 203 602 602 650 246 277
	32, 4 3 1 3 2 75, 4 4 3 2 75, 4 2 2 2 2 2 2	-33 600 666 79 620 602 602 602 602 650 646 77 -32
	32, 4	<ul> <li>33</li> <li>600</li> <li>666</li> <li>79</li> <li>20</li> <li>20</li></ul>
	32, 4	-33 600 666 79 620 602 602 602 602 650 646 77 -32
	32, 4	<ul> <li>33</li> <li>300</li> <li>366</li> <li>79</li> <li>320</li> <li>303</li> <li>402</li> <l< td=""></l<></ul>
	32, 4	<ul> <li>33</li> <li>300</li> <li>366</li> <li>79</li> <li>320</li> <li>303</li> <li>402</li> <l< td=""></l<></ul>
	32, 4	33         600         666         79         620         603         602         603         602         603         604         677         632         655         625         80         881
	32, 4       3	33         600         666         79         20
	32, 4	33         300           666         79           620         303           602         602           603         602           604         677           632         555           625         80           811         112           675         612
	32, 4	33         300           666         79           620         303           602         602           603         602           604         677           632         555           625         80           811         112           675         612
	32, 4	33         300           666         79           620         303           602         302           602         50           646         777           632         555           80         881           612         775           612         412           612         612
	32, 4	33         300           666         79           70         320           802         302           802         320           802         320           802         320           803         81           812         775           812         412           819         603
	32, 4	33         300         666         77         20         302         402         550         446         777         332         555         426         4275         412         412         419         403         405
	32, 4         33, 4         33, 3         31, 3         32, 2         775, 4         33, 2         22, 775, 4         33, 2         34, 2         35, 4         36, 4         37, 2         383, 4         33, 4         4	33         600         666         79         620         602         603         604         6350         646         777         632         655         80         811         112         1275         612         603         605         628
	32, 4	33         600         666         79         620         602         603         604         620         620         620         620         620         620         620         620         632         650         646         777         632         655         80         881         412         755         612         603         605         628         888
	32, 4	33         300         666         79         20         302         402         550         402         550         446         777         332         555         80         81         412         275         419         403         405         428         888         413
	32, 4	33         300         666         779         20         302         402         402         402         402         402         403         404         477         32         455         425         881         412         475         412         475         412         428         813         423         403         403         412         428         433         401
	32, 4	33         300         366         79         20         302         302         302         302         302         303         304         305         32         32         344         412         32         344         403         405         228         888         113         322         443         401         95
	32, 4	33         300         666         79         20         302         402         402         402         402         403         404         412         412         412         412         412         412         412         413         403         413         428         431         401         95         474
	32, 4       3         33, 3       3         11       3         22       75, 4         4       3         37, 2       2         21, 17, 4       4         33, 4       3         44       3         44       4         42       3         44       4         42       3         559, 4       1         3559, 4       3	33         300         666         79         20         20         20         302         402         402         402         403         404         412         412         413         403         404         403         404         403         404         403         404         405         428         430         401         95         474
	32, 4	33         300         666         79         20         302         402         402         402         402         403         404         412         412         413         403         404         410         424         410         454
	32, 4       3         33, 3       3         1       3         2       2         75, 4       4	33         300         666         79         20         20         20         302         402         402         403         404         412         412         412         412         412         412         412         413         414         401         95         443         401         95         410         54
	32, 4       3         33, 3       3         1       3         2       2         75, 4       4	33         300         666         79         20         302         402         402         402         402         403         404         412         412         413         403         404         410         424         410         454

Shaw, B A	409
Shaw, L L 202, 208,	346
Shcherbakov, A V	256
She, H	213
Sheen, S R	355
Shen, C	183
Shen, F	290
Shen, H	201
Shen, J	176
Shen, Y	408
Shepelyavyj, P E	451 180
Sheretz, R J	448
Shevade, S S	448 274
Shi, D 238,	448
Shi, D 258, Shi, X	179
Shi, X Q	339
Shi, Y	232
Shi, Z	357
Shian, S	291
Shibata, J 426, 427,	448
Shieh, Y C 199,	374
Shield, J E	388
Shields, J A 174,	215,
	400
Shiflet, G J 216,	217,
	442
Shigemastu, I	234
Shih, D 189,	416
Shih, M	179
Shih, P	338
Shiina, S	358
Shim, J	455
Shima, M 234,	334
Shimizu, T	358
Shin, D	221
Shin, D H	455
Shin, D H 254, 260,	350
Shin, D H 206, 208, 251,	253, 433
Shin. E	435 276
Shin, K S	270
Shinozuka, K 184,	301
Shiomori, K	449
Shizuo, N	269
Shobu, K	175
Shoji, T	294
Shreve, A 424,	447
Shrimpton, J	362
Shu, Y	380
Shuey, M S	364
Shuey, R T	347
Shukla, S	395
Shulan, W	367
Shull, R D	195
Shyam, A	418
Sichen, D	409
Sidhu, R	416
Sieck, L V	364
Siegel, R W	381
Siegert, K 234,	398 265
Siegfried, R M	365
Sikder A K	310
Sikder, A K Sikka, V	222 436
Sikora, M	430 321
Siljan, O 312,	400
~J, C	

Sim, G	214
Simak, S I	405
Sinclair, C S	307
Sinclair, I	
Sinclair, K	360
Singh, A K	429
Singh, P 235,	236
Singh, R J	312
Singler, T J 191,	417
Sinha, S K	250
Sinnott, M	218
Sinnott, S B	428
Sisneros, T 296,	297
Sisson, R 404,	423
Sisson, R D	409
Skar, J I	191
Skepper, I G 284,	372
Skibin, A P	318
Sklenicka, V	434
Skoptsov, A M	
Skripnyuk, V	260
· · · · · · · · · · · · · · · · · · ·	405
Skrotzki, W	401
Skyllas-Kazacos, M	267
Sleboda, T	413
Sluiter, M H	390
Slutsker, J 322, 334, 384,	425
Smith, D	273
Smith, F M	
Smith, S	
Smola, B	383
Smugeresky, J E 209,	261,
	418
Show D.C.	
Snow, R C	353
Snugovsky, P	331
Snugovsky, P Snurnitsyna, S S	331 312
Snugovsky, P Snurnitsyna, S S Snyder, A J	331 312 424
Snugovsky, P Snurnitsyna, S S Snyder, A J Snyder, G J	<ul> <li>331</li> <li>312</li> <li>424</li> <li>435</li> </ul>
Snugovsky, P Snurnitsyna, S S Snyder, A J Snyder, G J	<ul> <li>331</li> <li>312</li> <li>424</li> <li>435</li> <li>435</li> </ul>
Snugovsky, P Snurnitsyna, S S Snyder, A J Snyder, G J	<ul> <li>331</li> <li>312</li> <li>424</li> <li>435</li> <li>435</li> <li>214</li> </ul>
Snugovsky, P Snurnitsyna, S S Snyder, A J Snyder, G J Snyder, J So, C Sobkow, Z S	<ul> <li>331</li> <li>312</li> <li>424</li> <li>435</li> <li>435</li> <li>214</li> <li>321</li> </ul>
Snugovsky, P Snurnitsyna, S S Snyder, A J Snyder, G J	<ul> <li>331</li> <li>312</li> <li>424</li> <li>435</li> <li>435</li> <li>214</li> <li>321</li> <li>261,</li> </ul>
Snugovsky, P         Snurnitsyna, S S         Snyder, A J         Snyder, G J         Snyder, J         So, C         Sobkow, Z S         Sobyejo, W	<ul> <li>331</li> <li>312</li> <li>424</li> <li>435</li> <li>435</li> <li>214</li> <li>321</li> <li>261,</li> <li>377</li> </ul>
Snugovsky, P         Snurnitsyna, S S         Snyder, A J         Snyder, G J         Snyder, J         So, C         Sobkow, Z S         Sobyejo, W	<ul> <li>331</li> <li>312</li> <li>424</li> <li>435</li> <li>435</li> <li>214</li> <li>321</li> <li>261,</li> <li>377</li> <li>417</li> </ul>
Snugovsky, P         Snurnitsyna, S S         Snyder, A J         Snyder, G J         So, C         Sobkow, Z S         Soboyejo, W	<ul> <li>331</li> <li>312</li> <li>424</li> <li>435</li> <li>435</li> <li>214</li> <li>321</li> <li>261,</li> <li>377</li> <li>417</li> <li>275</li> </ul>
Snugovsky, P         Snurnitsyna, S S         Snyder, A J         Snyder, G J	<ul> <li>331</li> <li>312</li> <li>424</li> <li>435</li> <li>435</li> <li>214</li> <li>321</li> <li>261,</li> <li>377</li> <li>417</li> <li>275</li> <li>371</li> </ul>
Snugovsky, P         Snurnitsyna, S S         Snyder, A J         Snyder, G J	<ul> <li>331</li> <li>312</li> <li>424</li> <li>435</li> <li>435</li> <li>214</li> <li>321</li> <li>261,</li> <li>377</li> <li>417</li> <li>275</li> <li>371</li> <li>445</li> </ul>
Snugovsky, P         Snurnitsyna, S S         Snyder, A J         Snyder, G J	<ul> <li>331</li> <li>312</li> <li>424</li> <li>435</li> <li>435</li> <li>214</li> <li>321</li> <li>261,</li> <li>377</li> <li>417</li> <li>275</li> <li>371</li> <li>445</li> <li>410</li> </ul>
Snugovsky, P         Snurnitsyna, S S         Snyder, A J         Snyder, G J	331 312 424 435 435 214 321 261, 377 417 275 371 445 410 .382
Snugovsky, P         Snurnitsyna, S S         Snyder, A J         Snyder, G J	331 312 424 435 435 214 321 261, 377 417 275 371 445 410 382 441
Snugovsky, P         Snurnitsyna, S S         Snyder, A J         Snyder, G J	331 312 424 435 435 214 321 261, 377 417 275 371 445 410 .382 441 224
Snugovsky, P         Snurnitsyna, S S         Snyder, A J         Snyder, G J	331 312 424 435 435 214 321 261, 377 417 275 371 445 410 .382 441 224 400
Snugovsky, P         Snurnitsyna, S S         Snyder, A J         Snyder, G J	331 312 424 435 435 214 321 261, 377 417 275 371 445 410 .382 441 224 400 331
Snugovsky, P         Snurnitsyna, S S         Snyder, A J         Snyder, G J	331 312 424 435 435 214 321 261, 377 417 275 371 445 410 .382 441 224 400 331 283
Snugovsky, P	331 312 424 435 435 214 321 261, 377 417 275 371 445 410 .382 441 224 400 331 283 416
Snugovsky, P         Snurnitsyna, S S         Snyder, A J         Snyder, G J	331 312 424 435 435 214 321 261, 377 417 275 371 445 410 .382 441 224 400 331 283 416 318
Snugovsky, P	331 312 424 435 435 214 321 261, 377 417 275 371 445 410 .382 441 224 400 331 283 416 318 382
Snugovsky, P	331 312 424 435 435 214 321 261, 377 417 275 371 445 410 .382 441 224 400 331 283 416 318 382 350
Snugovsky, P	331 312 424 435 435 214 321 261, 377 417 275 371 445 410 .382 441 224 400 331 283 416 318 382
Snugovsky, P	331 312 424 435 435 214 321 261, 377 417 275 371 445 410 377 445 410 331 283 416 318 382 350 380 215
Snugovsky, P	331 312 424 435 435 214 321 261, 377 417 275 371 445 410 377 445 410 331 283 416 318 382 350 380 215
Snugovsky, P	331 312 424 435 425 4261, 321 261, 377 417 275 371 445 410 382 441 224 400 331 283 416 318 382 350 380 215 321 438
Snugovsky, P	331 312 424 435 435 214 321 261, 377 417 275 371 445 410 382 441 224 400 331 283 416 318 382 350 380 215 321 438 272
Snugovsky, P	331 312 424 435 435 214 321 261, 377 417 275 371 445 410 382 441 224 400 331 283 416 318 382 350 380 215 321 438 272 208
Snugovsky, P	331 312 424 435 425 426 435 214 321 261, 377 417 275 371 445 410 382 441 224 400 331 283 416 318 382 350 380 215 321 438 272 208 438 311
Snugovsky, P	331 312 424 435 425 426 435 214 321 261, 377 417 275 371 445 410 382 441 224 400 331 283 416 318 382 350 380 215 321 438 272 208 438 311

Spadafora, F	220, 278	, 406	Stree
Spaldin, N			Stroe
Spanos, G			Strog
Sparks, C J			Stron
Speakman, S Spelt, J K			Stucz Stulí
Spencer, D B			Sturn
Spencer, R			Sturn
Speyer, R F			Styre
Spolenak, R	188	, 394	Su, Y
Spreij, M			Subb
Spuskanyuk, A V			Subra
Srajer, G			 G . 1.
Sridhar, R Srinivasan, R			Suda Suda
Srinivasan, S G			Suda
			Sudb
Srinivasan, S S			Sudh
Srinivasan, V			Suem
Srivatsan, T S			Suery
Srolovitz, D J 182,			Suga
Stach, E A			Sugi
Staley, J T			Sui, Z
Stanbery, B J Stanciu, L A			Suk, Sulei
Stanton, K T			Sulli
Starke, E A			Sun,
Staudenmann, J			Sun,
Staudhammer, K P			Sun,
Stauffer, E			Sun,
Stefanescu, D M			Sun,
Steinbach, I			Sun,
Steiner, C Steiner, J			Sun, Sun,
Steingart, D A			Sun,
Stellacci, F			Sund
Stencel, J M			Sung
Stephens, C			Sung
Stephens, J J			Suni,
Stevens McFadden, F.			Sunk
Stevenson, J W			Supa
Stevenson, M E Steverson, W B			Sure! Sures
Steverson, W D			Surva
Stierman, R			Suss,
StJohn, D H			Süss,
			Sutor
Stober, F			Suyit
Stock, R			Suyit
Stockhausen, W			Suzu Suzu
Stoica, A D Stoica, G M			Suzu
Stoker, G			Suzu
Stölken, J S			Suzu
Stoloff, N S		. 413	Suzu
Stolyarov, V	208	, 350	Suzu
Stone, G A			Svob
Stone, I C			Swar
Stone, M O Stone, Z			Swar
Stone, Z			Swee Swer
Storm, D R			
Stoudt, M R			Swift
Stout, J		170	Swift
Stoyanov, S			Swis
Straatsma, E N			Swyg
Stratton, M		. 404	Synk
A 77	•		

Street, S C	
Stroeder, M	265
Stroganov, A G	245
Stronach, C E	
Stuczynski, T	403
Stulíková, I	383
Sturm, E	398
Sturm, P	265
Styrov, V V	169
Su, Y J	241
Subbanna, G N	239
Subramanian, K N 187, 188,	190,
	373
Suda, S	262
Sudakar, C	
Sudbrack, C K	
Sudhakar, K	
Sudhakar, N 196,	239
Suematsu, H	194
Suery, M	417
Suganuma, K 190,	338
Sugiyama, A	300
Sugryana, T	200
Suk, M	299
Suleiman, M	353
Sullivan, T M	435
Sun, D	263
Sun, F 278, 364,	440
Sun, H	440
Sun, W 320,	428
Sun, Y 520,	202
Sun, Y	176
Sun, Y	423
Sun, Z	232
Sun, Z Sundaresan, R	420
	224 428
Sung, P K Sung, Y	428 186
Suni, J P	347
Sunkara, M K 334,	
Supatarawanich, V	
Surek, T	169
Suresh, S 334,	420
Suryawanshi, A	450
Suryawanshi, A	312
Süss, R	
Suss, IX	270
	270 242
Sutou, Y	242
Sutou, Y Suyitno	242 220
Sutou, Y Suyitno Suyitno, X	242 220 203
Sutou, Y Suyitno Suyitno, X Suzuki, A	242 220 203 324
Sutou, Y Suyitno Suyitno, X Suzuki, A Suzuki, A	242 220 203 324 346
Sutou, Y Suyitno Suyitno, X Suzuki, A Suzuki, A Suzuki, M	242 220 203 324 346 384
Sutou, Y Suyitno Suyitno, X Suzuki, A Suzuki, A Suzuki, M Suzuki, S	242 220 203 324 346 384 194
Sutou, Y Suyitno Suyitno, X Suzuki, A Suzuki, A Suzuki, M Suzuki, S	242 220 203 324 346 384 .194 387
Sutou, Y Suyitno Suyitno, X Suzuki, A Suzuki, A Suzuki, M Suzuki, S Suzuki, T Suzuki, T	242 220 203 324 346 384 194 387 194
Sutou, Y Suyitno Suyitno, X Suzuki, A Suzuki, A Suzuki, M Suzuki, S Suzuki, T Suzuki, T Suzuki, Y	242 220 203 324 346 384 194 387 194 291
Sutou, Y Suyitno Suyitno, X Suzuki, A Suzuki, A Suzuki, M Suzuki, S Suzuki, T Suzuki, T Suzuki, Y Svoboda, J	242 220 203 324 346 384 194 387 194 291 405
Sutou, Y Suyitno Suyitno, X Suzuki, A Suzuki, A Suzuki, M Suzuki, S Suzuki, T Suzuki, T Suzuki, T Suzuki, Y Svoboda, J Swaminathan, S	242 220 203 324 346 384 194 387 194 291 405 259
Sutou, Y Suyitno Suyitno, X Suzuki, A Suzuki, A Suzuki, M Suzuki, S Suzuki, T Suzuki, T Suzuki, T Svoboda, J Swaminathan, S	242 220 203 324 346 384 194 387 194 291 405 259 405
Sutou, Y Suyitno Suyitno, X Suzuki, A Suzuki, A Suzuki, M Suzuki, T Suzuki, T Suzuki, T Svoboda, J Swaminathan, S Suzuf, Swaminathan, S Suzuf, Swan-Wood, T Suzuf, State S	242 220 203 324 346 384 194 387 194 291 405 259 405 403
Sutou, Y         Suyitno         Suyitno, X         Suzuki, A         Suzuki, A         Suzuki, M         Suzuki, T         Suzuki, T         Suzuki, Y         Svoboda, J         Swaminathan, S       207,         Swan-Wood, T       354,         Swenson, D J       198, 240,	242 220 203 324 346 384 194 387 194 291 405 259 405 403 241,
Sutou, Y Suyitno Suyitno, X Suzuki, A Suzuki, M Suzuki, S Suzuki, T Suzuki, T Svoboda, J Swaminathan, S Swam.Wood, T Sweet, E Swenson, D J 198, 240, 	242 220 203 324 346 384 194 387 194 291 405 259 405 403 241, 417
Sutou, Y Suyitno Suyitno, X Suzuki, A Suzuki, A Suzuki, M Suzuki, T Suzuki, T Suzuki, T Svoboda, J Swaminathan, S Swaminathan, S Swan-Wood, T Sweet, E Swenson, D J Swenson, D J Swaft, D	242 220 324 346 384 194 387 194 291 405 259 405 403 241, 417 201
Sutou, Y         Suyitno         Suyitno, X         Suzuki, A         Suzuki, M         Suzuki, S         Suzuki, T         Suzuki, T         Suzuki, Y         Svoboda, J         Swaminathan, S       207,         Swaeet, E         Sweet, E         Swenson, D J       198, 240,	242 220 324 346 384 194 291 405 259 405 259 405 403 241, 417 201 284
Sutou, Y         Suyitno         Suyitno, X         Suzuki, A         Suzuki, A         Suzuki, M         Suzuki, T         Suzuki, T         Suzuki, T         Suzuki, T         Svoboda, J         Swaminathan, S       207,         Swan-Wood, T       354,         Sweet, E       Swenson, D J         Swift, D       293, 338, 382,         Swift, G A       283,         Swisher, D L       283,	242 220 324 346 384 194 291 405 259 405 403 241, 417 201 284 252
Sutou, Y         Suyitno         Suyitno, X         Suzuki, A         Suzuki, M         Suzuki, S         Suzuki, T         Suzuki, T         Suzuki, Y         Svoboda, J         Swaminathan, S       207,         Swaeet, E         Sweet, E         Swenson, D J       198, 240,	242 220 324 346 384 194 291 405 259 405 259 405 403 241, 417 201 284

Szpunar, J A	221,	249,	254,
	281,	356,	452
Szymczak, R			321

# Т

<b>T</b> 1 <b>T</b>		1 7 5
Tabaru, T		175
Tabereaux, A T 170,		176,
	217,	218,
	272,	311,
	356,	360.
		439
Tada, S		420
Taua, 5	•••••	
Taghavi, S M		369
Takahashi, K		323
Takaku, Y		191
Takami, Y		426
Takamiya, H		440
Takano, H		415
Takashi, S		449
Takasugi, T		
	1/4,	401
Takeshita, H T 309,		436
Takeuchi, I		289
Talas, S		290
Talbot, D E         343,           Taleff, E M         184,         211,	427,	428
Taleff, E M 184, 211,	225.	226,
	326,	355,
		441
Talin, A		308
Tallant, D R		430
Tamura, M		301
Tamura, N 372,	394,	441
Tan, H		345
Tan, L		428
	335,	404
Tanabe, M		427
Tanaka, M		449
Tandon, S		196
Tandon, S C		317
Tang, J		380
Tang, W		296
Tarasov, A V		186,
		449
Tatalovich, J		352
Tatyanin, E V		253
Taub, M		240
Tavares, R P		320
Tavera, F J		378
Tawfic, S N		200
Тауа, М		201
Taylor, C		212
Taylor, J A		385
Taylor, M P		212
Taylor, P R		426
Tedstrom, R		222
Teigs, T N		372
Telang, AU 188,		229
Telesman, J		340
Téllez-Martínez, J S	408,	409
Tenhundfeld, G		185
Teramoto, S		401
Teranishi, K		406
Terpstra, R L		295
Teter, D F 233,		396
Tewari, R		400
Tewari, S N		248
Thibault, M		171

Thiel, G H	286
Thirumalai, N	183
Thom, A J 175,	215
Thoma, D J 253,	283
Thomas, B G 203,	218,
	446
Thomas, J	272
Thompson, L J	238
Thompson, S A	411
Thompson, S R	407
Thomson, P F 269,	333
Thonstad, J	437
Thuramalla, N V	398
Thurston, A K	360
Tian, B	254
Tian, H 184, 202, 226,	297
Tian, Z	357
Tikare, V	242
Tilly, D J	278
Timofeeva, V	369
Tin, S	174
Tiryakioglu, M	347
Tiwari, A 195,	237,
	336
Tiwari, R	248
Tizon, E	170
Toda, H	411
Todaka, Y	253
Tokar, V	348
Tokarz, M L	176
Tokimatsu, R C	368
Tomala, J	177
Tomasino, T	437
Tome, C N 207, 255,	339
Tommey, C	172
Tomokiyo, Y	390
Tong, L	243
Tonheim, J	172
Tonti, R T	217
Торро, В	368
Torbet, C J	418
Torek, P	172
Torosyan, A R	236
Torres, V 230, 231, 329,	443
Torsiello, S	171
Tortorelli, P F 174, 215,	269,
	400
Tran, S	416
Tratteberg, O	172
Trebuh, O A	267
Trichy, G R	256
Triessnig, A	404
Trinkle, D R 183,	431
Trivedi, P B	279
Trivedi, R 202, 247,	299,
	386
Trojanova, Z	425
Trubitsyna, I B	253
Trumble, K P 195, 207,	259
Tryon, B	270
Tsai, C M 332,	338
Tsai, D	332
Tsai, J Y 199,	374
Tsai, Y	285
Tsakiropoulos, P 175,	216,
13akiropoulos, 1	421
Tsau, C H	176
1 Jau, U 11	1/0

Tso, C	227
Tsuchida, N	328
Tsuchiya, K	253
Tsuchiyama, A	300
Tsui, F	238
Tsuji, N 207, 259, 351,	388
Tsunekane, M	315
Tsuzuki, R	418
Tszeng, C	314
Tu, K 187, 231,	294
Tuominen, M T	336
Turbini, L J 189,	231,
	416
Turchi, P E 192, 304,	348
Turner, J	329
Turpeinen, P	286
Tyagi, S A	268
Tyumentsev, A N 254, 256,	257

# U

Ubhi, H S	411
Uchic, M D 309,	352
Ucok, I 223, 323,	365
Udaykumar, H S	249
Udovic, T J	210
Ueda, M	324
Ueji, R	259
Uekawa, N	296
Ueshima, M	190
Uesugi, K	300
Uhrig, J R	318
Ulfig, R M	198
Umakoshi, Y	390
Umantsev, A	196
Umeda, T	
Umemoto, M 253,	305
Ungár, T	350
Unland, J	240
Unlu, N	363
Upadhaya, C	336
Upadhyay, V	274
	443
Urbani, M D	
Ustundag, E 176, 271, 272,	283,
	372
Utigard, T A	313
Utsunomiya, H	206
Utyashev, F Z	255

# $\mathbf{V}$

Vabishchevich, P	437
Vahed, A	329
Vaidyanathan, R 201,	246,
	342
Vainik, R	403
Valek, B C	394
Valiev, R Z 206, 251, 252,	253,
	258,
	307
	432
Valls, R A	230
van de Walle, A 304, 358,	430
Van Den Avyle, J J	342
van den Broek, B	312
Van der Giesen, E	. 377
van der Merwe, J H 228,	327

van der Meulen, D	329
Van der Ven, A	
Van Haaften, W	385
Van Humbeek, J	392
v all Hullideck, J	
van Klaveren, E P	219
Van Schaik, A	200
Van Vliet, K J	334
Van Weert, G	333
Van Wert, J	370
Vandermeer, R A	204
Vanderson, E	261
VanEvery, K J	219
Vanvoren, C	. 172
	. 172
Vardıll, W	. 188
Vardill, W	260
Vashishth D 410	
Vashishth, D 418,	419
Vasiliev, A L	346
	321
Vasquez, O 199,	
Vasudevan, A K 347,	348
Vasudevan, V K 175, 238,	301,
v asuac vali, v IX 175, 250,	
	400
Vaudreuil, S	361
Vega, S	215
Velgosova, O 296,	311
Vella, J B	229
Venkatesh, R	289
Venkatesh, V	407
Venkateswaran, S	422
Venskutonis, A 315,	358
Verlinden, B	392
Verma, H C	336
Verma, R	
Verma, V	233
Vetrano IS	355
Vetrano, J S	355
Vetrano, J S Vetrone, J M	355 238
Vetrone, J M	238
Vetrone, J M Vetter, R	238 . 195
Vetrone, J M Vetter, R Vianco, P T 331,	238 . 195 338
Vetrone, J M Vetter, R Vianco, P T 331,	238 . 195 338
Vetrone, J M Vetter, R Vianco, P T	238 . 195 338 448
Vetrone, J M Vetter, R Vianco, P T	238 . 195 338 448 . 272
Vetrone, J M Vetter, R Vianco, P T	238 . 195 338 448 . 272 384
Vetrone, J M Vetter, R Vianco, P T	238 . 195 338 448 . 272 384
Vetrone, J M Vetter, R Vianco, P T	238 . 195 338 448 . 272 384 361
Vetrone, J M Vetter, R Vianco, P T	238 . 195 338 448 . 272 384
Vetrone, J M Vetter, R Vianco, P T	238 . 195 338 448 . 272 384 361
Vetrone, J M Vetter, R Vianco, P T	238 .195 338 448 .272 384 361 208 422
Vetrone, J M Vetter, R Vianco, P T	238 .195 338 448 .272 384 361 208 422 392
Vetrone, J M Vetter, R Vianco, P T	238 .195 338 448 .272 384 361 208 422 392 444
Vetrone, J M Vetter, R Vianco, P T	238 .195 338 448 .272 384 361 208 422 392 444
Vetrone, J M Vetter, R Vianco, P T	238 .195 338 448 .272 384 361 208 422 392 444 410
Vetrone, J M Vetter, R Vianco, P T	238 .195 338 448 .272 384 361 208 422 392 444 410 299,
Vetrone, J M Vetter, R Vianco, P T	238 .195 338 448 .272 384 361 208 422 392 444 410
Vetrone, J M Vetter, R	238 .195 338 448 .272 384 361 208 422 392 444 410 299, 449
Vetrone, J M Vetter, R	238 .195 338 448 .272 384 361 208 422 392 444 410 299, 449 345
Vetrone, J M Vetter, R	238 .195 338 448 .272 384 361 208 422 392 444 410 299, 449
Vetrone, J M Vetter, R	238 .195 338 448 .272 384 361 208 422 392 444 410 299, 449 345
Vetrone, J M Vetter, R	238 .195 338 448 .272 384 361 208 422 392 444 410 299, 449 345 348 445
Vetrone, J M Vetter, R Vianco, P T	238 .195 338 448 .272 384 361 208 422 392 444 410 299, 449 345 348 445 213
Vetrone, J M Vetter, R Vianco, P T	238 .195 338 448 .272 384 361 208 422 392 444 410 299, 449 345 348 445
Vetrone, J M Vetter, R	238 .195 338 448 .272 384 361 208 422 392 444 410 299, 449 345 348 445 213 331
Vetrone, J M Vetter, R	238 .195 338 448 .272 384 361 208 422 392 444 410 299, 449 345 348 445 213 331 383
Vetrone, J M Vetter, R	238 .195 338 448 .272 384 361 208 422 392 444 410 299, 449 345 348 445 213 331
Vetrone, J M Vetter, R	238 .195 338 448 .272 384 361 208 422 392 444 410 299, 449 345 348 445 213 331 383 434
Vetrone, J M Vetter, R	238 .195 338 448 .272 384 361 208 422 392 444 410 299, 449 345 348 445 213 331 383 434 336
Vetrone, J M Vetter, R	238 .195 338 448 .272 384 361 208 422 392 444 410 299, 449 345 348 445 213 331 383 434 336 217
Vetrone, J M Vetter, R	238 .195 338 448 .272 384 361 208 422 392 444 410 299, 449 345 348 445 213 331 383 434 336
Vetrone, J M Vetter, R	238 .195 338 448 .272 384 361 208 422 392 444 410 299, 449 345 348 445 213 331 383 434 336 217 437
Vetrone, J M Vetter, R	238 .195 338 448 .272 384 361 208 422 392 444 410 299, 449 345 348 445 213 331 383 434 336 217 437 176
Vetrone, J M Vetter, R	238 .195 338 448 .272 384 361 208 422 392 444 410 299, 449 345 348 445 213 331 383 434 336 217 437 176 188
Vetrone, J M Vetter, R	238 .195 338 448 .272 384 361 208 422 392 444 410 299, 449 345 348 445 213 331 383 434 336 217 437 176 188
Vetrone, J M	238 .195 338 448 .272 384 361 208 422 392 444 410 299, 449 345 348 445 213 331 383 434 336 217 437 176 188 270
Vetrone, J M	238 .195 338 448 .272 384 361 208 422 392 444 410 299, 449 345 348 445 213 331 383 434 336 217 437 176 188 270 248
Vetrone, J M	238 .195 338 448 .272 384 361 208 422 392 444 410 299, 449 345 348 445 213 331 383 434 336 217 437 176 188 270 248
Vetrone, J M	238 .195 338 448 .272 384 361 208 422 392 444 410 299, 449 345 348 445 213 331 383 434 336 217 437 176 188 270 248 383
Vetrone, J M	238 .195 338 448 .272 384 361 208 422 392 444 410 299, 449 345 348 445 213 331 383 434 336 217 437 176 188 270 248 383 322
Vetrone, J M	238 .195 338 448 .272 384 361 208 422 392 444 410 299, 449 345 348 445 213 331 383 434 336 217 437 176 188 270 248 383 322 .270
Vetrone, J M	238 .195 338 448 .272 384 361 208 422 392 444 410 299, 449 345 348 445 213 331 383 434 336 217 437 176 188 270 248 383 322 .270
Vetrone, J M	238 .195 338 448 .272 384 361 208 422 392 444 410 299, 449 345 348 445 213 331 383 434 336 217 437 176 188 270 248 383 322 .270 350
Vetrone, J M	238 .195 338 448 .272 384 361 208 422 392 444 410 299, 449 345 348 445 213 331 383 434 336 217 437 176 188 270 248 383 322 .270 350

Vuik, C	248
Vulcan, M	398

# W

Wadley, H N 320	5, 352
Waghmare, U	304
Wagner, G J	
Wagnière, J 203	
Wagoner, R H 214	4, 314
WaKimoto, Y	. 200
Waku, Y	
Waldo, R A	
Waldron, D J	268
Walker, C A	
Walker, M S 235	
Wall, J J	372
Wallace, J P	365
Walters, R T	
Walukas, D M	
Wan, X	276
Wang, C 278	3, 406
Wang, D	
Wang, G 178, 190	), 387
Wang, G 202, 220	5, 271
Wang, G Y 272	1, 411
Wang, H 379	
Wang, H	302
Wang, H	424
Wang, J	
Wang, J	181
Wang, J	242
Wang, J 207, 251, 257, 258	3, 260
Wang, J	356
Wang, J C	
Wang, L	219
Wang, M	
-	
Wang, N	
Wang, P 310	5, 360
Wang, P T	412
Wang, Q	
Wang, Q	
Wang, Q 410	), 411
Wang, R	440
Wang, R J	
Wang, S	
Wang, S	243
Wang, S	. 233
Wang, S F	
Wang, S H	
Wenn CI	275
Wang, S J	. 3/3
Wang, T	322
Wang, T	322 3, 364
Wang, T	322 3, 364 426
Wang, T	322 3, 364 426
Wang, T         363           Wang, T         363           Wang, W         217	322 3, 364 426 7, 402
Wang, T         363           Wang, T         363           Wang, W         217           Wang, X         217	322 3, 364 426 7, 402 410
Wang, T       363         Wang, T       363         Wang, W       217         Wang, X       184, 297	322 3, 364 426 7, 402 410 7, 402
Wang, T       363         Wang, W       363         Wang, W       217         Wang, X       184, 297         Wang, Y       363	322 3, 364 426 7, 402 410 7, 402 197
Wang, T       363         Wang, W       363         Wang, W       217         Wang, X       184, 297         Wang, Y       384, 297	322 3, 364 426 7, 402 410 7, 402 197 291
Wang, T       363         Wang, W       363         Wang, W       217         Wang, X       184, 297         Wang, Y       384, 297	322 3, 364 426 7, 402 410 7, 402 197 291
Wang, T       363         Wang, W       363         Wang, W       217         Wang, W H       217         Wang, X       184, 297         Wang, Y       184, 297         Wang, Y       184, 297         Wang, Y       184	322 3, 364 426 7, 402 410 7, 402 197 291 4, 297
Wang, T       363         Wang, W       363         Wang, W H       217         Wang, X       363         Wang, X       184, 297         Wang, Y       184, 297         Wang, Y       184, 297         Wang, Y       184         Wang, Y       184         Wang, Y       184         Wang, Y       184	322 3, 364 426 7, 402 410 7, 402 197 291 4, 297 431
Wang, T       363         Wang, T       363         Wang, W       217         Wang, W H       217         Wang, X       184, 297         Wang, Y       184, 297         Wang, Y       184, 297         Wang, Y       184, 297         Wang, Y       184	322 3, 364 426 7, 402 410 7, 402 197 291 4, 297 431 421
Wang, T       363         Wang, T       363         Wang, W       217         Wang, W H       217         Wang, X       184, 297         Wang, Y       184         Wang, Y       305, 322, 363	322 3, 364 426 7, 402 410 7, 402 197 291 4, 297 431 421 3, 364
Wang, T       363         Wang, T       363         Wang, W       217         Wang, W H       217         Wang, X       184, 297         Wang, Y       184         Wang, Y       305, 322, 363	322 3, 364 426 7, 402 410 7, 402 197 291 4, 297 431 421 3, 364
Wang, T       363         Wang, T       363         Wang, W       217         Wang, W H       217         Wang, X       184, 297         Wang, Y       184         Wang, Y       305, 322, 363	322 3, 364 426 7, 402 410 7, 402 197 291 4, 297 431 421 3, 364
Wang, T       363         Wang, T       363         Wang, W       217         Wang, W H       217         Wang, X       184, 297         Wang, Y       184         Wang, Y       305, 322, 363         Wang, Y       174, 182, 183	322 3, 364 426 7, 402 410 7, 402 197 291 4, 297 431 421 3, 364 391 3, 224,
Wang, T       363         Wang, W       363         Wang, W       217         Wang, W H       217         Wang, X       184, 297         Wang, Y       184         Wang, Y       184         Wang, Y       184         Wang, Y       184         Wang, Y       305, 322, 363         Wang, Y       305, 322, 363         Wang, Y       174, 182, 183	322 3, 364 426 7, 402 410 7, 402 197 291 4, 297 431 421 3, 364 391 3, 224, 5, 407
Wang, T       363         Wang, T       363         Wang, W       217         Wang, W H       217         Wang, X       184, 297         Wang, Y       184         Wang, Y       305, 322, 363         Wang, Y       174, 182, 183	322 3, 364 426 7, 402 410 7, 402 197 291 4, 297 431 421 3, 364 391 3, 224, 5, 407
Wang, T       363         Wang, W       363         Wang, W       217         Wang, W H       217         Wang, X       184, 297         Wang, Y       184         Wang, Y       184         Wang, Y       184         Wang, Y       184         Wang, Y       305, 322, 363         Wang, Y       305, 322, 363         Wang, Y       174, 182, 183	322 3, 364 426 7, 402 410 7, 402 197 291 4, 297 431 421 3, 364 391 3, 224, 5, 407

Wang, Z	
Wang, Z	286
Wang, Z	417
Wang, Z X	
Wanjale, M	302
Wannasin, J	296
Wanashi, J Ward, W G	
· · · · · · · · · · · · · · · · · · ·	
Ward-Close, C M	407
Warren, J A 276, 322,	386
Waryoba, D R	205
Watanabe, M	432
Watanabe, T	390
Waterstrat, R M	304
Watkins, T R	400
Watson, T J	419
Watson, 15	401
Waz, E	437
Weaver, M L 262,	367,
	441
Webb, D A	220
Webster, T J	197
Wedde, G	398
Weertman, J	201
Weertman, J R	349
	353
Wegryzn, J	
Wei, C	382
Wei, C C	332
Wei, J	. 232
Wei, J H	290
Wei, L	421
Wei, M	243
Wei, W	260
Weil, K	235
Weil, K G	409
Weiland, H	277
Weinan, E	
Weirauch, Jr., D A	273
Weissmueller, J	346
Welch, B	267
Welch, B J 212,	399
Wellnitz, R	214
Wells, M A 268,	386
Welp, U	250
Welsh, G S 271,	272
Wen, S 280,	281
Wen, W	314
Wenderoth, M	270
Weninger, J A	251
Wenner, M	233
Wermer, J R 210, 262, 395,	436
Werner, J	.215
Werner, J H	447
Wetscher, F	254
	302
Wetteland, C J	
Wezyk, W	403
Wheeler, D 220,	280
White, B	
White, D	. 329
White, P	267
Whitfield, D S	267
Whiting, M	216
Whittington, B I	
Widjaja, A	
Widom, M	431
Wiench, J	
Wiezorek, J M	379
Wilde, G 346,	351

Wilkening, S	177
Wilkins, J W 183,	431
Wilkinson, D S	269,
	355
Willander, M	180
Williams, D B	432
Williams, F S	170
Williams, G A	242
	185
Williams, R K	
Wilson, O C	446
Winkelman, G	371
Winterscheidt, D L 278,	406
Winther, G 252,	302
Wirth, B D	183
Wiseman, M	189
	244
Withers, A	
Withers, J C 224,	278
Withers, P J	297
Wittig, J E	327
Wochner, P	250
Wolanski, R 172,	173
Wolf, A	266
	305
Wolf, D	
Wolfe, R C	
Wolverton, C 181, 205, 250,	277,
	430
Wolverton, C C	406
Wong, C K	232
Wong, G C	239
Wong, L L	246
Wong, P W	439
Woo, W	297
Wood, J R	173
Woodard, S	215
Woodman, R H	254
	416
Woods, J J	
Woods, J J Woodward, C	322
Woodward, C	322 430
Woodward, C	430
Woodward, C	430 174
Woodward, C	430 174 416
Woodward, C	430 174 416 354
Woodward, C	430 174 416
Woodward, C	430 174 416 354
Woodward, C	430 174 416 354 338 413
Woodward, C	430 174 416 354 338 413 286
Woodward, C	430 174 416 354 338 413 286 313
Woodward, C       183,         Wright, I G       183,         Wright, J       Wright, P K         Wright, R D       Wright, R N         Wright, W       Wright, W         Wright, W       181, 225, 226,	430 174 416 354 338 413 286 313 281
Woodward, C         Woodward, C       183,         Wright, I G       183,         Wright, J       183,         Wright, P K       183,         Wright, R D       181,         Wright, W       183,         Wright, W       181,         Wu, D T       181,       225,         Wu, E       181,       225,	430 174 416 354 338 413 286 313 281 348
Woodward, C         Woodward, C         183,         Wright, I G         Wright, J         Wright, P K         Wright, R D         Wright, R N         Wright, W         Wright, W         Wu, B         Wu, D T       181, 225, 226,         Wu, J	430 174 416 354 338 413 286 313 281 348 375
Woodward, C         Woodward, C       183,         Wright, I G       183,         Wright, J       183,         Wright, P K       183,         Wright, R D       181,         Wright, W       183,         Wright, W       181,         Wu, D T       181,       225,         Wu, E       181,       225,	430 174 416 354 338 413 286 313 281 348 375 322
Woodward, C         Woodward, C         183,         Wright, I G         Wright, J         Wright, P K         Wright, R D         Wright, R N         Wright, W         Wright, W         Wu, B         Wu, D T       181, 225, 226,         Wu, J	430 174 416 354 338 413 286 313 281 348 375
Woodward, C         Woodward, C         183,         Wright, I G         Wright, P K         Wright, R D         Wright, R N         Wright, W         Wright, W         Wu, B         Wu, D T         Wu, E         Wu, J         Wu, K	430 174 416 354 338 413 286 313 281 348 375 322
Woodward, C       183,         Wright, I G       183,         Wright, J J       Wright, P K         Wright, R D       Wright, R N         Wright, W       Wright, W         Wu, B       181, 225, 226,         Wu, E       Wu, J         Wu, J       Wu, J         Wu, K       Wu, K	430 174 416 354 338 413 286 313 281 348 375 322 240 421
Woodward, C         Woodward, C         183,         Wright, I G         Wright, J         Wright, P K         Wright, R D         Wright, R N         Wright, W         Wuight, W         Wu, B         Wu, D T         Wu, E         Wu, J         Wu, K         Wu, K         Wu, K         Wu, M         Wu, M         178, 247,	430 174 416 354 338 413 286 313 281 348 375 322 240 421 423
Woodward, C         Woodward, C         183,         Wright, I G         Wright, J         Wright, P K         Wright, R D         Wright, R N         Wright, W         Wuight, W         Wu, B         Wu, D T         Wu, B         Wu, Z         Wu, K         Wu, K         Wu, K         Wu, K         Wu, M         178, 247,         Wu, W	<ul> <li>430</li> <li>174</li> <li>416</li> <li>354</li> <li>338</li> <li>413</li> <li>286</li> <li>313</li> <li>281</li> <li>348</li> <li>375</li> <li>322</li> <li>240</li> <li>421</li> <li>423</li> <li>326</li> </ul>
Woodward, C         Woodward, C         183,         Wright, I G         Wright, J         Wright, P K         Wright, R D         Wright, R N         Wright, W         Wu, B         Wu, D T         181, 225, 226,         Wu, E         Wu, K         Wu, K         Wu, K         Wu, K         Wu, M         178, 247,         Wu, X	<ul> <li>430</li> <li>174</li> <li>416</li> <li>354</li> <li>338</li> <li>413</li> <li>286</li> <li>313</li> <li>281</li> <li>348</li> <li>375</li> <li>322</li> <li>240</li> <li>421</li> <li>423</li> <li>326</li> <li>287</li> </ul>
Woodward, C         Woodward, C         183,         Wright, I G         Wright, J         Wright, P K         Wright, R D         Wright, R N         Wright, W         Wu, B         Wu, D T         Wu, B         Wu, K         Wu, K         Wu, K         Wu, K         Wu, K         Wu, K         Wu, M         178, 247,         Wu, X	<ul> <li>430</li> <li>174</li> <li>416</li> <li>354</li> <li>338</li> <li>413</li> <li>286</li> <li>313</li> <li>281</li> <li>348</li> <li>375</li> <li>322</li> <li>240</li> <li>421</li> <li>423</li> <li>326</li> <li>287</li> <li>233</li> </ul>
Woodward, C         Woodward, C         183,         Wright, I G         Wright, J         Wright, P K         Wright, R D         Wright, R N         Wright, W         Wu, B         Wu, D T         Wu, B         Wu, U T         Wu, K         Wu, J         Wu, K         Wu, K         Wu, K         Wu, M         178, 247,         Wu, X         Wu, X	430 174 416 354 338 413 286 313 281 348 375 322 240 421 423 326 287 233 238
Woodward, C         Woodward, C         183,         Wright, I G         Wright, J         Wright, P K         Wright, R D         Wright, R N         Wright, W         Wu, B         Wu, D T         Wu, B         Wu, K         Wu, K         Wu, K         Wu, K         Wu, K         Wu, K         Wu, M         178, 247,         Wu, X	430 174 416 354 338 413 286 313 281 348 375 322 240 421 423 326 287 233 238

# X

Xi, J H	421
Xia, G 235,	236
Xia, X 276,	332
Xia, Z	232
Xia, Z C 397,	398
Xiang, X	290
Xiang, Y	182

Xiao, H 439
Xiao, J Q 290
Xiao, X 295
Xie, F 298
Xie, S
Xie, Y 265
Xihong, Y 269
Xing, Q
Xu, C 256, 258, 311, 392, 433
Xu, G 231
Xu, H
Xu, H 299, 318
Xu, J 176
Xu, J
Xu, K
Xu, Q
Xu, R
Xu, W
Xu, Y
Xu, Y
Xu, Y B 412
Xue, L
Xue, Q 326, 367
Xueyi, G 378
1100,1, 0
Y

Ya Ping, Y 3	325
	153
	+35 345
	269
	415
	401
	200
	148
	358
,	323
,	315
	95
	298
6,	271
8	130
	382
Yang, D	
Yang, F	
Yang, H4	
Yang, H2	
Yang, J	
Yang, J 4	
Yang, M 1	94
Yang, N Y 3	308
	312
	321
Yang, W 3	328
Yang, W 2	233
	87
	249
Yang, Y 2	265
Yang, Y 2	216
	362
	332
	93
Yang, Z G 235, 2	236
	133
	121
	350
<u> </u>	341
* * *	

Yassar, R S	•••••	347
Yasskin, P B		259
Yasuda, H		300
Yatsui, K		194
Yazami, R		
Ydstie, B		356
Ye, F		295
Yee, C E		
Yeh, A		
Yeh, H		440
Yeh, H H		440
Yeo, I		358
Yi, J		173
Yi, J		283
Yildirim, T		210
Yin, L	191,	417
Yin, Z		171
Yinbiao, Y		234
Ying, J Y		291
Yingjun, L		367
Yoko, Y		269
Yokobayashi, M		215
Yokoyama, Y		359
Yonamine, T		204
Yoon, C		
Yoon, J		
Yoon, K E		251
Yoon, M		293
Yoon, S		438
Yoon, S W		241
Yoon, Y B		412
Yoon, Y S		275
Yoshida, S		296
Yoshimi, K	215,	315
Yost, F G		368
Young, J A		183
Youssef, K M		391
Yu, A		447
Yu, J 189,		285
	382	416
Yu, K		406
Yu, L		
Yu, O		182
Yu, S		254
Yuan, H		319
Yuan, L		354
Yuan, W 202,		271
Yuan, Z		401
Yuanchi, D		368
Yücel, O		185
Yue, S		233
Yunyou, Z		325
Yurchenko, L I		260
Yurievich, B E		194
Yurko, J		
Yurkov, V V		
Yuzyuk, Y I		
Yvon, K		
1 . 511, 11		557

# Z

Zabaras, N	235,	237,	319,	428
Zacharia, T				223
Zaitsev, A				342
Zakharov, A E				245
Zakharov, ID				280
Zamiri, A				431

Zamkotowicz, Z	403
Zangari, G	237
Zantye, P	222
Zarembo, S	321
Zavalij, L 382,	416
Zawierucha, R	343
Zeh, J	266
Zehetbauer, M 252, 392, 391,	393
Zeipper, L	392
Zelenitsas, K	175
Zelin, M	355
Zender, G A	
Zeng, K	293
Zeng, X	383
Zerkle, R 213,	399
Zevgolis, E N 330,	373
Zhai, C	288
Zhai, T	410
Zhang, D 323,	413
Zhang, D L	406
Zhang, F	407
Zhang, G	
Zhang, G P	188
Zhang, H	223
Zhang, J	213
Zhang, J H 412,	421
Zhang, K 349,	413
Zhang, L	290
Zhang, M	295
Zhang, M	357
Zhang, M	228
Zhang, Q A	210
Zhang, R	259
Zhang, S 290,	445
Znang. S	
Zhang, W	
Zhang, W	
Zhang, W	432 370
Zhang, W 187, 295, Zhang, X 197, 239, 261,	432 370 291,
Zhang, W	432 370 291, 447
Zhang, W	432 370 291, 447
Zhang, W	432 370 291, 447
Zhang, W	432 370 291, 447 421 313
Zhang, W	432 370 291, 447 421 313 345
Zhang, W	432 370 291, 447 421 313 345 290
Zhang, W	432 370 291, 447 421 313 345
Zhang, W	<ul> <li>432</li> <li>370</li> <li>291,</li> <li>447</li> <li>421</li> <li>313</li> <li>345</li> <li>290</li> <li>375</li> </ul>
Zhang, W	432 370 291, 447 421 313 345 290 375 257
Zhang, W	<ul> <li>432</li> <li>370</li> <li>291,</li> <li>447</li> <li>421</li> <li>313</li> <li>345</li> <li>290</li> <li>375</li> <li>257</li> <li>451</li> </ul>
Zhang, W	432 370 291, 447 421 313 345 290 375 257 451 428
Zhang, W	432 370 291, 447 421 313 345 290 375 257 451 428
Zhang, W	432 370 291, 447 421 313 345 290 375 257 451 428 217
Zhang, W	432 370 291, 447 421 313 345 290 375 257 451 428 217 380
Zhang, W	<ul> <li>432</li> <li>370</li> <li>291,</li> <li>447</li> <li>421</li> <li>313</li> <li>345</li> <li>290</li> <li>375</li> <li>257</li> <li>451</li> <li>428</li> <li>217</li> <li>380</li> <li>322</li> </ul>
Zhang, W	<ul> <li>432</li> <li>370</li> <li>291,</li> <li>447</li> <li>421</li> <li>313</li> <li>345</li> <li>290</li> <li>375</li> <li>257</li> <li>451</li> <li>428</li> <li>217</li> <li>380</li> <li>322</li> <li>402</li> </ul>
Zhang, W	<ul> <li>432</li> <li>370</li> <li>291,</li> <li>447</li> <li>421</li> <li>313</li> <li>345</li> <li>290</li> <li>375</li> <li>257</li> <li>451</li> <li>428</li> <li>217</li> <li>380</li> <li>322</li> <li>402</li> <li>173</li> </ul>
Zhang, W	<ul> <li>432</li> <li>370</li> <li>291,</li> <li>447</li> <li>421</li> <li>313</li> <li>345</li> <li>290</li> <li>375</li> <li>257</li> <li>451</li> <li>428</li> <li>217</li> <li>380</li> <li>322</li> <li>402</li> <li>173</li> </ul>
Zhang, W	<ul> <li>432</li> <li>370</li> <li>291,</li> <li>447</li> <li>421</li> <li>313</li> <li>345</li> <li>290</li> <li>375</li> <li>257</li> <li>451</li> <li>428</li> <li>217</li> <li>380</li> <li>322</li> <li>402</li> <li>173</li> <li>454</li> </ul>
Zhang, W	<ul> <li>432</li> <li>370</li> <li>291,</li> <li>447</li> <li>421</li> <li>313</li> <li>345</li> <li>290</li> <li>375</li> <li>257</li> <li>451</li> <li>428</li> <li>217</li> <li>380</li> <li>322</li> <li>402</li> <li>173</li> <li>454</li> <li>265</li> </ul>
Zhang, W	<ul> <li>432</li> <li>370</li> <li>291,</li> <li>447</li> <li>421</li> <li>313</li> <li>345</li> <li>290</li> <li>375</li> <li>257</li> <li>451</li> <li>428</li> <li>217</li> <li>380</li> <li>322</li> <li>402</li> <li>173</li> <li>454</li> <li>265</li> <li>257</li> </ul>
Zhang, W	<ul> <li>432</li> <li>370</li> <li>291,</li> <li>447</li> <li>421</li> <li>313</li> <li>345</li> <li>290</li> <li>375</li> <li>257</li> <li>451</li> <li>428</li> <li>217</li> <li>380</li> <li>322</li> <li>402</li> <li>173</li> <li>454</li> <li>265</li> <li>257</li> <li>451</li> </ul>
Zhang, W	<ul> <li>432</li> <li>370</li> <li>291,</li> <li>447</li> <li>421</li> <li>313</li> <li>345</li> <li>290</li> <li>375</li> <li>257</li> <li>451</li> <li>428</li> <li>217</li> <li>380</li> <li>322</li> <li>402</li> <li>173</li> <li>454</li> <li>265</li> <li>257</li> <li>451</li> </ul>
Zhang, W	<ul> <li>432</li> <li>370</li> <li>291,</li> <li>447</li> <li>421</li> <li>313</li> <li>345</li> <li>290</li> <li>375</li> <li>257</li> <li>451</li> <li>428</li> <li>217</li> <li>380</li> <li>322</li> <li>402</li> <li>173</li> <li>454</li> <li>265</li> <li>257</li> <li>451</li> <li>350</li> </ul>
Zhang, W	<ul> <li>432</li> <li>370</li> <li>291,</li> <li>447</li> <li>421</li> <li>313</li> <li>345</li> <li>290</li> <li>375</li> <li>257</li> <li>451</li> <li>428</li> <li>217</li> <li>380</li> <li>322</li> <li>402</li> <li>173</li> <li>454</li> <li>265</li> <li>257</li> <li>451</li> <li>350</li> <li>249</li> </ul>
Zhang, W	<ul> <li>432</li> <li>370</li> <li>291,</li> <li>447</li> <li>421</li> <li>313</li> <li>345</li> <li>290</li> <li>375</li> <li>257</li> <li>451</li> <li>428</li> <li>217</li> <li>380</li> <li>322</li> <li>402</li> <li>173</li> <li>454</li> <li>265</li> <li>257</li> <li>451</li> <li>350</li> <li>249</li> <li>324</li> </ul>
Zhang, W	<ul> <li>432</li> <li>370</li> <li>291,</li> <li>447</li> <li>421</li> <li>313</li> <li>345</li> <li>290</li> <li>375</li> <li>257</li> <li>451</li> <li>428</li> <li>217</li> <li>380</li> <li>322</li> <li>402</li> <li>173</li> <li>454</li> <li>265</li> <li>257</li> <li>451</li> <li>350</li> <li>249</li> <li>324</li> </ul>
Zhang, W	<ul> <li>432</li> <li>370</li> <li>291,</li> <li>447</li> <li>421</li> <li>313</li> <li>345</li> <li>290</li> <li>375</li> <li>257</li> <li>451</li> <li>428</li> <li>217</li> <li>380</li> <li>322</li> <li>402</li> <li>173</li> <li>454</li> <li>265</li> <li>257</li> <li>451</li> <li>350</li> <li>249</li> <li>324</li> <li>354</li> </ul>
Zhang, W       187, 295,         Zhang, W       197, 239, 261,	<ul> <li>432</li> <li>370</li> <li>291,</li> <li>447</li> <li>421</li> <li>313</li> <li>345</li> <li>290</li> <li>375</li> <li>257</li> <li>451</li> <li>428</li> <li>217</li> <li>380</li> <li>322</li> <li>402</li> <li>173</li> <li>454</li> <li>265</li> <li>257</li> <li>451</li> <li>350</li> <li>249</li> <li>324</li> <li>354</li> <li>258</li> </ul>
Zhang, W       187, 295,         Zhang, W       197, 239, 261,	<ul> <li>432</li> <li>370</li> <li>291,</li> <li>447</li> <li>421</li> <li>313</li> <li>345</li> <li>290</li> <li>375</li> <li>257</li> <li>451</li> <li>428</li> <li>217</li> <li>380</li> <li>322</li> <li>402</li> <li>173</li> <li>454</li> <li>265</li> <li>257</li> <li>451</li> <li>350</li> <li>249</li> <li>324</li> <li>354</li> <li>258</li> <li>268</li> </ul>
Zhang, W       187, 295,         Zhang, X       197, 239, 261,	<ul> <li>432</li> <li>370</li> <li>291,</li> <li>447</li> <li>421</li> <li>313</li> <li>345</li> <li>290</li> <li>375</li> <li>257</li> <li>451</li> <li>428</li> <li>217</li> <li>380</li> <li>322</li> <li>402</li> <li>173</li> <li>454</li> <li>265</li> <li>257</li> <li>451</li> <li>350</li> <li>249</li> <li>324</li> <li>354</li> <li>258</li> <li>268</li> <li>256</li> </ul>
Zhang, W       187, 295,         Zhang, W       197, 239, 261,	<ul> <li>432</li> <li>370</li> <li>291,</li> <li>447</li> <li>421</li> <li>313</li> <li>345</li> <li>290</li> <li>375</li> <li>257</li> <li>451</li> <li>428</li> <li>217</li> <li>380</li> <li>322</li> <li>402</li> <li>173</li> <li>454</li> <li>265</li> <li>257</li> <li>451</li> <li>350</li> <li>249</li> <li>324</li> <li>354</li> <li>258</li> <li>268</li> <li>256</li> </ul>
Zhang, W       187, 295,         Zhang, X       197, 239, 261,	<ul> <li>432</li> <li>370</li> <li>291,</li> <li>447</li> <li>421</li> <li>313</li> <li>345</li> <li>290</li> <li>375</li> <li>257</li> <li>451</li> <li>428</li> <li>217</li> <li>380</li> <li>322</li> <li>402</li> <li>173</li> <li>454</li> <li>265</li> <li>257</li> <li>451</li> <li>350</li> <li>249</li> <li>324</li> <li>354</li> <li>258</li> <li>268</li> <li>256</li> <li>256</li> </ul>
Zhang, W       187, 295,         Zhang, X       197, 239, 261,	<ul> <li>432</li> <li>370</li> <li>291,</li> <li>447</li> <li>421</li> <li>313</li> <li>345</li> <li>290</li> <li>375</li> <li>257</li> <li>451</li> <li>428</li> <li>217</li> <li>380</li> <li>322</li> <li>402</li> <li>173</li> <li>454</li> <li>265</li> <li>257</li> <li>451</li> <li>350</li> <li>249</li> <li>324</li> <li>354</li> <li>258</li> <li>268</li> <li>256</li> <li>254</li> </ul>
Zhang, W       187, 295,         Zhang, X       197, 239, 261,	<ul> <li>432</li> <li>370</li> <li>291,</li> <li>447</li> <li>421</li> <li>313</li> <li>345</li> <li>290</li> <li>375</li> <li>257</li> <li>451</li> <li>428</li> <li>217</li> <li>380</li> <li>322</li> <li>402</li> <li>173</li> <li>454</li> <li>265</li> <li>257</li> <li>451</li> <li>350</li> <li>249</li> <li>324</li> <li>354</li> <li>258</li> <li>268</li> <li>256</li> <li>254</li> <li>368</li> </ul>
Zhang, W       187, 295,         Zhang, X       197, 239, 261,	<ul> <li>432</li> <li>370</li> <li>291,</li> <li>447</li> <li>421</li> <li>313</li> <li>345</li> <li>290</li> <li>375</li> <li>257</li> <li>451</li> <li>428</li> <li>217</li> <li>380</li> <li>322</li> <li>402</li> <li>173</li> <li>454</li> <li>265</li> <li>257</li> <li>451</li> <li>350</li> <li>249</li> <li>324</li> <li>354</li> <li>258</li> <li>268</li> <li>256</li> <li>254</li> <li>368</li> <li>245</li> </ul>
Zhang, W       187, 295,         Zhang, X       197, 239, 261,	<ul> <li>432</li> <li>370</li> <li>291,</li> <li>447</li> <li>421</li> <li>313</li> <li>345</li> <li>290</li> <li>375</li> <li>257</li> <li>451</li> <li>428</li> <li>217</li> <li>380</li> <li>322</li> <li>402</li> <li>173</li> <li>454</li> <li>265</li> <li>257</li> <li>451</li> <li>350</li> <li>249</li> <li>324</li> <li>354</li> <li>258</li> <li>268</li> <li>256</li> <li>254</li> <li>368</li> <li>245</li> </ul>

Zhou, B	323
Zhou, F	. 306
Zhou, G	325
Zhou, H	336
Zhou, N	383
Zhou, S	364
Zhou, W	339
Zhou, W	288
Zhou, X	352
Zhou, Y	451
Zhou, Y	449
Zhu, A 217,	376
Zhu, J	322
Zhu, J	422
Zhu, J 294,	364
Zhu, J	312
Zhu, S	. 445
Zhu, T	290
Zhu, W	323
Zhu, X	404
Zhu, Y	196
Zhu, Y T 206, 251, 253,	257,
	306,
	432
Zhuo, L	281
Zi, A	252
Ziegler, D P	437
Zikanov, O	437
Zindel, J W	403
Zinovev, A V	429
Zoeller, T	404
Zong, Z 261,	377
Zribi, A 179, 220, 274, 320,	326
Zunger, A 304,	389